Structure and dynamics of the penguin synnomes : understanding seabird life history and response to climate change through population genomics

Robin Cristofari

UNIVERSITÉ DE STRASBOURG

École Doctorale Vie et Santé
CNRS-IPHC-DEPE

THÈSE

présentée par :

Robin CRISTOFARI

soutenue le : **23 février 2016**

pour obtenir le grade de : **Docteur de l'Université de Strasbourg**

Discipline / Spécialité : Biologie / Écologie, Génétique des populations

Structure and dynamics of the penguin synnomes

Understanding seabird life history and response to climate change through population genomics

THÈSE dirigée par :
Dr LE MAHO Yvon — Profeseur émérite, CNRS-Université de Strasbourg
Dr ANCEL André — Directeur de recherches, CNRS-Université de Strasbourg

Co-encadrée par :
Dr LE BOHEC Céline — Chargée de recherches, CNRS-Université de Strasbourg
Dr TRUCCHI Emiliano — Associate researcher, Universität Wien

RAPPORTEURS :
Dr BEAUGRAND Grégory — Directeur de recherches, CNRS-Université de Lilles
Dr DAVEY John — Principal investigator, University of Cambridge

PRESIDENT DU JURY :
Dr POTIER Serge — Directeur de recherches, Université de Strasbourg

Acknowledgements

If ever a PhD was the fruit of an enthusiastic and supportive team, it is the work I present here. It was only made possible thanks to the unfailing dedication and patience of Dr Céline Le Bohec and Dr Emiliano Trucchi, who assumed the doubly essential roles of supervisors and friends. I sincerely thank you both, with the joyful certitude that this work is just the beginning of a long series..!

I warmly thank Pr Yvon Le Maho for giving me the chance to enter the insular world of polar biology, and for his continued guidance throughout this endeavour. His support made it possible not only to design this work, but also to realise it with the help of the Ecophy team: André Ancel, who co-directed this work, Julien Courtecuisse and Nicolas Chatelain, who invented every possible penguin-tracking contraption used here and there in this work, Aymeric Houstin, Matthieu Boureau, Gildas Lemonnier and Anne-Catherine Klein on the field. And, of course, the whole DEPE team in Strasbourg for their support and welcome every time I visited.

I spent the best days of this work on the research stations of Dumont D'Urville, in Adélie Land, and Alfred Faure, in Crozet Archipelago: I sincerely thank the French Polar Institute for this opportunity, as well as for their essential technical support that made this work possible, and Marie Pellé, Quentin Schull, Gaël Cardinal, Caroline Bost and Paco Decina for making these days the happiest ones.

I whole-heartedly thank Pr Nils C. Stenseth and the CEES team, who welcomed me at the University of Oslo, where almost all this work was done. Nanna Winger Steen and Emelita Rivera Nerli had the patience and kindness to help through the long and messy lab-work. The Norwe-

Table of contents

Index of tables

Index of figures

Articles and communications.

The following articles are included in this thesis:

- <u>Cristofari R,</u> Trucchi E, Whittington JD, Vigetta S, Gachot-Neveu H, Stenseth NC, Le Maho Y, Le Bohec C (2015) **Spatial heterogeneity as a genetic mixing mechanism in highly philopatric colonial seabirds.** PloS one 10: e0117981.

- <u>Cristofari R,</u> Liu X, Bonadonna F, Cherel Y, Le Maho Y, Pistorius P, Raybaud V, Stenseth NC, Le Bohec C & Trucchi E, **Stepping-stone range shifts in response to climate change in the Southern Ocean.** (*in prep.*)

- <u>Cristofari R,</u> Bertorelle G, Ancel A, Benazzo A, Le Maho Y, Ponganis PJ, Stenseth NC, Trathan PT, Whittington JD, Zanetti E, Zitterbart DP, Le Bohec C & Trucchi E, **Full circumpolar migration ensures evolutionary unity in the Emperor penguin.** (*Nature Communications - in prep*)

- Ancel A & <u>Cristofari R,</u> Fretwell PT, Trathan PN , Wienecke B, Boureau M, Morinay J, Blanc S, Le Maho Y, Le Bohec C (2014) **Emperors in Hiding: When Ice-Breakers and Satellites Complement Each Other in Antarctic Exploration.** PloS one 9:e100404

- <u>Cristofari R,</u> Fernandez-Zamora F, Gouin N, Le Bohec C, Plaza P, Trucchi E, Zavalaga C, Luna Jorquera G, **Unexpected population isolation in a critically endangered insular seabird, the Peruvian Diving Petrel** *(Pelecanoides garnotii).* (*in prep*).

The following communications also served as a basis for this work:

- Le Bohec C, Whittington JD, Ancel A, Chatelain N, Cornet C, Courtecuisse J, Crenner F, <u>Cristofari R,</u> Marpaux S, Allemand D & Le Maho Y (2014, August) **Predict changes in polar ecosystems : biological adaptation and technological innovation.** Oral presentation at the XXXIIIth SCAR Open Science Conference, Auckland, New Zealand.

- Cornet C, Amélineau F, Babel D, Boureau M, Courtecuisse J, Cristofari R, Descamps S, Marpaux S, Morinay J, Whittington JD, Le Maho Y. & Le Bohec C. (2014, July). **Personality and environmental heterogeneity in the Adélie penguin.** Oral presentation at the 15th Conference of the International Society for Behavioural Ecology, New York, USA.

- Cornet C, Amélineau F, Babel D, Boureau M, Courtecuisse J, Cristofari R, Descamps S, Marpaux S, Morinay J, Saraux C, Whittington JD, Le Maho Y. & Le Bohec C. (2013, September). **The adaptive capacities of Adélie penguins to face environmental variability : the role of heterogeneity within populations.** Keynote presentation at the 8th International Penguin Conference, Bristol, UK.

- Cristofari R, Trucchi E, Whittington JD, Vigetta S, Gachot-Neveu H, Stenseth NC & Le Bohec C (2015) **Spatial heterogeneity as a genetic mixing mechanism in highly philopatric colonial seabirds.** Poster presented at the XIth SCAR Biology Symposium : « Life in Antarctica : Boundaries and Gradients in a Changing Environment », Barcelona, Spain.

- Cornet C, Amelineau F, Babel D, Boureau M, Courtecuisse J, Cristofari R, Descamps S, Marpaux S, Morinay J, Whittington JD, Le Maho Y. & Le Bohec C. (2013, July). **Personality and its effect on fitness in the Adélie penguin.** Poster presented at the XIth SCAR Biology Symposium : « Life in Antarctica : Boundaries and Gradients in a Changing Environment », Barcelona, Spain.

- Le Bohec C, Cornet C, Cristofari R, Whittington JD, Courtecuisse J, Chatelain N, Crenner F, Allemand D & Le Maho Y. (2013, July). **Adaptive strategies and population trends of penguins to predict changes in polar marine ecosystems.** Oral presentation at the XIth SCAR Biology Symposium : « Life in Antarctica : Boundaries and Gradients in a Changing Environment », Barcelona, Spain.

Foreword

The work we present here lies in-between two poles of biological sciences - ecology and evolution. Increasingly well explored from a theoretical and laboratory perspective, the practical interface of these two disciplines, when applied to wild species and natural ecosystems, is at the core of intense contemporary investigation: for this reason, as will appear to the reader, the methods we use matter nearly as much as the conclusions we reach. To that aim, we will examine the particular stories of three seabirds of the Southern Seas, the Emperor penguin (*Aptenodytes forsteri*), the King penguin (*Aptenodytes patagonicus*), and the Peruvian diving-petrel (*Pelecanoides garnotii*), each of them confronted to environmental change in its own manner. Our primary line of investigation will be the way genetic data - an evolutionary exploration tool by excellence - can be integrated in the framework of ecological models, and in particular in numeric representations of climate.

This thesis is divided into eight main sections. A first introductory chapter will present the main concepts around which our work revolves, as well as its climatic and oceanographic framework. A second chapter will give an overview the methodological concepts that will be deployed in this particular study. The third and fourth chapters will focus on the King penguin, and its interactions with its habitat both at local, and global scale. The fifth and sixth chapters will repeat this exercise for the Emperor penguin. The seventh chapter, that presents the particular case of the little-known Peruvian diving-petrel, will showcase how these methods can be used as an exploratory tools in remote species where field data is scarce. Finally, an eighth and last chapter will sum-

marise the main findings of this work, and propose some conclusions, both for our three focal species, and for the development of more accurate investigation methods.

As already appears from its organisation, the question of scales - both spatial, and temporal - will be a structuring one throughout this manuscript. The complexity of temporal scales in speciation processes is still at the core of evolutionary investigations (see *e.g.* Gould & Eldredge 1972) - and this complexity only increases when considering ecological processes together with evolutionary ones. When focusing on a metazoan organism (a simple case compared to the bewildering organisation of plants), a point of relatively atomic singularity is reached with the *individual*[1]. Above that scale, the longer-lasting populations and species are increasingly complex ensembles obeying to stochastic processes; while below that scale, the rapid and minute scales of physiology bring us into yet another stochastic realm of populations, of cells or molecules this time: thus, going below or above the individual indistinctly leads us back from the most singular towards an increasing form of universality.

The nested temporal scales of *individuals*, *populations* and *species* also need to be thought of in the complex temporality of their environment. Metazoan life is directly characterised by the instantaneous interface between the individual, and the immediate conditions of its environment. At an instantaneous scale, this interface is highly variable, both externally (through the presence or absence of food, conspecifics, competitors, or the state of the weather, *etc*) and internally (*i.e.* through the physiological state of the individual), and leads to a wide variation of «*instantaneous fitness*» - or, more simply, immediate well-being. Yet this stochastic variation is averaged throughout the lifespan of the individual to a range of external and internal conditions, that results in a individual general *fitness*[2]. Further on, the large-scale fluctuations in average weather, or *climate*,

---

1.   The «*un-divisible*», by etymology.

2.   Fitness is first defined by Darwin 1859, together with the concept of *natural selection*, as the idea that «*individuals having any advantage, however slight, over others, [...] have the best chance of surviving and of procreating their kind. On the other hand, we may feel sure that any variation in the least degree injurious would be rigidly destroyed. This preservation of favourable variations, and the destruction of injurious variations, I call Natural Selection, or the Survival of the Fittest*» - fitness being here loosely conceived as the advantage conferred to an individual by its particular characteristics. As further noted by Barker 2008, «*fitness may refer to a*

together with the associated changes in biological communities[1], impose long-term patterns on the average relationship of large numbers of individuals to their changing environment - and, ultimately, *evolution*. Finally, in-between the immediate contact of the *individual* and the *instant*, and the slow change of the relationship of the *species* and the state of the world, lie the multiple facets of intermediate variations. The oscillating climatic phenomena that operate on a few years scale, the centennial variations of the Southern Annular Mode, or the slower pulse of Milanković cycles and Pleistocene glaciations, all blur any direct, linear extension of short-term phenomena to long-time scales. This fractal conception of the scales on which chronological processes operate is mirrored in space, through the local heterogeneity both of individuals and of environment: local adaptation or local extinction often occur at cross-current with the general stream of evolution.

The theory of population genetics seems to take all its sense at the light of this complex structure of time and space - with the curious meaning that *time* and *space* take there. A gene (this very material, real and transient fragment of a DNA molecule bounded both in space and in time) is progressively *abstracted* in the population genetics framework until it becomes a continuous time-object - a *sequence*. In this framework, the diversity of DNA molecules is relieved both from its synchronic and diachronic boundaries, as formalised through the approximations of the *continuous-time coalescent* and the *diffusion equations of drift* (see later on in §39 p. 99 and §40 p. 101). The resulting generalised object now transforms slowly and continuously over the evolution of the species, in an essentially Braudelian *longue durée* conception[2]. Yet this approximation requires the sacrifice of the most obviously discrete aspects of metazoan life: the individual and the generation.

---

genotype, an individual, a population or a species*», but may be broadly defined as « *the ability of organisms to pass on the genes they carry*».

1.   By «biological community», or *biocœnosis*, we refer to the ensemble of species that share a single habitat and interact within it (see Möbius 1877).

2.   See Braudel 1958, and §16 p. 60.

In parallel, however, a fundamental postulate of the modern synthesis is that evolution operates precisely at the level of the *individual* (Mayr & Provine 1998; Seehausen *et al.* 2014). At this level, genetic material is once again highly bounded: within the space of the individual's body, it is classically (although simplistically) considered *one*, and collectively subjected to fitness selection at the interface of the body and the environment. The sanction of this fitness selection on the space of the body is the shift of its boundaries in time: the frequency of *beginning* of a new organism carrying these genes, or *breeding*, and the delayed *demise* of that ensemble (or *death*): more beginnings and later demises are the way evolutionary success is sanctioned. Breeding and death have a position in time, yet they are also *spatial* boundaries, as they describe the beginning and end of the *body*, that *embodiment* of the abstract sequence along its continuous tree-like evolution.

And so, a *mise en abyme* occurs for the gene too: the processes that apply on the individual (a collection of identical DNA molecules) as *fitness selection* apply on the family group (an ensemble of highly similar molecules) as *kinship selection*, and on the species as *evolution*. And we are left wondering whether the variations in fitness that we document at the level of the individual (the variation in individual «quality» and life-history choices, and their direct consequences on that individual's life) are of the same nature as the broad trends in the adaptation of the species to an environment and a state of the climate, or whether the fitness of an individual is an essentially different concept from the fitness of a population, the one involving a stochastic, particular association of alleles, and the other a collective distribution of allele frequencies and expected fitness selected through repeated, but inaccurate, individual trajectories and accidents.

In fine, this amounts to asking how prevalent the individual should be in the study of the collective, and whether there is any sense at all in disregarding, even for theoretical purposes, that intuitively central figure when considering the fate of species. Although here purely methodological, this question ultimately converges towards ethical perspectives: indeed, the relative importance of the individual and the species is a difficult intuition, or decision, in our relationship to nature as

a whole. Conservation biology is mostly concerned with species, at the cost of disregarding individual trajectories: yet it may sometimes appear that this conception fails to capture the true complexity of our surroundings, by reducing to a handful of taxonomic categories what is really a rich spectrum of individual consciousnesses[1]. And paradoxically, despite its near-complete disappearance throughout the present manuscript, I finish with a clear intuition that only the individual makes absolute sense, and that the ultimate goal of my study was to better understand what exactly is the *experience* of the singular seabird who, against larger population trajectories and environmental changes, *« ever stands forth his own inexorable self »*[2]. However, these considerations must remain the salt of this work, and should not interfere with the detachment that is required by all sound scientific endeavours.

Thumbing through this manuscript, it will be evident that the diversity of methods is beyond a single person's work. The contributions of Dr Céline Le Bohec on the ecological side, and of Dr Emiliano Trucchi on the evolutionary side, have been determinant at every single step of this study. No less important was the expertise of Dr Giorgio Bertorelle, Dr Xiaoming Liu, and Dr Virginie Raybaud, in giving shape and soundness to the different parts of this manuscript: I want to thank them here once again.

Chapter 1: Introduction

Populations, philopatry and dispersal

§-1 Species: type and repetition. The systematic description of species can be seen as an extreme mediation of the *individual* and the *collective*. A single sample, the *holotype*, is taken as the explicit reference for bestowing the species' name - and the rest is essentially a *repetition*, in time and in space, of that individual type. That repetition, however, cannot be perfect (Kierkegaard 1843): variation, or *diversity*, plays a central role, both in time and in space (Mayr 1982). Intra-specific phenotypic variation only became the focus of biological sciences as «*individual differences*» with the works of Darwin, who famously understood them to «*afford materials for natural selection to act on and accumulate*» (Darwin 1859): the genetic basis of this diversity is now at the centre of the modern evolutionary synthesis (Mayr & Provine 1998; Seehausen *et al.* 2014). While not serving any pre-defined purpose, variation may *a posteriori* be organised along a spectrum ranging from *adaptive* to *neutral* diversity (Kimura 1983; Wagner 2008). At the molecular level, adaptive variation can be defined as the appearance of mutations with a beneficial phenotypic effect, that are positively selected in the population (Mayr 1963), while neutral variation is the appearance of mutations offering virtually no hold to natural selection (Kimura 1983). Without taking position as to the relative importance of neutral and adaptive variation in molecular evolution (a still debated topic, see *e.g.* Wagner 2008), the present work will mostly focus on *neutral variation*, as an insight into non-molecular ecological processes.

Introduction - §1

The organisation of molecular variation in space and time is the foundation of population genetics (Wright 1978; Kingman 2000), which can be defined as the study of genetic diversity within the conventional spatio-temporal bounds of a species - those «*merely artificial combinations made for convenience*» in the midst of «*intermediate gradations*» (Darwin 1859). The extent of this diversity and its organisation reflect basic characteristics of the species: genetic diversity itself has been linked to a variety of parameters, ranging from organismal complexity (Lynch & Conery 2003) to population size and history (Amos & Harwood 1998) or life-history strategies (Romiguier *et al.* 2014), while its organisation in space and time is largely a consequence of its demographic and migratory history (a point introduced in §41 p. 103). Therefore, studying species as a population-scaled system allows us to capture not only their intrinsic taxonomic diversity, but also the variety their ecological and evolutionary dynamics.

A most remarkable feature of the population genetic approach to within-species diversity, that has important methodological consequences, is (as far as metazoans are concerned) its necessarily ambivalent conception of the *individual*. Population genetics are, in a sense, pervaded with an overwhelming notion of singularity: as Ernst Mayr put it, «*wherever we look, we find uniqueness, and uniqueness spells diversity*» (Mayr 1982). The individual, as a singular (and likely unique) combination of alleles, is the only possible form upon which fitness selection may operate, and thus the only effective shape of genetic material - in that sense, a population, or a gene pool, is nothing else than an abstract representation of what is really only an aggregation of singular individuals. Although the concepts of species or populations (see §2 p. 25) are essential tools for understanding behavioural, demographic or evolutionary processes, the only observable, uninterpreted atomic unit of metazoan life is the individual. Hence, any empirical study that relies on the sampling of groups or populations really relies, in fact, on the sampling of a collection of unique individuals, the assignment to a group being a posterior decision of the observer (which poses very concrete questions of sampling design, see *Fine-scale colony structure*, p. 135).

And yet the *individual* is dissolved either *vertically*, or *transversally*, throughout the theoretical framework of population genetics. The central notion of *allele frequency* (see §45 p. 117), for example, exists only through the transversal analysis (*i.e.* at a single point of time) of a large number of chromosomes at a single genomic position, without retaining any information as to the particular associations of alleles within individuals - it can thus be conceived as a removal of the *synchronic*[1] boundaries between individuals - an idea that reaches its mathematical consecration in the diffusion equations approximating genetic drift (see §39 p. 99). The whole structure of the *coalescent* (see §40 p. 101 *sqq.*), on the other hand, relies on the vertical (*i.e.* cross-generation) analysis of sequences, throughout which the advent and demise of the individual (*i.e.* the *generation*) is an accident, and a mere unit of time: thus, the coalescent concept itself involves the dissolution of the *diachronic* separation between individuals - a conception that is formalised in the continuous-time representation of the coalescent, that completely discards the very notion of generation or individual (see §45 p. 117).

This paradoxical representation of singularity in the population genetic framework is in stark contrast with the prevalent concept of the individual both in the systematic framework (where singularity is reduced to dispersion around the holotype in morphospace), and in the ecological framework - where diversity is either replaced by homogeneous population parameters such as density (Bolnick *et al.* 2011), or on the contrary emphasised through attention to singular life-history choices (*e.g.* Le Bohec 2008; Weimerskirch 2013). One of the challenges of the modern evolutionary synthesis therefore remains the reconciliation of these different paradigms despite widely divergent tenets. In particular, the difference between the concepts of *population size* or *migration rate* in the ecological and the population genetic (henceforth «evolutionary») paradigms (see §41 p. 103 and Fig. 1 p. 24) makes the integration of cross-disciplinary sources difficult (see *The Emperor synnome*, p. 211) - and so do the very different time scales on which these

---

1.   *i.e.* boundaries between individuals occurring *at the same time*, or «physical» boundaries - as opposed to *diachronic* boundaries, that occur between *successive generations*.

1 different frameworks are based: in many respects, the population genetics framework occupies an

2 intermediate position between systematics (that operates on the speciation time scale) and ecolo-

3 gy (that focuses on the discrete lifespans of individuals). While the synthesis of these different

4 modes is, of course, beyond the scope of this work, the questions addressed here, being at the

5 crossroads of ecology and population genetics, will be best understood through this unavoidable

6 ambivalence.
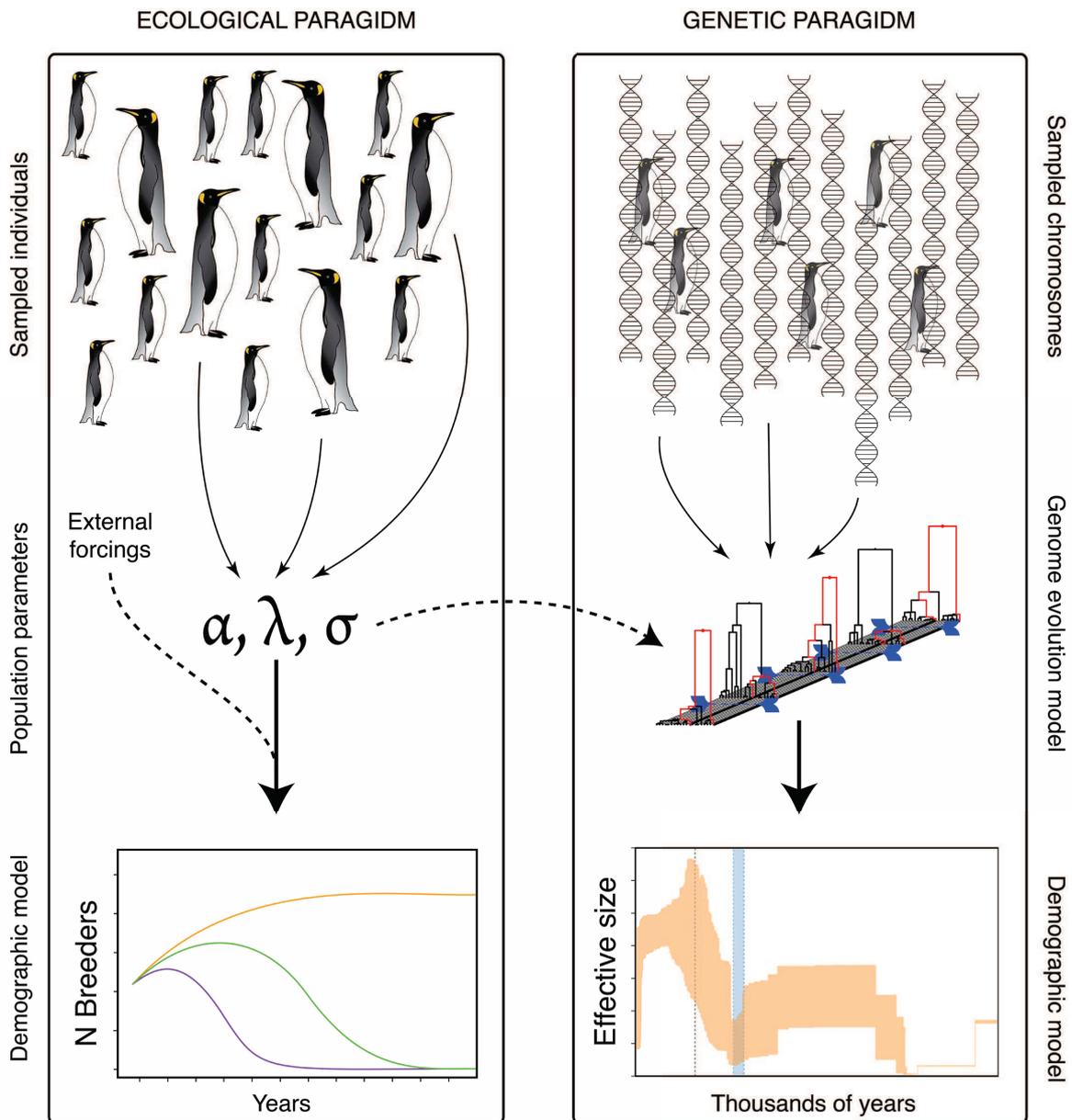
7 **Figure 1 | Demography in the Ecological and the Genetic paradigms.** In the ecological paradigm, a

8 subset of individuals is used to infer population-wide demographic parameters, and these define a general population

9 model, normally in units of number of breeders and at the decadal scale. In the genetic paradigm, a subset of

chromosomes is sampled, that integrates diachronic aspects of the population: this subset is used to fit a genome evolution model, that further defines a general demographic model, in units of *effective breeders* (see §41 p. 103) and usually at the scales of several thousand years.

§-2 Population, deme, colony. Just as the distribution of individual positions in the morphological, behavioural or genetic space defines a species' patterns of spatial and temporal diversity, the extent of the overlap between an individual's movement range on the one hand and the species' range on the other determines a spectrum of spatial structures, with homogeneous, *panmictic* ensembles on the one end, and highly heterogeneous and fragmented systems on the other. The particular architecture of a species integrates processes occurring on very different scales: and its description will change according to the framework in which analysis is conducted (Esler *et al.* 2006). The definition of a *population* - a central concept in a field such as population genomics - thus differs widely according to whether we place ourselves in a *genetic*, or an *ecological* paradigm (Waples & Gaggiotti 2006). In the ecological paradigm, the criteria retained are usually geography (individuals occurring *at the same place*, *e.g.* Krebs 2013), interactions between individuals (such as sharing food resources, *e.g.* Huffaker & Gutierrez 1984), or, importantly, demographic independence (*i.e.* migration between groups is not sufficient to force them into similar demographic trajectories, or influence extinction risk of one group, *e.g.* McElhany *et al.* 2000). Waples and Gaggiotti (Waples & Gaggiotti 2006) summarise the ecological definition as « *a group of individuals of the same species that co-occur in space and time and have an opportunity to interact with each other* » - a definition that relies on the examination of a species distribution, demography and behaviour at an observable timescale, *i.e.* in the order of magnitude of the observer's own lifetime.

In the genetic or « evolutionary » paradigm (Waples & Gaggiotti 2006), on the other hand, a population is rather defined as a breeding community, *i.e.* a group of individuals that have a higher probability of breeding with each other, than with an individual from another group (Hartl *et al.* 1988), and consequently as a group of individuals with correlated genotypes. The

quantitative aspect of the minimum correlation needed to achieve population status is debated: but whenever a standard criterion is proposed, it relies on a comparison of the relative influences of generic drift and migration in shaping a group's genetic diversity (see §39 p. 99 and §41 p. 103). For example, a threshold of one effective migrant per generation has been used in empirical studies (Mills & Allendorf 1996; Vucetich & Waite 2000; Wang 2004): if two groups exchange more than one effective migrant per generation, they are not considered separate. Higher thresholds have been proposed - *e.g.* a maximum of 5, or 25 effective migrants per generation (see Waples & Gaggiotti 2006 for a review). As these criteria are concerned with per-generation parameters, they can only apply when averaged over several generations - *i.e.* on a much longer time frame than the ecological definition.

The relationship between the concepts of population in the ecological and the evolutionary paradigms is not a trivial one. Although it would seem that behavioural and geographical isolation of a group of individuals naturally leads to reduced gene flow and genetic isolation, it is not clear how far the patterns observed on the decadal scale also apply over longer periods, as group cohesion may be heterogeneous over time or space, and lead to the apparent paradox of behaviourally very structured, yet genetically fully admixed species (*e.g.* Harlequin ducks, Esler *et al.* 2006, or Wandering albatrosses, Milot *et al.* 2008). In order to clearly distinguish between these different paradigms, in the present work, we will mainly use three related - but not equivalent - terms to describe the architecture of species: a *deme*, a *population*, and a *colony*.

A *deme* is a fully genetic definition of a group of individuals. It may be summarised as «*the largest area or collection of individuals where mating is (on average) random*» (Hamilton 2011). This definition does not necessarily include a spatial component, as several groups of random-mating individuals may occur in sympatry (*e.g.* Killer whales, Riesch *et al.* 2012). In particular, demes do not need to have boundaries (neither geographical nor behavioural), and may be defined in a «sliding window» fashion, *e.g.* in a classical isolation-by-distance system, where each individual may be taken as the focal point of a group or «genetic neighbourhood» (Crawford 1984) within

which alleles are highly correlated, and which decays gradually with distance. In that case the *deme* might be seen as the local approximation of a broader spatial autocorrelation system (Double *et al.* 2005; Epperson 2005). A threshold of 5% probability of mating has been proposed to define the limits of a deme (Hamilton 2011) - but this is obviously arbitrary, as the concept makes most intuitive sense in discretely distributed species, with strong discontinuities in mating probability. When defining a *deme*, we therefore assume that within the ensemble under scrutiny, mutation and drift, as opposed to migration, are the major contributors to genetic diversity.

A *colony* - especially for seabirds, see §18 p. 65 - is the conceptual counterpart of a *deme*: it is a completely geographical and behavioural concept, describing a spatial aggregation of breeding individuals over a period of time, and does not make any assumption as to the underlying genetic structure or evolutionary processes. The term is widely used in a variety of organisms, ranging from polyps (*e.g.* corals or siphonophores) to insects (*e.g.* ants, Giraud *et al.* 2002), each time with a different set of characteristics (in particular as to functional integration, which is extreme in siphonophores, see *e.g.* Dunn 2005, but minimal in corals, see *e.g.* Soong & Lang 1992). Coloniality is also well-spread in terrestrial vertebrates, whether in mammals (such as spermophiles, Armitage 1981; Johnson 1981), or in birds (Rolland *et al.* 1998). While some bird species' colonial behaviour extends to all aspects of their life (e.g. the well organised European starling *Sturnus vulgaris* colonies), most only exhibit colonial behaviour during reproduction (Lack 1968). This is especially the case in seabirds (see §18 p. 65), that may spend most of the year foraging alone or in small groups, out at sea, but gather in large colonies on land at the start of the breeding season. Paradoxically, philopatry is high in almost all seabirds (see §5 p. 32): although individuals roam far and wide during their foraging season, and have virtually no need for the shore, they keep a strong inner link to a particular patch of land, and return there regularly to breed. For some species with a limited foraging range, this may be the only available breeding grounds in the area (e.g. for the Black guillemot *Cepphus grylle*, see Ewins 1986). Yet in the widest-ranging seabird species, such as the great albatrosses (*Diomedea sp.*), or the *Aptenodytes*

penguins, colonial behaviour becomes a truly abstract conception: non-breeding foraging range overlaps widely between breeding colonies (and may in reality extent all around the world, see Croxall *et al.* 2005), while individuals will return to their birth-place with astounding regularity. Individual learning, and horizontal, or «cultural» (*sensu* Whitehead & Rendell 2014) transfer of information between birds breeding at the same place, may even lead to colony-specific idiosyncrasies, for example different foraging grounds for nearby colonies of the same species (Weimerskirch 2013). Thus, the *colony* can be seen as the most extreme representation of the population concept in the ecological paradigm: a spatially and temporally stable aggregation of individuals, that can be easily observed, defined and bounded (although not without conceptual choices, see §41 p. 103), but without assumed genetic characteristics.

Our use of *population* is at the intersection of *deme* and *colony.* In this work, a population will be defined as an ensemble that is bounded at the same time in the geographical, the demographical and the evolutionary spaces - in other words, a colony, or group of colonies, that also happens to be a deme. Rather than an anecdotical coincidence, speaking of a *population* implies that the processes that can be observed at the ecological scale (*i.e.* geographical clustering of individuals, use of common resources, or philopatric behaviour) are strong and stable enough through time to have an influence on evolutionary mechanisms, so that both the ecological and the genetic paradigms overlap. Thus, as opposed to a *deme*, our definition of population requires a *geographical* component - and as opposed to a *colony*, it also requires an *evolutionary* criterion.

Two antagonistic forces thus interact in shaping the wide variety of possible species architectures: *dispersal*, or the active or passive ability of individuals to move across their habitat, and *philopatry*, or the tendency for individuals to stay, or return, to their birth place (when fully passive, this may more accurately be called *inertia*). Taken together, these two forces may respectively be considered as the specific *fluidity* and *viscosity* of a species.

§-3 What is a Synnome? The particular architecture of the two *Aptenodytes* penguin species falls short of any existing concept. As will be exposed in detail in the following chapters (especially

The King synnome, p. 163 and *The Emperor synnome*, p. 211), *Aptenodytes* penguins display a startling tension between the ecological and the evolutionary definitions of a population. Colony structure is brought to an extreme, with highly discrete aggregations of individuals that appear fairly stable through time, at least at the centennial scale. Philopatry is high (see §19 p. 68), and is thought to extend not only to the colony, but also regularly to the very nesting site within that colony (see *Fine-scale colony structure*, p. 135 for details). Colonies have a high degree of demographic independence, as shown for example by the contrasting trajectories of the five rookeries on Possession Island, in Crozet Archipelago (Delord *et al.* 2004). However, none of the genetic criteria are met, and the long-term fluidity of the species appears to fully counteract any incipient genetic structuring, with migration asserting itself as a major evolutionary force in these species. Such a structure is distinct from a metapopulation system (see *e.g.* Hanski 1998), in which subunits are, to some extent, genetically separated - but it is also distinct from a panmictic system, since the extremely clustered spatial distribution of individuals, and high philopatry, contradicts the assumption of random mating at the generation-scale. Although extensive research remains to be done as to the underlying mechanisms, it is possible that heterogeneous demographic processes are involved - for example *pulsatile* dispersal, in which catastrophic local events would prompt massive dispersal during some generations, and no dispersal at all some others (see *Empirical evidence of heterogeneous dispersal*, p. 259 for a possible instance of this phenomenon). In order to describe this paradoxical structure, in this work, we use the term *synnome*, that we derive from the Greek σύννομος, «*a common grazing of flocks*», that has in particular been used for gathering flocks of birds[1], and which was commonly used by extension for «*reunions*», «*gatherings*», and even «*kindred*» (see §123 p. 236). The pivotal concept of *grazing together* (or συν - νομός, *syn-nomos*, «*shared pasture*») accurately renders the importance of central place foraging in the

---

1.   See for example Aristophanes' *Birds* (v. 1755 sqq.): « ἕπεσθε νῦν γάμοισιν ὦ | φῦλα πάντα συννόμων | πτεροφόρ᾽ ἐπὶ δάπεδον Διὸς | καὶ λέχος γαμήλιον.» - «*let them now gather, all the feathered flocks [synnómōn], and follow the brides to the houses of Zeus and to their wedding bed* ».

colony structure of seabird species, while distinguishing it from more deeply fragmented metapopulation systems. These different meanings together convey the particularity of the observed structure, that we here define as « *one single, nearly homogeneous pool of individuals is that distributed in a highly discrete way throughout its range. Local concentrations, or colonies, are highly consistent on the scale of a few generations, at which scale philopatry may be the norm. Yet, migration between these areas is high enough to maintain total homogeneity of the species' gene pool, so that, viewed on a micro-evolutionary time-scale, the only relevant unit is the species as a whole.* »

§-4 Dispersal and migration. Populations may be defined, as we exposed earlier, under two divergent paradigms - the *ecological* and the *evolutionary* ones (see §2 p. 25). Across both paradigms, a population is a *bounded* entity: either geographically or genetically, it is characterised by its *autarkic* aspect. Any kind of movement amongst groups works against the constitution of population units. Demographically, movement promotes the coupling of population trajectories, and counters the evolution of demographic independence. Genetically, movement provokes the transfer of alleles between demes, and works towards homogenising genetic variation and allele frequencies. However, the distinction between the ecological and the evolutionary paradigms also apply to inter-group movements, and, here again, prompted the choice of different terms. An unfortunate problem arises, however, because of the convergent choice of « migration » to describe very different phenomena, that we will clarify here.

The most common sense of *migration*, especially in a bird-biology context, is the seasonal movements of groups of birds (often *colonies*) between distinct breeding and overwintering grounds. Migratory species, in that sense, have evolved particular adaptations (see *e.g.* Berthold 1991) that allow them to achieve well-timed departure and arrivals to track the most beneficial environments year-round. Interestingly, migratory behaviour is a challenge to the definition of populations in the ecological paradigm, since groups may have different geographical and demographic boundaries in their summer, and winter ranges. However, migratory behaviour in that sense will not be examined in this work, mainly because it is not classically observable in our focal system

(although the inter-breeding foraging trips of penguins may arguably be related to migratory behaviour).

A more simple, one-way movement is the *dispersal* of individuals out of their original group. Dispersal was originally described by Howard 1960 as «*the movement the animal makes from its point of origin to the place where it reproduces*». From each individual's perspective, it is «*the greatest distance its genetic characteristics are transmitted, rather than the greatest distance the animal may have migrated or otherwise travelled away from the place it was conceived, hatched or born*». Dispersal can be defined both in the ecological and in the genetic paradigms. Ecologically, dispersal is the force working towards demographic linkage of populations, as an excess of juveniles in one location can compensate a low recruitment in another through direct displacement of individuals. Genetically, a dispersal event is the «unit» of gene flow, with each dispersing individual bringing a set of alleles from one location to another.

The second sense of *migration*, and the one we will use throughout this work, has been described by Dingle and Drake (Dingle & Drake 2007) in a biogeographical context as «*range expansions of faunas or individual species*», such as «*the northward extension of ranges following the retreat of glaciers at the end of the ice ages*». More specifically, in a population genetic context, the migration parameter M has been defined by the same authors as «*the exchange of genes among populations by whatever means, including but not limited to migration as we consider it here*». It is used in that sense in the coalescent framework, in particular by Beerli and colleagues (Beerli 2006; Beerli & Palczewski 2010, see more details in §41 p. 103). In this sense, *migration* is the averaged extent, on the long term, of individual dispersal events. Whereas dispersal is an individual- and generation-centred phenomenon that may be observed directly, migration is a time-averaged, population-centred event that is only detectable through indirect methods, such as gene flow reconstruction. Thus, while dispersal properly belongs to the life-history theory[1], and is expected to be

---

1.   In a word, the life history theory reconsiders traits of anatomy, physiology and behaviour in the light of «life history traits», *i.e.* reproductive, demographic or foraging strategies (see Stearns 1992 for details).

highly variable depending on individual characteristics and temporary environmental conditions, migration is a structural characteristic of the system, and is only expected to vary slowly according to broad changes in the organisation of a species.

§-5 Philopatry and site fidelity. Philopatry has first been described as *Ortstreue* («site fidelity») by von Haartman (Von Haartman 1949), as the tendency of the pied fly-catcher *Ficedula hypoleuca* to breed near its birth place, and has been generalised under the term *philopatry* by Huntington (Huntington 1951) as *«the tendency of an animal to return to its birthplace or breeding place, particularly for breeding»*. Thus, although the term has occasionally been used to describe adult fidelity to its breeding spot (Anderson *et al.* 1992), it describes, in the strict sense, the fidelity of adults to their birth place, or «natal philopatry», and is only properly used in that sense (Pearce 2007). Philopatry *sensu stricto* has important implications for the genetic processes that shape a species' architecture. The tendency to breed near one's birth place implies a significant departure from the panmixia hypothesis, since the probability of mating, for two randomly chosen individuals, becomes inversely proportional to their distance at birth. At a low level, this generates patterns of isolation by distance, where relatedness between individuals is a function of their geographical separation (Wright 1943; Wright 1946); at higher intensity, this may lead inbreeding and population fragmentation (Mayr 1963; Avise *et al.* 2000). However, the benefits of philopatry may be considerable. They may be behavioural, such as increased knowledge of the higher quality breeding spots or partners (Wheelwright & Mauck 1998; Heg *et al.* 2011; Arnaud *et al.* 2012), or enhanced selective value of proximal defensive behaviour (Dunford 1977) and allofeeding (Lecomte *et al.* 2006) through kinship selection; or they may be genetic, *e.g.* through the promotion of local micro-adaptation (Richardson *et al.* 2014) - which may apply either on land, or on the associated foraging areas, which are often specific to a colony (see Weimerskirch 2013). Philopatric behaviour is considered to be the basis of coloniality (Bowler & Benton 2005). However, there is an important discrepancy between the genetic and ecological time scales. On an ecological scale, the mean return rate of juveniles to their natal colony over a few generations is

generally taken as an estimator for the strength of philopatry. In several species, in particular seabirds, very high observed return rates seem to be inconsistent with the lack of genetic structure between colonies - the so-called *seabird paradox* identified by Milot *et al.* (Milot *et al.* 2008). However, based on simulation approaches, comparatively low (5% to 10%) migration rates have been shown to be sufficient to counterbalance the effects of local genetic drift on a longer time scale (Waples & Gaggiotti 2006). Moreover, the assumption that philopatry is a stationary process in colonial species, and that the mean return rate should converge over time to the species philopatry, does not take into account the possibility of pulsatile mass-dispersal events, that may reshuffle gene pools entirely amongst several populations. Philopatry, as opposed to the instantaneous probability of fidelity (F) or dispersal ($1 - F$), is not a directly estimable parameter (Kendall & Nichols 2004; Pearce 2007), but rather a long-term behavioural trait of the species, that may or may not lead to a choice of site fidelity, depending on the actual environmental conditions.

§-6 Philopatry and dispersal in oceanic systems. The dynamics of oceanic structures differ dramatically from terrestrial ones when it comes to dispersal (Steele 1985). Although at the lower levels of the trophic system, passive long-distance dispersal is equally present in terrestrial and marine environments, as atmospheric currents perform the same role as sea currents for seed or propagule dispersal (Cain *et al.* 2000; Nathan & Muller-Landau 2000; Cowie & Holland 2006; Nathan 2006; Nathan *et al.* 2008; Nikula *et al.* 2013), the difference in spatial organisation and structure becomes more important for larger organisms, especially vertebrates (Carr *et al.* 2003). Terrestrial ecosystems have typically higher habitat fragmentation, less dispersal and gene flow, and globally more closed systems (Waser & Jones 1983; Turchin 1998; Carr *et al.* 2003): the interaction between latitudinal and altitudinal gradients results in very complex habitat distributions that contrast with the mostly zonal pelagic habitats (Burrows *et al.* 2014). On the other hand, oceans may be considered as a *fluid landscape* in which both active and passive dispersal occurs on very large scales (Queiroz 2005; Cowie & Holland 2006; Nikula *et al.* 2013). Habitat fragmentation, al-

though documented (Acosta 1999; González-Wevar *et al.* 2010), is usually restricted to coastal or benthic species with extremely specialised niches (Rex *et al.* 1993; Whitlatch *et al.* 1998; Poulin *et al.* 2014). Long distance passive (*i.e.* current-driven) dispersal has been observed in organisms ranging from planktonic species (*e.g.* vagile stages of kelp, or invertebrates, see Fraser *et al.* 2011; Nikula *et al.* 2013) to larger vertebrates, especially at early life stages (*e.g.* turtles, see Gaspar *et al.* 2012). Active dispersal by vertebrate species is common at transoceanic scales (Bowen & Siniff 1999; Le Boeuf *et al.* 2000).

In oceanic systems dominated by strong currents (such as, in this study, the Antarctic Circumpolar Current system (ACC - see §7 p. 35, or the Humboldt Current system - see §147 p. 276), passive and active dispersal are general features of communities. In the ACC, it has been evidenced for species ranging from algæ and small invertebrates (Nikula *et al.* 2010), to benthic species (Arango *et al.* 2011) and fish (Matschiner *et al.* 2009; Damerau *et al.* 2012). However, the extent of genetic diversity along circumpolar ranges remains variable amongst taxa, and appears to depend largely on specific dispersal potential and life-history traits (Rogers 2007). In many cases, discontinuities such as the Antarctic Peninsula region (which extends North to almost 62°S) break these homogeneous dispersal systems, and stand out as distinct provinces, both in terms of climate (Mulvaney *et al.* 2012) and of biogeography[1] (Terauds *et al.* 2012).

The active dispersal power of vertebrates has, however, one paradoxical consequence: their higher ability to move around oceanic systems allows them to *not* disperse along the currents. While sessile species resist to dispersal by sheer inertia, active swimmers and flyers exhibit *philopatric behaviour* (see §5 p. 32 and Frederiksen & Petersen 1999; Steiner 2005; Bicknell *et al.* 2012; Fernández-Chacón *et al.* 2013), which can be thought of as counteracting the high fluidity of oceanic environments through opposed active movement. Philopatry thus allows for the perpetuation of relatively stable demes (*e.g.* in fur seals, see Bonin *et al.* 2013), family groups (as in killer

---

1.   Broadly considered here as the distribution and co-occurrence of species through space.

whales, see Hoelzel 1998), or colonies (as in most seabirds, see Friesen *et al.* 2007). Indeed, in most cases, natal philopatric behaviour is strong enough to promote genetic differentiation even between populations that largely overlap in their foraging or wandering areas (Dearborn *et al.* 2003; Friesen *et al.* 2007; Smith *et al.* 2007). Such patterns have been observed in marine mammals (both cetaceans and pinnipeds, see Hoelzel 1998; Baker *et al.* 2008; Bonin *et al.* 2013), in turtles (Molfetti *et al.* 2013), and in most seabirds (Friesen *et al.* 2007; Bicknell *et al.* 2012). Thus, the possibility of fast and unhindered movements in oceanic system has the unexpected consequence of allowing high return rates to particular breeding locations in most vertebrates, rather than promoting complete genetic mixing.

Antarctica and the Southern Ocean

§-7 Oceanography and geography. The Southern Ocean is the vast water mass encircling the Antarctic continent, and one of the major thermal exchange points between the oceans, the atmosphere and the cryosphere (Hofmann & Maqueda 2011; Meijers 2014). While its official definition fixes its northern limit at 60°S (International Hydrographic Organization 2000), its functional definition is usually extended at least to the Antarctic Polar Front, around 55°S (Moore *et al.* 1999; Gersonde *et al.* 2005), where it blends into the Southern Atlantic, Indian and Pacific oceans (see Fig. 2 p. 37 and Fig. 7 p. 77).

Southern Ocean oceanography is dominated by the influence of the strong planetary Westerly winds in the southern Ferrell cell (De Boer *et al.* 2008; Kohfeld *et al.* 2013) that blow continuously over the middle latitudes, unhindered by land barriers in the Southern Hemisphere, bringing the surface waters into motion. The resulting West Wind Drift, or Antarctic Circumpolar Current (ACC) is one of the largest ocean currents on earth, with a mean transport of 105 to 140 Sverdrups, and the only one to directly connect the three major ocean basins (Rintoul *et al.* 2001). Westerly wind stress' main effect is the eastward flow of the ACC, but it also causes im-

portant Ekman transport (in the Southern hemisphere, a counterclockwise deviation of up to 90° of the surface drift compared to the wind stress, see Toggweiler & Samuels 1998) that brings the surface waters equatorwards. In the Antarctic region, wind and evaporative cooling under katabatic wind stress, and salt concentration through brine rejection during sea ice formation around polynyas (Thomas & Dieckmann 2008, see §18 p. 65), make the surface waters especially cold and salty - and consequently dense. During their equatorwards transport, these water masses converge with the warmer and less dense northern water masses: the resulting steeper isopycnals[1] mean that the Antarctic surface waters ultimately sink to the sea floor at the Antarctic Convergence or Antarctic Polar Front (APF), forming the Antarctic Bottom Waters (AABW, see Rintoul *et al.* 2001). South of the APF, on the other hand, Ekman transport is divergent, and causes the upwelling of warm circumpolar deep waters (Warm Deep Water, WDW and Circumpolar Deep Water, CDW, see Sarmiento *et al.* 2004; Anderson *et al.* 2009 for details) south of the APF.

North of the APF lies the Subantarctic region, bounded to the North by the Subtropical convergence (STC) where Antarctic and Subantarctic waters become stratified under the tropical surface waters, around 40°S. While nowhere near as sharp as the APF, the STC is best defined by the disappearance of the permanent thermocline[2] (Tomczak & Godfrey 2003): north of the STC, temperature drops rapidly from the surface towards the bottom until ~1000 m. South of the STC, on the other hand, the temperature gradient between the surface and deep waters becomes less and less pronounced, with sometimes less than 1°C difference in the Antarctic region. The APF, however, remains characterised by minor seasonal thermoclines at the lower limit of the surface mixed layer (SMC, see *e.g.* Charrassin & Bost 2001). South of the ACC, and close to the Antarctic continent, on the other hand, the Antarctic Coastal Current, or East Wind drift, flows in the opposite direction of the ACC over the narrow continental shelf (Tchernia & Jeannin 1980;

---

1.   Or planes of equal water density. As opposed to pressure which is mostly determined by depth, density is determined primarily by temperature and salinity.

2.   The *thermocline* is the transition zone between the surface mixed layer, where diurnal solar radiation and wind- and tide-driven water mixing result in rather homogeneously warmer temperatures, and deeper and colder waters. It is characterised by a steep temperature gradient in the water column.

1   Fahrbach *et al.* 1994). Both currents form the two main gyres of the Southern Ocean, in the Ross

2   and Weddell seas (Gouretski 1999; Meredith *et al.* 2000), that have distinct oceanographic fea-

3   tures - for example the warmer deep water upwelling and resulting stable sensible heat polynya in

4   the Weddell sea (*i.e.* a polynya caused by water heat rather than wind stress, see Thomas &

5   Dieckmann 2008).
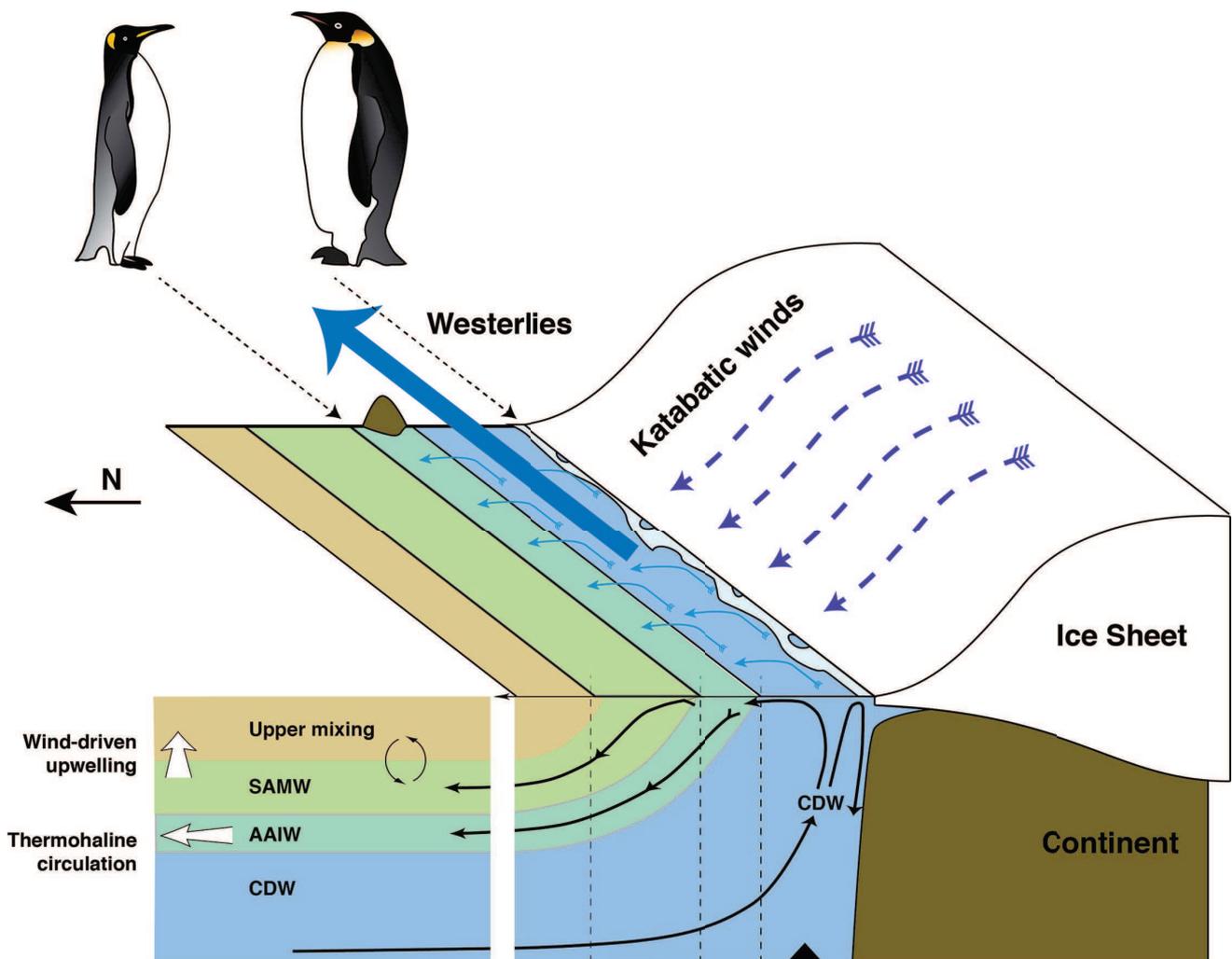
6   **Figure 2 | Structure of water masses in the Southern Ocean.** Main layers of the Southern Ocean:
7   Circumpolar Deep Water (CDW), Antarctic Intermediate Water (AAIW), Subantarctic Middle Water (SAMW) and
8   upper mixing layer. Thick blue arrow represents Westerly winds and the main flow of the Circumpolar current.
9   Lighter arrows in the Antarctic Circumpolar Current represent Ekman transport (*Based on Sarmiento et al. 2004*).
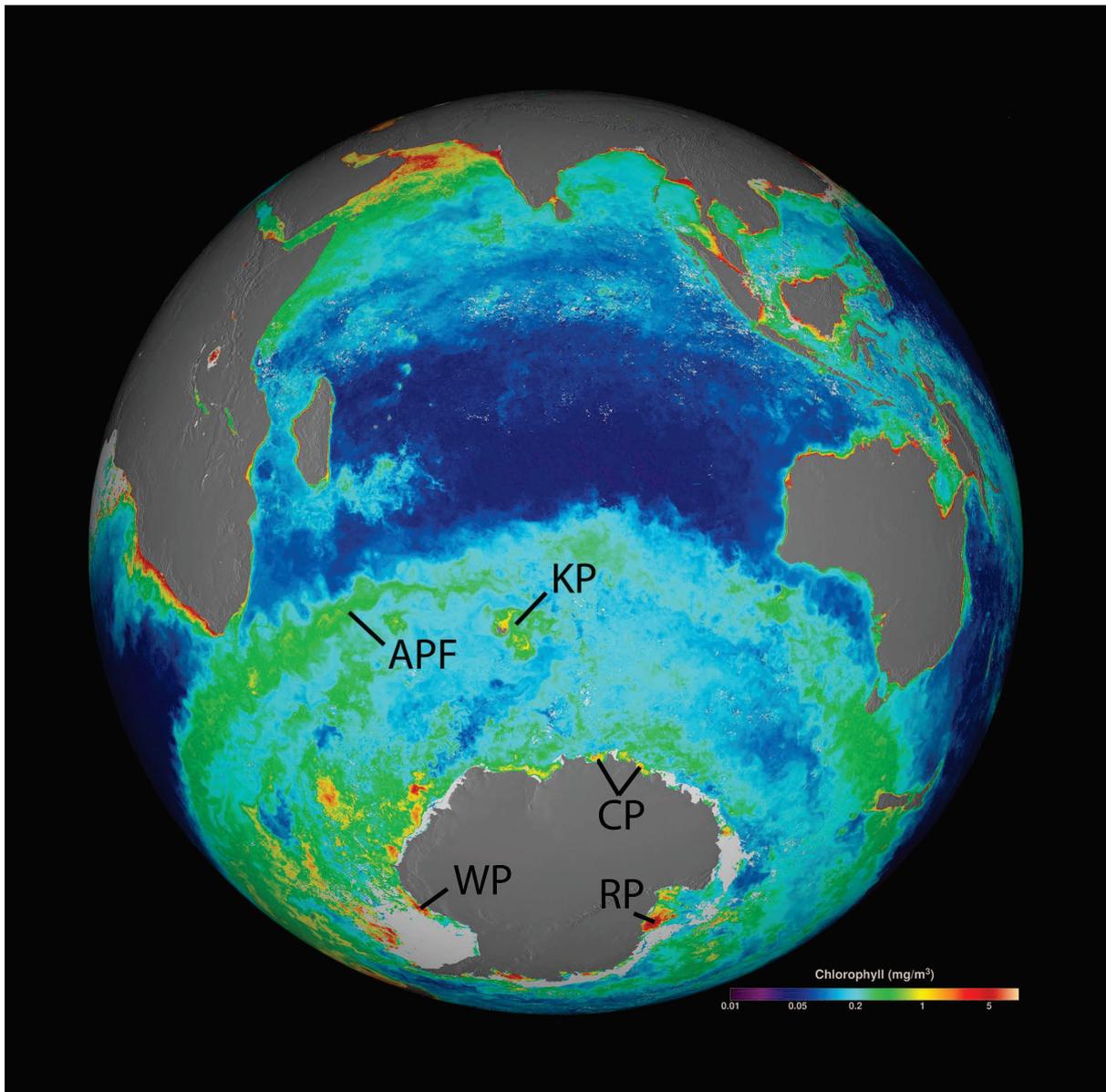
1 **Figure 3 | Primary productivity concentration on the Antarctic Polar Front.** Surface chlorophyll
2 concentration, 21 dec. 2011 to 20 mar. 2012. High chlorophyll concentration is visible all along the APF, with a lo-
3 cal peak on the Kerguelen plateau (KP), as well as in latent heat coastal Antarctic polynyas (CP), and in the sensible
4 heat Weddell polynyas (WP) and latent and sensible heat Ross Sea Polynya (RP) - see §18 p. 65 for details). Image
5 courtesy of NASA, Suomi NPP VIIRS satellite program.

6 The importance of the Southern Ocean and of the ACC, however, goes well beyond their region-

7 al effects. Together with the North Pacific, the ACC is the major upwelling area for ancient bot-

8 tom waters (Primeau 2005; Marshall & Speer 2012), and therefore a central contributor in the

9 thermohaline circulation, or Meridional Overturning Circulation (MOC, see Marshall & Speer

2012), which makes its importance central for global heat exchange and circulation. As it is one of the few areas were deep waters outcrop directly at the surface, it is also central for gas exchange between the deep ocean and the atmosphere, and enhanced upwelling activity has been linked to a rise in atmospheric CO_2 in the Southern Ocean (Anderson *et al.* 2009). But the Southern Ocean upwelling has also been identified, together with the North Pacific, as the major return path of nutrients towards the surface after downwelling at lower latitudes, which makes it a key component of the global biological pump[1], accounting for up to three quarters of the productivity north of 30°S (Sarmiento *et al.* 2004). Finally, being the only zonally unbounded water mass in the world, and blending into the three main ocean basins, the Southern Ocean functions as a central coupling mechanism between otherwise independent water masses, and allows for tele-connections between basins (White & Peterson 1996; Rintoul *et al.* 2001). It also spills out in the major northward Eastern Boundary Currents of the three Southern Hemisphere ocean basins (the Humboldt Current on the western shore of South America - see §147 p. 276, the Benguela Current on the western shore of Africa, visible on Fig. 3 p. 38, and the lesser West Australia Current).

The local influence of the ACC and of the APF on biological processes is tremendous. The up-welling of nutrient-rich deep waters to the surface, and their increased oxygen concentration in the surface mixed layer, is responsible for a massive concentration of primary productivity in the APF area (up to 20% of the world's marine primary productivity, see Laubscher *et al.* 1993; Bathmann *et al.* 1997; Carr *et al.* 2006, and Fig. 3 p. 38). Enhanced primary productivity in turns sustains stocks of krill (*Euphausia superbia*, see Murphy *et al.* 2007a) and fish (Pakhomov *et al.* 1996) - these being dominated by the myctophids (mostly *Electrona sp.*, *Protomyctophum sp.*, *Gymnoscopelus sp.* and *Krefftichthys sp.*, see Collins *et al.* 2008 for details). Several top predators take advantage of prey aggregation on the APF - for example elephant seals *Mirounga sp.* (Boyd

---

1.   Or, put simply, the global circulation of nutrients, that integrate both active components (*e.g.* animals themselves), and passive components (*e.g.* drift with water masses).

& Arnbom 1991) or king penguins *Aptenodytes patagonicus* (Charrassin & Bost 2001). At the southern boundary of the ACC, the extended winter sea ice cover also promotes blooms of marine productivity: years of increased sea ice have the highest krill biomass (Nicol *et al.* 2000), with direct consequences on the populations of top predators (*e.g.* the Adélie penguin *Pygoscelis adeliae*, Nicol *et al.* 2008), making the coastal pack-ice zone a distinct high-productivity area (Tynan 1998).

§-8 Climate variability in the Southern Ocean. The complex structure and global connections of the Southern Ocean make it respond strongly to the major modes of climate variability in the Southern Hemisphere: the circumpolar Southern Annular Mode (SAM), and the subtropical dipole events, of which the most important is the El Niño Southern Oscillation (ENSO), but which also include the Southern Indian Ocean Dipole (SIOD) and the South Atlantic Subtropical Dipole (SASD).

The Southern Annular Mode is the average pressure difference between the mid-latitudes and Antarctica. The resulting atmospheric circulation is the major cause of climate variability in the Southern Ocean (Marshall 2003; Abram *et al.* 2014), with important decadal-scale cyclicality, and broader centennial-scale oscillations (Abram *et al.* 2014). SAM has opposite effects in the polar and subtropical zones. During positive SAM events, the poleward shift of the westerlies strengthens the Ekman transport in the ACC, resulting in an equatorward shift of the APF, increased upwelling activity south of the APF, and increased marine productivity in the polar frontal zone (Lovenduski & Gruber 2005) - while in the subtropical zone, warm SST anomalies result in decreased productivity. Conversely, negative SAM events (*i.e.* northwards expansion of the Westerlies) have a strong effect on the whole food chain, up to top predators (Forcada & Trathan 2009; Bost *et al.* 2015).

While the impact of the SAM is essentially felt all around the Southern Ocean, each ocean basin is also subject to the more local (although tele-connected) effects of the dipole events. While the El Niño phenomenon differs qui significantly from the South Indian and Atlantic dipoles, its

general structure remains the oscillation of temperature differences between the East and the West of the subtropical zone. A steep zonal temperature gradient guarantees strong trade winds and intense Walker circulation[1]. The periodic diminution of winds off the West coast of South America diminishes cold deep water upwelling, reduces the east-west temperature difference across the Pacific, and, as a result, also diminishes the Walker circulation: this brings high precipitations so South America, and high sea surface temperatures across the whole Pacific (Tomczak & Godfrey 2003; Stuecker *et al.* 2013). More recently, similar cyclical events arising from zonal temperature gradients have been identified in the Southern Indian Ocean (the SIOD, Saji *et al.* 1999) and in the South Atlantic (the SASD, Taschetto & Wainer 2008; Wainer *et al.* 2014). Their link with the ENSO, and their global connections, however, still remain to be fully investigated (Saji & Yamagata 2003; Ashok *et al.* 2004; Abram *et al.* 2008). Together, the SAM, ENSO and dipole events also contribute to the variability in sea ice extent around Antarctica (Simmonds & Jacka 1995; Lefebvre 2004; Stammerjohn *et al.* 2008).

The integrated effect of the SAM, the ENSO, and the dipole events result in combined modes of variability in the Southern Ocean (Fogt & Bromwich 2006; Ciasto & Thompson 2008; Fogt *et al.* 2011), that have deep impact on biological communities. Primary productivity in the Southern Ocean responds both to the SAM (Lovenduski & Gruber 2005) and to ENSO (Beaufort *et al.* 2001; Behrenfeld *et al.* 2001), mostly mediated through changes in surface water temperature, sea ice, and nutrient availability. Both changes in the physical properties of surface waters and in trophic interactions also have an impact at trophic levels above phytoplankton, *e.g.* on the Antarctic krill (Murphy *et al.* 2007b): in turn, these effects are passed on to top-level predator species such as right whales (Leaper *et al.* 2006), elephant seals (McMahon & Burton 2005) or penguins (Bost *et al.* 2015). Although climate variability is a perfectly natural phenomenon, and should not threaten species resilience, the highly integrated character of the Southern Ocean climate makes it liable to entering large feedback mechanisms, thereby amplifying the effects of cli-

---

1.   *I.e.* a zonal circulation of air masses in the tropics, driven mostly by east-west temperature and pressure differences.

mate change (see §12 p. 52). It is therefore of the utmost importance to gain a good understanding both of the climatic processes themselves and of their effects on biological communities.
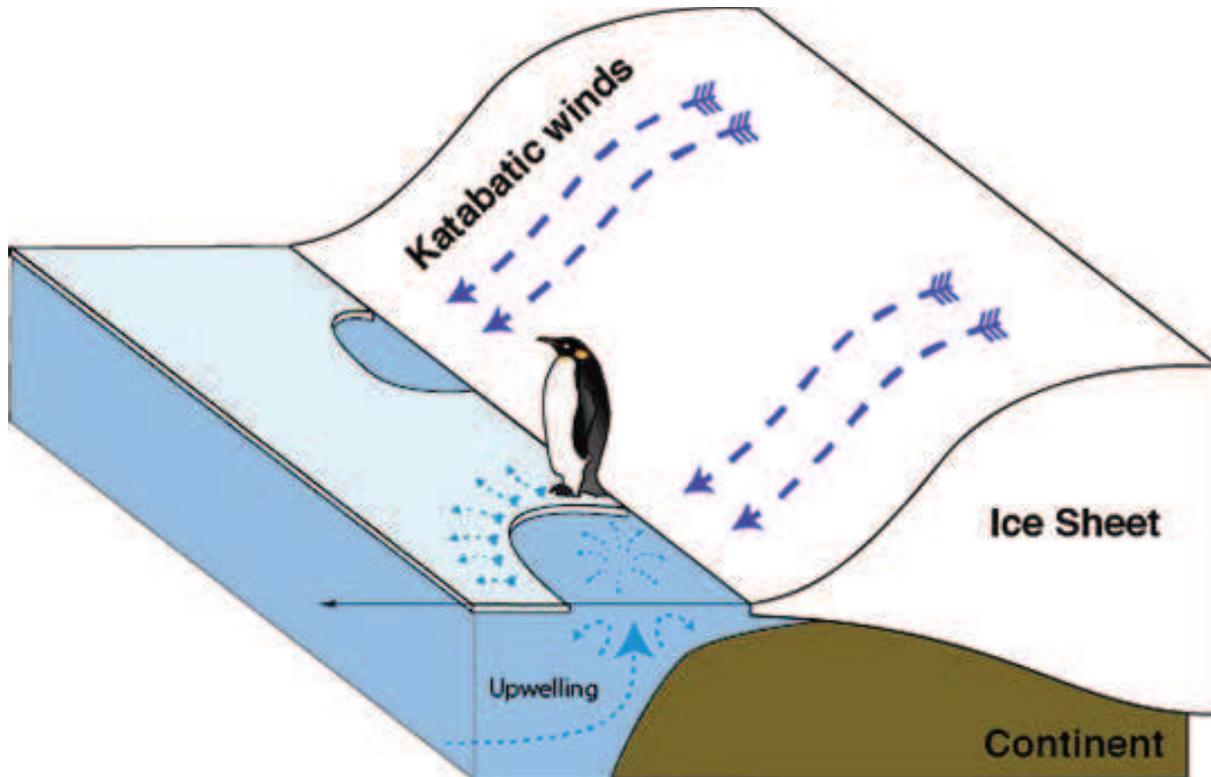
Figure 4 | The formation of sea ice in coastal polynyas. A schematic representation of coastal sea ice formation (light blue arrow on the ice) and local upwelling around polynya area (see §18 p. 65 for details).

§-9 Climatic history of the Southern Ocean. The Southern Ocean is considered to have taken its present-day shape by the onset of Pliocene (~5.3 Myr). The physical separation between Antarctica and South America is though to have occurred between the mid-Eocene (~41 Myr ago, Livermore *et al.* 2005) and the Oligocene-Miocene transition (~23 Myr ago, Pfuhl & McCave 2005), together with the slow onset of icehouse-earth conditions - the opening of the Drake passage itself having possibly contributed to the global temperature decrease (Nong *et al.* 2000; Livermore *et al.* 2004). The Antarctic Circumpolar Current (see §7 p. 35) is thought to have settled around the early Miocene (Pfuhl & McCave 2005), but the present-day water mass boundaries appear to have been established later, perhaps around the Middle Miocene Climatic Transition (MMCT,

~16-11.5 Myr, see Haywood *et al.* 2008; Knorr & Lohmann 2014). This idea is confirmed by the DNA-inferred radiation date of several marine taxa, for which Antarctic and Subantarctic clades have been isolated from each other around the MMCT (Poulin *et al.* 2014), which is also coincident with the radiation of crown penguins (see §21 p. 72).

Miocene marks the transition from greenhouse-earth conditions to present-day-like icehouse conditions. The Antarctic Ice Sheet is thought to have taken over the prevailing tundra environment by the early Miocene (Raine & Askin 2001), and developed to reach its current extent by the end of the period (Westerhold *et al.* 2005). Despite high (and still not fully understood) variability, prevalent marine conditions were warmer during the early Pliocene than today (Haywood *et al.* 2008) - although with high marine productivity. The SST was about 5°C warmer than today throughout the Southern Ocean (Whitehead 2003), and the APF lay about 6° South of its present position in the mid-Pliocene (Barron 1996), while the global thermohaline circulation may have been stronger than observed now (Haywood *et al.* 2008). By the late Pliocene (~2.5 Myr), however, Antarctic cooling strengthened, with increased Westerlies and equatorward migration of the APF, and possibly a reduction in the thermohaline circulation (McKay *et al.* 2012).

Most of the Subantarctic islands came to existence during that period. Apart from the continental-shelf South Georgia and Falklands (that are remnants of Gondwana, and as old as neighbouring South America), and sub-continental Kerguelen islands (that were formed during the Oligocene), the subantarctic islands are mostly young, volcanic mounds raised from the sea-floor. Crozet, Heard and Macquarie were thus formed during the late Miocene, and Prince Edward, Bouvet, Gough, etc. appeared between the Pliocene and the Pleistocene - and as late as 0.45 Myr ago for Prince Edward (see a complete review in Quilty 2007). Thus, both in terms of geography and of oceanography, we may consider that the Southern Ocean did not take its present-day shape before the Pleistocene.

Although better known, Pleistocene (~2.6 Myr to 11.7 Kyr BP) and Holocene (~11.7 Kyr BP to the present) history in the Southern Ocean is still subject to considerable uncertainties. General-

ly, reconstructing oceanographic and atmospheric processes at these relatively recent periods relies

on to different approaches. First, direct or indirect evidence may be obtained from cores, whether

of marine sediment throughout the Southern Ocean, of ice on the Antarctic ice sheet, or of peat

on the subantarctic islands. Alternatively, General Circulation Model (GCM) developed for the

historical period may perform rather well in that recent past, since the major features of Ocean-

Atmosphere circulation are assumed stable over that period: the Coupled Model Intercomparison

Project phase 5 (CMIP5, see §50 p. 130) panel thus includes Pleistocene Last Glacial Maximum

and mid-Holocene experiments (see Fig. 5 p. 45 and §50 p. 130 for details on these experi-

ments). Core evidence provides chemical, physical and biostratigraphic markers that may be used

as proxies for a variety of variables Gersonde *et al.* 2005; Armand & Leventer 2010; Hodgson *et

al.* 2014, either directly at the location of the core (which is how marine sediment and terrestrial

peat cores are usually interpreted, see Gersonde *et al.* 2005; Martínez Garcia *et al.* 2009; Armand

& Leventer 2010), or as a mixture of local and oceanic source area signal (see Wolff *et al.* 2003;

Wolff *et al.* 2006). Foraminiferan and diatom assemblages in marine sediment cores offer an ac-

curate index of the state of the surface water masses, that can be used to locate the position of the

Southern Ocean fronts through changes in surface temperature (*e.g.* the complex frontal structure

around the Campbell plateau, in Neil *et al.* 2004, or the APF in the Indian and Atlantic oceans,

in Kemp *et al.* 2010) or the extent of sea ice (*e.g.* Hodell *et al.* 2001; Gersonde *et al.* 2005). Fossil

pollen in terrestrial or marine cores provides direct evidence as to the prevailing climatic condi-

tions (*e.g.* McGlone *et al.* 2010). Chemical indices can be extracted from ice cores[1] and marine

sediment cores[2]. These multiple proxies are used either directly, or as an input in Atmosphere-

---

1. Considering they have been deposited at the core site as wind-borne aerosols, this requires hypotheses as to the atmospheric circulation at the core site (see Wolff *et al.* 2006): these normally include methanesulphonic acid (MSA, as a proxy for marine dimethyl sulphide, a biomarker that reflects algal growth and thence marine productivity - see Legrand *et al.* 1991), sea salt sodium (freed as high-salt brine at the surface of sea ice, and thus indicating sea ice extent, see Wolff *et al.* 2003), iron and calcium (transported as dust, and revealing atmospheric circulation, see Wolff *et al.* 2006). Deuterium/hydrogen ratio ($\delta D = {}_2H/{}_1H$) is commonly used as a proxy for temperature anomaly (Augustin *et al.* 2004; Wolff *et al.* 2006), and can be combined with the record of greenhouse gases (CO_2 and CH_4 mostly, see Fischer *et al.* 1999; Petit *et al.* 1999; Augustin *et al.* 2004).

2. Marine sediment cores, besides isotopic signatures ($\delta_{18}O$, see Lisiecki & Raymo 2005) and chemical signatures such as iron flux (from continental input, as a marker of marine productivity, see Martínez Garcia *et al.* 2009), also provide biomarker ev-

Ocean General Circulation Models, to reconstruct the prevailing oceanographic and climatic conditions. However, reconciling these diverse sources is still problematic, with mixed signals between the glacial, oceanic, and terrestrial environments (Armand & Leventer 2010; McGlone *et al.* 2010).
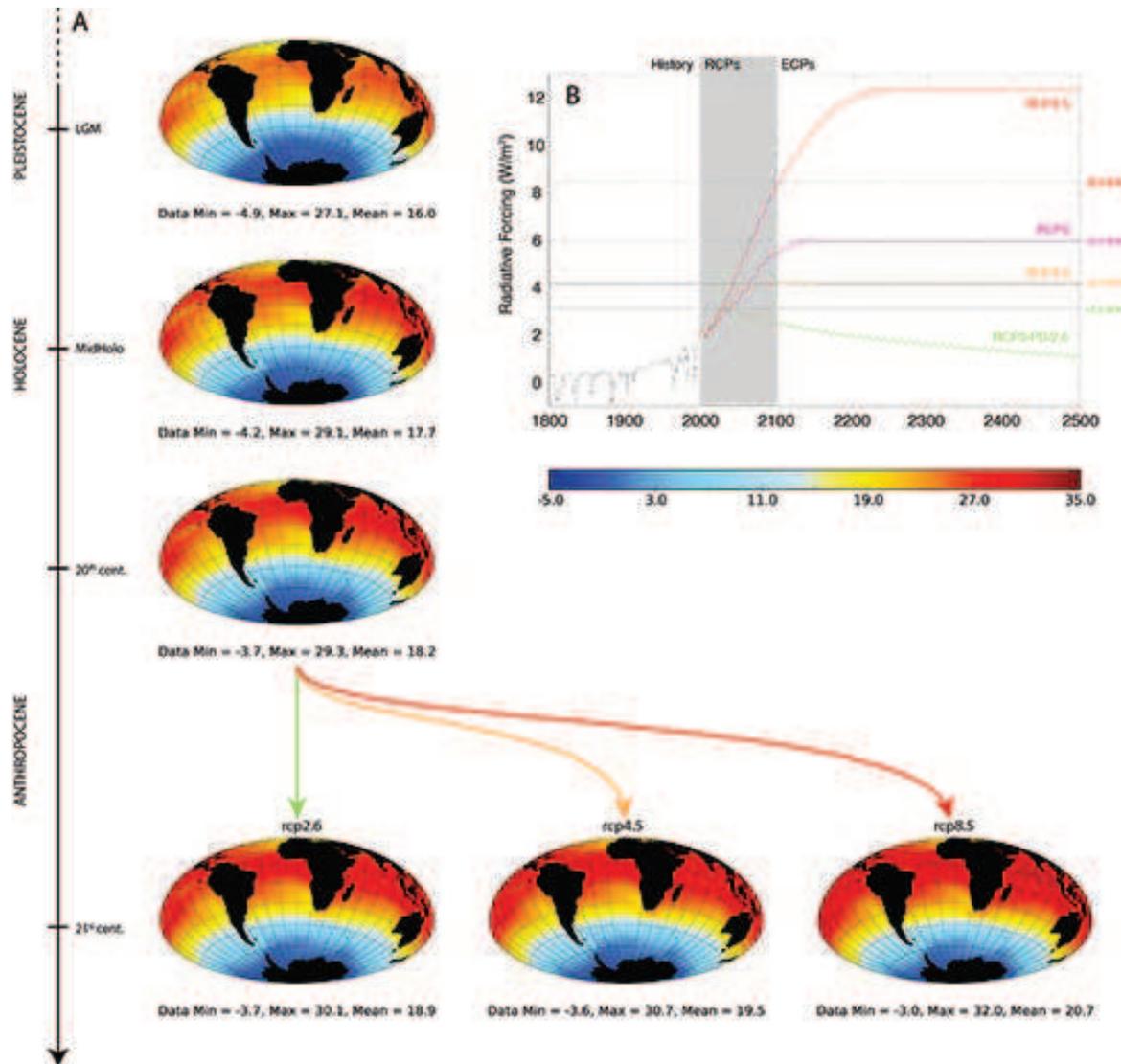
Figure 5 | Sea Surface Temperature changes in the Southern Ocean. A. 20-years mean sea surface temperature at four different time-points (from a 14-member ensemble, see §102 p. 201), from the CMIP5 panel (see §50 p. 130 for details), and under three different forcing scenarios (in B, adapted from Meinshausen *et al.* 2011).

---

idence such as alkenones or Mg/Ca ratio (as a proxy for sea surface temperature, see Kucera *et al.* 2005; MARGO 2009).

Despite local variations and alternating conditions in the different oceanic basins, we can separate four major periods in the Southern Ocean recent history, that appear consistent at the global scale: *(i)* Quaternary conditions (mid-Pleistocene to 22 Kyr BP), *(ii)* LGM conditions (21-18 Kyr BP), *(iii)* Pleistocene glacial retreat and early holocene optimum (17-9 Kyr BP), *(iv)* Holocene hypsithermal and neoglacial conditions (8-0 Kyr BP).

(i) Quaternary conditions (1.3 Myr - 22 Kyr BP) are characterised by the slow onset of glacial conditions, in the continuity of the Miocene-Pliocene icehouse trend (Haywood *et al.* 2008), although with marked glacial-interglacial cycles with a phase of ~100 Kyr (Petit *et al.* 1999; Augustin *et al.* 2004; Wolff *et al.* 2006), during which the APF exhibits important latitudinal variations (see Kemp *et al.* 2010). Winter sea ice cover already reached as far as ~56°S in the Pacific during the period (Gersonde *et al.* 2005). Little is known of land ice throughout the period, as the following LGM glacier growth obliterated most of the direct evidence (Hodgson *et al.* 2014).

(ii) Last Glacial Maximum (LGM, 21-18 Kyr BP) has been the focus of much research, in particular regarding the Antarctic ice sheet (*e.g.* Anderson *et al.* 2002; Denton & Hughes 2002), the Southern Ocean frontal structure and sea ice extent (*e.g.* Gersonde *et al.* 2005), land ice cover (*e.g.* Hodgson *et al.* 2014) and atmospheric circulation (*e.g.* Kohfeld *et al.* 2013). Late Pleistocene glacial conditions culminate for the last time during the LGM, with a ~5°C cooling in summer SST throughout the Southern Ocean (Gersonde *et al.* 2005; MARGO 2009) and associated equatorward movement of the APF that may have reached 40°S at some locations (Kohfeld *et al.* 2013). Precise dynamics of the APF still remain to be understood, however, as the strong bathymetric constraints at several locations (the Campbell Plateau, the Kerguelen Plateau, or the Drake passage) are thought to have prevented equatorward frontal displacement (Rosenthal *et al.* 1997; Neil *et al.* 2004; Kohfeld *et al.* 2013). Westerly wind change reconstruction is still uncertain, but available data point to strengthened circulation and equatorward widening of the westerlies (Kohfeld *et al.* 2013). Winter sea ice expanded greatly during the period, reaching at least

50°S in winter (CLIMAP 1981; Gersonde *et al.* 2005 - with variation between the icy Atlantic and Indian oceans, and the more ice-free Pacific). A shift in marine productivity has been inferred from the Antarctic to the Subantarctic region (Hodgson *et al.* 2014), without however a global reduction in biomass (Wolff *et al.* 2006). The islands of Heard, Crozet, Marion, and the Drake Arc were entirely covered by ice, while Kerguelen and South Georgia may have had some ice-free areas, and the Falklands and Macquarie underwent periglacial conditions, with a harsh tundra environment (Hodgson *et al.* 2014). Like in the Northern Hemisphere, the prevailing glacial conditions pushed the higher latitude terrestrial or semi-terrestrial biodiversity into a handful of refugia, mostly located in the now subtropical (but then subantarctic) islands of Gough and StHelena in the Atlantic, Amsterdam in the Indian Ocean, and Auckland and Campbell in the Pacific. The Falklands and the Patagonian Shelf area (where swathes of land emerged from the lower sea level) may also have granted ice-free refugia (see Fraser *et al.* 2009; Fraser *et al.* 2012). Marine diversity, on the other hand, was not severely affected (see *e.g.* Morin *et al.* 2015).

(iii) Pleistocene glacial retreat and early Holocene optimum (17-9 Kyr BP) is a period of global thawing and warming following the LGM. In the Southern Ocean, the deglaciation has very contrasting chronologies, in particular in relation to the local topography and bathymetry: while the dry land expanses of Kerguelen and South Georgia, and the shelf-less archipelagos of the Scotia Arc, saw ice retreating early, the shelves of Crozet and Prince Edward retained extensive land ice caps as late as the early Holocene (Hodgson *et al.* 2014). Sea ice retreated slowly during the late Pleistocene, with an important regain during the Antarctic Cold Reversal, around 14.7 Kyr BP (likely due to the massive influx of meltwater from the Antarctic Ice Sheet, see Weber *et al.* 2014). The Younger Dryas Northern hemisphere cold reversal corresponds, on the other hand, to a warm period in the Southern Ocean (Kaplan *et al.* 2010). Oceanic fronts moved poleward and reached their current position by the beginning of the Holocene, during the so-called Holocene Climatic Optimum (Kohfeld *et al.* 2013). Around ~9 Kyr BP, a second cold reversal in the

Antarctic waters led to a slight regain of sea ice (Nielsen *et al.* 2004) - although the state of the Southern Ocean may not have been homogeneous between ocean basins.

(iv) Holocene hypsithermal and neoglacial conditions (8-0 Kyr BP) mark the advent of the modern (pre-industrial) conditions throughout the Southern Ocean. Sea surface temperature reaches a maximum around 7.5 Kyr BP (Calvo *et al.* 2007), with subantarctic ice-free conditions at ~50°S around 6-5 Kyr BP (Hodell *et al.* 2001; Nielsen *et al.* 2004). Land ice conditions are then similar to the present, with complete deglaciation on Crozet and Prince Edward (Hodgson *et al.* 2014). There warmer hypsithermal conditions are followed by colder conditions as early as 5 Kyr BP in East Antarctica, and 3 Kyr BP in West Antarctica (Armand & Leventer 2010). However, the oceanographic landscape is not thought to have changed much, let aside minor variation in sea ice, and species distribution is thought to have been very similar to pre-industrial ranges.

§-10 Biogeography of the Southern Ocean. The present-day Southern Ocean has a rather simple biogeography, made of broad, often zonally bounded systems, but that host a considerable diversity of marine life (Smetacek & Nicol 2005; Chown *et al.* 2015). Four distinct areas may be distinguished: *(i)* the *Subantarctic zone*, which is outside the Southern Ocean proper, but biogeographically bound to it, is bounded by the Subtropical convergence to the North, and the APF to the South, *(ii)* the *Antarctic Ocean zone*, south of the Subantarctic zone, and bounded to the South by the Northern Limit of the Circumpolar Current, *(iii)* the *Coastal Antarctic zone*, which includes the Antarctic coastal countercurrent and shelf area, as well as the coastal ice area, and *(iv)* the *Antarctic peninsula* (Convey *et al.* 2012; Terauds *et al.* 2012). In this study, we are mostly concerned with the first three concentric zones. The Subantarctic area is characterised by mild air temperatures, high precipitation, absent sea ice cover, and prevailing Westerlies. Islands are dominated by peat and low vegetation, or periglacial habitat. Subantarctic islands are few and far in-between (from the Pacific to the Atlantic: Macquarie, Heard-and-McDonald, Kerguelen, Crozet, Marion-and-Prince Edward, Bouvet, the South Sandwich, South Georgia, Tierra del Fuego and the Falklands), and concentrate both avian and pinniped fauna. The Antarctic Ocean zone, South

of the Polar Front, has much colder surface waters and extensive winter sea ice cover, islands are rare and ice-covered (from the Pacific t o t he A tlantic: P eter I , S cott, B alleny, a nd t he South Orkneys). Vegetation is scarce and mostly limited to lichens, liverworts and mosses (Convey *et al.* 2012). The Antarctic coastal zone (Tynan 1998), finally, is a shelf environment, characterised by almost perennial pack-ice, and a strong influence of the Antarctic Ice Shelf. Vegetation is almost absent, and displays extreme adaptations, and breeding vertebrate fauna is limited to a handful of species: Adélie and emperor penguins, snow, cape, antarctic and giant petrels, Wilson's storm-petrels, southern fulmars and southern polar skuas, as well as a few pinniped species. Of these, only the Emperor penguin breeds during the Southern winter.

Foraging opportunities stem mostly from two sources. As mentioned earlier (see §7 p. 35), the tremendous upwelling areas associated with the APF are a major contributor to the world's marine productivity (Laubscher *et al.* 1993; Bathmann *et al.* 1997; Carr *et al.* 2006), and attract long-distance central-place foragers such as the King penguin (Péron *et al.* 2012). The pack-ice area in the Antarctic and Coastal Antarctic areas also concentrate massive primary productivity (Arrigo *et al.* 1997; Arrigo *et al.* 1998), and are an important food resource both for Antarctic Coastal foragers such as the Snow Petrel *Pagodroma nivea* (Barbraud & Weimerskirch 2001b) or the Adélie penguin (Wienecke *et al.* 2000). In particular, open-water and upwelling conditions around polynyas along the coast (see §18 p. 65 and Fig. 4 p. 42) concentrate sea-ice-linked productivity, and are critical foraging areas for several species (Ancel *et al.* 1992; Ancel *et al.* 1999). The most salient feature of the Southern Ocean biogeography is therefore its almost direct link to very broad climatic features. Unlike terrestrial environments, where the complex interaction of latitude and altitude may blur surface wind currents to a considerable extent and result in very heterogeneous patterns (Burrows *et al.* 2014), the zonal structure of the Southern Ocean places biogeographic boundaries in regular accordance with annular, circumpolar circulation patterns. As a result, the extent and location of these biozones are directly influenced by global circulation patterns (see §18 p. 65).

1   *Species' responses to anthropogenic climate change in the Southern Ocean.*

2   *§-11 Climate is changing.* Palæoclimate reconstructions teach us that climate change is, by itself, a

3   natural and unavoidable phenomenon at the millennial scale (see §9 p. 42), and may be linked to

4   external forcings (*e.g.* changes in solar activity or in Milankovitch orbital cycles, with positive

5   feedbacks such as the «snowball earth» loop, see *e.g.* Hyde *et al.* 2000; Berger 2013), or to inter-

6   nal biogenic modifications of atmosphere composition (*e.g.* Frolking & Roulet 2007). However,

7   the pace of these changes is slow. Even the LGM did not alter significantly the composition or

8   structure communities in Europe on the long term (see *e.g.* Yeakel *et al.* 2013). Current climate

9   change, on the other hand, sees modifications of the same magnitude as the Holocene transition

10   happening at the decadal - and not millennial - scale. Climate change in general has been unam-

11   biguously and rather intuitively defined b y t he I ntergovernmental P anel o n C limate Change

12   (IPCC) as a «*change in the state of the climate that can be identified (e.g. by using statistical tests) by*

13   *changes in the mean and/or the variability of its properties, and that persists for an extended period,*

14   *typically decades or longer. Climate change may be due to natural internal processes or external forcings*

15   *such as modulations of the solar cycles, volcanic eruptions and persistent anthropogenic changes in the*

16   *composition of the atmosphere or in land use*» (Solomon *et al.* 2007). During the last decades of the

17   20th century, accumulated evidence increasingly pointed towards unprecedented rapid changes

18   in the climate of the earth, starting shortly after the 19th century Industrial Revolution. The

19   combination of deforestation and large-scale use of fossil fuels led to higher production, and low-

20   er fixation, of greenhouse gases (GHG), in particular carbon dioxide and methane, to the point

21   that «*atmospheric concentrations of carbon dioxide, methane and nitrous oxide [...] are unprecedented*

22   *in at least the last 800,000 years*» (Pachauri *et al.* 2014). Increased GHG results in an increase in

23   greenhouse effect, or effective radiative forcing on global climate. Thus, a ll a vailable evidence

24   make it «*extremely likely that human influence has been the dominant cause of the observed warming*

25   *since the mid-20th century*» (Stocker *et al.* 2014).

Intense and coordinated effort is currently deployed to understand the underlying mechanisms, and possible outcomes, of ongoing climate changes (see §50 p. 130 for an overview of the Intergovernmental Panel on Climate Change) - the same can unfortunately not be said of political endeavours. The result of this scientific effort is a growing understanding of the articulation between three different domains: *climate change*, *environmental change*, and *meteorology*. Although deeply intertwined, these three paradigms should not be confused. *Climate change* alone is the object of the IPCC definition, and is limited to the atmosphere-ocean circulation effects - *i.e.* long-term changes in temperature, precipitation, wind regime, etc. These may be appropriately described and captured through physical investigation methods, such as Atmosphere-Ocean General Circulation Models (see §50 p. 130 for details), and are mostly bounded by uncertainties about the nature of physical processes at work, and the socio-economic hypotheses underlying our projections of greenhouse gas emissions. Yet while numerical climate models are increasingly successful at predicting the physical environment of the Earth in the 21st century, the response of biological communities, or «*environmental change*», is a more elusive topic (see §13 p. 55 *sqq.* for an overview), because of the lack of a prior example (although early Holocene climate change is often used as an example, its pace differs significantly from ongoing changes - see Petit *et al.* 2008; Blois *et al.* 2013; Moritz & Agudo 2013). The diverse mechanisms through which these changes occur in ecosystems make them particularly difficult to predict. They range from the disruption of developmental processes in lower-trophic-level organisms by higher sea surface temperatures (Gregg *et al.* 2003; Behrenfeld *et al.* 2006) or water acidification (Harvey *et al.* 2013), with cascading trophic-web effects (*e.g.* McMahon & Burton 2005), to shifts in species distribution and associated biodiversity loss (*e.g.* in Arctic copepods, see Beaugrand *et al.* 2002). Marine ecosystems, just as terrestrial ones, are already severely affected by human exploitation, which diminishes their resilience to climate change (see Halpern *et al.* 2008; Watson *et al.* 2013; McCauley *et al.* 2015). Thus, expected biodiversity collapse under the darker scenarios (see §50 p.

130) is projected to affect 50% to 70% of the oceans to a greater extent than all the changes that took place in the Pleistocene and Holocene (Beaugrand *et al.* 2015).

Concurrently, a several studies have investigated the effects of climate change on species through the cyclic variability of climate, which is especially prevalent in oceanic systems (see for example §8 p. 40). These studies have often exploited the high contrast between positive and negative phases of the El Niño Southern Oscillation (ENSO, *e.g.* Le Bohec *et al.* 2008), the Southern Annular Mode (SAM, *e.g.* Weimerskirch *et al.* 2012), or the North Atlantic Oscillation (NAO, *e.g.* Frederiksen *et al.* 2004). While this is often a reasonable approximation - and importantly the only proxy available anyway - these *meteorological changes* should not be fully equated to *climate change*. *Weather*, which is mostly at stake there, is only one interface between climate change and species. Warm phases of the ENSO may accurately reproduce warm-earth conditions in the Southern Ocean, but not additional coupling mechanisms with, *e.g.*, the Northern Hemisphere - despite the fact that Arctic-Antarctic couplings have been shown to be central to climate change *stricto sensu* (Barbante *et al.* 2006). While the approximation is often a methodological necessity, *meteorological change* should therefore not be confused with *climate change*.

§-12 Particularities of climate change in the polar regions. The effects of climate change are especially visible in the polar regions, a fact due to their climatological characteristics, as well as to the structure of their biological communities. From a purely climatological (or «*abiotic*», see §49 p. 127) perspective, the polar regions stand out as distinct from the rest of the planet. The singularities of Ocean-Atmosphere circulation in the Arctic, in particular the threshold change in albedo with the presence or absence of sea ice in the Arctic Ocean, leads to an «Arctic amplification» phenomenon of accelerated climate change (Serreze & Francis 2006; Pithan & Mauritsen 2014). Antarctica, on the other hand, exhibits rather mixed patterns: while Eastern Antarctica seems to «resist» climate change (possibly due to the buffering effect of the Southern Ocean, see Mulvaney *et al.* 2012 - although observation uncertainties may be hiding the true trend, see Hanna *et al.* 2013), West Antarctica and the Antarctic Peninsula are amongst the fastest-warming areas of the

1   Earth (Mulvaney *et al.* 2012; Bromwich *et al.* 2013). In the Southern Ocean, accelerated

2   warming both of the surface waters (Liu & Curry 2010) and of the deep water masses (Purkey &

3   Johnson 2010) has been observed, and the effects of the influx of fresh meltwater on upwelling

4   activity have already been documented (*e.g.* de Lavergne *et al.* 2014). The fundamental global

5   connections of the Southern Ocean also make it especially sensitive to changes in tropical circula-

6   tion patterns, such as the ENSO (see §8 p. 40 and Collins *et al.* 2010). Therefore, a generally in-

7   creased effect of climate warming is expected.
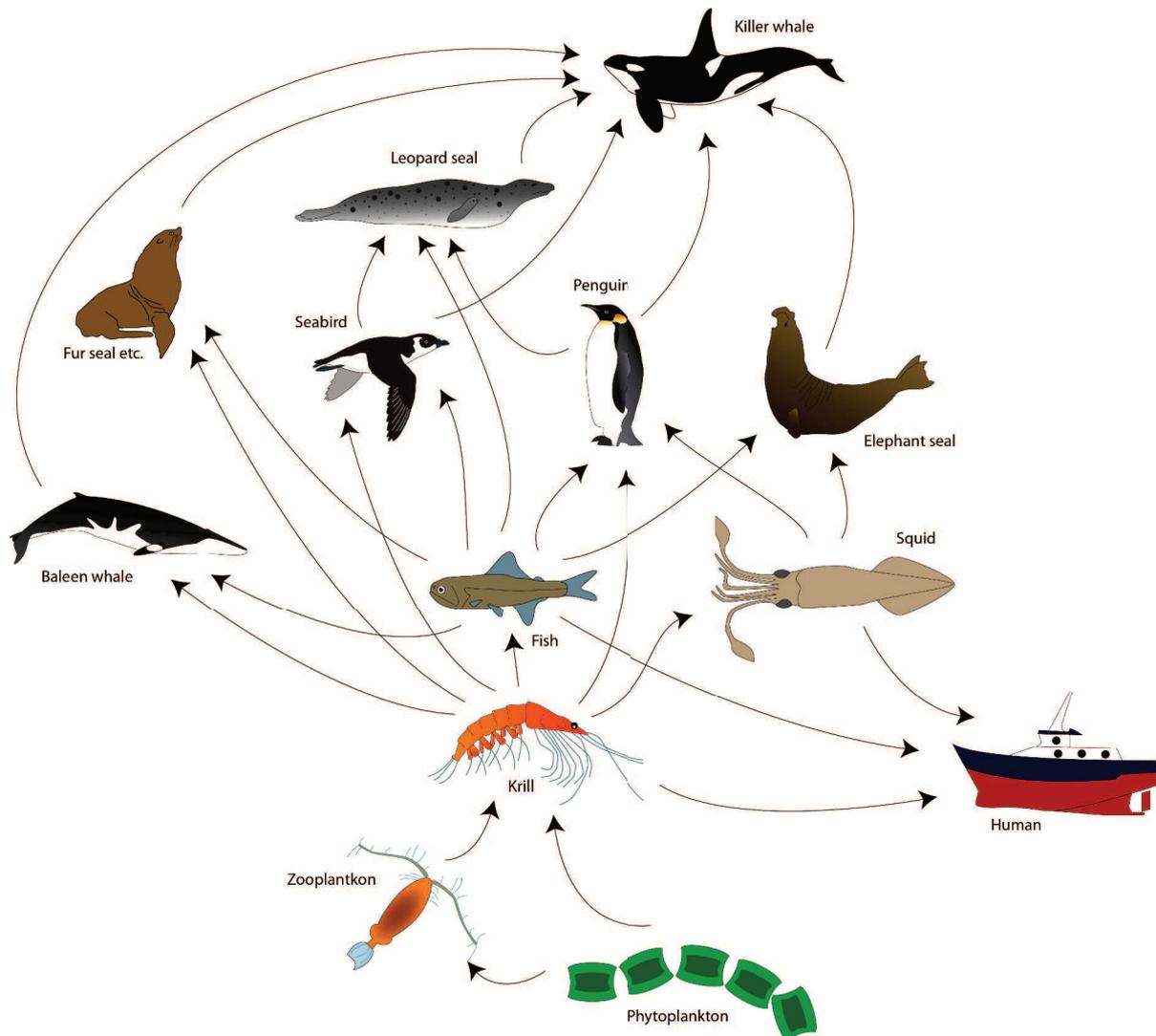
8   **Figure 6 | The Food web of the Southern Ocean.** A simplified structure of the food web of the Southern

9   Ocean. Arrows figure p redation l inks. Th e di versity of zo oplankton an d fis h str ategies is col lapsed in our

10 representation.

However, the biogeography of the Southern Ocean (see §10 p. 48) also contributes to aggravated effects of climate change. While habitats are generally expected to shift poleward in response to climate warming (see Williams *et al.* 2007; Fraser *et al.* 2012, and §15 p. 57), the polar ecosystems have little margin for further displacement, and the high latitudes are expected to become «climate sink areas» (Burrows *et al.* 2014) where habitats contract and ultimately disappear, rather than shift (see §15 p. 57). Further complexity arises from the fact that human activity has heavily influenced the Southern Ocean from the bottom of the food chain (*i.e.* through anthropogenic climate change and reduction in primary production) as well as from the top (*i.e.* through the massacre of top-level predators such as whales, seals and penguins - see Ainley *et al.* 2007), which results in an intricate combination of effects (Smetacek & Nicol 2005 - see also a spectacular and concrete example of this intricate system in Trivelpiece *et al.* 2011).

As a result, the seemingly pristine polar regions have largely come to concentrate the effects of climate change. For a long time, it has been thought that polar ecosystems were simpler, and with shorter trophic chains, than lower-latitude systems, thus leading to more easily understandable shifts. However, it is now recognised that both taxonomic diversity and trophic network complexity is just as high in the high latitudes than in the temperate regions (Smetacek & Nicol 2005; Chown *et al.* 2015 and Fig. 6 p. 53), and it has been suggested that the apparent specificities of the polar oceans are due more to the delayed human impact due to sheer inaccessibility, than to a unique character favouring, *e.g.*, marine macrofauna: indeed, Smetacek & Nicol 2005 have proposed that these regions rather represent a vestigium of the pre-historical global marine ecosystems - in their words, a «*Serengetis of the sea*». Thus, we may be currently witnessing in the high latitudes what happened already long ago closer to the equator and what is also happening in continental Africa, with the demise of mammalian macrofauna and its replacement by ubiquitous human exploitation. Whether climate change is really particular *per se* in the polar regions beyond its physically increased pace, or whether the nature of its effects on biotic communities is

rather a consequence of the relative integrity of these communities, is a question that may be urgent to answer.

§-13 Species' responses to climate change. The importance of the impact of current global changes on the world's biological communities is now recognised beyond question by the scientific community (see §11 p. 50 and Thomas *et al.* 2004; Warren *et al.* 2013; Pacifici *et al.* 2015), although the detail of its impact is complex and debated (Pereira *et al.* 2010; He & Hubbell 2011; Pacifici *et al.* 2015). The different levels of impact (ranging from physiology to community level, see §11 p. 50), the complexity of biotic interactions (Davis *et al.* 1998; Norberg *et al.* 2012; Midgley & Bond 2015), and the idiosyncratic character of each species' sensitivity and exposure to climate change (Moritz & Agudo 2013; Comte *et al.* 2014; Dickinson *et al.* 2014) contribute to apparently heterogeneous responses at the ecosystem level (Parmesan & Yohe 2003). Most studies, however, agree on the idea that three fundamental mechanisms interact in determining response to climate change at the species level: (*i*) *adaptive microevolution* through fitness selection (Bradshaw & Holzapfel 2006; Hoffmann & Sgrò 2011), (*ii*) *phenotypic plasticity* and in particular changes in phenology (Charmantier *et al.* 2008; Hoffmann & Sgrò 2011), and (*iii*) *range shift* to track habitat isolines (Walther *et al.* 2002; Chen *et al.* 2011; VanDerWal *et al.* 2013).

§-14 Micro-evolution and phenotypic plasticity. Micro-evolution and phenotypic plasticity share a common structure: in order to accommodate its changing environment, a species changes its physiological, phenological, or generally behavioural characteristics (Hoffmann & Sgrò 2011). The mechanisms involved, however, are very different. Micro-evolutionary response happens on a multi-generation scale, through selection of the fittest heritable features (either genetic or epigenetic): thus, it is a population-scale process. Phenotypic plasticity, on the other hand, is an individual-based phenomenon. Either through developmental, or through purely behavioural modifications, each individual optimises its fitness under the prevailing conditions - but its new state is

not heritable, if we let aside the comparatively rare cultural transmission of behaviour (White-head & Rendell 2014).

Evolutionary responses to anthropogenic climate change have already been evidence in several very short-lived species, such as mosquitoes (Gienapp *et al.* 2008; Hoffmann & Sgrò 2011). However, all studies conducted in vertebrates have up to now failed to detect any clearly evolutionary process (see Møller *et al.* 2010 for a complete review of the subject in birds). The mismatch between the very fast pace of climate change, the longer generation time of vertebrates, and their generally K-like reproductive strategies[1], makes true evolution difficult to achieve.

Plasticity, on the other hand, has been shown to play an important part in several species' short-term response (Charmantier *et al.* 2008; Hoffmann & Sgrò 2011). It is primarily known to affect phenology in order to match the meteorological conditions and most importantly the peak of nutrient availability, as has been evidenced in birds such as the Great tit (*Parus major* Charmantier *et al.* 2008; Husby *et al.* 2010) or the Collared flycatcher (*Ficedula hypoleuca*, Dunn *et al.* 2010), but also in plants (Anderson *et al.* 2012) - but is may also apply to metabolic traits (McKechnie *et al.* 2006; Nicotra *et al.* 2010) or morphology (Przybylo *et al.* 2000). The highly dynamic nature of the Southern Ocean system makes phenology a crucial condition of survival for most species. The seasonal temperature cycle brings about a latitudinal variation in the position of the Polar Front (see §7 p. 35), thus potentially changing the distance between foraging grounds and breeding locations along the breeding season for several species (*e.g.* Massom *et al.* 2009; Bost *et al.* 2015), or drives the strength of the upwelling activity, and thus the productivity, in the Humboldt Current System (Thiel *et al.* 2007). Thus, just as the timing of the insect abundance peak is a critical factor for several bird species (Dunn *et al.* 2010), the seasonal variation of foraging areas in oceanic systems may be a major constraint on their phenology, and its evolution is expected to

---

1.   Classically, K and r reproductive strategies are opposed: K-strategists have fewer offsprings, but a very high parental investment, and consequently high offspring survival, while r-strategists have numerous offspring with minimal investment and low survival.

force a plastic shift in the phenology of several species. Such shifts, however, have a high fitness cost (Van Buskirk & Steiner 2009), as they increase the likelihood of a mismatch between different ecological constraints (Both *et al.* 2006), and may therefore rapidly reach their limits (Visser & Both 2005; Both *et al.* 2006; Møller *et al.* 2008).

Microevolutionary response, since it relies on inter-generational selection in pre-existing variation, is a longer-time process. It has been evidenced for several short-lived organisms (Van Heerwaarden & Hoffmann 2007; Hoffmann & Willi 2008; Hoffmann & Sgrò 2011; Krehenwinkel *et al.* 2015), but the extreme velocity of current changes (Burrows *et al.* 2011; Mahlstein *et al.* 2013; Poloczanska *et al.* 2013) is a particular challenge for species that have long generation times (Hoffmann & Sgrò 2011) and low genetic diversity (Hoffmann & Sgrò 2011; Norberg *et al.* 2012), all the more as these two traits tend to be highly correlated (Romiguier *et al.* 2014). Micro-evolution and plasticity are, however, closely interwoven: only the strength of heritability may allow to distinguish between both (Réale *et al.* 2003), and more importantly, plasticity itself is increasingly recognised as an evolving trait (Nussey *et al.* 2005; Pelletier *et al.* 2007).

In this study, however, both the pace of current climate change and the life-history of long-lived seabirds exclude, *a priori*, any significant evolutionary response. A plastic response, on the other hand, is possible, and even to be hoped for. It is however beyond the scope of our work, as cross-generational data is required in order to build a clear picture of such a process. Up to now, evidence has been presented in several short-generation-time species (see *e.g.* Charmantier *et al.* 2008, etc.) - but several decades of phenological and behavioural observations would be necessary to build a clear picture given the long generation time of most seabirds.

§-15 Habitat displacement and range shift. Range shift is increasingly recognised as a major feature of short-term response to climate change (Davis & Shaw 2001; Chen *et al.* 2011; Burrows *et al.* 2014, etc.). While the main expression of plastic response concentrates on the phenology (see §14 p. 55), that is to say on a *temporal* frame shift in the breeding cycle of the species or population, range shift is a *spatial* frame shift in the distribution of the organism. As opposed to micro-

evolution and plasticity, it exclusively involves a change in geographical, and not temporal, physiological or morphological space - although cases of «pure» range shifts, not associated with phenological shifts, are scarce (Møller *et al.* 2010). Range shift can be conceived as the expression of different individual- and species-scale factors. On a functional level, *niche conservatism* can be defined as the tendency, for an individual, to remain within its physiologically and ecologically defined comfort zone (Wiens *et al.* 2010). Depending on the width of that niche, and on the evolvability of the species, niche conservatism may apply on very long time scales. For example, New World bird taxa exhibit a high degree of evolutionary-level niche conservatism, with the more derived species occupying the most specialised environments (Hawkins *et al.* 2006), while similar structures have been identified in stream fish (Comte *et al.* 2014) or land mammals (Martínez Meyer *et al.* 2004). This slow-time niche conservatism means that habitat preference is not a fast-evolving trait, and may be phylogenetically inherited within taxa, slowing down the colonisation of new habitats.

On shorter ecological time scales, on the contrary, niche conservatism is the main force that prompts individuals to follow their habitat rather than adapt to new conditions. As such, it results in *habitat tracking*, a movement by which a population will be displaced together with environmental conditions. Habitat tracking, when observed from a human perspective, results in *range shift*, a global modification of the species geographical distribution in response to trends in habitat change. Global warming, for example, typically (and schematically) results in a displacement of habitat and species towards the poles, or the higher altitude regions (Jump *et al.* 2009; Fraser *et al.* 2012).

In an ideal system, species may be expected to follow habitat displacement smoothly (Scheffer *et al.* 2001). However, the anisotropic character of biozones implies that habitats do not transform in a homogeneous manner (Diffenbaugh & Field 2013), and that changes are likely to be doubly heterogeneous - between ecosystems and between species within ecosystems. A recent study on Australian birds (VanDerWal *et al.* 2013), for instance, has shown that during the past 60 years,

species' range shifts had followed mostly idiosyncratic trajectories on the whole continent, only partly explained by habitat displacement. Such an example stresses the importance of biotic interactions in the determination of a species' range and range displacement, as several interspecific relationships can be affected simultaneously by climate change (*e.g.* feeding behaviour, see Charmantier *et al.* 2008, or and interspecific competition, see Stenseth *et al.* 2015), resulting in non-linear, and sometimes downright paradoxical habitat tracking (*e.g.* in the Barnacle goose *Branta leucopsis*, see Bauer *et al.* 2008; Eichhorn *et al.* 2009). Thus, understanding current and future species' distributions may not be properly achieved based solely on single-species (*e.g.* «climate envelope», see Pearson & Dawson 2003) models, but need to be extended to include essential biotic interactions (a point further developed in §49 p. 127).

The heterogeneity and idiosyncratic character of range shifts is exacerbated whenever discontinuities prompt *habitat convergences* (Burrows *et al.* 2014) or «subduction», for instance when possible climatic corridors, where range shift could theoretically happen linearly, are interrupted either by natural, or anthropogenic barriers. Habitat fragmentation, which is often a result of human influence (although it may be natural, in particular in insular environments, see *The King synnome*, p. 163 and *Unexpected philopatry in an insular seabird, the Peruvian diving-petrel*, p. 275) thus interacts with climate change and has rather unpredictable consequences. This is especially true around "climate sink areas" where local conditions disappear instead of being displaced (Burrows *et al.* 2014). Moreover, individual species are in reality not expected to respond linearly to habitat shift: insufficient dispersal possibilities may lead to a lagged range shift (Bertrand *et al.* 2011; Schloss *et al.* 2012), increased competition around sink areas may prevent range extension (Norberg *et al.* 2012), and compensatory metabolic processes may mask the effects of climate change until a tipping-point is reached (Doak & Morris 2010). These delayed effects can lead us to underestimate the depth of current changes, while placing species in a state of *climatic debt*, ultimately giving way to sudden ecosystem collapses (Scheffer *et al.* 2001; Hoegh-Guldberg & Bruno 2010; Barnosky *et al.* 2012).

1   Thus, the polar regions, which undergo accelerated environmental change (Serreze & Francis

2   2006; Turner *et al.* 2014; Chown *et al.* 2015) and have an extremely limited margin for habitat

3   shift (Burrows *et al.* 2014), are an extreme example of problematic habitat displacements

4   (Williams *et al.* 2007). Detecting lagged response to ongoing environmental changes before the

5   tipping-point is therefore critical if we are to develop appropriate and efficient management and

6   conservation strategies and to accurately forecast the actual distribution of future critical refugial

7   areas (Keppel *et al.* 2012; Hope *et al.* 2013; Watson *et al.* 2013), in particular for top-level preda-

8   tors that largely determine ecosystem resilience (Soulé *et al.* 2003; Heithaus *et al.* 2008) in order

9   to develop appropriate and efficient management and conservation strategies. Thus, range shift

10   predictions are becoming a major challenge in ecological modelling.

11   *Aims of this work*

12   *§-16 The scales of climate change.* One of the most challenging aspects of the biology of climate

13   change is the maze of scales on which it operates. Extant studies often oscillate between two ex-

14   tremes: the very *slow* time, in which geological climate change (such as the Pleistocene-Holocene

15   transition) is taken as a proxy for anthropogenic events, or the very *short* time, in which meteoro-

16   logical stochasticity and cyclic phenomena (for example the North Atlantic Oscillation) are used

17   to the same purpose[1]. In that context, one of the difficulties of understanding contemporary cli-

---

1.   An opposition theorised by Fernand Braudel in his study of the *History of the Mediterranean*, as the distinction between the *« longue durée »* (in which the interaction of humans with their geography and habitat prevail) and the *« short, fast and nervous oscillations »* of *« event history »* (Braudel 1949; Braudel 1969). Along this spectrum, Braudel stresses the *« increasingly precise notion of the multiplicity of time, and of the exceptional value of long time »* (Braudel 1958). Thus, *« every historical work decomposes past time, chooses between its chronological realities, according to more or less conscious preferences and exclusions. Traditional history, which is focused on the swift time, the individual, the event, has long since accustomed us to its precipitated, dramatic, gasping narrative. The newer economic and social history emphasises its search for cyclic oscillations and has tuned itself to them: it became entangled in the illusion, but also in the reality of the cyclical raises and falls of prices. Thus there is, next to the narrative (...), a recitation of the conjuncture that examines the past by thick slices: decades, scores and fifties. But well beyond that second recitation lies a history of a steadier breath still, and now of centennial scale: the long, longue durée history »* (Braudel 1958). This essential decomposition of history into layers of causes and events - structural, conjunctural and proximal - is now a tenet of modern history. Yet, it is hardly theorised in bio-logical sciences, where it only lives in the often unreconciled opposition of evolutionary and ecological paradigms (§1 p. 21).

mate change is that it operates on a scale for which we have little or no concepts, because it has no known precedent in the history of the earth, and that requires us to find a middle ground between ecological and evolutionary times. And so, a central question is whether the observations we extract from very long term (*i.e. palaedemographic*) studies are of the same *nature* as the ones we extract from short term (typically *monitoring*) studies - and whether any of these may explain and predict the events to be expected under anthropogenic climate change. In many respects, it may appear that the nearly instantaneous observations that we make on monitored populations, and that span a few generations at best, are dominated by several layers of stochasticity and mixed forcings - the stochasticity and cycles of meteorology around the trends of climate and its nested cycles, the stochasticity of demography around the cycles and trajectories of populations and species, the slow but chaotic restructuring of ecosystems when its parts move in different directions - and that these contradictory signals may hide for some time the inevitably directional trends of global change. At the other end of the spectrum, however, palæodemography, by its evening out of this very stochasticity and these high-frequency variations, retains only broad patterns of change, such as the slow pulse of Pleistocene glaciations, that leave time for evolution to occur. It may, however, totally fail to capture the now comparatively swift movement of man-made change.

For these reasons, what really occurs in a situation such as contemporary anthropogenic climate change can be conceived as a disruption of the pace and manner in which these nested scales are integrated, and an increasingly likely mismatch between layers of spatial and temporal variation. The duration of the generation, for example, may be simplistically considered as the time lapse over which an individual integrates environmental conditions and undergoes selection: it is long enough to average over the seasons, and sometimes the oceanic modes, but fast enough to let a consequential series of generations to adapt to geological changes. A new, intermediate pace of change may disrupt this timing, and be too fast for evolution to keep up. The organisation in space of individuals and species reflects the extent over which conditions make them most fit (see

§49 p. 127), and the size and mobility of individuals evolved to match this space: there again, the convergence and divergence of habitats disrupts this equilibrium. Thus, in many respects, it appears that the key to understanding contemporary climate change is understanding how the different chronological and spatial paradigms articulate themselves for ecosystems, for species, and for individuals.

§-17 Understanding the scales of organisation in seabirds. The primary focus of this work is the understanding of the different spatial and temporal scales in the demographic organisation and dynamics of seabirds - a group at the forefront of climate change, as presented in §18 p. 65 - using three contrasting species as models: the King penguin *Aptenodytes patagonicus*, the Emperor penguin *Aptenodytes forsteri*, and the Peruvian diving-petrel *Pelecanoides garnotii*. While set primarily from an evolutionary point of view, we explore the results provided by a broad set of population genetic methods in the light of the insights offered into different scales by alternative approaches, including bio-logging, habitat modelling, and direct field monitoring techniques. For each of the two *Aptenodytes* penguin species, we present two complementary studies: one focusing on worldwide, evolutionary-scaled patterns and based on genome-wide datasets (*The King synnome*, p. 163 and *The Emperor synnome*, p. 211), and one focusing on local, «*chronicle-scaled*»[1] phenomena (*Fine-scale colony structure*, p. 135 and *Empirical evidence of heterogeneous dispersal*, p. 259). These two approaches are combined in the more exploratory study of the Peruvian diving-petrel (*Unexpected philopatry in an insular seabird, the Peruvian diving-petrel*, p. 275).

(i) The comparative biogeography of these three species is the foundation of this study. A first task will be to understand how range-wide distributions are organised, at scales ranging from intra-colonial diversity to island and range-wide levels, and to establish what seems to be the relevant demographic unit for studying past, current and projected demographic trends. This will

---

1.   We borrow this term from Fernand Braudel (see above, §16 p. 60), as it accurately reflects the framework in which our monitoring data operates: like medieval *chronicles*, monitoring approaches are based primarily on recording individual birth, deaths, lineages, and memorable events, and are by definition set to the generation time of the focal model, by opposition to *histories*, scaled to a people - that is, a *population*.

also involve reviewing current estimates of population size, structure, and, in the case of the King penguin ,taxonomic diversity.

(ii) Predictions regarding the fate of these three species in the face of environmental change are rather grim. The Emperor penguin has recently been declared doomed throughout its range (Jenouvrier *et al.* 2014), the King penguin received dire forecasts for its best-studied colony (Le Bohec *et al.* 2008; Péron *et al.* 2012), and the Peruvian diving-petrel achieved the *Endangered* status since 1994 update of the International Union for Conservation of Nature (IUCN) Red List[1]. Nevertheless, achieving a better understanding of seabird population dynamics requires a critical examination of these predictions, and an integration of the methods that prompted them. We address this issue using the total available evidence for the best known of these three species, the King penguin, and propose a possible re-interpretation of the Emperor penguin's response to Southern Ocean warming. In both cases, we try to propose a likely consensus projection based both on *long-* and *short-time* observations, as a temptative framework to solve the difficult problem of ecological and evolutionary integration in the context of climate change.

---

1.   As will be exposed in details in **Concepts and methods** *(p. 65)*, different reasons prompted these three projections: the observed dependency on sea ice, and the modelled evolution of that same sea ice for the Emperor penguin, the correlation between foraging area and sea surface temperature for the King penguin, and the observed and partly unexplained (but likely only marginally climate-related) population decline for the Peruvian diving-petrel.

Chapter 2: Concepts and methods

A brief introduction to Seabirds.

§-18 Seabirds, and Penguins in particular, as sentinels for polar ecosystems. The effects of climate change (§13 p. 55) are but incipient, and, although they likely already involve all species and ecosystems on the planet (Barnosky *et al.* 2012), they are most clearly observable only in a subset of organisms that integrate and amplify these changes. Since several confounding factors may blur our understanding of the ongoing changes (see §13 p. 55), an accurate assessment of the true processes at work requires the selection of study models that integrate those changes across trophic levels and geographical areas in a significant way. Due to the particular speed and moment of climate change in the polar regions (see §12 p. 52), polar or sub-polar ecosystems are often used to that purpose: and within these, top-predator species are commonly chosen. Indeed, the structure of the trophic networks places apex predators in a particular position. Being downstream of the nutrient and energy flow, external forcing on the biomass of every trophic level (from the primary phytoplankton production to the upper fish or krill biomass) will ultimately affect the availability of their resource (Bakun 2006; Frederiksen *et al.* 2006; Hunt & McKinnell 2006; Ainley *et al.* 2007). For example, a decrease in upwelling activity south of the Polar Front (see §7 p. 35) will result in a reduced phytoplankton growth, and ultimately in a decrease of available prey biomass for top predators (in a classical «bottom-up» forcing scenario, Frederiksen *et al.* 2006). Yet, considering a constant primary productivity, a specific forcing, such as increased

ocean acidity, may reduce the growth of an intermediate organism, such as krill - also resulting in a decreased prey abundance for top predators (in a so-called «wasp-waist» forcing, see Bakun 2006). In parallel, other constraints may converge on top-predators: bio-accumulation, for example, increases along the trophic levels, with anthropogenic contaminants reaching the highest concentrations in long-lived apex predators.

Amongst top predators, most seabird species share some additional characteristics that make them particularly suitable to monitor environmental changes. As opposed to top-predator fish or shark species, and to cetaceans, that never touch land, seabirds and pinnipeds require firm ground (either land or ice) to breed, and usually exhibit a high degree of philopatry (see §6 p. 33 and §19 p. 68), which makes it possible to study individuals over long time periods, and to measure critical parameters, such as individual breeding success - a possibility made even more interesting by the long life span of most species (up to ~45 years for large penguins, see Bost *et al.* 2013, or more for several procellariiformes, and 15 to 40 years for most pinnipeds, see Shirihai & Kirwan 2008). However, seabirds have over pinnipeds the advantage of often very large population sizes, normally bi-parental offspring care, and typically central-place foraging, which makes them especially suitable for long-term monitoring programs (Cairns 1988; Croxall *et al.* 2002; Parsons *et al.* 2008; Grémillet & Charmantier 2010; Cury *et al.* 2011).

Amongst seabirds, the evolutionary history of spheniscids (see §21 p. 72) makes them a perfect model for understanding the changes in the Southern Ocean. Constrained to tight latitudinal zones, most penguin species are specialised in a narrow set of preys (*e.g.* squid for the Emperor penguin *Aptenodytes forsteri* - see §23 p. 78, or myctophid fish for the King penguin *Aptenodytes patagonicus*, see §25 p. 80) which reduces their short-term plastic response to modifications in the trophic network. But specific characteristics of the King and Emperor penguins are of particular interest. The Emperor penguin breeds during winter on the sea ice (see §23 p. 78 for details), and, during that period, it relies on coastal *polynyas* for foraging. These coastal open-water areas may occasionally be caused by warmer deep-water upwellings (they are then called *sensible heat*

polynyas, *e.g.* the Weddell sea polynya, see Thomas & Dieckmann 2008 and §7 p. 35), but are mostly the result of continental wind circulation patterns. The very large temperature and pressure difference between the extremely cold and high-altitude central Antarctic ice sheet, and the comparatively mild coastal zone, result in strong coastwards *katabatic* winds, that follow the topography of the ice sheet. These winds cause offshore drift of the coastal sea ice, and maintain ice-free areas at the breaking point between the grounded ice and the floating ice, before dying off a few miles from the coast - at the same time, the offshore drift of the ice draws a local upwelling of deeper shelf waters, resulting in increased marine productivity (see Fig. 4, and Ancel *et al.* 1999; Thomas & Dieckmann 2008). These *latent heat* polynyas are essential for the survival and breeding success of Emperor penguins, and can be affected either locally by icescape modifications (Ancel *et al.* 2014; Kooyman & Ponganis 2014), or globally by changes in the atmospheric circulation patterns, and reduction in katabatic wind activity.

The King penguin, on the other hand, relies for breeding-season foraging on the myctophid fish stock of the Antarctic Polar front (see §7 p. 35, §25 p. 80, and *The King synnome*, p. 163). The Antarctic Polar front position is directly determined by the strength of Westerly wind circulation and resulting Ekman transport, and by sea surface temperature in the Antarctic and Subantarctic zones (see §7 p. 35 and Fig. 2): higher temperatures and weaker Westerlies result in a increased mean latitude for the Polar Front (as is the case during negative Southern Annular Mode events, see §8 p. 40). Since the insular breeding locations of the King penguin, on the other hand, are fixed (see §25 p. 80, and *The King synnome*, p. 163), the foraging distance of the species varies with the latitude of the frontal zone. Thus, King penguins thrive when Westerlies are strong and surface temperature cold south of the Polar Front.

And so, *Aptenodytes* penguins share this fascinating characteristic that their survival, breeding success, and overall fitness are directly tied to the planetary atmospheric and oceanic circulation, rather than to local, finer scale proximal causes. While the sensitivity of *e.g.* Great tits to climate change happens through several mediations - the local climate change forced by global evolu-

tions, the combined effects of temperature and precipitation of the abundance of insect larvæ, etc (Charmantier *et al.* 2008), the relationship of large penguins to climate change is, so to speak, immediate: increased radiative forcing results in changes in the planetary wind circulation, and drives the King penguin foraging areas further South, or decreases polynya availability for the Emperor penguin. This characteristic has been exploited in both species to predict demographic evolution in relation to global changes (Le Bohec *et al.* 2008; Jenouvrier *et al.* 2014; Bost *et al.* 2015).

Other seabird species have been monitored in a similar way, for example the Wandering albatross *Diomedea exulans* (*e.g.* Weimerskirch *et al.* 2012), the Adélie penguin *Pygoscelis adeliae* (*e.g.* Ballard *et al.* 2010), or the Kittiwake *Rissa tridactyla* (*e.g.* Moe *et al.* 2009). Generally, we may consider that the value of a species as a bio-indicator is linked to the extent of its foraging areas (that may be the whole Southern Ocean, as for the Wandering Albatros, see Croxall *et al.* 2005) and breadth of its trophic basis: whereas colonies of large penguins integrate large swathes of Southern Ocean, some locally-foraging, highly philopatric species may rather be indicative of finer-scale changes. This is for example the case of the Peruvian Diving-petrel *Pelecanoides garnotii*, a small insular procellariid dependent on the coastal upwellings of the Humboldt Current System along the Pacific coast of South America, and mostly subject to the local variations in the El Niño Southern Oscillation (see §8 p. 40, and *Unexpected philopatry in an insular seabird, the Peruvian diving-petrel*, p. 275). Thus, whether they integrate large-scale, planetary processes, or more local tendencies of marine ecosystems, the sentinel role of seabirds makes the study of their demography, life history, and population dynamics a priority for understanding the ongoing changes in the earth's climate.

§-19 Philopatry and dispersal amongst seabirds. Seabirds are, in many respects, intermediate species between oceanic and terrestrial ecosystems (see §18 p. 65). While their foraging grounds are marine, and are subject to all the particularities of oceanic systems, their breeding grounds are terrestrial, and usually extremely fragmented (being insular, or coastal with very selective charac-

teristics). Thus, their ability to cover very large areas during their foraging trips is in contrast with the scarcity of available breeding habitat, and a strong tendency to return to the same location to breed year after year - although most of species have the ability to disperse well beyond the borders of their local grounds, and most have been observed to do so (e.g. Croxall *et al.* 2005; Milot *et al.* 2008, etc.). As a result, genetic population structure has been evidenced in most species (see Friesen *et al.* 2007), and often results in speciation (see Friesen 2015).

Thus, patterns of population structure are a result of the equilibrium established between dispersal and philopatry - and penguins are a particularly striking example of this equilibrium. Several studies have concluded in a high degree of philopatry in different species: in the King penguin, juvenile return rate is typically very high (up to 87% on Crozet archipelago, Saraux *et al.* 2011a). In the Emperor penguin, although estimated from flipper-banded individuals and therefore potentially underestimated (Le Maho *et al.* 2011), juvenile and adult return rate has also been shown to be important (Jenouvrier *et al.* 2012), and Adélie penguin *Pygoscelis adeliae* juveniles have a similarly high return rate (45% to 75% recruitment on their natal colony, Cornet *et al. in prep*). Thus, a natural expectation would be for populations to undergo significant reproductive isolation, and genetic drift. However, surveys have been conducted in most species, either at a local or a global scale, with contrasting results. Several species, such as the Magellanic penguin *Spheniscus magellanicus* (Bouzat *et al.* 2009), the Adélie penguin *Pygoscelis adeliae* (Roeder *et al.* 2001), the Chinstrap penguin *Pygoscelis antarcticus* (Freer *et al.* 2015), have been shown to exhibit very weak or absent isolation patterns amongst colonies. On the other hand, the Little penguin *Eudyptula minor* (Overeem *et al.* 2008; Peucker *et al.* 2009) or the Yellow-eyed penguin *Megadyptes antipodes* (Boessenkool *et al.* 2009a; Boessenkool *et al.* 2009b) show significant isolation patterns, while the Gentoo penguin *Pygoscelis papua* (De Dinechin *et al.* 2012), and the Rockhopper penguin *Eudyptes chrysocome* (Banks *et al.* 2006; Jouventin *et al.* 2006; De Dinechin *et al.* 2008) are thought to be engaged in a speciation process between isolated oceanic provinces. While morphological evidence points towards a certain degree of homogeneity in the Emperor

penguin, the King penguin's alleged subspecies structure (Mathews 1911; Barrat 1976 and §21 p. 72), points to much reduced gene flow - a conclusion supported by an early study (Viot *et al.* 1993). While the heterogeneity of methods and sampling designs used in these different studies prevents a systematic comparison of population structures, it appears that genetic homogeneity is higher in the pelagic-foraging species such as the Adélie and the Chinstrap, and that population isolation is characteristic of more coastal species such as the Gentoo or the Rockhopper.

However, the genetic structure of populations is not a direct reflection of their philopatric behaviour, as it also integrates other traits such as generation time, substitution rate[1], the extent of random mating within colonies, etc. And dispersal itself (§4 p. 30) is hardly a directly observable parameter (§5 p. 32) in wild populations. Most surveys of seabird demography are technically limited to one or a few colonies (Frederiksen & Petersen 1999; Barbraud & Weimerskirch 2001a; Gendner *et al.* 2005; Ponchon *et al.* 2015), and monitoring relies on the identification and recapture of marked individuals (commonly through the use of rings, or flipper-bands for penguins - or radio-identification tags, see §26 p. 81). Thus, while return rate is a direct observation (once tag loss is accounted for, see *e.g.* Olsson & van der Jeugd 2002), the only alternative observation is non-return - that is, either dispersal, or death. Distinguishing between these would ideally require that the marked individuals are recaptured elsewhere than on the studied colony - a methodological aporia at the present time. Some explicit modelling approaches have been developed for scalable systems where local dispersal can be used as an estimator for long-distance dispersal (see *e.g.* Cooper *et al.* 2008), but seabirds oppose this essential limitation that dispersal is either long-distance, or null - since intra-colony movement is inherently of a different nature than inter-colony movement (Frederiksen & Petersen 1999 and *Fine-scale colony structure*, p. 135). This difficulty is made much worse by the fact that several marking techniques have been shown to influence directly the return rate of individuals: this is notoriously the case in penguins,

---

1. Which can be defined as the observed number of substitutions (*i.e.* changes of DNA base) per single position in the genome, per million years - an estimator of the probability, for a given monomorphic position, to become polymorphic during the next million years.

where flipper-banding has been demonstrated to increase adult mortality (Froget *et al.* 1998; Sa-raux *et al.* 2011a). Beyond the obvious ethical question (Le Maho *et al.* 2011), this raises concerns as to the informative content of several studies based on recapture of banded penguins (Sa-raux *et al.* 2011a). Thus, a complementary approach to the study of dispersal, not based on individual recapture probability, is needed (see §41 p. 103).

§-20 Taxonomy of Penguins, and their relationship to other seabirds. Although treated until here as a consistent group, seabirds are a surprisingly diverse ensemble - both in terms of taxonomy, and of adaptation. In the broader sense, seabirds encompass the whole *Æquornithia* group, including *Procellariimorphæ*[1] (*i.e.* petrels, albatrosses, and penguins), *Pelecanimorphæ* (*i.e.* pelicans, herons and cormorants), and *Gaviimorphæ* (*i.e.* loons), as well as the *Charadriiformes* (*i.e.* seagulls, terns, skuas, and plover-like shorebirds), and in the vernacular sense also include a handful *Anseriformes* (*e.g.* the Common eider *Somateria mollissima*) - see Livezey & Zusi 2007; Hackett *et al.* 2008; Jarvis *et al.* 2014. All the species in these groups share some either plesiomorphic, or convergent traits. They rely on marine productivity for food, either directly preying on fish, crustaceans or mollusks, or foraging in the marine debris on the shore. Their plumage evolved advanced insulation and waterproofing properties. Their feet evolved interdigital webbing to facilitate paddling or steering. They are not usually territorial in their foraging areas, as opposed to most raptor or passerine species, and most of them breed colonially. However, their exploitation of the marine environment is highly diverse. Some species are mostly restricted to the shoreline (*e.g.* plovers or herons), and most usually occupy only the coastal waters (*e.g.* seagulls, pelicans, cormorans, etc).

Few species are truly pelagic, and most of these belong to the *Procellariimorphæ* or «storm-birds» - often called seabirds *stricto sensu*. Paradoxically, within that group, the colonisation of the high seas followed two opposite paths: *(i)* some species, within the *procellariiforme* family, developed

---

1.   Both recent and questionable compounds of Latin and Greek (*aequor*, the «high seas» and ὄρνις, «bird» for the first, and *procella*, «storm», and μορφή, «shape» for the second).

extraordinary gliding abilities, and started using the strong winds prevailing at sea to dispense with the metabolic costs of active flight - these are the petrels, fulmars, shearwaters, and above all albatrosses, that may circle the entire planet during a foraging voyage (Croxall *et al.* 2005). *(ii)* Some others, however, developed swimming abilitites instead, at the cost of reduction, or complete loss, of flight: these are first and formost the *Sphenisciformes* (the penguins), the *Alciformes* (the auks, puffins, mures and guillemots), and the *Pelecanoididæ* or diving-petrels (a part of the mostly gliding *Procellariiformes*). Morphological resemblances between these three families are due true convergence (see Grassé 1950 for details), and the most remarkable is the modification of the wings to facilitate underwater swimming: since the resistance of the water is much stronger than that of the air, wings have become shorter, more rigid, and the pectoral muscles have developed accordingly. The trade-off for this adaptation has been the complete loss of flight in modern penguins - as well as in at least one alcid, the now-destroyed Great Auk (*Alca impennis*) - and a costly and laborious flapped flight in the remaining Alcidæ, and in Pelecanoididæ. Posterior displacement of the hind limbs also accurred in all three groups, with an increasingly upright standing posture from Pelecanoididæ to Spheniscidæ. Finally, outstanding diving abilities have been observed in the three groups: the massive Emperor penguin may reach depths down to 500m (Kooyman & Ponganis 1998), while the intermediate-sized *Uria* guillemots can reach 180m (Piatt & Nettleship 1985), and the small Peruvian diving-petrel 80m (Zavalaga & Jahncke 1997)[1]. These common characteristics set apart the Northern Hemisphere Alcidæ, and the Southern Hemisphere Spheniscidæ and Pelecanoididæ, from the rest of the seabirds. This work will mainly focus on Spheniscidæ, and in particular on the two *Aptenodytes* penguin species. The Pelecanoididæ, due to their several convergence points with the penguins, will also be used as a reference outgroup in the seventh chapter, *Unexpected philopatry in an insular seabird, the Peruvian diving-petrel*, p. 275.

---

1.   Diving abilities being a direct function of myoglobin availability, and hence body mass.

§-21 Origin, evolution and radiation of sphenisciforms. Although penguins benefit from an outstandingly rich fossil record (Simpson 1975; Myrcha 2006; Clarke *et al.* 2007), their evolutionary history presents considerable uncertainties. The earliest stem penguin radiation is generally thought to have occurred just after (Baker *et al.* 2006; Clarke *et al.* 2007), or just before (Slack *et al.* 2006) the Cretaceous-Tertiary boundary, around ~65 Myr, with early flightless species such as the loon-like *Waimanu*. The dating of the crown group radiation, however, is much more uncertain. Based on morphological evidence, it was proposed around ~10 Myr (Clarke *et al.* 2007), but molecular evidence has set it back to ~40-50 Myr (Baker *et al.* 2006), or ~20 Myr for Subramanian *et al.* 2014, while extant species would have mostly diversified around 16-11 Myr. However, a recent total-evidence study including morphological and molecular data for fossil and extant species in a fossilised-birth-death model (Gavryushkina *et al.* 2015) reconcile these two sources of evidence, and imply a very recent radiation of the crown taxa around ~12.45 Myr, and a divergence of most extant species around ~2 Myr.

Eocene and Oligocene penguin diversity is dominated by «giant» taxa such as *Icadyptes* from South America or *Kairuku* from New Zealand, which probably originated in Tertiary temperate Gondwanaland (Baker *et al.* 2008). Early apomorphies that allowed for adaptation to cold waters, and in particular the humeral arterial plexus counter-current heat exchange structure (Thomas *et al.* 2011), are thought to have evolved in the Cenozoic greenhouse-earth, at lower latitudes, and independently from the current extreme-cold adaptation. Although theory predicts that larger taxa should be better adapted to cold climate due to a favourable body surface-to-volume ratio, only smaller taxa survived through the late Tertiary icehouse earth transition, which lead to suggest that *i)* giant penguin diversification was linked to increased upwelling activity and marine productivity during the Cenozoic (Clarke *et al.* 2007) and that *ii)* their demise was linked to the appearance of competing fish-eating small cetacean taxa (Fordyce *et al.* 1990; Williams 1995).

Crown penguins are thought to have originated at higher, subantarctic latitudes, and to have radiated back to lower subtropical and tropical latitudes in the recent past (Baker *et al.* 2006). Several adaptations to extreme cold have taken place in the recent evolutionary history, both on a molecular level (diversified keratin β genes, and modified phototransduction and lipid metabolism pathways, see Li *et al.* 2014), and on a behavioural level (e.g. the Emperor penguin's huddling behaviour, see Stonehouse & Glenister 1953). However the precise timing and structure of their radiation remains uncertain, and hybridisation is still commonly observed between extant species (e.g. between Humboldt and Magellanic penguins *Spheniscus humboldti* and *S. magellanicus* - see Simeone *et al.* 2009, or between Royal and Macaroni penguins *Eudyptes schlegeli* and *E. chrysolophus, pers. obs.*).

The *Aptenodytes* clade has been alternatively proposed as basal to all other crown penguins (Baker *et al.* 2006; Subramanian *et al.* 2014), or nested within the crown group (Gavryushkina *et al.* 2015). At any rate, the divergence between the Emperor penguin *Aptenodytes forsteri* and the King penguin *Aptenodytes patagonicus* is though to be very recent, during the mid-Pleistocene (1.52 Myr [0.73, 2.38] according to the total-evidence analysis, see Gavryushkina *et al.* 2015), although the place and conditions of this speciation event are still unknown. The King penguin has traditionally been separated in two subspecies on a morphometrical basis, with the autonym *Aptenodytes patagonicus patagonicus* in the southern Atlantic ocean, and *Aptenodytes patagonicus halli* elsewhere (Mathews 1911; Barrat 1976), although it is still unclear how far this classification reflects the true species architecture (see *The King synnome*, p. 163).

The most remarkable features of the known evolutionary history of the penguins are thus that *i)* the stem group is ancient and separated early from other *neornithes* species (Gavryushkina *et al.* 2015); *ii)* early penguin diversity is not associated with polar or otherwise cold environment, but rather with greenhouse-earth temperate habitats (Baker *et al.* 2006; Thomas *et al.* 2011); *iii)* the giant penguin fossil abundance and the co-occurrence of their demise with the radiation of small-

er fish-eating cetaceans makes it likely that they occupied a central top-predator role in the Ceno-zoic marine food-web (Fordyce *et al.* 1990; Williams 1995; Baker *et al.* 2006); *iv)* the adaptation of crown penguins to extreme cold conditions is secondary, and builds upon pre-adaptations (Thomas *et al.* 2011), and the colder-adapted species may have taken advantage of the glacial conditions onset, and of the lower competition in the polar areas, to diversify in the mid-Pleis-tocene, and *v)* the recent diversification within the major crown penguin groups (*Spheniscus*, *Eu-dyptes*, *Pygoscelis* and *Aptenodytes*) is shallow, and may still allow for interspecific gene flow.

§-22 Aptenodytes penguins in the historical period. The King penguin (*Aptenodytes patagonicus*) enters the historical records during Cook's second voyage in the southern seas (1772-75), when it is sketched by the ship's naturalist Forster in South Georgia, and later described by Miller as *Aptenodytes patagonicus.* We can hardly estimate how numerous the species was at the time: we only know that large colonies were described on Macquarie Island, Heard Island, Kerguelen and Crozet Archipelagos, Marion and Prince Edward Islands, and South Georgia, while smaller pop-ulations bred in Islas Hornos and Estados in Tierra del Fuego, and possibly in the Falklands (Bar-rat 1976). Yet, however populous they may have been, King penguins populations were massa-cred at industrial scales through most of their range by the whaling and sealing expeditions: the population on Macquarie was thus reduced to *ca* 3,400 birds (~0.7% of its current size) by the early 20th century (Rounsevell & Copson 1982), while most colonies were driven to near-extinc-tion throughout the species range (Murphy 1915; Murphy 1936; Barrat 1976; Lewis Smith & Tallowin 1979; Delord *et al.* 2004; Pistorius *et al.* 2012), and to complete extinction in Heard and Tierra del Fuego (Barrat 1976; Gales & Pemberton 1988) - although is difficult to ascertain the global extent of the reduction in population size. Following the end of slaughters in the mid-20th century, the King penguin population rebounded (Budd 2000; Delord *et al.* 2004; He-upink *et al.* 2012) at most breeding locations, possibly benefiting from the continued large-scale hunting of cetaceans and pinnipeds in the Southern Ocean throughout most of the 20th century (Cressey 2015), and subsequent reduction in competition for food resources (Ainley *et al.* 2010b;

Trivelpiece *et al.* 2011). However, populations seemed to have reached the end of their recovery by the early 21ˢᵗ century (Delord *et al.* 2004; Heupink *et al.* 2012), and are now once again challenged by large scale environmental changes in the Southern Ocean (Le Bohec *et al.* 2008; Péron *et al.* 2012; Bost *et al.* 2015).

As to the Emperor penguin *Aptenodytes forsteri*, which is endemic to Antarctica, it was first seen by Forster during the same voyage, but was then misidentified as belonging to the freshly discovered King penguin species (Wienecke 2010). It was classified as a separate species by the British zoologist G. R. Gray in 1844 (Gray 1844). But it was long before its winter breeding biology was understood, as the first breeding colony was only discovered in 1902 during the first of Scott's *Discovery* Expeditions (Wienecke 2010), and eggs during his fatal 1911 *Terra Nova* expedition, as romantically put by Cherry-Garrard - « *if you march your winter journeys you will have your reward, so long as all you want is a penguin's egg* » (Cherry-Garrard 1922). Eggs were also collected for study during Shackleton's last expedition (1914-17, as narrated in Shackleton 1919). Discovery of breeding colonies was slow and difficult, owing to the technical difficulties of winter expeditions in the most remote areas of Antarctica (Wienecke 2010), and has been substantially helped by satellite exploration (Fretwell & Trathan 2009; Fretwell *et al.* 2012; LaRue *et al.* 2015). However, it is believed that several colonies are still undiscovered (Ancel *et al.* 2014). In contrast with the large-scale massacres of king penguins, the direct impact of humans on Emperor penguins has been relatively small, a fact owing unfortunately more to the remoteness of its habitat than to any particular benevolence towards this remarkable species. However, an impact of research activities, in particular flipper banding, has been suggested on studied colonies (Le Maho *et al.* 2011), and, more importantly, the ongoing anthropogenic climate change is likely to have a tremendous impact on the near future of this species (Trathan *et al.* 2011; Jenouvrier *et al.* 2014, see §24 p. 79 for details).

Study sites and species

Although this work encompasses world-wide patterns of population history and geography, we have taken two particular areas as focal points: the Pointe Géologie Emperor penguin colony, near Dumont d'Urville research station, in Terre Adélie, East Antarctica (S66°39'46'' E140°0'07"), and the Baie du Marin King penguin colony, on Possession Island, Crozet Archipelago, in the Southern Indian Ocean (S46°24'41'' E51°45'22") - see Fig. 7. These two colonies have been the focus of long-term monitoring programs (Barbraud & Weimerskirch 2001a; Gendner *et al.* 2005), and their demography, although still not fully understood, is fairly well known compared to other penguin species.
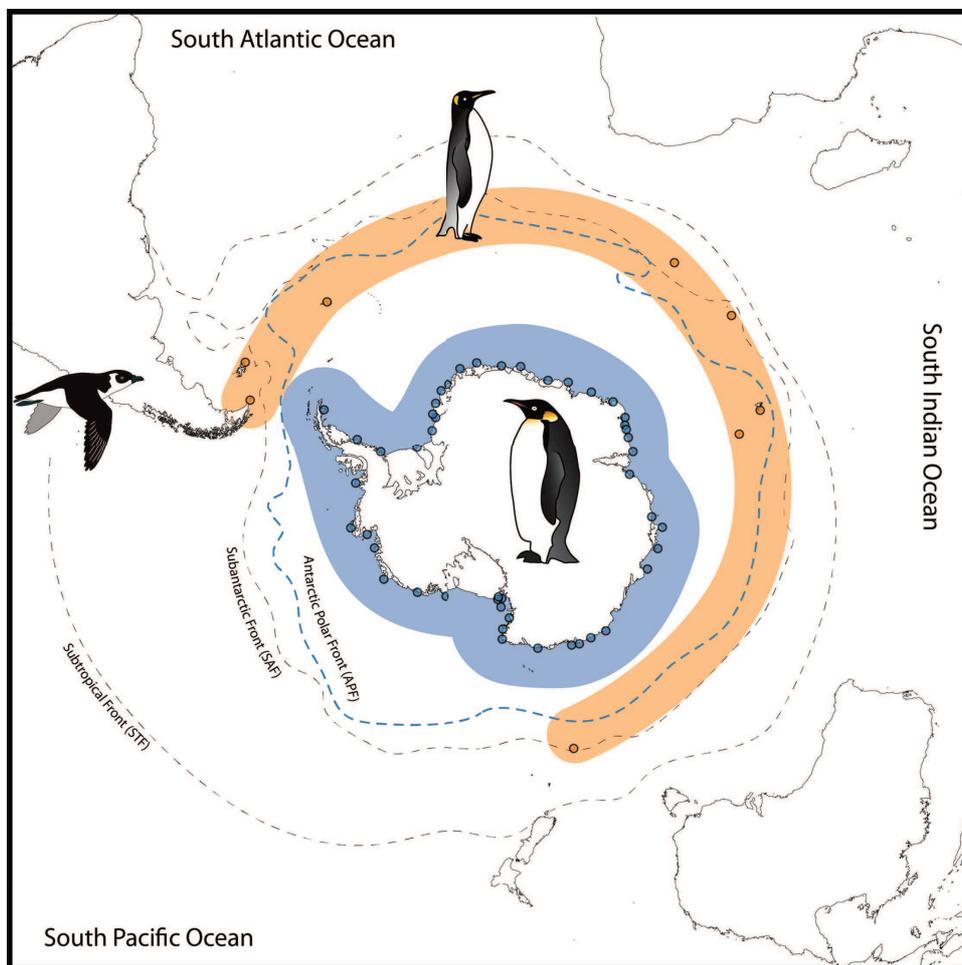
Figure 7 | Distribution of the two *Aptenodytes* species. Orange dots: King penguin breeding archipelagos, blue dots: Emperor penguin breeding colonies. Orange and Blue areas, general range of the species (schematic). Antarctic Polar Front, Subantarctic convergence and Subtropical convergence, approximate mean position (Australian Antarctic Division dataset, after Orsi *et al.* 1995).

§-23 *The Emperor penguin.* The Emperor penguin (*Aptenodytes forsteri*) is the largest extant penguin species, measuring up to 120 cm and weighting up to 45 kg (Stonehouse & Glenister 1953). It breeds during winter along the shoreline of mainland Antarctica, at latitudes comprised between 64°S and 77°S (Wilson 1983). All across this range, it reproduces in well-separated colonies that gather on the sea-ice at the beginning of the breeding season, in the first days of winter, and that dissolve again completely during the austral summer, as the chicks fledge and their breeding ground breaks up, only to gather again at the beginning of the next winter. The size of these colonies usually ranges from a few hundred, to dozens of thousands of breeding pairs (Fretwell *et al.* 2012). Despite their cyclical existence, however, each colony is considered to be a very stable unit, both in terms of location, and of individual identity: the Emperor penguin is thought to be a strongly philopatric species, both as a juvenile, and as an adult (Stonehouse & Glenister 1953; Budd 1961; Prévost 1961; Budd 1962; Isenmann & Jouventin 1970; Isenmann 1971; Le Maho 1977; Kooyman 1993; Ancel *et al.* 2013). Recent satellite surveys have shown that its present-day breeding range is made up of 52 colonies, distributed along most of the Antarctic shoreline (Fretwell & Trathan 2009; Fretwell *et al.* 2012; Ancel *et al.* 2014). The only significant interruption in this distribution is the Antarctic peninsula (see §10 p. 48), which extends North to almost 62°S, at the very limit of the specie's breeding habitat: indeed, the first documented loss of an Emperor colony happened at the northern end of the species' range, in Dion Island, as recently as the early 21st century, and has been directly associated with the region's important warming trend (Trathan *et al.* 2011). However, the species' high dependence on sea ice makes it a difficult task to accurately predict its future response to climate change (see §18 p. 65), the dynamics of which we still poorly understand in Antarctica (Turner *et al.* 2013; Shu *et al.* 2015).

The Emperor penguin's complex breeding system poses particular challenges to population modelling. This long-lived bird (the current lifespan estimate is unknown - see Borboroglu & Boers-

ma 2013 - but at least equal to 35-40 years, Jenouvrier 2004) has a very late reproductive maturi-
ty (ca. 4-8 years for males, and 3-6 years for females, Mougin & Van Beveren 1979, and a long
generation time (16 years, Jenouvrier *et al.* 2014), which implies that generations are largely over-
lapping, in contradiction with the assumptions of the Wright-Fisher population model (Wright
1931 and §39 p. 99). Although divorce rate is high in this serially monogamous bird (ca. 85%,
Isenmann 1971), mating is not likely to be fully random (Bried *et al.* 1999). Finally, the species'
particular spatial organisation during breeding make capture-mark-recapture technically chal-
lenging, so that even instantaneous demographic trends are not trivial to infer.

§-24 The Pointe Géologie colony and its regional and continental ties. The Pointe Géologie Emperor
penguin colony is by far the best-studied one in Antarctica. Its presence was one of the reasons
for the choice of location for the Dumont d'Urville research station, in 1952, and it has been
monitored continuously ever since (Prévost 1961; Isenmann & Jouventin 1970; Isenmann 1971;
Jouventin 1971a; Jouventin 1971b; Jouventin 1972b; Jouventin 1975; Le Maho 1977; Barbraud
& Weimerskirch 2001a; Jenouvrier *et al.* 2005; Ancel *et al.* 2009; Jenouvrier *et al.* 2009). As it is
also the most accessible colony during the winter breeding season, the breeding behaviour of the
Emperor penguin is mostly known through observations made on this colony (see references
above). The corollary is that our knowledge of the species is often restricted to local observations,
and that we may lack a global perspective on behavioural, phenological or demographic traits (see
The Emperor synnome, p. 211).

Of particular interest, for example, is the sudden decline in the number of breeders on the Pointe
Géologie colony, that abruptly dropped from *ca* 6,000 to *ca* 3,000 breeding pairs between 1975
and 1985 (Barbraud & Weimerskirch 2001a). Although it has been alternatively linked to local
effects of climate change (Barbraud & Weimerskirch 2001a; Jenouvrier *et al.* 2005; Barbraud *et
al.* 2011), or to increased predation pressure by killer whale as a consequence of the decline of
their usual prey, the minke whale, under whaling industry pressure (Ainley *et al.* 2010b), the pe-
riod also corresponds to heavy logistic and scientific activity on the colony, in particular large-

scale flipper banding (Jenouvrier 2004) which has been unambiguously shown to negatively affect survival (Gauthier–Clerc *et al.* 2004; Dugger *et al.* 2006; Le Maho *et al.* 2011; Saraux *et al.* 2011a). Interestingly, the decline of the Pointe Géologie Emperor penguin study colony has a parallel on Crozet archipelago, where the King penguin study colony in the Baie du Marin (see §26 p. 81), also subject to human disturbance and heavy flipper-banding (Delord *et al.* 2004; Saraux *et al.* 2011a), is the only one to have declined, while the four other colonies of the same island were undergoing very rapid growth (Delord *et al.* 2004) - thus leaving little doubt as to the effects of human activity on colony demographic trajectory.

But the decline of the Pointe Géologie colony also raised the question of the fate of the missing penguins. While their disappearance has usually been explained by increased mortality, we suggest that dispersal to other colonies may have played an important role (see *Empirical evidence of heterogeneous dispersal*, p. 259 and §135 p. 250) - a possibility that would change our interpretation of the global demographic trajectory of the species. However, the lack of both of direct evidence for dispersal, and of a broad comparative perspective in the Emperor penguin makes a global assessment of the species' status difficult, and will require an increased methodological effort (see *The Emperor synnome*, p. 211 and *Empirical evidence of heterogeneous dispersal*, p. 259). In the meantime, it is still unclear whether the Pointe Géologie colony can be taken as a reliable indicator of worldwide population trend or whether its importance is rather on a regional scale.

§-25 The King penguin. The King penguin (*Aptenodytes patagonicus*) is the second-largest extant penguin species, and sister species to the Emperor penguin. It is somewhat smaller, measuring up to ~90 cm and weighting up to ~15 kg at most (Bost *et al.* 2013), and its colouration is mode vivid than the Emperor's. It currently breeds on 7 subantarctic archipelagos, between 45°S and 55°S, located indifferently North or South of the Antarctic Polar Front (see §2 p. 35, and details in *The King synnome*, p. 163) - and small, incipient breeding colonies have been documented in Tierra del Fuego, in Bahia Inútil (Kusch & Marín 2012). Morphometric differences have justified the distinction between two subspecies: the autonym, *A. p. patagonicus*, that is found in

South Georgia, is slightly larger that the Indian and Pacific *A. p. halli* according to Mathews (Mathews 1911) and Barrat (Barrat 1976) - although this distinction has not been revisited by the modern literature (*i.e.* using more recent and systematic morphometric tests, or a genetic approach - see *The King synnome*, p. 163).

The King penguin's breeding system, although closely akin to that of the Emperor, offer some noteworthy differences. As opposed to the Emperor's fully vagrant incubation, the King penguin selects a local territory of ca. 1.5m^2 (Barrat 1976), and behaves there in a remarkably territorial way, although it does not build a nest and incubates its egg on its feet in the same manner as its sister species. The King's breeding system also extends over the winter, but egg-laying, hatching and brooding occur during summer, and chicks fast unguarded in «*crèches*» over the winter (Stonehouse 1960; Barrat 1976). During the early chick rearing period, king penguins forage mostly on the APF (see §18 p. 65), which becomes a critical food resource during the months of January and February (Péron *et al.* 2012; Péron *et al.* 2012; Bost *et al.* 2015).

Like the Emperor (see §23 p. 78), the King penguin presents interesting challenges to demographic modelling. This equally long-lived bird has a slightly shorter generation time (~10.5 years, see §95 p. 186), and usually only breeds successfully every second or third year (Le Bohec 2008). The King penguin also has a high yearly divorce rate (70% to 80% based on flipper-banding data - Olsson 1998; Bried *et al.* 1999, or 63% based on more reliable PIT-tagging data, Toscani *et al. in prep.*), yet random mating seems contradicted by several behavioural traits (Olsson *et al.* 2001, and field observations - see also *Fine-scale colony structure*, p. 135). Finally, like the Emperor penguin, the King penguin is highly sensitive to immediate environmental constraints (*e.g.* Le Bohec *et al.* 2008) and exhibits a high variability in breeding success (Saraux *et al.* 2011a, Le Bohec *et al. in prep.*), adding to the challenges of extracting reliable demographic parameters on short time series.

§-26 The Baie du Marin colony and long-term monitoring design. Most of the classical knowledge on the King penguin was gathered on South Georgia by Stonehouse (*e.g.* Stonehouse 1960), or

on Possession Island by Barrat (*e.g.* Barrat 1976). More accessible and better studied than the Emperor penguin - yet paradoxically almost absent from popular culture - the King penguin has been the object of several more or less large scale monitoring programs - on South Georgia (see Olsson & Brodin 1997; Olsson & van der Jeugd 2002), on Marion Island (Du Plessis *et al.* 1994), and most importantly on Possession Island, in Crozet archipelago (Gendner *et al.* 2005).

On this latter island, one colony, situated in the *Baie du Marin* (S46°24′ E51°45′) has been the focus of intensive research in the past decades - including physiology (*e.g.* Handrich *et al.* 1997; Thouzeau *et al.* 2003), demography (*e.g.* Le Bohec *et al.* 2008), parasitology (*e.g.* Gauthier-Clerc *et al.* 2003), life-history (*e.g.* Le Bohec et al. 2007; Saraux et al. 2011b; Saraux et al. 2012; Celia et al. 2014), foraging behaviour (*e.g.* Bost *et al.* 2015; Le Vaillant *et al.* 2015), *etc.* First studied since the seventies using flipper-bands, the discovery of their adverse effects (Froget *et al.* 1998) led to their replacement by subcutaneous radio-frequency identification (RFID) tags (Gendner *et al.* 2005). The current monitoring program involves the yearly RFID-tagging of ~ 450 nearly-fledged chicks, and the tracking of their movements in and out of their sub-colony using antennas buried under the ground on the major access paths to and from the sea. Informatic logging and treatment of these movements allow for the inference of individual life history patterns, such as recruitment and yearly return rate, or timing and success of the major stages of the breeding cycle: thus, fundamental population parameters such as instantaneous growth rate, age at first breeding, yearly breeding success, *etc.* can be extracted, and integrated in population models (see *e.g.* Le Bohec *et al.* 2008; Saraux *et al.* 2011a; Saraux *et al.* 2011b). This system currently represents the best trade-off between the reduction of disturbance to the birds, and the derivation of reliable information about population dynamics.

While relatively well known in comparison with the Emperor penguin, the King penguin's demography remains an elusive question. The long life span of the species, and the dramatic impact of human activities on the population (see in particular §22 p. 75) fundamentally limits the scope of human-scaled monitoring programs to almost instantaneous parameters: thus, comple-

mentary approaches are required if we are to understand long-term processes at work in the species.

§-27 The Peruvian diving-petrel. The last study of this work will focus on the case of the Peruvian diving-petrel *Pelecanoides garnotii*, that we briefly introduced in §20 p. 71. This small procellari-iforme weights around 200g (based on our field measurements), and is currently known to breed on 4 Northern Chilean islands (Islas Pan de Azúcar, Isla Choros, Isla Grande, and Isla Pájaros II Mattern *et al.* 2002; Simeone *et al.* 2003; Martinez Palma 2014), and a handful of Peruvian islands (Isla San Gallán and La Vieja, Zavalaga *et al.* 2010) - a drastic range reduction for this once-abundant seabird, that used to breed along the totality of the Humboldt Current, from 6°S to 42°S (see §147 p. 276 for references and details). Little is known of the natural history of the species (longevity, return rates, breeding success and strategies are all unexplored yet). It breeds in burrows dug in the soft guano of the islands Hays 1989, and occasionally, in Peru, in scree slopes where guano habitat has been destroyed (Carlos Zavalaga *pers. com.*). Burrow fidelity is unknown in the absence of any capture-mark-recapture study. It feeds mostly on anchovies *Engraulis ringens* and krill *Euphausia mucronata*, but also on fish larvæ and planktonic invertebrates during the breeding season (Jahncke *et al.* 1999; García-Godos & Goya 2006), when it remains in local waters (Zavalaga *et al.* 2010, Fernandez-Zamorra *pers. com.*). Its winter foraging strategy is unknown, but anecdotic sightings and the parallel of two sister-species (the South Georgian diving-petrel *P. georgicus* and the Common diving-petrel *P. urinatrix* - see Navarro *et al.* 2013; Navarro *et al.* 2015) suggest that it is probably a year-round coastal water resident.

The specialisation of the diving-petrel's nesting behaviour in the highly unique guano substrate makes it a very sensitive indicator of habitat destruction. Guano being a rich fertiliser for intensive agriculture (due to its concentration in nitrogen, phosphate and potassium), it has been exploited on a large scale since 19th century[1], and this resulted in the destruction of the majority of

---

1.   Incidentally leading to rather controversial political decisions such as the «US Guano Islands Act» of 18 August 1856, granting US citizens the exclusive property of the guano islands they would chance to discover anywhere in the world - or the

insular habitats of the *guanero* birds, such as the Peruvian diving-petrel and the Guanay cormorant *Phalacrocorax bougainvillii*. The large historical population sizes of the diving-petrel did not survive the exploitation, and the maybe up to 1,000,000 pairs dwindled to a few thousands nowadays (see *Unexpected philopatry in an insular seabird, the Peruvian diving-petrel*, p. 275 for more details). As a result of this chaotic demographic history, it is difficult to assess the true state of conservation of the species, that may be recovering, or, on the other hand, still dwindling beyond salvation. A more in-depth summary of the current state of knowledge will be presented in §149 p. 279-§150 p. 280.

Laboratory methods

§-28 Utility of classical markers. Since the advent in 2005 of «next-generation» or high-throughput sequencing, electrophoresis-based individual marker analysis has been slowly losing ground to massively parallel sequencing technologies. In this work, however, we make use of two such «classical» methods: Sanger-sequencing of mitochondrial markers, and analysis of nuclear variable number of tandem repeats (VNTR) or «microsatellite» markers. Microsatellite loci differ from single nucleotide polymorphisms (SNP) by their higher mutation rate, mutation process (usually approximated through a Brownian motion model[1]), and consequently higher allelic richness. Thus, a single microsatellite marker is, on average, 4 to 12 times more informative than a single SNP (Liu *et al.* 2005). However, the number of markers available in a typical SNP experiment is several hundred times higher than what can reasonably be achieved with microsatellite markers, and it has been shown that an increased number of markers contributed highly to detection power for several genetic patterns (Liu *et al.* 2005; Hoban *et al.* 2013b). Direct comparisons

---

«Chincha Islands war» of 1864-1866 between Spain and a Peru-Chile alliance for the possession of the Chincha guano islands.

1.   Brownian motion of particles is used as an approximation of the stepwise mutation in microsatellites: an *n*-mer allele can randomly mutate to *n+1* or to *n-1* at each mutation even, ultimately leading to an increasingly dispersed distribution of fragment lengths.

informed by empirical data, however, have alternatively concluded in an increased power (Hoffman *et al.* 2014) or an increased noise (Mesak *et al.* 2014) of SNP compared to microsatellite markers, so that the latter remain a valid option, at least whenever full transversal coverage of the genome is not of interest (e.g. for detecting population differentiation, see Gorospe & Karl 2013). Sanger sequencing, especially of haploid (e.g. mitochondrial) markers, retains one advantage over massively parallel sequencing: the possibility of obtaining a very long read without a very low error rate, up to 1,000 bp with 99.999% per-base accuracy (Shendure & Ji 2008), as opposed to 250 bp with a maximum of 99.9% accuracy for NGS (Wall *et al.* 2014), and mitochondrial DNA barcoding has been shown to retain sufficient resolution for several phylogeographical questions (Baker *et al.* 2009; Peucker *et al.* 2009) In the present work, microsatellite markers were mainly used as a cost-effective way to increase sample size where our primary interest laid in wide population coverage (see *Fine-scale colony structure*, p. 135). Sanger sequencing, on the other hand, was used in combination with Restriction-site-Associated DNA sequencing (RAD-seq data, see §29 p. 85), in order to provide an independent methodological take on the same dataset, free from potential undetected biases (see *The Emperor's gnome*, p. 211).

§-29 The RADseq approach. Although classical markers remain useful for addressing several population genetics questions, the rise of NGS methods has opened new horizons for molecular ecology (Allendorf *et al.* 2010). Thus, an important choice when setting up an experiment is the balance of high-resolution coverage of the genome, and high-resolution coverage of the populations: in other words, numerous markers in numerous individuals (Hoban *et al.* 2013b). Classical markers may lack sensitivity to resolve complex population parameters (see §28 p. 84), while whole-genome resequencing is, as yet, too costly to allow for large-scale surveys of populations. A trade off is offered by the Restriction-site-Associated DNA sequencing (RAD-seq), developed by Baird *et al.* 2008. Genomic DNA is cut at specific sites using a restriction enzyme, and flanking DNA sequences are analysed on a high-throughput platform: thus, a large number of markers

can be obtained with a nearly-random representation of the genome. The protocol is as follows: *(i)* Genomic DNA is first checked for degradation on a 1.5% agarose gel, and only samples with consistently high molecular weight are retained, and precisely quantified by fluorometry (Life technologies™ Qubit®). *(ii)* approximately 150 ng of genomic DNA per sample are digested with a restriction enzyme. Each enzyme cutting at a specific restriction site, the enzyme determines the density of markers along the genome. For this study, we used the Sbf-I HF enzyme (New England Biolabs), which is specific for the GC-rich CCTGCAGG pattern. *(iii)* each sample is then ligated to a unique barcoded P1 adapter prior to pooling in a single library. The library is then randomly sheared by sonication; *(iv)* sonicated libraries are concentrated by DNA capture on magnetic beads, and the target size range fraction (350-650 bp) is selected by gel electrophoresis; *(v)* DNA fragments are prepared for sequencing: single-stranded ends are repaired, a single A base is added to the repaired ends, and P2 sequencing adapters are ligated to these A-tails; *(vi)* the library is enriched by PCR amplification, *(vii)* the library was then quantified by quantitative PCR, controlled on a fragment analyser, and sequenced on an ILLUMINA HiSeq 2500 platform, spiked with 20% PhiX control library in order to reduce low-diversity bias introduced by the aligned restriction sites (see Fig. 29 p. 85).

§-30 Whole-genome resequencing. In order to complete the RAD sequencing data, we produced whole-genome resequencing (WGS) data for three King penguins, and three Emperor penguins. Samples were selected on the basis of DNA quality and efficiency of the corresponding RAD-sequencing libraries. For the King penguin, we selected three samples from South Georgia; for the Emperor penguin, three samples from the Neumayer colony (see Fig. 31 p. 217). Library preparation followed a standard PCR-free Illumina protocol (Illumina TruSeq low-throughput kit), and the sequencing was done on two lanes of a HiSeq 2500 V-4 sequencer, at the Norwegian Sequencing Centre facility. The two combined lanes yielded a total of 442,637,497 paired-end 125 base-pairs (bp) reads, or a total of 110,659,374,250 bp. Once demultiplexed and combined, we obtained a total of 73,772,916 (± 1,385,583) reads, or 18,443,229,042 (± 346,395,842) base

1 pairs per sample. Both species were mapped to the published Emperor penguin reference genome

2 (Zhang *et al.* 2011b), with a final coverage of ~14X per sample.
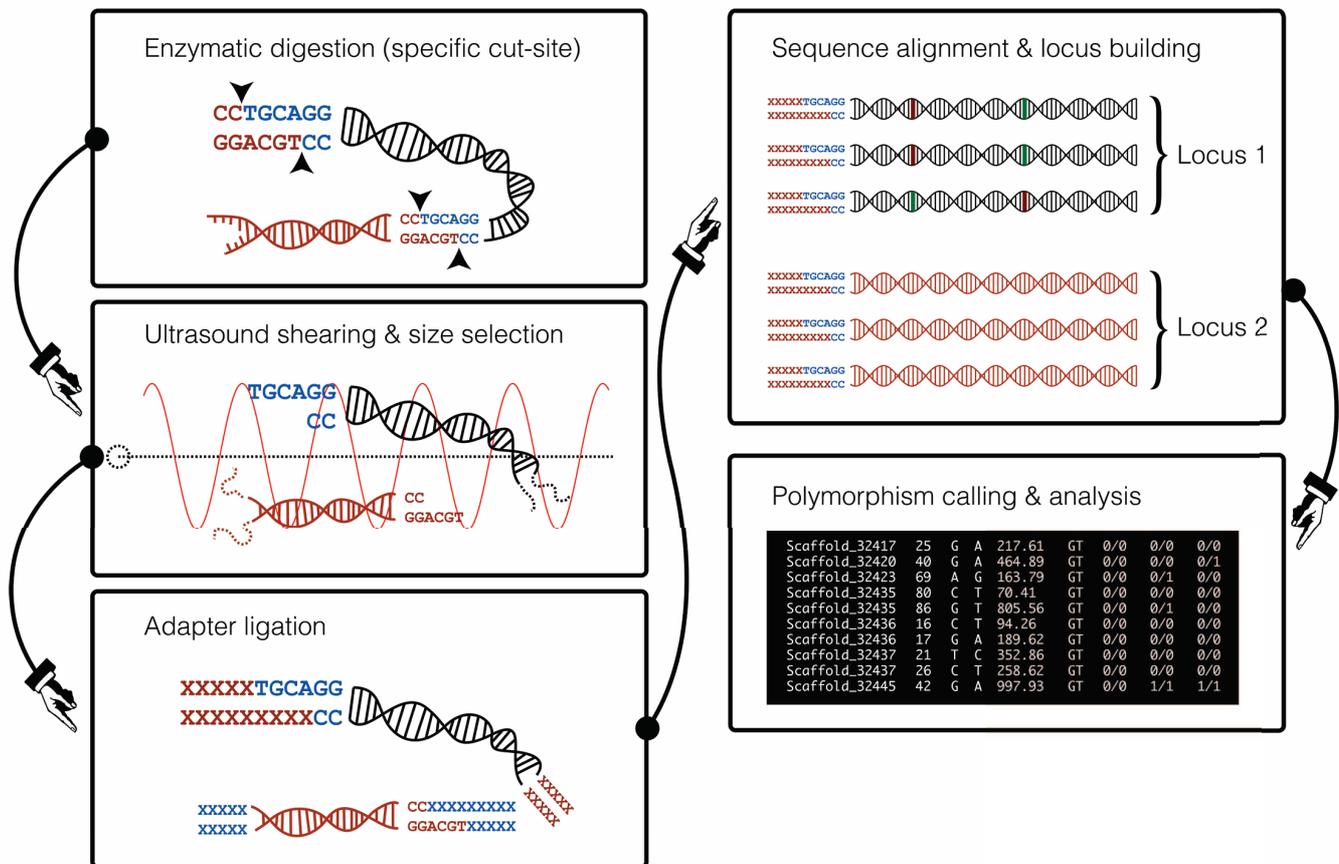
3 **Figure 8 | The RAD sequencing approach.** See details of the protocol in §29 p. 85.

4 *From DNA libraries to polymorphism data.*

5 *§-31 Particularity of RAD data for analysis.* An important strength of the RAD-sequencing ap-

6 proach (see §29 p. 85) is the possibility it offers to work on a genome-wide scale in non-model

7 species for which no reference genome is available (Baird *et al.* 2008). As every RAD locus is con-

8 strained by the location of cut-sites, first-in-pair read overlap is complete at each particular loca-

9 tion. It is thus possible to match the multiple reads covering a locus without any information

10 about its position in the genome. But even in the presence of a reference genome, the highly dis-

11 cretised character of the RAD-sequencing data changes substantially the analysis paradigm.

The « natural » structure of genomic data is shaped by two opposite processes - *coalescence* and *recombination*. The coalescence process can be described as the down-time branching of sequences through the occurrence of new mutations (see §40 p. 101). The recombination process, on the contrary, is the merging of sequences with different coalescent histories, through physical crossing-over during meiosis. Thus, a coalescent event can be seen as the fusion of sequences when going *backward* in time, a recombination event is, on the opposite, a fusion of two sequences going *forward* in time (see §42 p. 107). The direct consequence of a shared coalescence history is the linkage between different polymorphic sites: in the absence of recombination, and with an infinite-sites model, co-occurrence of derived alleles reflects the coalescent history of the sequences. Recombination, on the other hand, breaks this linkage, by physically linking derived alleles that did not arise in the same lineages in the first place. Since recombination is a relatively random process, the chances that it would happen between two given loci increases with the distance between these loci. Thus, two polymorphic nucleotide positions separated by only a few base-pairs are expected to keep their linkage much longer than two loci separated by several thousands of base-pairs. In continuous genomic data, this means that linkage between markers will decay continuously with increasing distance, until a point where distant loci may be considered effectively independent. Between very close and absolutely linked loci, and distant and effectively independent loci, virtually all states of linkage disequilibrium can be found.

RAD-sequencing data, on the other hand, has a strongly bimodal structure. Since only short fragments (95 to 125 bp) of DNA are sequenced, and since these are assumed to be evenly interspersed in the genome, two polymorphic positions that belong to the same locus can be considered non-recombining, and their allele distribution is solely the consequence of the coalescent history of the locus, while polymorphic positions belonging to different loci are effectively independent, and their co-occurrence on a chromosome is mainly driven by the recombination process. Thus, while the « classical » polymorphism calling framework assumes continuity in the data, and therefore works on a per-base rationale, RAD data can also be handled in a discrete

way, first identifying reads belonging to the same RAD locus, and then treating these loci as non-recombining units.

§-32 The Stacks pipeline. This latter approach is implemented in the popular Stacks pipeline (Catchen *et al.* 2011; Catchen *et al.* 2013). Stacks builds upon the discretised RAD paradigm, and makes the RAD locus a self-standing unit. The analysis pipeline runs in three steps: *(i)* identifying exactly matching reads, that come from a single genomic location and a single allele (a «stack» in the program's lexicon), and match those stacks within individuals to identify polymorphic loci, and *(ii)* match loci across individuals to build a common catalog, and *(iii)* reference all data to this common catalog.

The first step can be achieved in two different ways: either (a) by direct local *de novo* assembly, without a reference genome (using the ustacks program), by matching the reads against each other, or (b) by mapping the raw reads against a reference genome (using an independent mapping program, in our case *Bowtie2*, Langmead & Salzberg 2012), and collating reads that map at the same genomic position (using the pstacks program). While both approach are valid, mapping reads to a reference genome is preferable whenever possible, first because it allows for polymorphism data to be compared between Stacks and other methods through the mapping co-ordinates, and second because it guarantees that sequenced contaminants (bacterial DNA, etc) are not retained in the analysis, as these are not expected to align to the reference genome. It is this second approach that we used in this work, using as a reference the published Emperor penguin genome (Zhang *et al.* 2011b), both for the Emperor and for the King penguin sequencing data.

The second and third steps are done using the cstacks and sstacks programs, and allow the building of a MySQL database containing RAD loci (as opposed to polymorphic sites) as individual entries. A particularity of this approach is that polymorphic sites are identified early in the pipeline (at step *(i)*), within individuals, when matching stacks to form diploid loci. Thus, SNP calling does not integrate information from the whole population as a basis for the likelihood

function - therefore there is an increased probability of mistakenly scoring sequencing errors as legitimate polymorphisms in low-coverage data. A final correction has been implemented in the rxstacks program, that correct genotype calls based on information from the whole dataset. However, this two-steps procedure only re-evaluate genotypes at already identified SNP loci, as opposed to the SNP positions themselves, and is therefore more error-prone than a native joint SNP and genotype calling algorithm such as Samtools' mpileup (Li *et al.* 2009) or GATK's HaplotypeCaller (DePristo *et al.* 2011) pipelines.

The strength of the Stacks approach, however, remains the rapidity and ease of querying and filtering offered by the MySQL database structure, that allows for efficient data mining, before deploying more robust and computationally-intensive analysis methods.

§-33 SNP-calling approach. Although the locus-based paradigm offered by the Stacks framework (see §32 p. 89) is an efficient representation of RAD data structure, it is also possible to handle RAD-sequencing data as conventional high-throughput sequencing data, provided the bimodal linkage structure is taken into account in downstream analysis. This approach involves three successive steps: *(i)* raw read mapping and filtering, *(ii)* SNP and genotype calling, and *(iii)* data filtering.

For the initial read mapping, we use *Bowtie2* (DePristo *et al.* 2011), allowing only for fully mapped read pairs, respecting the observed length of our paired-end libraries (250 to 1,000 bp). While other tools, such as the Burrow-Wheeler transform alignment (BWA, Li & Durbin 2009), perform a comparable task, not all support end-to-end read mapping: BWA, for example, allows for missing bases at both ends of the raw reads. This is suitable for most short-read mapping situations, but not for RAD sequencing, which relies on the presence of a cut-site, and thus puts a strong constraint on the correct alignment of the first six (in our case) bases of the raw reads. Using Bowtie2, we have typically high alignment rates (75% to 85%). The resulting alignment files (see §38 p. 98) are filtered for mapping quality, sorted, and indexed using Samtools (Li *et al.*

2009) and Picard Tools (picard.sorceforge.net), including a step of duplicate removal (see §35 p. 93 and §36 p. 95).

Current genotype and SNP calling algorithms can be broadly divided into two categories: « clip-off » or read-count-based calling, and probabilistic calling (Nielsen *et al.* 2011). While count-based calling simply relies on the relative proportion of reference and alternate bases to assign a genotype, probabilistic methods rely on a polymorphism model as a prior, to assign likelihood scores to each possible genotypes - this latter family of methods being generally considered much more accurate, although the details of the prior can vary widely (e.g. assuming or not Hardy-Weinberg equilibrium, etc, see Nielsen *et al.* 2012). In this work, we use two different algorithms for calling SNPs and genotypes from alignment files. A robust and accurate approach is implemented in GATK's HaplotypeCaller pipeline (DePristo *et al.* 2011): each individual alignment file is converted to a gVCF format (see §38 p. 98) that includes information about physical phasing (see §37 p. 97), using the HaplotypeCaller java program. These individual gVCF files are then scanned all together on a per-site basis by the GenotypeGVCF program, that makes use of individual depth, base quality, variant frequency, and variant phasing information to call genotypes in a maximum-likelihood framework. The main drawback of this approach is its extremely time-consuming character, as computation time grows exponentially with the number of included individuals: thus, on our platform, genotyping ~200 individuals for the whole RADome on 48 threads can take up to 10 days. Another faster, and equally accurate method is the Samtools mpileup/bcftools pipeline (Li *et al.* 2009), which is also deployed in two steps: first the collating of all alignment files into a single « pileup » format, and then a genotype calling and filtering step, also in a maximum-likelihood framework. While the Samtools pipeline can not be multithreaded, it can easily be split in chunks along the genome, and the results merged after genotype calling.

The final filtering of called genotypes is mostly done in VCFtools (Danecek *et al.* 2011). The details of filtering greatly depends on the analysis for which data is prepared, although some aspects

are invariant. For one, a form of *ensemble* calling may be highly desirable. All maximum-likeli-
hood genotype calling algorithms are model-based: they implement an explicit model describing
the likelihood of a particular genotype given the observed data. Yet these models differ between
algorithms: while they overlap very closely in the «central» part of the genotype calling problem,
they may differ quite widely at its limits - for example, under very high or very low coverage, or
when both alleles are represented with very asymmetric depth. However, while it is possible to as-
sess the accuracy of genotyping using an ascertained SNP panel in model data (*e.g.* human ge-
nomic material), there is no straightforward method for ranking genotype models in more exotic
organisms. A robust method to address the potential lack of agreement between SNP models is
to retain only consensus SNPs, i.e. loci and genotypes called the same way by a panel of models,
as the most reliable set of loci (Greminger *et al.* 2014).

Within this consensus SNP set, further filtering may be necessary, relative, this time, not to the
model after which genotypes have been called, but rather to the structure of the available popula-
tion dataset. Some analyses may be overly sensitive to missing data (e.g. non-assignment bias in
principal component analysis), in which case only loci genotyped in a high proportion of individ-
uals should be retained. Some analyses, on the other hand, are very sensitive to genotype mis-as-
signment (e.g. erroneously calling a homozygous site, where the true underlying genotype is het-
erozygous), in which case it is critical to impose a minimum depth, e.g. 10x, over retained
genotypes (see §35 p. 93) in order to obtain reliable results. However, all such filtering always
comes at the cost of reducing the number of loci available for analysis: therefore, a tradeoff often
needs to be made between the quality of the data necessary for the analysis, and the quantity of
data required for robust results (see §36 p. 95).

§-34 Genotype-free approach. Most current model-based calling algorithms implement a maxi-
mum-likelihood framework (see §33 p. 90). Genotype calling thus commonly happens in two
steps: first, at each position, a likelihood score is calculated for all 10 possible genotypes (AA, AC,
AG, AT, CC, CG, CT, GG, GT, and TT) - this score being defined as the probability of the se-

quencing data given each possible genotype (Korneliussen *et al.* 2014). Then, the genotype with the best likelihood score is retained as the «true» genotype, provided the contrast with the second-best likelihood score is steep enough. However, this second step, by choosing one single genotype, suppresses the information contained in the genotype likelihood distribution (Nielsen *et al.* 2005; Fumagalli *et al.* 2013). In many cases, this gives a false sense of certainty to data that did not, in reality, support any positive genotype call: thus, it has been proposed that analysis may often be more accurately performed by focusing on the genotype likelihood distribution, rather than on called genotypes (Nielsen *et al.* 2005; Nielsen *et al.* 2011; Nielsen *et al.* 2012; Fumagalli *et al.* 2013). This approach has recently been implemented in the ANGSD program (Korneliussen *et al.* 2014). This approach is particularly powerful for low-coverage data, where the genotype likelihood distribution tends to make little difference between homozygous and heterozygous calls. Therefore, it was preferred for our RAD sequencing data, whenever suitable analysis algorithms were implemented for downstream data treatment (e.g. principal component analysis and fixation index in Fumagalli *et al.* 2014, admixture analysis in Skotte *et al.* 2013, or derived-allele frequency spectrum estimation in Korneliussen *et al.* 2014).

§-35 Exploring the duplicate bias. Accurate estimation of SNP positions and individual genotype likelihoods is further complicated by the technical challenges of Illumina platforms, such as we use in the present study. Two important characteristics of high-throughput sequencing platforms, in particular of Illumina type, are *(i)* the random sampling process that occurs during fragment binding and cluster generation and *(ii)* the relatively high error rate, with possibly more than 0.1% erroneous base calls. Thus, every analysed fragment must be sequenced several times independently, in order to ensure that *(i)* both alleles have been sampled, and *(ii)* sequencing errors can be accurately filtered out.

Genotype under-sampling occurs when, at a heterozygote position, only one of the two possible bases is sampled across the whole sequencing coverage (Nielsen *et al.* 2012). At a sequencing depth of one, this is necessarily the case. At a depth of n, this occurs with a probability of (1 /

$2^{(n-1)}$). Thus, at a depth of 5, the probability of under-sampling the true genotype is 0.0625 (in other words, out of a very large number of heterozygous positions, ~6.25% will erroneously be called as homozygous); at a depth of 10 that probability falls to $9.77e^{-4}$. This, however, refers to «effective» or «true» sequencing coverage, where 5X means that 5 independent genomic copies of a DNA region have been sequenced in the same individual. Yet observed coverage may be significantly overestimated compared to effective coverage.

Indeed, in case of sub-optimal library preparation efficiency, too few individual DNA fragments are prepared compared to the flow cell capacity. During PCR library enrichment, multiple clonal copies of these fragments are generated. Normally, the random sampling process occurring during flow cell clustering would ensure that ~1 copy of each fragment only is represented in the sequenced library. However, in case of a low-diversity library, several PCR-copies of each fragment will be sequenced. Although these fragments, or «PCR duplicates», contribute to the total sequencing depth, they do not stem from independent genomic copies. Thus, if each independent fragment is, on average, sequenced along with 1 duplicate (50% of the library is thus made up of duplicates - or 50% duplication rate), an observed coverage of 10X will, in reality, only give information as to 5 independent genomic copies: its effective depth is 5X. The probability of under-sampling genotypes will therefore be $1 / (2^{(5-1)}) = 0.0625$, and not $1 / (2^{(10-1)}) \approx 9.77e^{-4}$. This problem can become more important in case of drastic scenarios of PCR duplication, where the rate can reach up to 90% (a coverage of 10X will represent only one genomic copy, and will not be enough to identify a heterozygote).

The most visible consequence of genotype under-sampling will be the loss of heterozygosity despite acceptable coverage (10 to 20X, see Hoffman *et al.* 2014). Under ideal conditions, observed heterozygosity increases with depth of sequencing at low coverage, and converges towards true heterozygosity at 15 to 20X (when virtually every site has a nearly-null probability of having been under-sampled). However, if a large number of duplicates are present, correlation between heterozygosity and depth of coverage is heterogeneous, or absent.

If left unfiltered, PCR duplicates are likely to introduce a strong bias in several analyses, by leading to overly confident genotype calls where, in reality, evidence is scarce. In more extreme cases, it will also lead to homozygous calls where both alleles have been sampled, by artificially increasing the depth of coverage of one allele only, and leading to discarding the low-coverage alternate allele as a sequencing error.

Fortunately, the original RADseqprotocol allows for efficient duplicate removal. Since DNA is randomly sheared after restriction, the length of individual fragments is expected to be broadly distributed; at medium to high coverage, no two fragments are expected to have the exact same length in the same individual, at the same locus. Thus, if two fragments of the same individual share the same mapping coordinates both on their front-read an reverse-read, these may be considered to be duplicates, and one of them (the one with the overall lowest quality) may be removed. An approach implemented in the popular pipeline Stacks (Catchen *et al.* 2011; Catchen *et al.* 2013) uses as a filtering criterion the fact that both front-read and reverse-read must match exactly in order to discard the lowest-quality read pair as a duplicate. This approach, however, assumes that sequencing errors are absent, which is a very unrealistic hypothesis in the case of high-throughput sequencing data: the consequence is that all duplicate reads including sequencing errors will be kept as original genomic copies, together with genuine reads, which may lead to many false-positive SNP calls. Another approach, implemented in PicardTools (http://picard.sourceforge.net), relies instead on prior read mapping: two read pairs will be flagged as duplicate only if their mapping coordinates and mapping descriptors (as symbolised in a CIGAR string[1]) are identical. This approach has the advantage of not being sensitive to sequencing errors; however it necessitates a reference genome of some kind in order to perform read mapping. We preferred the latter approach for this study.

---

1.   A character string summarising the structure of the alignment - number of consecutive matching bases, gaps, etc. (see https://samtools.github.io/hts-specs/SAMv1.pdf).

§-36 The duplicate bias in our data. RAD library preparation involves several sensitive steps that may contribute to decreasing the overall protocol efficiency (see §29 p. 85), and thus lead to increased presence of PCR duplicates in the raw sequencing output (see §35 p. 93). In our data, the presence of duplicates was first noticeable because of the heterogeneous regression between heterozygosity and depth of sequencing between libraries, and generally the strong correlation between individual inbreeding estimators and library identity. Removing PCR duplicates efficiently solved this problem, however, the resulting effective coverage was consequently decreased. As a result, the number of sites that could be reliably called by conventional (e.g. maximum-likelihood) SNP and genotype calling algorithms (see §33 p. 90) was much reduced. Thus, in order to keep a SNP-based analysis framework, we must balance two antagonistic parameters, *(i)* the minimum depth of coverage to retain a genotype and *(ii)* the number of loci necessary for the analysis. While low coverage is reducing the certainty of genotypes (see §35 p. 93), and thus potentially introducing noise in the data, increasing the minimum genotype depth effectively amounts to increasing the amount of missing data, and thus decreasing the number of exploitable loci (see §33 p. 90). We tested this tradeoff on a dataset containing RADseq data from two well-separated populations of Peruvian Diving-petrels *Pelecanoides garnotii* (see *Unexpected philopatry in an insular seabird, the Peruvian diving-petrel*, p. 275), by running the Structure clustering algorithm (Pritchard *et al.* 2000) on filtered datasets with a minimum depth ranging from 20X to 40X, and a minimum proportion of genotyped individuals per locus ranging from 40% to 90%. While structure is perfectly recovered for balanced datasets (e.g. 30X and 60% representation), it decays with more stringent filtering (e.g. 90% representation) due to the low number of remaining loci. This particular algorithm being especially sensitive to missing data, it highlights the importance of finding a good compromise between genotype certainty and missing genotypes - the main problem posed by PCR duplication and loss of sequencing efficiency.

Being PCR-free, our whole-genome resequencing libraries are immune from the duplication issues identified in our RAD-sequencing data (see §35 p. 93): therefore, the data processing steps

could be greatly simplified. For each sample, we pooled the data from both sequencing lanes (see §30 p. 86), and mapped it to the published Emperor penguin reference genome (Zhang *et al.* 2011b) using Bowtie2 (Langmead & Salzberg 2012), allowing only for unique, concordant paired-end alignments. Output BAM files were sorted and filtered using Samtools 0.1.19 (Li *et al.* 2009) and PicardTools 1.113 (http://picard.sorceforge.net).

§-37 Phasing of the WGS data. A particular difficulty, in WGS data analysis, is the inference of the correct phase for the pre-established polymorphism. Two main methodological approaches have been proposed (Browning & Browning 2011): *(i)* an observed-linkage approach, and *(ii)* a computational approach. The observed-linkage or read-based approach (i) exploits the naturally phased base calls in the paired-end Illumina reads, in a process similar to scaffolding, but using the prior positional information provided by the read mapping step. At sufficiently high coverage, the overlap between reads may allow the reconstruction of long stretches of phased haplotypes. However, the process is often broken - either necessarily whenever the distance between two successive heterozygous sites exceeds the library insert length, or stochastically through variation in read overlap distribution. Thus, at medium coverage, read-based phasing tends to produce short blocks of phased haplotypes, separated by stretches of unphased sequence. The computational approach (ii), on the other hand, relies on a prior model of recombination to estimate the most likely local haplotypes given the observed linkage data. Ideally, a specific recombination model is established beforehand in the form of a genetic map, or an ascertained phased reference panel is used. In a non-model species, however, computational phasing may rely on population data: across a large number of individuals, assuming a constant recombination rate, the measure or linkage disequilibrium between closely located SNPs is considered informative of their physical phasing, and used to infer the most likely underlying local haplotypes.

Ideally, both approaches should be combined, as is the case in the ShapeIt PIRs pipeline (O'Connell *et al.* 2014): read-based physical linkage is assessed first in order to build local haplotypes, and the phasing between those is further assessed computationally using population data.

In our case, however, the low number of sequenced individuals (3 per species) prevented the use of any computational method. Therefore, we reconstructed the local haplotypes using the graph-based algorithm implemented in HapCompass (Aguiar & Istrail 2012), and used the resulting partially-phased data whenever phase information was necessary. However, the resulting phasing proved insufficient, and results visibly lacked robustness, presenting artefact patterns similar to those encountered in unphased data: we therefore did not retain it for final analyses (see *The King synnome*, p. 163 for details).

§-38 A point on data management. Handling of high-throughput sequencing data presents important scale challenges, both in terms of computational power and of data storage and management. The methods used to address these challenges vary according to the specific analysis stages, although some general guidelines can be retained. When processing sequencing data, four main «generations» of data files can be identified, of increasing specificity and decreasing redundancy: *(i)* raw data formats, *(ii)* alignment formats, *(iii)* variant formats, and *(iv)* analysis input formats.

(i) **Raw data** is mostly stored as (compressed) fasta or fastq format - a sequencer-output format listing sequence base calls (as performed, in our case, by Illumina's CASAVA software), physical read coordinates on the flow cell, and base quality encoded as Phred33 quality scores. Redundancy is high, as several reads, or dozens of reads, may cover the same position in the target genome.

(ii) **Alignment files** are output by read mapping algorithms, usually formatted as SAM (Sequence Alignment Map), or as its binary equivalent BAM (Binary Alignment map). After alignment, the complete information from read sequence and quality scores is retained, but mapping coordinates are added, relative to a reference genome: at that stage, redundancy is still high, as each individual read is represented by a single entry (and not collapsed by genomic position). SAM/BAM files are typically handled using the flexible Samtools package (Li *et al.* 2009), or the Broad Institute's Picard Tools package (http://picard.sorceforge.net). BAM format is the preferred data storage format in this work, as it retains all the necessary information for alternative SNP calls.

(iii) **Variant calls** are produced through SNP and genotype calling algorithms (see §33 p. 90), usually stored as a VCF (Variant Call Format, or its binary version, the BCF) file, and usually handled using VCFtools (Danecek *et al.* 2011). The VCF format removes most of the redundancy of raw and aligned formats, as each genomic position is represented by a single entry, and the number of reads covering that position is summed numerically for each individual. Thus, a major shift of paradigm occurs between the aligned and the called formats: the identity of the original reads is lost, and information switches from a « horizontal » (sequence) format, to a « vertical » (per-site) format. Usually only polymorphic sites are retained at that step, although the Broad Institute gVCF (genomic Variant Call Format) includes also the sequence at non-polymorphic sites, as « blocks » of sequence data. The main characteristic of VCF formats is that it is an « analysed » format, storing an interpretation of the raw genetic data, rather than the data itself: it contains information that is the intersection of a dataset, an analysis protocol, a particular variant calling model, filtering decisions, etc.

(iv) **Input formats** are usually particular to each analysis program. They are, in their vast majority, a reformulation of the VCF format, with or without data loss (e.g. 0/1 coding of alleles instead of ATCG coding, etc). They are too specific to an individual program or version to be detailed in this work.

Genetic analysis framework

The detail of the particular analyses and models used in each chapter will be detailed in the corresponding Methods sections. Here, however, we present the conceptual framework of the methods used repeatedly throughout this work.

§-39 Populations, random mating and neutral drift. As we introduced earlier (see §2 p. 25), the basis of population genetics is the *deme*, which, whenever it has a strong geographic component, is described as a *population*. A population, in the population genetic framework, is oftentimes ap-

proximated through the *Wright-Fisher model* (Wright 1931; Ewens 1979), as an ensemble of *randomly mating* («*panmictic*») individuals, where each individual will be replaced by one offspring at the next generation, and where generations do not overlap. Although seemingly rather unrealistic, this model has repeatedly been proved to perform surprisingly well under most empirical situations (Hamilton 2011), at the only cost of the necessary re-definition of some concepts, such as *population size* (see §41 p. 103 for a development).

One essential feature of the Wright-Fisher model is the way the transmission of alleles is conceived. The Wright-Fisher model describes a simple Markovian process: at each generation event, allele frequencies are re-sampled from the ancestral gene pool to the offspring gene pool under a binomial law, with stochastic variation in frequencies; thus, the gene pool at time *T+1* only depends on the gene pool at time *T* and on a stochastic sampling event, without memory from previous states. The expectation for the binomial sampling is that, in the absence of selection pressure, allele frequencies remain the same across generation (the *Hardy-Weinberg propriety*, see Edwards 2008) - an expectation marginally contradicted by the stochastic nature of the sampling, which allows frequencies to vary in a random direction at each generation. The extent of this variation, or *genetic drift*, is a function of the *size* of the Wright-Fisher population: a larger population will undergo less drift than a smaller one.

Drift thus becomes the main tenet of the Wright-Fisher neutral molecular evolution model: new alleles, that occur randomly and after an *infinite sites model* (*i.e.* no two mutations ever occur at the same site, see Kimura & Crow 1964 for details), can either be lost through random sampling, or on the contrary see their frequency increase in the population; so that the probability of loosing an allele through drift decreases as the frequency of the allele increases.

As opposed to the *coalescent* framework (see §40 p. 101), the Wright-Fisher Markovian model does not integrate evolution over the history of the population: there is a succession of states, but no *origin* in the process. Thus, the discrete generation steps of the Markov chain can be approximated as a continuous process, in what is known as the *diffusion approximation of genetic drift*

(Kimura 1955). Under the Kimura model, alleles are idealised as *particles*, their frequencies as *co-ordinates*, and drift as *movement*. The diffusion process results in a change in the location of alleles in the frequency space, under a probability law determined by the allele's *diffusion coefficient* - itself a reflection of the population size and demographic events that may vary through time. While the expectation for the movement of the allele remains zero for any diffusion coefficient and any length of time (in keeping with the Hardy-Weinberg expectation), the *variance* of the final position increases with increased diffusion coefficient - in other words, over a large set of loci, a sharply clustered frequency distribution is expected to spread out over time. The diffusion approximation becomes especially useful in N-dimensional frequency spaces, *i.e.* when the frequency of an allele is considered in several populations simultaneously, with limited diffusion allowed between populations (see §45 p. 117 for applications of this propriety).

Although powerful conceptual tools, the Wright-Fisher model and Kimura diffusion theory have the limitation of being, by default, a site-based paradigm: alleles are represented as (usually independent) entities whose relationship is merely complementarity in the frequency space. In other words, the drift paradigm does not take the genealogical evolution of sequences into account - thus, it can not exploit one of the richest information sources in the genome structure.

§-40 The Coalescent theory. Developed by Kingman in the 1980s, the coalescent theory is a diachronic take on the previously dominantly synchronic paradigm of population genetics, and the Wright-Fisher approximations of neutral drift (Kingman 1982; Kingman 2000). As opposed to essentially atemporal descriptive statistics such as fixation indices (Wright 1965) or analyses of molecular variance (Excoffier *et al.* 1992b), the coalescent explicitly models the history of the observed state of genetic diversity. When considering the tree-like history of a short DNA sequence, each new mutation appears as the branching of the ancestral lineage into two new sequences: one unchanged, and one new mutated sequence. If we happened to know the «true» history of that sequence in a population, we would witness several such branching events, as well as several extinction events, when a lineage becomes lost by the effects of random sampling, or natural selec-

tion. But considering a realistic experimental situation, we really only sample the final state of

that history, *i.e.* the present state. When reconstructing that history from the data contained in its

present state, each *branching* event now appears as the *merging* of two lineages into one ancestral

lineage - a *coalescence* event.
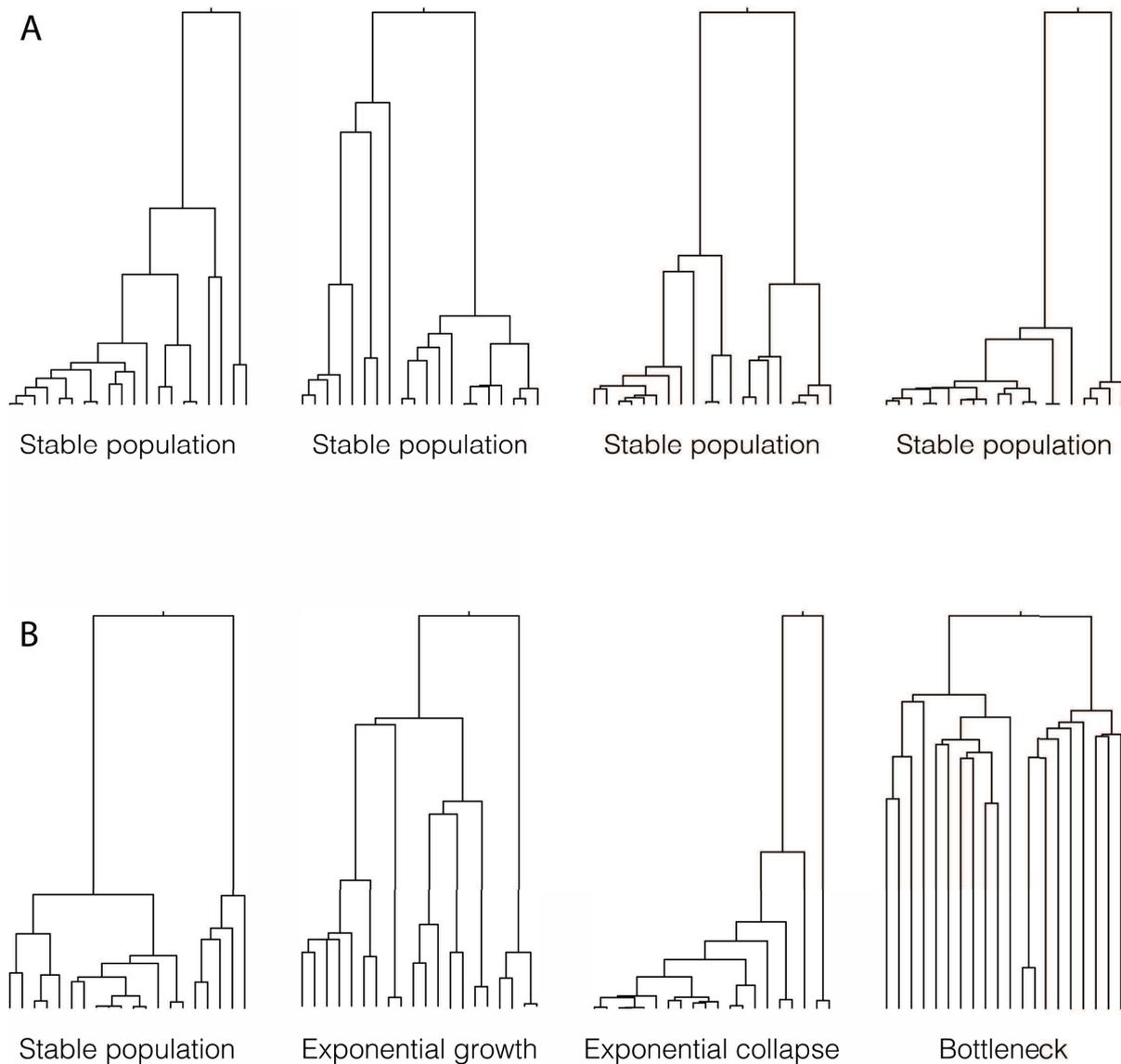
Figure 9 | Stochasticity and demography in the coalescence process. Gene trees simulated under different demographic models using *ms*HOT (Hellenthal & Stephens 2007). **(A)** Constant population: all four trees are replicates of the same simulation parameters. **(B)** Four different demographic histories.

Coalescence is an essentially stochastic phenomenon (Fig. 9A p.102): interestingly, although the actual coalescence events are random, the probability of two lineages coalescing (*i.e.* having a common ancestor) at any given point of the past is a direct function of the effective population size. Given a diploid population of constant effective size *Ne* (thus 2.*Ne* lineages in the gene pool at each generation), and a constant evolution rate of one substitution per generation, the probability of any two lineages sharing a common ancestor at the previous generation is (1 / 2.*Ne*), and the probability of *not* sharing a common ancestor is 1 - (1 / 2.*Ne*). Expanding this to any generation *t*, the probability of two lineages having a common ancestor at generation *t* is the product of their probability of having a common ancestor given the population size at generation *t*, and their probability of not having already had a common ancestor at any previous generation, or $(1 - (1 / 2.Ne))^{(t-1)} . (1 / 2.Ne)$. If *Ne* is constant and large enough, the instantaneous probability of coalescence is very small, and the cumulative probability of two lineages coalescing at or before generation *t* can be approximated by the exponential function, as $1 - e^{-(1/2Ne).t}$.

Thus, the coalescence theory sets an expectation for the rate of coalescence of lineages in a random sample, which follows an exponential distribution if the population size remains constant through time. As it gives a diachronic picture of the evolution of sequences in a Wright-Fisher population, it allows us to step from the earlier synchronic paradigm of population genetics, into the reconstruction of time-dependent events such as demography and migration history.

§-41 Coalescence, population size and migration. The probability of coalescence at any given generation is a function of the population size at that generation (see §40 p. 101). This has two important consequences: *(i)* the neutral, exponential coalescent provides us with a null model against which we can assess the neutrality of observed coalescent histories, and *(ii)* we can further develop the coalescent framework to explicitly model population size changes through time. But an important first step is to clarify what we mean by *population size* - since, as we already discussed

earlier (see §2 p. 25), the fundamental concept of *population* is defined very differently in the ecological, and the evolutionary frameworks.

Revolving essentially around the notion of *individual*, the ecological paradigm naturally considers the *population size* to be the *number of individuals alive at the same time* in the group under scrutiny. Here, we call *census size* this direct observation of the population size. While the census size of a full species is a rather understandable concept («*how many king penguins are there at this moment on Earth?*» does have a true answer), the census size of a population is a rather more abstract idea as soon as life history strategies become elaborate (see Lecomte *et al.* 2009 for an interesting practical example): in these seabirds, adults will only breed up to two years out of three, and will probably not come ashore at all during the third year - so that the maximum number of adults in reproductive age on the colony will only represent two-thirds of the total number of breeders who «belong» in that colony. Juveniles that are born on a colony regularly spend several traveling years at sea, and may or may not choose to disperse after that time: should they be counted as part of the colony in advance, or not until they effectively settled? What about juveniles in *r-strategy* species, where the number of juvenile is very high, but mortality tremendous? Thus, although the concept itself appears fairly straightforward, its application is much more subjective in wild populations - all the more so if we lack precise knowledge about the recruitment and the proportion of non-breeders that may be temporarily away.

The evolutionary paradigm, on the other hand, is based on the notion of *gene pool*. Thus, is only counted as part of the genetic population an individual that actively contributes to the gene pool: population size is there defined as the *number of successfully breeding individuals*. To distinguish it from the census size, we call this measure the *effective size* of the population. Here again, this definition is simple in the ideal case of a Wright-Fisher population, with non-overlapping generations and replacement of each parent by one offspring (see §39 p. 99). But it becomes more difficult to estimate whenever life history diverges from this abstract state - *e.g.* when a breeder may have several offsprings, or when breeding success is heterogeneous within the population. Effec-

tive population size also diverges widely from census size (sometimes by orders of magnitude, see

for example *The Emperor synnome*, p. 211) as soon as non-breeding individuals are an important

part of the species, *e.g.* when sexual maturity is delayed (as in most long-lived species), or when

an adult may choose to not breed if its body condition is not adequate - or when a senescent in-

dividual chooses not to die (as in humans and albatrosses). As it then becomes increasingly diffi-

cult to define the number of individuals contributing to the species' genetic diversity through ex-

ternal evidence, the effective population size is commonly defined as a direct index defining the

characteristics of the observed gene pool, in other words, as the *size of a theoretical Wright-Fisher*

population of similar genetic characteristics (Hamilton 2011). As we mentioned earlier (§40 p.

101), in a population of constant size, and with a unit substitution rate, the probability of two

lineages coalescing at generation t is $(1 - (1 / 2.Ne))^{(t-1)} . (1 / 2.Ne)$. Provided the sample is

large enough, this probability can be approximated by the observed density of coalescence events,

and allows us to estimate the effective population size. Yet since substitution rate μ is, in reality,

never equal to 1, this estimated population size is scaled by the substitution rate as $\vartheta = 4.Ne.\mu$ (in

a diploid organism) - with the underlying idea that a small, but slowly mutating population will

undergo the same amount of genetic drift as a larger, but faster evolving one.

Thus, assuming that substitution rate is constant through time (which is reasonable at the in-

traspecific level), the distribution of times to coalescence throughout gene trees is an estimator of

the probability of coalescence throughout the history of the population - and hence of the popu-

lation size through time. This is the fundamental idea of the Skyline Plot approach (Fig. 10 p.

107): in its simplest form, each coalescence interval in a single gene tree is converted by maxi-

mum-likelihood into a population size during a time interval. Of course, the stochasticity of coa-

lescence events is directly transferred to the population size estimates (as can be seen on the first

row of Fig. 10 p. 107). Several approaches have been proposed to filter out this noise - ranging

from simple ideas such as the generalised skyline plot (which imposes thresholds for taking

changes into account, and filters out excessively quick «jumps» in population size), to more com-

plex ones line the Bayesian Skyline Plot (which tries to estimate a general demography with a low number of epochs, that maximises the likelihood of the observed gene tree - with a set of assumptions, like the autocorrelation of the population size through time, reducing the demography space to be explored). More complex and accurate approaches have been proposed to better address the problem of estimating past population size changes (see §44 p. 112 to §47 p. 122), but most of them ultimately rely on this basic tie between coalescence rate and scaled effective population size.

A fundamental feature of the link between coalescence and population size, as it is currently conceived, is the irrelevance of gene tree topology - reconstructed topology is only a means to accurately estimate coalescence intervals. Migration, on the other hand, mostly affects the structure of gene trees through the topology of the coalescent. In geographically complex groups of individuals, migration (as defined in §4 p. 30) interacts with population size in shaping the gene pool: in a given deme, genetic diversity may only arise through *(i)* mutation and drift (both functions of the effective population size) or *(ii)* migration. Unlike population size, however, migration is not estimated absolutely from the genetic data, but rather in reference to the present-day distribution of the sequences. In the coalescent framework, if we consider two present-day *demes* (see §2 p. 25 for a definition), *migration* can be defined as the probability (as usual looking back in time) for a given lineage to move from its current deme to the other at the previous generation - *i.e.* the probability of any «effective individual» to have one of its parents being an immigrant. Thus, the *probability of coalescence* is, within each deme, the probability of a lineage merging with another from the same deme at a given generation (a function, as we exposed, of population size) - and the *probability of migration* is the probability of a lineage stemming back to another deme at the same period. Identifying migration through the coalescent structure across several demes has some limitations: in particular, it requires that deme identity is stable throughout species' analysed history (*i.e.* within ~ 4Ne generations), and that during that time gene flow is low enough, that back-and-forth lineage migration is separated by at least one coalescence event.

1   Technically, accurate estimation is restricted to demes *stricto sensu* (see §2 p. 25), where mutation

2   and drift are major contributors to genetic diversity, an migration a marginal contributor.
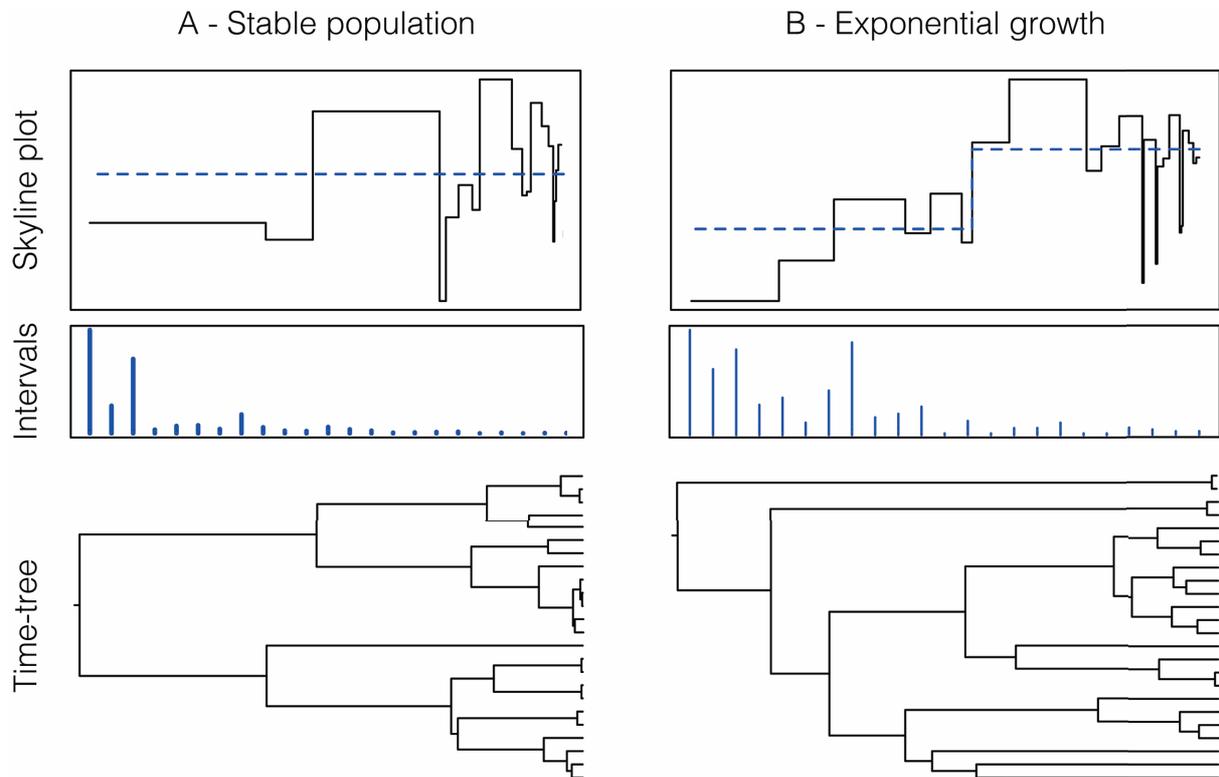
Figure 10 | Coalescence and population size. Reconstruction of the past population size of two simulated populations after the original Skyline Plot model (Pybus *et al.* 2000). (**A**) Constant size population, and (**B**) Exponential growth population. *Bottom row:* simulated gene trees, generated using *ms*HOT (Hellenthal & Stephens 2007), *Middle row:* length of the coalescence intervals along the tree, *Upper row:* direct demographic function (black line) and generalised skyline plot (dashed blue line).

8   *§-42 The Ancestral Recombination Graph.* The coalescence process gives an accurate description of

9   the evolution of a non-recombining sequence of DNA, for which, under an infinite-sites model,

10   the only possible event is a divergence due to a mutation (when looking forward in time), *i.e.* a

11   coalescence event when looking backwards in time (as presented in details in §40 p. 101). How-

ever, the recombination process interferes with the pure coalescence process when we consider longer sequences, and *a fortiori* genomic-scale data. During recombination events (usually the manifestation, at the sequence level, of the crossing-over of chromosomes during meiosis), sequences sharing different ancestries (and thus different coalescent histories) become concatenated into one new sequence. By reshaping the associations between alleles, recombination is a major driver of genome evolution (Reich *et al.* 2001; Zhang *et al.* 2002), and must be accounted for when reconstructing the evolutionary history of a set of haplotypes. In the context of sequence evolution, recombination events can be seen as the counterpart of coalescence events: looking back in time, a coalescence event is the merging of two different sequences into one ancestral sequence, while a recombination event is the splitting of one single sequence into two distinct ancestral sequences.

The *Ancestral Recombination Graph* (ARG) is the representation of the full ancestry of a set of sequences, that includes both coalescence, and recombination events (Rasmussen *et al.* 2014). Just like a classical phylogenetic tree, it is constituted of nodes, and edges - however, unlike a in phylogenetic tree, nodes can be of two different types: *coalescent* nodes, or *recombination* nodes. When estimated over a very short stretch of non-recombining DNA, the ARG is essentially a coalescent tree, but its complexity increases when it is estimated over longer, recombining sequences. The full ARG of population-scale genomic data virtually encompasses all the possible information about population size changes, migration events, selection processes, *etc*. However, the complexity of the structure makes it extremely challenging to reconstruct and analyse, and it is mostly simplified down to a lower-dimensionality representation, such as the multi-dimensional allele frequency spectrum (see §45 p. 117).

The Sequentially Markovian Coalescent (SMC, Wiuf & Hein 1999 - see §47 p. 122) is a transversal interpretation of the ARG. As a set of orthologous[1] sequences is considered transversally,

---

1.   *I.e.* stemming from a single common ancestral copy.

the coalescent process is «pure», i.e. without recombination, at each single nucleotide position. As long as successive nucleotides share the same ancestral history, a single coalescent tree holds. However, a recombination event will introduce a change in the tree topology, as the ancestral relationships between sequences are shuffled - and this new topology will hold until the next recombination point. This structure can be summarised as a Markovian process: a single coalescent tree is a state in the process, a recombination event is a state change, and the topology of the coalescent tree before the state change has no bearing on the topology after the state change. One particularity of the SMC model is that it allows inference of multiple tree topology, *i.e.* coalescent histories, when sampling along a single set of recombining sequences.

Sampling along the SMC can be conducted in several ways in order to infer population history:

(a) A «classical» approach relies on the extreme discretisation of the genome to sample virtually independent states of the ARG. Thus, when sampling short sequences separated by very large chromosomic distances, we can assume that 1) no recombination occurs within the sequences under consideration, and 2) recombination occurred freely between the sequences, so that their coalescent histories are fully independent draws from the population's ARG. Since, in that case, sampled topologies are comparatively few and far in-between, it is possible to estimate the full coalescent tree for each locus, and to draw information from every node. This is the approach implemented in several multi-locus algorithms, for example the Extended Bayesian Skyline Plot (Heled & Drummond 2008, see §44 p. 112), or the Migrate-n algorithm (Beerli 2006; Beerli & Palczewski 2010).

(b) A continuous approach, on the contrary, is based on the reconstruction of the states and state changes in the hidden SMC model through transversal scanning of the set of sequences. Thus, a coalescent tree is reconstructed for each non-recombining interval between two state changes, decomposing the full ARG into a set of coalescent-only graphs. This is the approach implemented in the «SMC» family of models (see §47 p. 122) *(c)* the ARG may also be sampled indirectly,

through a set of summary statistics - for example the distribution of allele frequencies , either represented as a spectrum (see §45 p. 117) or as single statistics, such as Wright's F-statistics or Tajima's D (see §43 p. 110). These different approaches will be developed below.

§-43 What is a summary statistic? The full complexity of population genomic data could ideally be represented without loss in a highly dimensional structure such as the Ancestral Recombination Graph (see §42 p. 107). However, such an endeavour has limitations both in means, and in aims. Accurately reconstructing a population's ARG would require flawlessly ascertained genomic data - which we can not yet produce - and monumental computational resources (see Lam *et al.* 2010). On the other hand, the full ARG is hardly intelligible by itself (Arenas 2013), and its major characteristics need to be extracted in order to produce meaningful information. The need to reduce the ARG to a simpler object therefore stems both from the failure to gather exhaustive data and computational resources, and from the necessity of obtaining more easily comparable indices. Thus, the common character of most population genetic approaches - several of which have been devised long before the theorisation of the ARG - is to be in some respect a reduction of the full graph into a lower-dimensionality object, such as a tree, a distribution, or a single statistic.

In the «classical» population genetics approach (see §28 p. 84), the nature of the markers used (single mtDNA sequence or low number of nuclear loci) naturally makes the ARG a very distant concept. The low information content of the data only allows for the estimation of «point» indicators, not of the shape and extent of variation in signal across the genome. Thus, low-dimensionality statistics have initially been devised to match the information content of the data that was possible to produce: these focus on describing the amount and distribution of polymorphism between a set of samples. As we mentioned above (§40 p. 101 and §42 p. 107), the present-day distribution of genetic variation is a result of the history of *coalescence*, *recombination*, and *migration* within the species - if the sequences under scrutiny are not evolving neutrally, *selection* must be added to that list, but neutrality is normally verified, or assumed. In the Wright-Fisher «drift»

framework (see §39 p. 99), on the other hand, only that final state is really considered and described at all.

A first and essential descriptor of an instantaneous state of genetic variation is the *density of segregating sites*, often called *S*, that is a measure of the depth of the local coalescent tree in a perfect Wright-Fisher constant-size population - and therefore an indirect estimator of ϑ, the mutation-scaled population size, also described as Watterson's estimator ϑ_W (Watterson 1975). However, Watterson's ϑ technically discretises allele frequencies as a binary character («minor allele frequency > 0»), and thus discards the obvious informative content of the observed allele frequency distribution. Therefore, a more refined estimator is *nucleotide diversity*, normally designated as π, and defined as the *average number of pairwise differences* in a set of sequences - *i.e.* the mean value of the *mismatch distribution* (Nei & Li 1979). Shifting from the polymorphism in a full set of sequences to the average polymorphism in pairs of sequences sampled from that set, π retains information as to the allele frequency distribution in the sample, and is also an estimator of ϑ under a neutral model, as ϑ_π.

These two estimators of ϑ become inaccurate when the true population departs from the Wright-Fisher model: interestingly, however, the inaccuracy of these indices does not arise in the same way, and is in itself informative. ϑ_π is sensitive to the frequency of alleles, and intermediate-frequency variants will weight most in the estimator: thus, histories with a high density of ancient coalescence events will lead to higher values of ϑ_π. ϑ_W, on the other hand, since it handles allele frequencies in a binary way (*i.e.* «polymorphic» or «monomorphic»), is not sensitive to the depth of pairwise coalescence of sequences, and hence is not affected by the structure of the coalescent: it only reflects the depth of the full local coalescent. Thus, the difference of ϑ_π and ϑ_W is an indicator of the neutrality of the coalescence process, as proposed by Tajima 1989: if both estimators are similar, a neutral constant-size coalescent process cannot be rejected, but if ϑ_π is larger than ϑ_W, we can infer an excess of ancient coalescence events, and therefore population growth. Other indicators (Fu's F_S, Fay and Wu's *H*, *etc.*) have been devised with a similar idea, all reflect-

ing, in some way or some other, skews in the coalescent structure, and consequently directional departures from the neutral population model.

Another central (and still very much in use) application of point-value summaries of the ARG is the quantification of population structure, or, in other words, of the amount of difference between allele frequencies in distinct sets of samples. The most common approach is the family of «*F*-statistics» or *fixation indices* (Wright 1950), initially described in the synchronic drift framework (see §39 p. 99), but that can be re-thought in the coalescent framework. In the original formulation, the fixation index idea relies on the *Wahlund effect* (Wahlund 1928), a corollary of the Hardy-Weinberg principle that implies that observed heterozygosity is reduced by sub-population structure. By comparing the observed heterozygosity in a pair of populations to the expected heterozygosity under Hardy-Weinberg equilibrium across that combined set of individuals, one can obtain a measure of the Wahlund effect, and hence of the strength of sub-population structure, or population separation. Fixation statistics are declined at several levels (individual *vs.* total heterozygosity, *etc.*), and more refined estimators have been proposed for practical sampling cases, to increase robustness to *e.g.* asymmetric sample sizes, or missing data (see Reynolds *et al.* 1983; Weir & Cockerham 1984; Reich *et al.* 2009; Willing *et al.* 2012; Bhatia *et al.* 2013, and §129 p. 242), and are also the basis of the Analysis of Molecular Variance approach (Excoffier *et al.* 1992a). In the coalescent framework, fixation statistics are a function of the N-dimensional Allele Frequency Spectrum (see §45 p. 117), and therefore a translation of the relative coalescence and migration probabilities (see §41 p. 103).

Although summary statistics, by the low dimensionality, necessarily miss a large part of the informative content of genomic data, they have the important propriety of being easily comparable across organisms, markers, or genomic regions (*e.g.* genome-wide statistics *vs.* mitochondrial DNA statistics, *etc.*), and therefore to provide a more unified (with the trade-off of being simplistic) picture of genetic variation.

§-44 The Extended Bayesian Skyline Plot approach. The Extended Bayesian Skyline Plot (EBSP) method was proposed by Heled and Drummond (Heled & Drummond 2008), as a Bayesian multilocus extension of the Skyline Plot (SP). In its orignal form (Pybus *et al.* 2000), the Skyline Plot is a maximum-likelihood non-parametric method that exploits the relationship between population size and coalescence probability (see §41 p. 103) to reconstruct effective population size at different time points. The density of coalescence events is therefore indicative of the population size (a higher rate of coalescence generally means a smaller population). However, the classical Skyline Plot has severe limitations: for example the fact that the gene tree is assumed error-free, and estimated independently, or the fact that, as a single-locus approach, it may be severely affected by the random sampling processes - a true random coalescent may diverge vastly from the neutral expectation by mere chance (Ho & Shapiro 2011). The first limitation was overcome by the replacement of the maximum-likelihood framework by a Bayesian approach (as Bayesian Skyline Plot or BSP, Drummond *et al.* 2005), in which gene tree and demographic history are co-estimated, and averaged over a very large Markov-chain Monte-Carlo (MCMC) sampling. However, the locus-by-locus stochasticity limitation of the Skyline Plot remains with the BSP. Another limitation of the BSP is that it is not fully model-flexible: the number of demographic groups needs to be fixed *a priori*. The EBSP, as implemented in BEAST2 (Bouckaert *et al.* 2014), overcomes all these major limitations. As a natively multilocus approach, EBSP relies on the Bayesian co-estimation of gene trees and demographic histories from a set of unlinked loci, thus considering large pannel of stochastic representations of the underlying « true » coalescent history of the population. EBSP is also a truely model-flexible approach, in the sense that the number of periods in the demographic function is informed solely by the genetic data. In its current form, its main limitation is that, as it relies on the full likelihood of the DNA sequences, it is computationally intensive, and hardly scalable to full-genome-scale sequence data.

In this work, we exploit the specific features of RAD sequencing to deploy EBSP demographic reconstructions (see Supplementary sections of *The King synnome*, p. 163, and of *The Emperor*

synnome, p. 211), as first proposed by Trucchi *et al.* (Trucchi *et al.* 2014). RAD sequencing (see §29 p. 85) allows the production of a large number of short sequenced loci that are widely interspersed in the genome, so that they can be assumed unlinked. Within loci, recombination rate can also be assumed null, and the random sampling process in the genome allow us to consider the loci as neutrally-evolving (a condition rarely met in traditional multilocus approaches, that often rely on gene sequencing). Thus, the three main assumption of EBSP are *a priori* verified by RAD data. However, two characteristics of RAD sequencing require some adaptation: *(i)* the sequencing process makes locus- and allele-dropout a significant problem and *(ii)* short loci necessarily have less segregating sites than longer loci, so that a selection must be made in order to base the analysis on informative data.

Allele dropout happens either as a result of cut-site mutation, that prevents one of the alleles to be sampled during the RAD library preparation (see §29 p. 85), or of under-sequencing, that causes one allele only to be sampled during the sequencing process (see §35 p. 93). The direct consequence of allele dropout is a mis-representation of true haplotype frequencies (see §35 p. 93), that is likely to bias the reconstruction of the coalescent history of the population, through an over-representation of null branch lengths in the gene tree topologies. A simple workaround is to sample only one haplotype per individual: while halving the dataset, this guarantees that the distribution of coalescence events will be faithfully reproduced. Locus dropout is a different issue, that is more easily solved: both during library preparation and during sequencing, loci may be lost in some individuals. Thus, it may be difficult to find a sufficient number of informative loci that are sequenced in the same set of individuals. However, coalescent reconstructions are not individual-, but rather population-centred: as long as panmixia is verified in the population, the identity of the individuals from which haplotypes were sampled has no bearing on the sampling of the haplotype pool. In order to avoid potential skews due to, for example, the sampling of related individuals (i.e. individuals with correlated haplotypes at all loci), it may actually be desir-

able to choose haplotypes randomly from the full (haploid) population for each locus, rather than to choose individuals.

The information content of loci is a different problem. Since RAD loci as considered neutrally evolving, we suppose that the general genome background substitution rate applies to the RADome. However, since substitution is essentially a rare, stochastic process, we expect the actual number of substitutions occurring in a given genomic interval to follow a Poisson distribution, with a parameter λ equal to the genome-wide background substitution rate (see §48 p. 124). Given the low substitution rate in long-lived vertebrates, most short (here 95 bp) loci are expected to contain zero or 1 SNP. However, the general Skyline Plot rationale implies that several coalescence events must be reconstructed in order to obtain information on the variation of coalescence probability (i.e. population size) through time. Indeed, in the absence of recombination, the number of coalescence events is, at most, equal to the number of polymorphic sites: a locus with 3 SNPs is, at best, informative as to 3 coalescent nodes (less if multiple substitution occurred on the same branch). In our experience, loci with less than 4 SNPs are not informative enough to robustly infer population history. In the same population, the number of SNPs observed at a locus is a function of the number of haplotypes sampled and of the haplotype frequency distribution: generally, sampling more individuals will increase the number of polymorphic sites discovered, until all extant alleles have been represented. However, loci with excessive diversity are also suspicious: in a Poisson process, the probability drops rapidly towards the upper tail of the distribution - in our case, very few loci are expected to have more than 7 or 8 SNPs. Processing artefacts, on the other hand, such as a low-quality read, or collapsed paralogous loci[1], can have the effect of increasing the observed number of SNPs at a given locus. For that reason, we restrict the analysis to loci that have from 4 to 6 SNPs amongst 50 randomly sampled haplotypes. As this selection is only made amongst neutrally evolving loci, the underlying substitution and diversification

---

1. That is, regions of the genome that stem from a common ancestral copy through a duplication event. Each paralogous copy further evolves separately, in a generally tree-like way. If the duplication event is recent, paralogs may retain enough similarity to be merged or confused during analysis, resulting in a chimæric, non-tree-like ensemble.

processes are not different from those at work in the rest of the RADome. By doing so, we are only filtering the stochastic output of the substitution Poisson process.

This locus selection also has implications for the parametrisation of the EBSP model. EBSP, like any other model, may be easily subject to over-parametrisation: however, due to the huge computational burden of the MCMC algorithm, precisely estimating the number of necessary parameters (through, e.g. Bayes factor comparison of path-sampled alternative models' marginal likelihoods) is a difficult task. However, the structure of RAD data allows for a particularly efficient parametrisation. In Trucchi *et al.* (Trucchi *et al.* 2014), an independent substitution model was defined for each locus in the analysis: even reducing the sites model to a simple HKY+G with empirical base frequencies, a substitution rate and a transition/transversion ratio (*kappa*)[1] had to be defined of each locus (or 100 parameters for a 50-locus analysis), each of them informed with very little data. On the other hand, if we assume the RADome to be a globally neutral ensemble, we may assume that a single substitution model holds for all loci: we need only, in theory, define one substitution rate and one *kappa* parameter for all 50 loci, informed this time by the full dataset. Substitution rate, however, is strongly biased in our model by the selection of loci with higher observed polymorphism: although the full RADome verifies the expectation of a Poisson-distributed number of polymorphisms per locus with a single parameter, we use a truncated distribution that is not accounted for by a single substitution rate. Therefore we use a single *kappa* parameter for all sites, but a different substitution rate for each class of loci (by « class », we mean whether the locus includes 4, 5 or 6 polymorphic sites). This reduced parametrisation scheme has two advantages: since we use 4 instead of 100 parameters, MCMC convergence time is greatly reduced. And since we obtain a single consensus substitution rate for each locus class, it is possi-

---

1.　　A transversion being the replacement of a purine base (A or G) by a pyrimidine base (C or T), and a transition the replacement of a purine by the other purine, or of a pyrimidine by the other pyrimidine. Thus, there are 8 possible transversions, and only four possible transitions. The ratio of the transition to transversion rates, or κ (*kappa*) is characteristic of a mutation model.

ble to link the observed RAD substitution rates, and the whole-genome background substitution rate (see §48 p. 124).

We use this much simplified parametrisation in *The King synnome*, p. 163, and *The Emperor synnome*, p. 211, and find that the slow MCMC convergence issues encountered by Trucchi *et al.* are mostly solved, and that repeatability is high between different random sets of loci. However, large improvements could be achieved by designing a RAD-specific parametrisation for the EBSP, that would take into account the observed distribution of polymorphisms in the whole RADome, and use its λ parameter as an underlying rate for the loci included in the analysis.

§-45 The Allele Frequency Spectrum approach. The Allele Frequency Spectrum (AFS) is a rich summary of the Ancestral Recombination Graph. This data structure gathers the counts (or proportions) of sites in the genome for which the derived allele has a frequency f in the population under consideration. While the «true» AFS for a population could only be compiled through exhaustive sampling, the AFS can also be estimated from a random subset of individuals sampled from a panmictic population. Thus, the maximum resolution of the reconstructed spectrum will be 1/(2S+1) (with S being the number of sampled diploid individuals). Since usually the sample size is much smaller than the effective population size, only alleles that are already present in a significant fraction of the population (*i.e.* $f \gtrsim S/Ne$) are effectively represented in the spectrum. Under its most simple expression, the AFS can be reconstructed directly from allele counts in the sample, with the observed frequency taken as an estimator of the true frequency in the population. However, the difficulty of ascertaining genotypes reliably at a large number of loci, in a large number of individuals, makes such a direct estimation rather error-prone. Maximum-likelihood estimates of the AFS, that take into account the possibility of genotype errors, and the impact of missing data, are used whenever possible, and have been shown to provide a much more robust estimate of the «true» population AFS (Nielsen *et al.* 2012). The ML estimate of the AFS is not a direct transformation of the observed sites counts, and should better be interpreted as the distrib-

ution of probabilities, for a given allele, to be found with a frequency f in the population - here, we used this latter method as implemented in ANGSD (Korneliussen *et al.* 2014).

Another difficulty of AFS estimation lies in the correct identification of ancestral and derived states at each position. Accurately estimating the full AFS for a population requires that we can determine whether a given site should be considered as having a frequency $f = 1/2Ne$, or rather $f = 1 - (1/2Ne)$. In order to do this, it is necessary to reconstruct the state at each position in the genome at the parent node for the taxon, thus requiring sequence and polymorphism data for a sister taxon, and for an outgroup. If this is not possible, the AFS may be *folded*: instead of considering the frequency of the *derived* allele, one considers the frequency of the *minor* allele (the allele with the lesser frequency - which raises additional problems when considering multiple populations). Although this approach removes the errors due to ancestral state mis-identification, it greatly increases the number of possible scenarios leading to the same observed AFS, thus reducing the robustness of inferences.

The AFS is highly informative as to demography and gene flow. When starting from a single ancestral sequence, each new mutation appears as single copy in the whole population, *i.e.* with a frequency $f = 1/(2Ne)$. If the fitness value of that new mutation is neutral, its frequency is expected to vary only due to the stochastic process associated with binomial sampling at each generation, with variations in population size being a major forcing on allele frequency drift. For example, a population bottleneck will have the immediate effect of removing rare variants from the population, and biasing the AFS towards intermediate allele frequencies. Thus, the AFS for a given population reflects the successive demographic events in the population. But more informative is the N-dimensional AFS, that summarises the distribution of alleles frequencies amongst N populations, with $P(i,j,k)$ being the probability, for a given allele, to have the frequency i in population I, the frequency j in population J, and the frequency k in population K. If populations I, J and K are three random subsets of one single panmictic population, we expect the frequencies i, j, and k to be highly correlated for all sites, since the only source of variation is the stochastic er-

ror due to the sampling process. Isolation between populations, on the other hand, will manifest itself as a decay in the correlation between allele frequencies between these populations. The N-dimensional AFS (or «multi-AFS») is therefore a result both of the populations' demographic history, and migration history (see Fig. 11 p. 120).

Whereas the ARG explicitly represents population history by integrating time as a variable in its topology, the AFS is a «*temporally flat*» object, that only contains the outcome of demographic and migratory events. Inferring population history from the AFS therefore requires a more elaborate procedure than would be needed using an explicit coalescent history. The first approach that has been proposed to exploit the full N-dimensional AFS is that of Gutenkunst *et al.* 2009. This approach, implemented in δ*a*δ*i*, uses a diffusion approximation to represent the AFS: the discrete structure of real populations (discrete number of individuals - hence discrete frequency classes - and discrete generations) is approximated in continuous time, with continuous frequency transitions, as proposed by Kimura 1955 (see above §39 p. 99), so that demographic parameter values become parameters in a diffusion equation, of which the observed AFS is the numerical solution. In order to find the most likely parameter values, δ*a*δ*i* uses a composite-likelihood approach (*i.e.* a method where the true log-likelihood function is approximated by a simpler function, see Lindsay 1988), and the uncertainty of the results is assessed through parametric or non-parametric bootstrapping (*i.e.* either through resampling of the AFS itself, or by simulating new datasets based on the estimated parameters, and estimating new parameters based on these simulations - both approaches described by Gutenkunst *et al.* 2009).

Recently, a different approach has been suggested to infer population history from the observed N-dimensional AFS, based on coalescent simulations. This approach, proposed by Excoffier *et al.* 2013, overcomes the previous limitations of the simulation-based methods by implementing a continuous-time coalescent simulation (as opposed to the «natural» generation-by-generation coalescent, too slow to be used for demographic inference). Thus, the composite likelihood of the model is calculated based on a large number of simulated coalescent histories and resulting AFS -

typically 100,000 simulations per step in an Empirical Bayes approach, in the *fastsimcoal2* implementation (Excoffier & Foll 2011; Excoffier *et al.* 2013). Thus, as opposed to the δ*a*δ*i* approach, the *fastsimcoal2* approach explicitly models the coalescence process that underlies the observed AFS.
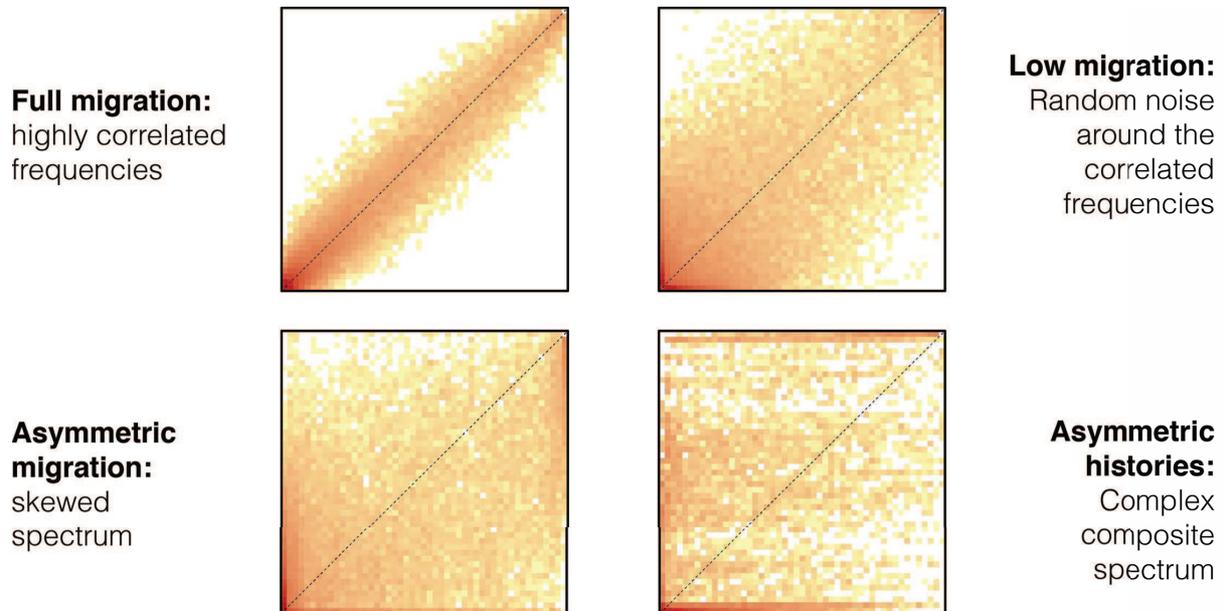
Figure 11 | Influence of demographic processes on the joint AFS. Four different pairwise situations, simulated using fastsimcoal2. Under **full migration**, allele frequencies are highly correlated between the two populations. With **low migration**, random dispersion increases around the full correlation line. With **asymmetric migration**, dispersion becomes skewed, and the correlation departs from the diagonal. Our last example is an **asymmetric history**, where the first population(vertical marginal spectrum) underwent a strong bottleneck biasing it towards intermediate allele frequencies, while the second population remained stable.

One limitation of both methods is that they are strongly model-constrained: the parameter space has to be carefully defined from prior knowledge. Since possible population histories can be extremely diverse, and since the AFS does not represent the temporal component of the ARG, it is necessary to define a demographic function, with a fixed set of free parameters that will be optimised by maximum composite likelihood - these parameters including the timing of major events, the population size and growth rate before and after those events, and the migration rates

between populations. Thus, the general structure of the population history is set beforehand, and only the value of the parameters may be optimised over. Although it is possible to compare different historical models (normally through AIC model choice), it may happen that only models that are fully incompatible with the true underlying history have been tested: thus, strong external evidence is required to formulate relevant historical hypotheses before testing them.

§-46 The Stairway plot approach. The Stairway plot (STY) model has been recently proposed by Liu & Fu 2015 as a model-flexible alternative to the general AFS-based methods (see §45 p. 117). By considering only a 1-dimensional AFS, marginalised for a single population, the STY excludes all information relative to historical migration rates, and focuses on population size change events, which allows for a considerable simplification of the parameter space. Thus, instead of requiring the specification of a number of demographic events, epochs, or growth rates, it is able to use a piecewise-constant population size prior, with a flexible number of population size changes informed by the data (through a likelihood ratio test, as models with decreasing numbers of demographic epochs are fully nested within each other) - a characteristic shared with the EBSP approach (see §44 p. 112, although EBSP includes the number of population size changes as a parameter to be co-estimated together with substitution models, gene trees and population sizes during the MCMC sampling, rather than a likelihood ratio test).

Instead of explicitly modelling recombination events (as the PSMC approach does, see §47 p. 122), the STY assumes each single variable site to be independent, and to stem for a separate coalescence process (a simplification defining the composite likelihood function). The probability of a site having a derived allele frequency f is a function of population size at each point of time in the past: thus, we can search for population size values (mutation-scaled as ϑ) that maximise the composite likelihood of the observed spectrum. Although the STY approach does not explicitly model the full coalescent process as EBSP does, it is able to use information from a much larger number of loci, and thus may better capture the information contained in the full dataset.
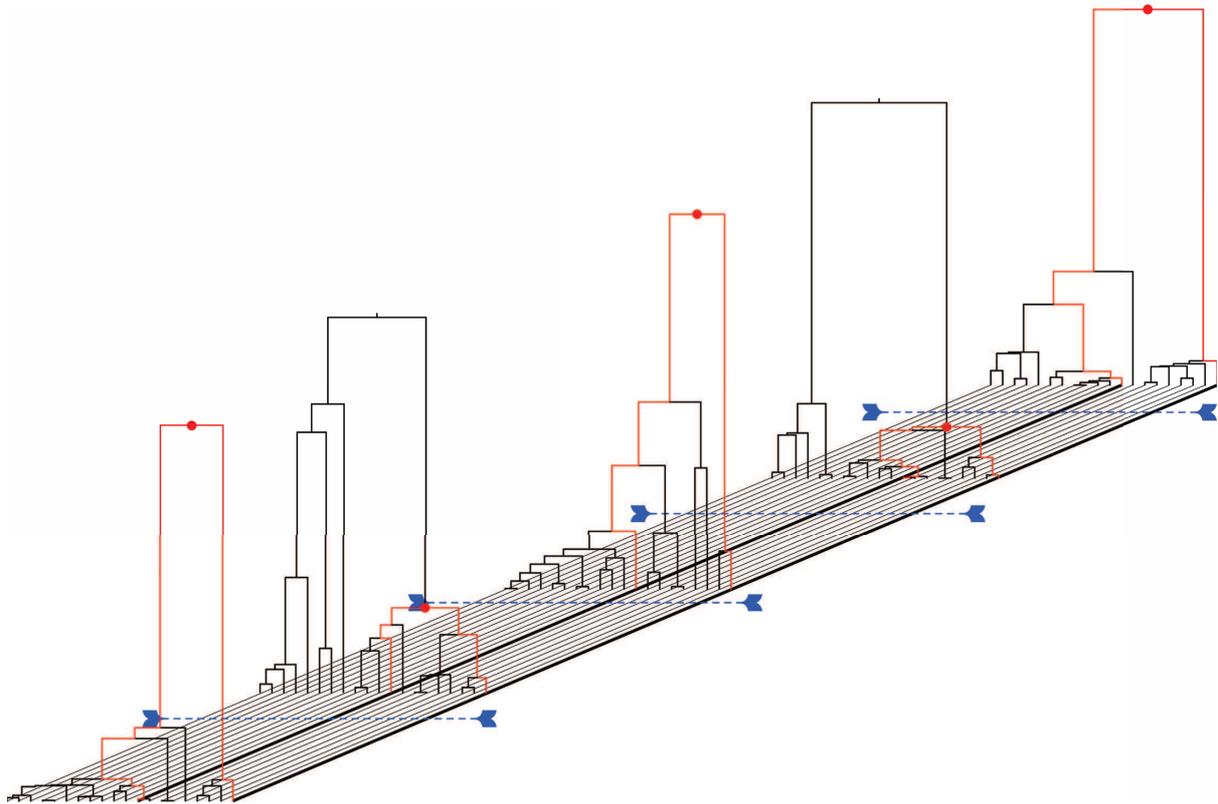
Figure 12 | The Pairwise Sequentially Markovian Coalescent model. We represent the independent local trees along a set of recombining sequences. Each blue arrow figures a recombination event, or state change in the hidden Markov model. The bolder lines are the two sampled chromosomes, and their pairwise coalescence is outlines in red in the local trees. The result of the pairwise sampling is a distribution of TMRCAs (see §47 p. 122 for details).

§-47 Sequentially Markovian Coalescent approaches. Another, independent take on the problem of estimating past population size changes has been proposed by Li & Durbin 2011, and recently extended by Schiffels & Durbin 2014. In its original form, the Sequentially Markovian Coalescent (SMC) model is a transversal interpretation of the classical coalescent, with recombination, introduced by Wiuf & Hein 1999, and can be interpreted as a reduction of the general Ancestral Recombination Graph (see §42 p. 107), in which recombination density is retained, but recombination topology is discarded. Considering that the distribution of times to the most recent common ancestor (TMRCA) along two chromosomal sequences follows a Markov model, where

changes of states represent recombination events (McVean & Cardin 2005; Li & Durbin 2011), the pairwise sequentially Markovian coalescent approach treats the «true» coalescence and recombination history of a pair of chromosomes as a hidden Markov model, where the hidden states are the TMRCA, the state transitions the recombination events, and the observed states are the densities of SNPs along the sequence (a higher density implying a more remote MRCA - see Fig. 12 p. 122). Past population size is assumed piecewise-constant, but can change state at time intervals: these intervals need to be specified beforehand, as opposed to the approach implemented in the STY (see §46 p. 121). Considering the number of recombination events in a typical population, any pair of chromosome contains thousands of independent coalescent samples. However, recent history is difficult to retrieve, since fewer recombination events can be detected, which is the main shortcoming of the method. To overcome this problem, the multiple sequentially Markovian coalescent approach (MSMC, Schiffels & Durbin 2014), considers more than two haplotypes at a time. Thus, instead of considering the TMRCA between a pair of chromosomes as an indicator of the ARG, it takes the shallowest TMRCA amongst any pair of chromosomes in the sample as its hidden Markov state. The structure of the coalescent (see §40 p. 101) implies that this TMRCA tends to become shallower as the sample size becomes larger. Thus, switching from PSMC to MSMC increases considerably the resolution over the most recent periods. A particularity of the MSMC algorithm, consequently, is the link between sample size and reconstruction depth. Since MSMC focuses on the first coalescence event between any two sequences in the sample, a larger sample size will increase the amount of information about recent coalescent structure, at the cost of older events, while reducing sample size will increase accuracy for deep-time events (Schiffels & Durbin 2014). However, this requires precise phasing of each haplotype, which is a considerable challenge in non-model species (see §37 p. 97): indeed, reconstructing the local mismatch distribution is impossible without an accurate representation of the local haplotypes. If phasing is not accurate, the precise local distribution of pairwise differences will be averaged to its mean value, and the estimated local MRCA will consistently be closer to

the population's average MRCA, thus loosing nearly all the informative content of the distribution of TMRCAs along the genome. Thus, the MSMC seems more suited for cases where the phasing can be established with high confidence - which is nearly never the case in non-model species (see §37 p. 97).

§-48 Rate of evolution. Accurate reconstruction of past and present population size changes requires an accurate estimate of the substitution rate - a notoriously difficult parameter to assess (Warnock *et al.* 2012; Warnock *et al.* 2015). A robust estimate of the substitution rate of the mitochondrial hyper-variable control region (HVR) or the Adélie penguin, based on mitochondrial heteroplasmy transmission through lineages, has been proposed by Millar *et al.* (Millar *et al.* 2008). In order to infer the genome-wide evolution rate, we performed a joint analysis of mitochondrial HVR and RAD data in a multilocus Extended Bayesian Skyline Plot framework, using the HVR rate as a calibration, by setting a normally-distributed prior reflecting the published point estimate and 95%CI interval, with a high sampling rate along the MCMC (10x the sum of sampling rates for all other substitution rates) in order to ensure free sampling of the prior.

In a coalescent framework, we need to assess the frequency of coalescence events along time: thus, calibration must address the rate of transmitted mutations only, i.e. the species' substitution rate, as opposed to its intrinsic mutation rate (a purely physiological parameter of little relevance here). However, the germ line cell divisions are, within a taxon, independent from the generation time - thus, what we may assume constant is the number of substitutions per generation, rather than per units of calendar time. Since the generation time differs widely between the Adélie penguin (6.46 years, see Millar *et al.* 2008) and the King penguin (10.48 years, see §95 p. 186), we must thus convert the established rate (in substitutions per site per Myr: median = 0.55, 95% CI = 0.29–0.88, see Millar *et al.* 2008) in order to reflect the generation time of the King penguin, to 0.34 substitutions.site^{-1}.Myr^{-1} (95% CI = 0.18–0.54).

1 The EBSP analysis was setup as exposed in *The Emperor synnome*, p. 211, and is briefly reminded

2 here. We downsampled the data to haploid individuals, and using independent 50 loci with 50

3 haplotypes each, with 3 to 6 polymorphic sites, in addition to 50 randomly selected HVR hap-

4 lotypes. We specified one independent site model for each locus class (3, 4, 5 or 6 SNPs, and

5 HVR). For each class, specified a HVR model, allowing for invariant sites for the HVR, but not

6 for the short nuclear loci, and for gamma-distributed rate heterogeneity discretised in 4 classes.

7 Transition-transversion ratio *kappa* was linked across nuclear models. All chains were run in du-

8 plicate to check for convergence and for a sufficient length to gather ESS[1] > 200 for all parame-

9 ters, which necessitated 500,000,000 to 1,000,000,000 steps.

10 Since we parametrised each locus class separately, we expect our model to fit a class-specific sub-

11 stitution rate as a function of the observed number of segregating sites, rather than a common

12 substitution rate. However, as we focus on neutrally evolving regions of the genome, we expect

13 the number of segregating sites to follow a Poisson distribution, of parameter λ equal to the mean

14 number of segregating sites per RAD locus. On a large number of sequences, the expected value

15 $E(\lambda)$ converges towards the "true" underlying constant mutation rate, multiplied by the total tree

16 length for each locus. Thus, if we fix the tree length, λ becomes an estimator of the substitution

17 rate μ. However, under the EBSP model, the observed number of segregating sites is taken as an

18 estimator of λ, and consequently of the substitution rate μ. Therefore we expect the inferred value

19 of μ for each locus class to be a posterior probability of the "true" substitution rate, conditional

20 on the mean number of segregating sites observed for that class (Trucchi *et al.* 2014). In order to

21 retrieve the underlying common substitution rate μ, we first fitted a log-linear model to the in-

22 ferred substitution rates (μ_3= 0.0159, μ_4= 0.0218, μ_5= 0.0275, μ_6= 0.0389. Fitted model: inter-

23 cept *i* = -5.02, slope *s* = 0.292, R^2=0.997). A Poisson model of parameter λ equal to the mean ob-

24 served number of segregating sites was a good fit for the empirical distribution of number of

---

1.   ESS or *Effective Sample Size* is the number of uncorrelated states sampled along the Markov chain. Correlation between successive states indicates a trend in the state of the model, and hence incomplete mixing. Thus, the number of steps needed for the correlation between states to decay, or *lag vector*, is indicative of the efficiency of the mixing for the MCMC.

segregating sites per locus (λ=1.47 , chi-squared test of goodness-of-fit p-value= 0.232). Thus, we extracted μ as $e^{(s.λ+i)}$ ~ 1.02e-2 substitutions per site per Myr, or 1.08e-7 substitutions per site per generation. This rate is ca. twice slower than the one reported by Trucchi *et al.* (2.6e-7 subst.site^{-1}.generation^{-1}, see Trucchi *et al.* 2014), but much faster than the one reported by Li *et al.* (8.11e-9 subst.site^{-1}.generation^{-1}, see Li *et al.* 2014). While the former was not used in Trucchi *et al.*'s analysis, but rather derived from it, Li *et al.*'s result, on the other hand, relies on two exterior and uncertain assumptions: 1) the divergence time between the Emperor and the Adélie penguin is set to ~23 Myr, which may be a large overestimate (based on a state-of-the-art total evidence bayesian analysis, Gavryushkina *et al.* 2015 proposes ~9 Myr instead), and 2) the generation time is taken to be 5 years in both species; however it has been shown to be 16 years in the Emperor penguin (Jenouvrier *et al.* 2014), and 6.46 years in the Adélie penguin (Millar *et al.* 2008) - thus 11 years would be a closer (although inaccurate because assuming a single rate) estimate of a common generation time. Applying these corrected estimates to Li *et al.*'s findings would give a rate of ~4.55e-8, which is more than five times faster than proposed, and ca. half our estimate. And still, this calculation does not take into account the possible rate heterogeneity between lineages, and most importantly the changes in generation time between the *Aptenodytes*/*Pygoscelis* common ancestor and the extant species, which may explain the remaining difference.

Generally, the rate of evolution of penguins has been a rather challenging subject, with a wide discrepancy between the paleontological and molecular evidence (see §1 p. 65). While fossil data has been recognised to support a very recent radiation of penguins (about 10 Myr BP, see Slack *et al.* 2006), molecular data has been interpreted as implying a much more ancient origin (~45 Myr for Baker *et al.* 2006). This molecular-derived radiation has successively been brought to a closer agreement with the fossil evidence by Subramanian *et al.* (~20 Myr, Subramanian *et al.* 2013) and Gavryushkina *et al.* (~12.5 Myr, Gavryushkina *et al.* 2015). The rate that we propose here is in accordance both with the hypothesis of a very fast diversification of the spheniscids, and with the findings of Trucchi *et al.*

Habitat and climate analysis.

The set of external conditions required by a species to thrive define its *habitat*. Generally, these conditions include both *abiotic*, and *biotic* factors - *i.e.* factors that are only dependant on *(a)* physical and chemical characteristics, or *(b)* interactions with other living organisms. Abiotic habitat determinants usually include temperature and precipitation mean and variability, a range of elevations, sometimes wind or currents regime, but also the length and variability of the photoperiod or the intensity of insolation. These parameters (although some, such as temperature and precipitation, are themselves in a certain measure influenced by biotic communities), may be accurately estimated, and predicted on medium time scales, and are the focus of general circulation models (see §50 p. 130). Their impact on biological system is multiple. They primarily interact with species' physiology: each organism has an optimum set of abiotic conditions in which its metabolic processes are least costly, and in which it thrives. But they also impact species indirectly, through direct effects on other organisms which themselves interact with the focal organism - in other words, through the mediation of *biotic interactions*. For example, prey or food resource availability, predation pressure, vegetal cover for shelter, parasites and pathogens, *etc.* play a central role in defining the suitable habitat for a species. The respective parts of abiotic and biotic factors in the definition of a habitat are debated: their contribution is certainly species-dependent, but may also vary across the different margins of a species distribution - for example, it has been proposed that the polar boundaries of habitats are more often defined by abiotic limits (*e.g.* physiologic effects of the coldest winter temperatures), while the equatorial boundaries are rather defined by biotic constraints (such as an increasing density of competitors and parasites equatorwards - themselves prevented from a polewards spread by their own abiotic limits). Biotic and abiotic factors may also interact across phases (*e.g.* overwintering and summer grounds, foraging and breeding areas, *etc.*), or evolve through time - a habitat main-

ly determined by biotic factors may come under increasingly strong abiotic constraints as a result of climate change.

The geographical extent of a species' habitat defines its *potential range* - that is, the range it would occupy if biological systems were fully mechanistic. Several factors may prevent a species from occupying its whole potential range: for example, suitable habitat may occur outside of the species' dispersal range, or the species may have gone locally extinct through hunting pressure, *etc.* The actual range occupied by the species, which is necessarily fully nested within its potential range, is its *realised range* (Hutchinson 1957) - the one provided in atlases and distribution maps (*e.g.* Fig. 7). A mismatch between the *potential* and the *realised* range is common at the global scale, especially in continental taxa: while similar ecosystem are normally found zonally around the world, dispersal across ocean basins is a rare event for larger organisms. Thus, the abundant endemic fauna of Australia and New Zealand owes more to the lack of connectivity between similar habitats than to restricted potential ranges. Indeed, the ease and rapidity of biological invasions shows that once the (often punctual) barrier-to-dispersal problem is solved (*e.g.* once the ocean has been crossed in some way), whole swathes of new habitat may be colonised rapidly (Thuiller *et al.* 2005; Trucchi *et al.* 2015), bringing the realised range closer to the potential range. The dispersal problem is less drastic in marine systems (see §6 p. 33), and is most important meridionally - while connectivity is rather large between ocean basins at the same latitudes (especially at higher latitudes were connectivity is enhanced by inter-ocean circulation, see §7 p. 35), the equatorial region may constitute an important barrier between the Arctic and the Antarctic, resulting in fully independent organisms occupying similar ecological functions and displaying convergent traits (for example the auklets and the diving-petrels, see §20 p. 71).

This convergence, in similar habitats, of species fulfilling similar ecosystem functions, allows us to define the concept of *niche* (Hutchinson 1957). Whereas a *habitat* is a species-focused, and largely geographical concept («is that place, given its biotic and abiotic constraints, suitable for that species ?»), a *niche* is a functional, ecosystem-focused concept («is there already a species here

that can eat anchovy in the coastal waters while nesting on these scree slopes ?»). Although both

concepts are often confused, they are extremely different. Modelling a niche would rely on explic-

it modelling of each relevant species and their relationships in the ecosystem (Wiens *et al.* 2009;

Chevin *et al.* 2014) and is very seldom done in climate change biology. Modelling a habitat is a

slightly easier task, as the problem may be restricted with a reasonable level of approximation to

non-functional aspects (*e.g.* static distribution of abiotic parameters, and a few key biotic parame-

ters such as prey abundance). Yet even within the approximation of habitat modelling, a funda-

mental distinction arises between fully *correlative*, and what we could call *causal* models. The

overwhelming majority of studies of species' response to climate change use the «climate enve-

lope» or «climate space» approach (Box 1981; Berry *et al.* 2002): through a multivariate correla-

tive approach, the observed distribution of a species is correlated to a set of (usually abiotic only)

environmental parameters, and this set is used to project the species' future distribution (*e.g.*

Virkkala *et al.* 2008; Durner *et al.* 2009) or demography (*e.g.* Jenouvrier *et al.* 2012; Jenouvrier *et

al.* 2014) based on numerical climate models predictions. One obvious limitation of this ap-

proach is that it takes the species *realised range* as an estimator of its *potential range* - in some cas-

es, this can be just an approximation, but in some other it can be a true error (Pearson & Daw-

son 2003). This becomes even worse when only abiotic habitat characteristics are included in the

model (as it is the case in the 2015 Audubon society report on future North American bird dis-

tributions, for example - see Langham *et al.* 2015), since biotic constraints are expected to reduce

the set of abiotically exploitable areas. Thus, the abiotic habitat estimated from the realised range

is very likely to underestimate the range of abiotic conditions that a species can tolerate, as it con-

fuses the abiotic limitations of the biotic interactors with the abiotic limitations of the focal

species itself. For example, a species may be limited to a very little part of its otherwise potential

habitat by the presence of a strong competitor: the future distribution of that species will then

mostly depend on the future evolution of the competitor, and not of the local climate. If, by

chance, the competitor is less tolerant to changes in abiotic conditions, then climate change may

manifest itself as a range extension of our example species. If we had in the first place modelled that species habitat by hypothesising that it can only tolerate the precise abiotic conditions in which it is found, it is very likely that this overly precise set of conditions will be disrupted by any change of climate, and that we will forecast that species' extinction. The same goes to demographic, rather than distributional, modelling: there again, observed correlations are assumed, but not shown, to imply a causal relationship between environmental parameters and the species' growth rate. However this line of thought is usually flawed, as has been convincingly exemplified by Trivelpiece *et al.* 2011 using the Chinstrap penguin *Pygoscelis antarctica* as a model: the penguin's breeding success is explained primarily by krill abundance, and the krill abundance is partly explained by sea ice extent. A climate-envelope model would therefore find a rather robust correlation between penguin breeding success and sea ice extent. However a disruption of the correlation between sea ice and krill can be introduced by cetacean demography (cetaceans are important competitors, and their demography is also controlled by lower-latitude breeding-ground conditions) or by human exploitation (a notoriously difficult parameter to forecast in our days): thus, the observed correlation between sea ice and penguin demography is in fact fallacious, and may change abruptly whenever cetacean demography or human exploitation of krill will change regime.

A *causal* approach to modelling, on the other hand, will endeavour to identify parameters that have a know, direct influence on the species' demography. In the case of the Chinstrap penguin, this would mean including krill abundance, and not sea ice extent, as an explanatory variable. This is the approach we use in *The King synnome*, p. 163, as we are convinced it allows for much more robust forecasts of population trajectories.

§-50 Climate projections in the Coupled Model Intercomparison Project. Our current understanding of the Earth's climate system is summarised in Earth System models, that mainly implement General Circulation Models (GCM) - i.e. numerical models which reproduce energy transfer between atmospheric, oceanic, land and ice masses. These models usually involve a discretisation in

cells of varying dimensions, and the state of each cell is computed for each time step as a function of the other cells in the system. The Coupled Model Intercomparison Project (CMIP) proposes an international framework to assess and understand the differences between the representation of climate in different models, by defining standard experiments that can be compared between systems. The current framework, the CMIP phase 5 (CMIP5, detailed in Taylor *et al.* 2012), builds upon the previous CMIP3 ensemble to achieve more consistent and accurate model predictions. In particular, CMIP5 models have a generally higher resolution, and a more accurate representation of bathymetry, than the previous generation of models, which leads to a much improved simulation of the Southern Ocean (Meijers 2014). While most CMIP5 models perform generally well, sea ice representation in the Antarctic Ocean remains a weakness, as most models predict a slight decrease in sea ice extent in East Antarctica in the early 21st century, while the observed trend is a slight increase (Zhang 2007; Turner *et al.* 2013; Xu *et al.* 2013; Wang *et al.* 2014) - a discrepancy that may be linked to different factors. First, most current GCMs treat ocean, atmosphere and sea ice as three separate models, with boundary interfaces at the surface of the ocean, and the upper and lower surfaces of the sea ice layer. Relative to its own internal dynamics, boundary conditions are thus comparatively very important for sea ice, and the current approach may lead to incorrect representation. Secondly, the spatial resolution of most CMIP5 models (usually a 1°x1° grid) may be too coarse to explicitly model latent-heat polynya, that act as sea-ice formation zones (see §118 p. 225 and Kusahara *et al.* 2015). But lastly and most importantly, the input of freshwater (with a higher freezing temperature) from the melting continental ice sheet has an important impact on the sea ice formation: however, the Antarctic ice sheet itself is not modelled in the CMIP5, but merely treated as a specified boundary condition, which is likely to lead to an incorrect representation of sea ice (see Bintanja *et al.* 2015 and §118 p. 225).

As CMIP5 models include different representations of climatological phenomena, their outputs may vary, both for the reconstruction of past climate, or for the prediction of future changes. A

common way to handle these divergences is the *ensemble* approach, in which several different models are used jointly (Ainley *et al.* 2010a; Doak & Morris 2010; Péron *et al.* 2012; Raybaud *et al.* 2013; Jenouvrier *et al.* 2014; Raybaud *et al.* 2015). Thus, it may be expected that the most robust features, represented similarly in all models, will be preserved, while the model-specific and possibly artifactual divergent traits will be evened out (Cabré *et al.* 2015). Of course, this «democratic» approach to model selection is not failsafe: first, because despite the controls included in the CMIP5 validation process, not all model are of similar «quality» at a given location - the degree of precision and realism varies between models, and so does the size of the spatial grid over which phenomena are represented. Another source of imprecision is the similarity between different models, that may in some cases amount to pseudo-replication when several models of related architecture give similar outputs because they represent climate in the same way (Cabré *et al.* 2015). In order to assess the robustness of the predicted trends to the choices in model parametrisation, an ensemble approach may be used within the framework of a single model, by using multiple equally possible parameterisations in a *perturbed physics ensemble* approach (Ackerley *et al.* 2009). But a more common approach is to use altogether different models when the focus it the prediction itself, and not its robustness.

Although ensembles of AO-GCMs usually perform better than single models, their aim is to represent the earth system as a whole: thus, their still may not accurately capture local aspects of certain parameters. In the case of less reliably represented areas, it is common to include only models that already accurately describe the state of climate during the historical period on a few accurately observed parameters (Ainley *et al.* 2010a; Raybaud *et al.* 2013), *e.g.* satellite-derived measures of surface temperature or sea-ice cover, which are directly comparable to model outputs.

§-51 The Representative Concentration Pathways. While the uncertainty arising from climate representation within models can be partly addressed through the ensemble approach, another important source of uncertainty is the nature of future forcings. Atmospheric greenhouse gas (GHG) concentration, in particular, is a major driver of effective radiative forcing (Pachauri *et al.* 2014;

Stocker *et al.* 2014), but their future concentration is largely determined by political and socio-economical trajectories. Thus, four different forcing scenarios or *Representative Common Pathways* (RCP) have been established, each corresponding to a different atmospheric concentration of GHG in 2100 (Meinshausen *et al.* 2011). Under the RCP-2.6 scenario, efficient political action leads to a peak in radiative forcing at ~ 3 W/m^2 before 2100, followed by a decline. Under the RCP-4.5 and RCP-6 scenarios, radiative forcing stabilises before 2100, either at 4.5 W/m^2 or at 6 W/m^2. Under the RPC-8.5, no political action is taken and radiative forcing follows the current trend, reaching 8.5 W/m^2 by 2100. These four scenarios lead to widely different predictions as to global temperature increase (Meinshausen *et al.* 2011) - yet the direction taken by political decisions is difficult to forecast. Thus a common practise when assessing species response to climate change is to repeat predictions under several RCPs, in order to assess the range of possible responses (see e.g. Péron *et al.* 2012; Raybaud *et al.* 2013; Jenouvrier *et al.* 2014; Jenouvrier *et al.* 2014; Raybaud *et al.* 2015). However, variability between models under a single forcing scenario remains high, so that ensemble predictions may overlap between different RCPs (Goberville *et al.* 2015). Thus, CMIP5 RCP experiments should not be understood as a positive take on future climate: rather, «*the goal of working with scenarios is not to predict the future, but to better understand uncertainties in order to reach decisions that are robust under a wide range of possible futures*» (Moss *et al.* 2010).

§-52 Palæoclimate experiments. In order to assess the current GCMs' ability to represent different climatic conditions, it has been proposed that comparatively well-known ancient climate periods could be used as a benchmark. Thus, the Palæoclimate Modelling Intercomparison Project (PMIP, currently in phase 3, see Braconnot *et al.* 2012) has been developed as a counterpart to the CMIP experiments. PMIP3 experiments focus on past climatic periods with abundant available data, in particular the LGM («21 kyr experiment), the Early Holocene («8.2 kyr experiment»), the mid-Holocene period («6 kyr experiment»), and the last millennium («past1000 experiment»). Further back, Interglacial and mid-Pliocene experiments are also included. Of these,

three have been included in the CMIP5 panel: the 21 kyr, 6 kyr, and past1000 (Braconnot *et al.* 2011). While model parametrisation follows the same rules as piControl, historical and rcp runs, initial conditions, specification of external forcings, and boundary conditions are different, and are determined as part of the experiments definition. These rely either on direct computation (*e.g.* the state of solar radiative forcing at each point of time conditional on Milankovitch cycles, etc.), or on evidence from palæontology and sedimentology (see §9 p. 42 for more details). In the Southern Ocean, one particularly important parameter needs to be addressed, in the configuration of the Antarctic Ice Sheet. The continental ice sheets themselves (either in Antarctica or in Greenland) are currently not explicitly modelled in the PMIP3/CMIP5 panels (Kusahara *et al.* 2015), and need to be specified as *boundary conditions*, *i.e.* fixed states at the limit of the dynamic cells of the models. Reconstruction of the Antarctic Ice Sheet in the PMIP3 experiments relies on external evidence, in particular the CLIMAP multiproxy reconstructions (CLIMAP 1981). Overall, PMIP3 experiments support the current generation of AO-GCMs, as reconstructed palæoclimate reconstructions closely match the available direct evidence (Braconnot *et al.* 2011; Braconnot *et al.* 2012; Harrison *et al.* 2015).

In this work, we use PMIP3/CMIP5 palæoclimate experiments as an explanatory framework for our coalescent-based palæodemographic reconstructions for the King and the Emperor penguin (*The King synnome*, p. 163 and *The Emperor synnome*, p. 211).

Chapter 3: Fine-scale colony structure

This chapter has been published as: <u>Cristofari R,</u> Trucchi E, Whittington JD, Vigetta S, Gachot-Neveu H, Stenseth NC, Le Maho Y, Le Bohec C (2015) **Spatial heterogeneity as a genetic mixing mechanism in highly philopatric colonial seabirds.** PloS one 10: e0117981.

Context

§-53 Local structure and random sampling in population genetics. Population genetic studies rely on the molecular analysis of individuals sampled from one or several demes or populations (see §2 p. 25). With very few exceptions, these individuals represent a small fraction of the focal populations: therefore, when comparing different ensembles through reduced subsets of individuals, an underlying assumption is that the population-level sampling process is unbiased, and that fundamental parameters (such as allele frequencies, see §45 p. 117) observed in the sampled individuals are reliable estimators of the same parameters are the population scale. While this hypothesis is normally verified when true random sampling is possible, it is often only assumed in less easily accessible wild species.

Thus, an important first step before engaging in large-scale population genetic studies is to establish whether variation in local sampling schemes is likely to influence results on a broader geographic scale. Previous studies of colonial seabirds have suggested that natal philopatry could ex-

tend not only to the colony, but also to the sub-area within the colony where the individual was born (e.g. in Black guillemots *Cepphus grylle*, see Frederiksen & Petersen 1999). In turn, strong fine scale philopatry may lead to very heterogeneous genetic landscapes, and in particular to strong spatial autocorrelation of genotypes at short distances (e.g. as has been observed in Superb Fairy-wrens *Malurus cyaneus*, see Double *et al.* 2005). A direct consequence of this is that uninformed local sampling would be likely to oversample autocorrelated genetic groups (*i.e.* loosely related individuals), and therefore to overestimate the amount of genetic drift between demes, while also violating the genetic independence assumption of most models. Indeed, very local patterns of genetic variation do not occur on the same level as between-deme genetic structure. Broad-scale genetic structure between demes normally involves long-term reduction of gene flow and random drift in allele frequencies: population-scale genetic sampling, rather than direct kinship, plays the main part in the process. Thus, although strong local genetic heterogeneity (e.g. kinship structure) at the local level is likely to promote larger-scale genetic structure (*e.g.* through reduction of dispersal between demes), this is not necessarily the case, as local kinship structures may be regularly dissolved into the broader deme gene pool.

§-54 Impact of local habitat on populations. While anthropogenic climate change is a global phenomenon (see §11 p. 50), its realisation is heterogeneous, and its variability happens at all scales - from continental to local ones (§15 p. 57). Understanding the relationship of species with their environment, whether in a context of stability or of change, therefore requires the integration of very broad-scale patterns (that will be examined later, in *The King synnome*, p. 163), but also of fine-scale, extremely local parameters. Heterogeneity between seabird colonies and breeding locations is a rather straightforward phenomenon that can be intuitively hypothesised, and that implies contrasts between groups of individuals (see *e.g.* Kauffman *et al.* 2003) - but heterogeneity between singular breeding places and individual fitness and breeding success within a colonial framework is a rather new concept in the study of coloniality (see Cornet 2014). Here, we con-

sider the link between local habitat heterogeneity, and the shape of genetic variation at the individual level.

§-55 Aims of this chapter. In the King penguin, fine scale local philopatry has been anecdotally documented (Nesterova *et al.* 2010), yet the importance of this behaviour in shaping the species genetic landscape is unknown. In this study, we use a dense local sampling of king penguins chicks to assess the importance of very-fine-scale spatial patterns in the structure of the species' colonial units. Our aim is twofold: first, assessing the strength of local genetic heterogeneity at the colony level will allow us to set an upper limit on the strength of philopatric behaviour in the King penguin from a dense local sample, and thus to set a prior expectation for the study of world-wide gene flow. Second, it will allow informed sampling for larger-scale genetic studies in the following chapters of this work (see *The King synnome*, p. 163 or *The Emperor synnome*, p. 211).

Abstract

How genetic diversity is maintained in philopatric colonial systems remains unclear, and understanding the dynamic balance of philopatry and dispersal at all spatial scales is essential to the study of the evolution of coloniality. In the King penguin, Aptenodytes patagonicus, return rates of post-fledging chicks to their natal sub-colony are remarkably high. Empirical studies have shown that adults return year after year to their previous breeding territories within a radius of a few meters. Yet little reliable data are available on intra- and inter-colonial dispersal in this species. Here, we present the first fine-scale study of the genetic structure in a king penguin colony in the Crozet Archipelago. Samples were collected from individual chicks and analysed at 8 microsatellite loci. Precise geolocation data of hatching sites and selective pressures associated with habitat features were recorded for all sampling locations. We found that despite strong natal and breeding site fidelity, king penguins retain a high degree of panmixia and genetic diversity.

Yet, genetic structure appears markedly heterogeneous across the colony, with higher-than-expected inbreeding levels, and local inbreeding and relatedness hotspots that overlap predicted higher-quality nesting locations. This points towards heterogeneous population structure at the sub-colony level, in which fine-scale environmental features drive local philopatric behaviour, while lower-quality patches may act as genetic mixing mechanisms at the colony level. These findings show how a lack of global genetic structuring can emerge from small-scale heterogeneity in ecological parameters, as opposed to the classical model of homogeneous dispersal. Our results also emphasise the importance of sampling design for estimation of population parameters in colonial seabirds, as at high spatial resolution, basic genetic features are shown to be location-dependent. Finally, this study stresses the importance of understanding intra-colonial dispersal and genetic mixing mechanisms in order to better estimate species-wide gene flows and population dynamics.

Introduction

§-56 Coloniality and population structure. How colonial systems are maintained in non-cooperative species remains an important question in evolutionary biology (Danchin & Wagner 1997; Bowler & Benton 2005). Philopatric behaviour is usually considered to be the basis of coloniality (Bowler & Benton 2005). It is thought to offer several selective advantages, such as a good knowledge of the higher quality breeding spots and of the pool of breeding partners linked to these spots (Wheelwright & Mauck 1998; Heg *et al.* 2011; Arnaud *et al.* 2012), and it favours the selective value of proximal defensive behaviour (Dunford 1977) or allofeeding (Lecomte *et al.* 2006) through kinship selection. However, the drawback of such behaviour is the fragmentation of genetic diversity at the colony level (Banks & Peakall 2012), which leads to an increase in inbreeding within clusters of closely-related individuals, in turn potentially leading to local inbreeding depression (Frankham 1995; Frankham 2005). Dispersal is therefore an essential balancing force in the conservation of colonial systems (Serrano *et al.* 2004; Bowler & Benton 2005; Bick-

nell *et al.* 2012; Fernández-Chacón *et al.* 2013). It is known to promote gene flow (Winters & Waser 2003) and genetic adaptability (Bowler & Benton 2005) as well as plasticity in response to habitat changes (Travis & Dytham 1999; Serrano *et al.* 2004).

Both philopatry and dispersal occur at all spatial scales in many colonial species (Murrell *et al.* 2002; Barlow *et al.* 2013), yet it has often been assumed that strong philopatric behaviour is a common trait of most pelagic seabirds (Frederiksen & Petersen 1999; Bried *et al.* 2007; Dugger *et al.* 2010). Indeed, the benefits of philopatry and coloniality (Coulson 2002), the barriers to dispersal (Friesen *et al.* 2007) and the dynamics of colony formation and extinction (Matthiopoulos *et al.* 2005) have traditionally been explored under that hypothesis. Thus several studies have documented a lack of genetic structure amongst distant colonies, which, in this context, seemed incompatible with assumed philopatric behaviour (the so-called "seabird paradox" of Milot *et al.* 2008).

It is often considered that the relatively weak evidence for structure, together with the high level of genetic diversity observed in many seabird species (e.g. Akst *et al.* 2002; Bouzat *et al.* 2009; Gómez-Díaz *et al.* 2009), are mostly the consequence of the random dispersal of a few juveniles. On the other hand, the importance of intra-colonial dispersal in fitness enhancement has been studied through phenological methods (Steiner 2005), and dispersal distance, even at very fine scale, has been shown to depend on species-specific ecological dynamics (Murrell *et al.* 2002; Banks & Peakall 2012). However, strict correlation between dispersal, site fidelity, and population structure has been questioned (Pearce *et al.* 2008), and the importance of intra-colonial movements on genetic mixing has received comparatively little attention.

§-57 The King penguin as a model. The King penguin, *Aptenodytes patagonicus*, which breeds in large colonies all around the sub-Antarctic area, is an ideal model to investigate these aspects of coloniality. While the King penguin's sister-species, the Emperor penguin, *Aptenodytes forsteri*, does not display territorial behaviour (Williams 1995), the King penguin is known to choose and defend a breeding territory within the colony, even though it does not build a nest (Bried & Jou-

ventin 2001). Breeders of this species have been described as having a marked philopatric behaviour across reproductive seasons and have been observed to use the same breeding site, within a radius of a few meters, year after year within their colony (Barrat 1976; Bried & Jouventin 2001). Return rates of juveniles to their natal colony are also typically high (Le Bohec *et al.* 2008; Saraux *et al.* 2011b). However, it is not yet clear whether natal philopatric behaviour also extends to the specific birth site within the colony, and whether this behaviour may result in local structuring of populations. In order to test this, a genetic study was conducted in the "Baie du Marin" colony on Possession Island, Crozet Archipelago. If philopatric behaviour indeed extends to breeding territory selection, it is expected that the colony will have a non-random genetic structure, with closely related individuals distributed in spatial clusters, as has already been observed in several non-avian philopatric species (e.g. Rivers *et al.* 2005; Kanno *et al.* 2011). However, even in known philopatric species, detection of genetic structure can be hindered by a variety of behaviours, such as juvenile and adult dispersal or extra-pair paternity (Double *et al.* 2005); therefore, the methods used to study it must be sensitive enough to detect even a weak signal (Jones & Wang 2012).

§-58 Expectations and hypotheses. When considering the genetic structure of a species, expected patterns may be analysed according to *(i)* global homogeneous processes or *(ii)* local heterogeneous processes whose effect varies across the area (Osborne *et al.* 2007). *(i)* The predictions associated with strong and consistent philopatric behaviour belong to the former class. Without taking spatial distribution of individuals into account, a skew in global population inbreeding descriptors may be expected (Wright 1965), with an excess of homozygosity reflecting higher-than-random relatedness between paired individuals. However, a prior to F-statistics is that populations are in a state of equilibrium, which may be in contradiction with fine spatial and temporal scale analysis, such in our study (Whitlock & McCauley 1999; Paetkau *et al.* 2003). Alternatively spatial autocorrelation should be detected at the colony level, reflecting a gradual isolation-by-distance trend, though this should only hold true if the process leading to spatial structure is ho-

mogenous at the individual level (Osborne *et al.* 2007). *(ii)* If, on the other hand, philopatric behaviour is a more variable trait dependent on local ecological conditions, the processes involved in colony structure are expected to belong to the second class. Local heterogeneous signatures should therefore be found, such as divergent population parameters for different areas of the colony (Jones & Wang 2012). Although inbreeding is not in itself an indicator of spatial structure, higher-than-expected individual inbreeding levels may reveal a non-random mating system, favouring relatives as potential partners. In such cases, a spatially-correlated distribution of inbreeding suggests a space-driven mating system (Ruzzante *et al.* 2002; Vogl *et al.* 2002). Pairwise relatedness, calculated across spatially-defined windows, is another insight into the same phenomenon (Ruzzante *et al.* 2002; Stevens *et al.* 2011).

In this study, we use a combined approach including genetic, spatial and local ecological data to investigate the mechanisms of genetic mixing inside a seabird colony. We focus in particular on how fine-scale habitat heterogeneity patterns may influence local dispersal behaviour, and how lack of genetic structuring can emerge from small-scale heterogeneity in ecological parameters.

Materials and Methods

§-59 Permits and ethics statement. All animals in this study were handled only once in order to mark them with a plastic tag and to conduct morphological measurements. All procedures employed during this field work were approved by the Ethical Committee of the French Polar Institute (Institut Paul Emile Victor – IPEV) and conducted in accordance with its guidelines, also complying with French laws including those relating to conservation and welfare. Authorizations to enter the breeding site (permits n°2009-57 issued on august 26th 2009) and handle birds (permits n°2009-59 issued on august 29th 2009) were delivered first by the French "Ministère de l'Aménagement du Territoire et de l'Environnement" and then by the Terres Australes et Antarctiques Françaises (TAAF).

Handled animals were removed from the colony in order to minimize the disturbance to neighbouring birds and taken to a shelter a few meters away for manipulation. They were hooded to reduce their stress and manipulations lasted between 5 and 10 minutes. All blood-sampling and tagging material was sterilized (either sealed, or through chemical sterilization). Moreover, Védine soap and alcoholic antiseptic solutions were used to disinfect the skin before bleeding and tagging. Flesh wounds did not seem infected thereafter (personal observations on a subset of recaptured birds).

§-60 Study site and sampling. Our study was conducted during the summer season 2010/2011 in the king penguin colony of "La Baie du Marin", on Possession Island, Crozet Archipelago (46°25'S, 51°45'E), which comprises around 16,000 breeding pairs (Delord *et al.* 2004). Chicks born in a sub-section of the colony comprising approximately 10,000 breeding pairs (Antavia, Gendner *et al.* 2005) were randomly selected and captured along a peripherical 120m-transect, in order to maximise separation distance. To minimize disturbance of breeding penguins, sampling was conducted no deeper than 4-5 nests towards the center the colony. Sampling was conducted at a high spatial resolution (~2 m between successive samples, i.e. every second nest at the time of sampling) in order to assess fine-scale genetic structure of the colony (sampling map is given in Fig. 13). The sampling area was partitioned according to natural terrain discontinuities (such as tussocks, rocks, or flooded patches), in a total of 6 clusters encompassing all sampled nests (Fig. 13). 175 early-hatched chicks were thus sampled during early brooding (~ 2 week old chicks) and temporarily tagged with a small external plastic pin (Floytag®). Each chick's hatching site was geolocated with a Global Positioning System device (Garmin eTrex®), and further confirmed using visual grid markings in the field (*ca.* 10x10m cells). King penguins are monogamous during a reproductive season and lay a single egg each year (Stonehouse 1960; Barrat 1976), thus we exclude the possibility of full siblings in the study population. Blood (~ 100 μL) samples were collected from the brachial veins using heparin-coated tubes, transferred to a Whatman filter paper, dried, and later frozen at -20°C for the genetic analysis.

1
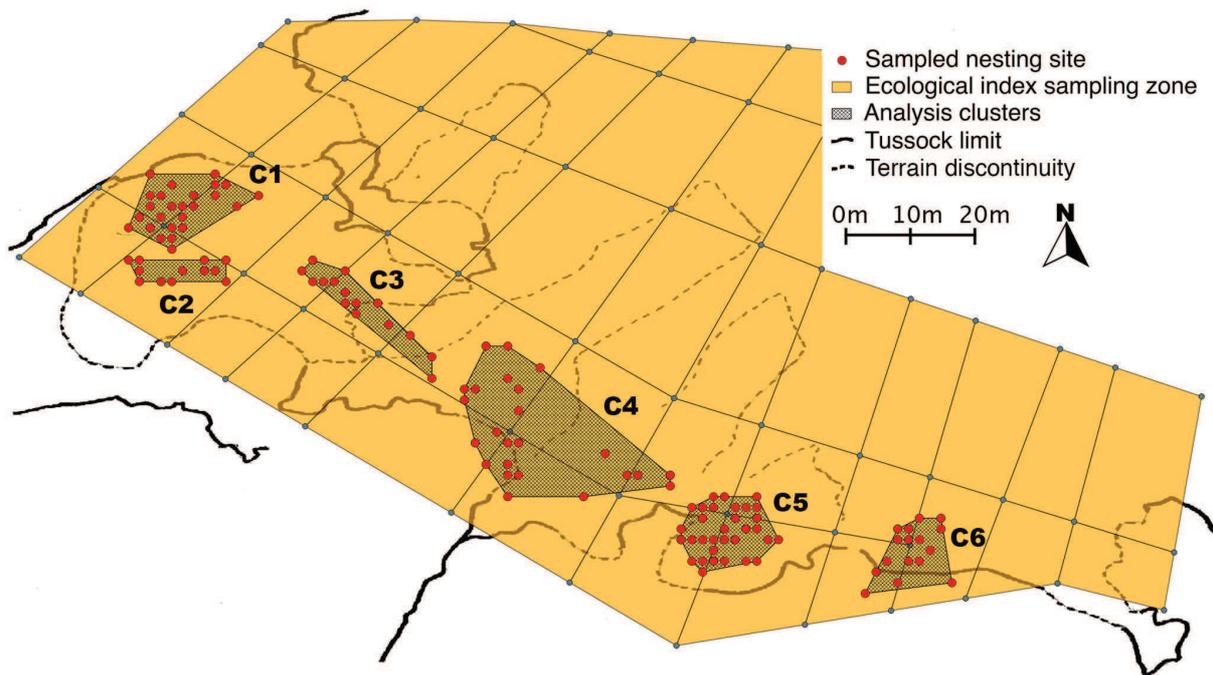
Figure 13 | Sampling distribution. Sampling was restricted to the periphery of the colony. Orange zone boundaries are marked on the ground for remote parameter assessment. Shaded clusters run from C1 (north-west) to C6 (south-east). Orange zone: extent of the colony at the peak of the breeding season.

§-61 DNA extraction, PCR and genotyping. DNA was extracted using a DNeasy® Blood and Tissue Kit (Qiagen) with a modified protocol. A prolonged initial incubation of the impregnated Whatman paper in PBS buffer (24 h) was used to dissolve dried blood cells, and a final elution in 50 μL instead of 100 μL was made to obtain higher DNA concentration. The final DNA concentration was assessed by spectrometry and adjusted to 25 ng.μL^{-1}.

Genotyping was performed with 10 microsatellite loci (Akst *et al.* 2002; Billing *et al.* 2007; Ahmed *et al.* 2009; Hart *et al.* 2011). PCR was conducted using MasterMix® (Qiagen) premixed TAQ-polymerase, dNTPs and MgCL$_2$, in a total reaction volume of 12.5 μL (6.75 μL Master-Mix, 2 μL of each primer pair, 0.5 μL DNA, H$_2$O up to a final volume of 12.5 μL). Amplification followed a touchdown protocol, with a 5-minute denaturation at 95°C, 12 amplification cy-

cles of a 30 second denaturation at 95°C, 30 seconds of annealing beginning at 63°C in the first cycle and decreasing one degree at each cycle until 52°C, and 30 seconds of elongation at 72°C, followed by 23 cycles of 30 seconds at 95°C, 30 seconds at 52°C, and 30 seconds at 72°C. Amplification was finished with 10 minutes at 72°C. The same protocol was used for all primers. FAM and HEX fluorochrome-labelled primers were used for sequencing: several microsatellite loci could be multiplexed in the same reaction (Table 1). When multiplex amplification failed, samples were amplified at each locus separately, and pooled together for electrophoresis. Sequencing was performed on an ABI3730 capillary sequencer. 1 μL of PCR product was diluted in 9 μL H2O, and 1 μL of this solution was added to 10 μL formamide and 0.2 μL GeneScan 500-ROX size standard (Applied Biosystems). Output files were analysed on GeneMapper (Applied Biosystems). A random 10% of the samples were amplified and genotyped a second time to check the repeatability and accuracy of the readings.

Table 1 | Microsatellite analysis: multiplexing parameters and summary statistics.

	Ech030		Ech036		Ech051		Ech071		AM13		B3-2		Emm4		RM3	
PCR	Multi_A		Multi_A		Multi_B		Multi_B		Single		Multi_C		Single		Multi_C	
Genotyping	Seq_A		Seq_A		Seq_B		Seq_B		Seq_C		Seq_C		Seq_A		Seq_C	
Label	HEX		HEX		FAM		FAM		HEX		HEX		FAM		FAM	
Pattern	$(CTAT)_n$		$(GT)_n$		$(GT)_n$		$(CTCAT)_n$		$(GT)_n$		$(GT)_n$		$(CT)_n$		$(CA)_n$	
Allele count	9		8		8		13		6		9		9		4	
Gene diversity	0.773		0.750		0.544		0.866		0.702		0.642		0.658		0.541	
Allelic richness	8.988		7.994		7.988		12.994		6.000		8.994		9.000		4.000	
	Allele	Freq.	Allele	Freq.	Allele	Freq.	Allele	Freq.	Allele	Freq.	Allele	Freq.	Allele	Freq.	Allele	Freq.
	267	0.024	190	0.024	188	0.012	215	0.009	109	0.006	285	0.009	233	0.003	202	0.012
	271	0.045	194	0.179	192	0.006	220	0.027	111	0.066	288	0.033	235	0.012	207	0.518
	275	0.232	196	0.003	194	0.580	225	0.051	115	0.326	290	0.009	237	0.407	208	0.438
	279	0.330	198	0.015	196	0.345	230	0.057	117	0.371	292	0.238	239	0.410	210	0.033
	283	0.223	200	0.244	198	0.039	235	0.152	119	0.228	294	0.536	241	0.087	-	-
	287	0.113	202	0.378	200	0.012	240	0.185	121	0.003	296	0.113	243	0.033	-	-
	291	0.027	204	0.125	204	0.003	245	0.176	-	-	298	0.039	245	0.024	-	-
	295	0.003	206	0.033	206	0.003	250	0.176	-	-	300	0.021	247	0.015	-	-
	299	0.003	-	-	-	-	255	0.092	-	-	302	0.003	249	0.009	-	-
	-	-	-	-	-	-	260	0.048	-	-	-	-	-	-	-	-
	-	-	-	-	-	-	265	0.015	-	-	-	-	-	-	-	-
	-	-	-	-	-	-	270	0.012	-	-	-	-	-	-	-	-
	-	-	-	-	-	-	280	0.003	-	-	-	-	-	-	-	-

§-62 Analysis of microsatellite data. Hardy-Weinberg equilibrium was tested in *adegenet* (Jombart 2008) with 100,000 permutations, and in Fstat (Goudet 1995). F-statistics were assessed in Fstat together with microsatellite summary statistics (allele range, count and frequencies, and linkage disequilibrium). Global intrinsic differentiation in the sample, regardless of any spatial grouping, was tested in Structure (Pritchard *et al.* 2000), with 200,000 burn-in and 1,000,000 steps, under Admixture model, with K values ranging from 1 to 6 (allele frequencies correlated). Log-probability of the data was calculated in Structure Harvester (Earl 2012).

§-63 Spatial autocorrelation analyses. In a population with limited, yet homogeneous, internal dispersal and gene flow, genetic drift is expected to generate a pattern of isolation by distance. Related genotypes will tend to become clustered in spatial patches, and correlation between genotypes will decay with distance (Epperson 2005). In this case, correlation between genetic and spatial distance between samples should be observed. In order to test that prediction, spatial autocorrelation analysis was performed across the whole sampling area using Genalex (Peakall & Smouse 2006), through multivariate analysis of pairwise euclidean and square genetic distances, regardless of any spatial grouping. Significance of autocorrelation was assessed through random permutation of samples across the whole area, and subsequent bootstrapping of the samples contained within pre-defined distance-classes around each individual: permutation tests are used to assess the randomness of the distribution, while bootstrapping allows for the evaluation of the weight of potential individual outliers. We used distance classes starting at 2 meters (the average minimum distance between two sampled nests), and no longer than 8 meters (the average radius of our clusters). Longer distance classes were excluded as they would give too much weight to cross-cluster comparisons. 100,000 random permutations were performed.

However, heterogeneous spatial processes may not always be detected by global spatial autocorrelation analyses (Miller 2012). Heterogeneous fine-scale genetic structure was therefore assessed in Genalex using the 2D-Local Spatial Analysis algorithm (2D-LSA, Double *et al.* 2005): each individual was tested for genetic relatedness to its *n* nearest neighbours in order to identify fine-scale

patches of lower genetic diversity. This method differs from standard autocorrelation tests in that it completely removes further distance classes from the analysis, and gives the same weight to all individuals considered as neighbours. Thus, it takes into account the possibility of locally restricted areas, within which all individuals are equivalently related and therefore do not exhibit spatial autocorrelation. Once again, significance levels were estimated through random permutation of the samples. Analyses were performed with a number of neighbours ranging from 8 to 10 (the approximate closest 5% of the colony), and 100,000 random permutations.

§-64 Inbreeding and relatedness. Individual inbreeding coefficients and pairwise relatedness were also taken as an index of local genetic structure: if potential mates are more related to each other in some areas, then offspring sampled in that area are expected to be more inbred, and potentially related to each other. Inbreeding was studied both at population and individual levels. At population level, Ballou's maximum likelihood method was preferred (Ballou 1997), since it has been shown to better estimate population parameters provided sample is large enough (Weir 1990). However, MLE methods are known to be sensible to small sample size, and they are therefore less suitable for estimating individual parameters. Individual inbreeding and relatedness were thus calculated using Ritland's method-of-moments estimators (Ritland 1996). Ballou's MLE index was calculated in *adegenet* (Jombart 2008). Individual means were extracted from a subset of 2,000 values sampled from 20,000 estimates, and were then averaged across the whole sample. Ritland's MME estimators were computed in *Coancestry* (Wang 2011). As expectations for individual inbreeding levels vary, and cannot be reliably imported from another study organism, expected inbreeding distribution was estimated through simulation. A virtual population of entirely non-related individuals (as is the expectation for a large, ideal and randomly sampled population) was generated with the same allele frequencies and per-locus homozygosity levels as the sampled colony, and empirical data was compared to the simulated individual inbreeding distribution. Difference in average individual inbreeding between the observed and the simulated distribution was assessed through a bootstrapping method as implemented in *Coancestry*: 10 independent

simulated datasets were generated. For each of them, both observed and simulated individuals were pooled, and 100,000 randomly redistributed partitions were generated. Group-averaged inbreeding difference was computed for each of these partitions, and significance of the observed result was checked against this random distribution. Observed individual inbreeding was then mapped onto the colony to identify potential high-inbreeding clusters using *Quantum GIS* (Quantum GIS Development Team, 2013).

§-65 Pairwise cluster analysis. If our second hypothesis (heterogeneous structuring processes) holds true, we expect these processes to apply differently in specific areas of the colony depending on local characteristics. We therefore performed the following analyses on the discrete natural clusters defined in the sampling area (Fig. 13), as opposed to the continuous models applied above. Genetic differentiation between clusters was tested in *Genepop* (exact G-test, default Markov chain parameter values) and *Fstat* using chi-square assessment of genotypic frequencies. Pairwise divergence in inbreeding and relatedness distribution between clusters was also assessed: pairs of individuals belonging to one cluster were compared to pairs of individuals belonging to different clusters, and significance of distribution divergence was tested in *Coancestry* (10,000 bootstrapping samples).

§-66 Site-quality descriptors analysis. To measure breeding site quality, several ecological variables were used as proxies. *(i)* For 3 consecutive breeding seasons (2010-2012), chick survival rate between hatching (January/February t) and fledging (November/December t) was measured as the proportion of marked chicks still alive at fledging (Weimerskirch *et al.* 1992). *(ii)* Parasite infestation has been shown to influence breeding success and adult survival rate in king penguins (Mangin *et al.* 2003). Thus, for 8 consecutive years (2005-2012), tick infestation was measured as the proportion of infested adults in a randomly-selected sample (N=50) within each colony grid zone. *(iii)* Finally, as early breeders lay eggs in November/December, and late breeders after January (Brodin *et al.* 1998; Descamps *et al.* 2002), an estimate of the ratio of incubating and brooding birds in early March was used, as preferred nesting sites are expected to be occupied first by

early breeders, while late breeders will occupy remaining, lower-quality areas. For 8 consecutive years (2006-2013), site occupancy timing was thus indexed as the proportion of brooding birds among 50 randomly-chosen breeders (i.e. incubating or brooding birds, leaving non-breeders aside). This results in a score of 1 for preferred early-breeding sites, and a score of 0 for locations only occupied by late breeders.

Correlation between successive year per unit of space was assessed for all three variables (Pearson's *r* test performed between successive years with all grid zones), and spatial autocorrelation of the data was assessed in *spdep* (Bivand 2013, Moran's I, two-sided test, using the closest 5%, or 8 nearest neighbours). Our underlying hypothesis being that the breeding-site location choice of an individual breeder depends on its long-term experience and knowledge of breeding-site quality, ecological data were then concatenated for all available sampling years on each space unit. Adult tick infestation on each grid-location was averaged across all 8 sampling years. Chick survival rate was spatially averaged through local spatial analysis: each sampling location was weighted with the mean survival of the closest 5% of the colony (8 nearest sampling sites) within each breeding year, and data for all years were simultaneously mapped onto the colony. Areas with generally high score therefore have a consistently high local survival rate across several breeding seasons. Spatial autocorrelation within each dataset was assessed through Moran's I test implemented in *spdep* R package (Bivand 2013), with the closest 5% of the colony defining the spatial weights. For representation purposes, each nesting location was attributed its local tick load, chick survival score and occupancy score, and values were interpolated across the whole colony in Quantum GIS, using squared inverse distance algorithm.

In order to assess the relation and overlap of the three included ecological variables, we performed a principal component analysis (as implemented in R package FactoMineR, Lê *et al.* 2008). Since we focus on three variables that seem to determine habitat quality on the periphery of the colony, but omit some factors that may interfere in other zones than our study area (e.g. vulnerability to flooding, or density pressure), we restricted the PCA to the peripheral area where

our genetic sampling is restricted. Each variable was averaged by grid zone, across all available years. The first principal component was plotted on the colony using Quantum GIS.

Results

§-67 Microsatellite data. Of the 10 microsatellite loci tested for genotyping, only 8 were successfully amplified, and were used in the subsequent analyses. Ech011 amplified irregularly in king penguins under the tested PCR conditions, and Ech081 was repeatedly scored as more than 2 alleles per genotype. Only Ech030, Ech036, Ech051, Ech071, AM13, B3-2, Emm4 and RM3 were therefore retained for genotyping. For these, scoring repeatability was of 100% across our random replicates.

The total population was found to be in Hardy-Weinberg equilibrium. After 100,000 randomisations, no locus showed significant departure from Hardy-Weinberg equilibrium (*P-values*: Ech030 = 1; Ech036 = 0.9997; Ech051 = 0.3880; Ech071 = 1; AM13 = 1; B3-2 = 0.4948; Emm4 = 1; RM3 = 0.0697). F_{IT} was not found to be significantly different from zero for the whole sample (F_{IT} = 0.0259), although it was significantly higher for one locus (Ech071: F_{IT} = 0.1275). Considering this might be a sign of weak linkage to a region under selective pressure, subsequent analyses were therefore tested both including and excluding this locus. No locus was found to be under linkage disequilibrium. Allele frequencies, counts, and genetic diversity are given in Table 1.

Population inbreeding indicator mean value across our sample was F = 0.2321 ± 0.0958 (Ballou's MLE estimator, standard error: 0.0074). At the individual level, MME inbreeding coefficients were found to deviate from a random distribution. In 80% of our simulations, the empirical data fell outside the 95% interval of the random distribution, and in all cases the difference was clearly positive (empirical mean inbreeding clearly higher than simulated). In particular, the lower (outbred) range was strongly under-represented as compared to a random, non-related sample as

simulated in *Coancestry* (Fig. 14b-c). Ritland's inbreeding coefficient was then mapped on the

colony. Two more inbred regions appeared, at the south-east and in the centre of the sampling

area (Fig. 15a), corresponding to clusters C3 and C5-C6.
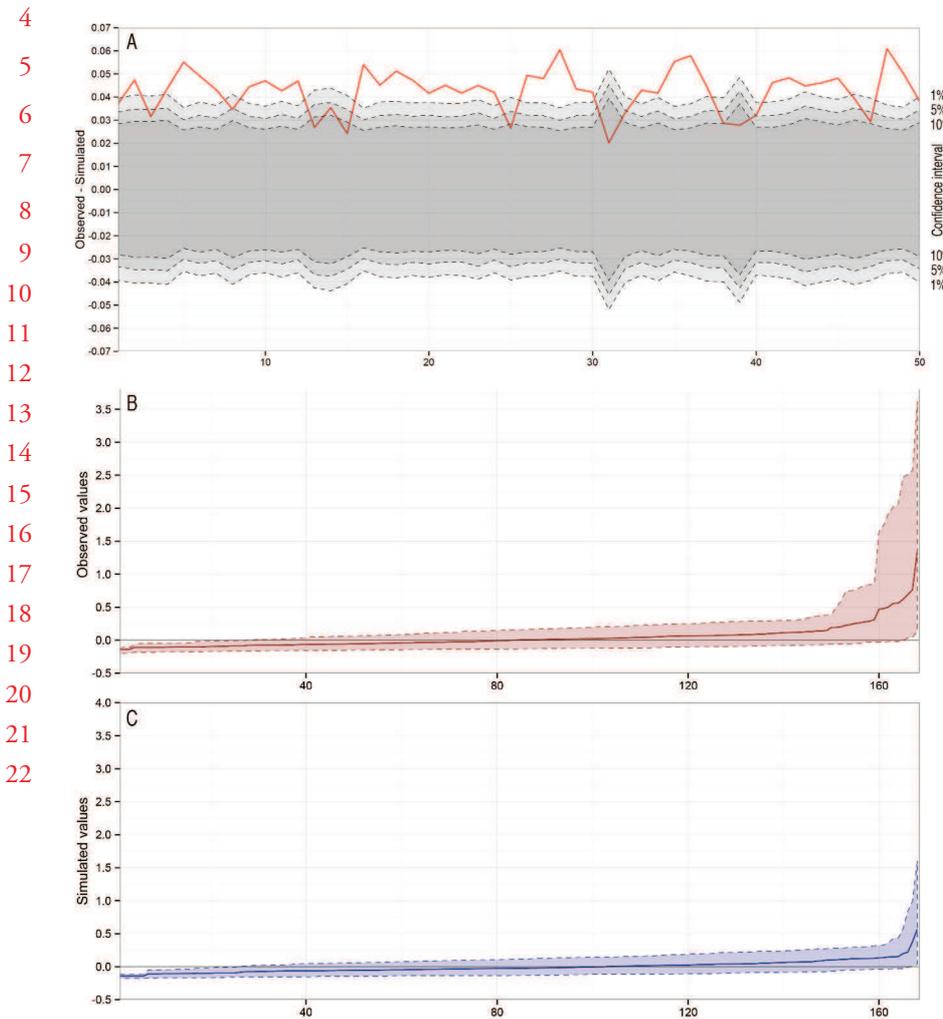
Figure 14 | Observed individual inbreeding distribution deviates from expected distribution in a non-related sample. (A) Difference between simulated and observed mean population inbreeding level (Ritland's coefficient) for 50 simulated datasets. Solid red line: observed difference. Gray intervals: 1%, 5% and 10% confidence intervals. (B) Observed distribution in the sample. (C) Expected distribution in a non-related population, given the same parameters as the observed population.
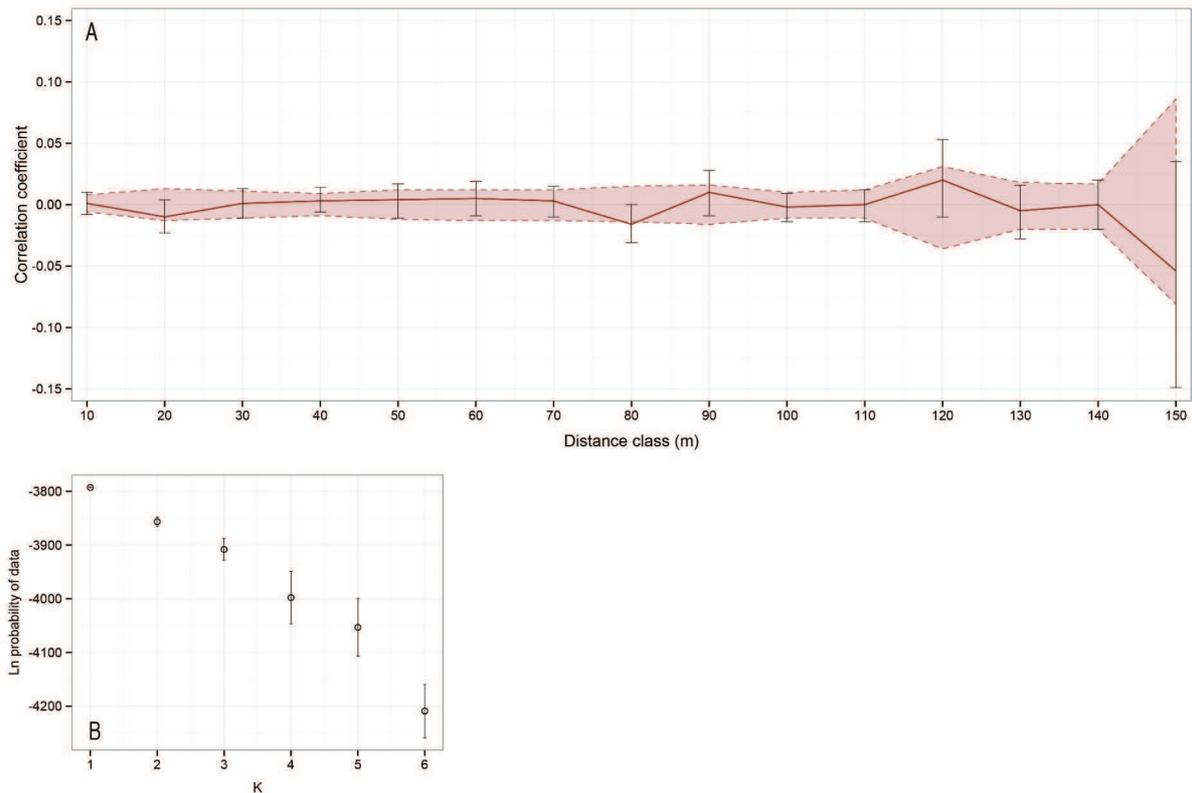
Figure 15 | Individual inbreeding and nearest-neighbours-relatedness tend to have a clustered distribution throughout the colony. (A) Distribution of Ritland's individual inbreeding coefficient along the sampling area. Shaded zones represent analysis clusters C1 to C6. Gray circles signal point displacement for representation purposes (B) 2D-LSA scores (9 neighbours analysis). Red triangles represent individuals that are significantly more related to their 9 nearest neighbours than to random individuals.

§-68 Spatial analysis. Spatial autocorrelation tests performed on the whole population in *Genalex* did not yield any significant structure across the sampling area (Fig. 16a), suggesting no visible decay in correlation in the first distance classes, as would be expected if genetic diversity varied along a gradient across the colony. Intrinsic clustering of the dataset, assessed in Structure, did not yield any significant results either (Fig. 16b). In our 2D-LSA analyses however, a maximum of 10 individuals across our sample were found to have significant genetic correlation with their 9 nearest neighbours ($P < 0.05$). It is noteworthy that these individuals were clustered in two groups that strongly overlapped with the higher-inbreeding regions identified previously (clusters

C3 and C5, see Fig. 15b). Genetic correlation decayed quickly when we increased the number of neighbours used in the analysis above the nearest 5% of the colony.
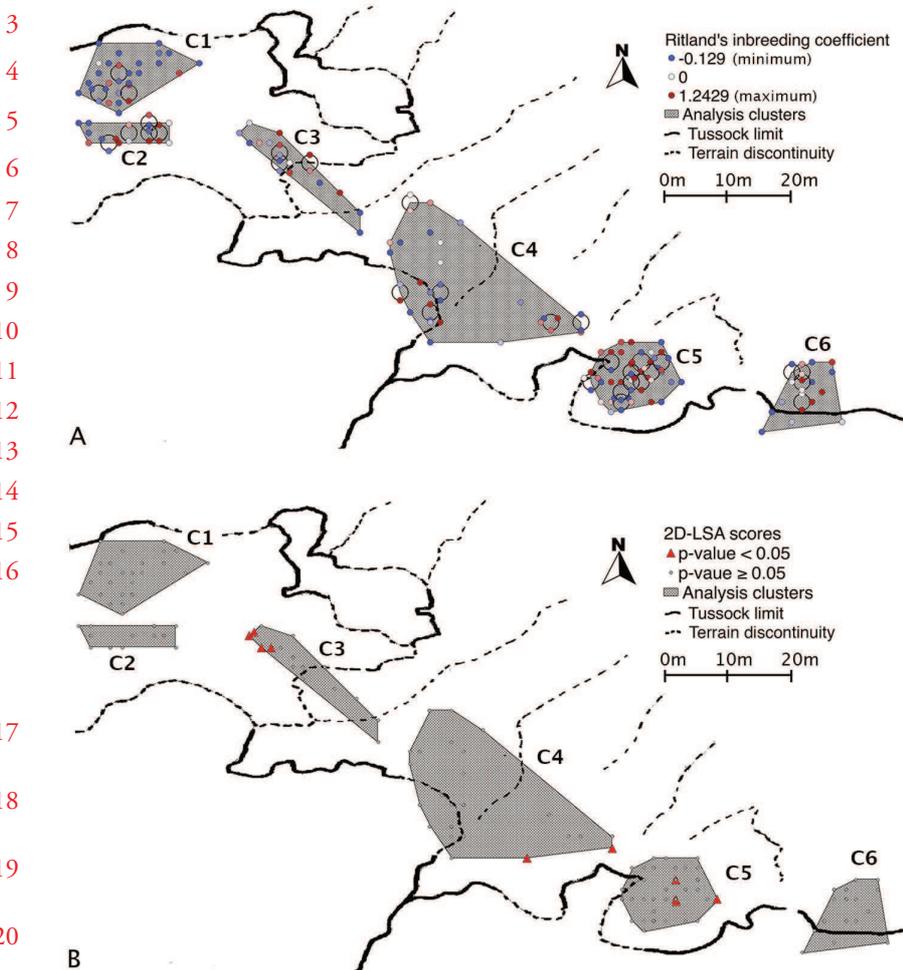
Figure 16 | Spatial correlation and Intrinsic clustering tests do not support strong structure. (A) Spatial correlogram. Solid red line: observed correlation, by distance classes. Dashed red lines: random expectation confidence interval, determined by bootstrapping. (B) Ln probability of the genetic data under six different clustering situations (from 1 to 6 populations).

Cluster differentiation analyses performed in *Genepop* showed that cluster C3 was significantly different from three other clusters (genotypic differentiation, exact *G*-test: P_{C1} = 0.0277, P_{C4} = 0.0326, and P_{C5} = 0.0268). However, pairwise F_{ST} comparisons did not yield any significant result.

Heterogeneity in inbreeding distribution across different clusters was tested pairwise in *Coancestry* (bootstrapping: 10,000): cluster C1 was found to have significantly (P_{C1} < 0.05) less inbreeding than clusters C2, C3, C5 and C6 (but not C4). Most significant was the comparison between C1 and C5 (Table 2). In the same way, pairwise individual relatedness was found to be signifi-

cantly higher in C6 than in C1 and C4 (other pairwise comparisons were non-significant, see Table 2).

Table 2 | Pairwise cluster comparison of inbreeding and relatedness distributions reveal genetic heterogeneity in the sampling area. *Upper triangle*: Ritland's individual inbreeding coefficient. *Lower triangle*: Ritland's pairwise relatedness coefficient. The empirical coefficient is shown in bold, followed by the 95% confidence interval. Significantly divergent comparisons are shown in bold type with asterisks.

	Cluster 1	Cluster 2	Cluster 3	Cluster 4	Cluster 5	Cluster 6
Cluster 1		**-1.1002e-1** *8.4695e-2* **C1<C2*** *-8.5559e-2*	**-1.5355e-1** *1.0299e-1* **C1<C3*** *-1.2204e-1*	**-3.9188e-2** *4.0492e-2* C1=C4 *-4.3607e-2*	**-7.0628e-2** *5.2465e-2* **C1<C5*** *-5.1926e-2*	**-6.3993e-2** *5.8778e-2* **C1<C6*** *-5.8408e-2*
Cluster 2	**1.0118e-2** *2.0834e-2* C1=C2 *-2.3307e-2*		**-4.3531e-2** *1.5727e-1* C2=C3 *-1.6080e-1*	**7.0834e-2** *7.9085e-2* C2=C4 *-7.1760e-2*	**3.9394e-2** *8.1326e-2* C2=C5 *-7.3237e-2*	**4.6029e-2** *1.0041e-1* C2=C6 *-9.9416e-2*
Cluster 3	**-4.0898e-3** *2.1038e-2* C1=C3 *-2.3405e-2*	**-1.4208e-2** *3.2650e-2* C2=C3 *-3.4437e-2*		**1.1436e-1** *1.1821e-1* C3=C4 *-8.6573e-2*	**8.2925e-2** *1.1181e-1* C3=C5 *-8.5461e-2*	**8.9560e-2** *1.4201e-1* C3=C6 *-1.2877e-1*
Cluster 4	**4.5949e-3** *1.1684e-2* C1=C4 *-1.1589e-2*	**-5.5231e-3** *1.9016e-2* C2=C4 *-1.6720e-2*	**8.6848e-3** *-1.7182e-2* C3=C4 *1.7959e-2*		**-3.1439e-2** *4.7974e-2* C4=C5 *-4.4700e-2*	**-2.4804e-2** *4.7573e-2* C4=C6 *-5.3248e-2*
Cluster 5	**8.1903e-3** *1.4813e-2* C1=C5 *-1.3828e-2*	**-1.9277e-3** *2.4833e-2* C2=C5 *-2.0848e-2*	**1.2280e-2** *2.7328e-2* C3=C5 *-2.2622e-2*	**3.5953e-3** *1.2583e-2* C4=C5 *-1.1928e-2*		**6.6350e-3** *5.8991e-2* C5=C6 *-6.3224e-2*
Cluster 6	**1.8131e-2** *1.6586e-2* **C1<C6*** *-1.7630e-2*	**8.0130e-3** *2.6127e-2* C2=C6 *-2.4755e-2*	**2.2221e-2** *2.3997e-2* C3=C6 *-2.3723e-2*	**1.3536e-2** *1.3248e-2* **C4<C6*** *-1.3465e-2*	**9.9407e-3** *1.8263e-2* C5=C6 *-2.1122e-2*	

Our analyses revealed strong overlap between this clustered pattern and spatial distribution of ecological site-quality indicators. Tick infestation and site occupancy timing showed strong year-to-year correlation across all 8 sampled years (slope c_t, intercept i_t and significance level of the correlation p_t for tick load from one year to the previous one, starting in 2004: $c_{2004}=0.400$ $i_{2004}=0.006$ $p_{2004}\approx0$; $c_{2005}=0.465$ $i_{2005}=0.034$ $p_{2005}\approx0$; $c_{2006}=0.146$ $i_{2006}=0.058$ $p_{2006}<0.05$; $c_{2007}=0.406$ $i_{2007}=0.021$ $p_{2007}\approx0$; $c_{2008}=0.577$ $i_{2008}=0.068$ $p_{2008}<0.001$; $c_{2009}=0.424$ $i_{2009}=0.062$ $p_{2009}<0.01$; $c_{2010}=0.192$ $i_{2010}=0.037$ $p_{2010}<0.01$; $c_{2011}=0.743$ $i_{2011}=0.063$ $p_{2011}\approx0$. For site occupancy timing from each year to the previous one, $c_{2007}=0.526$ $i_{2007}=0.279$ $p_{2007}\approx0$; $c_{2008}=0.712$ $i_{2008}=0.112$ $p_{2008}\approx0$; $c_{2009}=0.462$ $i_{2009}=0.331$ $p_{2009}\approx0$; $c_{2010}=0.664$ $i_{2010}=0.226$ $p_{2010}\approx0$; $c_{2012}=0.159$ $i_{2012}=0.062$ $p_{2012}<0.01$; $c_{2013}=0.010$ $i_{2013}=0.250$ NS. Too much missing data in 2011 led us to discard this year, and to

correlate 2012 values with 2010). Chick survival was found to be correlated between 2010 and 2011 (slope 1.548, intercept 0.168, p-value 0.0427), sampling did not overlap suffienciently between years 2011 and 2012 for comparison. All three variables showed a markedly structured, gradient-driven distribution across our sampling range (Bivand 2013) and were found to be strongly autocorrelated (Moran's I, two-sided test, using the closest 5%, or 8 nearest neighbours, all p-values < 0.01). Occupancy timing and chick survival distributions appeared to largely overlap, and to be partly complementary to tick infestation distribution. Comparison between C1 and C5 was especially significant for all variables: tick infestation varied from 0.188 ± 0.095 in C1 to 0.083 ± 0.019 in C5, while averaged chick survival ranged from 0.208 ± 0.058 in C1 to 0.398 ± 0.130 in C5, and occupancy timing index from 0.303 ± 0.206 in C1 to 0.488 ± 0.056 in C5 (Fig. 17). Principal component analysis results support this view: the first axis, which accounted for 40.5% of the total variation (correlation coefficients, contributions: chick survival 0.82, 55.6%, occupancy timing 0.62, 31.6%, tick load -0.39, 12.8%), separates between the south-eastern end of the colony, of higher habitat quality, and the western end, of lower habitat quality (Fig. 18). However, neither of the individual habitat quality descriptors correlates directly with individual-level or cluster-level genetic descriptors.
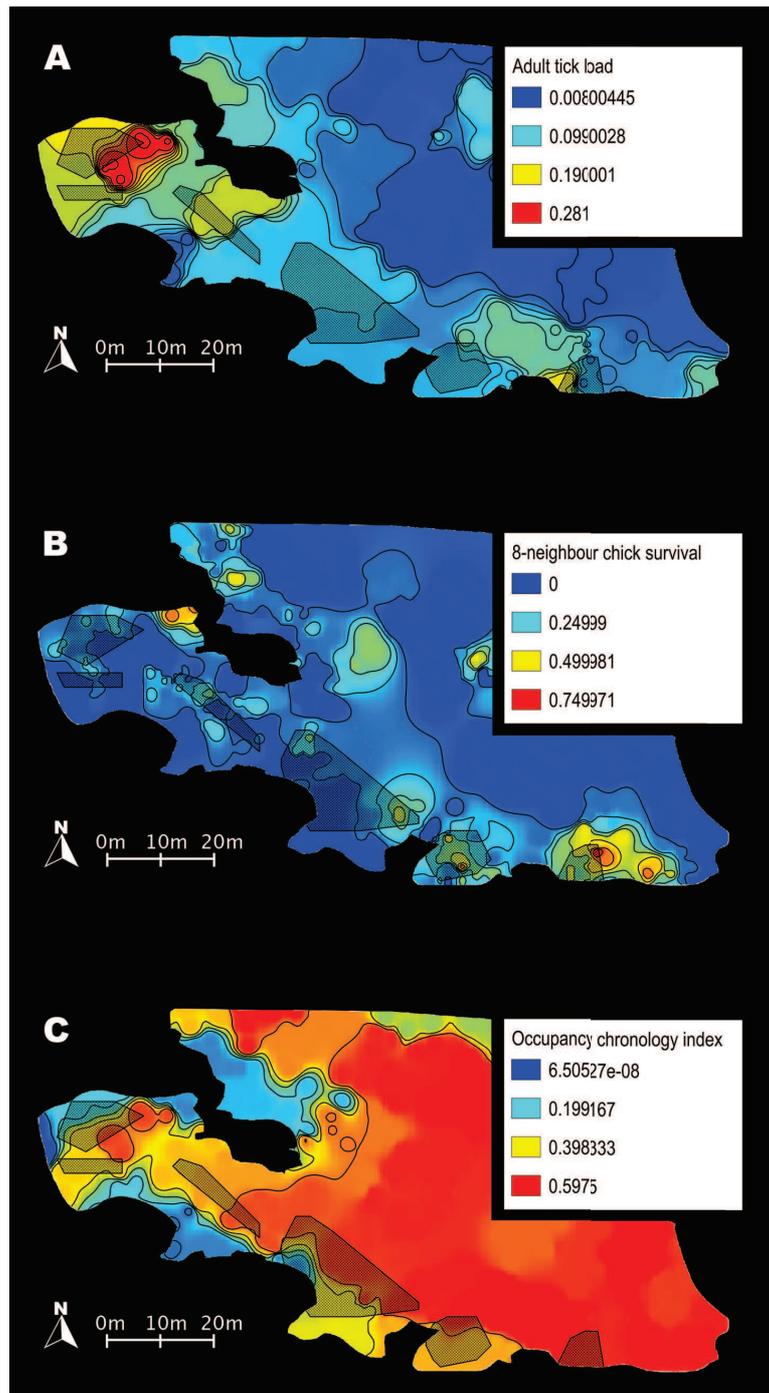
Figure 17 | Ecological descriptors of breeding-site quality exhibit a strongly heterogeneous distribution across the colony. (A) Adult tick load, averaged for years 2005-2012. Contour lines: 0.02 steps. (B) 8-neighbour chick survival, averaged for years 2010-2012. Contour lines: 0.1 steps. (C) Site occupancy chronology, averaged for years 2006-2013. Ratio of brooding birds amongst 50 randomly selected breeders. Contour lines: 0.1 steps.
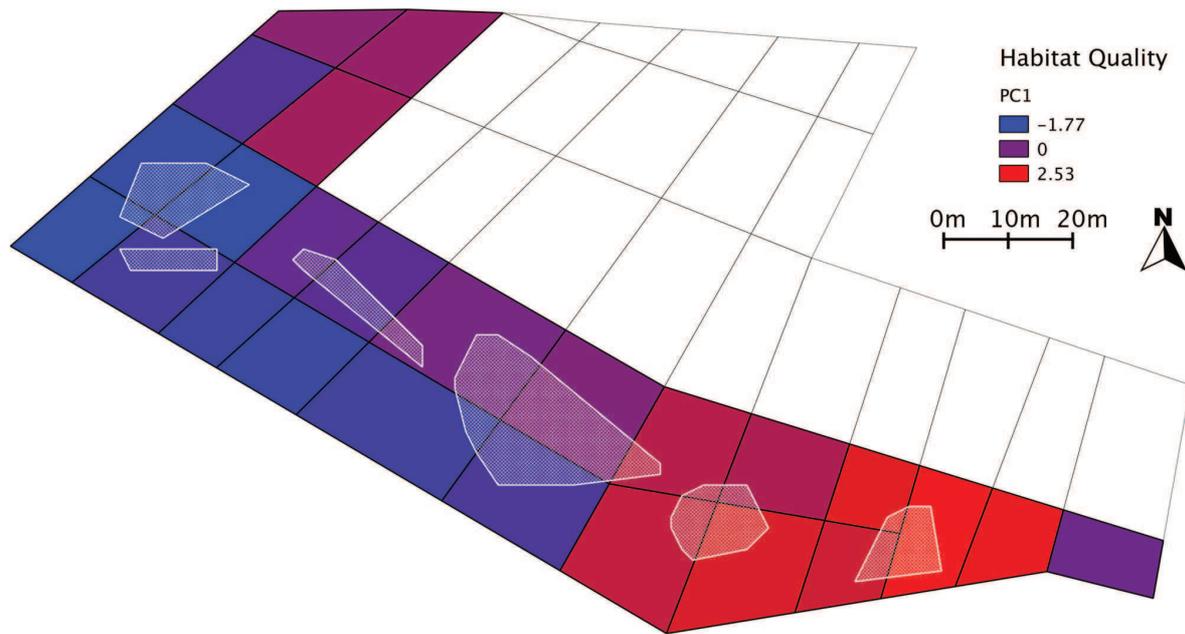
1 **Figure 18 | First axis of principal component analysis as a summary habitat-quality index.** White
2 polygons: clusters C1 to C6.

Discussion

4 *§-69 A near-panmictic population.* Our data on colony-wide spatial structure appear to contradict

5 the hypothesis of a strong, homogeneous process shaping the genetic structure of our studied

6 king penguin sub-population. Hardy-Weinberg equilibrium held across all loci, population-wide

7 F_{IT} was not significantly skewed (Wright 1965; Holsinger & Weir 2009), and spatial autocorrela-

8 tion tests performed across the whole sampling area were non-significant (Epperson 2005; Kanno

9 *et al.* 2011). Analyses of intrinsic partitioning indeed systematically pointed to a non-structured

10 population (Falush *et al.* 2003). Although tests of genotypic differenciation did yield significant

11 results for cluster C3, this finding is subject to caution, as it is not confirmed by pairwise Fst

12 comparisons. This discrepancy may be due to the non-homogeneous inbreeding probability, as in

13 inbred individuals, genotype distribution departs from the neutral expectations (and thus be bio-

14 logically menaningful); however, G-test has been shown to often be over-sensitive (Balloux &

Lugon-Moulin 2002), and to yield numerous false positives (Ryman *et al.* 2006), this result should therefore be taken with caution, as it is not supported by other tests. These findings allow us to reject strong underlying structure resulting from constant, homogeneous processes such as multi-generation isolation of sub-colony units. Yet, in wild populations, a lack of global visible genetic structure does not necessarily imply the absence of structuring processes (Osborne *et al.* 2007). Indeed, spatial structure may evolve as a secondary dependency to heterogeneous habitat features (Majumdar *et al.* 2011; Miller 2012).

§-70 Heterogeneity in inbreeding probability. Our investigations of inbreeding probability high-light the fact that analyses taking into account possible heterogeneity in structuring processes do point towards a non-panmictic population. Observed population inbreeding descriptor $F = 0.231$ is remarkably high - it implies a homozygosity level close what is expected in a half-sibling relatedness context, for example (Wright 1978; Ballou 1997). Although homozygosity-based in-breeding calculations do not necessarily imply true (i.e. pedigree-deduced, Keller & Waller 2002) inbreeding (Balloux *et al.* 2004), our result shows a strong bias in the mating system, resulting in non-random gene mixing. This interpretation is supported by the individual inbreeding distribu-tion, which significantly deviates from an equivalent random distribution, with outbred classes being strongly under-represented as compared to a non-related group of individuals (Keller & Waller 2002). Moreover, more inbred individuals tend to be concentrated at the south-eastern end of the sampling range of our sub-colony (clusters C5 and C6), while more outbred individu-als are more frequent at the north-west end (cluster C1). Pairwise relatedness within spatially de-limited areas has also been shown to reflect weak genetic structure in wild populations (Jones & Wang 2012). Not surprisingly, we found that individuals that are significantly related to their di-rect neighbours tend to cluster in areas that largely overlap more inbred areas.

§-71 Pairwise cluster differentiation. Our pairwise cluster analysis supports such a structure. Geno-typic differentiation points towards structural divergence between the centre and the extremities of our sampling range. Yet, the genotypic structure detected is globally weak. This is an expected

result, as Waples and Gaggiotti (Waples & Gaggiotti 2006) showed that microsatellite-based genotypic cluster divergence faded out when movement among clusters exceeded 10%, which is likely the case in seabird colonies (e.g. Steiner 2005). More importantly, the north-west cluster (C1) appeared significantly less inbred than any other cluster. Similarly, C1 and C4 both showed low internal pairwise relatedness levels. This trend was not marked enough to be significant throughout all pairwise comparisons (comparison between C1 and C5, for instance, was near-significant).

These different elements outline an underlying structure in which the north-west end of the colony (cluster C1 in particular) appears more outbred, with lower pairwise-relatedness levels, and the south-east end (especially cluster C5) is more inbred, with higher relatedness levels. Such a structure implies that the probability for a breeder to mate with a related individual is not constant across the colony: potential mates are more likely to share identical alleles (either by descent or by state) at the south-east end of the colony than at the north-west end. This result is in accordance with the findings of Steiner and Gaston (Steiner 2005), who showed, on phenological grounds, that, in colonial seabirds, even a very short-distance intra-colony dispersal may significantly impact breeding success and inbreeding avoidance.

§-72 Heterogeneity in breeding site quality. Interestingly, the observed heterogeneity in genetic structure we found within this king penguin colony appeared to be related to the quality of the breeding sites. Tick infestation has a local maximum around C1, i.e. at the north-west end of the range, and lower values elsewhere. In contrast, chick survival has local maxima around C5 and C6, and very low values in C1. The chronology of settlement-site occupancy also appeared to be strongly associated with the quality of the breeding sites. Indeed preferred areas at the south-east end of the colony were occupied first, and less-favoured spots at the north-east end were occupied by late breeders. The fact that no significant correlation could be found between habitat descriptors and genetic parameters may be a consequence of very limited sample size, as our sampling area is not large enough to allow for replicate situations. It may also be explained by the limited

number of ecological parameters monitored, as several other constraints (such as flooding, fine-scale variations in predation pressure, or heterogeneous inter-annual variability) may also interact to define high- and low-quality habitat.

However, overall, principal component analysis reveals a gradient from higher habitat quality at the south-eastern end of the colony, around clusters C5 and C6, to lower quality at the western end (clusters C1 and C2), and this pattern globally mirrors genetic heterogeneity structure. This fact may be explained as being a consequence of differences in fine-scale philopatric behaviour: while king penguins have been shown to select their breeding location according to site-specific characteristics at the breeding-season scale (Bried & Jouventin 2001), our results suggest that breeding experience may drive settlement site choice across multiple generations, and that this process may be widespread enough to impact genetic patterns in the colony.

§-73 Effects of demography and life-history. Part of the relative weakness in the genetic signal may be explained by the limited number of markers used; however microsatellite loci have a high mutation rate in spheniciforms (Shepherd & Lambert 2005; Hart *et al.* 2011), and generally enough polymorphism to allow for fine-scale genetic comparisons within a population (Gorospe & Karl 2013).

A possible bias due to the exclusively peripheral sampling design (required in order to minimize colony disturbance) may also be considered: indeed, the peripheral areas have generally higher tick load and later settling dates. However, central areas do suffer from specific pressure, such as higher density and associated stress levels (Viblanc *et al.* 2014). Predation pressure, on the other hand, is not expected to differentiate peripheral and central areas. Although it has been shown that immediately peripheral birds spend twice as much time interacting with predators than central birds (Coté 2000), most of the chick mortality has been shown to happen during winter, especially through predation by the giant petrel (*Macronectes giganteus*, Hunter 1991), at a time when chicks have gathered in creches. Moreover, our field observations tend to show that summer predation on eggs and small chicks by the subantartic skua (*Stercorarius antarcticus*) is not

more frequent at the periphery than at the center of the colony. Finally, the overall breeding success has been shown to be independent of central or peripheral location (Descamps *et al.* 2009), which supports the idea that the purely geometric location in relation to the colony (such as center-to-periphery gradients) is not the main determinant of habitat quality. We can therefore assume that spatial processes driving breeding site choice identified on the edges of a colony should also apply at its centre.

Another possible limit to our study may arise from our choice of sampling pre-dispersal chicks, as opposed to adults, and to analyze nuclear autosomal markers (as opposed to sex-specific ones). Indeed, a constant bias such as sex-specific dispersal may lead to more genetic structure in one sex than the other, a phenomenon which may be blurred by our sampling of pre-dispersal individuals of undetermined sex. Yet, although sex-specific dispersal is a common phenomenon in birds (Clarke *et al.* 1997), on a mutli-generation scale it is only expected to influence the structure of sex-specific markers, and not of autosomal loci, which are subject to admixture (Prugnolle & De Meeûs 2002). Thus, our sampling design should only reduce our ability to detect instantaneous sex-specific phenomenons, and not population-wide, sex-independent structures.

However, a more likely explanation of the weakness of the detected signal may lie in inter-annual habitat variability: if local philopatric maxima are conditioned by the past breeding experience of individuals, they may be subject to medium time-scale variation, that is, higher-quality breeding sites may change every few generations, depending on flooding variations, ground erosion, or parasite pressures. These very fine-scale shifts may be sufficient to weaken genetic structure at the colony level on longer time scales.

Moreover, at the individual scale, it may be difficult for a breeder to retain its breeding site consistently across all breeding seasons. Indeed, the complex breeding cycle of the King penguin extends for more than a year, implying that birds are alternately early or late breeder (Stonehouse 1960; Stonehouse 1960; Barrat 1976), regardless of individual quality (Le Bohec *et al.* 2007). Therefore, even experienced breeders might sometimes be forced to settle in lower-quality spots

due to site-occupancy contingency at the season-level, and the output of their previous breeding season. This process could maintain a sufficient rate of genetic mixing in the whole colony despite a general trend towards local structure.

Finally, king penguin population genetic structure may still bear the imprint of recent demographic history. Most of the sub-Antarctic king penguin colonies suffered a drastic reduction at the turn of the nineteenth century, as sealers slaughtered them to near-extinction on most of the archipelagos for oil production. They recovered, but recently (Rounsevell & Copson 1982; Gales & Pemberton 1988). Similar colonies on Macquarie island were reportedly reduced to less than 1,600 breeding pairs in 1937 (Falla 1937). Rapid recovery followed the cessation of slaughtering (Rounsevell & Copson 1982; Delord *et al.* 2004), and population growth rate is suggested to have neared intrinsic growth rate for three decades (Delord *et al.* 2004). This complex demographic history is also expected to have had an impact on colonial genetic patterns. Even under the assumption of strong, consistent processes driving structure across several generations, recent rapid growth may weaken a long-term signal in present-day colonies (Waples & Gaggiotti 2006), though in that case, the use of more markers or more individuals may increase the strength of the signal (Banks & Peakall 2012).

§-74 Heterogeneity as a mixing mechanism. Despite these different factors, the convergence of genetic and ecological indicators outlines the structural heterogeneity inherent to penguin colonies, and probably to other colonial seabirds (such as guillemots or eiders, Frederiksen & Petersen 1999; Pearce *et al.* 2005). However, our data point towards generally transient processes, which are not homogenous and stable enough in time to impact colony structure on a large spatial and temporal frame. Local heterogeneity appears to be dependent on medium-scale factors, such as individual experience and breeding history, but also present-day site quality, and should therefore be considered as a fundamental feature of coloniality in seabirds: local philopatric hotspots are counterbalanced by active outbreeding regions, thus preserving global genetic diversity and mixing at the colony level. Instead of being an exception in an otherwise strongly philopatric system,

we therefore believe that these lower-quality, strongly outbred areas are playing an active role in mitigating the potentially drastic effects of strong natal philopatry on local genetic drift and loss of diversity. Our findings illustrate how individual life-history decisions, such as site-fidelity or dispersion, are related at the colony level with local environment features. These constitute true colony processes that actively enhance higher-scale population functions such as genetic mixing and inbreeding avoidance, thereby allowing the persistance over time of philopatric colonial systems.

Appendices

Chapter 4: The King synnome

This chapter is based on Cristofari R, Liu X, Bonadonna F, Cherel Y, Le Maho Y, Pistorius P, Raybaud V, Stenseth NC, Le Bohec C & Trucchi E, **Stepping-stone range shifts in response to climate change in the Southern Ocean**. (*in prep.*)

Context

§-76 From local to global gene flow. In the previous chapter, we investigated the patterns of very fine-scale local dispersal within a colony of king penguins. The absence of intra-colonial genetic structure suggests that philopatry does not apply to particular areas within the colony beyond a handful of generations. However, at the colony level, philopatry is a strong and fairly well documented behaviour (see *e.g.* Barrat 1976; Bried & Jouventin 2001; Saraux *et al.* 2011b). Juvenile return rates to the natal colony may reach up to 87% in that species (Saraux *et al.* 2011a). Yet, while return rate may be measured accurately, assigning the respective roles of mortality and dispersal in the non-returning fraction of the population is a challenging task. At the single-generation scale, this may be a methodological dead-end: however, a lower bound may be placed on average dispersal rates at the coalescent scale using gene flow as an indicator of the migration patterns of individuals. In the present chapter, we assess the extent of genetic structure between colonies of King penguins on a global scale. Based on direct observation of philopatric behaviour

(Le Bohec *et al.* 2008; Saraux *et al.* 2011b) and on the parallel with other seabird species (Friesen *et al.* 2007), a certain degree of genetic isolation would be expected in this species. However, the high dispersal potential of the King penguin, that is known to travel considerable distances outside of its breeding season (thousands of kilometres, see Bost *et al.* 2013), may promote long-distance gene flow and counteract the drift consequences of local philopatry: so that it is uncertain which force, of philopatry and dispersal, has the upper hand in shaping the genetic patterns in the species.

§-77 Understanding the dynamics of contemporary structures. As sentinel species of the Southern Ocean (see §18 p. 65), King penguins are the object of a long-term monitoring program on Possession Island (see §26 p. 81). However, extrapolating the findings of local surveys to the whole species requires a set of assumptions that may not be easily verified. The degree of demographic independence of the colonies, in particular, raises central concerns. Direct comparison of the demographic trend of the five King penguin colonies on Possession Island showed that colonies followed different demographic trajectories (Delord *et al.* 2004). However, true demographic independence requires not only divergent, but fully uncorrelated trends between demes (Waples & Gaggiotti 2006). In other words, the transfer of individuals from one colony to another results in divergent demographic patterns, but also demographic dependency. Delineating the one from the other is essential if we are to draw global conclusions from single-colony surveys: *(i)* true demographic independence would imply that the main driver of colony trajectory is the local environmental conditions, while *(ii)* complex demographic correlation between colonies may blur the direct relationship between environmental conditions and local demographic patterns. In the first case, climate-envelope-type model may be applied successfully, while more complex modelling procedures may be necessary in the second case. Moreover, our understanding of the demographic trajectory of the King penguin is further complicated by its recent history of near-extinction, as steep population growth in the recent past is mostly an artefact of population recovery (see §22

p. 75 for details): thus, our knowledge both of population structure, and of demographic trends, should be rooted in a longer time frame in order to detach itself from these recent events.

§-78 Integrating genetics with climate models. Evolutionary and ecological proxies of species demography are grounded in very different conceptual frameworks (see §2 p. 25 for an overview). While the ecological paradigm relies on the short-term, local observation of the species in order to extract larger order parameters, evolutionary studies use the information contained in the species' coalescent structure to infer long-term demographic events. Relating these demographic histories with environmental variables (typically climate) thus also relies on very different principles. A commonly used approach for ecological-scale surveys is the «climate-envelope» approach (*e.g.* Pearson & Dawson 2003; Hunter *et al.* 2010; Péron *et al.* 2012; Jenouvrier *et al.* 2014), in which precise, fully quantitative demographic data is the response variable explained by a wide set of loosely correlated environmental parameters: the resulting correlative models can be extended into future climate projections, with a rather large set of of assumptions (*e.g.* fully realised potential niche, or «relevant» - as opposed to coincidental - observed correlations, see Pearson & Dawson 2003). Genetic data, however, will not usually lend itself to such an approach: demographic reconstructions are more qualitative than quantitative (in particular because both the size of population and the extent of changes are scales by an unobserved long-term substitution rate, and because of the loose relationship between effective and true population size, see §41 p. 103), and few environmental variables are available on a comparable time scale (see §9 p. 42) - so that the lack of correlation between reconstructed demography and climate (*e.g.* Morin *et al.* 2015) may be either explained by the low sensibility of the species, or of the methods. The preferred approach must be robust to these shortcomings: for example, a hypothesis-testing framework may be used instead of an agnostic exploratory one. Prior conceptions about the determinants of a species' range or demographics may be examined throughout the history of the species, and their long-term validity can be assessed, without necessarily establishing a direct, quantitative relationship between them. This is the approach that we develop in this chapter. Relying on the general

characteristics of the King penguin's breeding and foraging biology, we extract traits that appear to be proximal determinants of its survival and breeding success, and broad, easily observable indices related to these traits, in order to assess their (mostly qualitative) realisation at different periods of time.

Abstract

Range shift is the primary short-term response of species to rapid climate change, but may be challenged by natural or anthropogenic ecosystem fragmentation. Using the global King penguin (*Aptenodytes patagonicus*) population as a model for top-predator climate-induced range shift in a fragmented landscape, and integrating a large set of ecological and genomic data with general circulation models, we show that the panmictic King penguin population responded strongly to climate change throughout the late Quaternary, and predict that up to 70% of the present-day population will be threatened before the end of the century if no immediate step is taken. By showing how habitat fragmentation can exacerbate the effect of global warming towards biodiversity collapse, we stress the urgency of tangible actions to limit global temperature increase.

Results

§-79 Expected responses to climate change. While the impact of anthropogenic global changes on biological communities is beyond question (Thomas *et al.* 2004; Pacifici *et al.* 2015), the nature and extent of species responses are generally still imperfectly understood (Pereira *et al.* 2010; He & Hubbell 2011; Pacifici *et al.* 2015). At the species level, three fundamental mechanisms interact in determining the response to climate change: (*i*) *phenotypic plasticity* (Charmantier *et al.* 2008; Hoffmann & Sgrò 2011), (*ii*) *adaptive microevolution* (Bradshaw & Holzapfel 2006; Hoffmann & Sgrò 2011), and (*iii*) *range shift* (Chen *et al.* 2011; Beaugrand *et al.* 2015). Although important in the short-term, plasticity has a high fitness cost (Van Buskirk & Steiner 2009) and may rapidly reach its limits (Auld *et al.* 2009). On the other hand, the fast rate of current climate

change (Mahlstein *et al.* 2013) may outpace the potential rate of microevolutionary responses, especially for species that have long generation times (Hoffmann & Sgrò 2011) and low genetic diversity (Hoffmann & Sgrò 2011; Norberg *et al.* 2012). Thus, range shift is emerging as a major feature of species response to fast environmental change (Wiens *et al.* 2010). However, the fragmentation of ecosystems, mostly due to a growing anthropogenic pressure, implies that newly available habitats may be beyond reach for most of the species. Moreover, the uncoupling of climate change between geographical areas (Burrows *et al.* 2014) imposes additional constraints on species that rely on different territories (*e.g.* migratory species, or long-distance central-place foragers). This is especially true in the Alpine and Polar Regions (Williams *et al.* 2007), which may act as "climate sink areas" where local suitable ecological conditions disappear instead of being displaced (Burrows *et al.* 2014). In addition, habitat fragmentation may exacerbate the effect of climate change for higher trophic level taxa: in particular, the complex response of top predators, which integrate changes occurring at all levels of the trophic network (Zarnetske *et al.* 2012) and largely determine ecosystem resilience (Heithaus *et al.* 2008), may be the key to understanding the depth of current changes, and forecasting ecosystem collapses (Scheffer *et al.* 2001; Barnosky *et al.* 2012).

§-80 Habitat constraints for the King penguin. The highly constrained niche of the long-lived sub-antarctic King penguin (*Aptenodytes patagonicus*) makes this species a useful model of top-predator response to environmental change (Le Bohec *et al.* 2008). While a poleward range shift is the predicted response to climate warming for cold-adapted species, the highly fragmented nature of the King penguin's habitat precludes continuous population displacement. Because the species breeds exclusively on year-round ice-free areas on islands scattered throughout the Southern Ocean (Bost *et al.* 2013), it may only disperse in a stepping-stone manner amongst the few available islands. The species' foraging grounds, on the other hand, move together with the myctophid fish stock that strives around the Antarctic Polar Front (APF) (Cherel *et al.* 2002; Bost *et al.* 2015). Since the King penguin's breeding system, that spans over 12 months, makes it espe-

cially sensitive to the duration of its central-place foraging trips during the early chick rearing pe-

riod (Barrat 1976; Bost *et al.* 2015), foraging distance at the peak of summer is a critical driver of

breeding success (Le Bohec *et al.* 2008; Péron *et al.* 2012; Bost *et al.* 2015). The most extensively

studied colony, belonging to the most important breeding area for the species (the Crozet archi-

pelago, Bost *et al.* 2013), appears to have benefited from Holocene warming (Trucchi *et al.*

2014). However, recent tracking studies have revealed a southward extension in their foraging

ranges as a result of climate change (Péron *et al.* 2012; Bost *et al.* 2015). As a result of the associ-

ated increase in energy expenditure, the Crozet population is expected to decline within the com-

ing decades (Le Bohec *et al.* 2008; Bost *et al.* 2015). The continuous poleward displacement of

the species' foraging grounds, combined with the discrete distribution of its breeding locations,

implies that King penguin populations must undergo abrupt location shifts from one island to

another to follow their habitat, thereby increasing the risk of mismatched strategies.

§-81 A Synnome species. In order to predict the limits and opportunities for this species to track

its fragmented habitat, we adopted here a cross-disciplinary approach, integrating information

from ecology, behaviour and genomics, together with multi-proxy paleoclimate reconstructions

and numerical climate models. The most striking feature of the present-day King penguin popu-

lation is its worldwide panmixia, that we explain by a high inferred migration rate among

colonies. Our genome-wide data, including ~35,000 independent polymorphic DNA loci gener-

ated using a RAD-sequencing approach (Baird *et al.* 2008), and gathering 163 individuals from

13 different locations covering most of the King penguin's contemporary range (see S-0 p. 177,

and Fig. 22), strongly contradict the alleged separation between the South Atlantic *patagonicus*

and the South Indian and Pacific *halli* subspecies (Mathews 1911; Barrat 1976), suggesting that

the traits used as a basis for subspecies delineation are better explained by phenotypic plasticity

than by reproductive isolation. Both classical descriptors of genetic variation and structure analy-

sis unambiguously support a fully-panmictic worldwide population (see S-1 p. 181 for details).

Full admixture among colonies is also clear when repeating these analyses at the island level (see

S-1 p. 181). Furthermore, bio-logging experiments and empirical observations suggest that short and long distance movements are significant contributors to the ongoing genetic mixing. Recently reported new colonies (Convey *et al.* 1999; Budd 2000; Pistorius *et al.* 2012) indicate that immigration-fuelled colony establishment can occur at a decadal scale. Contrary to previous hypotheses, recapture of tagged individuals (see S-2 p. 196 for details) shows that dispersal is also strong at the generation-scale: thus, dispersal ability is not a limiting factor in the King penguin's response to environmental change, and the species can be assumed to realise its fundamental habitat efficiently, and to follow a single, unified demographic trajectory.

§-82 Palæodemography of the Aptenodytes penguins. The value of the King penguin as a climatic bio-indicator is confirmed by its strong demographic response to Quaternary climate change, that we reconstructed using RAD-sequencing and full-genome data. We relied on a novel model-flexible approach (the Stairway plot; §95 p. 186), based on the composite likelihood of the derived-allele frequency spectrum (Liu & Fu 2015), as well as on extended Bayesian skyline plot (§96 p. 187) and pairwise sequentially Markovian coalescent (§97 p. 190) approaches. The King penguin population experienced two bottlenecks: (a) a recent one during the Last Glacial Maximum (LGM), and (b) a more ancient one overlapping with the previous Pleistocene glacial episode (Fig. 19). During the late Pleistocene and early Holocene, a period of steep population growth is followed by a long plateau. In order to assess the importance of general marine productivity variation in this response, we repeated the analysis for the high-Antarctic Emperor penguin (*A. forsteri*), the only other extant large penguin species, using 110 individuals and an identical sequencing approach. In contrast with the King penguin, the Emperor penguin shows no detectable demographic response to the recent Pleistocene and Holocene climatic events (Fig. 19 and S-3 p. 197), but rather a slow increase during the Pleistocene, with a possible population maximum after the Valdivian interglacial (Fig. 19). The large King penguin population fluctuations are not mirrored in the Emperor penguin, excluding interspecific food competition. Yet, all reconstruction methods support the replacement of the cold-adapted Emperor penguin by the

1 warmer-adapted King penguin as the major *Aptenodytes* species already during the early

2 Holocene.
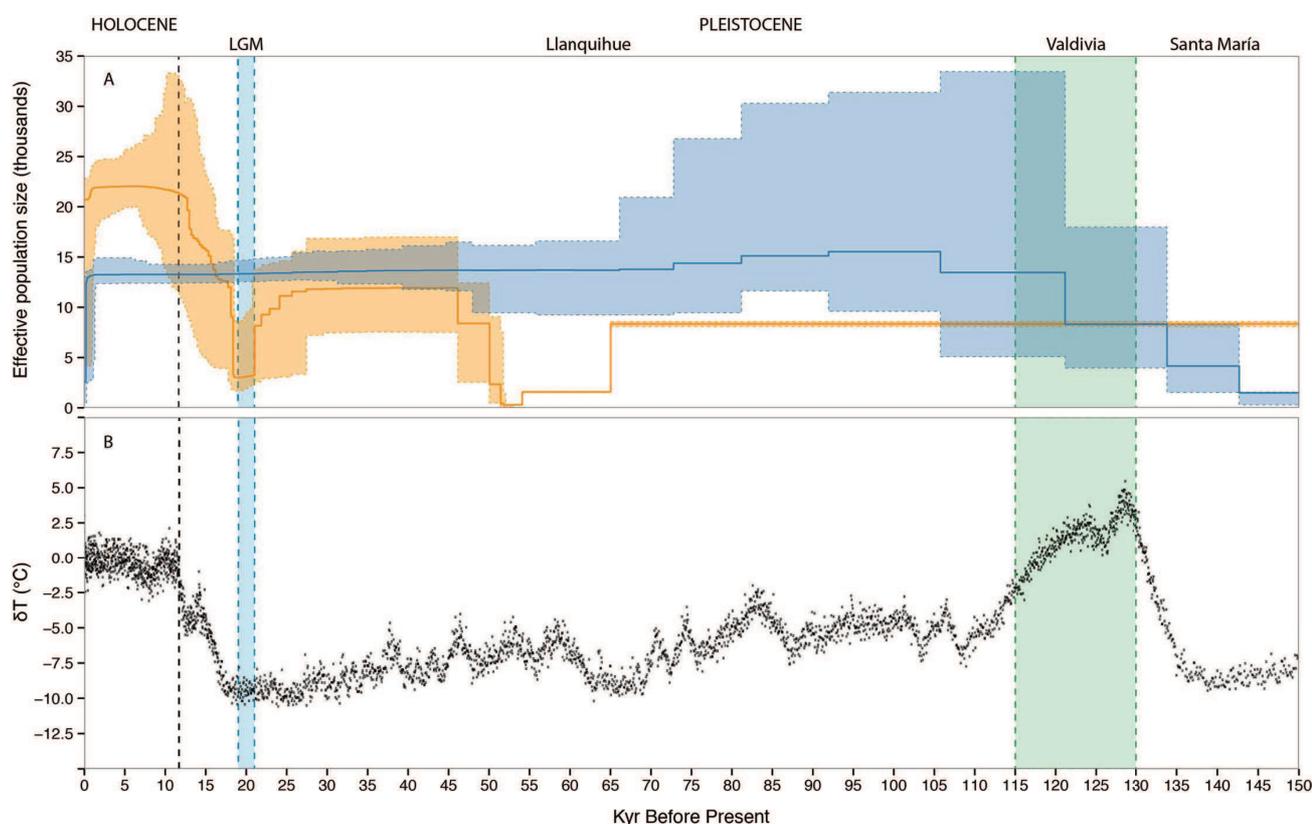
3 **Figure 19 | Penguin paleodemography in response to Quaternary climate change. A. Stairway plot**
4 **reconstruction of population size changes** for the King penguin (orange) and the Emperor penguin (blue). Solid
5 line: median population size; shaded area: 95% confidence interval. **B . Temperature a nomaly i n t he l ate Qua-**
6 **ternary**, as inferred from the EPICA Dome C ice core (Augustin *et al.* 2004). Highlighted areas: Last Glacial Maxi-
7 mum (LGM, ~21-19 Kyr BP) and Valdivian interglacial period (~130-115 Kyr BP). Dashed line: Pleistocene-
8 Holocene transition (~11.7 Kyr BP).

9 The King penguin's response to past climate change is best explained by variations in the extent

10 of suitable habitat (see S-4 p. 200 for details). We relied on both observed and modelled paleocli-

11 matic data to identify the extent of the King penguin's past fundamental niche, which we defined

12 based on three major traits that directly determine habitat suitability: *(a) within foraging distance*

13 *of the prey stock at the APF* (Bost *et al.* 2009), *(b) reduced sea ice extent to allow for overwinter*

14 *chick-rearing* (Barrat 1976), and *(c) insular and ice-free land* (Barrat 1976). As confirmed by the

absence of LGM impact on the Emperor penguins (Fig. 19), the overall productivity of the Southern Ocean did not change significantly during the Pleistocene and Holocene periods (Wolff *et al.* 2006; Kohfeld *et al.* 2013). On the contrary, the location of the APF zone and the extent of land ice and winter sea ice cover exhibited important latitudinal variation over the period (Gersonde *et al.* 2005; Kohfeld *et al.* 2013; Hodgson *et al.* 2014). Thus, the location of optimal King penguin breeding areas changed vastly between warm and cold conditions. APF and foraging range predictions, based on historical period (1981-2005) experiments from an ensemble of IPCC CMIP5 models (see S-4 p. 200 for details), closely matched both observed APF and empirical foraging distances derived from bio-logging experiments (§103 p. 202). Our model is able to capture the full present-day range of the King penguin, and our paleohabitat reconstructions are also in close agreement with the species' reconstructed demography (Fig. 19 and Fig. 20). Under LGM conditions, the equatorward displacement of the APF and increased land and sea ice cover (Kohfeld *et al.* 2013; Hodgson *et al.* 2014) reduced the King penguin's range to a fraction of its current extent (Fig. 20A), as suggested by the inferred population bottleneck (Fig. 19A). Assuming a 700-km February foraging distance as the upper limit for successful breeding (Péron *et al.* 2012), the only two possible refugial areas were found in the Falklands, and in the Campbell plateau region, a much reduced refugial range compared to the eight pre-industrial breeding areas (Bost *et al.* 2013). By mid-Holocene, on the other hand, the King penguin already occupied most of its pre-industrial range (Fig. 20B-C). The APF occupied a position close to its present-day state at most locations, while all present-day breeding archipelagos (except for South Georgia) were free from sea ice, and land ice receded early on Kerguelen and South Georgia - although it persisted until early Holocene on Crozet and Prince Edward archipelagos (Hodgson *et al.* 2014). The King penguin rapidly exploited these newly available locations, as evidenced by the steep growth and following plateau in our demographic reconstructions. Thus, the King penguin's response to past climate change strongly supports the idea that modifications in the posi-

tion of the APF and in the distribution of land and sea ice, by modifying the extent of available

habitat, have a major impact on the species' demographic trajectory.
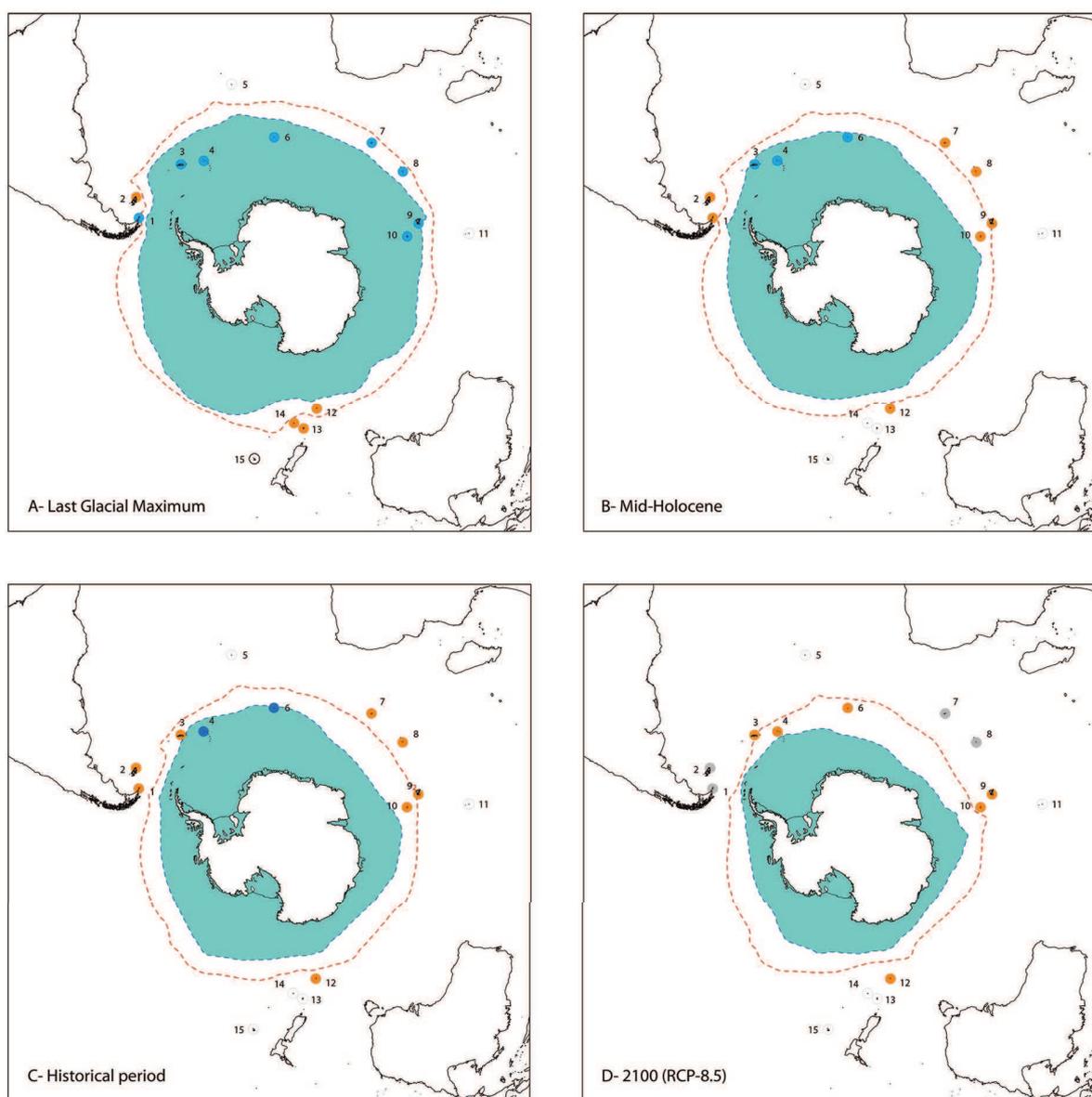
Figure 20 | Past and future breeding range of the King penguin. Reconstructed position of the Antarctic Polar Front in February (SST = 5°C, dashed red line), and extent of sea ice in September (SIC > 15%, light blue area) at four contrasting time periods: **A. Last Glacial Maximum** (21-19 Kyr BP), **B. Mid-Holocene** (6 Kyr BP), **C. Historical period** (1981-2005), **D. Projection for 2100** (RCP-8.5 forcing scenario). Occupation status of the islands: **orange:** presence of King penguin breeding colonies, **blue:** sea and/or land ice preventing colony foundation, **grey:** too far from the Antarctic Polar Front for foraging, **white:** never occupied by King penguins. **Islands:** 1: Tierra del Fuego, 2: Falklands, 3: South Georgia, 4: South Sandwich, 5: Gough, 6: Bouvet, 7: Marion and Prince Edward, 8: Crozet, 9: Kerguelen, 10: Heard and McDonald, 11: Amsterdam, 12: Macquarie, 13: Auckland, 14: Campbell, 15: Chatham.

§-83 21st century range shifts. Projected changes for the 21st century are expected to have a deep impact on the King penguin's range and population size (see S-4 p. 200 for details). The uncoupled trends in *(i)* the mobile food resources of the APF and *(ii)* the static breeding locations may have opposite effects depending on the initial state (Fig. 21): foraging distance increases steadily until the end of the century for the world's largest colonies, located north of the APF; but the conditions become more favorable on the colder archipelagos south of the APF, with shorter foraging distances and decreased sea ice - a trend that is consistent across individual models (Fig. 21, see §104 p. 204), and supported by three different Representative Concentration Pathways (rcp) forcing scenarios (Meinshausen *et al.* 2011). With its low genetic diversity and long generation time, the species is not expected to undergo rapid adaptive evolution to adapt to the new conditions at the northern end of its range (Hoffmann & Sgrò 2011; Norberg *et al.* 2012): local extinction or dispersal, rather than adaptation, is therefore the forecasted outcome.

Colony loss is likely to bring about a decrease in population size, although high dispersal ability also implies that newly available locations may be colonised rapidly. Under the "*business-as-usual*" rcp-8.5 scenario, 70% of the present-day 1.6 million King penguin breeding pairs (Bost *et al.* 2013) are expected to abruptly relocate or disappear before the end of the century. Forty-nine percent of the world population are projected to lose their habitat completely by 2100 (on Crozet and Prince Edward), and ~21% may also see their habitat degrade strongly due to regularly nearlimit foraging distances (on Kerguelen, Falklands and Tierra del Fuego). These losses may be partly compensated by the predicted colonisation of Bouvet, and by a possible additional growth on Heard and South Georgia due to improved foraging conditions. These last two locations, together with Macquarie Island, are likely to become the major refugia for the King penguin in the coming decades. Under the low-emission rcp-2.6 scenario, however, only Crozet and Falkland populations come under direct threat, while other colonies may retain good foraging conditions

(Fig. 21), and undergo minimal demographic impact: thus, our results stress the importance of immediate action to limit radiative forcing, as efficient attenuation strategies may still have a positive outcome for the Southern Ocean biodiversity. We also insist on the importance of taking preemptive conservation measures in areas of the Polar Regions, such as Bouvet, that may act as cold biodiversity refugia for the coming warm-earth conditions if we fail to limit radiative forcing in time.

§-84 Uncertainties and perspectives. Thus, although the impact of these changes on the global King penguin population size will largely depend upon the relative roles of dispersal, breeding failure, and mortality in colony extinctions, the forecasted re-shaping of the species' distribution is considerable. Nevertheless, our projection is likely to be an underestimate, as we only take into account the maximum foraging distance after which no successful breeding may take place. However, increasing foraging distances even below the 700 km-limit have been shown to impact breeding success strongly, and may trigger a colony decrease well before the extinction threshold is reached (Le Bohec *et al.* 2008; Bost *et al.* 2015). In addition, our model does not take into account aggravating effects of climate change, such as sea level rise (Rahmstorf 2007) or decrease in ocean productivity due to ocean acidification (Jackson 2008) and reduction of the global thermohaline circulation (Kuhlbrodt *et al.* 2009). The abrupt nature of the predicted King penguin range shift may additionally accelerate the restructuring and concentration of biotic interactions (*e.g.* range overlap and competition with other penguin species): this in turn can generate complex feedback effects (Davis *et al.* 1998; Norberg *et al.* 2012), thereby decreasing the predictability of Southern Ocean biodiversity, and prompting us to adopt an explicitly precautionary approach to marine resource management.
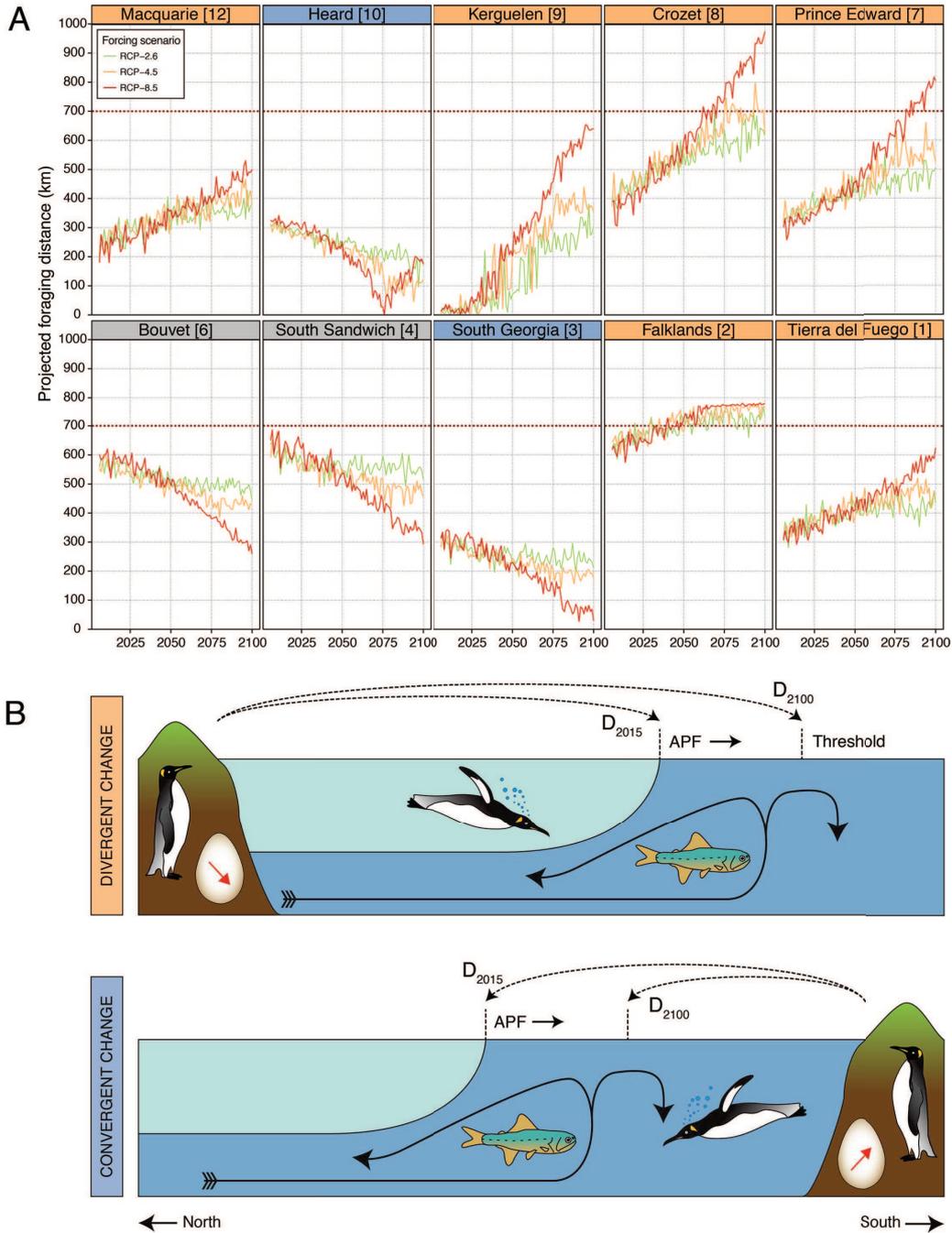
Figure 21 | Projected foraging distance under three RCP scenarios. (A) *Mean projected summer foraging distance* for an ensemble of 15 CMIP5 general circulation models, over the 21st century, for the 8 currently occupied archipelagos, and the two possible future breeding archipelagos (Bouvet and South Sandwich), under three different forcing scenarios (for inter-model variability, see S5). Horizontal red line: 700 km limit, beyond which no successful breeding is expected. *Header numbers* refer to Fig. 21. *Header colour* according to present-day status and projected trend at the location; **orange**: north of the APF, increasing foraging distance, **blue**: south of the APF, decreasing foraging distance, **gray**: currently unoccupied islands south of the APF. **RCP-8.5**: colonies are predicted to (i) disappear from Crozet and Prince Edward, (ii) undergo significant population decline or disappear in Kerguelen and newly-colonised Tierra del Fuego, (iii) remain unchanged in Macquarie Island, (iv) grow on South Georgia and Heard, and (v) settle on Bouvet, and possibly the South Sandwich, as the winter sea ice disappears. **RCP-2.6 and**

RCP-4.5: only Crozet and Prince Edward are too far from the APF to sustain large breeding colonies by 2100, while Kerguelen retains a favourable situation. (**B**) *Schematic representation of the different results of climate change in the Southern Ocean*. Dark and light water masses: cold antarctic deep water and warmer subantarctic surface water (major circulation as a black arrow). APF: Antarctic Polar Front. Dashed arrows: foraging trips in 2015 and 2100. The red arrow in the egg represents the trend in breeding success.

The penguin example illustrates how data about habitat distribution and connectivity, dispersal abilities, trophic interactions, and past range shifts need to be integrated into atmospheric and oceanographic scenarios in order to capture the full extent of human impact on threatened ecosystems. Beyond its implications for the Southern Ocean, the King penguin's complex stepping-stone trajectory offers a paradigmatic representation of the impact of global warming on species distributions, whenever heterogeneous environmental change leads to the uncoupling of a species' different critical areas (*e.g.* breeding, foraging, or overwintering grounds), and thus results in mismatched strategies. As we show here, mismatching between feeding and breeding strategies is strongly aggravated in fragmented habitats - a growing pressure in urban or agricultural matrices, that has been identified as the pivotal aspect of species extinction worldwide (Haddad *et al.* 2015). Habitat fragmentation increases the risk of divergent trends in the different aspects of a species' niche, while reducing corridors that may allow continuous niche tracking: by forcing species to undergo tipping-point range-shifts, it has the double effect of aggravating the impact of environmental change, but largely masking it, placing populations in a situation of climatic debt well before the critical threshold is reached. Thus, the King penguin's cautionary tale should invite us to explore further the complex and sometimes paradoxical effects of climate change, even in those ecosystems that may still appear most remote and pristine.

1 *Supporting information*

2 *S-0: Supplementary methods: from sample collection to SNP typing.*
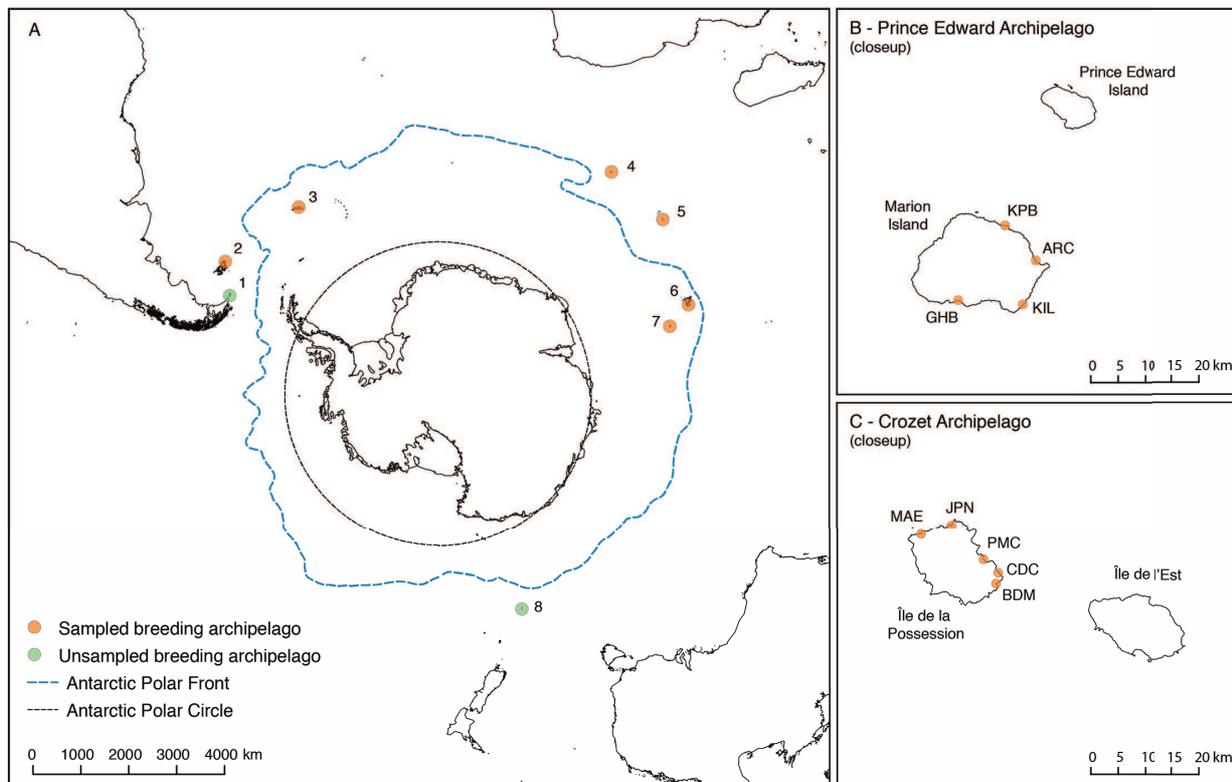
3 **Figure 22 | Sampling design.** **A**) The King penguin's range and sampling: (1) Tierra del Fuego, (2) Falklands,
4 (3) South Georgia, (4) Prince Edward archipelago, (5) Crozet archipelago, (6) Kerguelen archipelago, (7) Heard is-
5 land, (8) Macquarie island. **B**) and **C**) local sampling on Prince Edward and Crozet archipelagos (see §184 p. 347 for
6 details).

7 *§-85 Sample collection and DNA extraction.* A total of 163 blood samples were collected from

8 fledged King penguin juveniles, or from breeding adults, on thirteen colonies covering most of

9 the species' range, between 2010 and 2014. In order to assess fine-scale patterns, we sampled all

10 five colonies from Possession Island, on Crozet archipelago (S46°24′ E 51°45′ - Baie du Marin

11 "BDM", N=15, Crique de la Chaloupe "CDC", N=16, Petite Manchotière "PMC", N=15,

12 Jardin Japonais "JPN", N=16, and Mare aux Elephants "MAE", N=16 - all samples were fledged

13 juveniles), and all four colonies from Marion Island (S46°54′ E37°44′ - Good Hope Bay "GHB",

N=10, Kildalkey Bay, Archway Bay "ARC", N=10, and King Penguin Bay "KPB", N=10 - all samples were fledged juveniles). We sampled one colony from Kerguelen archipelago (S49°20' E69°20' "KER", N=16 - all samples were fledged juveniles), from Falkland archipelago (S51°45' W59°00' - "FLK", N=10 - all samples were breeding adults), from South Georgia (S54°15' W36°45' - "GEO", N=12 - all samples were moulting adults), and from Heard Island (S53°00' E73°30' - "HEA", N=7 - all samples were breeding adults). See Fig. 22 for the geographical location of these colonies. Blood was stored in Queen's lysis buffer at +4°C (Crozet, Marion, Kerguelen), or centrifuged, and red blood cells stored in ethanol at -20°C (Falklands, South Georgia, Heard). DNA was extracted using a spin-column protocol (Qiagen DNEasy© Blood and Tissue kit) with minor modifications.

§-86 Genome-wide Single Nucleotide Polymorphism (SNP) typing. SNP discovery and sequencing followed a single-digest RAD-sequencing protocol (Baird *et al.* 2008). Genomic DNA was checked for degradation on a 1.5% agarose gel, and only samples with consistently high molecular weight were retained and quantified by fluorometry (Life technologies™ Qubit®). The 163 samples was retained and sequenced in 6 distinct libraries. *(i)* approximately 150 ng of genomic DNA per sample were digested with the restriction enzyme Sbf-I-HF (NEB); *(ii)* each sample was then ligated to a unique barcoded P1 adapter prior to pooling in a single library. The library was then sheared by sonication (7 cycles 30'' ON – 30'' OFF); *(iii)* sonicated libraries were concentrated to 25 μl by DNA capture on magnetic beads (beads solution:DNA = 0.8:1), thus further reducing the carry-over of non-ligated P1 adapters, and the target size range fraction (350-650 bp) was then selected by automated gel electrophoresis (BluePippin®); *(iv)* capture on magnetic beads using the same beads:DNA ratio (0.8:1) was then employed in all following purification steps (after blunt-end repairing, poly-A tailing, P2 adapter ligation and library enrichment by PCR). Magnetic beads were kept together with the library throughout the pre-PCR steps, and DNA was re-bound to the beads for purification using a PEG-8000 binding solution; *(v)* PCR amplification was performed in 8 x 12.5 μl aliquots pooled after the amplification in or-

der to reduce amplification bias on few loci due to random drift. PCR was performed using NEB Phusion® polymerase with the following cycles: 30" denaturation at 98°C, 18 cycles of amplification (10" at 98°C, 30" at 65°C, and 30" at 72°C), and a final elongation of 5' at 72°C; *(vi)* the library was then quantified by a fluorimetry-based method (Life technologies™ Qubit®), and molarity was checked on an Agilent Bioanalyzer chip (Invitrogen™). A final volume of 20 μl for each library was submitted for paired-end sequencing on an Illumina HiSeq2000 sequencer (V3 chemistry, libraries 1-3), or HiSeq2500 (V4 chemistry, libraries 4-6), at the Norwegian Sequencing Centre, University of Oslo, spiked with 20% PhiX control library in order to reduce low-diversity bias.

§-87 Sequence alignment and genotyping. Data processing was performed using the following workflow: *(i) S equence d emultiplexing.* R ead q uality a ssessment w as m ade i n F astQC (http://www.bioinformatics.babraham.ac.uk/projects/fastqc/). Samples were de-multiplexed according to in-line barcodes using Stacks v1.28 (Catchen *et al.* 2011; Catchen *et al.* 2013), low-quality reads were discarded, and sequences trimmed to 95 bp. *(ii) Read mapping and filtering.* Demultiplexed fastq files were mapped to the published contigs of the Emperor penguin genome (Zhang *et al.* 2011b) using Bowtie2 2.2.35, with standard settings, allowing only end-to-end mapping. Resulting SAM files w ere fi ltered us ing Sa mtools 0. 1.196, Pi cardTools 1. 113 (picard.sorceforge.net), and custom R and shell scripts (github.com/rcristofari/RAD-Scripts.git) in order to discard unpaired reads and full read pairs where at least one mate has a mapping quality score below 30. The resulting BAM files were then filtered for PCR and optical duplicates by comparing mapping position and CIGAR string, using Picard MarkDuplicates. This process also allowed to filter out most sequencing errors, since MarkDuplicates only retains the read with the highest average Phred score in each duplicate cluster. *(iii) SNP calling and genotyping.* A draft SNP-calling was done in Stacks v1.28 for the general assessment of the dataset, using the "rxStacks" correction algorithm, with a maximum of 5 mismatches allowed between alleles at a single locus (both within and between individuals). For SNP-based analysis, joint SNP and genotype calling was per-

formed using the GATK HaplotypeCaller pipeline (DePristo *et al.* 2011), with standard parameters, except for population heterozygosity which was set to 0.01. We retained only SNPs genotyped in at least 75% individuals, or 90% for AMOVA and PCA analyses. *(iv) Allele-frequency likelihood and allele frequency spectra.* ANGSD 0.9008 (Korneliussen *et al.* 2014) was used to compute per-site probability of being variable, and raw genotype likelihoods, using the Samtools mpileup/bcftools algorithm, and the complete sample allele frequency information as a prior. Per-site allele-frequency likelihood distribution was used to produce a maximum-likelihood estimate of the derived allele frequency spectrum, either unidimensional at the population or species level, or pairwise joint spectrum between pairs of populations.

§-88 Ancestral state reconstruction. In order to polarize allele-frequency spectra, we reconstructed the most likely ancestral base for all positions in the RADome. We selected 12 high-quality King penguin samples covering the whole species' range, and 12 Emperor penguin samples processed according to the same protocol (see *The Emperor synnome*, p. 211). We used BEDtools (Quinlan & Hall 2010) and GATK's FastaAlternateReferenceMaker to update the published Emperor penguin genome and establish a reference RADome for both the King penguin, and the Emperor penguin, using only high-quality polymorphisms (phred-scale genotype quality ≥ 80). We aligned this RADome to the Adélie penguin genome (*Pygoscelis adeliæ*, Zhang *et al.* 2011a) using Bowtie2, and extracted the corresponding regions. For each RAD locus, a maximum-likelihood unrooted tree was built in PhyML (Guindon *et al.* 2010), and maximum-likelihood ancestral sequence for crown-Aptenodytes was reconstructed using PAML (Yang 2007) and Lazarus (project-lazarus.googlecode.com/), using PhyML tree topology as a prior. Downstream analysis was restricted to the sites that could be reliably polarized. All sites that were identified as belonging to coding regions (Zhang *et al.* 2011b), or to sex chromosomes (Zhou *et al.* 2014), were excluded from the analysis.

1 *S-1: Analysis of genetic data.*

2 *§-89 Summary statistics.* Summary statistics were calculated in Arlequin (Excoffier *et al.* 2005)

3 and with custom R scripts either from filtered SNP calls, or from short RAD haplotypes. Pairwise

4 fixation index (Fst), calculated using Reich's estimator (Reich *et al.* 2009), is close to zero (mean

5 pairwise Fst 0.0132 ± 0.00567). Nucleotide diversity π and Tajima's D were computed for full

6 RAD haplotypes. In order to avoid possible biases due to low coverage, we randomly sampled

7 one haplotype for each individual, and performed calculations on this haploid subset. Tajima's D

8 is slightly negative, and homogeneous across locations (D_{all}: -1.094 ± 0.672, D_{HEA}: -0.329 ±

9 0.925, D_{KER}: -0.518 ± 0.899, D_{CRO}: -0.546 ± 0.890, D_{MAR}: -0.404 ± 0.00307, D_{GEO}: -0.448

10 ± 0.925, D_{FLK}: -0.312 ± 0.953), and nucleotide diversity is low (π_{ALL}: 0.00209 ± 0.00258, π_{HEA}:

11 0.00201 ± 0.00326, π_{KER}: 0.00215 ± 0.00304, π_{CRO}: 0.00218 ± 0.00307, π_{MAR}: 0.00200 ±

12 0.00306, π_{GEO}: 0.00199 ± 0.00295, π_{FLK}: 0.00182 ± 0.00294), in keeping with the prediction of

13 Romiguier *et al.* 2014 for long-lived species.

14 *§-90 Clustering analysis.* Clustering was performed in ngsAdmix (Skotte *et al.* 2013), based on

15 genotype likelihoods calculated in ANGSD with a SAMtools model, and allowing for a maxi-

16 mum of 50% missing data in order to process a site, and keeping only positions inferred as vari-

17 able with a high likelihood (p-value threshold 1e-6). We performed 100 bootstrap replicates,

18 with K values ranging from 1 to 10. Best-fitting K was chosen using Evanno's δK method. An in-

19 dependent clustering was performed in FastStructure (Raj *et al.* 2014) using a filtered SNP

20 dataset (minimum depth of coverage of 4x, and minimum 80% individuals genotyped at each lo-

21 cus, leaving 4,784 polymorphic loci for analysis), again with 100 replicates and K ranging from 1

22 to 10. Both approaches unambiguously supported a K=1 model.
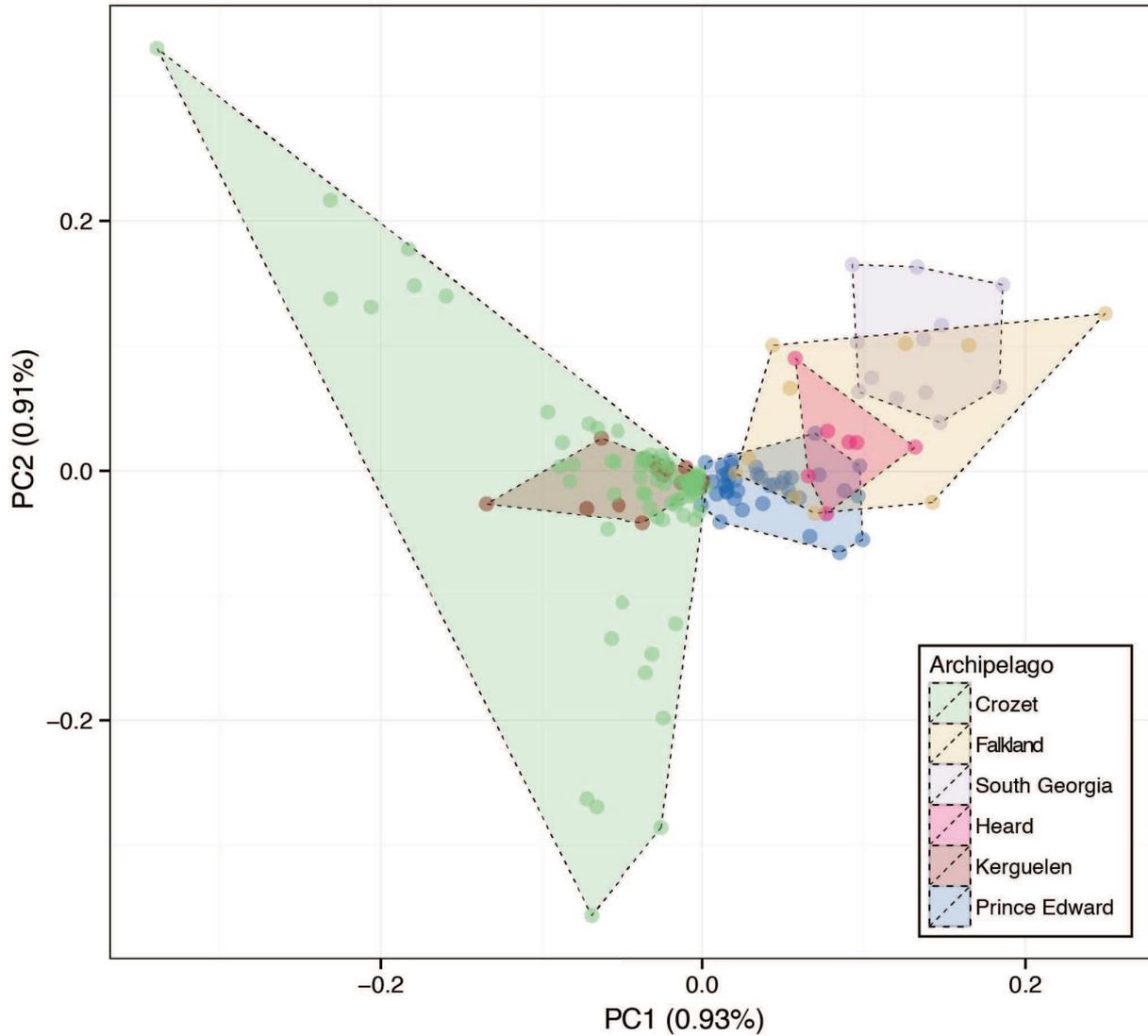
3 *§-91 Principal component analysis.* Genotype posterior probabilities calculated in ANGSD (§87 p.

4 179) were used to perform a principal component analysis (PCA) in ngsTools (Fumagalli *et al.*

5 2014), including only variable sites with a maximum-likelihood derived allele frequency at least

6 equal to 1/2N (with N being the number of included samples). PCA was repeated in the R pack-

7 age *adegenet* (Jombart 2008), using a filtered SNP dataset (minimum depth of coverage of 4x,

8 and minimum 80% individuals genotyped at each locus, leaving 4,784 polymorphic loci for

9 analysis). PCA does not resolve strong geographical structure (Fig. 23): although samples tend to

1   gather by archipelago, there is considerable overlap between locations, and no single principal

2   component explains more than ~0.9% of the total variation.
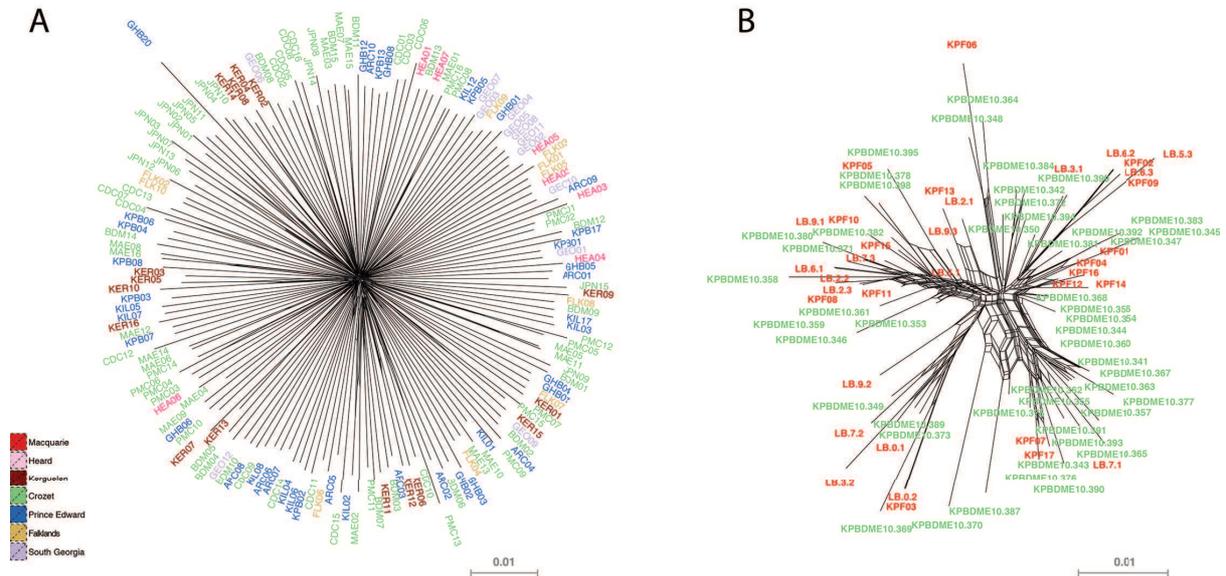
3   **Figure 24 | Neighbour-net.** Calculated **A**) from pairwise Hamming distances, based on genome-wide SNP

4   data, for 6 breeding archipelagos, and **B**) from the mitochondrial control region of 40 individuals from Crozet, and

5   39 individuals from Macquarie island.

6   *§-92 Analysis of molecular variance.* Analysis of molecular variance was performed in Arlequin

7   3.5.2.1 (Excoffier *et al.* 2005), using a filtered SNP set that included only sites genotyped in 90%

8   individuals. Amova was performed on a per-locus basis, with 10,000 permutations. We tested

9   four different grouping schemes: *(i) colonies grouped by archipelago*: ((HEA), (KER), (BDM,

10   CDC, PMC, JPN, MAE), (GHB, KIL, ARC, KPB), (GEO), (FLK)) *(ii) A. p. patagonicus vs A. p.*

11   *halli*: ((HEA, KER, BDM, CDC, PMC, JPN, MAE, GHB, KIL, ARC, KPB), (GEO, FLK)) *(iii)*

12   *Crozet-only*: ((BDM), (CDC), (PMC), (JPN), (MAE)) *(iv) Marion-only*: ((GHB), (KIL), (ARC),

13   (KPB)). Under all four groupings, the overwhelming majority of variance is explained at the indi-

14   vidual level: *(i)* 92.9% within individuals, 6.20% amongst individuals, 0.989% amongst popula-

15   tions, -0.124% amongst groups. *(ii)* 92.9% within individuals, 6.20% amongst individuals,

0.904% amongst populations, -0.0370% amongst groups. *(iii)* 94.1% within individuals, 4.57% amongst individuals, 1.30% amongst populations. *(iv)* 85.1% within individuals, 14.8% amongst individuals, 0.0309% amongst populations.

§-93 Pairwise Hamming distance network. We calculated pairwise Hamming distance between individuals based on genotype calls using PLINK v1.9 (Purcell *et al.* 2007), and calculated the corresponding neighbour-net in SplitsTree (Huson & Bryant 2006) - see Fig. 24A. In keeping with the results of AMOVA and PCA, the terminal branches explain most of the variance, and samples do not cluster geographically.

§-94 HVR comparison with Macquarie. Comparison of mitochondrial hypervariable control region (HVR) haplotypes from Crozet (Trucchi *et al.* 2014, Genbank accession number KF530582-KF530621) with published sequences from Macquarie Island (Heupink *et al.* 2012, Genbank accession number JQ256379-JQ256413) confirms the idea of a single, worldwide and fully panmictic population. Pairwise Fst is low (Fst=0.032), and a haplotype network does not support any population separation between the two islands (Fig. 24B).
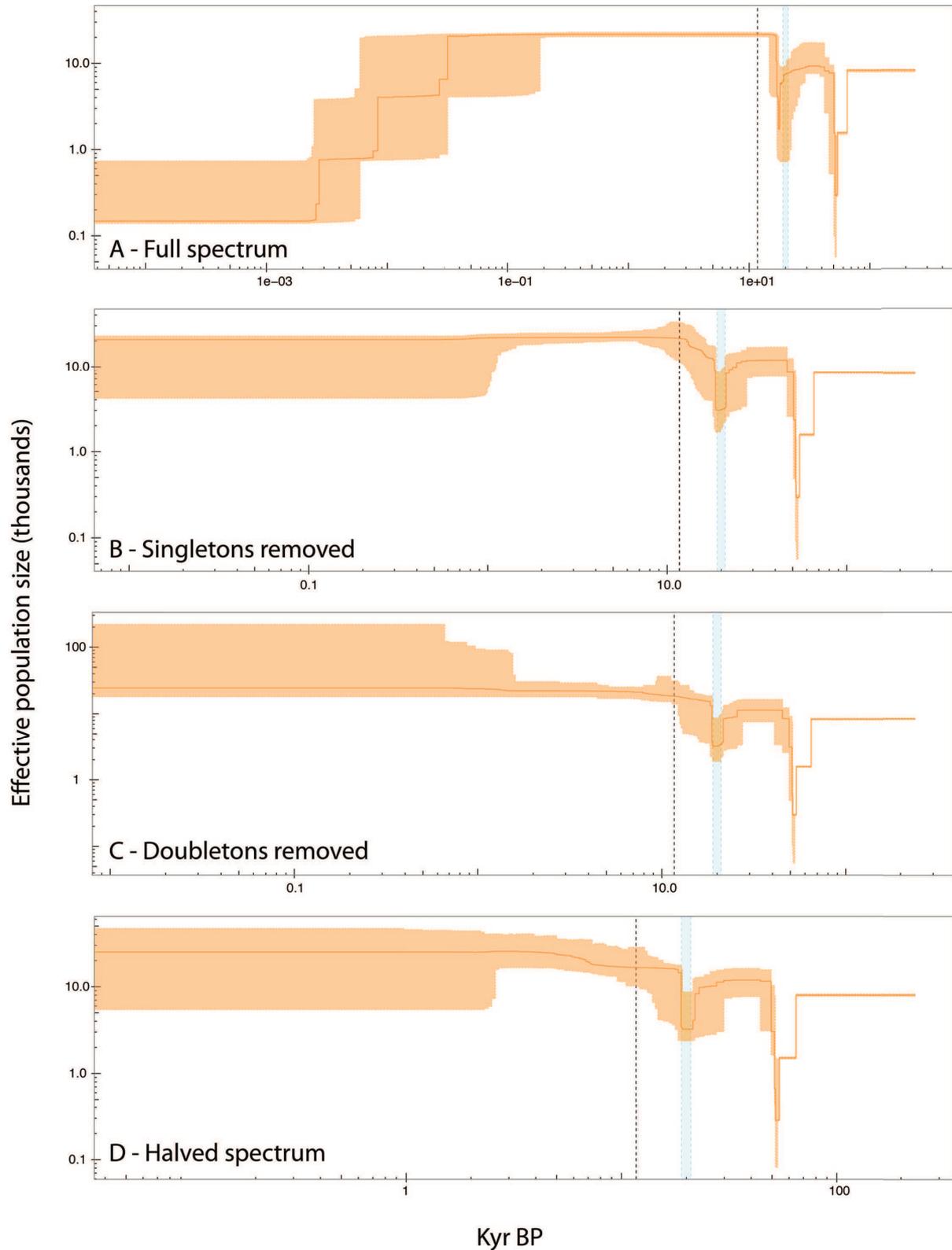
Figure 25 | Robustness of the Stairway plot method. Stairway plot reconstructions with the same set of King penguin individuals, but based on **A)** the full spectrum as inferred from 140 samples, **B)** masking the singleton loci, **C)** masking both singletons and doubletons, and **D)** masking singletons, and using only a random subset of 70

individuals. Dashed black line: Pleistocene-Holocene boundary. Shaded blue band: last glacial maximum.

§-95 Demographic reconstructions: the Stairway plot method. The Stairway Plot method is a novel method for demographic inference developed by Liu & Fu (Liu & Fu 2015). This model-flexible method relies on the maximisation of the composite likelihood of the observed derived-allele frequency spectrum, without prior hypothesis on demographic history, as opposed to previous spectrum-based demographic inference methods (*e.g.* Gutenkunst *et al.* 2009). Maximum-likelihood estimation of the allele frequency spectrum was performed in ANGSD-0.901 under a SAMtools model, for 140 high-quality King penguin samples, and 90 high-quality Emperor-penguin samples. Each spectrum was run along with 500 bootstrap replicates. Singletons were found to be the least robustly estimated frequency class, due in particular to the confounding effect of sequencing errors, and were consequently masked from the reconstructions - although comparison of reconstructions *(i)* including all frequency categories, *(ii)* excluding singletons, or *(iii)* singletons and doubletons show that only the reconstruction of the most recent demographic events are affected by the low-frequency variants (Fig. 25A-C). Similarly, using only a randomly picked subset of half of the individuals did not affect the reconstructions (Fig. 25D) **Generation time:** In a long-lived species, generation time is not a fixed parameter, but rather a function of the demographic trend. An estimator has been defined by Saether *et al.* 2005 as $\alpha + (S / (\lambda - S))$, where α is the age at first breeding for females, S is the yearly adult survival rate, and λ is the yearly growth rate of the population, defined as $\lambda=1$ for a stable population. Using long-term monitoring data, we extracted both yearly growth rate, and adult survival, from a pool of 400 adults of known age (Le Bohec *pers. com.*), for the 1999-2010 period. S and λ were found to be strongly correlated over that period (intercept: -0.2454, slope: 1.0936, $R^2=0.6$): therefore, we extended the empirical relationship between both parameters to our reconstruction. For each generation, the generation time in years was therefore defined as $T_{t+1} = \alpha + (S_t / (\lambda_t - S_t))$, where λ_t and S_t are the growth

rate and adult survival rate for the previous generation, defined as $\lambda t = (N_{t+1} / N_t).e(1/T_t)$,
where N_{t+1} and N_t are the population sizes at generations $t+1$ and t, and T_t is the generation
time in years at generation t, and S_t is a linear function of λt, using empirically derived parameters. This correction was applied recursively from the oldest generation in the reconstruction assuming $\lambda = 1$, and towards the present. In order to calibrate other analyses, the mean generation
time over the whole reconstruction T = 10.6 years was retained.

§-96 Demographic reconstructions: the Extended Bayesian Skyline Plot (EBSP) method. Accurate reconstruction of past and present population size changes requires a robust estimate of the substitution rate. We performed a joint analysis of mitochondrial HVR and RAD data, in a multilocus
EBSP framework, using the robustly established substitution rate for the Adélie penguin HVR
(in substitutions per site per Myr: median = 0.55, 95% CI = 0.29–0.88 Millar *et al.* 2008) as a
calibration. Since the generation time differs widely between the Adélie penguin (6.46 years Millar *et al.* 2008) and the King penguin (10.48 years, see §95 p. 186), and since we are considering
the rate of substitution as determining the frequency of coalescence events, as opposed to the rate
of mutation (a purely physiological parameter - see Gibb & Hills 2013), we converted that rate
to reflect the difference in generation time, to 0.34 substitutions.site^{-1}.Myr^{-1} (95% CI = 0.18–
0.54).

We followed the protocol presented in §44 p. 112 and applied in §136 p. 252, a development of
the protocol of Trucchi *et al.* 2014, downsampling the data to haploid individuals, and using independent 50 loci with 50 haplotypes each, with 3 to 6 polymorphic sites, in addition to 50 randomly selected HVR haplotypes. We specified one independent site model for each locus class (3,
4, 5 or 6 SNPs, and HVR). For each class, specified a HVR model, allowing for invariant sites for
the HVR, but not for the short nuclear loci, and for gamma-distributed rate heterogeneity discretised in 4 classes. Transition-transversion ratio *kappa* was linked across nuclear models. All chains

1   were run in duplicate to check for convergence and for a sufficient length to gather ESS > 200 for

2   all parameters, which necessitated 500,000,000 to 1,000,000,000 steps.

3   Since we parametrised each locus class separately, we expect our model to fit a class-specific sub-

4   stitution rate as a function of the observed number of segregating sites, rather than a common

5   substitution rate. However, as we focus on neutrally evolving regions of the genome, we expect

6   the number of segregating sites to follow a Poisson distribution, of parameter λ equal to the mean

7   number of segregating sites per RAD locus. On a large number of sequences, the expected value

8   $E(\lambda)$ converges towards the "true" underlying constant mutation rate, multiplied by the total tree

9   length for each locus. Thus, if we fix the tree length, λ becomes an estimator of the substitution

10 rate μ. However, under the EBSP model, the observed number of segregating sites is taken as an

11 estimator of λ, and consequently of the substitution rate μ. Therefore we expect the inferred value

12 of μ for each locus class to be a posterior probability of the "true" substitution rate, conditional

13 on the mean number of segregating sites observed for that class (Trucchi *et al.* 2014). In order to

14 retrieve the underlying common substitution rate μ, we first fitted a log-linear model to the in-

15 ferred substitution rates (μ_3= 0.0159, μ_4= 0.0218, μ_5= 0.0275, μ_6= 0.0389. Fitted model: inter-

16 cept i = -5.02, slope s = 0.292, R^2=0.997). A Poisson model of parameter λ equal to the mean ob-

17 served number of segregating sites was a good fit for the empirical distribution of number of

18 segregating sites per locus (λ=1.47 , chi-squared test of goodness-of-fit p-value= 0.232). Thus, we

19 extracted μ as $e^{(s.\lambda+i)}$ ~ 1.02e-2 substitutions per site per Myr, or 1.08e-7 substitutions per site per

20 generation.

21 This rate is ca. twice slower than the one reported by Trucchi *et al.* (2.6e-7 subst.site[-1].genera-

22 tion[-1], Trucchi *et al.* 2014), but much faster than the one reported by Li *et al.* (8.11e-9 sub-

23 st.site[-1].generation[-1], Li *et al.* 2014). While the former was not used in Trucchi *et al.*'s analysis, but

24 rather derived from it, Li *et al.*'s result, on the other hand, relies on two exterior and uncertain as-

25 sumptions: 1) the divergence time between the Emperor and the Adélie penguin is set to ~23

Myr, which may be a large overestimate (Gavryushkina *et al.* 2015, based on a state-of-the-art total evidence Bayesian analysis, proposes ~9 Myr instead), and 2) the generation time is taken to be 5 years in both species; however it has been shown to be 16 years in the Emperor penguin (Jenouvrier *et al.* 2014), and 6.46 years in the Adélie penguin (Millar *et al.* 2008) - thus 11 years would be a closer (although inaccurate because assuming a single, constant rate) estimate of a common generation time. Applying these corrected estimates to Li *et al.*'s findings would give a rate of ~4.55e-8, which is more than five times faster than proposed, and ca. half our estimate - although this calculation does not take into account the possible rate heterogeneity between lineages, and most importantly the changes in generation time between the *Aptenodytes*/*Pygoscelis* common ancestor and the extant species, which may explain the remaining difference. Generally, the rate of evolution of penguins has been a rather challenging subject, with a wide discrepancy between the paleontological and molecular evidence. While fossil data has been recognised to support a very recent radiation of penguins (about 10 Myr BP, see Slack *et al.* 2006; Clarke *et al.* 2007), molecular data has been interpreted as implying a much more ancient origin (~45 Myr for Baker *et al.* 2006). This molecular-derived radiation has successively been brought to a closer agreement with the fossil evidence by Subramanian *et al.* (~20 Myr, see Subramanian *et al.* 2013) and Gavryushkina *et al.* (~12.5 Myr, Gavryushkina *et al.* 2015). The rate that we propose here is in accordance both with the hypothesis of a very fast diversification of the spheniscids, and with the findings of Trucchi *et al.* Our reconstruction supports the evidence provided both by the Stairway plot analysis (§96 p. 187) and the PSMC analysis (§97 p. 190, with a fast expansion of the King penguin population in the late Pleistocene, and a stable Emperor penguin population throughout the period (Fig. 26).
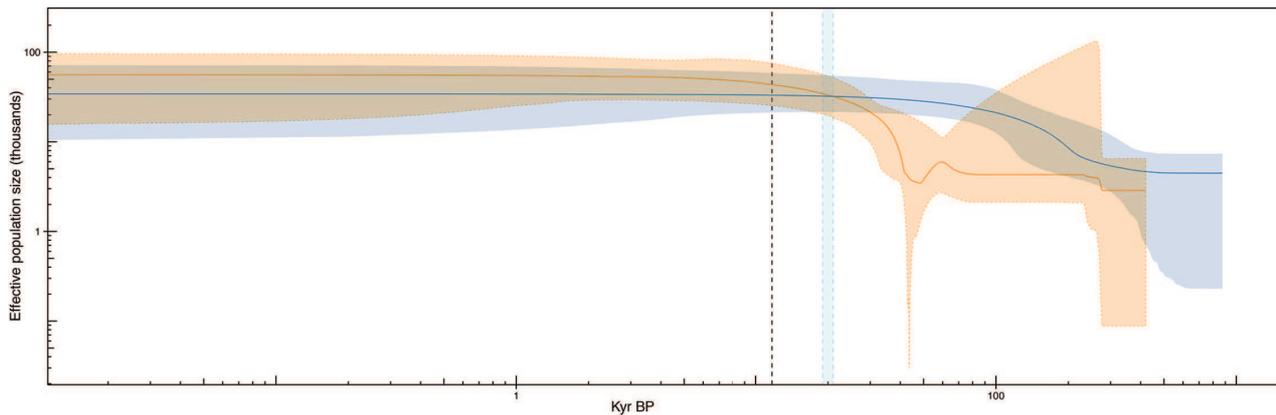
Figure 26 | Extended Bayesian Skyline Plot. Reconstruction of past population size changes for the King penguin (orange) and the Emperor penguin (blue). Solid line: median population size; shaded area: 95% confidence interval (see S2.4 for details). Dashed black line: Pleistocene-Holocene boundary. Shaded blue band: last glacial maximum.

The EBSP demographic reconstruction shows only one bottleneck, and places it around 40 Kyr BP - between the two Stairway-inferred bottlenecks. The contrast between the King and the Emperor penguin is maintained, with the Emperor experiencing only a slow and moderate expansion before 100 Kyr BP, and the King going through more diverse demographic events in the late Pleistocene. Our simulation tests (see §98 p. 192) show that, even when two bottlenecks are really present, the EBSP's expected behaviour is to smooth them out as one single broad population depression (Fig. 28B). Thus, our reconstruction, although with a lower resolution, supports the Stairway-inferred demography. The EBSP's lower resolution is not surprising, given that it only includes a subset of 50 short loci (*i.e.* 250 to 300 SNPs), where the Stairway plot is using the information from every single genotyped SNP.

§-97 Demographic reconstructions: the Pairwise Sequentially Markovian Coalescent (PSMC') method.
Like the Stairway Plot and the EBSP methods, PSMC (Li & Durbin 2011; Schiffels & Durbin 2014) is a model-flexible method, that does not require prior specification of demographic epochs or events. Instead of maximising the composite likelihood of the derived-allele frequency spectrum (Liu & Fu 2015) or the full likelihood of short, non-recombining sequences (Heled &

Drummond 2008), the PSMC algorithm summarises the full ancestral recombination graph through the depth of the most recent coalescence event (time to most recent common ancestor, TMRCA) and total length of singleton branches, as a hidden Markov model in which recombination events mark state changes. It allows for accurate reconstruction of deeper-time demographic events, although it lacks power for more recent time periods in its pairwise form (Li & Durbin 2011; Schiffels & Durbin 2014). The full Multiple Sequentially Markovian Coalescent approach (MSMC, Schiffels & Durbin 2014), which has a much improved resolution for recent time periods, relies on the accurate phasing of haplotypes, which unfortunately is not possible in a non-model species, in the absence of a large transmission or population dataset. In order to exploit unphased haplotypes, analysis must be restricted to the pairwise case, as PSMC'. However, since recombination events are treated as a Markovian process along the sequence, it is still possible to increase the likelihood of the reconstruction by concatenating several genomes together, thus increasing the independent sampling of TMRCA. We selected three high-quality samples for the King penguin, and the Emperor penguin. Libraries were prepared with a standard Illumina(c) TruSeq™ PCR-free protocol, and multiplexed on two lanes of a HiSeq 2500 V4 sequencer at the Norwegian Sequencing Center facility, University of Oslo. Reads were mapped to the published Emperor penguin genome (Zhang *et al.* 2011b) with high success (unique concordant alignment rate, King penguin: ~86%, Emperor penguin: ~81%). We retained only longer scaffolds (length ≥ 2 Mb, i.e. 188 scaffolds making up for ~80% of the total reference length) for the analysis. Analysis was run on all three samples from each species simultaneously, with 200 bootstrap replicates. Substitution rate and generation time were defined as above (§95 p. 186-§96 p. 187). Results (Fig. 27) are very similar to the EBSP analysis (§96 p. 187, Fig. 26): the King penguin population grows rapidly in the late Pleistocene, while the Emperor penguin population is mostly stable. However, the resolution of the PSMC' analysis is low in the recent periods, and the last 4 to 5 time bins exhibit considerable instability when compared across reconstructions (Fig. 27A), as opposed to older time periods. Thus, the precise timing of the LGM bottleneck is not precisely

1 retrieved for the King penguin: the two-step expansion since the mid-pleistocene (Fig. 19A) ap-

2 pears smoothed in one single growth trend. A similar behaviour can be reproduced when simu-

3 lating data with two bottlenecks in a rapid succession (see §98 p. 192): thus, our PSMC' analysis

4 is in accordance (although with much lower precision) with our general demography.
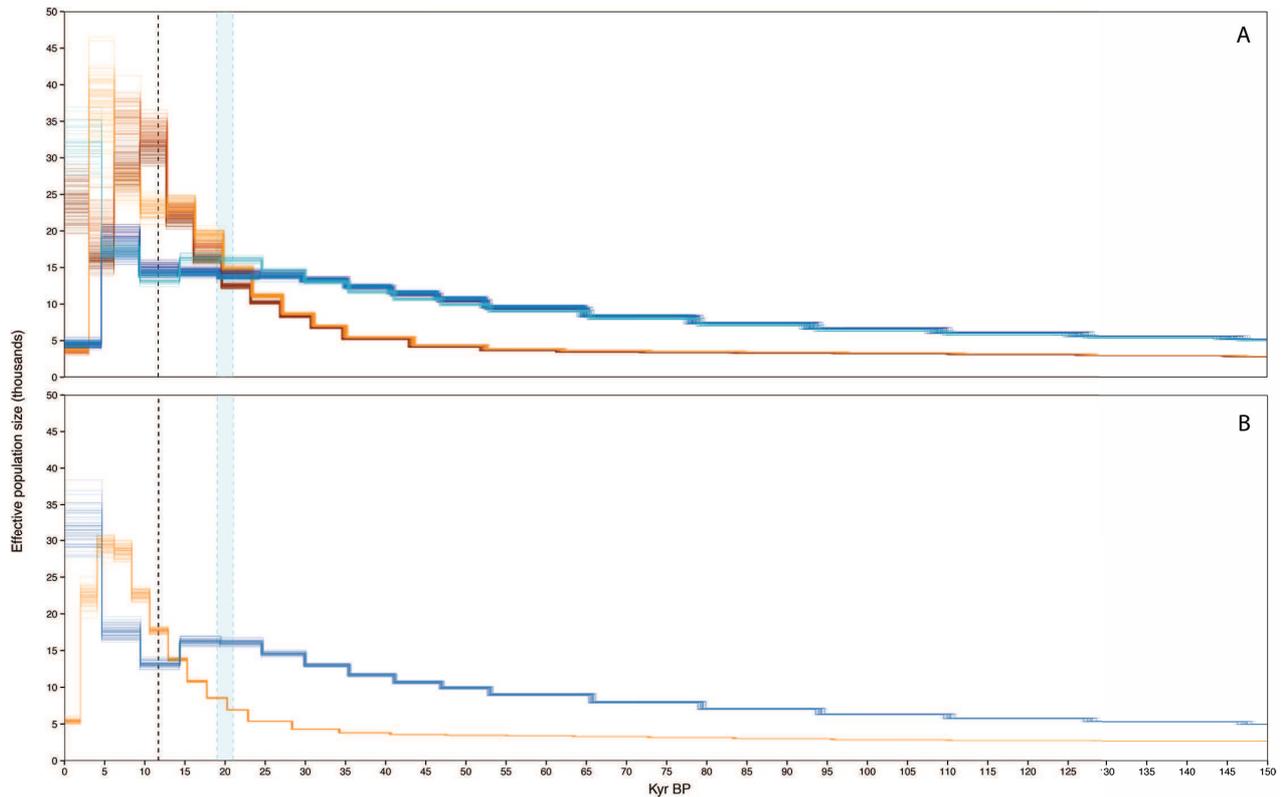
5 **Figure 27 | Pairwise Sequentially Markovian Coalescent.** Reconstruction of past population size changes

6 for the King penguin (orange) and the Emperor penguin (blue). Each individual line represents one bootstrap repli-

7 cate. Reconstruction was performed either **A)** for each individual separately (each shade represents one individual),

8 or **B)** concatenating genomic data from all three individuals for each species. Dashed black line: Pleistocene-

9 Holocene boundary. Shaded blue band: last glacial maximum.

10 *§-98 Reconstruction validation through simulation.* In order to assess the consistency of our recon-

11 struction, we simulated genetic data under the Stairway-plot demographic model for the King

12 penguin, and analysed it using all three algorithms (Stairway plot, EBSP, and PSMC'). Data was

generated under a sequential Markovian coalescent model, either assuming equal substitution and recombination rates (for the Stairway plot and PSMC'), or 95bp non-recombining haplotypes (for EBSP), using scrm (Staab *et al.* 2015), to match the characteristics of the empirical data, and was either directly converted to an allele-frequency spectrum (for the Stairway plot analysis), or to sequence data, under an HKY model, using seq-gen (Rambaut & Grass 1997) (for EBSP). Both the Stairway plot and the PSMC' approaches rely on bootstrapping, rather than MCMC sampling (as EBSP does), for confidence interval estimation. Whereas the empirical data was bootstrapped directly in a non-parametric way (see §96 p. 187 and §97 p. 190), here, we replicated the full simulation 200 times to estimate the confidence intervals.

(i) The Stairway plot retrieves the principal events in the simulation (Fig. 28A). The main difference lies in the attenuation of the LGM bottleneck, that is mainly visible in the shape of the 95%CI. This is of importance, since it indicates that the Stairway approach may underestimate, rather than overestimate, the bottleneck signal in the data: thus, the bottleneck inferred from the empirical data is likely to be at least as deep as reconstructed. The demographic peak that is visible in the 95%CI at the beginning of the Holocene in our reconstruction from the empirical data (Fig. 19A), on the other hand, although not simulated, is also present in the simulation's 95%CI. Thus, that secondary peak rather appears to be entirely artefactual.

(ii) EBSP on simulated data globally matches the expected demographic history (Fig. 28B), with the true demography nearly entirely included in the EBSP CI95% interval. However, the double bottleneck in our simulated data is smoother out as one single depression in the reconstruction, that matches neither bottleneck, but rather averages them - although additional complexity is visible in the shape of the lower CI95% interval. When comparing the empirical-data EBSP (Fig. 26), and the simulated reconstructions, CI95% overlap entirely although median effective population size differs, and uncertainty is much larger in the empirical EBSP. Interestingly, however, the empirical run exhibits some features of our simulated model that the simulated-data run fails

to retrieve - in particular the low population size during the Llanquihue glacial episode. Due to the low number of SNPs in the loci we include in EBSP analysis, however, less resolution is expected for ancient time periods, so neither the observed discrepancy between simulated and empirical runs, not the loss of precision compared to the simulated scenario, is surprising.

(iii) PSMC' reconstruction, on the other hand, exhibits a more unexpected behaviour when applied to our data. When assuming equal substitution and recombination rates, none of the bottlenecks is retrieved, but one single bottleneck is inferred instead around 40 Kyr BP, while a large population size peak (absent from our simulation) is inferred in the early holocene (Fig. 28C). Decreasing the recombination rate down to 1/16th of the substitution rate allows us to recover both bottlenecks, yet the artefactual additional population depression remains around 40 Kyr BP, as well as a sharp artefactual population peak after the most ancient bottleneck (Fig. 28D). None of the reconstructions performed on simulated data matches the true demography in a satisfactory way: however, the very recent events on which we focus may be at the limit of the PSMC' method (Li & Durbin 2011). It is noteworthy, however, that the empirical PSMC' inference follows the expected general demographic trend as given by both the Stairway plot analysis and the EBSP analysis, smoothing out both bottlenecks in one single population increase from the early Pleistocene to the late Holocene.
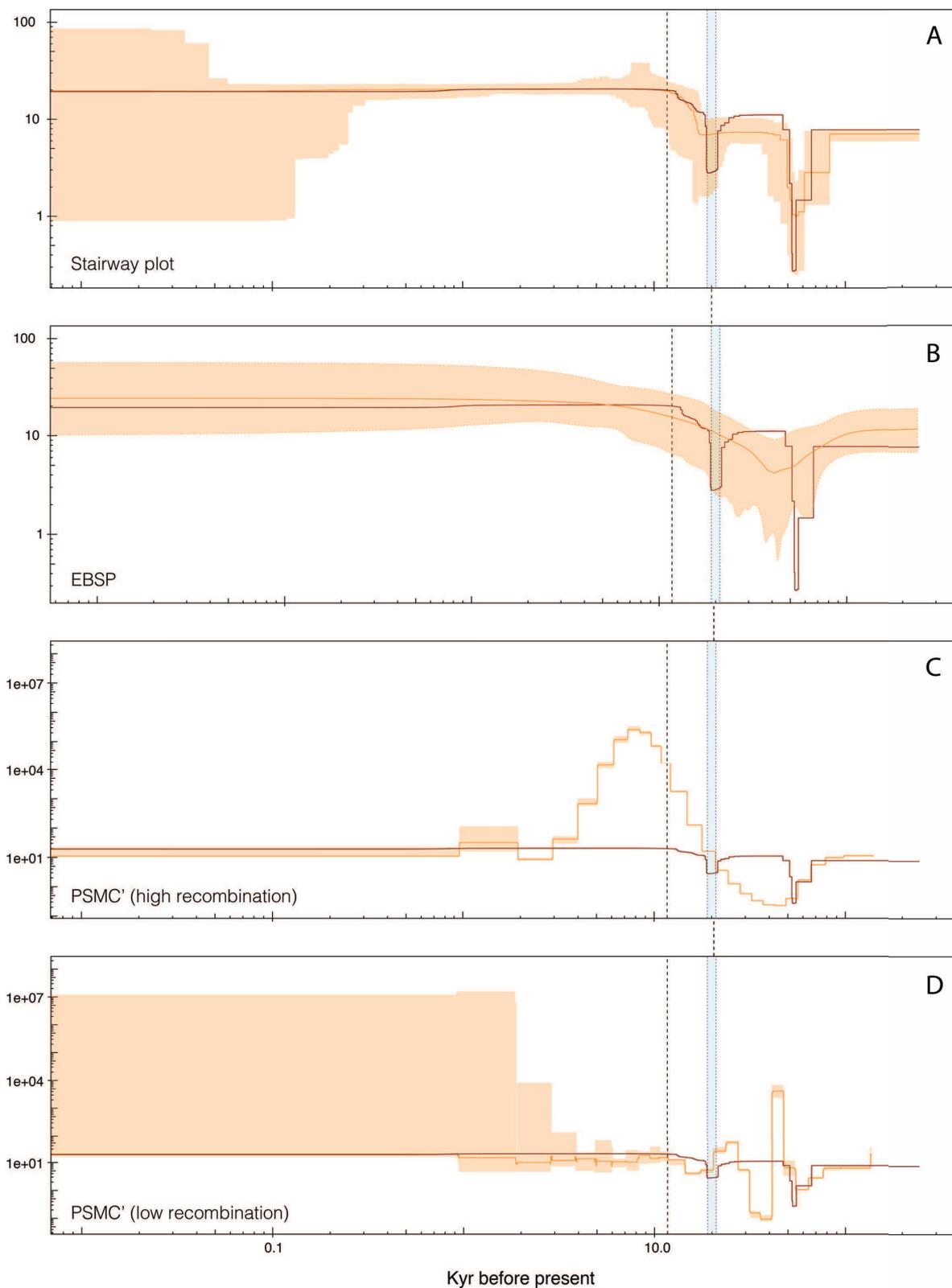
1 **Figure 28 | Validation of the demographic reconstructions through simulation.** Median effective
2 population size and confidence interval (in thousands of breeders) as a function of time, as reconstructed from simu-
3 lated data (simulated scenario is represented by the red line on each graph). **A)** Stairway plot reconstruction, **B)**

EBSP reconstruction, **C-D**) PSMC' reconstruction, with either high (**C**) or low (**D**) recombination rate. Dashed black line: Pleistocene-Holocene boundary. Shaded blue band: last glacial maximum.

S-2: Field observation data.

§-99 Capture-mark-recapture experiments. In order to verify the hypothesis of high dispersal between colonies, we deployed a capture mark recapture (CMR) experiment on Possession Island, Crozet archipelago, and Ratmanoff beach, Kerguelen archipelago. Ca. 9,832 king penguins were equipped with passive radio-frequency identification (RFID) t ags s ince 1 990 o n t he BDM colony, in Crozet archipelago within the framework of a long-term monitoring program (see Gendner *et al.* 2005 for details). We deployed mobile detection antennas on all other colonies of Possession Island, as well as on Ratmanoff beach. These antennas have a low detection distance (ca. 60 cm), and are buried in the ground on paths frequented by penguins when they travel in and out of the colony. Each antenna is ~5 m wide, and records the identification number of any RFID-tagged individual crossing the detection zone. On average, each antenna works for ~12 hours. Antennas were deployed in the evening, in order to record the activity peak around sunrise. In the current state of development of this system, it is impossible to assess how many individuals (tagged or not) crossed the detection zone during the deployment period: thus, recaptures can only be analysed as presence-absence data, and not as quantitative CMR results. Due to the harsh field conditions, deployments were also in some measure opportunistic; and it is generally impossible to ascertain the status of detected individuals (breeding or moulting), except when their age excluded a breeding attempt. This data, however, provides us precious insights into the behavioural mobility of the species, since antennas were usually located well within the target colonies, and not directly at the seaside: thus, only penguins wandering into a colony distinct from their birth colony were detected.

We performed a total of 28 12-hours deployments during the field s easons 2011-2012, 2012-2013, 2013-2014, and 2014-2015 (Per-colony detections/deployments: CDC: 11/5, PMC: 44/10, JPN: 9/5, MAE:1/1). Out of the 9,832 individuals marked as chicks, an average of 2.3 birds per 12-hour antenna deployment were detected on other colonies of the same island. One anecdotic recapture, in 2014, of a tagged individual born on Crozet in 2009 (and therefore reaching age of first b reeding a t t he t ime o f r ecapture) a lso h appened o n t he R atmanoff beach colony, on Kerguelen archipelago. Although a single event has hardly any statistical value, the Ratmanoff colony counts ~140,000 breeding pairs (Delord *et al.* 2015), and only two 5m-long antennas were deployed along the beach: thus, this single recapture suggests that dispersal from Crozet to Kerguelen may not be a rare event.

S-3: Palæoclimate of the Southern Ocean.

§-100 Definition and constraints of the Antarctic Polar Front. The Southern Ocean is characterised by a strong circular Westerly current that flows u ninterrupted b y l and b arriers, t he Antarctic Circumpolar Current (ACC). Strong westerly winds generate important northward Ekman transport in the surface water layer, resulting in a convergence of the cold Antarctic surface waters, and warmer Subantarctic surface waters, where the colder southern water masses sink below the northern water mass, at the Antarctic Polar Front (APF). This convergence is compensated by a divergence area, where upwelled deep water masses rise to the surface, creating an intense marine productivity area (Mackintosh 1946; Peterson & Whitworth 1989; Meijers 2014). This a rea is characterised by a steep surface temperature gradient, between 5°C and 3°C (Moore *et al.* 1999).

Generally, a cooling of surface waters in the Southern Ocean is reflected in a northward displacement of the APF, while a warming brings the APF southward. However, as the APF is defined by the interaction of deep and surface water masses, it is strongly constrained by the sea bottom topography (Moore *et al.* 1999). Important bathymetric features, such as the Campbell Plateau,

the Drake passage, or the Kerguelen plateau, may constrain the position or structure of the APF. In other areas, most importantly the Southern Indian Ocean and Southern Atlantic Ocean, APF displacement is mostly free from bathymetric constraints, and exhibits the largest latitudinal variation (Kohfeld *et al.* 2013).

The Campbell Plateau may be the best studied case of bathymetric constraint on the APF. Both flow models and sediment core evidence showed that the APF remained south of the plateau throughout the Pleistocene, despite important changes in sea surface temperature and frontal positions throughout the Southern Ocean. Whereas the APF is free to move south to greater depths, it is constrained to the North by the sea floor rise (Hayward *et al.* 2008; MARGO 2009; Kohfeld *et al.* 2013). Similarly, the Drake passage constrains both the northern and southern boundaries of the APF (Moore *et al.* 1999; Dong *et al.* 2006; Chereskin *et al.* 2012). Finally, the Kerguelen plateau has been shown to alter the subsurface structure of the front, with its deeper manifestations moving North of the islands, while the surface expressions move South (Moore *et al.* 1999; Park *et al.* 2014). These features, however, are now well modelled in the CMIP5 panel, which has a much improved bathymetric resolution (Meijers 2014), and the influence of the Drake Passage and Campbell Plateau on the frontal structure is accurately reproduced in our reconstructions (Fig. 20).

§-101 Current state of knowledge. There are still considerable uncertainties as to the Pleistocene and Holocene history of the Southern Ocean. Available evidence relies on different types of proxies (Gersonde *et al.* 2005; Thomas & Dieckmann 2008; Kohfeld *et al.* 2013; Hodgson *et al.* 2014). (**a**) Ice core data (e.g. EPICA Dome C and Vostok) provide direct evidence for chemical conditions at the core site, and indirect evidence for the oceanic source areas, provided transfer models are accurate enough (Wolff *et al.* 2003; Wolff *et al.* 2006). Parameters derived from ice core evidence mostly covers air temperature, sea ice extent, and marine productivity (Wolff *et al.* 2006) (**b**) Benthic sediment core provide more direct evidence for marine conditions (tempera-

ture, sea ice cover, productivity) at the core location (Gersonde *et al.* 2005; Martínez Garcia *et al.* 2009). (**c**) Peat cores and geological evidence on the subantarctic islands and surrounding continental shelf are mostly informative for land ice cover (Hodgson *et al.* 2014). Taken together, this evidence allows for a general palæoclimatic reconstruction in the Southern Ocean. However, there is still much progress to be done in reconciling the different sources of evidence, as variability amongst core locations (especially benthic sediment cores) is high, and several land-sea coupling mechanisms are still poorly understood (McGlone *et al.* 2010). In the current state of knowledge, we can distinguish four major periods in the Southern Ocean late-Pleistocene and Holocene history: (i) Quaternary conditions (59-22 Kyr BP), (ii) Last Glacial Maximum conditions (21-18 Kyr BP), (iii) Pleistocene glacial retreat and early holocene optimum (17-9 Kyr BP), (iv) Holocene hypsithermal and neoglacial conditions (8-0 Kyr BP).

(i) Quaternary conditions (59-22 Kyr BP) were mostly glacial-like, with slow onset of glaciation from ~35 Kyr BP, and winter sea ice cover reaching as far as ~56°S in the Pacific. Little is known of land ice throughout the period, as further glaciation obliterated most of the direct evidence.

(ii) Last Glacial Maximum conditions (21-18 Kyr BP) were characterised by extensive land and sea ice cover throughout the Southern Ocean. **The Antarctic Polar Front** is thought to have moved northward to 40-50°S, a movement associated with a ~5°C cooling in summer SST (Gersonde *et al.* 2005; MARGO 2009), although frontal movement is thought to have been constrained by bathymetry south of the Campbell plateau (Neil *et al.* 2004; Kohfeld *et al.* 2013). **Winter sea ice** is also thought to have reached ~50°S or further northward, or the approximate position of the present-day polar front (CLIMAP 1981) (between 47°S in the Atlantic and Indian Oceans, and 57°S in the Pacific Ocean, see Gersonde *et al.* 2005). **Marine productivity** is thought to have shifted from the Antarctic to the Subantarctic region (Hodgson *et al.* 2014), while not changing significantly in total biomass (Wolff *et al.* 2006; Kohfeld *et al.* 2013). **Islands of Heard, Crozet, Marion, and the Drake Arc were entirely covered by ice**, while Kerguelen and

South Georgia may have had ice-free areas. Falklands and Macquarie underwent periglacial conditions (Hodgson *et al.* 2014). Likely faunal refugia were the currently subtropical islands of Gough, Auckland and Campbell, as well as the Falklands and more generally the Patagonian shelf area (Fraser *et al.* 2012).

(iii) Pleistocene glacial retreat and early holocene optimum (17-9 Kyr BP) saw a gradual thawing of most land ice, with contrasting chronologies. **Antarctic and subantarctic fronts** retreated south to their current location (Kohfeld *et al.* 2013). **Sea ice** retreated until the Early Holocene climatic optimum (~11.5-9 Kyr BP), with an episodic increase during the Antarctic Cold Reversal around 14.5 Kyr BP, reaching its current position by ~10 Kyr BP. Kerguelen and South Georgia archipelago bear signs of early deglaciation, while Crozet and Marion islands are thought to have carried extensive land ice until the end of the period (Hodgson *et al.* 2014). The end of the period is marked by a first cold reversal in the Antarctic waters and a short increase in sea ice cover, of unknown extent (Nielsen *et al.* 2004).

(iv) Holocene hypsithermal and neoglacial conditions (8-0 Kyr BP) were characterised by a warmer climate, similar to historical conditions, interrupted by minor cold reversals. The subantarctic region is ice-free, and the northernmost islands of Gough, Auckland and Campbell are located north of the Subantarctic front (Hodgson *et al.* 2014). Temperature reaches a maximum around ~7.5 Kyr BP in the South Pacific (Calvo *et al.* 2007). Marine conditions are warm and ice free at ~50ºS until around 6-5 ka BP (Hodell *et al.* 2001; Nielsen *et al.* 2004), and temperature drops slightly after ~3 Kyr BP, although with no change in the glacial landscape. **Neoglacial conditions** arise after 5 Kyr in East Antarctica, and 3 Kyr in West Antarctica: open water conditions are still prevalent throughout the Southern Ocean, although with possible winter sea ice episodes at 53°S at some periods (~1-2 Kyr BP).

S-4: Atmosphere-Ocean General Circulation Models (AOGCMs)

§-102 AOGCMs choice and multi-model ensemble approach. We used the latest generation of AOGCMs from the IPCC Coupled Model Intercomparison Project Phase 5 (CMIP5, see Taylor *et al.* 2012), which represent a significant improvement over CMIP3 in the Southern Ocean (Meijers 2014). We applied a multi-model ensemble approach, a common improvement over single-model projections, as only the trends present in most models are retained in the final ensemble mean (Meijers 2014). We selected 15 AOGCMs based on the range of available outputs and their coverage of the Southern Ocean (see Table 3). All model outputs were downloaded from the ESGF nodes (pcmdi9.llnl.gov/). In our study, we used the following variables: Sea Surface Temperature (SST) and Sea-Ice Concentration (SIC). For each variable, we calculated the multi-model ensemble mean and standard deviation using the Climate Data Operators toolset (CDO 2015, available at: http://www.mpimet.mpg.de/cdo).

Reconstructions were performed under Last Glacial Maximum, mid-Holocene, and Historical conditions, and projections according to three Representative Concentration Pathways (rcp) scenarios, the rcp2.6, rcp4.5, and rcp8.5, corresponding respectively to the strong emissions reduction scenario, a moderate emissions profile and the "business-as-usual" scenario. We excluded the rcp6.0 as too few model outputs are available yet.

Table 3 | Ensemble members used in habitat predictions. Model outputs were downloaded from the IPCC archive (http://www.ipcc-data.org/sim/gcm_monthly/AR5/Reference-Archive.html). Only one ensemble member was used for each model (r1i1p1 whenever available). Not all models outputs for both 21st century and paleoclimate experiments, thus different ensembles were used for LGM, mid-Holocene and 21st century reconstructions.

Model	Institution	LGM	mid-Holocene	21st century
BCC-CSM1	*Beijing Climate Center (China)*	N/A	r1i1p1	r1i1p1
CanESM1	*Canadian Centre for Climate Modelling and Analysis (Canada)*	N/A	N/A	r1i1p1
CCSM4	*National Center for Atmospheric Research (USA)*	r1i1p1	r1i1p1	r1i1p1
CESM1-CAM5	*National Center for Atmospheric Research (USA)*	N/A	N/A	r1i1p1

#	Model	Institution			
1	CNRM-CM5	*Centre National de Recherches Météorologiques, Centre Européen de Recherche et de Formation Avancée en Calcul Scientifique (France)*	r1i1p1	r1i1p1	r1i1p1
2	CSIRO-Mk3-6-0	*Australian Commonwealth Scientific and Industrial Research Organization (Australia)*	N/A	r1i1p1	N/A
3	EC-EARTH	*EC-EARTH consortium published at Irish Centre for High-End Computing (Netherlands/Ireland)*	N/A	N/A	r8i1p1
4	FIO-ESM	*The First Institute of Oceanography, SOA (China)*	N/A	N/A	r1i1p1
5	FGOALS-G2	*Institute of Atmospheric Physics, Chinese Academy of Sciences, and Tsinghua University (China)*	r1i1p1	r1i1p1	N/A
6	GFDL-ESM2M	*Geophysical Fluid Dynamics Laboratory (USA)*	N/A	N/A	r1i1p1
7	GISS-E2-R	*NASA/GISS (Goddard Institute for Space Studies) (USA)*	r1i1p1	r1i1p1	r1i1p2
8	HadGEM2-ES	*Met Office Hadley Centre (UK)*	N/A	r1i1p1	r1i1p1
9	IPSL-CM5A-MR	*Institut Pierre Simon Laplace (France)*	r1i1p1	r1i1p1	r1i1p1
10	MIROC5	*Atmosphere and Ocean Research Institute, National Institute for Environmental Studies, and Japan Agency for Marine-Earth Science and Technology (Japan)*	N/A	N/A	r1i1p1
11	MPI-ESM-MR	*Max Planck Institute for Meteorology (Germany)*	N/A	N/A	r1i1p1
12	MPI-ESM-P	*Max Planck Institute for Meteorology (Germany)*	r1i1p1	r1i1p1	N/A
13	MRI-CGCM3	*Meteorological Research Institute (Japan)*	r1i1p1	r1i1p1	r1i1p1
14	NorESM1-M	*Bjerknes Centre for Climate Research, Norwegian Meteorological Institute (Norway)*	N/A	N/A	r1i1p1

§-103 Sea Surface Temperature (SST). For palæoclimate as well as 21st century projections, we followed a protocol similar to that of Péron *et al.* 2012. The 5 °C Sea Surface Temperature (SST) isotherm was used as a diagnostic of the position of the Antarctic polar front (APF, see Moore *et al.* 1999) where the King penguin is known to forage (Péron *et al.* 2012). The particular breeding cycle of the King penguin makes the constraints on foraging behaviour especially strong during the early chick rearing stage, when the juveniles have not yet reached thermal independence, and need regular feeding while not being able to survive without an adult (Barrat 1976), which happens around the month of February. This is supported by observed foraging trips, which show a much greater geographic constraint during the month of February (Péron *et al.* 2012; Bost *et al.* 2015). Thus, we focused our analysis to the position of the APF in February, as representative of the maximum constraint on foraging trips.

Before using SST outputs derived from AOGCMs, we assessed the accuracy of the representation of the Southern Ocean by comparing each model SST-output for historical runs to satellite-measured SST from december 1981 to december 2005, using the NOAA Optimal Interpolation v2 SST dataset (Reynolds *et al.* 2002). Cell-by-cell (1°x1°) linear correlation of SST was assessed and R^2, slope and intercept were plotted in order to assess the spatial distribution of model departure from observed values.

As modelled SST was generally found warmer than observed SST in the APF zone over the historical period, we followed the correction applied by Péron *et al.* 2012. In order to maximise the fit between observed and modelled SST for each archipelago, we defined four oceanic sectors: South Atlantic Ocean (45°W to 18°E), South Indian Ocean (18°E to 80°E), Macquarie (135°E to 180°E), and Falkland region (75°W to 45°W), ranging in latitude from 45°S to 55°S, but extended to 60°S in the Falkland region to account for the higher latitude of the APF around Cape Horn. For each of these sectors, we tested the linear correlation between modelled and observed SST, and we corrected the model value linearly when needed (Table 4). The 5°C SST isotherm was then calculated in GDAL (www.gdal.org), and kilometric distance between each island and the 5°C isotherm was calculated using the OGR Python library. Correctness of our model was assessed through 1) correlation the observed and modelled distances to the 5°C isotherm on the 1981-2005 period and 2) consistency between these distances and published data on King penguin foraging areas.

Table 4 | Correlation of observed and modelled SST in the Southern Ocean. Slope, intercept and correlation coefficient for linear correlation of our ensemble model and observed SST data over the historical period (1981-2005), in four sectors of the Southern Ocean.

Sector	R^2	Slope	Intercept
Drake	0.903 ± 0.0291	0.683 ± 0.0472	1.84 ± 1.19
South Atlantic	0.945 ± 0.0259	0.785 ± 0.0571	1.84 ± 1.04
South Indian	0.945 ± 0.0157	0.791 ± 0.0730	2.27 ± 0.876

Macquarie	0.945 ± 0.0160	0.805 ± 0.0687	1.80 ± 0.705

Foraging range predictions for the historical period closely matched both observed historical SST, and observed foraging distances at most locations: ~380 km on Crozet (observed: 300-500 km, see Péron *et al.* 2012), ~320 km on Marion (observed: 300 km three decades ago, see Adams & Klages 1987), ~20 km in the Kerguelen (observed: 270 km in the APF along the 4 and 5°C isotherms, see Koudil *et al.* 2000; Pütz 2002 - the APF is reached immediately, but foraging trips extend further in the productivity zone), ~310 km on Heard (observed: 370 km a decade ago, see Moore *et al.* 1998), ~300 km in South Georgia (observed: 300-600 km over the whole breeding season, see Pütz 2002). Predicted distance for Macquarie Island (~240 km) is slightly lower than the observed summer range (300-500 km, see Wienecke & Robertson 2002), however, recorded foraging trajectories meet the APF in the higher-productivity areas on the edge of the Campbell plateau, where upwelling is increased, rather than southward along the shortest route. Finally, the predicted and observed ranges differ most strongly in the Falklands (predicted: ~640 km and ob-served: 300-500 km, see Pütz & Cherel 2005), a discrepancy explained by the fact the small Falk-land population frequently forages on the Patagonian Shelf break, and not directly on the APF (Pütz & Cherel 2005). This different behaviour of the Falkland population makes its response to APF displacement more uncertain, as other productivity areas may remain available. However, it seems that the Patagonian Shelf could never sustain a large King penguin population (Pistorius *et al.* 2012), and it is sustaining a high, and increasing, anthropogenic pressure from overfishing and climate change (Halpern *et al.* 2008). It is therefore unlikely that the Falklands may sustain a significant King penguin population on a centennial time scale.

§-104 Winter sea-ice concentration (SIC). Winter Sea-Ice Concentration (SIC) is known to limit the southward expansion of the King penguin's breeding range, as the species overwinter breed-ing cycle makes open-water conditions a requisite throughout the year (Barrat 1976). Although

SIC may still be subject to biases in its representation compared to SST, it has improved since CMIP3 (Turner *et al.* 2013; Xu *et al.* 2013; Shu *et al.* 2015). We take the 15% concentration iso-line as being representative of the effective sea ice edge (Turner *et al.* 2013). We only consider the sea-ice concentration at their maximum, during the months of august and September. Compared to satellite-derived historical measures from the NOAA Optimal Interpolation dataset, ensemble reconstruction gives a winter sea ice that tends to be more dense than observed values (mean density of sea ice above 15% concentration over the 1981-2005 period: reconstructed 85 ± 20 %; observed 61 ± 22 %, t-test p-value < 2.2e-16), but less extended (reconstructed extent of september SIC > 15% on the 1981-2005 period occupies 90% of observed SIC > 15% extent), although correlation is strong on a per-cell basis (mean R^2 = 0.67 ± 0.27). Winter sea ice extent is projected to decrease in all forcing scenarios. While sea ice cover should still be relatively important even at the northern tip of the South Sandwich islands during the last two decades of the century (rcp2.6: 0.26 ±0.058, rcp4.5: 0.22 ±0.044, rcp8.5: 0.045 ±0.040), Bouvet island is projected to become ice-free all year round by 2080 under all forcing scenarios (rcp2.6: 0.058 ±0.037, rcp4.5: 0.028 ±0.024, rcp8.5: 0.00041 ±0.00053). However, sea ice projections may not be quite as reliable as SST projections. Indeed, although geographical distribution is modelled rather accurately, CMIP5 ensemble models fail to reproduce the increase in sea ice extent observed in East Antarctica over the last decades, suggesting that some processes are not yet adequately accounted for in the current models (Turner *et al.* 2013) - in particular, the impact of the influx of fresh meltwater from the Antarctic ice sheet on the extent of winter sea ice may still be widely underestimated. If such a bias exists, however, it underestimates the true extent of sea ice: in that case, the King penguin's range reduction may be even more drastic than we forecast here, as Bouvet may not be ice-free and suitable for colony establishment by the end of the century.

§-105 Uncertainties assessment. Although the use of a multi-model ensemble mean approach is considered to outperform the use of a single climate model, it is also essential to assess the uncertainties related to AOGCMs to evaluate the confidence that can be attached to our results. Out-

puts of the different AOGCMs may diverge across time and space because they are based on diverse parameterization of natural processes, downscaling approaches, spatial resolutions, etc… To assess the uncertainties associated with our projections, we calculated, for each rcp scenario, the projected foraging distance derived from each climate model separately. We followed the protocol developed by Goberville *et al.* 2015 by calculating the density distribution of projected foraging distance for each island *(i)* for the current period (2006-2015), *(ii)* for the middle of the century (2041-2050) and *(iii)* for the end of the century (2091-2100) (Fig. 29). In addition, for the same periods, we also calculated the percentage of models forecasting local King penguin population collapse (February foraging distance > 700 km; Fig. 30), as proposed by Raybaud *et al.* 2013. The latitude of the APF, and therefore the duration of the King penguin's foraging trips, is subject to a high interannual variability, in particular under the influence of the cyclical El Niño Southern Oscillation and Southern Annular Mode, with year-to-year latitudinal fluctuations of up to 200 km (Bost *et al.* 2015). Therefore, we considered that a location had reached its critical foraging distance when foraging distance was higher than 700 km for at least 20% of a consecutive decade.

Figure 29 | (NEXT PAGE) Foraging distance from single models. Projected distance between subantarctic archipelagos and the Antarctic Polar Front in February extracted from IPCC CMIP5 models taken separately. Colours correspond to rcp scenarios: rcp-2.6 (green), rcp-4.5 (orange) and rcp-8.5 (red). Dashed line represents the 700-km limit. **A)** yearly projection, **B)** density distribution per rcp scenario, at three different time steps.
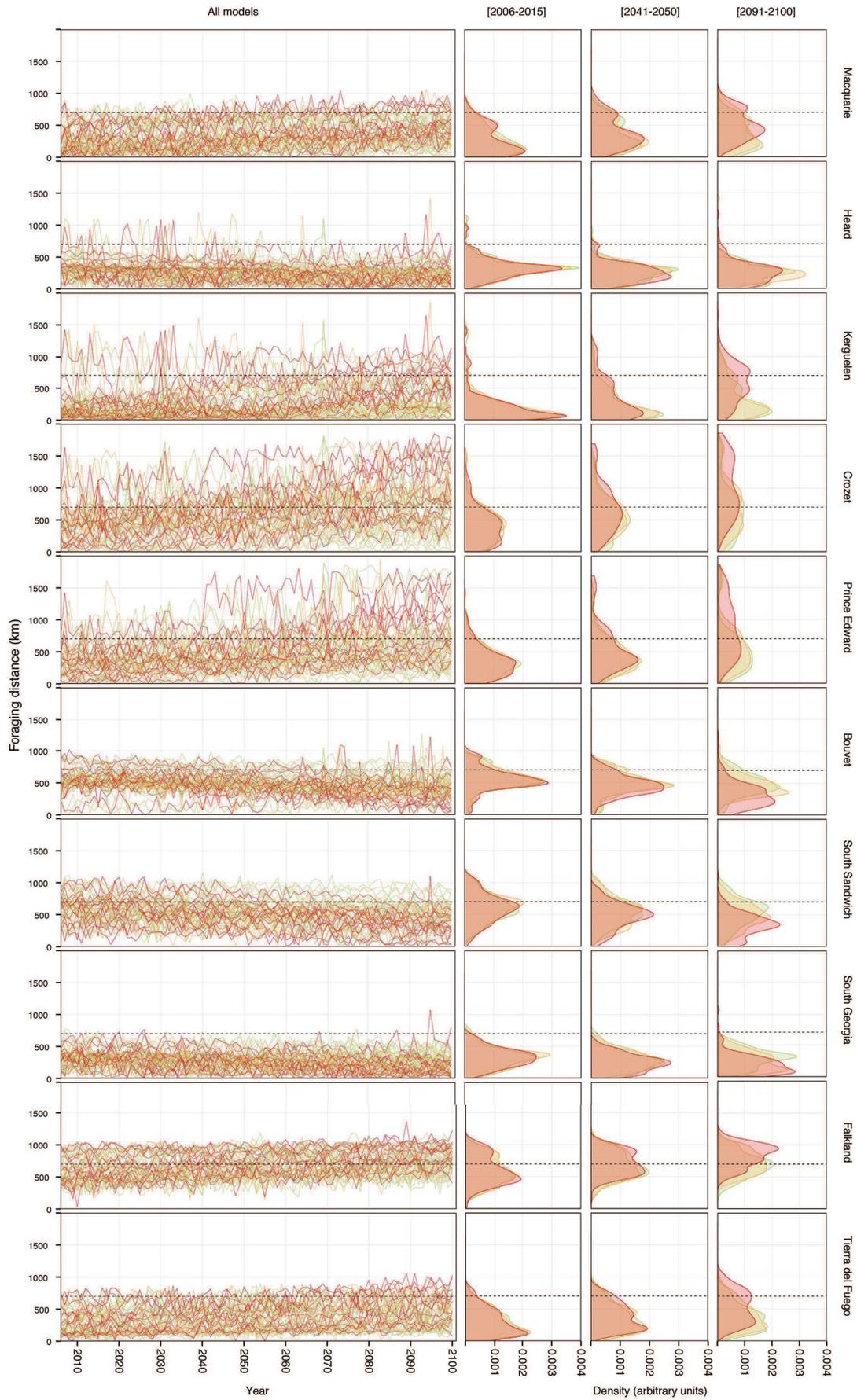
Variability between models remains relatively high, as has already been observed in previous studies (Cabré *et al.* 2015; Goberville *et al.* 2015 - see Fig. 30). At all locations, predictions overlap entirely between rcp scenarios for the first decade of our projections, as is expected. This is still mostly the case in the middle of the century (2041-2050). Most of the divergence between scenarios appear by the end of the century. This may take the form of *(i)* a strong divergence of the rcp-8.5 projections as opposed to rcp-4.5 and rcp-2.6 (as in Kerguelen and Bouvet); *(ii)* an increased dispersion on rcp-8.5 projections (as in Crozet and Prince Edward), or *(iii)* a more gradual panel of possible outcomes from rcp-2.6 to rcp-8.5 (at most other locations), or *(iv)* no strong difference between scenarios in Heard Island. This contrast between scenarios is also noticeable when considering the proportion of individual models predicting a local extinction at each time period (Fig. 30). In the last decade of the century, the 'business-as-usual" rcp-8.5 scenario stands out compared to the "controlled-emissions" rcp-2.6 and rcp-4.5 in Kerguelen, Crozet, Prince Edward, Bouvet and South Georgia, while all three scenarios make up a gradient in Macquarie, South Sandwich, the Falklands, and Tierra del Fuego. Under rcp-8.5, more than 50% of the models predict extinction in Crozet, Prince Edward and the Falklands by the end of the century, and the difficult position of Kerguelen and Tierra del Fuego is confirmed by the fact that a large proportion of models predict extinction on these islands too. Overall, although inter-model variability remains high, and alternative outcomes are possible, the strong consensus both in the increasing foraging distance trend, and in the actual prediction for local extinction, stress both the very likely nature of the threats upon the Southern Ocean ecosystems under the rcp-8.5 scenario, and the possibility of yet avoiding the most destructive effects of these threats if immediate action allows us to bring greenhouse-gas emissions closer to the rcp-2.6 forcing scenario.
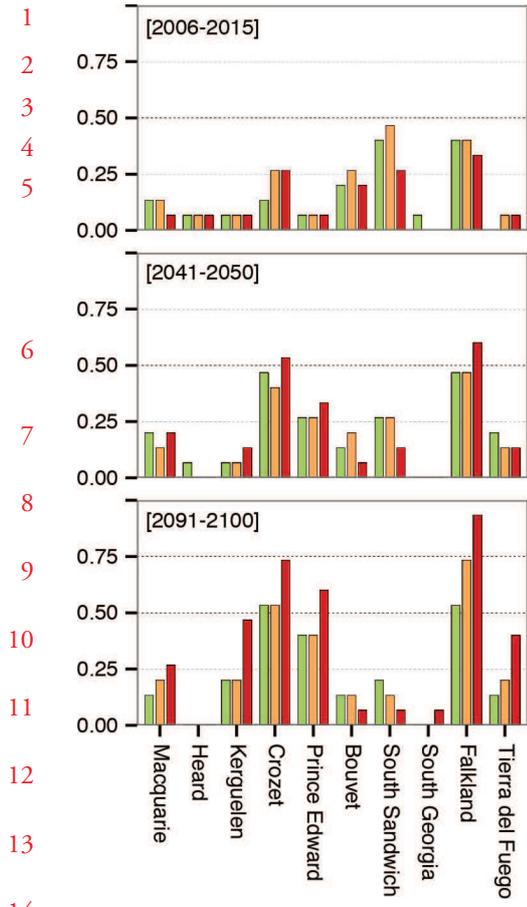
Figure 30 | Proportion of models predicting extinction of King penguin colonies. Proportion of the 15 selected models predicting a February foraging distance > 700 km for 20% of the decade, at three different time points. Colours correspond to rcp scenarios: rcp-2.6 (green), rcp-4.5 (orange) and rcp-8.5 (red).

Acknowledgements

Chapter 5: The Emperor synnome

Cristofari R, Bertorelle G, Ancel A, Benazzo A, Le Maho Y, Ponganis PJ, Stenseth NC, Trathan PT, Whittington JD, Zanetti E, Zitterbart DP, Le Bohec C & Trucchi E, **Full circumpolar migration ensures evolutionary unity in the Emperor penguin.** (*Nature Communications - in prep*)

Context

§-106 Can a species be studied from a single colony? Most studies investigating the effects of climate change on population dynamics have relied either on «anonymous» count data (*i.e.* unmarked individuals treated as a group - see for example VanDerWal *et al.* 2013 or Langham *et al.* 2015), or capture-mark-recapture, individual-based data (*e.g.* Le Bohec *et al.* 2008, Jenouvrier *et al.* 2014, or Durner *et al.* 2009). The latter approach is considerably more precise, as it is able to identify some misleading compensatory effects (such as local decline masked by density-dependent immigration) - however, fieldwork constraints typically restrict this approach to a single study colony or population (as is the case in Charmantier *et al.* 2008; Le Bohec *et al.* 2008; Jenouvrier *et al.* 2014) or to a handful of populations in optimal cases (*e.g.* Dunn *et al.* 2011). Although oftentimes highly informative, these studies all run the risk of misestimating local idiosyncrasies. For example, the characteristic plastic response of Great tits to food peak advance, observed in Great Britain by Charmantier *et al.* 2008, is in strong contrast with observations, al-

beit in very similar conditions, made in Netherlands by Visser *et al.* 1998. Similarly, the recent study of Stenseth *et al.* 2015 found important differences in the response to climate change of different neighbouring Belgian and Dutch Blue and Great tit (*Pares cœruleus* and *P. major*) populations. From a functional standpoint, the observation of Weimerskirch 2013 of fully segregated foraging grounds in two nearby booby colonies suggests that different alimentary strategies may lead to different exposure to environmental change. Thus, before extrapolating the results of local observations to species-level predictions, it is necessary to assess the nature and extent of the coupling between local and global processes.

§-107 Linking generation-scale and coalescent-scale demography. Amongst the hypotheses that allow the extensions of local demographic models to global trends is the assumption of *demographic independence*, that Jenouvrier *et al.* 2014 proposes, in the case of the Emperor penguin, as the idea that «*inter-colony dispersal is extremely unlikely [...]. Thus, neither dispersal nor demographic source–sink dynamics will change our main conclusion about global population declines*» - census and capture-mark-recapture data is thus considered self-contained, and the authors «*do not consider movement among populations; it is unlikely to be demographically important in this species*». Although hardly an avoidable assumption in that case, since almost no demographic data is available for other colonies, this postulate presents a risk: it does not acknowledge the possibility that *(i)* the population trend in the Pointe Géologie Emperor penguin colony may be particular to that colony for stochastic, or for idiosyncratic reasons (that is, not directly because of the observed local sea ice conditions - some elements even make this a very likely possibility, see §24 p. 79), and *(ii)* part of the observed population processes may be better explained by migration than by mortality or growth - that is, without assuming a direct link between local colony size and global population size. Measuring the importance of dispersal in field conditions is a considerable challenge (see §19 p. 68), and can only be done with massive recapture effort (see *e.g.* Barlow *et al.* 2013). Population genetics approaches, on the other hand, allow us to access the long-term migration parameter for a set of populations (see §41 p. 103), and to set, if not a point estimate

of instantaneous dispersal rate, at least a bracket for averaged migration ability in the species, that can help us define reasonable assumptions for developing more accurate demographic models.

Abstract

The rate of ongoing environmental change is now thought to exceed the rate at which most species (Hoffmann & Sgrò 2011), including humans (Díaz *et al.* 2006), are able to adapt, with significant consequences for their resilience and for ecosystem sustainability. In a recent review, Chown *et al.* 2015 reported that despite the pristine appearance of Antarctica, its species and ecosystems are also under considerable threat. Investigating trends and risks in such a remote area relies mostly on a handful of bio-indicator species: the Emperor penguin *(Aptenodytes forsteri)* often fulfills this task, as it integrates the multiple effects of climate change (Ainley *et al.* 2010a). A recent study suggests that populations of this flagship Antarctic species may be at high risk continent-wide within the next 100 years (Jenouvrier *et al.* 2014). However, predicting the dynamics of species adaptation and persistence requires a more complete understanding of the temporally and spatially complex ecological processes shaping the structure of worldwide populations, and can greatly benefit from the synergy amongst disciplines and methods. The projected decline of the Emperor penguin population (Jenouvrier *et al.* 2014) relies on the explicit assumption, based on behavioural observations, that inter-colony dispersal is negligible. Yet, using genome-wide data from individuals belonging to several colonies encompassing the whole Antarctic continent, we reveal that Emperor penguin populations are characterised by a high level of gene flow, with migration rates reaching up to 4.2% between colonies separated by more than 8,000 km of coastline, and a shared common

demography over the last quaternary climate change period. Thus, the population structure in this polar top-predator is better explained by one single global population rather than by a fragmented colonial system. By rejecting the view of the local colony as a relevant demographic unit, our results highlight that *i*) robust demographic projections and extinction risk estimations will only be possible by including dispersal rates in the models, and *ii*) population size fluctuations in single colonies should rather be taken as indicative of local stochastic events, since the species' response to global environmental change will likely follow a shared evolutionary trajectory.

Results

§-108 Studying demography in the context of climate change. The importance of global warming is now a central subject of international concern, and an increasing number of studies seek to understand its impact on the world's ecosystems and to predict likely scenarios in response to climate projections (Thomas *et al.* 2004), either in order to set up more efficient conservation strategies, or as a means to prompt urgent political action (Watson *et al.* 2013; Chown *et al.* 2015). One of the main difficulties of this task lies in the fact that only a handful of species have been monitored for more than a few decades, and, in most cases, our knowledge of their demography is limited to short-term (i.e. generation-scale) responses (Saether *et al.* 2005). Yet, in order to establish reliable projections, larger-scale population parameters must be integrated into demographic models. Recent development of high-throughput sequencing allows the analysis of genome-wide and population-scale data and provides the genomic signature of the important demographic parameters that can be used to accurately predict species responses to global change (Allendorf *et al.* 2010).

Extracting species-wide projections from time-series collected on a single population requires a precise understanding of how local events relate to species-scale demographic processes. We need for instance to establish whether the observed local extinctions or fluctuations occur as a consequence of mortality peaks, massive dispersal events, or a combination of both. Adult mortality has traditionally been proposed as the primary factor (through changes in resource availability and subsequent starvation, see Barbraud & Weimerskirch 2001a, or increased predation, see Ainley *et al.* 2010b), and several models have been built on that basis (Jenouvrier *et al.* 2014). Yet, these models mostly rely on the explicit assumption that movement amongst populations is negligible (Jenouvrier *et al.* 2014), leaving adult and juvenile survival and breeding output as the sole factors driving population dynamics. This assumption, however, is not based on direct evidence, but is rather motivated by technical difficulties in discriminating emigration from mortality of tagged individuals (Hunter *et al.* 2010; Ehrlén & Morris 2015).

§-109 Instability of Emperor penguin colonies. The Emperor penguin, the only winter-breeding top-predator species of Antarctica (Prévost 1961), stands at the forefront of the impacts of climate warming (Ainley *et al.* 2010a). Emperor penguins breed nearly exclusively on sea ice: this unstable habitat makes the species immediately sensitive to local environmental changes. One of the northernmost colonies, located on the Antarctic Peninsula, vanished during the last decades, as sea ice retreated in that area (Trathan *et al.* 2011). Other colonies underwent a dramatic drop in breeding success and population size shortly after a modification in local sea ice topology (Kooyman & Ponganis 2014). The colony breeding on the tongue of the Mertz glacier, for instance, disappeared after the 2010 calving of that glacier (Ancel *et al.* 2014), and the following changes in local ice movements also had catastrophic consequences on the nearby Pointe Géologie colony, where the number of fledged chicks dropped from ~2,500 in 2010 to ~100 in 2014 (*personnal observation*). All of these events have in common an identified proximal cause, usually linked to modifications in the local sea-ice landscape that either forced adults to make longer trips over the sea ice to reach open waters for foraging, with subsequent breeding failure resulting

from heightened energy expenditures (Massom *et al.* 2009; Kooyman & Ponganis 2014), or removed the usual colony location (Ancel *et al.* 2014). On the other hand, recent empirical evidence increasingly points to an important effect of dispersal in that species' respond to habitat disruption (Forcada & Trathan 2009). The rapid recovery of the emperor penguin population in Coulman Island confirms this assumption and excludes a peak in adult mortality followed by regrowth (Kooyman & Ponganis 2014). Recent satellite and ground surveys have also shown that whole emperor penguin colonies are able to relocate with or without an identified cause (Ancel *et al.* 2014; LaRue *et al.* 2015). Finally, biologging experiments have emphasized the outstanding distances regularly traveled by adult and juvenile emperor penguins (Thiebot *et al.* 2013). Here, we demonstrate that dispersal is a fundamental component of demography in this long-lived species, and propose that it does play a central role in its adaptive response at the continental scale. As such, migration amongst colonies needs to be incorporated into demographic models in order to achieve accurate projections.

§-110 Study design. We produced genome-wide RAD-sequencing data for 110 individuals from 6 Emperor penguin colonies representing the whole species' range (Fig. 31A). In order to assess both fine- and large-scale processes, we sampled three colonies in a tight cluster around Terre Adélie, in Eastern Antarctica: Eastern and Western Mertz colonies (Ancel *et al.* 2014 - 'MZE' and 'MZW'), as well as the Pointe Géologie colony, near Dumont d'Urville research station ('DDU'), all three within ~300 km. Two colonies were sampled in the Weddell Sea area, across the continent: Atka Bay colony, near Neumayer research station ('NEU'), ~6,500 km away from Terre Adélie, and Halley Bay colony ('HAL'), ~700 km further. Finally, one colony was sampled from the Ross Sea area (Cape Washington, 'WSH'), ~1,700 km from Terre Adélie and ~8,000 km from Halley Bay.
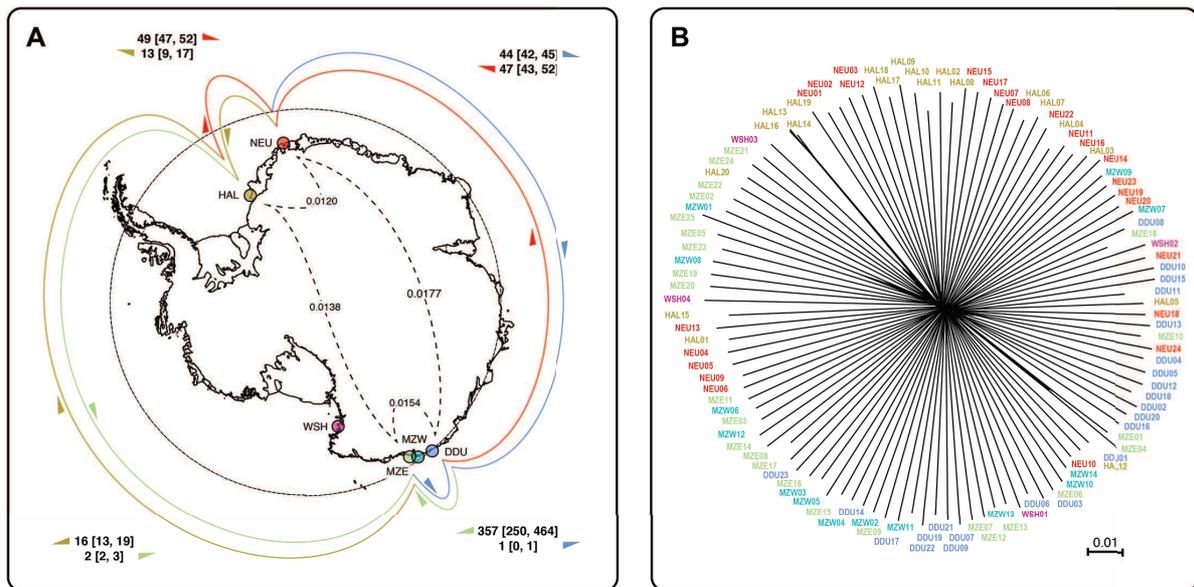
Figure 31 | Drift and mixing concur to keep a high degree of worldwide homogeneity in the Emperor penguin. (A) Estimated pairwise migration rates (outer coloured links) and Fst (inner dashed links) between sampled colonies. Migrations as estimated from joint allele-frequency spectra. Colours refer to the receiving populations. (B) Neighbour-net of all sampled individuals. Colours correspond to colonies on map (A).

§-111 A panmictic species. In striking contrast both with its fragmented geographical distribution and with our current knowledge about other marine predators (Hoelzel 1998; Friesen *et al.* 2007; Molfetti *et al.* 2013), the Emperor penguin exhibits a remarkable degree of genetic homogeneity at the continent scale. Pairwise fixation index (Fst) values, calculated either as a function of allele frequency covariance between populations over variable sites, or from called genotypes using Reich's estimator (Reich *et al.* 2009), are very low (see details in Supplementary methods §129 p. 242 and Table 6), and only about 0.5% of total variance is explained by colony structure (as per AMOVA, see §129 p. 242). A neighbour-net based on pairwise Hamming distances shows considerable admixture between areas: individuals are roughly sorted according to geographical location, but inter-individual variability is largely dominant (Fig. 31B). Inference of population split topology based on allele frequency variation amongst populations (§132 p. 246) also supports this view: neutral genetic differentiation from the ancestral population increases eastward from

WSH to MZE, but with numerous migration events inferred between most colonies (Fig. 38). Finally, high genetic mixing is supported by all classical descriptors of genetic variation (Hardy-Weinberg equilibrium, heterozygosity, nucleotide diversity, Tajima's D - as estimated for non-coding regions of the genome from downsampled haplotypes, see §129 p. 242, as well as principal component analysis, see §131 p. 245). The very limited genetic drift observed between colonies separated by several thousands of kilometers suggests intense gene flow in this flightless seabirds along the coast of Antarctica.

§-112 Demographic reconstruction. The existence of a common, homogeneous gene pool for the entire species also implies that all present-day colonies share a common demographic history. In order to test that, we reconstructed past Emperor penguin population size changes in BEAST2 (Bouckaert *et al.* 2014) under an extended Bayesian skyline plot model. In accordance with our expectation, reconstructions based either on a single colony or on haplotypes sampled randomly from the whole continent converge to the same estimate of effective population size and to the same demographic history. All show a moderate increase in population size over the past 100,000 years, as well as in the full sample (Fig. 32A, §136 p. 252), regardless of the very different present-day colony size (Fig. 32B). This trend is in accordance with the findings of Li *et al.* 2014 based on a single-genome pairwise sequentially Markovian coalescent approach. Emperor penguin population size does not appear to have been affected by the last glacial period. This is in stark contrast with the sudden post-glacial population expansion of the Emperor's sister species, the King penguin (*Aptenodytes patagonicus*) from the sub-Antarctic region (Trucchi *et al.* 2014), a difference likely explained by the contrasting breeding habitats and strategies of the two species, the King penguin being dependent on year-round ice-free breeding sites. The agreement of coalescent histories at both local and global sampling scales supports the idea that all extant colonies share the same genetic pool, and that the effects of neutral genetic drift between distant areas are mostly counterbalanced by the intensity of gene flow.
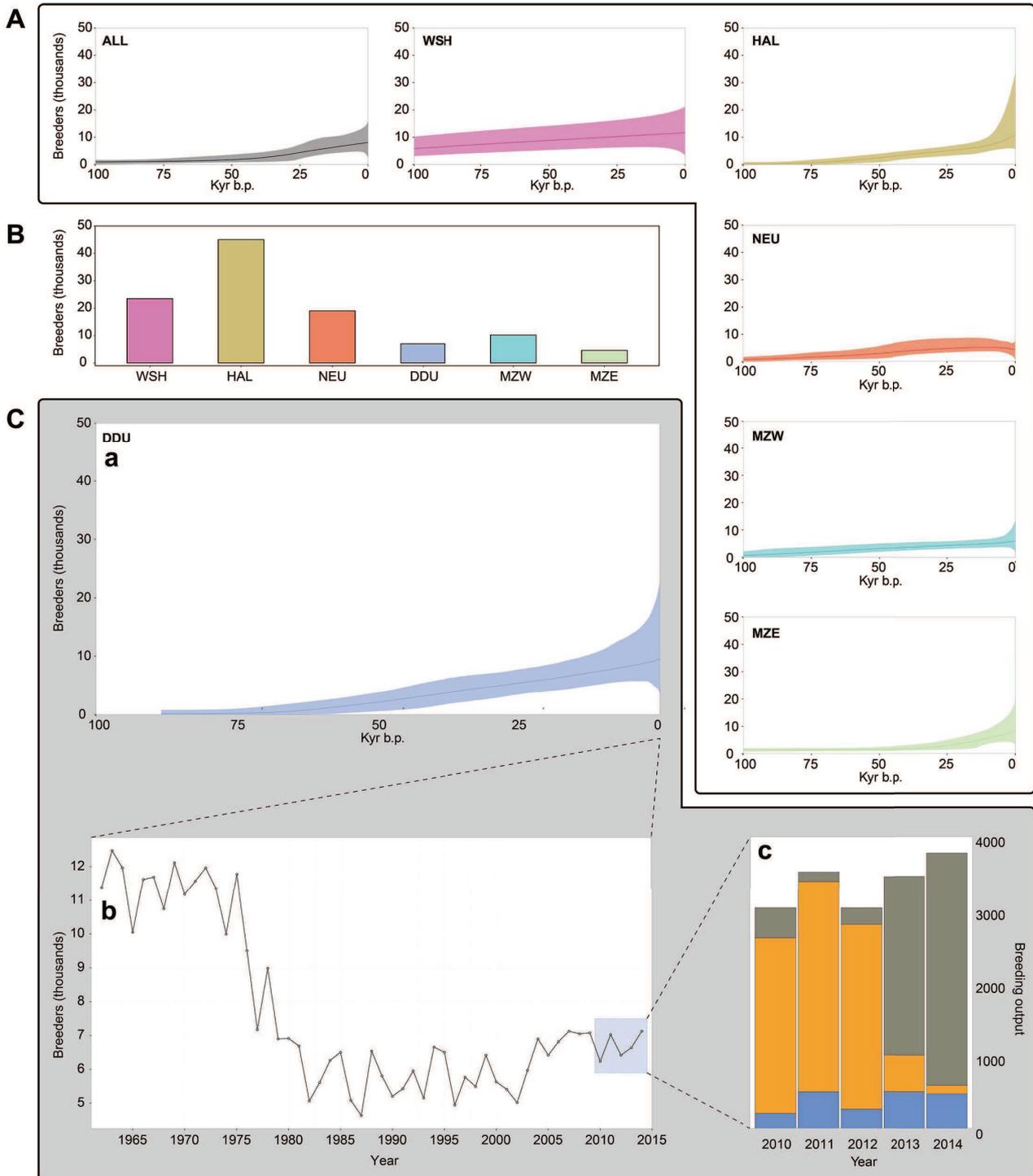
Figure 32 | Demography is a matter of scales. (A) Demographic reconstructions (extended bayesian skyline plots), for all samples, and per-colony. Solid line: mean population size. Shaded area: 95% confidence interval. Blue area: Last Glacial Maximum (LGM). (B) Census size for the six analysed colonies (from Fretwell *et al.* 2012 and Ancel *et al.* 2014) (C) Three different demographic times-scales for DDU colony: a. coalescent-scale (EBSP reconstruction, see 2A), b. monitoring-scale (from Jenouvrier *et al. 2006* and unpublished data), c. current catastrophic breeding failure: blue, eggs lost during brooding, gray, chicks found dead, orange, successfully fledged chicks.

§-113 Continental-scale migration. In order to quantitatively assess the importance of continental

dispersal, we modelled the inter-colony migration rates required to generate such a level of genet-

ic admixture. We first co-estimated effective population size and bidirectional migration rates be-

tween a subset of four colonies representing our whole sampling area by simulating genetic data

under a continuous-time Markovian coalescent model against the observed two-dimensional al-

lele frequency spectra, using a composite-likelihood approach (Excoffier *et al.* 2013, see §135 p.

250). Analysis was calibrated using a RADome mutation rate as estimated for King penguin

(Trucchi *et al.* 2014) and a generation time of 16 years (Jenouvrier *et al.* 2014). Effective popula-

tion sizes all converge to an average of ~4,000 (from 1120 to 7640) breeding individuals (de-

tailed estimates in supplementary Table 7 and Fig. 31A), in keeping with the observed median

size of extant colonies (Fretwell *et al.* 2012). Each colony is estimated to receive, on average, be-

tween ~0.7% and ~4.2% of its effective population size in migrants every generation. Thus, if we

were to scale these results to present-day observed census size, a colony such as Pointe Géologie

(DDU), with a count of ~7,000 breeding adults, would exchange, on average, between ~260 and

~300 migrants (3.8% to 4.2%) per generation with the rest of the continent. We further validat-

ed these results using a haplotype-based multilocus Bayesian approach as implemented in Mi-

grate-n (Beerli & Palczewski 2010, see §134 p. 247). Model ranking using Bayes factor model

choice gives clear support for a full-migration model with very high gene flow. Estimated migra-

tion rates (M) and population sizes (Θ) are highly homogeneous (mean mutation-scaled (μ) mi-

gration rate M = m / μ = 2,358 ±130, mean mutation-scaled effective size Θ = 0.0018 ±8.2e^{-5}).

Considering a conservative range of μ for our subset of loci (Trucchi *et al.* 2014), we can estimate

that each colony receives on average from 5.40% (±0.22) to 10.00% (±0.42) of its total effective

size as migrants from other colonies at each generation (see §134 p. 247). Although slightly high-

er, this estimate is of the same order of magnitude as the one derived from the joint allele fre-

quency spectra. We highlight the fact that these are estimates of the migration parameters aver-

aged over many generations, not of instantaneous dispersal rate (see S-0 p. 236): neither population sizes, nor migration rates, should be interpreted as referring literally to the immediate state of extant colonies but rather to the average coalescence-based population size and migration rate over time. Dispersal rate itself may also be very heterogeneous at any given point of time, with individual colonies showing positive or negative dispersal balance according to the current local habitat conditions and modifications.

§-114 Consequences of high dispersal. Dispersal thus appears to be a central aspect of the Emperor penguin's coloniality, and recent observations suggest that this view may be extended to other seabird species (Friesen *et al.* 2007). For example, we have repeatedly recaptured King penguins tagged at one colony in the Crozet archipelago at different colonies in the same archipelago, and as colonies in the Iles Kerguelen, 1,500 km away (*unpublished data*). As pointed out by Mayr (Mayr 1970), *« a high dispersal ability is a necessity for occupants of temporary habitats »*. Since dispersal has been the immediate response for colonies facing habitat disturbance in the recent past (Forcada & Trathan 2009; Trathan *et al.* 2011; Kooyman & Ponganis 2014), it may therefore be thought to play an important role by adding flexibility to an otherwise rigid philopatric system, and by allowing the species to dynamically exploit the best breeding locations in rapidly changing polar environments. Yet, such demographic events are of local rather than global significance. Population trends extracted from a single colony reflect the immediate quality of the focal location on a generation scale, rather than species-wide parameters (Fig. 32C). In this context, the colony is not a truly relevant demographic unit, but rather a transient aggregation of individuals at a particular point of time. In order to distinguish this structure from panmictic and metapopulation systems, we propose the term *synnome* for this combination of an exceptionally fragmented space and a very fluid gene pool (see full definition in Supplementary methods S-0 p. 236).

§-115 Future prospects. Our findings highlight the importance of adopting a cross-disciplinary approach, integrating population genomics and behavioural ecology, to the study of population dy-

namics. Such an approach should help in the development of more robust and accurate demographic projections at the whole species level. These refined projections will then be more likely to allow estimation of the extent of threats to vulnerable species and identifying the proximal causes of their decline. Our results also highlight the absolute novelty of the Emperor penguin's single fully-panmictic population. Although exceptional if compared with current knowledge about other marine predators, such as turtles (Molfetti *et al.* 2013), marine mammals (Hoelzel 1998), and most seabird species (Friesen *et al.* 2007), intense dispersal is expected to be a common evolutionary strategy in unstable high-latitude environments (Friesen *et al.* 2007), especially under ongoing climate warming. As a single genetic population, Emperor penguins will respond to climate change through a unified evolutionary trajectory. This insight thus presents new challenges to our understanding of how current climate scenarios will impact upon the future of the most cold-adapted species in the world, an iconic bio-indicator of the delicate Antarctic ecosystem.

Methods Summary

Samples were collected from fledged chicks or frozen carcasses at the end of the breeding season. RAD sequencing followed Baird and colleagues' original protocol (Baird *et al.* 2008) with minor modifications (see Supplementary methods §126 p. 237 for details). Sequences were aligned on the Emperor penguin's reference genome (Zhang *et al.* 2011b) and cleaned using standard tools. Genotyping was performed using GATK's HaplotypeCaller (DePristo *et al.* 2011) pipeline, Stacks (Catchen *et al.* 2011; Catchen *et al.* 2013), and ANGSD (Korneliussen *et al.* 2014). Genotype likelihoods and site-allele-frequency likelihood distributions were calculated in ANGSD (Korneliussen *et al.* 2014) under a samtools/mpileup model (§127 p. 238 and §128 p. 241). Only autosomal, high-quality loci were retained. Summary statistics were calculated in ngsTools (Fumagalli *et al.* 2013; Fumagalli *et al.* 2014), *adegenet* (Jombart 2008), and custom R

and shell scripts (§129 p. 242). For haplotype-based analyses, each individual was randomly downsampled to a haploid genome by discarding one haplotype at each locus, in order to avoid low-coverage biases. Hamming distances and identity-by-descent estimation were calculated in PLINK (Purcell *et al.* 2007, see §130 p. 244). For population size and migration rate estimates, we used Migrate-n (Beerli & Palczewski 2010), using downsampled haplotypes (§134 p. 247), and *fastsimcoal2* (Excoffier & Foll 2011; Excoffier *et al.* 2013), using empirical joint-frequency spectra calculated in ANGSD (§135 p. 250). BEAST2 (Bouckaert *et al.* 2014) was used to co-estimate effective population size and population size changes through time (§136 p. 252). See online supplementary material for more detailed information.

Modelling the changes in Emperor penguin habitat.

§-116 Aim of this study. The following part was not included in the original article « *Full circumpolar migration ensures evolutionary unity in the Emperor penguin* ». The strong contrast between the marked demographic response of the King penguin on the one hand (see *The King synnome*, p. 163) and the lack of detectable response of the Emperor penguin on the other, however, raises the question of the direct environmental determinants of demographic trends in the second species. Here, we propose a preliminary model to explore the relationship of the Emperor penguin to its direct abiotic environment, defined both by sea ice, and by atmospheric variables. Although the conclusions of this study are very consistent with the demographic trends inferred from genetic data, further work may still be required, outside the framework of the coarser CMIP5 models, in order to understand the finer local dynamics of sea ice formation and coastal polynya activity.

§-117 How to model the Emperor's habitat? Our survey of the Emperor penguin's genetic architecture brings to light two important traits: *(i)* the whole species is organised as a single synnome, and migration between colonies is a central demographic process, and *(ii)* the Emperor penguin

population was not affected by the late Pleistocene and Holocene climatic events (which is also confirmed by our reconstructions in *The King synnome*, p. 163). A corollary of the Emperor's high dispersal ability, is the possibility that colonies may relocate when local habitat conditions become unsuitable, provided better conditions can be found anywhere in the vicinity (see *Empirical evidence of heterogeneous dispersal*, p. 259, and LaRue *et al.* 2015).

These findings redefine the way the Emperor's habitat may be modelled. In a previous attempt that we discussed earlier in this chapter, Jenouvrier *et al.* 2014 used the observed complex correlation between sea ice conditions and Emperor penguin survival and breeding success on the Pointe Géologie colony to define a population dynamic model, that is extended to the whole continent using present-day colony locations as the focal points for assessing local environmental conditions. We showed that a first shortcoming in this approach is the assumption that dispersal was not interfering with local dynamics in response to icescape changes (or to other forcings such as human disturbance) - which may result in a biased estimate (and hence model) of survival and breeding output.

But a second, and equally important difficulty lies in the nature of the Emperor penguin's habitat. Indeed, the Emperor needs both dense and firm ice for establishing its breeding colonies, and open-water polynyas (see §18 p. 65) for foraging during the breeding season. Since only coastal (usually *latent heat*) polynya are a requisite, the total sea ice extent around the continent is of comparatively little importance, as long as offshore wind stress maintains open-water conditions at regular intervals along the shore (Ainley *et al.* 2010a). However, the mobility of Emperor penguin colonies imply that the distance between a particular present-day colony location and a polynya is not a hard constraint: as opposed to the King penguin whose breeding locations are fixed (see *The King synnome*, p. 163), the Emperor is free to select a colony space that will optimise both the strength of the ice for chick rearing, and the proximity of polynyas for foraging.

Ultimately, this means that although the local icescape has a strong impact on short-term colony demography, the species as a whole is sensitive to changes in the global state of the coastal Antarctic sea-ice rather than to local conditions: as long as an equivalent breeding location is available, the expected response is relocation rather than extinction (see also Forcada & Trathan 2009 on that point). For example, while an increasing distance between a subantarctic island and the Polar Front translates as an increased foraging constraint on the King penguin (see §80 p. 167), an increasing distance between a given present-day Emperor penguin rookery and the nearest polynya will most likely encourage the penguins to change their colony location accordingly to track their optimal habitat conditions, with no predictable cost for the population. Thus, the local, colony-based paradigm we adopted for the analysis of the King penguin's habitat in *The King synnome*, p. 163, and that Jenouvrier *et al.* 2014 deployed for predicting the Emperor penguin's future demography does not seem to be appropriate for the latter. Here, we explore an alternative approach, based on the global sea ice conditions around the coast of Antarctica.

§-118 Sea ice in the CMIP5 experiments. An additional difficulty in predicting the Emperor penguin's response to climate change is a technical limitation: the current CMIP5 AO-GCMs (see §50 p. 130) normally provide outputs mapped on a 1° grid, which, under the higher polar latitudes, is a rectangle of ca. 111 x 50 km - too coarse a grid to explicitly model polynyas, which are often less than 50km wide. Moreover, the current representation of Antarctic sea ice in the CMIP5 ensemble members still fails to capture important aspects of the observed conditions, such as the significant positive trend in sea ice extent (Zhang 2007; Turner *et al.* 2013; Shu *et al.* 2015) - a shortcoming that may be due to the fact the Antarctic Ice Sheet is currently specified as a boundary in the CMIP5 ensemble, and not explicitly modelled (Kusahara *et al.* 2015). Due to these constraints, it is currently impossible to accurately determine the distribution on polynya along coastal Antarctica in the CMIP5 framework.

However, our reconstructions of past population size changes give us an alternative viewpoint on the question. Although variation in habitat quality through space can be alleviated by dispersal, variations through time are rather final, and oblige the species to adapt or decline. Thus, the lack of response of the Emperor penguin to Pleistocene and Holocene climate change implies that the global sea ice conditions that prevailed at these periods provided suitable habitat for the species. Comparing the CMIP5 predictions for sea ice conditions during the Last Glacial Maximum, at midHolocene, during the historical period, and at the end of the 21st century should therefore allow us to simplify the complex spatial component of the Emperor's relationship to sea ice, and to consider several successive states of global sea ice distribution and characteristics. However, the identified biases in sea ice representation in CMIP5 models restricts the scope of this study: we expect it to be highly informative regarding how far CMIP5 models support a scenario in which changes in sea ice configuration brings the Emperor penguin to large-scale decline throughout the continent - but less so as to the species' actual demographic trend.

§-119 Model and variable selection. Our choice of models, within the CMIP5 ensemble, is limited by the availability of outputs and the difficulty of performing objective model-choice based on outputs. Only six models so far provide outputs for the PMIP3 palæoclimate experiments, the historical period, and three RCP scenarios (RCP-2.6, RCP-4.5 and RCP-8.5 - see §102 p. 201): the CCSM4, CNRM-CM5, the GISS-E2-R, the IPSL-CM5A-LR, the MPI-ESM-P, and the MRI-CGCM3 (see Table 5 for details). Analysis was performed on six 20-years period, during the LGM, at midHolocene, in 1980-1999 for historical runs, and 2080-2099 for the three RCP runs. Outputs were further divided into five yearly breeding stages (based on Jenouvrier *et al.* 2014): interbreeding (January to March), parading and egg-laying (April-May), incubating (June-July), hatching and small-chick rearing (August-September) and rearing of the thermally independent chick (October to December).

Table 5 | Ensemble members used in sea ice modelling. Model outputs were downloaded from the IPCC archive (http://www.ipcc-data.org/sim/gcm_monthly/AR5/Reference-Archive.html). Only one ensemble member was used for each model (r1i1p1 whenever available).

Model	Institution	LGM	mid-Holocene	21st century
CCSM4	*National Center for Atmospheric Research (USA)*	r1i1p1	r1i1p1	r1i1p1
CNRM-CM5	*Centre National de Recherches Météorologiques, Centre Européen de Recherche et de Formation Avancée en Calcul Scientifique (France)*	r1i1p1	r1i1p1	r1i1p1
GISS-E2-R	*NASA/GISS (Goddard Institute for Space Studies) (USA)*	r1i1p1	r1i1p1	r1i1p1
IPSL-CM5A-MR	*Institut Pierre Simon Laplace (France)*	r1i1p1	r1i1p1	r1i1p1
MPI-ESM-P	*Max Planck Institute for Meteorology (Germany)*	r1i1p1	r1i1p1	r1i1p1
MRI-CGCM3	*Meteorological Research Institute (Japan)*	r1i1p1	r1i1p1	r1i1p1

Sea Ice Concentration. We focused primarily on Sea Ice Concentration (SIC), as proposed by Jenouvrier *et al.* 2014. Considering that Emperor penguins are primarily affected by the local ice conditions around their coastal breeding site, and not by the total sea ice extent (Ainley *et al.* 2010a), we restricted the analysis to a zone of 3° from the coastline and offshore - which corresponds to a distance of ~330 km, largely including the maximum length of an Emperor penguin's walking trip to the nearest polynya (~100km at most before systematic breeding failure, see Massom *et al.* 2009). Within that zone, we considered four global descriptors of SIC: *(i)* the mean concentration, *(ii)* the variance of concentration, *(iii)* Moran's global index of spatial autocorrelation, and *(iv)* the sea ice extent within the coastal zone, defined as the ratio of the total surface with a SIC > 15% (Ainley *et al.* 2010a). For each of these parameters, we calculated multi-model mean and across-model standard deviation. In order to quantify the relative importance of changes in sea ice conditions through time, compared to model uncertainties, we also calculated the coefficients of variation - either between periods (*i.e.* geological periods, and RCP scenarios) within models, or between models within periods.

Sea Ice Thickness and Wind Stress. Three other complementary model output variables were assessed in order to capture possible variation in the icescape that would not be reflected in SIC.

First, Sea Ice Thickness (SIT) was taken as a different proxy for the presence of polynya. SIC describes the fragmentation of sea ice, which is normally high in polynya areas, but may be inaccurately represented in the current models. SIT is also expected to be low in polynya areas, due to the ongoing sea ice formation and offshore drift (Ainley *et al.* 2010a), and may not be subject to the same biases as sea ice concentration in the current models. For SIT, multi-model mean and across-model variance were calculated for the continent-wide mean thickness, standard deviation, and Moran's index. Across-models and across-periods coefficients of variations were also calculated.

Offshore wind stress is the proximal cause of polynya formation (see §18 p. 65). Since sea-ice models are usually independent sub-models within the CMIP5 AO-GCMs (see *e.g.* Gent *et al.* 2011), we account for the fact that wind patterns themselves may be accurately modelled, but that the sea-ice response at expected polynya areas may be less reliably predicted. We consider two variables representative of offshore wind stress in Antarctica: the Northward surface wind speed component (VAS, in m.s^{-1}) and the Surface northward downward wind stress (TAUV, in Pa). For both variables, we extracted multi-model mean and across-model variance for the continent-wide mean, standard deviation, and Moran's index for both VAS[1] and TAUV. Across-models and across-periods coefficients of variations were also calculated. All computations relied on the Climate Data Operators toolset (CDO 2015, available at: http://www.mpimet.mpg.de/cdo) and custom R scripts.

§-120 Is coastal sea ice really changing? SIC is predicted to decrease in all 6 included models, while its variance increases from LGM conditions until RCP-8.5 conditions (Fig. 33A). SIT, on the other hand, shows divergent trends across models, either slightly decreasing (in CCSM4 and MRI-CGCM3), or stable from LGM to 21st century (in the other models), while its variance decreases or remains unchanged (Fig. 33B). For both variables, homogeneity of spatial distribution,

---

1.　　　VAS is not output by the CCSM4 model - for this variable, we therefore only use a 5-member ensemble.

as summarised by Moran's global index, remains unchanged throughout Pleistocene and Anthropocene - the rather high value ($0.5 < I < 1$) is consistent with a local clustering of low-ice areas in polynya around the continent. As expected, SIC changes most during the warmer months - in summer (interbreeding period), autumn (egg-laying) and spring (rearing). Overall, despite the known bias towards sea ice reduction in the CMIP5 models, the *extent* of coastal sea ice only decreases during the interbreeding period, and marginally the egg-laying period, in most models.

Wind patterns, on the other hand, are remarkably constant on the Antarctic coastal band from LGM to RCP projections. Let aside the widely divergent GISS-E2-R model, offshore surface wind stress (TAUV) remains unchanged, in terms of absolute average value, spatial variance, and distribution (Fig. 33C). Wind speed decreases most noticeably between at the LGM-Holocene transition, but only decreases during the interbreeding period in the RCP projections (Fig. 33D). Since offshore wind stress is the primary cause of polynya formation, the stability of coastal offshore wind patterns may be an indication that polynya dynamics did not change much during the Pleistocene and the Holocene, and may not change much in the coming decades either. This is consistent with our reconstruction of Emperor penguin population size through the past millennia (see §82 p. 169 and §112 p. 218): the lack of demographic response to the glacial maximum and following deglacial period implies that the species' habitat was not significantly changed, and that Emperors were able to find a sufficient number of polynya for overwinter foraging throughout the period.

Figure 33 | (NEXT PAGE) Changes in sea ice configuration along coastal Antarctica from Pleistocene to the 21st century. Mean, variance and Moran's global index for sea ice concentration in % (**A**) and thickness in meters (**B**), and offshore surface wind stress in Pa (**C**) and speed in m.s^{-1} (**D**). In (**A**), sea ice extent is additionally defined as the ratio of sea ice surface with a concentration below 15%.

A - Sea ice concentration (SIC)

B - Sea ice thickness (SIT)
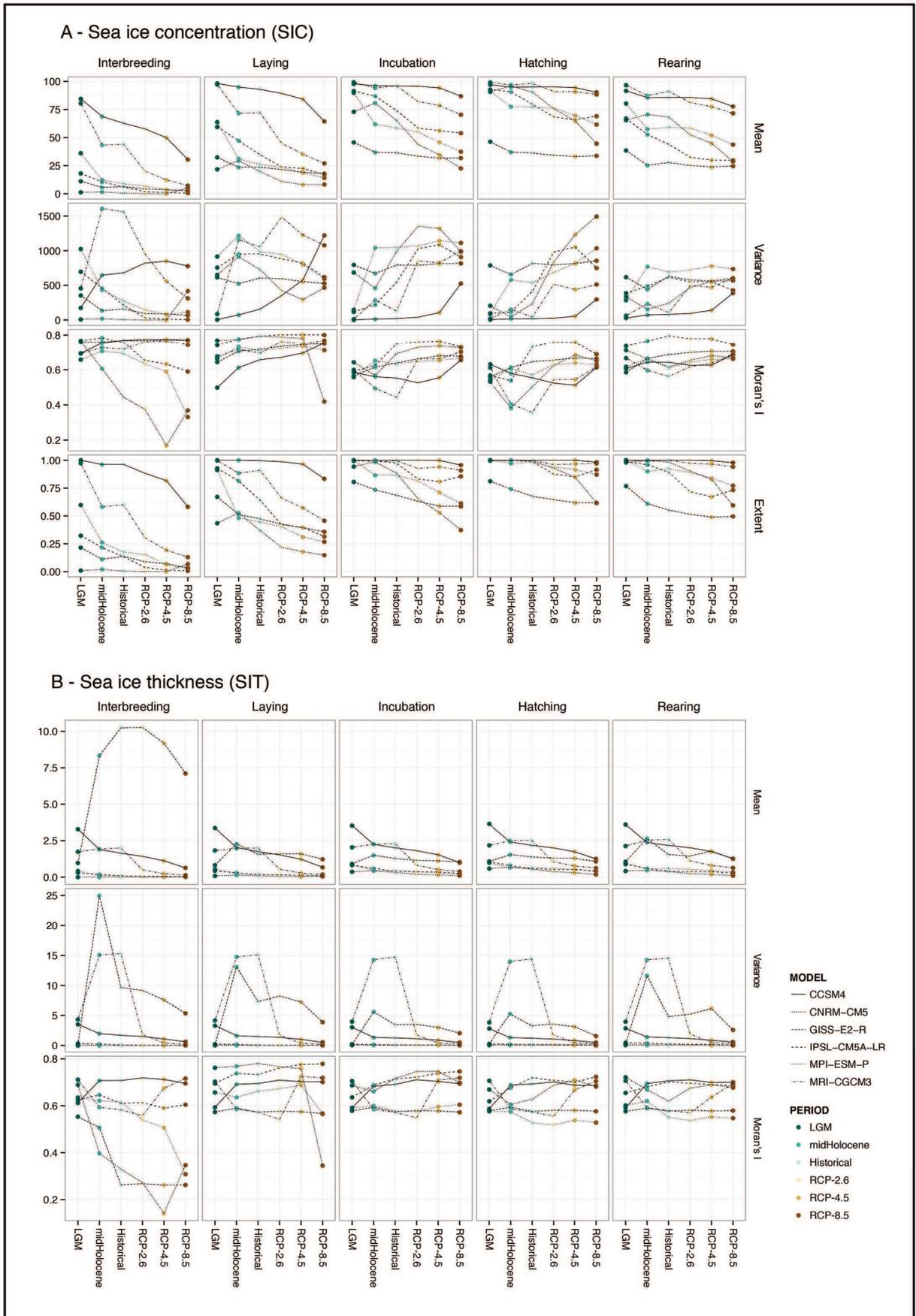
C - Surface wind stress (TAUV)
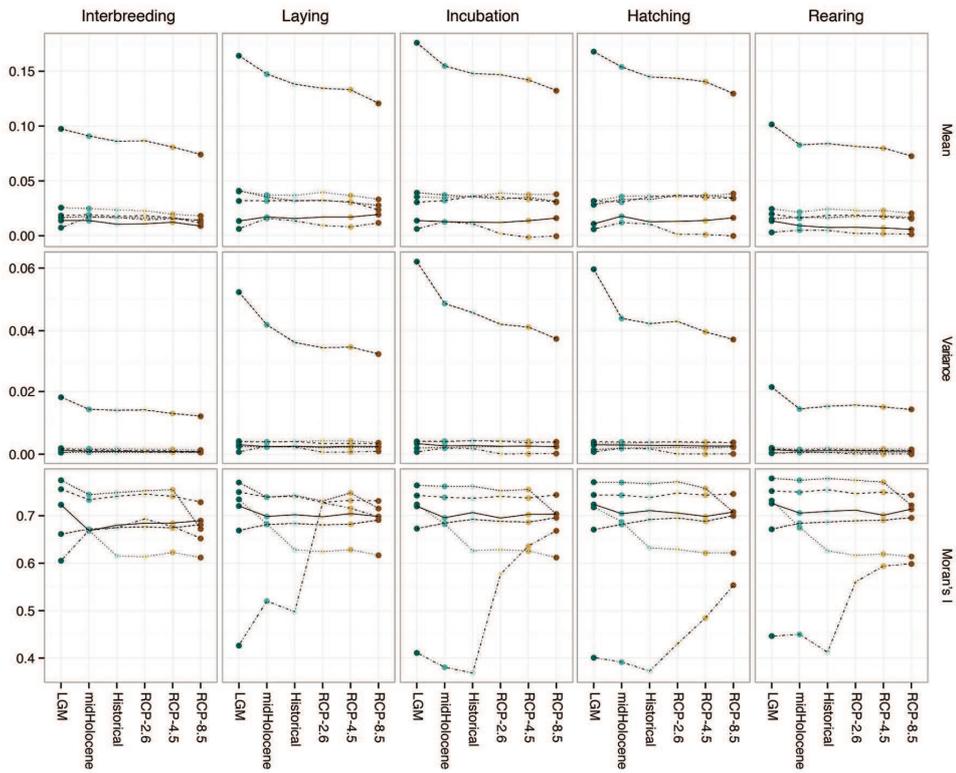
D - Suface wind speed (VAS)
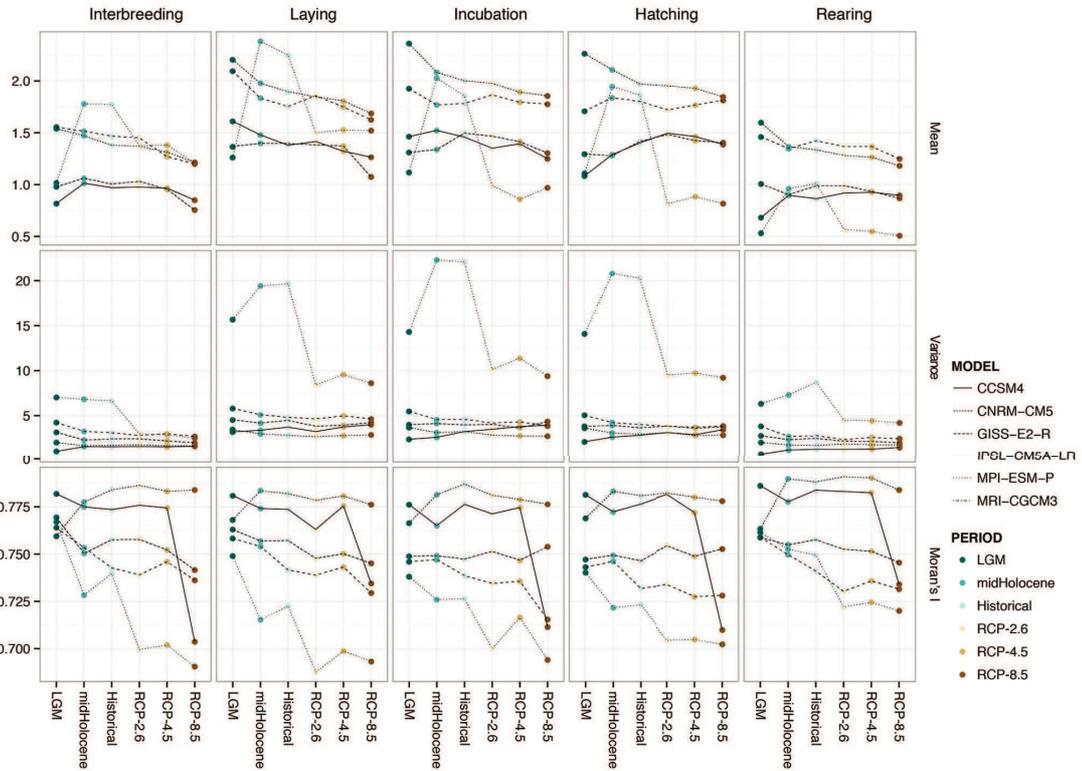
§-121 *Uncertainties in the CMIP5 models.* Comparison of per-model and per-period coefficients of variation (CV) stresses the large uncertainty that remains in the current AO-CGMs for the sea-ice zone around the Antarctic. For all four variables, CVs per period are equal or greater than CVs per model (Fig. 34) - in other words, the reconstructed and predicted changes are of the same order, or smaller, than the uncertainty in the models. Although such a comparison is not a direct assessment of the significance of trends in the models, it means that any detected trend still remains within the bounds of possible model uncertainty. In keeping with previous assessments (see *e.g.* Ainley *et al.* 2010a; Turner *et al.* 2013; Shu *et al.* 2015), wind patterns exhibit far less across-model variation than ice patterns, and may thus appear more robustly represented than ice patterns. Taken together, these different observations indicate that *(i)* the current generation of models disagrees strongly on the future ice patterns, and to a lesser extent wind patterns, around coastal Antarctica, prompting the development of more detailed local models (integrating the dynamics of the ice sheet in particular, see Kusahara *et al.* 2015), and *(ii)* taking this observed uncertainty into account, the evidence from the assessed models does not indicate any strong change in ice and wind patterns since the LGM, even in under the more pessimistic RCP-8.5 scenario.

Figure 34 | (NEXT PAGE) Uncertainty in the representation of sea ice in the CMIP5 models. Coefficients of variation (CV) for sea ice concentration in % (**A**) and thickness in meters (**B**), and offshore surface wind stress in Pa (**C**) and speed in m.s^{-1} (**D**). In (**A**), sea ice extent is additionally defined as the ratio of sea ice surface with a concentration below 15%. CV are computed per model, or per periods.

A - Sea ice concentration (SIC)

B - Sea ice thickness (SIT)

C - Surface wind stress (TAUV)

D - Suface wind speed (VAS)
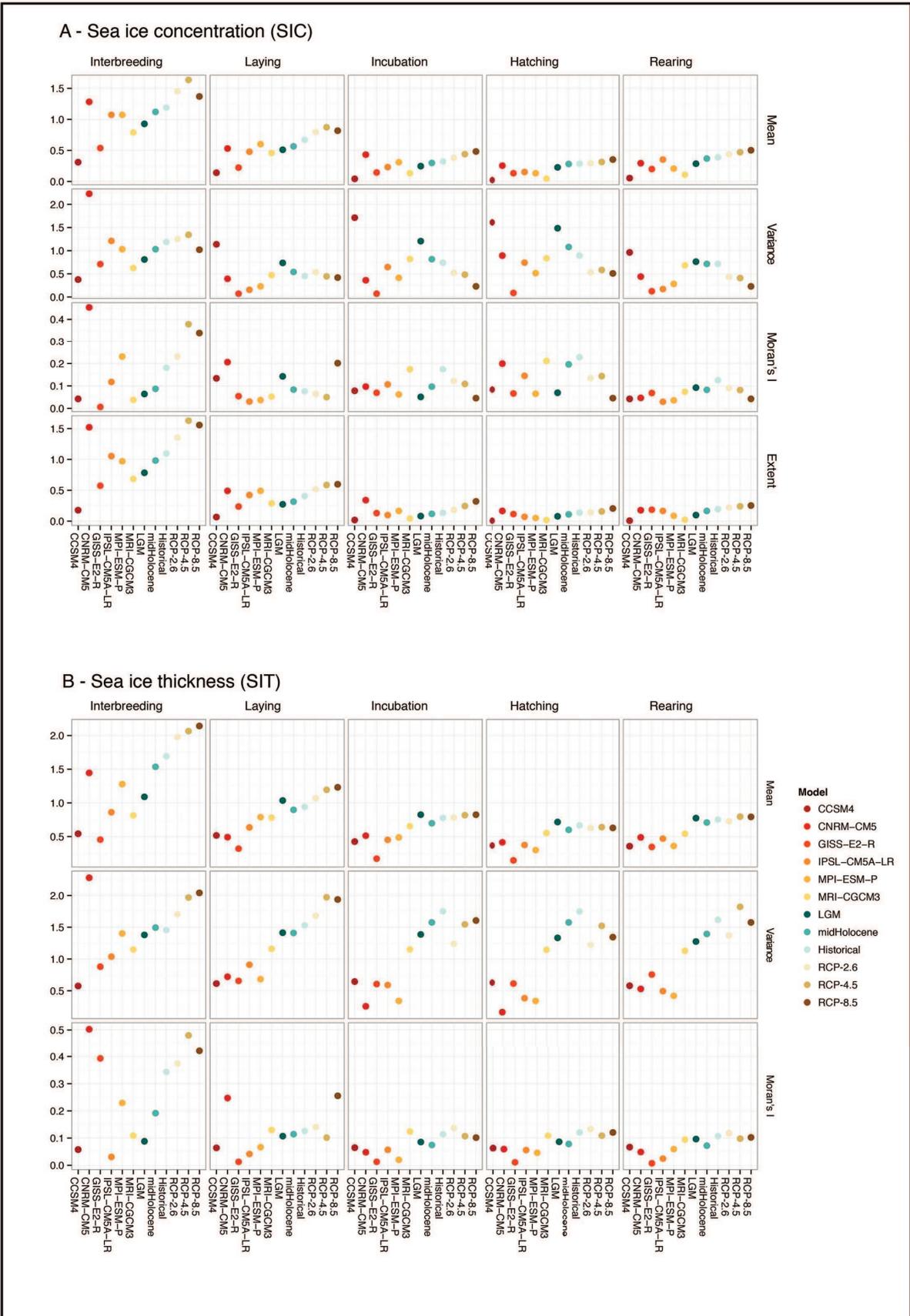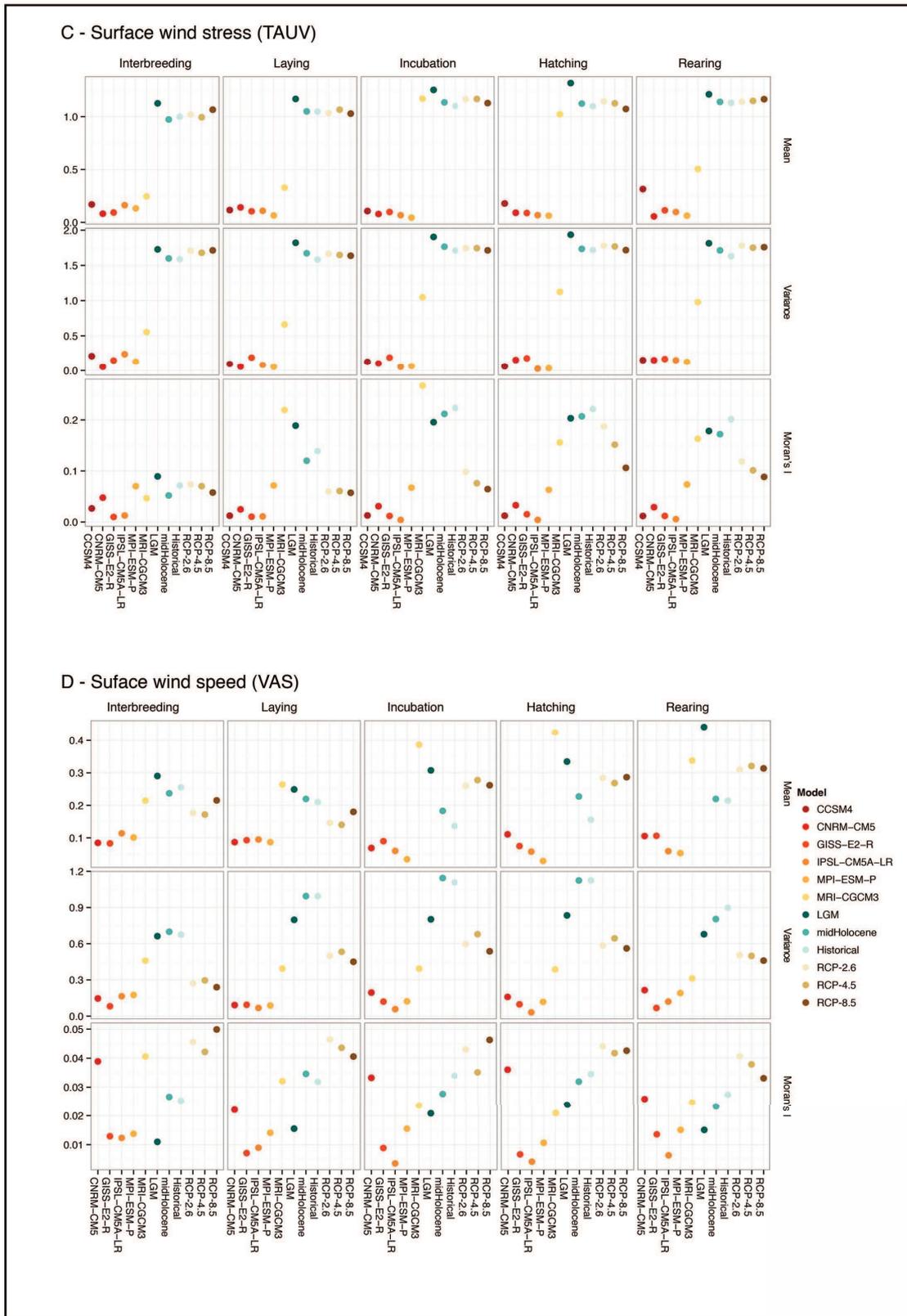
§-122 Can we predict Emperor penguin demography based on sea ice? Our examination of the habitat of the Emperor penguin shows the strong difference that oppose the two *Aptenodytes* species. While the King penguin's fixed and fragmented breeding locations forces it to undergo drastic range contractions and expansions in response to Southern Ocean chances, it appears that the Emperor penguin's ability to relocate when the local icescape changes, together with the paradoxical stability of the coastal Antarctic habitat, allowed it to maintain a constant population size throughout the main climatic events of the Pleistocene.

Although the Antarctic sea-ice area as a whole underwent large changes during the Pleistocene glacial-deglacial cycles (see §9 p. 42 and *The King synnome*, p. 163), the coastal zone stands out as a particular region. First, as it is buffered by the large expanses of pack ice that shield it from the lower latitudes, changes that occur at the edges of the ice remain mostly silent in the coastal area.: this is visible in the fact that even the projected changes in SIC are mostly visible in summer, when this buffer zone is reduced. Second, because the most important sea ice features, for the Emperor penguin, are not directly linked to the total amount of sea ice, but rather to the dynamics of its formation in the coastal wind-stress-driven divergence zones: thus, provided wind stress remains constant, an increase or decrease in total sea ice extent may have but little impact on the Emperor's ability to find accessible foraging areas. Indeed, on very short time scales (*i.e.* shorter than a generation), it is possible that abrupt changes in the repartition of sea ice may result in adverse effects for a single colony, as have been documented in Pointe Géologie (Barbraud & Weimerskirch 2001a) or in Coulman Island (Kooyman & Ponganis 2014), however, relocation to a more favourable location in the area seems to be rapid (see LaRue *et al.* 2015 and *Empirical evidence of heterogeneous dispersal*, p. 259). Overall, the long-term stability of the Emperor penguin population implies that local events have little influence on the resilience of the species as a whole.

These results do not imply that Emperor penguins will not be threatened by global warming. As we pointed out earlier (see §84 p. 174), the impacts of climate change have multiple aspects, that go well beyond the local changes in icescape. Changes in the trophic web of the Southern Ocean and an overall decrease in productivity (due to changes in upwelling activity on the Polar Front, to acidification, and most importantly to sheer temperature effects on plankton communities, see *e.g.* Beaugrand *et al.* 2002) may have a much deeper impact on the Emperor penguin population than changes in polynya distribution. However, addressing these changes will require very different approaches, such as ecosystem modelling - a central topic, but unfortunately beyond the scope of this work.

Supporting information

S-0: Main concepts in use

§-123 Choice and definition of a « synnome ». For the lack of an appropriate term that would be currently in use, we chose to designate by the word *synnome* the particular colonial system that can be observed in the Emperor penguin, and possibly in other species. We derive this term from the Greek σύννομος, « *a common grazing of flocks* », used in particular for gathering flocks of birds (e.g. Aristophanes' *Aves*, v. 1756-7), and which was commonly used by extension for « *reunions* », « *gatherings* », and even « *kindred* ». These different meanings together convey the particularity of the observed structure: *one single, nearly homogeneous pool of individuals is distributed in a highly discrete way throughout its range. Local concentrations, or colonies, are highly consistent on the scale of a few generations, at which scale philopatry may be the norm. Yet, migration between these areas is high enough to maintain total homogeneity of the species' gene pool, so that, viewed on a micro-evolutionary time-scale, the only relevant unit is the species as a whole.*

§-124 Dispersal and migration. **Dispersal** was originally described by Howard (Howard 1960) as « *the movement the animal makes from its point of origin to the place where it reproduces* ». From each

individual's perspective, it is «*the greatest distance its genetic characteristics are transmitted, rather than the greatest distance the animal may have migrated or otherwise travelled away from the place it was conceived, hatched or born*». **Migration**, on the other hand, has been described by Dingle and Drake (Dingle & Drake 2007) in a biogeographical context as «*range expansions of faunas or individual species*», such as «*the northward extension of ranges following the retreat of glaciers at the end of the ice ages*». More specifically, in a population genetics context, the (mutation-scaled) migration parameter M has been defined by the same authors as «*the exchange of genes among populations by whatever means, including but not limited to migration as we consider it here*» (Dingle & Drake 2007). It is used in that sense in the coalescent framework, in particular by Beerli and colleagues (Beerli 2004; Beerli & Palczewski 2010). Thus, in that context, migration is distinguished from dispersal by its larger scale: whereas dispersal is an individual- and generation-centred phenomenon that may be observed directly, migration is a time-averaged, population-centred event that is only detectable through indirect methods, such as gene flow reconstruction.

S-1: Supplementary methods and analysis

§-125 Sample collection and DNA extraction. Material was collected from six locations of East Antarctica, between 2004 and 2012: Cape Washington in the Ross sea area («WSH»), Pointe Géologie («DDU») in Adélie Land, Mertz East («MZE») and Mertz West («MZW») in George V Land, Atka bay («NEU») in Dronning Maud Land area, and Halley Bay («HAL») in the Weddell Sea area. On the DDU colony, blood samples were collected from 23 chicks prior to fledging. In WSH, MZE, MZW, NEU and HAL, muscle samples were collected from frozen chick carcasses collected around the colony (WSH: N=4, MZE: N=25, MZW: N=14, NEU: N=24, HAL: N=20). DNA was extracted using a spin-column protocol (Qiagen DNEasy© Blood and Tissue kit) with minor modifications.

§-126 Genome-wide Single Nucleotide Polymorphism (SNP) typing. SNP discovery and sequencing followed a single-digest RAD-sequencing protocol (Baird *et al.* 2008). Genomic DNA was checked for degradation on a 1.5% agarose gel, and only samples with consistently high molecular weight were retained and quantified by fluorometry (Life technologies™ Qubit®). A total of 110 samples was retained and sequenced in 5 distinct libraries. (i) approximately 150 ng of genomic DNA per sample were digested with the restriction enzyme *Sbf*-I-HF (NEB); (ii) each sample was then ligated to a unique barcoded P1 adapter prior to pooling in a single library. The library was then sheared by sonication (7 cycles 30'' ON – 30'' OFF); (iii) sonicated libraries were concentrated to 25 µl by DNA capture on magnetic beads (beads solution:DNA = 0.8:1), thus further reducing the carry-over of non-ligated P1 adapters, and the target size range fraction (350-650 bp) was then selected by automated gel electrophoresis (BluePippin®); (iv) capture on magnetic beads using the same beads:DNA ratio (0.8:1) was then employed in all following purification steps (after blunt-end repairing, poly-A tailing, P2 adapter ligation and library enrichment by PCR). Magnetic beads were kept together with the library throughout the pre-PCR steps, and DNA was re-bound to the beads for purification using a P EG-8000 binding solution; (v) PCR amplification was performed in 8 x 12.5 µl aliquots pooled after the amplification in order to reduce amplification bias on few loci due to random drift. PCR was performed using NEB Phusion® polymerase with the following cycles: 30'' denaturation at 98°C, 18 cycles of amplification (10'' at 98°C, 30'' at 65°C, and 30'' at 72°C), and a final elongation of 5' at 72°C; (vi) the library was then quantified by a fluorimetry-based method (Life technologies™ Qubit®), and molarity was checked on an Agilent Bioanalyzer chip (Invitrogen™). A final volume of 20 µl for each library was submitted for paired-end sequencing on an Illumina HiSeq2000 sequencer (V3 chemistry, libraries 1-3), or HiSeq2500 (V4 chemistry, libraries 4-5), at the Norwegian Sequencing Centre, University of Oslo, spiked with 20% PhiX control library in order to reduce low-diversity bias.

§-127 Sequence alignment and genotyping. Data processing was performed using the following workflow: (**i**) **Sequence demultiplexing.** Read quality assessment was made in FastQC (http://www.bioinformatics.babraham.ac.uk/projects/fastqc/). Samples were de-multiplexed according to in-line barcodes using Stacks v1.20 (Catchen *et al.* 2011; Catchen *et al.* 2013), low-quality reads were discarded, and sequences trimmed to 95 bp. (**ii**) **Read mapping and filtering.** Demultiplexed fastq files were mapped to the published contigs of the Emperor penguin genome (Zhang *et al.* 2011b) using Bowtie2 2.2.3 (Langmead & Salzberg 2012), with standard settings, allowing only end-to-end mapping. Resulting SAM files were filtered using Samtools 0.1.19 (Li *et al.* 2009), PicardTools 1.113 (http://picard.sorceforge.net), and custom R and shell scripts in order to discard unpaired reads and full read pairs where at least one mate has a mapping quality score below 30. The resulting BAM files were then filtered for PCR and optical duplicates by comparing mapping position and CIGAR string, using Picard MarkDuplicates. This process also allowed to filter out most sequencing errors, since MarkDuplicates only retains the read with the highest average Phred score in each duplicate cluster. (**iii**) **SNP calling and genotyping.** Three independent algorithms were used for SNP and genotype calling, all of them built on a maximum-likelihood framework. 1) First-in-pair reads were exported as BAM files for the maximum-likelihood-based genotype caller built in the Stacks pipeline (ref_map.pl), with a maximum of 5 mismatches allowed between alleles at a single locus (both within and between individuals), correcting genotype calls using the information from the whole dataset in the rxstacks program. 2) We used the same cleaned BAM files to simultaneously call both mismatch and indel polymorphisms in all samples using the GATK HaplotypeCaller pipeline (DePristo *et al.* 2011), with standard parameters, except for population heterozygosity which was set to 0.01. 3) ANGSD 0.900 (Kim *et al.* 2011; Nielsen *et al.* 2012) was used to call SNPs and genotypes using a maximum-likelihood process with the Samtools mpileup/bcftools algorithm, using the complete sample allele frequency information as a prior. Genotype calls were only retained for comparison purposes with Stacks and GATK, however, downstream analysis was performed directly on raw genotype likeli-

hoods, as this approach has been shown to be much more sensitive to weak structure than classi-cal SNP-calling analysis (Nielsen *et al.* 2011; Fumagalli *et al.* 2013). Genotype calls from all three processes were formatted into VCF format using software-specific (Stacks and GATK) or custom scripts (ANGSD); further filtering and manipulation was done using VCFtools 0.1.12 (Danecek *et al.* 2011). For analyses relying on SNP calls, an additional filtering step was per-formed by a) extracting the list of consensus loci called as SNPs by all three independent algo-rithms, b) discarding genotypes with a coverage under 3X for analyses sensitive to sequencing de-pth, c) removing loci genotyped in less than 75% of all individuals, and finally d) thinning down loci to keep only polymorphism distant of at least 1 kb, in order to minimise linkage between markers. **(iv) Sex-linked marker analysis.** In order to check for sex-specific dispersal or structure patterns, we repeated analyses for each sex separately, using either autosomal loci only or Z-linked loci only. We used the published genome annotations for bird gametologs (Zhou *et al.* 2014) to identify potentially Z-linked scaffolds. Since females are heterogametic in birds, we ex-pect non-pseudo-autosomal Z-linked regions to be fully homozygous in females, but to neutrally heterozygous in males. We therefore retained only scaffolds that had a clearly bimodal distribu-tion of heterozygosity, with one mode at or close to 0 (a slight tolerance was allowed to account for misalignment, sequencing errors mistyped as SNPs due to low coverage, or presence of a tran-sposable elements with autosomal homologs). Fifteen scaffolds were ultimately retained. Scaffolds containing candidate Z-linked coding DNA sequences, but with no visible bimodal heterozygosi-ty distribution, were excluded altogether from the analysis. Sex assignment was performed inde-pendently from each of the non-recombining Z scaffolds, and consistency of sex calls between scaffolds was checked manually.
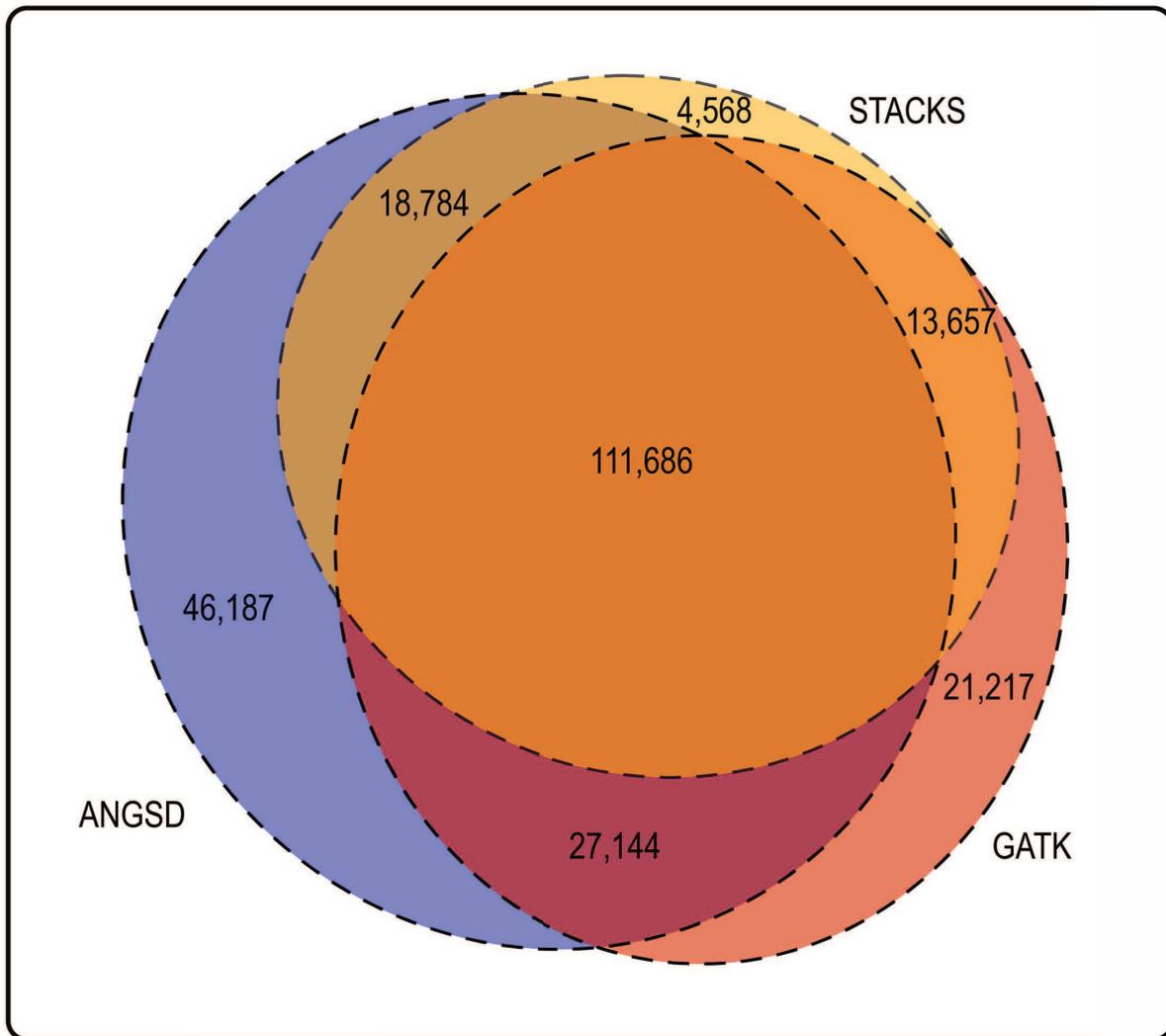
1 **Figure 35 | Consensus SNP calling.** Venn diagram of SNP calls by three different algorithms: GATK,
2 ANGSD with Samtools model, and Stacks.

3 *§-128 RAD data description.* Each HiSeq sequencing lane yielded an approximate 201,000,000
4 paired-end reads (±16,000) with a mean Phred score of 37, only part of which was dedicated to
5 that project. After barcode demultiplexing and quality filtering, w e r etained a n average
6 147,000,000 read pairs per library (±13,000,000). Concordant alignment rate was high (70.7%
7 ±9.1%). However, after filtering, a large proportion of the reads was identified as duplicates and
8 removed from further analysis. On average, 479,000 read pairs were retained per individuals. We
9 built an average 78,000 loci per individual (±17,000). Overlap between SNP calling methods was

high: 111,686 SNPs were called by GATK (173,704 SNPs total), ANGSD (203,801 SNPs total), and Stacks (148,721 SNPs total) (Fig. 35). After filtering by coverage (minimum 3x) and missing data (minimum 75% representation), 59,037 highly confident SNPs were retained for analysis, with a mean depth of 6.8x. Of these, 582, spread across 15 scaffolds, were identified as unambiguously belonging to the non-recombining region of the Z chromosome.

§-129 Pairwise FST, AMOVA, and summary statistics. Pairwise fixation index was estimated by two independent methods. We calculated Reich's estimator (Reich *et al.* 2009 - which has been shown to be most robust to small and uneven sample sizes, see Willing *et al.* 2012) on called genotypes, using custom R scripts. Without calling genotypes, we calculated Reynolds' estimator (Reynolds *et al.* 1983), taking into account uncertainty in site-allele-frequency, according to the method implemented in ngsTools (Fumagalli *et al.* 2013; Fumagalli *et al.* 2014). Both methods were performed on a per-site basis and averaged over 1-kb non-overlapping sliding windows, as the ratio of the windowed sum of inter-population variance over the windowed sum of total variance. For the genotype-call-free method, only sites with a probability of being variant at least equal to 0.95 were included in the estimation. Nucleotide diversity and Tajima's D were calculated on a per-locus basis. In order to avoid possible biases due to low coverage, we randomly sampled one haplotype for each individual, and performed calculations on this haploid subset. Calculations were made using *adegenet* and *pegas* packages, as well as custom R scripts. We found that the Hardy-Weinberg equilibrium holds across 466 out of 590 scaffolds with all colonies assessed together (out-of-equilibrium scaffolds all have less than 5 SNPs). The mean homozygosity across all individuals is low ($F=0.051 \pm 0.094$) and does not exhibit any inter-colony difference. The nucleotide diversity is low and highly similar across all colonies ($\pi_{DDU}=0.0026$; $\pi_{MZE}=0.0023$; $\pi_{MZW}=0.0023$; $\pi_{NEU}=0.0023$, $\pi_{HAL}=0.0023$; $\pi_{WSH}=0.0026$), going along with the expectation for long-lived high-investment species (Romiguier *et al.* 2014), and despite very different colony census sizes. Finally, Tajima's D averaged across the whole genome does not deviate from neutral expectations ($D_{DDU}=-0.87$; $D_{MZE}=-0.66$; $D_{MZW}=-0.578$; $D_{NEU}=-0.64$; $D_{HAL}=-0.68$; $D_{WSH}=-0.28$).

1 We used SplitsTree (Huson & Bryant 2006) to build a neighbour-net based on pairwise Fst dis-

2 tances between colonies. In order to quantify the proportion of variation at each organisation lev-

3 el, AMOVA was performed on unlinked SNP data (§131 p. 245) using Arlequin (Excoffier *et al.*

4 2005), on a per-locus basis, with 1,000 permutations.
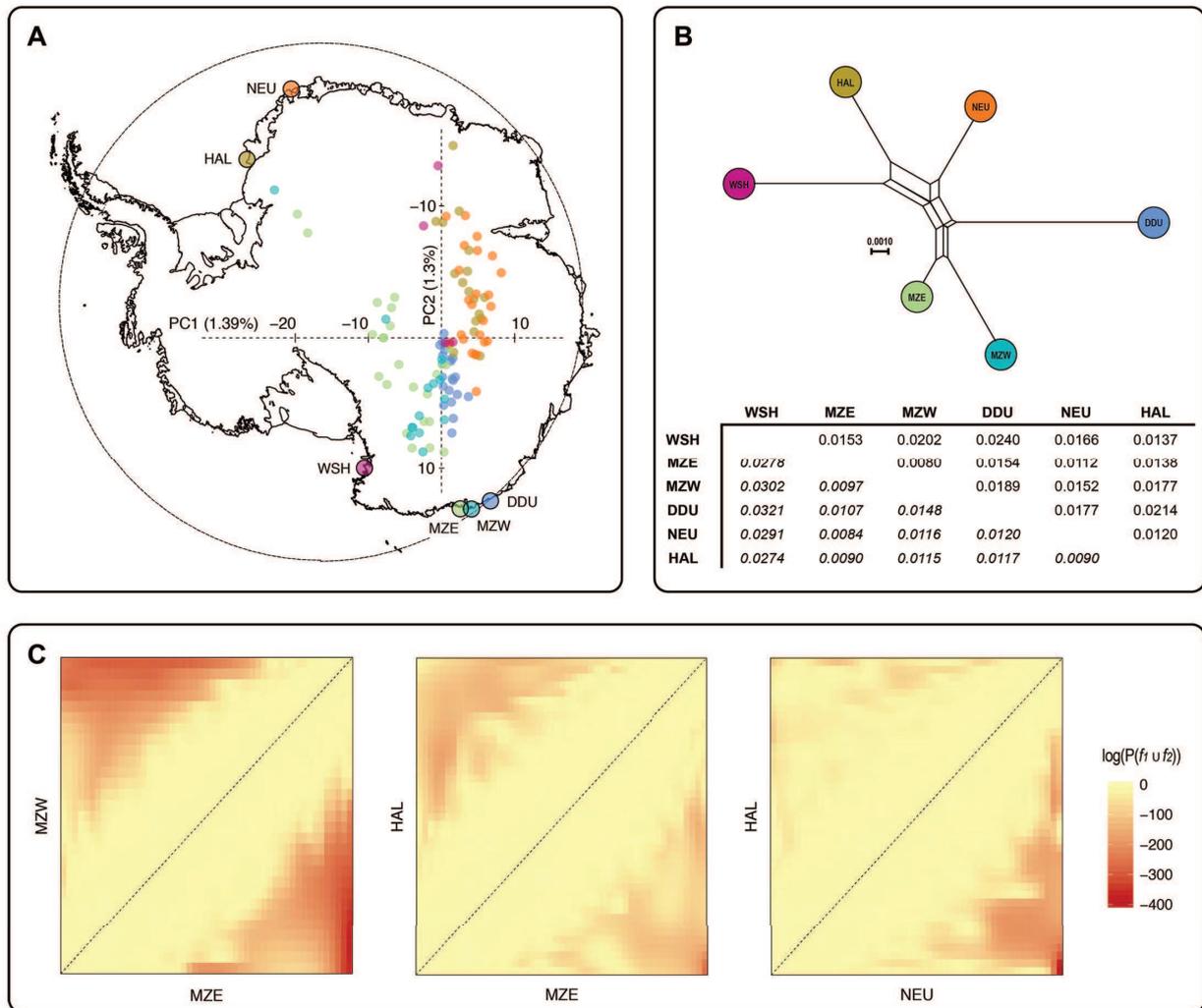
5 **Figure 36 | The imprint of geography on the Emperor synnome.** (**A**) Principal component analysis

6 (percentage of explained variance along the axes) - the colours on the plot refer to the colours used on the colony lo-

7 cations. (**B**) NeighbourNet built from Fst values according to Reich's estimator (table: upper triangle, point esti-

8 mates, lower triangle, standard deviation). (**C**) Three examples of pairwise derived-allele frequency spectra, between

9 two nearby South Pacific colonies (MZE and MZW), two distant colonies (HAL and MZE), and two South Atlantic

10 colonies (HAL and NEU).

Table 6 | Pairwise Fst, according to Reich's estimator. *Upper triangle*: mean value, *lower triangle*: standard deviation. DDU: "Dumont d'Urville", HAL: "Halley Bay", MZE: "Mertz East", MZW: "Mertz West", NEU: "Neumayer", WSH: "Cape Washington".

	DDU	HAL	MZE	MZW	NEU	WSH
DDU		0,0214	0,0154	0,0189	0,0177	0,0240
HAL	*0,0117*		0,0138	0,0177	0,0120	0,0137
MZE	*0,0107*	*0,0090*		0,0080	0,0112	0,0153
MZW	*0,0148*	*0,0115*	*0,0097*		0,0152	0,0202
NEU	*0,0120*	*0,0090*	*0,0084*	*0,0116*		0,0166
WSH	*0,0321*	*0,0274*	*0,0278*	*0,0302*	*0,0291*	

§-130 Identity-by-state (IBS) and identity-by-descent (IBD). Pairwise indicators of IBS and IBD were calculated in PLINK v1.9 (Purcell *et al.* 2007). Allelic distance for pairs of individuals is rather sensitive to uneven coverage (Fig. 37, lower triangle), with lower-depth individuals appearing more similar to all other individuals than higher-depth ones. However, IBD inference, which takes into account the total genetic variance in the whole sample, appears more robust to coverage variation (Fig. 37, upper triangle). Three individuals in the HAL colony (HAL13, HAL14 and HAL16, visible on Fig. 37 and Fig. 39), as well as two in the MZE colony (MZE01 and MZE04, visible on Fig. 37 and Fig. 39), appear markedly more related to each other than to the rest of the sample. Of these two clusters, only one individual was retained for inbreeding-sensitive analyses, such as principal component analysis. Pairwise IBS distances were also used to generate a neighbour-net using SplitsTree (Huson & Bryant 2006).
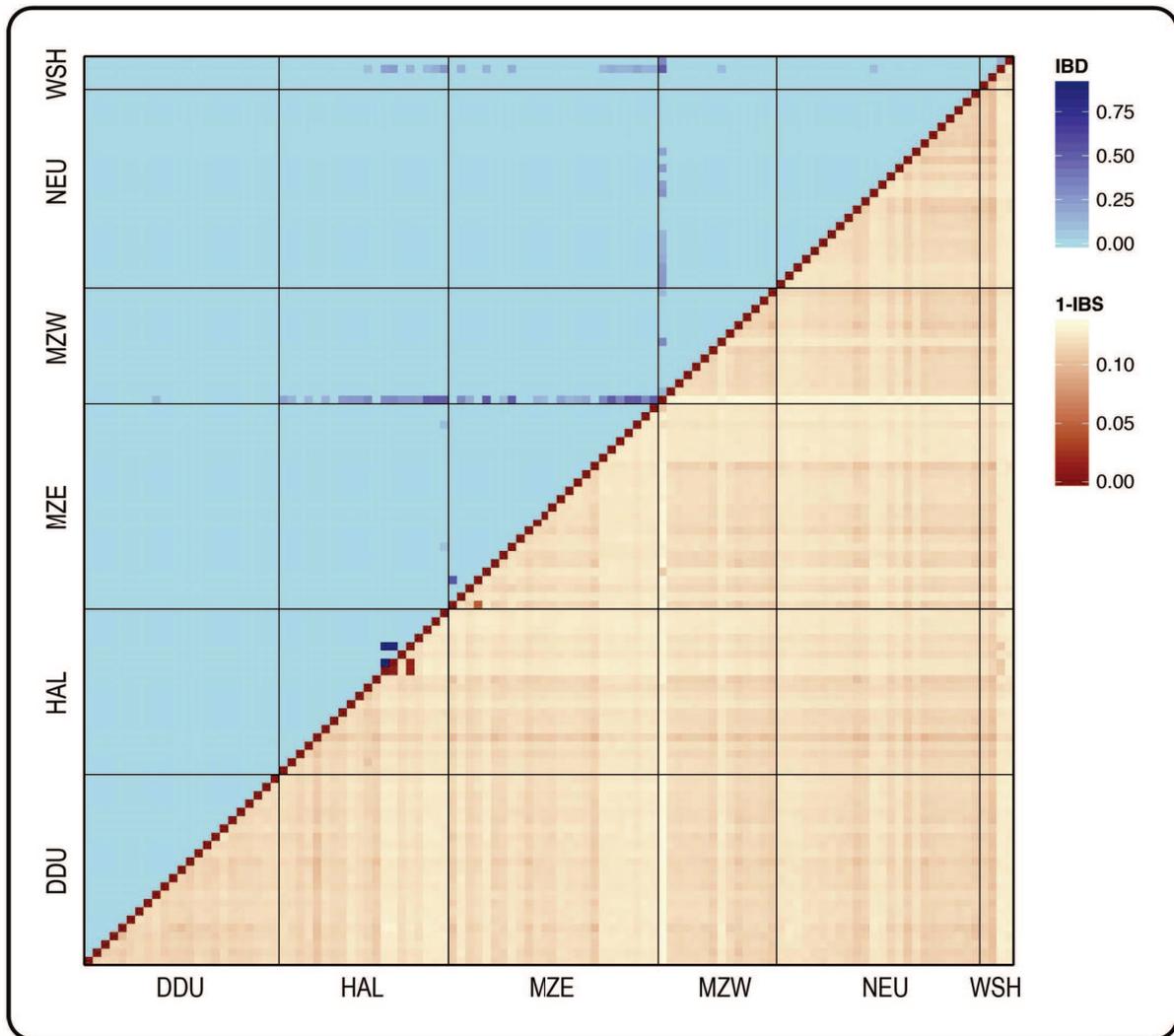
1 **Figure 37 | Pairwise genetic distance matrix. Upper triangle:** identity-by-descent inference (IBD). **Lower**
2 **triangle:** identity-by-state pairwise (IBS).

3 *§-131 Principal Component Analysis (PCA).* PCA was performed on called genotypes using R li-
4 brary adegenet (Jombart 2008), and on genotype likelihoods using ngsCovar (Fumagalli *et al.*
5 2014). Analysis was performed either on all samples or keeping only one individual for each
6 highly related cluster. When performed on all samples, analysis was mostly driven by the HAL re-
7 latedness cluster, with that first PC accounting for 2.84% of total variance. Interestingly, these
8 outliers are also identified as a separate group in admixture analyses (see below, §132 p. 246),
9 with high repeatability, although with only a slight gain in model fit compared to a single-popu-

lation model (Evanno's ΔK over 10 replicates). However, discriminant analysis of principal components (Jombart 2008) performed in adegenet, contrasting these outliers and the main sample group, showed that single-locus contributions were very low and evenly spread across the genome, thus excluding any strong directional selective phenomenon. After removal of all samples but one in each high-relatedness cluster, variation did not appear to be driven by outliers anymore. Overall, the variance explained by geographical structure is extremely low. After outlier removal, the first PCA component of variance shows a weak general pattern of isolation-by-distance along the coast. Mertz colonies stand on the one end, Pointe Géologie in the centre, and Atka Bay and Halley Bay at the other end, yet Ross sea samples do not stand out, as would be expected in case of strong, systematic distance-driven drift. However this pattern remains extremely marginal: the variance explained by the first component barely amounts to 1.4% of the total variance, and colonies can not be distinguished on the basis of PCA.

§-132 Population splits and migration topology. We used TreeMix (Pickrell & Pritchard 2012) to infer the topology of population splits and migrations from allele frequency variation among colonies. We produced RAD-sequencing data for the Emperor's sister species, the King penguin *Aptenodytes patagonicus*, and processed it with the same protocol as for our Emperor penguin samples. We genotyped 15 King penguins from the Baie du Marin colony, on Crozet archipelago, that were used as an outgroup for the analysis. We restricted our dataset to ca. 15,000 highly confident, unlinked SNPs shared between the two species. 3-population and 4-population tests did not allow us to reject a tree-like topology in our data. Analysis was performed first using the King penguin outgroup, and bootstrapping over blocks of 500 SNPs, in order to assess the topology of relationships between our 6 Emperor penguin colonies. We used this topology to re-run TreeMix without the King penguin samples, but fixing the root according to our first results, in order to increase the resolution of the analysis (Fig. 38).
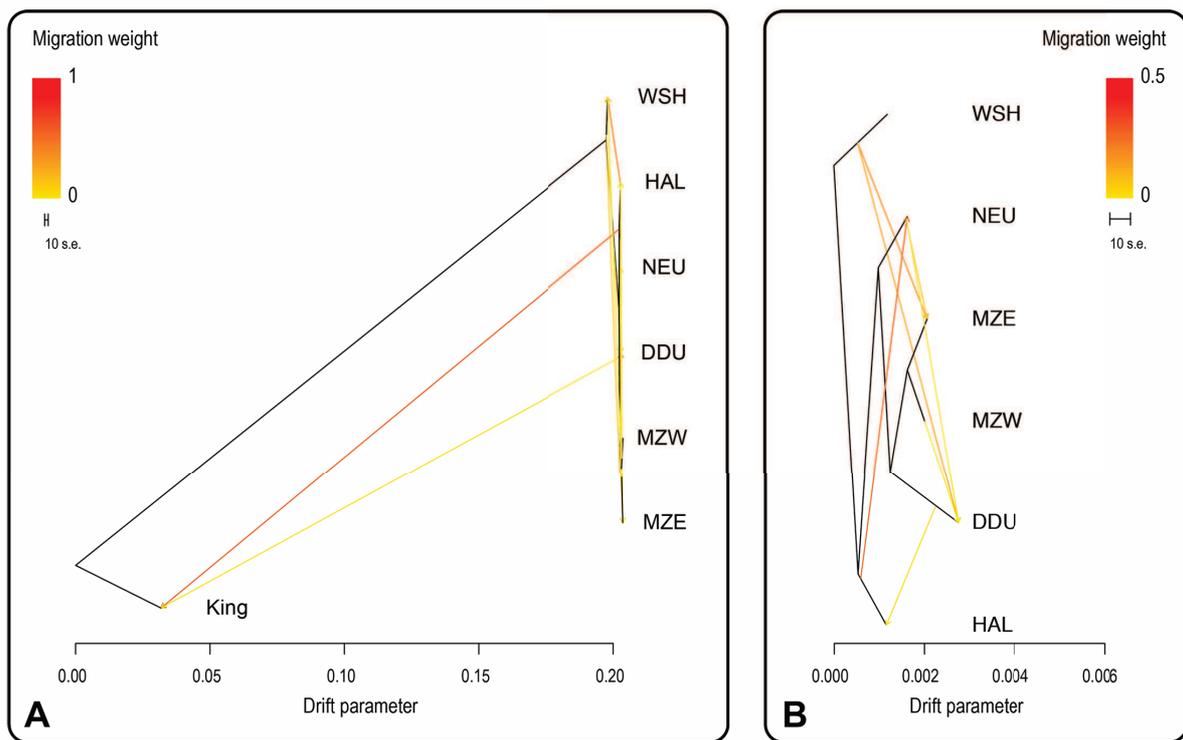
Figure 38 | Inference of population splits. Population tree reconstruction based on the *TreeMix* model. (**A**) Including polymorphism data from the King penguin as an outgroup. (**B**) Without the King penguin and fixing the root as the same position as inferred in **A**.

§-133 Clustering analysis. Clustering analyses were performed both on called genotypes, using fastStructure (Raj *et al.* 2014), and on genotype likelihoods, using ngsAdmix (Skotte *et al.* 2013). For both algorithms, only consensus polymorphic loci were retained. We tested a number of components ranging from 1 to 10, with 3 independent replicates. For fastStructure, we used a simple prior for K values ranging from 1 to 10, and a logistic prior for values from 1 to 3. Most likely number of components was chosen using fastStructure's chooseK.py script for fastStructure models, and Evanno's ΔK method (Evanno *et al.* 2005) for ngsAdmix models. For both algorithms, the preferred model consistently had K=1, i.e. no inferred clusters in the data.

§-134 Coalescent-based analysis: Migrate-n. All methods used above provide a robust framework for identifying groups even in weakly structured populations. However, all are, to some extent,

functions of the covariance of allele frequencies between populations. In the hypothesis that our estimate of the frequency spectrum may be biased is some way, e.g. by moderate sample size, we also performed a coalescent-based structure analysis using Migrate-n (Beerli & Palczewski 2010). As opposed to frequency-spectrum based approaches, coalescent-based analysis relies on phased polymorphisms to infer population parameters. After verifying that the number of polymorphisms in each RAD locus followed a Poisson distribution of λ equal to the mean number of polymorphisms per locus, we selected 50 random loci comprising between 5 and 6 polymorphisms as an unbiased representation of the neutrally evolving part of the genome (Trucchi *et al.* 2014). In order to correct for potential over-representation of sequences in case a heterozygous individual was mis-called as homozygous, we randomly sampled one allele only for each individual. For all colonies except WSH, we randomly picked a set of haplotypes in the population (16 in MZE, DDU, HAL, and NEU, 14 in MZW, and 4 in WSH). We ran a cold chain and 3 heated chain of 50,000,000 generations, recording every 500 generations, with a 5,000,000-generation burn-in. We used a static heating scheme, raising the cold chain to a power of 1.5, 3 and 1e6, and proposing chain swapping every 100 steps. We used a uniform prior for population sizes (Θ), bounded between 0 and 0.1 (with a δ of 0.01), and for the migration rates (M), bounded at 4,000 with a δ of 400. Proper mixing under these conditions was ensured using the highest parametrisation model (model 2). We compared 5 models of increasing complexity: 1) a panmictic model, in which all colonies were gathered in one population, estimating only a general Θ, 2) a full-matrix model, in which asymmetric migrations were allowed between all pairs of colonies, 3) a step-wise model, in which asymmetric migrations were allowed, but only between neighbouring colonies, in a closed circle, 4) a first meta-population model, in which the Ross Sea (WSH), Adélie and George V Lands (MZE, MZW and DDU), and the South Atlantic (NEU and HAL) were treated as three populations, with an asymmetric migrations between them, 5) a second meta-population model, in which the northernmost colonies (MZE, MZW,

DDU, and NEU) were separated from the Weddell Sea (HAL) and the Ross Sea (WSH). Models were ordered by log Bayes factor defined by Kass and Raftery (Kass & Raftery 1995) as lnBF = $2[ln(\text{mL(model1)})-ln(\text{mL(model2)})]$, with mL(model1) and mL(model2) being the marginal likelihoods for the two compared models, as calculated by thermodynamic integration.

Best support goes to the full migration matrix model (model 2). Estimated migration rates M and population sizes Θ are highly homogeneous (mean mutation-scaled migration rate m / μ = 2,358 ±130, mutation-scaled effective sizes Θ_{WSH}=0.0017, Θ_{MZE}=0.0018, Θ_{MZW}=0.0019, Θ_{DDU}=0.0019, Θ_{NEU}=0.0018, Θ_{HAL}=0.0019).

Under this model, each migration rate can also be expressed as a proportion of the receiving population's effective size as $m = 4.M.\mu$. Hence, the relative demographic importance of immigration for any given colony can also be expressed as $\Sigma_i=n(4.M_i.\mu)$, with n being the total number of populations identified as gene sources for the focal population. In order to convert mutation-scaled estimates of M and Θ, we therefore need an estimate of μ (the mean number of substitutions.site^{-1}.Myr^{-1}) for the set of loci used in the analysis. Since the number of sites in each locus is mainly due to the stochastic nature of the mutational process, and follows a Poisson distribution of parameter λ equal to the mean SNP density per locus (see above), we can consider that a single true mutation rate (μ) applies to the whole RADome. However, since our analysis is restricted to loci containing 5 to 6 SNPs, our estimates of Θ and M are not directly scaled by μ, but rather by posterior probabilities of μ conditional on the number of SNPs in each locus class. We used the class-specific mutation rate posterior probabilities as calculated for the King penguin (Trucchi *et al.* 2014). As a conservative estimate, we used a range of rates fitting the 3-SNPs to 6-SNPs class loci. Using a generation time of 16 years (Jenouvrier *et al.* 2014), these are μ_{3snps}= 1.14e^{-6} and μ_{6snps}= 2.16e^{-6}. Since these were estimated from a subset of 16 haplotypes, and we included 82 haplotypes in our analysis, we considered that variability was likely to be underestimated by Truc-

chi and colleagues (Trucchi *et al.* 2014) compared to our sample. Thus, we did not consider higher estimates than those made for 6-SNPs loci.

§-135 fastsimcoal2 analysis. Joint derived-allele frequency spectra were generated in ANGSD 0.900 (Kim *et al.* 2011; Nielsen *et al.* 2012) for a subset of four colonies that encompass the whole continent (MZE, DDU, NEU and HAL). In order to polarize these spectra, we reconstructed the most likely ancestral base for all positions in the RADome. We selected 12 high-quality Emperor penguin samples covering the whole species' range, as well as 12 high quality King penguin samples processed according to the same protocol (see *The King synnome*, p. 163). States at all positions were determined using GATK's Haplotype Caller pipeline (DePristo *et al.* 2011). We used BEDtools (Quinlan & Hall 2010) and VCFtools' vcf-consensus script (Danecek *et al.* 2011) to update the published Emperor penguin genome and establish a reference RADome for both the King penguin, and the Emperor penguin, using only high-quality polymorphisms (phred-scale genotype quality ≥ 80), and including variable sites as IUPAC ambiguity codes. We aligned this RADome to the Adélie penguin genome (Pygoscelis adeliae, see Zhang *et al.* 2011b) using Bowtie2 (Langmead & Salzberg 2012), and extracted the corresponding regions. For each RAD locus, a maximum-likelihood unrooted tree was built in PhyML (Guindon *et al.* 2010), and maximum-likelihood ancestral sequence for crown-*Aptenodytes* was reconstructed using PAML (Yang 2007) and Lazarus (https://project-lazarus.googlecode.com/), using PhyML tree topology as a prior. There ancestral states were then used to determine the ancestral and derived alleles in the Emperor penguin.

Reconstruction of population sizes and migration events was performed through composite-likelihood maximisation, by simulating joint-spectra under a continuous-time Markovian coalescent model in fastsimcoal2.5.11 (Excoffier & Foll 2011; Excoffier *et al.* 2013). For each run, we performed a maximum of 80 ECM optimisation cycles over the 12 retained parameters (population sizes and asymmetric migration rates between the four analysed colonies), each parameter optimi-

sation step requiring the generation of 100,000 simulated joint-spectra. We generated 50 non-parametric bootstrap replicates for each spectrum. For each bootstrap dataset, and for the original dataset, we ran 50 independent replicates, and retained the one with the highest log-likelihood. We assumed a mutation rate of 2.6e-7 subsitutions.site-1.generation-1 as calculated for the King penguin (Trucchi *et al.* 2014), and a generation time of 16 years (Jenouvrier *et al.* 2014). Computation was performed on the high-performance Abel cluster at the University of Oslo, and required a total of ~30,000 CPU-hours.

We chose to restrict our analysis to a stepwise migration model for two main reasons. First, computational load increases rapidly with the number of estimated parameters, and higher complexity models could not be run with the necessary amount of replication. Secondly, since our model is not supposed to represent precisely the present-day state of the colonies, but rather parameters averaged over a long period of time, we do not expect the intensity of the migration flow to be much affected by the structure of the connectivity. However, in one particular case, the estimate seems to deviate from the general pattern of migration in our analysis, and may be indicative of a very recent event, still directly linked to the present-day states of the colonies. Indeed, the gene flow between DDU and MZE is estimated to be much higher, and much more asymmetrical than the rest of the rates (Fig. 31, Table 7), with almost all of the gene flow being directed from DDU to MZE. Although this may be a circumstantial effect of our sampling, it is noteworthy that the DDU colony has indeed lost nearly half its breeding population in the very recent past, with no definitive explanation (Barbraud & Weimerskirch 2001a). Although it has been suggested that this sudden decrease may have been caused by local environmental effects (Barbraud & Weimerskirch 2001a; Barbraud *et al.* 2011), the disturbance caused by the Dumont D'Urville research station, including its research activities on the colony, and in particular the effect of flipper-banding of the Emperor penguins (Le Maho *et al.* 2011) have also been mentioned as potential causes for high emigration from the DDU colony. It is thus possible that the high gene flow

inferred from DDU to MZE indicates that this decrease was at least partly caused by emigration to the nearby Mertz glacier area in response to human-induced disturbance, rather than as by environment-induced mortality.

Table 7 | Migration rates and sizes as estimated from the joint allele frequency spectrum.

	MEAN	L95	U95
Population sizes and directional gene flow			
N_HAL	4040	3990	4080
N_NEU	3060	2920	3200
N_DDU	1120	1100	1150
N_MZE	7640	6150	9130
mHALNEU	0.0166	0.0153	0.0179
mNEUHAL	0.00323	0.0023	0.00416
mNEUDDU	0.0391	0.0376	0.0407
mDDUNEU	0.016	0.014	0.018
mDDUMZE	0.0416	0.0379	0.0452
mMZEDDU	0.000868	0.000372	0.00136
mMZEHAL	0.00397	0.00327	0.00466
mHALMZE	0.000413	0.000283	0.000544
Immigration rate (ratio of receiving population)			
HAL	0.0072	0.00557	0.00882
NEU	0.0326	0.0293	0.0359
DDU	0.039968	0.037972	0.04206
MZE	0.042013	0.038183	0.045744
Immigration size per receiving population (in effective breeders)			
HAL	29	22	36
NEU	132	117	146
DDU	161	152	172
MZE	170	152	187

§-136 Coalescent-based analysis: BEAST2. An independent estimate of population size changes through time was performed in BEAST2 (Bouckaert *et al.* 2014). We proceeded as above for locus selection and haplotype downsampling. In order to remain agnostic as to population structure, we performed analysis on each colony separately, as well as on the whole dataset, as the lack

of strong population structure, evidenced by all other analyses, allowed us to sample haplotypes from the whole species without violating the model's assumptions. We used an extended bayesian skyline plot model (Heled & Drummond 2008) in order to co-estimate present-day Θ and possible past fluctuations. We followed the protocol of Trucchi and colleagues (Trucchi *et al.* 2014), but reduced the parameter space by defining only one site-model per locus class (5 or 6 SNPs), using HKY models with empirical base frequencies, and allowing for rate variation in 4 discrete gamma categories. Kappa was linked across site models, according to our expectation for neutral variation, in order to alleviate computational load (A. Drummond, *personal communication*). All chains were run in duplicate to check for convergence and for a sufficient length to gather ESS > 200 for all parameters, which necessitated ca. 1,000,000,000 steps on all models. Reconstruction for WSH colony is much less precise due to the very small number of haplotypes (N=4) sampled per locus. However, present-day population size estimate converges with reconstructions based on the other colonies. It is also noteworthy that our results point to a gradual increase in population size over the last ~100,000 years (with some uncertainty as to the precise dating of the beginning of the expansion, due to the difficulty of precisely calibrating mutation rates in a multilocus approach), which confirms the findings of Li and colleagues (Li *et al.* 2014) based on a single-genome pairwise sequentially Markovian coalescent approach.

§-137 mtDNA analysis. A recent study by Younger and colleagues (Younger *et al.* 2015) focused on Emperor penguin mitochondrial DNA population structure. Their conclusion was that colonies from the Ross sea area are significantly isolated from the rest of the continent, and had a different demographic history. Our genome-wide SNP data does not support this view: however, our low sampling size in the Ross Sea region does not permit any definitive conclusion. In order to assess how far this result could be reproduced from mtDNA alone, we sequenced a 792 bp fragment of mitochondrial cytochrome-B gene and a 414 bp-long HVR fragment for our RAD samples, following the same protocol as Younger et al. Primers were the following: Cyt-b forward

primer 5'-GCCCCAAACCTCCGAAAATCCCA-3' and reverse primer 5'-TGTGGAG-GAGGGGGATTAGG-3'; HVR forward primer 5'-GGAACCTCCCAAAGAGTACCA-3' and reverse primer 5'-CCAACCAGATGTATCGGTGA-3'. PCR conditions were thus: for Cyt-b, 5' denaturation at 94°C, 35 cycles of amplification (30" denaturation at 94°C, 30" annealing at 57°C, and 1' elongation at 72°C), and 5' final elongation at 72°C; for HVR, 5' denaturation at 94°C, 35 cycles of amplification (30" denaturation at 94°C, 30" annealing at 59.5°C, and 1' elongation at 72°C), and 5' final elongation at 72°C. PCR product was then purified using Illustra™ ExoStar™, and Sanger sequencing was performed at the ABI lab of the University of Oslo. Quality assessment, trimming, and manual checking were performed in Geneious® v6.1.2. Unfortunately, our HVR sequences were of consistently low quality and thus could not be used reliably in analysis. Many double peaks were observed, possibly explained by HVR duplication (as previously observed in *Thalassarche* albatrosses, see Abbott *et al.* 2005), together with possible instances of polynucleotide repeat number variation. The uncertainties regarding base calls and site phasing in the case of double peaks made it impossible to extract any reliable data from these sequences.

We also re-analysed the data from Younger and colleagues (GenBank accession numbers KP644787-KP645015 and KP640645-KP640873). Considering no reliable and controlled model can account for diploid sites in mitochondrial DNA, we masked all ambiguous sites from analysis. We also considered that the higher reported similarity between Ross Sea mtDNA samples may be biased by the fact that, after masking ambiguous sites, two haplotypes are overly represented compared to the average haplotype diversity. Indeed, when concatenating HVR and Cytochrome B sequences for each individual, and putting aside the two over-represented sequences, each mitochondrial haplotype is present in an average 1.4 ±0.9 copies per colony. The two over-represented haplotypes, on the other hand, are found in 14 samples from Cape Washington, and 15 from Cape Crozier. Not surprisingly, however, these samples are the only "shed feathers [...] collected from the Ross Sea between 2010 and 2012 [...] at least 10 m apart to minimize sam-

pling the same bird" as opposed to blood samples for the other locations. It indeed may seem rather likely that the precaution was not sufficient, and that the same birds were sampled multiple times, as it is common for a moulting penguin to shed feathers on a great surface. Once miscalled bases are masked, and potentially pseudo-replicate samples are removed, the resulting pattern does not exhibit the clear bipartite organisation found by Younger and colleagues, but rather a gradual differentiation, in keeping with the general pattern we observe in genomic SNP data (Fig. 39B). As a side note, the over-representation of pseudo-replicate sequences in the Ross sea region, by violating the random-sampling assumption of coalescent reconstructions, may also account for the differences in past demographic trends inferences found by the authors (Younger et al. figure 2).

Cytochrome-B sequences, on the other hand, showed a standard level of variation in our dataset, as assessed in DnaSP (Rozas & Rozas 1999 - 10 haplotypes, gene diversity=0.634, nucleotide diversity=0.003, Fu's Fs=-0.948, Tajima's D=-0.216, non-significant). Haplotype network was built based on Fitch distances between sequences, using Fitchi (Matschiner 2015), using a maximum-likelihood bifurcating tree built in RaxML (Stamatakis 2014). In keeping with the results of Younger and colleagues, Cytochrome-B sequences do not reflect geographical distribution of the samples in any way (Fig. 39A).

The particular case of the Ross Sea area may require further analysis, as mitochondrial HVR alone seems too unreliably sequenced to provide positive information. The available data only support the extension of a low-level isolation-by-distance model to the whole continent, in keeping with our observations on genome-wide polymorphism. However, the intensity of the gene flow between the Ross Sea region and the rest of the continent has little impact on our ability to model immigration rates at the colony level. Indeed, the origin of the immigration flux is less relevant than its intensity if we are to accurately model population dynamics from colony-level data.
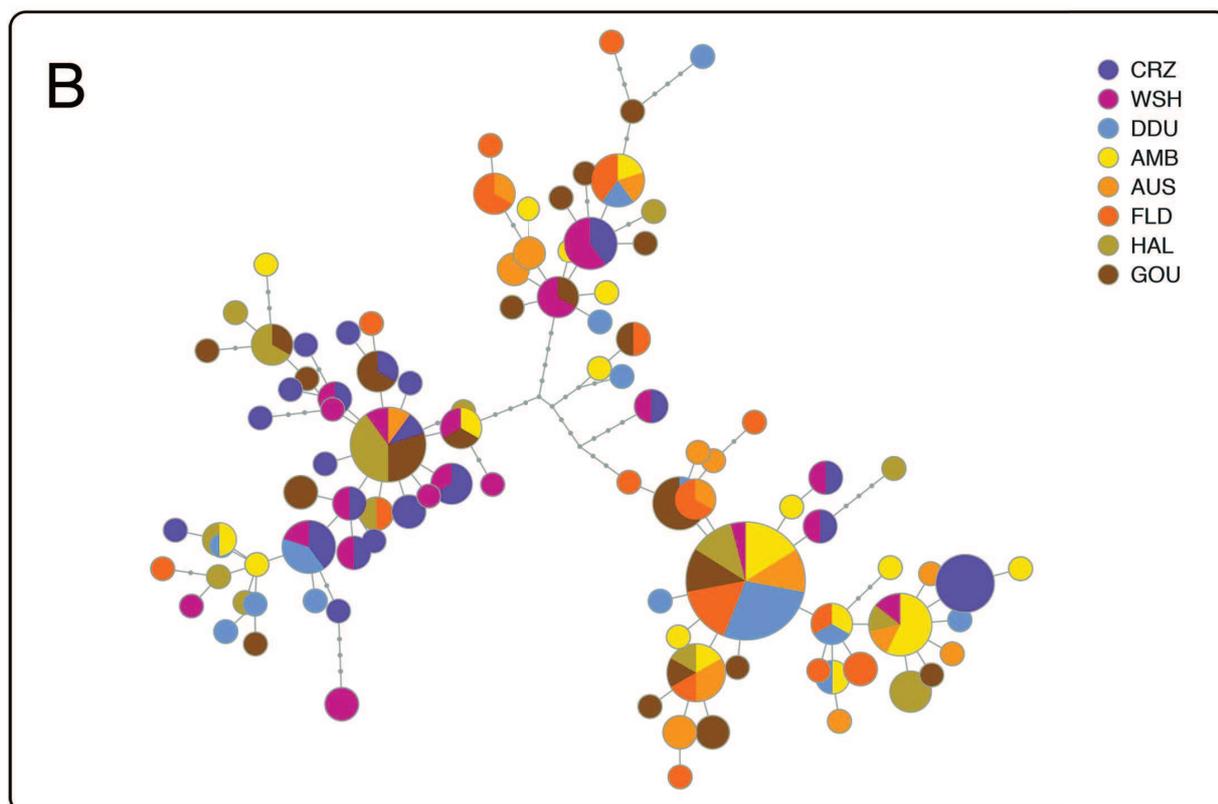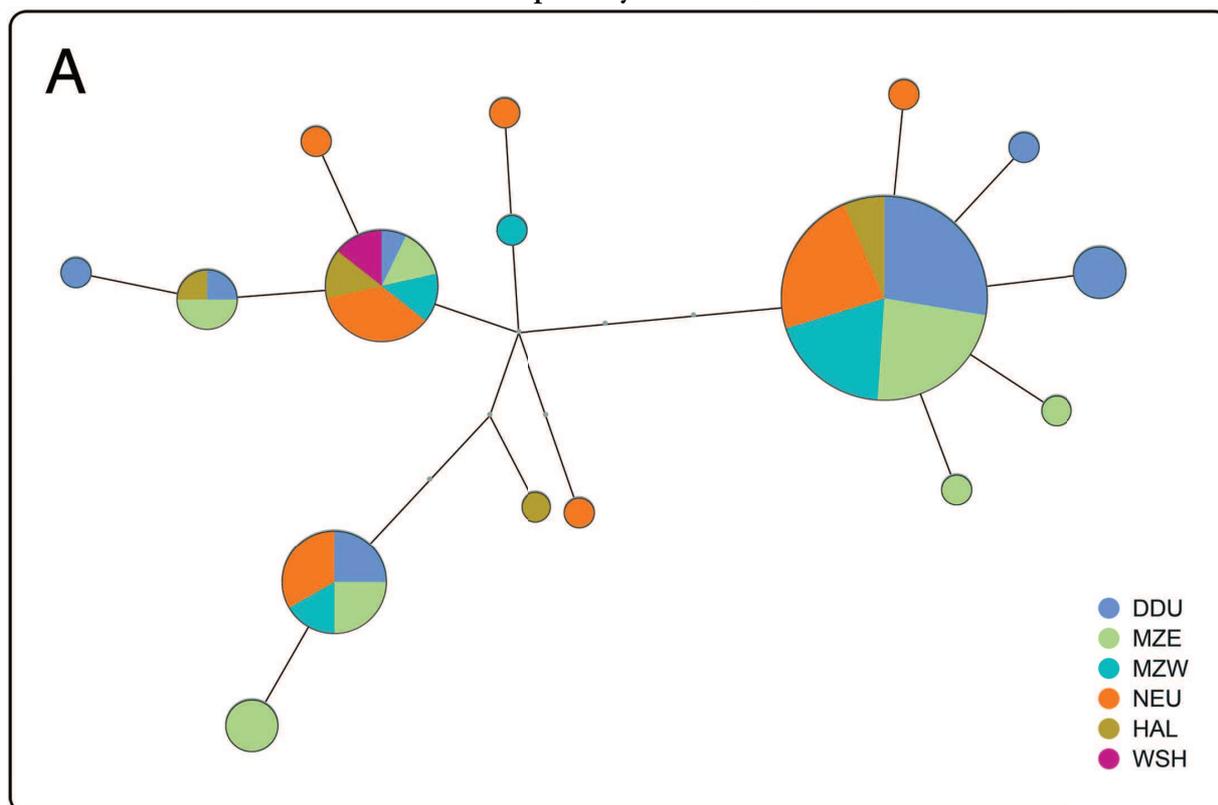
Figure 39 | Haplotype network for mitochondrial sequences. Each dot represents a mutation. The areas of the discs is proportional to the number of copies found in the sample. Coloured sectors indicate the geographical

repartition of these haplotypes. (**A**) Cytochrome B sequences produced for the present study. (**B**) Cytochrome B and HVR sequences from Younger *et al.* 2015, reanalysed for this study (S-13). Colony labels as follows: CRZ=Cape Crozier, WSH=Cape Washington, DDU=Dumont d'Urville/Pointe Géologie, AMB=Amanda Bay, AUS=Auster, FLD=Fold Island, HAL=Halley Bay, GOU=Gould Bay.

Acknowledgements

Chapter 6: Empirical evidence of heterogeneous dispersal

This chapter has been published as: Ancel A, <u>Cristofari R,</u> Fretwell PT, Trathan PN , Wienecke B, Boureau M, Morinay J, Blanc S, Le Maho Y, Le Bohec C (2014) **Emperors in Hiding: When Ice-Breakers and Satellites Complement Each Other in Antarctic Exploration.** PloS one 9:e100404

Context

§-138 How do coalescent-scale migration translate at the ecological scale? In the previous chapter (*The Emperor synnome*, p. 211), we showed how continent-wide genomic data allows us to reconstruct large-scale migration patterns in the Emperor penguin. Inferred gene flow is outstandingly high, with colonies receiving between ~1% and ~5% of their effective population size as migrants every generation (see §113 p. 220). However, these estimates are averaged over the period spanned by the coalescent history, *i.e.* up to 4.Ne generations (see §41 p. 103): their distribution in time may be homogeneous, with a low and constant trickle of migration, or on the other hand highly heterogeneous, with periods of high or complete dispersal alternating with periods of «*stasis*» and philopatric isolation. Similarly, dispersal may be homogeneous, or heterogeneous in space: the determinants of the strength of dispersal may be global (*e.g.* planetary climate change and modifications of the glacial or oceanographic landscape), and affect every colony equally, or

local (*e.g.* accidental changes in the ice landscape following a particular event) and affect only one or a few colonies at a time.

Understanding the structure of migration in time and space at such scales, however, is well beyond the power of genetic approaches. The particular synnome structure of the *Aptenodytes* penguins (see §3 p. 28) implies that, although colonies as geographical units may persevere for long periods (see §2 p. 25), particular lineages do not reside in the same colony for more than a few generations. Thus, the spatial coordinates of a lineage are to some extent anecdotal: each may be traced back from its current position to the previous one, but thence no further. Thus, events such as the merging of two nearby and barely isolated colonies, temporary interruption of gene flow, or the disappearance of a group dispersing into the neighbouring colonies are beyond the resolution of our analysis methods. Understanding the dynamics of dispersal thus requires direct field observations, grounded in an ecological, rather than an evolutionary framework (see §2 p. 25). In the present chapter, we use a direct, observational method, based on ground surveys, aerial and satellite photography, and a long-term monitoring program (see §24 p. 79) to shed light upon the possible mechanisms underlying migration in *Aptenodytes* penguins.

Abstract

Evaluating the demographic trends of marine top predators is critical to understanding the processes involved in the ongoing rapid changes in Antarctic ecosystems. However, the remoteness and logistical complexity of operating in Antarctica, especially during winter, make such an assessment difficult. Satellite imaging is increasingly recognised as a valuable method for remote animal population monitoring, yet its accuracy and reliability are still to be fully evaluated. We report here the first ground visit of an emperor penguin colony first discovered by satellite, but also the discovery of a second one not indicated by satellite survey at that time. Several successive remote surveys in this coastal region of East Antarctica, both before and after sudden local

changes, had indeed only identified one colony. These two colonies (with a total of ca. 7,400 breeding pairs) are located near the Mertz Glacier in an area that underwent tremendous habitat change after the glacier tongue broke off in February 2010. Our findings therefore suggest that a satellite survey, although offering a major advance since it allows a global imaging of emperor penguin colonies, may miss certain colony locations when challenged by certain features of polar ecosystems, such as snow cover, evolving ice topology, and rapidly changing habitat. Moreover our survey shows that this large seabird has considerable potential for rapid adaptation to sudden habitat loss, as the colony detected in 2009 may have moved and settled on new breeding grounds. Overall, the ability of emperor penguin colonies to relocate following habitat modification underlines the continued need for a mix of remote sensing and field surveys (aerial photography and ground counts), especially in the less-frequented parts of Antarctica, to gain reliable knowledge about the population demography and dynamics of this flagship species of the Antarctic ecosystem.

Introduction

The emperor penguin (Aptenodytes forsteri), a flightless seabird endemic to Antarctica, was probably first seen on James Cook's second voyage, in 1773–1774 Yet the first breeding colony was only discovered in 1902 during the first of Scott's Discovery Expeditions (Wienecke 2009b). For the colonies that could be reached from research stations, population trends usually involved ground counts (Budd 1962; Peter *et al.* 2008). The census of those not accessible by ground surveys was usually obtained using aerial photography (Wilson *et al.* 2001). The first estimation from space was carried out in 2005 and 2006 for the western Ross Sea area (Barber-Meyer *et al.* 2007), while the first global survey was performed in 2009 (Fretwell & Trathan 2009; Fretwell *et al.* 2012). Today, 52 colonies of emperor penguins have been identified (Fretwell and Trathan, unpublished data), all of them being distributed along the coastline of Antarctica between 64°S

and 77°S (Wilson 1983; Woehler 2001; Lea & Soper 2005; Ancel *et al.* 2013). However, our present knowledge of the biology of the emperor penguin falls far behind the picturesque notoriety of this iconic species. The breeding behaviour and phenology of the species have been described from only a few sites, e.g. from the Dion Islands (Trathan *et al.* 2011) and Pointe Géologie archipelago (Prévost 1961), usually settled in the vicinity of overwintering research stations. Indeed, most colonies are just too remote from permanently occupied research stations, and because of the unique breeding cycle of this species (in which egg laying, hatching, and early chick rearing all occur during the austral winter, see Prévost 1961), ground visits to most breeding colonies are virtually impossible for most of the breeding season (Budd 1962). Yet, because the French station in Adélie Land, Dumont d'Urville, has been located next to the Pointe Géologie colony, this is the only colony which has been visited almost every day for more than 45 years (Prévost 1961; Isenmann & Jouventin 1970; Isenmann 1971; Jouventin 1971a; Jouventin 1972a; Jouventin 1975; Le Maho 1977; Ancel *et al.* 2009). However, it has been shown that demographic studies extrapolated from the colony-level can be strongly misleading as they tend to give too much weight to local stochastic events (Lynch *et al.* 2012).

The recently developed satellite-based remote-sensing methods (Barber-Meyer *et al.* 2007; Fretwell & Trathan 2009; Fretwell *et al.* 2012) are a major breakthrough. By detecting faecal deposits on the sea ice in satellite images, it is possible to locate emperor penguin colonies. However, present-day satellite technology is constrained in Polar Regions as the darkness of the polar winter and the frequent cloud cover during winter and early spring limit window of opportunity for satellite-surveys. Further, wind-blown snow may obscure the faecal signal. Therefore, to expand our knowledge of this species beyond the boundaries of the few available local observations, it is critical to corroborate and calibrate these remote-sensing methods through ground visits with detailed and precise observations of breeding colonies.

The ground survey of the Mertz Glacier area was initiated within this context and became logistically possible in November 2012. The existence of an emperor penguin colony near the Mertz Glacier had been suspected for almost a hundred years, and Mertz himself perished in an attempt to locate the colony. More recently, during August 1999, sightings of thousands of emperor penguins traversing the northern part of the Mertz Glacier tongue (Ancel *et al.* 1999) confirmed that a colony must be located close to the glacier.

By using Landsat and QuickBird2 Very High Resolution Landsat imagery, confirmation of the colony site at 66°54'S, 146°37'E at the tip of the Mertz glacier tongue was obtained in November 2009 (Fretwell & Trathan 2009; Fretwell *et al.* 2012). The high resolution of the satellite imagery allowed counting 4,781 pairs at the time of image acquisition. However, before a field survey could take place, the Mertz Glacier tongue calved in mid-February 2010 presumably inducing the colony to relocate or merge with another colony. New satellite images obtained since then suggested that the birds might attempt to breed on different sites depending on the year. Still, since the exact colony location and colony size appeared to change between successive observations, ground-based assessments were difficult and needed to be conducted over several seasons.

Our objective was to validate the presence of one or more emperor penguin colonies near the Mertz Glacier, to locate them, to estimate their population size (breeding adults) and breeding success (number of chicks), and to obtain other biological information.

Materials and Methods

§-139 Animal ethics were not an issue as we counted the birds from aerial pictures. No manipulation or experimentation was con- ducted on live birds and care was taken to avoid any disturbance. The French Polar Institute (IPEV) and the Terres Australes et Antarctiques Françaises (TAAF) are the authorities that issued the permit to visit the colonies.

During the 2012–2013 austral summer, the French Polar Institute's resupply ship MSS *L'Astro-labe* visited the Antarctic coastline near to the Mertz Glacier. *L'Astrolabe*'s classification is ice class 1A super, the highest class of vessels that can operate in difficult polar conditions without the assistance of an ice breaker. On November 1st and 2nd, using a Eurocopter Squirrel B-3 single-engine helicopter, aerial surveys were conducted along the northern edge of the Mertz Glacier in an attempt to locate the new breeding sites of the emperor penguin colonies. Aerial photographs, used for recording penguin location and for counting the chicks and adults, were taken obliquely in clear weather from an altitude of 300 meters, with a 35-mm Canon 40D digital camera fitted with a 200 mm f/4 lens.

§-140 Aerial photographs were stitched together to form photo- mosaics in PTGui(c) software, and both chicks and adults were counted separately using the count tool in Photoshop CS5©. This was repeated by two different observers. The total number of individuals was estimated using two different methods to provide a probable range for each colony census: 1) under the hypothesis that inter-annual climatic effects are largely dominant over fine- scale local effects, we made the assumption that breeding success is approximately similar in nearby colonies for any given year. We therefore estimated the number of breeding pairs from the early November chick-counts using the population parameters deter- mined from the nearby Pointe Géologie colony (66°40'S, 140°01'E) over the whole breeding season; 2) following Budd (Budd 1962), who proposed that, based on a census at several different colonies, adult counts between October and November equate to approximately one-third (26% to 40%) of the total adult population, independently of the actual breeding success. For comparison, the Pointe Géologie colony was counted at different times, from photographs, using the same methodology. The total number of incubating males in mid-June was taken as a proxy for the total number of breeding pairs: and chicks were counted in early November, to allow comparison with the census of the Mertz colonies.

To avoid potential disturbance, no low altitude flights were made over or near to the Mertz colonies, and a brief landing was made ca. 1 km from the breeding sites to minimize further disturbance. Each colony was visited by 4 or 5 people on foot, and surveyed for approximately 3 hours each. No direct ground counts of chicks or adults were made during the visits due to the lack of any satisfactory vantage point. Observations focused on assessing the habitat, chick abundance and health (though no direct measures were taken in order to avoid unnecessary disturbance). Observations were also made to search for flipper-banded individuals, potentially originating from the Pointe Géologie colony, located at only ca. 250 km to the west.

To find colony locations, satellite observations were made using freely available reduced resolution "quicklooks" from the com- mercial satellite provider DigitalGlobe (https://browse.digital-globe.com/imagefinder/). These images have an approximate on-the-ground resolution of ,10 m per pixel. Colonies were located visually from the images by detecting the brown signature of the bird's faecal stains on the ice. Once located, raw Very High Resolution imagery with a resolution of 0.5 m per pixel was acquired. This resolution allows areas of penguins to be differentiated from guano using a multivariate supervised classification method (Barber-Meyer *et al.* 2007; Fretwell & Trathan 2009; Fretwell *et al.* 2012).

Results

§-141 Habitat and Chick Census. First or eastern colony. The existence of a breeding colony of emperor penguins near the Mertz Glacier was confirmed and located at 67°19'S, 145°52'E on November 1st, 2012 (Fig. 40). The eastern colony was breeding on fast ice amidst grounded icebergs, 250 km east of Dumont d'Urville research station. The colony was composed of numerous sub-groups, which appeared to have moved short distances, as confirmed by the clustered guano deposits. The topography of the breeding site was very uneven with numerous icebergs embedded in the sea ice, offering protection from the prevailing high winds. Layers of droppings were found

between layers of snow on top of the icebergs (Fig. 41), providing evidence of numerous snow-fall episodes. Many icebergs, ca. 10-meter high, were also covered with guano, thus demonstrating that breeding birds had spent some time on the top of these icebergs (Fig. 41). This colony had three former incubation areas, identified by stained sea ice, numerous egg shells and carcasses of newly hatched chicks. During our 3-hour visit, no birds other than penguins, and no sign of predation (e.g. predated or scavenged carcasses) were found. Two Weddell seals Leptony- chotes weddelli were sighted along tidal cracks in the vicinity. Our survey yielded a count of 1,750 downy chicks, and 1,520 adults. Approximately 300 dead chicks, ranging in age from a few days (frozen) to 3-month-old (both frozen and fresh) were found. Most of them were found at the incubation sites, and on the top of small icebergs.
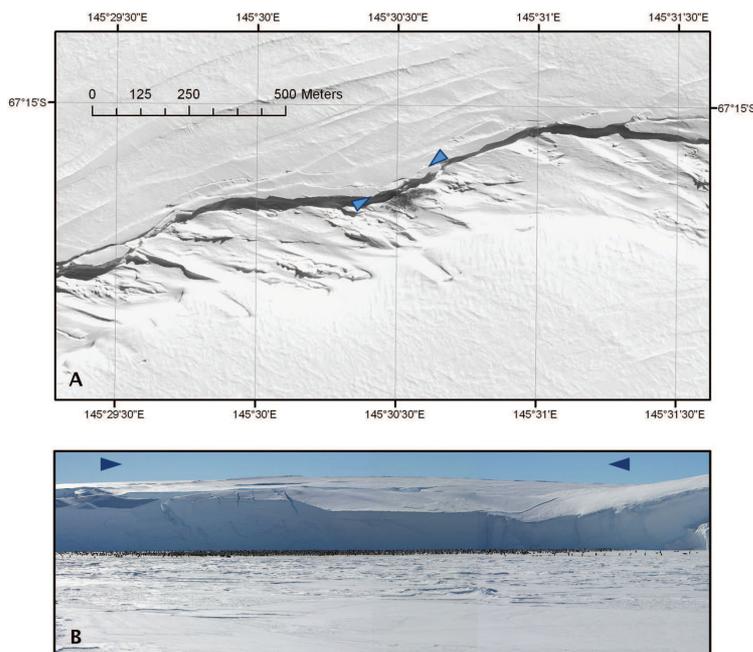
Figure 40 | Western Emperor penguin colony. A. Quickbird satellite view of the eastern emperor penguin colony (67°199S, 145°529E) showing adults and chicks present on November 1st, 2012. B. Ground view of the same (blue arrows at matching locations). Photograph by Robin Cristofari.

Second or western colony. On November 2nd, 2012, a second colony was discovered by chance from an altitude of ca. 500 m during a helicopter flight involved in resupply operations. This western colony was located on a large and flat fast ice sheet extending from the Mertz glacier, ca. 20 km west of the first colony, at 67°14'S, 145°30'E (Fig. #). This colony was bordered on the north-west by a high ice cliff of the Mertz glacier. Numerous large tabular icebergs were grounded in the fast ice, south of the colony. This habitat was similar

to that generally found in the Ross Sea area, characterized by stable fast ice, nearby open water and access to fresh snow (Kooyman 1993). The site was poorly sheltered from the wind. The colony comprised one single group of ca. 3,980 downy chicks, and 2,300 adults. From empirical observation, these chicks seemed bigger, and better fed, than those of the eastern colony. Three Antarctic skuas Catharacta maccormicki and one giant petrel Macronectes giganteus were sighted flying over the colony. Only 17 dead chicks and one abandoned egg were found during our 3-hour survey, some of them partly buried. The ice surface was of heavily compacted and abraded snow, and it is therefore most likely that more dead chicks were buried beneath the snow surface. Guano traces were restricted to the area currently occupied by the birds, and its direct surround-ings. Due to these difficult conditions, we were unable to precisely locate the incubation area. As for the first colony, we did not observe any individuals bearing flipper-bands.

Figure 41 | Eastern Emperor penguin colony. A. Location of the eastern colony (67°199S, 145°529E) on the sea-ice at the time of our visit and previous locations of the colony on top of icebergs, ca. 10 m high, covered with guano (arrow). B & C. Layers of drop-pings (arrows) covered by several layers of snow indicate abundant snow-covered episodes during the breeding season. Photographs by Robin Cristofari.

§-142 Extrapolation to Total Colony Size. Our average 2012 breeding season count for the Pointe Géologie colony was ca. 3,200 breeding pairs, and we counted ca. 2,500 chicks in early November 2012, which gives a pair-to-chick ratio of ca. 1.28. Applying this ratio to the chick counts for the Mertz colonies, we estimated the population size to be ca. 2,300 breeding pairs for the eastern colony, and ca. 5,100 for the western colony (Table 8).

Moreover, a total of 1,864 individual adults were counted at the Pointe Géologie colony on October 31st, 2012, which implies a total count of ca. 2,330 to 3,580 breeding pairs according to Budd's method. This is consistent with our average 2012 winter count of ca. 3,200 breeding pairs, thus allowing us to apply this method to the Mertz Glacier census.

Adult counts from photographs were 1,520 for the eastern colony and 2,300 for the western colony, respectively (Table 8). When applying Budd's method (Budd 1962), the estimated population size was 2,300 breeding pairs for the first colony (ranging from 1,900 to 2,900) and 3,500 for the second (from 2,900 to 4,400), hence a total of ca. 5,800 breeding pairs for the Mertz emperor penguin population.

Table 8 | 2012 census of the Mertz emperor penguin colonies.

	Lat. (S)	Lon. (E)	Chicks	Adults	Chicks-to-adults ratio	Pairs (from chicks)*	Pairs (from adults)
Eastern	67°19'	145°52'	1,750	1,520	1.15	~2,300	1,900-2,900
Western	67°14'	145°30'	3,980	2,300	1.73	~5,100	2,900-4,400

*Breeding pairs were obtained by applying a pair-to-chick ratio of ca. 1.28 obtained from the emperor penguin colony at Pointe Géologie, Adélie Land.

Discussion

§-143 Strength and Shortcomings of the Remote-sensing Technique. Our study confirmed sightings made 15 years ago of thousands of emperor penguins going back and forth at the northern part of the tongue of the Mertz Glacier, suggesting the presence of a colony in this area (Ancel *et al.* 1999). Moreover, our ground visit to the two Mertz colonies demonstrates the reliability of the remote-sensing method developed by researchers (Barber-Meyer *et al.* 2007; Fretwell & Trathan 2009). Although the method successfully identified several previously known emperor penguin colonies, this is the first time that the existence of three colonies identified solely from satellite images have been accurately corroborated in the field: two at the new edge of the Mertz Glacier

in late 2012 (present study) and one on Princess Ragnhild coast (69°54'S, 27°09'E) in early 2013 (visit http://www. antarcticstation.org/for more information).

However, the locations from satellite surveys of the two colonies at the edge of the Mertz Glacier were not determined during the same year, therefore suggesting the existence of only one colony in this area. This fact suggests that further refinement of the present- day remote-sensing method may be advantageous. Only the western colony was located in December 2011, while the eastern one remained invisible. In contrast, only the eastern colony was located in 2012. Failure to identify both colonies at the same time may be attributed to different factors. To locate colonies, the remote-sensing method relies on guano staining on the sea-ice surface, and heavy snow cover may obliterate the signal. The western colony, which could not to be detected just a few weeks before our visit, was largely covered by snow during the last weeks of winter. Hence, almost no guano stains, abandoned eggs, or dead chicks were found. The location of this colony along a high glacier edge may also have kept it hidden from the satellite, if the image was taken at too shallow an angle. In addition, a previous study (Gilbert *et al.* 2008) has shown that the density of emperor penguin colony can vary considerably, i.e. from 2 to 9 birds per square meter, and this within only a few hours. This means that census estimates based on colony area may be inaccurate in some circumstances due to variability in density and to inter-annual variability. This suggests that this colony was not the only one to be missed by the 2009 and 2012 satellite surveys, and that more colonies remain to be discovered in other parts of the continent. Although not always possible each season due to cloud cover and the availability of the satellite, our results suggest that satellite surveys should be conducted repeatedly and combined with field surveys to ensure that colonies are not missed. Our paper shows that to allow confidence in satellite observations, a multi-temporal/multi-year approach has to be used to ensure that breeding sites are not missed due to heavy snowfall, deep shadows or topographic features such as ice cliffs. If possible, these observations should be backed up with aerial or ground counts as the limited special resolution of satellite imagery results in large inherent variances when calculating breeding

populations. Innovative cameras combined with biologging would also be very useful to complete the satellite survey. For instance, since the satellite survey based on 2009 imagery, four more emperor penguin colonies have been discovered: two on the West Ice Shelf detected by aerial survey (Wienecke 2012), and two others on the West Ice Shelf and near the Jason Peninsula identified by satellite survey (Fretwell *et al.* 2014).

Due to the discrepancy between the coordinates given by satellites (66°54'S, 146°37'E, see Fretwell *et al.* 2012) and our land based ones (67°19'S, 145°52'E and 67°14'S, 145°30'E), we may assume that the colony initially detected from space in 2009 has been split into two colonies. Following the calving of the Mertz Glacier, the birds may indeed have attempted to settle in new favourable surroundings. The two new colonies are separated by 20 km along the new northern edge of the Glacier (Fig. 42). Taking into account the proximity of the two breeding sites, these colonies might however reunite in the future, especially if one or other of the sites eventually proves to be more reliable for breeding and/or foraging.

All satellite surveys conducted up to now, before and after the Mertz calving, had concluded the presence of a single emperor penguin colony, even if grouped into three close sub-colonies in 2009, in the Mertz Glacier area. It may also be that two nearby colonies already existed at the current location(s) before the 2010 calving. This is supported by the fact that the best population estimate of the Mertz Glacier colony located by Fretwell et al. (Fretwell *et al.* 2012) was estimated to be 4,781 adults (or 5,976 pairs if we considered that 80% of the total breeding population was present during the satellite survey, see Fretwell *et al.* 2012), a figure which is relatively close to our assessment of 5,100 breeding pairs for the western colony alone (Table 8) but lower than the sum of the two colonies we found (7,400 breeding pairs; Table 8). In such a scenario, the second colony we discovered might be the one found before at the nearby Ninnis Glacier (Wienecke 2009a), which would have been missed in all further surveys (see Fretwell & Trathan 2009).
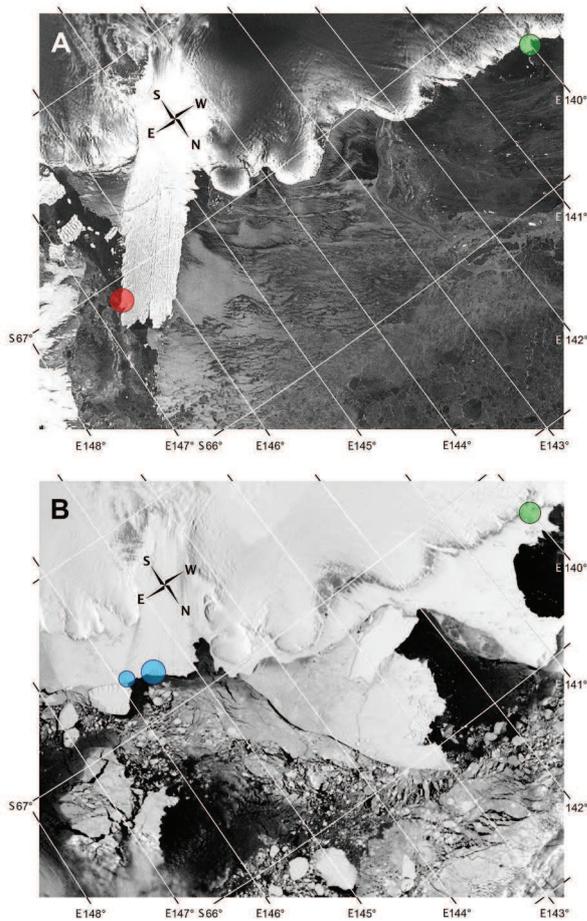
Figure 42 | Satellite images of the Mertz glacier. Circle area is proportional to colony size. Continent is on top, open sea at the bottom. **A.** Estimated location of the Mertz emperor penguin colony on November 13th, 2009 (red circle) on the eastern flank of the Glacier tongue. A large crack in the Mertz Glacier is visible (red arrow). The green circle corresponds to Pointe Géologie colony. **B.** Location of the two new colonies of emperor penguins on December 3rd, 2012 (blue circles), 2 years after the 2010 calving of the Glacier tongue. The berg (overall length of 80 km and a width of 40 km) broke off the Mertz Glacier after being rammed by another iceberg. The green circle corresponds to Pointe Géologie colony. Images downloaded from the USGS website (https://lta.cr.usgs.gov).

§-144 Influence of the Breeding Location at Fine-spatial Scale. It is important to note that the two colonies appeared to differ slightly in their breeding stage. The chick-to-adult ratio was higher in the western colony than in the eastern one (1.73 vs. 1.15, respectively: Table 8). This result may be interpreted as a difference in breeding success, with higher chick mortality in the eastern colony than in the western one. This hypothesis is supported by the much higher number of dead chicks in the eastern colony. Moreover, while the two colonies were visited on two consecutive days, the western colony appeared more advanced in its breeding cycle, as indicated by the generally better health and bigger size of the chicks than in the eastern colony. Finally, the western colony was much closer to the open water than the eastern one at the time of our visit, and a recent study (Massom *et al.* 2009) has shown that the distance between an emperor penguin colony and the open water may tend to correlate negatively with breeding success.

Budd (Budd 1961) proposed that "each rookery can be regarded as a compromise, and not always a very successful one, between the emperor's sometimes conflicting requirements of safety from sea- ice breakouts, shelter, and access to food". Finding a suitable trade-off may well be an

arduous matter of trial-and-error, since inter-annual variations make it difficult for the birds to evaluate rapidly the consistency of ice conditions at a particular location. Therefore, after the loss of their original habitat, some birds are probably breeding in a sub-optimal location, which may explain the difference in breeding success between neighbouring and possibly related colonies.

§-145 Status of the Emperor Penguins Census. Emperor penguins breed almost around the entire coastline of the Antarctic Continent (Melick & Bremmers 1995; Coria & Montalti 2000; Woehler 2001; Todd *et al.* 2004; Fretwell *et al.* 2012). Their known breeding distribution extends from Snow Hill Island (64°31'S, 57°26'W) to Gould Bay (77°43'S, 47°41'E) in the Antarctic Peninsula, and Cape Crozier on Ross Sea (77°28'S, 169°19'E). The Snow Hill Island and Gould Bay (Woehler 2001) colonies are the most northerly and the most southerly known emperor penguin colonies, respectively. Colony sizes vary from more than 20,000 pairs (Coulman Island, Cape Washington, Halley Bay) to just a few hundred pairs (Umbeashi Rock, Amundsen Bay, Fold Island, Cape Crozier). The two largest known colonies are in the Ross Sea: Cape Washington with ca. 24,000 pairs and Coulman Island with ca. 28,000 pairs (Kooyman 1993).

The closest colonies to the Mertz Glacier are at Pointe Géologie (66°40'S, 140°01'E) and Davis Bay (69°21'S, 158°29'E). While ca. 2,500 chicks of emperor penguins were raised at the Pointe Géologie colony during the 2012 breeding season, the two new colonies together numbered ca. 5,700 chicks. Since a pair of emperor penguins may only successfully raise one chick per year, the population of breeding emperor penguins in this area of Antarctica can therefore be estimated, based on these chick counts, to more than ca. 16,400 breeding adults, about a fourth more than previously estimated (Fretwell *et al.* 2012). This count represents a minimum estimate for the breeding population, given uncertainty about the mortality rate of chicks prior to our visit.

Because of the persistence of the sea ice, few ships are able to reach the Antarctic coasts before post-breeding adults disperse from their colonies between December and early January. Except for colonies close enough to research stations, during the breeding season (from March-April to

December-January, depending on the latitude), access to colonies is difficult or impossible due to adverse weather and/or extensive pack ice (Kooyman 1993). Consequently, many emperor penguin colonies have never been counted and some have presumably not even yet been discovered. Further- more, in addition to the Mertz colonies, another colony, on the Princess Ragnhild coast and for which location was reported in 2009 by satellite images (Fretwell *et al.* 2012), was first visited in early January 2013 by Belgian scientists, who surveyed ca. 20,000 adults, compared to 6,870 adults detected from satellite survey (Fretwell *et al.* 2012). The current global emperor penguin population can therefore be estimated to be, at least, ca. 260,000 pairs from 52 breeding colonies (Fretwell *et al.* 2012 and present study), or ca. 25% more than estimated only 15 years ago (Woehler & Croxall 1997).

Over the past five years satellite surveys have proved a very effective method for finding new emperor penguin colonies. However, as our visit to the western colony demonstrated, the nitrogen-signature of snow-covered droppings around colonies that underwent numerous snowfalls, and the shade of an ice front indicate that at certain times of year, under challenging environmental conditions it is virtually impossible to detect some colonies from satellite images. Importantly, several colonies have not been observed since they were first reported. This problem, of missing colony locations by satellite survey may be solved by taking multiple satellite images within a breeding season and especially towards the end of the breeding season when the guano is more apparent. Multi-temporal and multi-year satellite surveys, backed up with confirmation and further ground truthing from aerial or ground based counts are essential if we wish to fully understand the population demography and dynamics of emperor penguins. As a consequence, we can still hope to discover more emperor penguin colonies in the future if further investigations are conducted along the Antarctic coast.

Acknowledgements

Chapter 7: Unexpected philopatry in an insular seabird, the Peruvian diving-petrel

This chapter is based on <u>Cristofari R,</u> Fernandez-Zamora F, Gouin N, Le Bohec C, Plaza P, Trucchi E, Zavalaga C, Luna Jorquera G, **Unexpected population isolation in a critically endangered insular seabird, the Peruvian Diving Petrel** *(Pelecanoides garnotii).* (*in prep*).

Context

§-146 The Peruvian diving-petrel as a reference species. In the previous chapters, we introduced the particular case of the *synnomes* of the King and Emperor penguins - a highly original population organisation, in which the whole species, despite its fragmented colonial distribution, remains fully panmictic. This structure may be seen as an extreme case in the broad spectrum of seabird genetic and spatial organisations (see *e.g.* a review in Friesen *et al.* 2007): in the previous chapters (see *The King synnome*, p. 163 and *The Emperor synnome*, p. 211), we argue that this particular form of transient philopatry is a significant behavioural trait that allows *Aptenodytes* penguins to cope with the unstable polar environment, driven either by the extent of coastal upwelling and polynya activity, or by the latitudinal variations in the Polar Front location. In order to test that prediction, we review here the contrasting case of the Peruvian diving petrel *Pelecanoides garnotii*. A procellariimorphe like the penguins (Zhang *et al.* 2014), this small auk-like procellariform bird

offers several convergent traits with the spheniscids. Like them, its wings are derived and adapted to underwater swimming (Luna-Jorquera *et al.* 2003 - a trait it shares with *e.g.* Alcids) - albeit greatly reduced, flight function is however not totally lost. This diving bird feeds mostly on fish and krill (Jahncke *et al.* 1999) and may reach great depths relative to its small size (routinely 30m but depths of more than 80m have been recorded, see Zavalaga & Jahncke 1997). Finally, localised upwellings seem to be a major determinant of foraging behaviour in this central-place forager (Zavalaga *et al.* 2010, Fernandez-Zamora *in prep.* and Luna Jorquera, *pers. com.*). However, contrary to *Aptneodytes* penguins, *P. garnotii* enjoys a mostly stable oceanographic landscape. It breeds on a handful of offshore islands of central Northern Chile and Southern Peru (Hays 1989; Simeone *et al.* 2003), that are part of the Humboldt Current System.

§-147 The Humboldt Current System. The Humboldt Current System (HCS) is a Northward extension of the Pacific subantarctic watermasses. Like the Benguela Current in the Atlantic basin, it is one of the world's major Eastern Boundary Currents: North of the West Wind Drift zone (see §7 p. 35), the Southern Pacific anticyclonic gyre drives nearly constant equatorwards winds along the coast of South America. These winds result in a strong northward drift of cold subantarctic surface waters along the coast, and in offshore Ekman transport: near the shore, the drifting surface waters draw the upwelling of tropical nutrient-righ subsurface waters, which result in one of the most highly productive oceanic systems on the planet (see Thiel *et al.* 2007 for details). Upwelling activity is regulated by the seasonal displacement of the Pacific anticyclonic gyre, and is constant only in Northern Central Chile and in Peru. It is also strongly influenced by the topology of the South American continental shelf, where local cape and island systems promote upwelling activity - *e.g.* in the Coquimbo Coastal System (Montecino *et al.* 2006). Thus, although the El Niño Southern Oscillation (see §8 p. 40), just like in the Southern Ocean, has a deep impact on local productivity, it does not influence the location of upwelling hotspots, that remain at the same distance from breeding islands. This relative stability of the HCS topological and

oceanographic features sets a very different expectation for the population structure of seabirds[1].
An overview of the general behaviour of procellariimorphes makes philopatry a likely ple-
siomorphic trait in these species (Friesen *et al.* 2007), that may be counteracted by specific con-
straints, such as an excessively unstable environment: we therefore expect a «stable» species such
as the Peruvian diving petrel to represent the other extreme along the seabird population struc-
ture spectrum.

Abstract

Seabirds are often used as reliable sentinels of oceanic environments: however, idiosyncratic life
history traits strongly influence both their response to ecosystem changes and our capacity to as-
sess and interpret the extent of this response. In particular, the strength of philopatric behaviour
and dispersal ability are important determinants of each species' evolutionary response. Here, we
show that a representative endemic species of the Humboldt Current System, the once abundant
but now critically endangered Peruvian diving petrel (*Pelecanoides garnotii*), exhibits extreme
philopatric behaviour. Mitochondrial and genome-wide SNP data provide evidence for strong
isolation and low migration at very short distance. We suggest that behavioural and morphologi-
cal adaptations to coastal insular habitat and underwater foraging are the main drivers of the ex-
ceptionally strong philopatry in this aulk-like species. Importantly, range fragmentation, com-
bined with ongoing anthropogenic pressure, are expected to put the Diving-petrel under
continued high risk, as the full demographic independence between colonies is likely to preclude
local population rescue through migration. The independence of each island's breeding popula-

---

1.   Here, it is important to note that *stability* is only relative to a particular species' *habitat* (see §49 p. 127) within a
geographic or oceanic system. For example, we stated earlier that the Emperor penguin's sea ice habitat appeared as extremely un-
stable (see **Empirical evidence of heterogeneous dispersal**, p. 259): yet within the precise same area, the habitat of *e.g.* bottom-
dwelling notothenioid fish may be totally stable. Thus, it makes more sense to think about the stability or instability of *habitats*
than of *environments*. Here, therefore, the stability of the HCS is only considered *relative to the standard seabird habitat*, that is
heavily dependant on local upwellings and guano insular breeding locations.

tion should be a key element in the conservation strategy for this key species of the Humboldt Current System coastal archipelagos.

Introduction

§-148 Seabirds as terrestrial animals. Seabirds are an important link between marine and terrestrial ecosystems (Blais *et al.* 2005; Ellis 2005; McCauley *et al.* 2012): but that double bond makes them highly susceptible to changes on both sides of the shoreline. Their sensitivity to changes in marine ecosystems is now a well-documented subject: it involves either long-term, indirect impact of human activities through climate change (Le Bohec *et al.* 2008; Sydeman *et al.* 2012), or direct impact through fisheries which compete with seabirds for food resource (Tasker *et al.* 2000; Becker & Beissinger 2006; Karpouzi *et al.* 2007; Cury *et al.* 2011; Wagner & Boersma 2011) or even cause massive direct seabird mortality (Weimerskirch *et al.* 1999; Lewison *et al.* 2004). Yet the often overlooked disruption of terrestrial breeding habitats can also have a very significant impact on population dynamics. Impacts may range from spread of diseases on the colony areas (Barbosa & Palacios 2009) to sudden habitat disappearance (Ancel *et al.* 2014): yet the most common cause of habitat loss remains the growing interaction with terrestrial predators, including humans (see Croxall *et al.* 2012 for a review). Unlike marine environment modifications, increasing disturbance on land may be very restricted locally, and affect only one or a few breeding colonies. Therefore, both environmental compartments need to be taken into account when studying seabirds. This applies to the understanding of population dynamics, since locally-based monitoring programs and studies may largely misjudge global tendencies by mistaking local effects for general trends (Mallory *et al.* 2010; Lynch *et al.* 2012) - but also, importantly, when devising conservation strategies, since marine and land pressures need to be mitigated separately.

§-149 Recent history of the Peruvian diving-petrel. The Peruvian diving petrel (*Pelecanoides garnotii*) is a dramatic, although by no means unique, example of the combined effect of these multiple direct and indirect threats. According to historical records, this small insular procellariid was one of the most abundant endemic seabird of the Humboldt Current System, and presented a broad distribution {Coker 1919; Murphy 1936} from ~ 6°S (in Isla Lobos de Tierra, Peru) and ~ 42°S (in Isla Chiloé, Chile) along the Pacific coast of South America. Yet the species declined rapidly during the 20th century as a result of guano extraction (Murphy 1936; Hays 1989; Figueroa *et al.* 2011), hunting (Hays 1989), bycatch (Hays 1989; García-Godos & Goya 2006), human-introduced predators (Araya Modinger & Duffy 1987; Simeone *et al.* 2003) and habitat competitors (Fernández Zamora 2011), food competition with fisheries (Hays 1989; Jahncke & Goya 1998), and the increased effects of ongoing climate change on the productivity of the Humboldt Current System (HCS, see Thiel *et al.* 2007). This led to the decline of their nesting habitats, from thirteen colonies reported in the past to seven nesting sites at present (Araya Modinger & Duffy 1987; Vilina 1992; Figueroa & Stucchi 2008; Figueroa *et al.* 2011). Its breeding range has then been reduced and fragmented into two main areas, divided by a 1,300 km gap - one on the central Peruvian coastline, around 8°S and 14°S (Isla Corcovado, Isla San Gallán and Isla La Vieja (Jahncke & Goya 1998; Valverde Romero 2006), and one in northern Chile, between 26°S to 29°S (Islas Pan de Azúcar, with ~220 pairs, Isla Choros, with ~9,516 pairs, Isla Grande, with ~200 pairs, and Isla Pájaros II, with ~120 pairs (Mattern *et al.* 2002; Simeone *et al.* 2003; Martinez Palma 2014). Historical population sizes are little known, but all available information points to a critical decline: while 100,000 pairs bred on Isla Chañaral, Chile, in 1938 (Araya Modinger & Duffy 1987), this population is now completely extinct (Simeone *et al.* 2003); and the now recovering Peruvian population (Jahncke & Goya 1998) was estimated to a total of ca. 4,000 individuals in 1989 (Hays 1989).

Figure 43 | Full distribution of Pelecanoides garnotii. (A) Peruvian and (B) Chilean range of the species. To the left, close-up of the Chilean range of the species (dashed lines indicate discontinuity in our representation of the shoreline). Isla Chañaral is currently unoccupied. Sampled islands (Pan de Azúcar and Choros) are marked by coloured circles.

§-150 Present-day status of the species. Although the Peruvian diving-petrel's colonies have declined and even gone extinct during recorded history, marginal range re-expansion and local population regrowth have been documented in the past decades (Figueroa *et al.* 2011). Thus, small colonies have been discovered on Corcovado Island, Perú (Valverde Romero 2006), and non-breeding in-

dividuals have been sighted on Lobos de Afuera islands (Figueroa & Stucchi 2008; Figueroa *et al.* 2011). A rapid growth of observed census size was also documented in the past decade in Perú, on La Vieja Island (IUCN Red List) and in the Chilean islands (Simeone *et al.* 2003; Fernandez *et al.* 2014). However, the processes underlying this possible population recovery are poorly understood, and assessing true regrowth is made difficult by our very limited knowledge of the species' life history traits. It has been suggested that the diving-petrel's poor flight abilities greatly reduces its dispersal possibilities (Luna-Jorquera *et al.* 2003), and that the high investment required for burrow nest construction is likely to promote a strong philopatric behaviour (Furness 1978; Cortés Labra 2007). It has thus been proposed that diving petrels occupy a coastal niche and are thought to be year-round residents (Murphy 1936; Figueroa *et al.* 2011), which would further reduce its dispersal opportunities.

§-151 Panmixia in the Humboldt Current System. While most studies conducted in seabirds have emphasized the importance of genetic or phylogeographic structure in species dynamics (see Friesen *et al.* 2007 for a review), the Humboldt Current System stands out as an exception. Genetic surveys conducted in its major seabird species have concluded in a lack of genetic structure at the continental scale (*e.g.* in the Peruvian booby (*Sula variegata*, see Taylor *et al.* 2010) or the Peruvian pelican (*Pelecanus thagus*, see Jeyasingham *et al.* 2013), or in very high gene flow between colonies in the flightless Humboldt penguin (*Spheniscus humboldti*, see Schlosser *et al.* 2009). High dispersal, possibly promoted by foraging concentrations around localised upwellings (Jeyasingham *et al.* 2013), has therefore been proposed as a central underlying mechanism. It has also been suggested that high dispersal is one of the keys to the higher resilience of these species to habitat change compared to other seabirds (Jeyasingham *et al.* 2013). Thus, it is unclear whether the Peruvian diving petrel follows the expectation of high dispersal and panmictic population set by other seabirds of the Humboldt Current System, or rather the highly philopatric and low-dispersal life history strategy that its behaviour suggests.

§-152 Aims of the study. If *P. garnotii* exhibits the same degree of panmixia as the other seabirds of the Humboldt Current System, demographic independence of colonies may not be assumed. In that case, observed local population growth may rather be interpreted as the result of a complex process (for example, several local extinction or exodus events, anecdotally causing census increases in a handful of refugial areas through immigration). This would imply that only range-wide census may be informative as to the status of the species. Alternatively, however, if the hypothesis of high philopatry and low dispersal is verified, demographic independence may be expected between breeding locations throughout the species' highly fragmented range. In that case, population trends observed at single locations may reflect true demographic responses, *e.g.* to local conservation measures (such as reduced guano extraction in several protected islands, and creation of marine protected areas), rather than range-wide and species-scale processes. In order to understand the current demographic trends for the Peruvian diving-petrel, and the extent of the threats to the remaining populations, it is therefore necessary to establish whether observed local growth is a result of *(i)* intrinsic local population growth, or *(ii)* immigration-fueled refugial concentration. Here, we use both mitochondrial and genome-wide genetic markers to distinguish between these two hypotheses, and assess the current degree of demographic independence between diving-petrel colonies throughout its Chilean range.

Results

§-153 Sequencing data. Genome-wide short-locus RAD-sequencing and mitochondrial data (see *Methods*) are in good agreement in *Pelecanoides garnotii*. The Illumina sequencing lane yielded 182,319,948 paired-end reads with a mean phred-scaled quality score of 37, of which 144,048,478 were retained after barcode and cut-site sequence filtering. The final database included 65,582 distinct RAD loci, of which 37,170 were polymorphic, with an average of 1.3 SNPs per locus. After PCR-duplicate removal, SNP calling from the higher-quality reads in

GATK yielded 43,175 SNPs, of which 32,964 were genotyped in at least 75% of individuals, with a mean depth of 3.2X, and a median depth of 3.1X. Nucleotide diversity computed from genome-wide SNP data was very similar across islands, with π_{CHR} = 0.00224 and π_{AZR} = 0.00226 (and pooled diversity π_{ALL} = 0.00233), at a level in accordance with the expectation for long-lived seabirds (Romiguier *et al.* 2014), and Tajima's D supported neutral evolution at the selected sites (D_{CHR} = -0.364 D_{AZR} = -0.361). mtDNA-based indices support this view: nucleotide diversity was of the same order of magnitude for both islands, although slightly higher in Choros (π_{CHR} = 0.00232 and π_{AZR} = 0.00161, and pooled diversity π_{ALL} = 0.00218). Both Tajima's D and Fu & Li's F indices supported neutral evolution of the polymorphic sites (D_{CHR} = -0.463 and D_{AZR} = -0.649, P > 0.10; F_{CHR} = -1.26 and F_{AZR} = -1.34, P > 0.10). The sequenced cytochrome-b fragment contained 13 polymorphic sites, only 6 of which were polymorphic at both locations.

§-154 Population structure. All analyses support an outstandingly high level of genetic divergence at such a short geographical distance. Fixation index is high for genome-wide SNP data (Fst = 0.049 ±0.0082, averaged over 500-SNPs windows), and higher from mtDNA data (Fst=0.158). Analysis of molecular variance also supports significant differentiation between Isla Choros and Isla Pan de Azúcar. Based on SNP data, difference between islands account for 2.51 % of the total variation, while difference between colonies within each island accounts for -0.099 %. According to mtDNA data, these components account respectively for 14.28 % and 0.95 % of total variation. Differentiation between islands is significant according to both datasets (ΦST_{mtDNA} = 0.152 and ΦST_{SNP} = 0.0251, both p-values < 0.05), but differentiation between colonies within islands is not (ΦSC_{mtDNA} = 0.0111, p-value = 0.297; and ΦSC_{SNP} = -0.00101, p-value = 0.795).

Principal component analysis clearly supports a two-population structure (Fig. 44A). Although the first component only accounts for 6.62% of total variance, it discriminates widely between individuals from Isla Choros and Isla Pan de Azúcar - while the second and next components

only outline inter-individual variance. The idea of a low-level but highly consistent separation is

also supported by a Hamming-distance-based neighbour net (Fig. 44B): terminal edges are much

longer than structural inner edges, yet sorting is complete between the two islands (a structure

supported, although to a lesser extent, by a mtDNA haplotype network, see Fig. 44D). Finally,

clustering analyses, whether genotype likelihood based (Fig. 44C) or K-means based strongly

supports a two-population model, both over panmixia, and over higher complexity models.
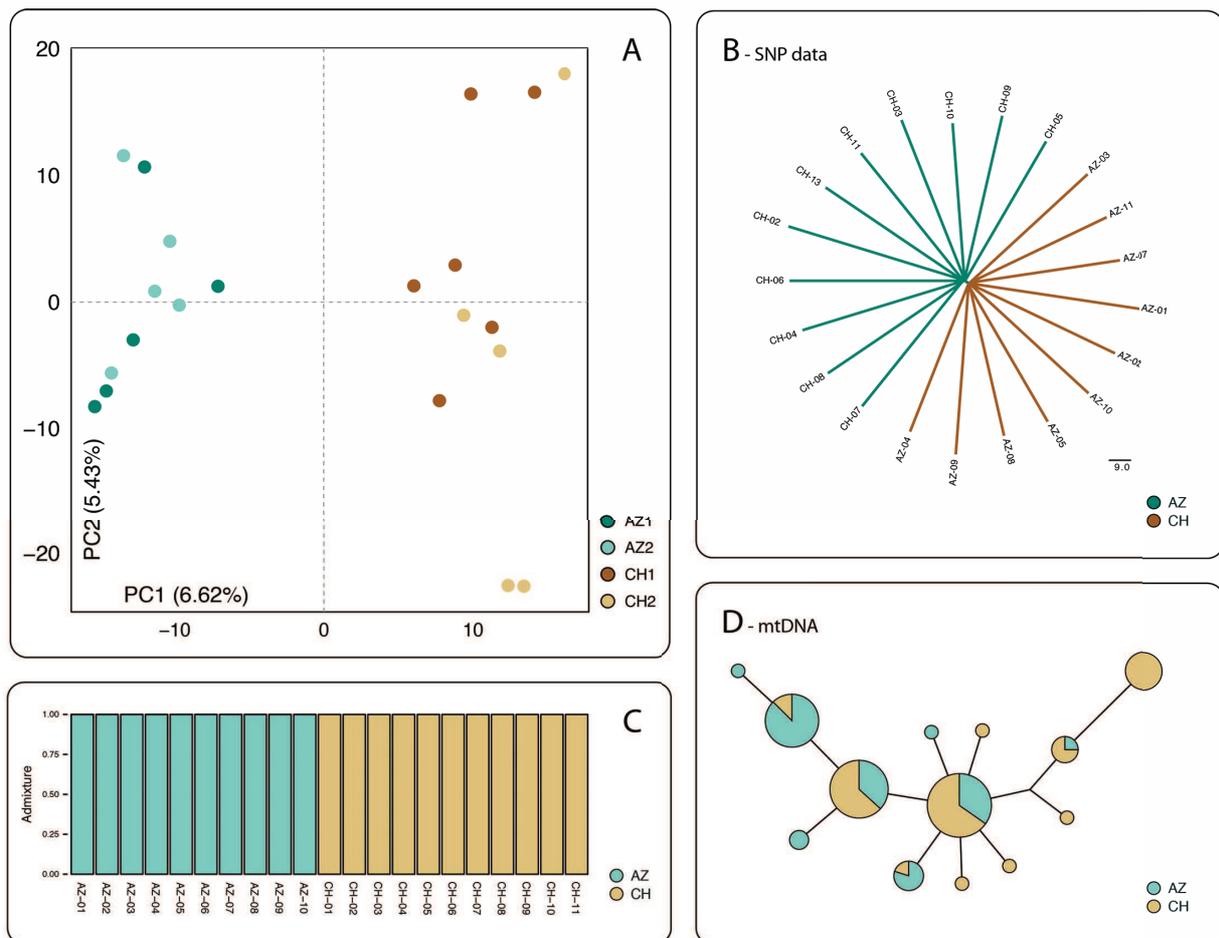
Figure 44 | Consistent genetic structure within the Chilean range. (**A**) Principal component analysis performed on genome-wide genotype likelihood data; (**B**) NeighbourNet built from nuclear SNP data; (**C**) Individual components of admixture as inferred from genome-wide genotype likelihood data (median values from 500 bootstrap replicates); (**D**) Fitch-distance haplotype graph for the mitochondrial cytochrome-b gene (disc area proportional to the number of haplotype copies). In all panels, "AZ" stands for Isla Pan de Azúcar and "CH" for Isla Choros. AZ1 and AZ2, and CH1 and CH2 respectively stand for two colonies of each island.

§-155 Isolation and migration analysis. Migrate-n models of connectivity support a structure with low migration between separated populations. Bayes factor (BF) model comparison across three independent replicates allows unambiguous rejection of both panmixia, and full isolation hypotheses. BF does not allow for a clear choice between symmetric, and asymmetric migrations - although BF does not take into account the number of estimated parameters: thus, the lower-parametrised symmetric migration model should be preferred. Under this model, Θ_{CHR}= 0.00697 ±8.0829e^{-5}, Θ_{AZR}= 0.00747 ±0.000212 and M= 2075 ±10.6. Using the reconstructed substitution rate for highly polymorphic RAD loci μ = 3.55.e^{-8} substitutions.site^{-1}.generation^{-1}, inferred effective population sizes scale to N_{CHR} ≈ 58,600 and N_{AZR} ≈ 62,800, with a symmetric migration rate of M ≈ 3% effective migrants per generation.

Joint minor-allele frequency spectrum based inferences are globally consistent with this model. AIC supports our fifth model - a model with a recent change in the migration regime (median: 207 generations ago, CI 95% [82; 375]), but no population size change. Population sizes are widely asymmetric (median sizes and CI95%; Choros: 91,350 [87,977 ; 95,509]; Pan de Azúcar 1,013 [1,010 ; 1,018]). Migration from Choros to Pan de Azúcar is inferred stable (before the change: 1.146e^{-5} [1.121e^{-5}; 1.209e^{-5}]; after the change: 1.170e^{-5} [1.124e^{-5}; 1.240e^{-5}]), but increases at least ten-fold from Pan de Azúcar to Choros (before the change: 2.756e^{-4} [2.397e^{-4}; 3.025e^{-4}], after the change: 4.268e^{-3} [2.553e^{-3};1.041e^{-2}]). The second-best AIC score supports a model with changes in migration regime and in population size: inferred migration patterns are similar (Choros to Pan de Azúcar, before change: 1.135e^{-5} [1.018e^{-5}; 1.207e^{-5}], after change 1.224e^{-5} [1.122e^{-5}; 2.226e^{-5}]; Pan de Azúcar to Choros, before change: 2.853e^{-4} [2.466e^{-4}; 3.128e^{-4}], after change: 1.103e^{-2} [3.724e^{-3}; 1.116e^{-1}]), and population size in Pan de Azúcar is stable or increases slightly (before change: 1,014 [1,010; 1,019], after change: 1,027 [1,011; 17,702]), but population is reduced strongly in Choros (before change: 95,542 [88,815; 101,124], after change: 23,832 [10,068; 36,104]).

Discussion

§-156 A highly structured population. The Chilean populations of *Pelecanoides garnotii* stand out as remarkably isolated, despite short geographical distances and a tumultuous recent history. All available evidence supports the idea of a distinct population per island, with limited gene flow. Genome-wide polymorphism based analyses concur on a complete sorting of individuals between Isla Choros and Isla Pan de Azúcar, albeit with limited differentiation: the variance accounted for by the first component of PCA (6.62%), although highly consistent with the geographical structure, is only slightly above the neutral expectation. This is fully in line with the relative lengths of internal and terminal edges, and the location sorting, in the neighbour-net (Fig. 44B). There is a good agreement between the genome-wide nuclear and the mitochondrial signal: some aspects, however, deserve consideration. The clearer sorting of individuals observed from nuclear data compared to mtDNA (see *e.g.* Fig. 44B *vs* Fig. 44D) is most likely a consequence of the much higher resolution of the large neutral nuclear marker dataset, compared to the relatively short, and non-recombining, functional cytochrome-b gene sequence. For F-statistics based analysis (pairwise Fst, or analysis of molecular variance), on the other hand, mtDNA gives a stronger signal than nuclear markers. Although higher dispersal in males than in females has often been proposed as an explanation in similar cases, this interpretation of discrepancies between nuclear and mitochondrial signals has been questioned (Zink & Barrowclough 2008), and the difference in coalescence rate of haploid and diploid markers has been convincingly proposed instead. In our case, the much larger sample size used for mtDNA analysis (83 individuals) compared to nuclear analysis (21 individuals) may also account for a large part of this apparent difference. The resolution and the strength of the signal, however, should not be confused: the weaker, but clearer nuclear signal may characterise the true isolation processes more accurately than the larger and more contrasted mitochondrial dataset (Hoban *et al.* 2013b).

§-157 Population size and gene flow. Reconstructed population sizes and gene flow between sampled locations are globally consistent between haplotype-based and spectrum-based approaches, although with a considerably higher precision for the spectrum-based inferences. Migrate-n and fastsimcoal2 models allow us to reject panmixia as well as full isolation between colonies, and support partial isolation, with ongoing gene flow. However, the models differ on two important points. First, Migrate-n suggests equal population sizes, with Ne ≈ 60,000 for each population, while fastsimcoal2 infers unequal (yet stable) population sizes, with $N_{CHR} \approx 90,000$ and and $N_{AZR} \approx 1,000$. Despite these contrasting results, however, both models propose an effective population size that is considerably higher than the present-day census: the cumulated population of ~90,000 to ~120,000 effective breeders is in stark opposition with the currently observed population of ~ 19,000 breeders in Isla Choros (Martinez Palma 2014) and ~ 220 in Isla Pan de Azúcar (Mattern *et al.* 2002), but more in tune with the historical populations (*e.g.* 100,000 breeders on the major breeding location of Isla Chañaral in 1938, and similarly large colonies elsewhere, Araya Modinger & Duffy 1987): a dire testimony to the rapidity and extent of the population collapse in the past decades (Roman & Palumbi 2003).

Second, Migrate-n infers symmetric, and relatively high gene flow (~3% per generation), whereas fastsimcoal2 supports much lower, asymmetric gene flow: n orthward m igration (from Isla Choros to Isla Pan de Azúcar) is stable and very low (~0.001% per generation), while southward migration is higher, and increases from ~0.03% to ~0.4% in the recent past. Although the historical records are too scarce to draw any definitive conclusion, it is noteworthy that on Isla Pan de Azúcar, a thousands of decaying, unoccupied burrows can still be observed (Fernandez *in prep.*) - a possible sign of one or several recent massive emigration events. Thus, generally, the haplotype-based reconstruction suggests a "homogenised" system, with population sizes averaged by higher gene flow: in contrast, the spectrum-based approach offers a more nuanced reconstruction, that better reflects the observed state of the populations. The higher resolution of the spectrum-based approach, however, is expected. First, it is able to use the information from the full RADome,

and not only from a random subset of loci. Second, haplotype-based methods chiefly capture events occurring at a substitution (*i.e.* millennial) scale, while spectrum-based approaches also capture drift in allele frequencies that may occur in a few generations, thus making them more suitable for the recovery of recent population history. Therefore, we may more appropriately consider Migrate-n reconstructions as a general framework, that does not contradict the more precise reconstruction given by our fastsimcoal2 model.

§-158 Evolution of philopatry. The high differentiation between two assessed sites at such close range is remarkable for seabirds in general (Friesen *et al.* 2007), but all the more so for the guano-seabirds ("*aves guaneras*") of the Humboldt Current System. The observed structure is in strong contrast with the HCS-wide panmixia of the Peruvian booby (*Sula variegata*, see Taylor *et al.* 2010) or the Peruvian pelican (*Pelecanus thagus*, see Jeyasingham *et al.* 2013). Weak genetic structure has indeed also been detected in the Humboldt penguin (*Spheniscus humboldti*), but only at a range of ~2,000 km (Schlosser *et al.* 2009), as opposed to the ~350 km separating the two assessed diving-petrel breeding islands. Since both the Peruvian pelican and the Humboldt penguin share with the Peruvian diving-petrel a recent history of dramatic population decline, the contrast in population structure can hardly be explained by their recent collapse. Morphological and metabolic aptitude to flight may, on the other hand, influence dispersal patterns - indeed, it has been proposed that the diving-petrel's adaptation to underwater wing-propelled swimming, and the necessary trade-off of poor flying abilities (Luna-Jorquera *et al.* 2003), reduced the species' activity radius. Although no data is available for the Peruvian diving petrel, its two sister species, the Common diving petrel (*P. urinatrix*) and the South Georgian diving petrel (*P. georgicus*), have been shown to forage more locally than similar-sized, sympatric "gliding" Procellariiformes, both during the breeding season (Navarro *et al.* 2013), and in the inter-breeding period (Navarro *et al.* 2015). Further studies, however, will be necessary to decide how far the lack of dispersal ability is involved in the Peruvian diving petrel's genetic fragmentation. An alternative explanation may be purely behavioural: while philopatric behaviour is the norm in Procellariiformes (see *e.g.* Milot *et*

al. 2008), the higher investment needed for burrow construction (Furness 1978; Cortés Labra 2007), together with the scarcity of available habitat, may reinforce that behaviour in the diving petrel.

§-159 Implications for conservation. The observed level of population isolation has important implications for the conservation of the species. Whereas the panmictic character of the HCS population of Peruvian pelican or Peruvian booby has been suggested to increase their robustness in the face of environmental change (Jeyasingham *et al.* 2013, see also *The Emperor's synnome*, p. 211*)*, the high fragmentation of the *P. garnotii* population, on the other hand, is expected to add to their already great vulnerability to land habitat destruction and marine environment degradation. Indeed, high philopatry and low dispersal imply that the loss of a combined safe breeding island and productive foraging area can not be mitigated by mass dispersal, but will rather lead to a local extinction, and the irremediable loss of the associated genetic diversity. An associated prediction is that current populations are demographically independent (Waples & Gaggiotti 2006). Therefore, the observed local trajectories are unlikely to be an artifact of labile migratory fluxes, but rather represent the true local demographic trend: thus, the local census increases that are observed (in particular in Isla Choros, Martinez Palma 2014) may be interpreted as the positive outcome of successful conservation measures, such as the creation of the Humboldt Penguin National Reserve (that includes Isla Choros and the surrounding marine area) - an encouragement to persevere in such endeavours.

Our results make it especially clear that any conservation strategy in the Humboldt Current System should focus on each island (and the surrounding marine areas, Luna-Jorquera *et al.* 2012) as a significant unit. Within islands, colonies do not stand out as genetically separate entity, although philopatric behaviour may still apply at that scale for stretches of a few generations. But the distinctness of each island's gene pool, as well as their inferred demographic independence, makes the conservation of each single one of the four remaining Chilean breeding islands an ab-

solute necessity for the survival of this once extremely abundant, and now critically endangered seabird species. Indeed, despite the positive trend observed in the last decade on Isla Choros, important threats remain both for the nesting sites and for the marine habitats of diving petrels. One of the four islands where petrels nests (Isla Pájaros II, currently with no legal protection) is still under a valid permit of guano extraction (Ministerio de Minería 1988), and ongoing extraction of guano was confirmed on the island as recently as 2003 (Simeone *et al.* 2003). Additionally, future plans for mining projects include the building of a large harbour in the close vicinity of the two central breeding locations of the species, Isla Choros and Isla Grande de Atacama (Servicio de Evaluación Ambiental 2015). This could significantly affect both the coastal foraging areas of the species (through increased marine transit) and nesting areas (through direct effects of increased human intrusion). However, our results clearly show that the conservation of each single breeding location is essential for preserving the full remaining genetic diversity of this already severely reduced species, and maximizing the chances of a recovery after its massive historical decline.

Material and Methods

§-160 Sample collection and DNA extraction. Access to the protected areas and sampling were performed under permit N°38/2012, delivered by the CONAF authority (Atacama region). Sampling was performed between april and may, outside the reproductive peak season (Fernández com. pers.) to minimise disturbance.

§-161 Sampling and DNA extraction. Four colonies of *Pelecanoides garnotii* were sampled throughout its Chilean breeding range: two in Isla Choros (Fig. 43 - Ch1 and Ch2: 32 and 11 individuals respectively), and two in Isla Pan de Azúcar (Fig. 43 - Az1 and Az2: 27 and 11 individuals respectively). Adults were captured using a mist net placed at the entrance of the colony at dusk. Blood was sampled from the *retia* in the interdigital membrane of the foot, using a he-

parinized microcapillary, dried, and frozen. DNA extraction was performed using a standard spin-column protocol (Qiagen DNeasy® Blood & Tissue kit).

§-162 Mitochondrial marker sequencing. A fragment of the mitochondrial cytochrome-b gene was amplified for all samples using either two or four specific primers designed from the published sequence (Nunn & Stanley 1998 - as 5'-3', yun1f: GCCCCAAACCTCCGAAAATCCCA and yun2r: GGTGATGGAGGCTAGTTGGCCG or with internal primers yun1r: GCCTGATTCGTGAAGGAAGGTGAGG and yun2f: CCACCCTAACCCGATTCTTCGCC). Amplification required the following conditions: 5' at 94°C, followed by 35 cycles of 30" at 94°C, 30" at 57°C, and 1' at 72°C, and finally 5' at 72°C. PCR product was then purified using Illustra™ ExoStar™, and Sanger sequencing was performed at the ABI lab of the University of Oslo. Quality assessment, trimming and manual checking were performed in Geneious® v6.1.2.

§-163 RAD library preparation and SNP typing. SNP discovery and sequencing was performed on a subset of individuals (11 from Isla Choros and 10 from Isla Pan de Azúcar) following a single-digest RAD-sequencing protocol (Baird *et al.* 2008). High quality samples were selected using a 1.5% agarose gel, and quantified by fluorometry (Life technologies™ Qubit®). *(i)* for each sample, 125ng of genomic DNA were digested with the restriction enzyme SbfI (NEB); *(ii)* each sample was ligated to a unique barcoded P1 adapter prior to pooling in a single library. The library was then sheared by sonication (7 cycles 30" ON – 30" OFF); *(iii)* sonicated libraries were concentrated to 25 μl by DNA capture on magnetic beads (beads solution:DNA = 0.8:1), and the target size range fraction (300-500 bp) was then selected by gel electrophoresis and manual excision; *(iv)* capture on magnetic beads using the same beads:DNA ratio (0.8:1) was then performed in all following purification steps (after blunt-end repairing, poly-A tailing, P2 adapter ligation and library enrichment by PCR); *(vi)* PCR amplification was performed in 8 x 12.5 μl aliquots pooled after the amplification in order to reduce amplification bias on few loci due to random drift. PCR was performed using NEB Phusion® polymerase with the following cycles: 30" denat-

uration at 98°C, 21 cycles of amplification (10" at 98°C, 30" at 65°C and 30" at 72°C), and a final elongation of 5' at 72°C; *(vii)* the library was then quantified by fluorimetry (Life technologies™ Qubit®) and molarity was checked on an Agilent Bioanalyzer chip (Invitrogen™). A final volume of 20 μl was submitted for paired-end sequencing on an ILLUMINA HiSeq2000 sequencer (V3 chemistry) at the Norwegian Sequencing Centre, University of Oslo, and spiked with 20% PhiX control library in order to reduce low-diversity bias.

As no reference genome is available for *P. garnotii*, data processing followed a two-step protocol. First, loci were built *de novo*, using the Stacks v1.28 pipeline (Catchen *et al.* 2011; Catchen *et al.* 2013), and a synthetic reference RADome was built. Second, this reference RADome was used to perform alignment-based SNP typing. The workflow was as follows: *(i)* Sequence de-multiplexing and *de novo* locus assembly was done according to in-line barcodes using the Stacks *denovo_map.pl* pipeline, with a maximum of 5 mismatches allowed between alleles at a single locus (both within and between individuals). The corresponding paired-end contigs were assembled using Velvet (Zerbino & Birney 2008) and Stacks, setting a minimum contig length of 200bp in order to filter out multiple non-overlapping short paired-end reads. *(ii)* Resulting loci were concatenated, together with their respective paired-end contigs, to form the scaffolds of a reduced reference genome, or RADome. At that point, loci comprising multiple paired-end contigs (a potential sign of collapsed paralogous loci) were removed. The raw paired-end fastq files were then mapped onto this RADome using Bowtie2 (Langmead & Salzberg 2012). The resulting alignments were processed using Samtools 0.1.19 (Li & Durbin 2009), PicardTools 1.113 (http://picard.sorceforge.net), and custom R and shell scripts in order to discard orphaned reads and low-quality pairs. These cleaned alignments were further filtered for PCR and optical duplicates using Picard MarkDuplicates. *(iii)* SNP and genotype calling was restricted to the first-in-par reads. We then used GATK's HaplotypeCaller pipeline (DePristo *et al.* 2011) to simultaneously call SNPs and genotypes in all samples, using first reads only, with standard parameters, except for population heterozygosity which was set to 0.01, and retaining only di-allelic, non-indel sites sequenced

in at least 75% of samples. We repeated key analyses using ANGSD 0.900 (Kim *et al.* 2011; Korneliussen *et al.* 2014) to estimate allele frequency and genotype likelihoods, without hard-calling genotypes, an approach that has been shown to be much more robust for low-coverage data (Nielsen *et al.* 2012; Korneliussen *et al.* 2014).

§-164 Analysis of population structure. Summary statistics were calculated in DnaSP (Rozas & Rozas 1999) for mtDNA, and R package *adegenet* (Jombart 2008) and custom scripts for SNP data. Analysis of Molecular variance was performed for both datasets using Arlequin v3.5 (Excoffier *et al.* 2013) (in a locus-by-locus rationale for SNP data, and haplotypic for mtDNA, and 15,000 permutations to assess significance levels). A neighbour-net was built in SplitsTree (Huson & Bryant 2006) either directly from the mtDNA sequences, or from a matrix of pairwise Hamming distances, as calculated in PLINK v1.9 (Purcell *et al.* 2007) from SNP data. Principal component analysis was performed on genome-wide data either using called genotypes in *adegenet*, or raw genotype likelihoods in ngsTools (Fumagalli *et al.* 2014). In order to understand the contribution of individual loci to the overall structure, we performed a discriminant analysis of principal components (Jombart *et al.* 2010), as implemented in *adegenet*. Admixture between populations was estimated using two different approaches. First, we used a classical model-based clustering approach relying on the hypothesis of Hardy-Weinberg equilibrium (HWE) (Pritchard *et al.* 2000), as implemented with an empirical Bayes algorithm either in fastStructure (Raj *et al.* 2014) for called genotypes, or in ngsAdmix (Skotte *et al.* 2013) for raw genotype likelihoods, retaining only sites that did not violate HWE, with a number components ranging from 1 to 4, and 100 bootstrap replicates. Model complexity was chosen using Evanno's ΔK method (Evanno *et al.* 2005). Second, in order to assess the impact of the HWE assumption, we used a model-free approach, as implemented in the *adegenet* k-means clustering (Liu & Zhao 2006).

§-165 Model-based estimation of population history. We relied on two separate coalescent-based approaches to estimate the amount of gene flow between the North and the South of the species

Chilean range. First, population sizes and migration rates were co-estimated based on multilocus haplotype data in a Bayesian framework, as implemented in Migrate-n (Beerli & Palczewski 2010). We selected three sets of 50 random nuclear loci with 4 to 6 polymorphisms, as an unbiased representation of the neutrally evolving part of the genome (Trucchi *et al.* 2014). In order to correct for potential allele dropout, we randomly sampled one haplotype only for each individual, at each locus. We ran a cold chain and 3 heated chain under a static heating scheme, raising the cold chain to a power of 1.5, 3 and 1e6, and proposing chain swapping every 100 steps. Chains were run for 50,000,000 generations, recording every 500 generations, with a 5,000,000-generation burn-in, specifying uniform priors both for population sizes (Θ, bounded between 0 and 0.1 with a δ of 0.01), and for the migration rates (M, bounded at 4,000 with a δ of 400). Proper mixing under these conditions was ensured using the highest parametrisation model, and checking convergence between the three independent random datasets. Models were ordered by log Bayes factors, as defined by Kass and Raftery (Kass & Raftery 1995), u sing thermodynamic integration approximation of marginal likelihoods. Four models were tested: (1) the two islands are fully isolated populations, (2) the two islands are independent population exchanging migrants with symmetric gene flow, (3) the two islands are independent population exchanging migrants with directional gene flow, a nd (4) t he t wo i slands b elong t o a s ingle, panmictic population.

Co-estimation of population size, gene flow, and population history was performed through explicit model testing in fastsimcoal2 (Excoffier *et al.* 2013), through Akaike Information Criterion (AIC) comparison of the optimised composite likelihood of the two-dimensional folded allele frequency spectrum under six different models. We first tested two simple models: (1) a full isolation model with two stable, independent populations, and (2) a classical isolation-with-migration model, with population sizes, migration rates and divergence time as free parameters. We then tested four more complex scenarios (3-6), in which the two population diverge after the last glacial maximum, ca. 7,000 generations ago (a conservative biogeographic estimate for most

taxa). Under model (3), human activities have no impact on the populations, and constant gene flow is maintained between the islands until the present, with no population size changes. Under models (4), population size do not change, but gene flow is disrupted at some point during the past, presumably by the expansion of guano exploitation. Under models (5) and (6), population size changes during the past, and either gene flow remains constant (model 5) or gene flow also changes (model 6). We generated 50 nonparametric spectrum bootstrap replicates, and performed 50 parallel runs for each model and each bootstrap replicate, keeping only the one with the highest composite log-likelihood. Each run necessitated a maximum of 80 ECM cycles, simulating 100,000 spectra at each step.

Models were calibrated using the general background genomic mutation rate for waterbirds, $1.6e^{-3}$ substitutions.site^{-1}.Myr^{-1}, as established from a wide panel of genomic data by Zhang *et al.* (Zhang *et al.* 2014), or $\mu = 9.6\ e^{-9}$ substitutions.site^{-1}.generation^{-1} considering a generation time of 6 years, as suggested by Welch *et al.* 2011. Migrate-n models, however, were based on loci with 4 to 6 polymorphic sites: these can not be calibrated directly using the general background substitution rate. Considering that the RADome is assumed to evolve neutrally, the number of polymorphic sites per locus is expected to follow a Poisson distribution, and the background substitution rate μ applies for the expected value λ of that distribution. Therefore, after verifying the goodness-of-fit of that the Poisson model, we extracted the expected substitution rates for loci with $S=4$, $S=5$ or $S=6$ SNPs, as $(S/(\lambda/\mu))$, and used their weighted average to calibrate our reconstructions.

Acknowledgements

Chapter 8: Discussion

Population structure in colonial seabirds

§-166 Aptenodytes penguins are synnome species. The most consistent and unexpected aspect of our results is the similar, and original structure of the worldwide Emperor and King penguin populations. Both species have circumpolar, zonal distributions, with large and well defined colonies, that are either homogeneously distributed along the coast of Antarctica, for the Emperor penguin, or clustered together on the subantarctic archipelagos, for the King penguin. As exposed in *The King synnome*, p. 163 and *The Emperor synnome*, p. 211, within these circumpolar distributions, each species is made up of one single, range-wide panmictic population, with all evidence consistently and unambiguously converging to that conclusion. Interestingly, however, in both species, principal component analysis does show a hint of sorting by distance. In the Emperor penguin (Fig. 36A), a rough gradient is visible between the colonies of the Adélie Land area and those of the Dronning Maud Land area, that may correspond to an underlying isolation-by-distance pattern. In the King penguin (Fig. 23), although no firm structure can be extracted, individuals from the same archipelago are consistently grouped together - even though groups overlap largely. Yet in both species, the variance explained by the first principal components is extremely low: the first component explains 1.39% of the total variation in the Emperor penguin, and 0.93% in the King penguin - in both cases, this is barely above the expectation for full homogeneity. This observation, instead of supporting the idea of structured metapopulations,

makes a case for the importance of taking the full evidence into account when describing a species' genetic architecture. Restricting the analysis to the sole observations that support some kind of genetic structure could allow us to suggest that an isolation by distance process is at work in both species: however, extensive model-based testing clearly shows that this is not the case.

In the Emperor penguin, the slightly more gradual geographical pattern does retain information as to the intensity and directionality of gene flow between colonies: both haplotype-based and spectrum-based approaches converge on similar estimates. In the King penguin, however, the even higher extent of panmixia obliterates any quantitative information as to the intensity of gene flow: model-based approaches hardly converge, but propose very high and seemingly random values for all migration parameters - an expected behaviour, since full mixing can inform a lower bound, but not an upper bound on gene flow parameters. The slight difference in intensity of genetic mixing between the two species may be interpreted in several ways. First, it may be an artifact of our sampling design: our geographical representation of the King penguin being far more complete than that of the Emperor penguin, it is possible that our view of the latter is overly contrasted by the artificial break in the sampling distribution (between the Adélie Land and the Dronning Maud Land groups), and that sampling intermediate colonies would bring the ensemble closer to a mixed whole. Indeed, the four sampled Ross Sea individuals hint to that direction, as they do not seem to fit in even a slight isolation-by-distance pattern (see Fig. 36A). Alternatively, the contrasting demographic histories of the two species may have played a role in this difference. Whether the Pleistocene bottleneck in the King penguin (see *The King synnome*, p. 163) «reset» a state of full panmixia 20,000 years ago that light drift could not yet disrupt, or rather (a more likely hypothesis in our opinion) the 20th century history of massacres and the subsequent recovery (see §22 p. 75) involved a very recent increase in gene flow for the recolonisation of the most severely affected archipelagos, it seems certain that the King penguin had a more tumultuous history than the Emperor - which could justify even slightly higher genetic mixing. However, we can not insist enough on the fact that, for both species, any kind of struc-

ture signal is far below significance - and that interpreting differences at that level may be perfectly vain.

Nevertheless, field observations and genetic data agree at the local, and the global scales. In the King penguin, equally high return rates have been evidenced at the level of the nest (Barrat 1976; Bried & Jouventin 2001) or the colony (Le Bohec *et al.* 2008; Saraux *et al.* 2011b): yet genetic structure is equally absent at both levels. A simple explanation seems, as we proposed in §71 p. 157, the difference in standpoint when considering return rate from an ecological or a genetic perspective. Indeed, if 90% precise local return will doubtlessly be considered a case of extreme philopatry by any field ecologist, because of the allowance made for mortality at sea, and of the one-sided character of the implicit test, this observation may be reversed as up to 10% of yearly dispersal: a flow that is high enough to obliterate any hint of populations structure. This bias, the « *seabird paradox* » of Milot *et al.* 2008, is in fact only a paradox as long as we do not really examine the bridge between the generation-scale and the evolutionary scale: a phenomenon that seems negligible when considering the lifespan of a few individuals becomes a major process on the evolutionary level. Moreover, the empirical case of the Emperor penguin (see *Empirical evidence of heterogeneous dispersal*, p. 259) provides us with additional indications on how heterogeneity in dispersal probability can be organised in time: the likely splitting of the Mertz colony following changes in the local icescape, and the repercussions on the neighbouring colony of Pointe Géologie, lift the veil on the events of catastrophic dispersal that may punctuate the history of penguin colonies, and maintain genetic mixing even in the case of temporarily reduced gene flow.

§-167 Genetic landscapes in the Southern Ocean. As exposed in introduction (see §19 p. 68), most seabird species exhibit a certain degree of phylogeographic structuring, and species with a worldwide distribution are all the more likely to have marked demes - at least one per ocean basin (Friesen *et al.* 2007). In the Southern Hemisphere, and especially at higher latitudes where inter-basin circulation is high (see §6 p. 33 and §7 p. 35) and biogeographic zones often have a strong

zonal component (see §10 p. 48), most species retain a colonial circumpolar distribution similar to that of the *Aptenodytes* penguins. Yet a marked genetic structure normally evolves, and may result in zonally separated populations that sometimes reach the subspecies level - as in the Giant petrel *Macronectes giganteus*, in which a Northern and a Southern form have been identified (as *giganteus* and *halli*, see Techow *et al.* 2010), or most commonly location-specific populations, as in also the case in the Giant petrel (Techow *et al.* 2010), the Snow petrel *Pagodroma nivea* (Barbraud & Jouventin 1998), or the lesser Sheathbill *Chionis minor* (Viot *et al.* 1993). More remarkable is the evolution of fully separate species along the circumpolar range. This is for example the case of the Wandering Albatross *Diomedea sp.* species complex, in which at least three different clades can be distinguished, each with a full species status - *D. exulans* in Crozet, Kerguelen, Marion & Prince Edward, and South Georgia archipelagos and Macquarie Island, *D. dabbena* on Tristan da Cunha, and *D. antipodensis* on Antipodes, Adams and Campbell islands (Burg & Croxall 2004): a structure that is made more surprising by the fact that Wandering albatross easily circumnavigate the Southern Ocean during one foraging season (Croxall *et al.* 2005). The Southern Skua *Catharacta sp.* species complex offers a similar picture, with both zonal and regional differentiation between species (*C. maccormicki* in Antarctica, *C. antarctica lonnbergi* in the subantarctic belt, *C. a. antarctica* in the Falklands and the Patagonian shelf area, *C. a. hamiltoni* in Gough and Tristan da Cunha, and *C. chilensis* in Tierra del Fuego and Patagonia), despite ocean-wide seasonal migration (Weimerskirch *et al.* 2015), and ongoing gene flow at the contact zones of species (Ritz *et al.* 2008). The Diving-petrel *Pelecanoides sp.* species complex, with *P. urinatrix* and *P. georgicus* breeding in sympatry throughout the subantarctic belt, *P. magellani* in Tierra del Fuego, and *P. garnotii* along the Humboldt Current (Shirihai & Kirwan 2008; Onley & Scofield 2013), also offers a clear example of local isolation both through distance, and through foraging niche specialisation (Navarro *et al.* 2013). The Common diving petrel *P. urinatrix* is itself separated in six subspecies that follow geographical areas (*P. u. urinatrix* in Australia and Northern New Zealand, *P. u. chathamensis* in the southern New Zealand archipelagos, *P. u.*

exsul in South Georgia and the Southern Indian and Pacific archipelagos, *P. u. dacunhae* in Tristan da Cunha and Gough, *P. u. berard* in the Falklands, and *P. u. coppingeri* in Southern Chile, see Onley & Scofield 2013). In the present study on the Peruvian diving-petrel *P. garnotii* (see *Unexpected philopatry in an insular seabird, the Peruvian diving-petrel*, p. 275), we demonstrate how this oceanic-scale structure in diving-petrels is likely the consequence of very strong local philopatry: even at the scale of a few hundred kilometers, populations may evolve near-complete isolation. In *Pelecanoides* petrels, genetic structure therefore appears to organise itself in a complex hierarchical system, with very closely related and partly sympatric species subdivided in subspecies (as in *P. urinatrix ssp.*), and locally in strongly differentiated demes.

Penguins are no exception here, and phylogeographic structure has been identified in several species across oceanic boundaries, often reaching subspecies or even speciation levels. The Little penguin *Eudyptula minor*, for example, exhibits strong isolation between populations, and has been divided six subspecies (Kinsky & Falla 1976), at least three of which are genetically monophyletic (Peucker *et al.* 2009), and exhibit local isolation-by-distance patterns (Burridge *et al.* 2015). The Rockhopper penguin *Eudyptes chrysocome* has similarly been separated in a Northern and a Southern group by De Dinechin *et al.* 2008, and the same applies for the Gentoo penguin *Pygoscelis papua* (De Dinechin *et al.* 2012). Finally, two groups have been proposed in the Adélie penguin, in the Ross Sea and in the rest of East Antarctica (Roeder *et al.* 2001). In the *Spheniscus sp.* group, the geographically isolated *S. demersus* in southern Africa, *S. magellanicus* in Tierra del Fuego and Patagonia, and *S. humboldti* in the northern Humboldt Current are identified as fully separate species with traces of ongoing gene flow between the latter two species at their contact point (Simeone *et al.* 2009). Similarly, the *Eudyptes* species complex may be considered as mostly structured by allopatry between breeding islands, as species have very well defined, and usually non-overlapping breeding range, with *E. pachyrhynchus* along the Fiorland coast of New Zealand, *E. robustus* on the Snares islands, *E. sclateri* on Bounty and Antipodes islands, the extinct *E. chathamensis* on Chatham island, *E. schlegeli* on Macquarie island, *E. chrysolophus* in the Southern

Atlantic Ocean and Crozet archipelago, *E. chrysocome chrysocome* around the Patagonian shelf area, *E. c. moseleyi* on Gough, Inaccessible, Tristan da Cunha, Saint-Paul and Amsterdam islands, and *E. c. filholi* on Marion & Prince Edward, Crozet, Kerguelen, Heard, Macquarie and the Campbell Plateau area (Williams 1995; Borboroglu & Boersma 2013).

Considering this general picture, it appears that Southern Ocean seabirds (penguins included) have a marked geographic structure of genetic diversity, where the intensity of gene flow will determine the level of structure. Higher gene flow keeps groups on a purely intraspecific phylogeographic level (as in *Eudyptula minor*), while a decreasing level of admixture gradually leads to subspecies systems (as in the *Eudyptes chrysocome ssp.* or the *Pelecanoides urinatrix ssp.* complexes) and full species systems (as in the *Diomedea sp.* or the *Spheniscus sp.* complexes). As suggested in our introduction (see §6 p. 33), the balance between philopatry, dispersal, and at larger scale incipient local adaptations, appears to vary along a gradient of increasingly strongly structured biogeographies. The continuous nature of this gradient, however, does raise the question of the significance of observed structures. While full speciation may be rather easy to observe when morphological, behavioural, and genetic cues converge, the lower reaches of phylogeographic structure are more unclear (Waples 1998; Waples & Gaggiotti 2006), especially as genetic and ecological separation entertain a rather blurred relationship in the lower differentiation areas (Esler *et al.* 2006; Waples & Gaggiotti 2006). In those lower ranges, it may sometimes appear that very subjective factors - such as publication pressure - influence the interpretation of observed structures. Publication bias is a recognised confounding factor in several domains, including genetics (Munafò *et al.* 2004; Pan *et al.* 2005), and usually takes the form of a bias towards reporting significant results over nonsignificant ones - or, more often, of reporting barely significant results as indicative of a strong process. In the particular field of phylogeography and ecological population genetics, it also often leads to the overinterpretation of barely significant results,

where otherwise insignificant signal is presented as having a tendency towards significance[1]. In seabirds, we may mention the study of Bouzat *et al.* 2009, in which colonies of Magellanic penguin (*S. magellanicus*) amongst which 99% of variation was explained by inter-individual differences, with Fst levels below 0.01, are presented as « metapopulation system »; or the study of Freer *et al.* 2015, in which non-significant Fst values are presented as « *consistent with female bias dispersal* ». In these cases, the lack of a strong conceptual and hypothesis-testing framework often results in misleading interpretations. The probability of observing similar values because of random sampling variation is rarely examined, and a selection of statistically significant indicators over statistically nonsignificant ones is common. All of these choices often result in overly constrated population structures - often easier to publish, but at the cost of loosing the more nuanced aspects of the interspecific variations in demographic organisations.

In §137 p. 253, we discussed such a case, in a previous analysis of population structure in the Emperor penguin, using mtDNA, by Younger *et al.* 2015, where a combination of biased sampling and not fully reproductible analysis led to the conclusion that Emperor penguins were separated in two different clades. Similarly, a pioneer study by Viot *et al.* 1993, using protein gel electrophoresis and a short fragment of the cytochrome-b gene[2], concluded in a strong isolation between Crozet and Kerguelen king penguins. Thus, prior findings using « classical » (*sensu* §28 p. 84) markers set the expectation of significant population structure in both species, on the tem-

---

1.   This often comes down to a subjective decision as to the *side* from which results will be presented. For example, even if significant, an Fst value or 0.01 is strongly indicative of a high gene flow: but it is more often cited as « significant evidence for separation ». This statement is not wrong in itself, since any given state of population connectivity is a balance between some degree of isolation, and some degree of mixing: but it is misleading, as it focusses on the minor isolation instead of the more meaningful high migration process.

2.   As we discussed in §156 p. 286, the characteristics of « classical » mitochondrial markers also makes them likely to overestimate population structure, due to their halved effective population size, and consequently shallower coalescence time, compared to nuclear data. If this distinction is not kept in mind, mtDNA results can yield largely overestimated population structure.

plate of other penguins, or seabirds in general[1]. Our results (see §166 p. 297) bring clear evidence against both mtDNA-based studies.

§-168 Synnomes and speciation. Amongst all Southern Ocean seabirds for which genetic data has been published, the two *Aptenodytes* species are thus, for the time being, the only two for which no relevant population structure could be identified. In terms of biogeography, with their full circumpolar distribution (Fig. 7), each of the *Aptenodytes* species should be more appropriately compared to the full *Diomedea* species complex: in the latter, the small population sizes and high philopatry of Wandering albatrosses has lead to full speciation between oceanic areas, whereas both large penguin species have maintained a high connectivity and full homogeneity at the same geographical scale. Indeed, preliminary analyses even emphasize the relatively low degree of divergence between the King and the Emperor penguin: inter-individual intraspecific variance may be almost of the same order of magnitude as interspecific variance, and shared polymorphism is important compared to fixed differences. Although the question of speciation and possibly incomplete lineage sorting between *A. forsteri* and *A. patagonicus* will require further investigation, based amongst other things on whole-genome resequencing data[2], the present study support the view of Gavryushkina *et al.* 2015, who place the divergence of the two *Aptenodytes* lineages in the relatively recent past (1.52 million years ago, but possibly as recently as 730,000 years ago), at a slightly more recent period than the divergence of the still-hybridising *Spheniscus magellanicus* and *S. humboldti*. The question of the extent of prezygotic isolation between the two *Aptenodytes*

---

1. As a side note, the example of the evolution of laboratory and analysis methods over the past two decades should act as a twofold caution for present studies. First, conclusions drawn from less reliable material, or analysed using less robust approaches, should not systematically be taken for granted: re-analysis using more advanced methods may yield very different results. Second, it should also serve as a reminder to the fact that contemporary approaches may also become outdated soon enough, and that our conclusions only hold until then. We mentioned earlier how theoretical frameworks like the ARG are yet in their early development, both from a conceptual point of view, and from sheer technical limitations (*e.g.* the lack of an accurate and very-high-throughput sequencing platform, or the limits of contemporary computational power). It may well happen that further methodological and technical developments will lead us to reconsider our results - a somewhat tiresome, but absolutely unavoidable possibility.

2. Which we already produced, but still remains to be analysed, see §30 p. 86.

species if ever their ranges were to overlap, in particular, is currently unresolved, and will be of particular interest for understanding the future of those species if ever climate change and subsequent range contraction brought them into close contact again.

The *synnome* structure of the two *Aptenodytes* species also raises questions as to the mechanisms involved in their recent speciation. Indeed, reduced gene flow and local adaptation under allopatry is often invoked in the case of sister species currently occurring in allopatry, as is the case of the King and Emperor penguins. However, the *synnome* structure that appears to be plesiomorphic in large penguins makes allopatric speciation a rather counter-intuitive event. A strong disruption of this structure may have been necessary at the time of speciation: either through colonisation of hew habitats on the Antarctic continent, or through a sudden interruption of a previously much borader range (for example through changes in the structure of the Southern Ocean water masses, although no such event has been documented yet in the stratigraphic record).

Seabirds on the evolutionary scale.

§-169 Inferring demography in synnome species. The synnome structure of both species offers a considerable advantage for reconstructing the demographic history of *Aptenodytes* penguins. Indeed, population structure is a major determinant of genetic diversity: with a constant combined census population size, fragmented populations undergo considerably more genetic drift than one single panmictic population (see §39 p. 99), with an increased loss of rare alleles and a bias towards intermediate allele frequencies in the full sample as a result. Thus, the subdivision of a large population in two subpopulations, with low gene flow, even with no loss of individuals, has essentially the same effect as a reduction in the total effective population size (Chikhi *et al.* 2010). This is an important *caveat* for the inference of population history, since population size and metapopulation dynamics are by no means independent parameters. Migration, for one, is often

a density-dependent parameter: a common prediction is that migration increases with density, *i.e.* usually with population size (Sæther *et al.* 1999; Taylor & Norris 2007). Range reduction, on the other hand, often results in habitat fragmentation, and consequently in population divergence through reduced gene flow (Hanski 1998; Hanski & Ovaskainen 2000; Keller & Largiader 2003), but also in total population decrease (see *The King synnome*, p. 163) and associated loss of genetic diversity (Arenas *et al.* 2012). Thus, there is an intricate connexion between census population size change, population fragmentation, gene flow, and effective population size change, and external (*e.g.* climatic) forcings are likely to influence all these parameters jointly. A typical example of this difficulty is the European refugial structure that is often proposed for the Last Glacial Maximum (Schmitt 2007). The Pleistocene continental ice sheet is thought to have forced most species into fully isolated coastal refugia: concurrently, several studies have inferred drastic population reductions during that period (*e.g.* in the Wild boar, see Groenen *et al.* 2012 or in the Brown bear, see Miller *et al.* 2012) - however, disentangling the respective roles of census size reduction, and population fragmentation in refugial areas, in the observed effective population size reduction, remains quite a challenge.

Although several studies have proposed, as a workaround, to start by establishing the genetic structure of the extant populations, and then reconstruct the demographic history of each population separately (see *e.g.* the remarkable work of Wallberg *et al.* 2014 on the honey bee *Apis mellifera*), this is only possible when population structure has a clear-cut phylogeographic component, that is to say, when populations have diverged in a tree-like manner, and remained isolated ever since, and that divergence happened much before the demographic events of interest, so that isolation and demographic processes do not interfere in shaping genetic diversity. A more realistic case is that the degree of isolation between populations is fluctuating together with population size and species density during the history of the population, and that the present-day population structure, if ever it exists, does not fully reflect the past population structure - as groups that have come in secondary contact may have totally re-shuffled in the meantime. Thus, suspicion of past

population structure may be an important hindrance to successful inference of past demography solely from contemporary genetic data uninformed by, for example, paleontological or ancient DNA data.

The *Aptenodytes* breeding system and genetic organisation is particularly favorable to past population size inference. The present-day *synnome* structure appears to be rooted in behavioural characteristics of the species (such as high dispersal ability) rather than being solely the result of recent population history (see §167 p. 299): so that there is no compelling grounds to suspect that population fragmentation was ever an important trait in the past. However, we should be cautious about the interpretation of strong population reduction events, such as the one observed during the Last Glacial Maximum in the King penguin (see *The King synnome*, p. 163). What we really reconstruct, in this study, is a reduction in *effective* population size, likely brought about by range contraction and refugial fragmentation of the species. This explicitly involves a form of population subdivision, and likely an associated reduction - even minor - in gene flow between refugial areas. Thus, translating the observed reduction in *effective population size*, as a reduction in *census population size* is not as straightforward as it would seem, even considering that the life history of the species remained fully unchanged during the period. On the contrary, the observed restructuration of genetic diversity during the Pleistocene is the joint consequence of all the forces we mentioned earlier. Yet, our observed baseline (the present-day state of the species) allows us to go further. With an effective population size of ~20,000 to 25,000 breeders, density is currently such that gene flow precludes any population structure. Situation is likely to have been similar prior to the LGM bottleneck, when inferred effective population size was strong. Thus, the state change during the LGM gives us at least one crucial qualitative information: disruption of the King penguin's habitat was strong enough to provoque a combination of population fragmentation and decline.

In contrast with the *Aptenodytes* synnomes, the very strong population structure that we observe in a strongly philopatric seabird such as the Peruvian diving-petrel (see *Unexpected philopatry in an insular seabird, the Peruvian diving-petrel*, p. 275) makes any attempt at inferring past demography rather risky. Indeed, present-day isolation patterns are a convincing testimony to the behavioural capacity of the species to evolve strongly isolated structures: but it does not imply that these structures have remained the same during the whole history of the species. Thus, even if we restricted ourselves to one single present-day colony, that did not bear any signs of internal fragmentation, we would not be able to ascertain whether that population was, at any time in the past, split into several units and later recast into its present shape. It is possible that further methodological developments will alleviate that important limitation: it has been argued that the full ancestral recombination graph (see §42 p. 107) should contain enough information to reconstruct not only past population size, but also past population structure and admixture patterns. An attempt has been made in that direction by Schiffels & Durbin 2014, although still within the Sequential Markovian Coalescent framework - that is to say, still without taking the topology of recombination events into account, which effectively limits reconstructions to tree-like divergence patterns. We suggest that integrating the local recombination topology may be more informative as to past admixture events, since the probability of two given haplotypes merging through recombination at any point of time is conditional on their probability of co-occurring in a given deme. However, this would imply stepping out of the SMC framework, and would probably require considerable computation effort (Song & Hein 2005; Rasmussen *et al.* 2014). Alternatively, within the multiple-SMC framework, reconstructing ancestral states at each node of each inferred independent local tree, and performing admixture analysis (*e.g.* through K-means clustering, see Jombart *et al.* 2010) for each reconstructed state at ancestral points of time may give us an insight into the evolution of admixture complexity in along the past history of the species. However, this is a broad endeavour, an far beyond the scope of our study. In the meantime, the wisest course would appear to be *(i)* to safely apply demographic reconstruction meth-

ods only to essentially panmictic species such as the *Aptenodytes* penguins, and *(ii)* when dealing with structured populations such as can be found in *Pelecanoides* species, to either avoid such approaches altogether, or to restrict the analysis to a single population and to stay aware of the considerable uncertainty that propensity to genetic isolation imposes on the results.

§-170 Pleistocene history of the Aptenodytes penguins. The various methods we applied in this work to reconstruct the demographic history of the King and Emperor penguin (in *The King synnome*, p. 163 and *The Emperor synnome*, p. 211) showed a satisfactory degree of consistency, (although all did not perform as accurately for the more complex history of the King penguin, see §98 p. 192): we can thus obtain a general picture of the recent past of the two species with relative confidence.

According to our reconstruction, the Emperor penguin population did not vary significantly during the past 100,000 years - a trait found consistently by three independent methods, and based on data either from the whole Antarctic continent, or from six individual colonies. The more accurate EBSP and Stairway Plot approaches (see §44 p. 112 and §46 p. 121) also suggest a population growth before 100,000 years, and back to 1,000,000 years according to the EBSP - however, these are deep times by the yard of penguin evolution, and at these scales demographic and speciation processes may start to interfere. This confidently stable population during the later Pleistocene contrasts with the findings of Younger *et al.* 2015: however, as we suggested in §137 p. 253, the steep population growth inferred from mtDNA data by Younger and colleagues rather seems to stem from inadequate analysis. Indeed, the use of unexplained diploid sites in haploid mitochondrial DNA (likely sequencing errors caused by secondary structures in the Emperor penguin control region) is expected to artificially increase recent population size by overestimating the importance of low frequency variants. Other improper choices, such as treating mitochondrial cytochrome-b gene and mitochondrial HVR as unlinked, independent markers in an EBSP framework (instead of concatenating them and remaining within the frame of a simple sin-

gle-locus Bayesian Skyline Plot), are likely to have biased this reconstruction: thus, they do not contradict our findings convincingly. This stable effective population size also implies that metapopulation structure was never prevalent in the species (see §169 p. 305, and let aside a very unlikely hypothesis of balanced compensation between census size and gene flow) - not even during the Last Glacial Maximum, when extensive winter sea ice cover and Antarctic ice sheet expansion could have been thought to have disrupted the Emperor's breeding cycle. Interestingly, the persistence of the Emperor penguin population throughout the period seems to imply that the conditions on the major part of the Antarctic shoreline were not significantly out of the species' optimum - *i.e.* somewhere between the harsh conditions now found at the high latitudes of the Ross Sea, and the milder ones that prevail at the lower latitudes of Wilkes Land in Eastern Antarctica. Importantly, the stability of the Emperor penguin population means that coastal polynya activity was comparable to what we observe nowadays (see §18 p. 65) despite very different global sea ice conditions (see §9 p. 42) - a hypothesis confirmed by our preliminary analysis of ice conditions in the coastal Antarctic area (see §116 p. 223 to §122 p. 235). It also confirms the hypothesis of Wolff *et al.* 2006 who, based on iron flux reconstructed from the EPICA ice core (Augustin *et al.* 2004), suggested that marine productivity did not change significantly during the last Pleistocene glacial cycles: indeed, the robustness of the Emperor penguin population implies that food resource was never a limiting factor for the species, even during the coldest times of the last era.

The King penguin offers a very different picture (detailed in *The King synnome*, p. 163). Allowance made for the possibly complex interplay of population decline and range fragmentation (see above, §169 p. 305), the King penguin differs from the Emperor by its drastic demographic response to the Last Glacial Maximum, and likely also to the previous Llanquihue glacial maximum - beyond which coalescence signal is lost in our sample, and possibly in the whole extant gene pool of the species. A previous study by Trucchi *et al.* 2014 had proposed a strong postglacial expansion of the species based on RAD data for 8 individuals, with strong support based

both on EBSP, and a diffusion-approximation based spectrum approach (see §45 p. 117): but that first study could not retrieve any signal past the LGM low-population-size period, an unsurprising consequence of the low sample size. The novel and more accurate method established by Liu & Fu 2015, that we deploy in *The King synnome*, p. 163, fully confirms that finding - but significantly changes its interpretation by making the post-glacial population expansion event a recovery rather than a *de novo* colonisation. The oscillating population size that we reconstruct in the King penguin offers a striking contrast with the Emperor penguin: as we demonstrate, the periods of strong population reduction are caused by a drastic reduction in available habitat under LGM conditions. The difference between the essentially fluid habitat of the Emperor penguin, that may follow the sea ice, and the semi-rigid habitat of the King penguin, that can only breeds on the available islands, but, just as the Emperor, is also sensitive to changes in the oceanic and atmospheric spheres, appears as an important evolutionary divergence - which gave a clear advantage to the most extreme adaptation, against the more generalist one, during the whole Pleistocene.

Interestingly, all our demographic reconstructions suggest that the Emperor penguin was the most abundant *Aptenodytes* penguin species during the late Pleistocene, but was replaced by the King penguin during the early Holocene. The early Holocene climatic optimum is one of the periodic interglacials that punctuate the Pleistocene (Wolff *et al.* 2006 - or at least it resembles them in every respect, but anthropogenic climate change might decide otherwise), and our demographic reconstructions suggest that the King penguin's breeding system and physiology evolved to provide highest fitness under these conditions, at the cost of much diminished populations during the regular glacial maximums. The specialisation in a relatively unstable niche (at the milenial scale) thus forces the King penguin into cycles of growth and decline, while the paradoxically more stable (because less firmly anchored in the midst of its unstable surroundings) niche of the Emperor allowed it to go through the Pleistocene unhindered. However, current projections seem to indicate that the Holocene-optimum conditions indeed provide the fitness optimum for the

King penguin, and that further increase in temperature beyond these conditions is equally likely to bring about population decline. Indeed, the replacement of the Emperor penguin by the King penguin as the dominant *Aptenodytes* biomass during the early Holocene implies that the latter is already the «warm adapted» species of the clade - and its glory days may well be behind it.

Seabird response to Anthropocene environmental change.

§-171 Seabird response to climate change. Evidence is accumulating for a negative response of penguins in general, and *Aptenodytes* penguins in particular, to ongoing climate change (Ainley *et al.* 2010a). Recent studies on the Emperor penguin (Barbraud & Weimerskirch 2001a; Jenouvrier *et al.* 2009; Jenouvrier *et al.* 2012; Jenouvrier *et al.* 2014), the King penguin (Le Bohec *et al.* 2008; Péron *et al.* 2012), or the Adélie penguin (Jenouvrier *et al.* 2006) have emphasised the vulnerability of these species to climate warming. Our results on the King penguin (see *The King synnome*, p. 163) clearly support this view. However, the two penguin species examined in this work are predicted to respond to climate change for very different reasons, and based on very different mechanisms - and both are subject to considerable uncertainties. The gaps in our knowledge of the Emperor penguin are maybe the most clearly visible. All of the data used in recent projections come from the single Pointe Géologie colony (see *The Emperor synnome*, p. 211), that has undergone tremendous disturbance in the recent past (see §24 p. 79 for an overview), so that the part of climatic, and direct influences in its demography are very blurred to say the least. Adding to these uncertainties are the basic assumptions of climate envelope modelling approach (Pearson & Dawson 2003), which are correlative, and may or may not reflect true causal processes (see §49 p. 127) - and do not integrate the possibility of (lagged) plastic adaptation. Finally, in the study of Jenouvrier *et al.* 2014, sea ice emerged as the main forcing on the Emperor's demography: however, the representation of sea ice in the CMIP3 and CMIP5 ensemble models is still inaccurate, and show trends that are contrary to the observations over the historical periods (Turner *et al.* 2013; Shu *et al.* 2015). Combined, these three layers of uncertainty (in the reliability of flip-

per-banded, disturbed birds, in the robustness of the correlative envelope approach, and in the accuracy of the CMIP sea ice projections) amount to a considerable lack of knowledge, that leaves room for about any hypothesis.

The King penguin's response seems, at first glance, to be more robust. The negative correlation between sea-surface temperature and adult survival and breeding success is well established (Le Bohec *et al.* 2008), and its causal mechanism is equally well understood: the warmer the sea surface temperature, the further South the Antarctic Polar Front and associated foraging areas, and the longer the foraging trips for the Northern King penguin colonies (see Péron *et al.* 2012, Bost *et al.* 2015, and *The King synnome*, p. 163) - a mechanism observed directly using GPS loggers placed on penguins. However, a possibly important flaw in this model is the fact that until now, the main driver of sea surface temperature variation is not directly anthropogenic climate change[1], but the natural oscillations of the Southern Hemisphere Ocean-Atmosphere circulation, such as the Southern Annular Mode, the El Niño Southern Oscillation or the Southern Indian Ocean Dipole (see §8 p. 40 for a summary of these phenomena). The changes in temperature associated with these oscillations can reasonably be taken as proxies for global change (although this is, in itself, subject to some uncertainties, see §11 p. 50). But approximating the response of seabirds to global long-term change by their response short-term oscillations is another matter. Indeed, oscillating phenomena such as the ENSO force the alternance of «warm» and «cold» periods over 3 to 6 years cycles: while breeding success is very low during the warm years, it may be partly compensated during the cold years. Considering that the most exposed populations (on Crozet archipelago, see *The King synnome*, p. 163) are still stable demographically (Delord *et al.* 2004; Saraux *et al.* 2011a), it is possible that the cyclic character of the changes makes even plastic adaptation un-necessary for the time being: put simply, «waiting for better times» can still be

---

1. While anthropogenic climate change clearly has an influence on Southern Ocean sea surface temperature, as we showed for example in **The King synnome**, p. 163, it mostly affect the *mean* temperature, and its underlying trend. But interanual variability is still central in local processes, and is of the same, or of a larger order than man-made trends.

a beneficial strategy for a bird like the King penguin. Whether this strategy will still hold under long-term irreversible changes, is another question. Several alternative strategies will still be possible: altogether not trying to breed during the warmer phases of ENSO (as has been reported in the Galapagos islands, see Duffy & Siegfried 1987) and building up reserves for increased breeding success during the more favorable years, developing nearshore foraging strategies, etc. Whether King penguins will react differently to linear changes than to cyclic changes is of course speculative, but it does add to the uncertainty of predicted demographic trajectories. If the actual timing and extent of climate change effects is far from certain, the reality of these effects is, at any rate, beyond doubt. Indeed, Pleistocene changes in King penguin population are qualitatively consistent with the expectations set by oscillative climate change *The King synnome*, p. 163: in our case, long term data validates hypotheses set by very short-term data, both converging to emphasise the importance of climate change in shaping the future of penguin.

§-172 Seabird response to environmental change. Despite the overwhelming evidence for a deep impact of climate change on biological communities (and that our work clearly supports), reducing the current threats to the sole effects of climate change is misleading. In a recent study, Trivelpiece *et al.* 2011 demonstrated how direct anthropogenic effects, such as the hunt of cetaceans to near-extinction, or the present-day overexploitation of krill stocks (*e.g.* for farmed-fish food), had a considerable effect on Chinstrap penguin *Pygoscelis antarctica* breeding success and recruitment, that outweighed the impacts of climate change. Generally, overfishing has been identified as the major cause of decline in seabird populations, far before the change in climate (Cury *et al.* 2011). This observation may, in a sense, be an optimistic one, as recovery from overfishing may happen faster and more fully than recovery from greenhouse-gas induced global warming (which may not happen at all on a human time scale).

In that respect too, the Peruvian diving-petrel is an extreme case. For that species, several well identified direct factors have contributed to reducing large populations to vestigial colonies in a

matter of decades: in the current state of knowledge, direct habitat destruction, predator and competitor introduction, overfishing, and hunting (see §149 p. 279) are responsible for the drastic population decline more than any effect of climate change, *e.g.* the intensification of the El Niño dipole oscillation. This again is a rather hopeful situation: indeed, since the threats are mostly local, local conservation measures such as land and marine habitat sanctuarisation and reintroduction may still save the species and help it recover. Comparing the King penguin and the Peruvian diving petrel gives a clear picture of the spectrum of threats weighing on seabirds in the anthropocene: one century ago, the main threat on both species was direct destruction by humans (see §22 p. 75 and §149 p. 279). Full protection granted to the King penguin allowed it to recover almost entirely, while insufficient or failing protection maintains the Peruvian diving-petrel populations at a critical level. Yet currently, because of the species' deep connexion to global circulation mechanisms (§18 p. 65), climate change has become the main threat to the King penguin - while climate effects are dwarfed, in the diving-petrel, by the comparatively overwhelming direct human impact.

Further work on the penguin synnomes.

§-173 A final examination of penguin population structures. Our studies explored most of the geographical range of both the Emperor and the King penguin, and concluded in the remarkable level of mixing in these two *synnomes* (§167 p. 299). However, the findings of Younger *et al.* 2015, if they lack robustness for methodological reasons (see §137 p. 253), invite us to explore further possible (yet unlikely) reduced-gene-flow areas in the Emperor penguin, *e.g.* in the Ross Sea, Marie Byrd and Ellsworth lands, or the Antarctic peninsula. Similarly, two areas were not fully covered by our study of the King penguin (Macquarie Island only through mtDNA, and Tierra del Fuego not at all). Interestingly, Tierra del Fuego is a newly founded colony (Kusch & Marín 2012), and could give us fascinating insights into the genetic aspects of colony foundation

(in particular the respective roles of intrinsic growth and immigration)[1]. Finally, the precise question of the subspecific taxonomy in the King penguin (see §25 p. 80), although we consider it as good as settled here, may require explicit testing, including morphometric measurements to match the observations of Barrat 1976.

In the Peruvian diving-petrel, on the other hand, additional sampling[2] will likely improve greatly our understanding of ongoing population processes. Our Chilean sampling shows that isolation is a major population process in this species, but an additional «outgroup» sample, distant from out sampling by ~1,500 km, should allow us to set bounds on the migratory flow, and to understand wether it is mainly driven by geographical distance (in which case we should observe a clear phylogeographic structure, driven by islotion-by-distance gradients), or by more complex mechanisms.

§-174 Extending palæodemographic reconstructions. Our final reconstructions for population size changes in the King and the Emperor penguin use a currently state-of-the-art method (Liu & Fu 2015), and are a large improvement over previous studies (Trucchi *et al.* 2014). However, coalescent-based reconstructions are inherently limited by the very structure of genetic diversity: once all examined sequences have found a single common ancestor, no further information can be retrieved. This is expected to happen, in a stable population, around $4.N_e$ generations back in the past (which, in *Aptenodytes* penguins, would be as considerable as 1 million years) - but much sooner if demographic events, such as bottlenecks, temporarily increase the probability of coalescence at given points of time. This phenomenon is easily visible when contrasting the King and the Emperor penguins (Fig. 19): although population sizes and generation times are comparable,

---

1. Sampling has been done in Tierra del Fuego, in Chile, with the collaboration of Dr Juliana Vianna, but will not be processed and integrated in the present work.
2. Sampling is currently underway in Isla San Gallán, in Peru, with the collaboration of Dr Carlos Zavalaga, but will not be finished in time to be processed and integrated in the present work.

the Emperor penguin population size can be reconstructed further back in time due to the absence of intermediate bottlenecks.

In order to retrieve evidence about more ancient times, two lines of action are possible. First, we may try to enlarge the sample size, in the hope that the increased diversity may retain information as to more ancient ancestors. However, past a modest sample size (as low as ~16 individuals), the full coalescent should already be reasonably well described, and increasing sample size is not expected to help much (Felsenstein 2006; Hoban *et al.* 2013a; Hoban *et al.* 2013b). Second, we may directly try to shift the time limit by integrating ancient samples in our reconstructions. In a «pure» coalescent framework, like the EBSP (see §44 p. 112), this may take the form of serial sampling (*i.e.* individuals from different points of time can be integrated in a single time-tree) in order to use the full evidence jointly. In a derived framework like the Stairway plot approach (see §46 p. 121), however, serial sampling is not directly possible, since the model is fitted to a time-flat object, the allele frequency spectrum (see §45 p. 117). Extending this method to serial sampling would require *(i)* that several ancient, but mutually contemporaneous samples are available, in order to establish a «palæospectrum». This is a rather drastic restriction imposed on the experimental design, and would only be possible in rather specific cases (*e.g.* the ice-core sampling of penguin moult feathers and remains, as performed by Emslie *et al.* 2007 for isotopic niche studies), and *(ii)* to have some knowledge about the relationship between the sampled palæo-population, and the modern population (see *e.g.* Heupink *et al.* 2012). If these two conditions can be met, further implementation could involve *(i)* a simple model in which independent reconstructions would be performed for modern and ancient samples, using the current algorithms, *(ii)* preferably, an integrated reconstruction, in which population size at each point of time would be chosen in order to maximise the likelihood of SNP classes in both spectra simultaneously (thus assuming that the modern population is the direct descendant of the ancestral one), or *(iii)* more

accurately still, by estimating the joint allele-frequency spectrum of the two *chronodemes*[1], and modelling allele inheritance as well as other demographic processes as unidirectional diffusion parameters (from the more ancient chronodeme to most recent one). In a Stairway plot framework, this would considerably widen the parameter space (since the number of SNP classes become the product, and not the sum, of the dimensions of the two spectra), but there is no obvious impossibility there.

Technically, this would also probably require shifting to a whole-genome resequencing, rather than RAD-sequencing, approach, as enzymatic digestion is notoriously unpredictable in ancient DNA. But King penguin DNA, for example, has been successfully extracted for samples as ancient as 8,000 years old conserved in peat (Heupink *et al.* 2012), so that there is hope to retrieve information prior to the most ancient of our reconstructed bottlenecks, and most importantly to verify whether the oscillating population size pattern may be extended to the whole Pleistocene period.

§-175 From neutral to adaptive genomics. RAD sequencing, since its original formulation in 2007 (Miller *et al.* 2007; Baird *et al.* 2008; Davey *et al.* 2011), has been successfully used in a wide range of genomic applications. These have focused, as we did in this work, on the informative content of neutrally evolving regions, in particular in the fields of phylogenetics (Cariou *et al.* 2013; Cruaud *et al.* 2014), phylogeography (Emerson *et al.* 2010), palæodemography (Trucchi *et al.* 2014), and generally population genetics (Davey & Blaxter 2010) - but also on speciation analysis (Gagnaire *et al.* 2013b), and on more resolutely functional aspects of genome evolution, such as quantitative trait locus analysis and association mapping (Hohenlohe *et al.* 2010; Gagnaire *et al.* 2013a), genetic maps (Amores *et al.* 2011; Amores *et al.* 2014), quantitative genomics (McGuigan *et al.* 2010). In a preliminary study, Trucchi *et al.* 2014 proposed an extension of the

---

1.   We propose this neologism to describe the extension in time of the *deme* idea, on the model of the *chronospecies* concept.

RADseq analysis paradigm to take advantage of its short-haplotype structure in a coalescent framework (§29 p. 85 and §31 p. 87), using a subset of highly variable loci for EBSP reconstruction of past population size changes. In this work, we developed this idea further, and applied it to population size and migration reconstruction, concurrently with SNP-based analyses. Based on our results (see *e.g.* the demographic reconstructions in *The King synnome*, p. 163), RAD-sequencing offers clear advantages over whole-genome resequencing: data can be gathered for a much larger number of individuals for a similar sequencing effort, and the accuracy of demographic reconstructions is increased using this wide dataset.

However, we did encounter a number of methodological limitations. Besides the random biases that do occasionally appear during library preparation (see §35 p. 93), the main *caveat* of RADseq is its discontinuous character (§31 p. 87): the unsequenced gaps between markers make it difficult to identify continuous structural processes in the genome. Thus, while focusing on neutral processes, we left aside functional phenomena - in particular the signature of local selection (that may be detected through clues like selective sweeps - see Nielsen *et al.* 2005, or long runs of homozygosity - see Kirin *et al.* 2010), or properly genomic processes such as the evolution of recombination hotspots (Smagulova *et al.* 2011) or replication origins (Lucas *et al.* 2007). However, now that a strong neutral framework has been established for both *Aptenodytes* species, further understanding may be gained from the functional and adaptive aspects of their genome. In particular, understanding whether speciation was the result of allopatric isolation and neutral drift (see §168 p. 304), or rather of a strong and sudden local selection pressure, may give us insights into the forces that shaped the Southern Ocean biodiversity during the Pliocene and the Pleistocene. For these processes, whole-genome resequencing is likely to offer a framework for the more precise interpretation of RAD data, *e.g.* by allowing us to locate RAD markers in relation to genome landmarks. Further investigation methods, such as bisulfite-conversion (Deng *e t al.* 2009), possibly in a RADseq framework (Trucchi *et al. in prep.*) can offer insights into epigenetic phenomena (*e.g.* methylated cytosine residues). RNAseq (*e.g.* Mortazavi *et al.* 2008) may allow us

to go further, by identifying very short-term local plastic responses though modulation of gene expression levels and patterns, for example during development.

Yet the plethora of new techniques in the field of genome analysis should not divert us from the real originality of the *Aptenodytes* model. The wealth of life-history data made accessible by the advanced monitoring program on Possession Island (see §26 p. 81 and Gendner *et al.* 2005; Le Bohec 2008) offers a unique framework for studying the interconnection of ecological and genomic processes in the wild, and further research will highly benefit by exploring this interface on a large number of individuals. In particular, the study of QTL associations between behavioural traits (such as breeding output, foraging efficiency, or partner and site fidelity) and genomic or epigenomic features may shed new lights on the evolution of life histories. In this respect too, our work lays a strong foundation for further investigation, since the identification of neutral population structure is a pre-requisite to the study of adaptation (Price *et al.* 2006) - in our particular case, the synnome structure also has implications on the possible realisation of processes such as positive selection (see §176 p. 320).

§-176 Synnomes and gene swamping. Delving into functional and adaptive processes may also allow us to shed light on the relationship that short- and long-term processes entertain in the species' dynamics and evolution. In §95 p. 186*,* we reconstructed the King penguin synnome growth rate along its Pleistocene and Holocene history: despite the very large amplitude of the fluctuations in population size, the growth parameter λ[1] remained very stable, ranging from a minimum $\lambda_{min} = 0.999$ in the decline periods to a maximum of $\lambda_{max} = 1.002$ in the growth periods. In comparison, when growth rate is extracted over a short period on a yearly basis (1999-2010, Le Bohec *et al in prep.*), variation is larger by one order of magnitude ($\lambda_{min} = 0.99$ and $\lambda_{max} = 1.08$). This is an expected observation, since growth rate is a highly stochastic parame-

---

1.   The growth rate λ is the ratio of the population size between two successive years (in our case - otherwise any other time interval may be used).

ter, and decade-scaled variability is dominated by yearly environmental effects, that are evened

out at longer scales. Yet, this raises the question of the methodological link that can be estab-

lished between local demographic monitoring surveys and evolutionary processes. As we men-

tioned in our introduction (see in particular §16 p. 60), most studies focusing on response to cli-

mate change, in particular in vertebrates, are necessarily restricted to the observation of a limited

number of individuals and generations: this individual-based monitoring is by nature focused on

individual responses to changes. But as we see, making a transition from individual to collective

responses, even in such a basic parameter as growth rate, is not trivial. Or, in Tolstoy's words: «*a*

human lives consciously for himself, but is an unconscious instrument in the accomplishment of the his-

toric, universal, aims of humanity. A deed done is irrevocable: and its result, coinciding in time with

the actions of millions of other men, assumes a historical significance [...]. As long as we will only write

the history of singled-out characters - be they Cesar, Alexander, Luther or Voltaire - and not the history

of every *man without exception who took part in the event, we will not be able to explain the move-*

ments of mankind without conceiving a force constraining men to strive towards a common end» (Tol-

stoy 1869). Put simply, individual responses matter less than the synchronised, convergent re-

sponse of great numbers of individuals: population phenomena can be represented as global,

species-scaled trends, yet the essence of these phenomena lies in the joint individual trajectories

that underly the common response.

Thus, for penguins, which are not organised in «nations» or populations, only the consensus re-

action of the whole species should really be considered meaningful: local trajectories may lead

(from a local perspective) to «local extinctions», or (from a global perspective) to «range shifts»,

but the species' eventual evolutionary (and adaptive) response can only be determined globally.

Indeed, free movement of alleles between colonies implies that *migration load*[1] certainly reaches

---

1.   *Migration load* can be defined as the «decrease in mean fitness of a population because of immigration. This occurs because the phenotypic mean of the population is different from the local optimum value» (Lenormand 2002). Thus, in the case of positive selection leading to local adaptation, migration load is the counteracting force bringing random alleles into the local gene pool through migration events, and making local adaptation less efficient.

1 the point of *gene swamping*[1] (see a complete review of these concepts in Lenormand 2002): for a

2 gene to be positively selected, it needs to offer consistent selective advantage throughout the

3 whole species' range - and, to undergo purifying selection[2], it needs to be consistently detrimental

4 everywhere. In short, the *migration-selection equilibrium* is brought to an extreme of *averaged se-*

5 *lection*, where local habitat conditions are integrated over the whole distribution of the species.

6 Whereas individual fitness selection occurs relative to the match of individual traits and local

7 habitat characteristics, the final selective pressure on the allele will, on the contrary, be the result

8 of its average selective advantage under the species' total habitat. This has two important conse-

9 quences: *(i)* even though there may be drastic local selection for certain alleles, local adaptation

10 will be prevented by the migration load*,* and *(ii)* as long as «*gene refugia*» (*i.e.* local conditions

11 where a gene retains a positive or neutral selective coefficient) are maintained in the species'

12 range, fixed adaptation is unlikely.

13 Shifting from a neutral evolution paradigm, such as the one we explored in the present work, to a

14 functional and adaptive one, should enable us to identify such processes. Rapid local micro-adap-

15 tation, for example, should be detectable through particularly shallow coalescence times at locally

16 selected loci, and spatial homogeneity in the patterns of selection may be an important clue on

17 ongoing gene swamping. Comparison with highly philopatric species such as the Peruvian

18 diving-petrel might be especially informative: in that case, the full genetic sorting between even

19 closely neighbouring colonies makes local adaptation a likely possibility. And the fitness benefit

20 can be easily understood in the stable Atacama coast environment, where both the insular breed-

21 ing grounds and the climate exhibits relatively high stability (*e.g.* in the ENSO cycles, see Moy *et*

22 *al.* 2002): investing on a particular local evolutionary strategy can pay off, since the is good

23 chance that the match between adaptation and environment will be maintained for some time.

1.　　*Gene swamping* can be used to describe « the situations where there is no significant response to selection because gene flow is too high » (Lenormand 2002) - in other words, when the migration load fully counteracts the effects of local selection.

2.　　Or «negative selection » - *i.e.* active removal of detrimental alleles from the local gene pool.

Thus, the contrast between high philopatry and reduced gene flow in the Diving petrel's stable environment, and the large penguins' panmictic system amidst unstable oceanic structures is double-sided: from a «*neutral*» point of view, unstable environments are likely to promote higher dispersal, in particular in response to local habitat destruction, as we showed in *Empirical evidence of heterogeneous dispersal*, p. 259, and therefore to bias population systems towards panmixia, whereas stable environments allow for perpetuation of colonial units on the long term, and consequently allow for drift and genetic isolation. But from an «*adaptive*» standpoint, stable environments allow species to benefit from local adaptation, and are expected to select for lower dispersal in order to reduce migration load on the efficiency of selection (Billiard & Lenormand 2005), while unstable environments will rather enhance the benefit of conserving a more generalist gene pool, that is globally suited to the range of possible conditions, although it may not be optimal in the current state of affairs - that is, ultimately, full *gene swamping*. Of course, distinguishing one line of explanation from the other is a lost cause, since these are probably but two ways of describing the same, unified phenomenon[1].

Conclusion

Bringing together the tools of population genomics, numerical climate models and field ecology allowed us to sketch a general picture of the effects of climate change on three remote seabird species. And whereas the general perception of the Southern Ocean is often that of a pristine and extreme environment, one of our most remarkable conclusions may be that it is, in fact, neither. As we exposed throughout this work, even species as rarely met by humans as the King and the

---

1.   Or, to pursue on Tolstoy's thought, «*when an apple has ripened and falls, why does it fall? Because of its attraction to the earth, because its stalk withers, because it is dried by the sun, because it grows heavier, because the wind shakes it, or because the boy standing below wants to eat it? Nothing is the cause. All this is only the coincidence of conditions in which all vital organic and elemental events occur. And the botanist who finds that the apple falls because the cellular tissue decays and so forth is equally right with the child who stands under the tree and says the apple fell because he wanted to eat it and prayed for it. Equally right or wrong is he who says that Napoleon went to Moscow because he wanted to, and perished because Alexander desired his destruction*» (Tolstoy 1869).

Emperor penguin are nonetheless at the forefront of anthropogenic change. The first and most direct effect of these changes is, of course, the increase in temperature, both at the sea surface (which results in polar front migration and loss of foraging grounds for the King penguin) and in the atmosphere (which results in modified sea ice formation patterns, and potentially loss of foraging grounds too for the Emperor penguin). But, as we presented earlier (see §84 p. 174), climate change itself has other, more indirect effects: by affecting the physiology of plankton, it changes the global primary productivity of the Southern Ocean; by modifying sea ice patterns, it affects the blooms of Antarctic Krill (Brierley *et al.* 2002 - with cascading effects on seabirds, see Nicol *et al.* 2008; Chapman *et al.* 2010; Trivelpiece *et al.* 2011); by changing the heat exchange between sea surface and atmosphere, it is likely to change the circulation patterns of water masses, with immediate effects on ecosystem structure (Nicol *et al.* 2000).

Nor does the remoteness of the Southern Ocean mean that it is isolated: directly connected to the three major ocean basins, it is at the heart of the global thermohaline circulation (see §7 p. 35), and a major input into the lower latitudes (in particular through the eastern boundary currents such as the Humboldt Current, see §147 p. 276) - and changes in its circulation patterns have strong consequences on the world's ocean circulation and productivity patterns. Thus, the effects of climate change that we document here in three seabird species are by no means limited to their particular ecosystems, but must rather be interpreted as a marker of large-scale changes in the global state of the Oceans.

Indeed, the extreme adaptations of polar species often motivate the misleading impression that they reveal equally extreme, and perhaps *marginal* effect of climate change. Yet although we can, from a phylogenetic standpoint, infer that *Aptenodytes* penguins' adaptations are extreme compared to their avian ancestors, there is nothing extreme in the species themselves, as seen from within their own habitats: they are, in that sense, strongly representative of the world's ecosystems at large. If the effects of climate change are more visible in polar regions than anywhere else, it is

also, as noted by Smetacek & Nicol 2005, because direct human impacts occurred later in the high latitudes than in the tropical and temperate belts, and that less climate change is to some extent visible there in a more «raw» form. Yet it seems that we are now rapidly catching up on these delayed impacts - to mention only the steep rise in marine overexploitation in the Southern Ocean (Myers & Worm 2003; Ainley & Blight 2009), and the increasing concentration of contaminants at high latitudes (Nash 2011).

Thus, regarding the fate of penguins and other seabirds in the face of man-made climate change, our study may have brought us as many questions as answers. Yet there may be some optimism in cases such as the one of the Peruvian diving petrel, in which resolute conservation measures appear to be having actual effect. Yet in all cases, the disproportionate effect of direct human impact (through population decimation in the King penguin, habitat destruction in the Diving-petrel, and human disturbance on the Emperor penguin) competes with indirect impact through anthropogenic climate change, so that it may be vain to separate both questions. Indeed, in the present state of things, climate change, ecosystem overexploitation and habitat destruction are but different faces of one general stance, that doubtlessly needs to be renewed.

This is however a fully different topic, that we will hopefully have the opportunity to explore further on. In the meantime, I wish to finish this work by thanking the reader for his patience and perseverance, and by expressing once again all my gratitude to Dr Céline Le Bohec and Dr Emiliano Trucchi for their guidance, and to Dr Beaugrand and Dr Davey for accepting the heavy task of reviewing it.

Discussion - §176

Annexes

King penguin demography since the last glaciation inferred from genome-wide data

The following work was performed during the earliest stages on this PhD, with a limited participation on my side - but it served as an important methodological basis throughout this thesis. We therefore include it here, mostly for reference:

Trucchi E, Gratton P, Whittington JD, Cristofari R, Le Maho Y, Stenseth NC, Le Bohec, C (2014) **King penguin demography since the last glaciation inferred from genome-wide data.** *Proceedings of the Royal Society B: Biological Sciences*, 281, 20140528.

Abstract

How natural climate cycles, such as past glacial/interglacial patterns, have shaped species distributions at the high-latitude regions of the Southern Hemisphere is still largely unclear. Here, we show how the post-glacial warming following the Last Glacial Maximum (ca 18,000 years ago), allowed the (re)colonisation of the fragmented sub-Antarctic habitat by an upper- level marine predator, the king penguin Aptenodytes patagonicus. Using restriction site-associated DNA se-

quencing and standard mitochondrial data, we tested the behaviour of subsets of anonymous nuclear loci in infer- ring past demography through coalescent-based and allele frequency spectrum analyses. Our results show that the king penguin population breeding on Crozet archipelago steeply increased in size, closely following the Holocene warming recorded in the Epica Dome C ice core. The following population growth can be explained by a threshold model in which the eco- logical requirements of this species (year-round ice-free habitat for breeding and access to a major source of food such as the Antarctic Polar Front) were met on Crozet soon after the Pleistocene/Holocene climatic transition.

Introduction

Environmental variation through time is one of the drivers of the evolutionary process and a key mechanism in shaping biodiversity. Both short- and long- term climate shifts dramatically affect the geographical distribution of species/populations according to their own dispersal abilities and ecological requirements (Hewitt 2000; Parmesan & Yohe 2003). Understanding how past fluctuations impacted the demography of key species in different ecosystems is essential for predicting the response of communities to ongoing and future change, including anthropogenic-induced climate forcing (Hoffmann & Sgrò 2011; Bellard *et al.* 2012). Using genomic data, we investigate the impact of the last glaciation on the past demography of a king penguin (*Aptenodytes patagonicus*) colony from the most important breeding areas for this species (the Crozet archipelago).

While the biological impacts of recent Quaternary glaciation events on the largely terrestrial Northern Hemisphere have been relatively well documented (Bellard *et al.* 2012), the oceanic Southern Hemisphere, particularly at higher latitudes, remains poorly described (Fraser *et al.* 2012) owing to its relative inaccessibility. Recent hypotheses suggested that winter sea ice during the Last Glacial Maximum (LGM) could have extended as far north as South Georgia, Crozet,

Kerguelen and Macquarie Islands, while Falkland, Gough and New Zealand Islands may have acted as ice-free refugia (Fig. 45 p. 330, and Fraser *et al.* 2009). As southern ocean conditions fluctuated between glacial and interglacial periods, local species had to contend with changes in both habitat and resource availability. In particular, the dis- tribution of most seabirds is primari- ly constrained by the spatial location of suitable breeding sites on land and foraging areas in the ocean (Hunt 1991). For a population to thrive, productive foraging areas must exist within reach of a suitable breeding site. Climate oscillations affect both these key ecological constraints. On one side, these fluctuations cause glaciers to expand and retreat, thus covering or exposing poten- tial breeding sites, on the other side, they affect the location and intensity of oceanic currents and fronts that in turn determine marine primary production. According to (Thatje *et al.* 2008) the large-scale Southern Ocean productivity may have been nearly shut down during the LGM, at least at the latitude where it is currently present. Highly dispersive species negatively affected by glacial conditions could have moved northwards to more suitable ice-free breeding habitats dur- ing the LGM, while low-dispersive ones may have been strongly reduced in population size or may even have gone extinct (Baroni & Orombelli 1994). Therefore, post-glacial warming and the subsequent retreat of glaciers and sea ice, probably favoured the re-colonization of Antarctic and sub-Antarctic territories by dispersive species dependent on ice-free breeding sites (Fraser *et al.* 2009; Van der Putten *et al.* 2010; Fraser *et al.* 2012).

Although some marine mammals or seabirds from Antarctic and sub-Antarctic areas have shown dispersal responses to long-term climatic variations (e.g. southern elephant seal *Mirounga leonina*, see de Bruyn *et al.* 2009, or Adélie penguin *Pygoscelis Adeliae*, see Roeder *et al.* 2001), the future rate of environmental changes inducedby a warming climate may outpace the ability of most up- per-trophic-level predators to adjust. In this context, projections simulated according to future global warming scenarios given by the latest Intergovernmental Panel on Climate Change Fourth Assessment Report (Solomon *et al.* 2007) reveal that the genus Aptenodytes may be under serious threat of extinction before the end of the twenty-first century (Le Bohec *et al.* 2008; Jenouvrier *et*

al. 2012). Indeed, an abrupt increase in sea surface temperature (SST) has been demonstrated to be detrimental to king penguin survival and reproductive rates in populations breeding in the Crozet archipelago in the southern Indian Ocean (Le Bohec *et al.* 2008; Saraux *et al.* 2011a). This is caused by the longer distance the individuals have to swim to get to their main foraging ground (the Antarctic Polar Front during the summer season) whose latitudinal location is influenced by SST (the higher the SST, the higher the latitude , see Péron *et al.* 2012). However, when SST was lower, and food resources probably closer, the Crozet Islands were probably not suitable for the king penguin to complete their breeding cycle as this species needs year-round ice-free grounds for reproduction.
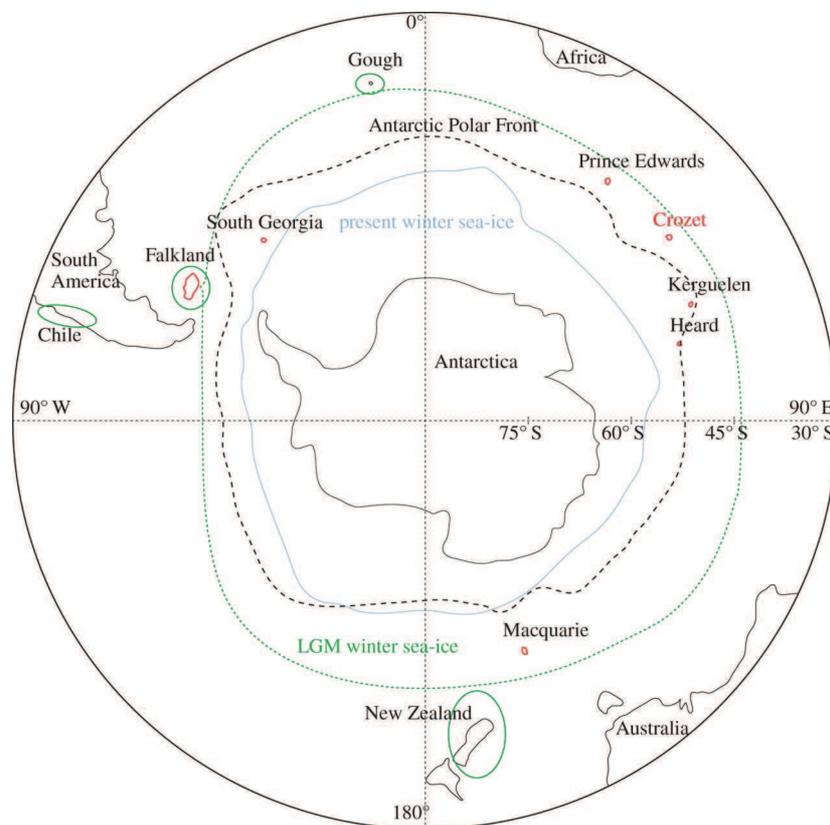
Figure 45 | Winter sea ice extent today (*pale blue solid line*) and during the Last Glacial Maximum (LGM; *green dashed line*), current position of the Antarctic Polar Front (*black dashed line*), putative refugia during the LGM (*solid green line*), and current location of king penguin populations (*red solid line*) and of the colony of 'La Baie du Marin' on Possession Island, Crozet archipelago, monitored in this study (*red text*); adapted from Fraser *et al.* 2012.

Although ca half of the global king penguin population is resident in the Crozet basin, and this top predator represents one of the largest components of the sub-Antarctic marine ecosystem as measured by biomass and energy flux (Charrassin & Bost 2001), the long-term response of this species to the warming period following the LGM remains entirely unknown. Here, we use a genomic-based demographic reconstruction to test whether the king penguin population from the Crozet archipelago ('La Baie du Marin' colony, Possession Island) was strongly affected by the colder conditions characterising the LGM. We tested the applicability of genome-wide data produced by restriction site-associated DNA (RAD) sequencing (Baird *et al.* 2008; Davey *et al.* 2011) within a multi-locus coalescent-based framework (Extended Bayesian Skyline Plot, EBSP, see Heled & Drummond 2008) that aims to average the stochasticity of mutation and drift across tens of genomic loci and to overcome the idiosyncrasy of the results obtained from one or a few molecular markers.

We first demonstrated that genomic regions with different levels of polymorphism consistently show a similar pattern of diversity, and that a consistent demographic signature is recognizable across the entire genome, thus providing evidence that a reduced subset of anonymous genomic loci can be safely employed to estimate past population trends. Historic demography was then inferred by employing a random selection of RAD loci sequenced in multiple individuals and time calibrated according to the mitochondrial substitution rate as estimated in the Adélie penguin Control Region (CR) (in substitutions.site^{-1}.Myr^{-1}: median = 0.55, 95% interval = 0.29–0.88, see Millar *et al.* 2008). Our data show that the king penguin population from Crozet was strongly reduced on this potentially ice-covered sub-Antarctic archipelago before the end of the LGM, or king penguins may have been totally absent, but they (re)colonized the island as soon as the ecological conditions required by this species were met during the following Holocene warming.

Results

ILLUMINA sequencing of a paired-end RAD library from eight king penguins yielded ca 65 million, 100 bp reads. Front reads only were used in our analyses and are available on GenBank at the Sequence Read Archive (Run Num.: SRR942341). After quality filtering, trimming of the last 5 bp, and barcode sorting, 101,115 anonymous loci (each as a 95 bp nucleotide sequence) with 50 average coverage were aligned in an unreferenced catalogue. GC content of this dataset was estimated as 50.45%. According to our quality criteria, the catalogue was further filtered to 66,172 loci (of which 31 452 were polymorphic) matching all eight individuals without missing data. This dataset was then used in downstream statistical analyses.

First, we tested whether genomic regions with different degrees of polymorphism carried consistent information about the demographic history of the king penguin population from Crozet. Polymorphic RAD loci were sorted into six different classes according to the number of single nucleotide polymorphisms (SNPs) observed (from 1 to 6 SNPs), and separate analyses were performed for each category: 20,458 loci with 1 SNP; 7,750 loci with 2 SNPs, 2,417 loci with 3 SNPS; 652 loci with 4 SNPs; 154 loci with 5 SNPs; and 21 loci with 6 SNPs. None of the loci with more than 6 SNPs passed our quality criteria. The signature of the past demography in the 1-SNP class was investigated using the allele frequency spectrum (AFS) (Fig. 46 p. 334) in δaδi (Gutenkunst *et al.* 2009). A likelihood ratio test strongly supported a 2-epoch sudden demographic expansion model over a constant-size model (χ^2 = 8063; p < 0.0001). When scaled by our estimated mutation rate for the 1-SNP class (see below), estimates of the parameters from the best model indicate a demographic expansion from ca 1,400 to ca 7,000 breeders around 18500 years ago. The mismatch distribution density was then checked for the loci in the 2- to 6-SNP classes (Fig. 46 p. 334). A unimodal distribution of mismatches, characteristic of a recent population expansion, was typical across loci in all SNP classes, though more evident in those classes with higher number of SNPs. Notably, the number of outlier loci (in this case, loci showing high

frequency of mismatch at the highest number of differences) was negligible in all classes, high-

lighting the consistent mismatch distributions across loci, which is expected in a population that

has recently undergone a demographic expansion. The same 2- to 6-SNP classes of loci were then

used to reconstruct the demographic function through time by a multi-locus coalescent-based

Bayesian approach (EBSP, see Heled & Drummond 2008). Highly consistent results were ob-

tained using separate datasets with 2, 3 or 4 – 6-SNP loci (c supplementary material, Fig. 47 p.

335). However, loci from 4- to 6-SNP classes were chosen for further analyses because of their

higher information content.

Figure 46 | Demographic inference based on the AFS. (a) Minor AFS analysis performed on 1-SNP class loci: observed (*blue*) and simulated (*red*) spectra and deviation (*green*) are given. (b) Mismatch distribution density analysis performed on 2- to 6-SNP class loci: mean values (*red*) and number of loci in each class (*in brackets*).

Ten independent datasets including 50 loci selected at random from 4- to 6-SNP classes were compared in order to check the consistency of the results over multiple loci. No significant linkage among the selected loci was detected in any dataset: the minimum p-value in the set of pairwise comparisons analysed in each dataset (0.004 − 0.006) was about two orders of magnitude higher than the Bonferroni-corrected threshold (0.00004) for a set of 50 loci. The substitution rate for each locus was set as a wide uninformative uniform prior (0.005 − 0.5 substitutions.site-1), without any absolute calibration, and the EBSP reconstructions were thus unscaled. The same pattern of population growth is clearly evident in all runs (supplementary material, Fig. 47 p. 335). Test analyses including subsets of 10, 25, 50 and 100 loci selected at random from the same set of 100 loci were also run. Smaller subsets resulted in broader credibility regions, although the median value of the population size through time was not substantially different (supplementary material, Fig. 49 p. 345). All runs showed highly consistent EBSP trends, but the effective sample size of the posterior increased very slowly in chain increments from 50 to 200 million generations, showing a general poor mixing. However, likelihood, substitution model parameters and clock model parameters

1   were adequately sampled in all runs. When analysing 100 loci in the same run, the length of the

2   analysis and the poor mixing of the Markov chain Monte Carlo (MCMC) simulations (meaning

3   that it should run much longer) were the limiting factors making the demographic analysis im-

4   practical on our computational resources (see Material and methods).
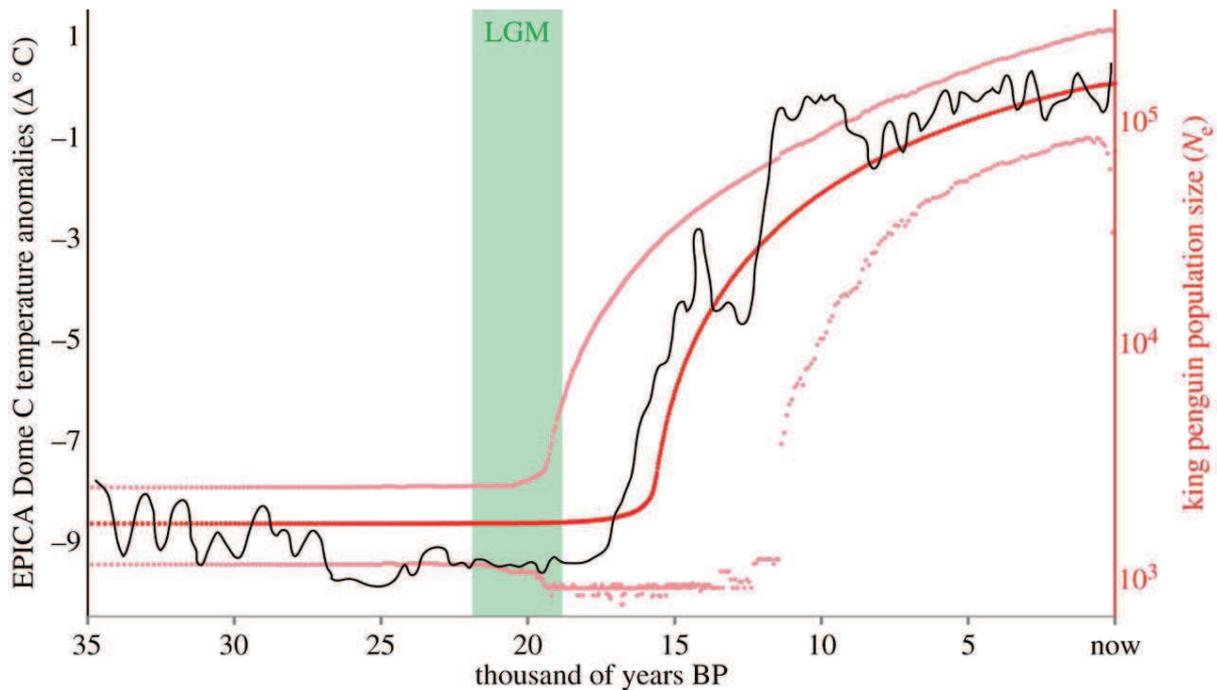
5

6   **Figure 47 | Demographic reconstructions of the Crozet king penguin colony** employing the Ex-

7   tended Bayesian Skyline Plot analysis. Consistency in the pattern inferred is compared among different data selec-

8   tions including 50 loci chosen at random from different classes of variation: a) 2 SNPs, 4 independent datasets; b) 3

9   SNPs, 4 independent datasets; c) 4-6 SNPs, 9 independent datasets. In order to facilitate comparison of uncalibrated

10   EBSP reconstruction and solely for visualization purpose, all runs were scaled to have the same value of the demo-

11   graphic function at t0. To do so, we divided all demographic estimates by the ratio Ki = Ni(t0)/max(Ni(t0)), where

12   Ni(t0) is the median value from the posterior distribution of the demographic function at t0 for each run. Corre-

13   spondingly, the time intervals of each run were multiplied by the same ratio Ki, reflecting the assumption that the

14   actual population size is the same across all runs. Median (black), 95% HPD lower (red) and upper (green) values

15   are reported.

16   In order to calibrate our reconstruction, the mitochondrial CR dataset was included in the EBSP

17   analysis together with 50 randomly selected nuclear loci (4- to 6-SNP classes), using the substitu-

tion rate (0.55 substitutions.site^{-1}.Myr^{-1}) published for the Adélie penguin (Millar *et al.* 2008). When analysed on its own, the mitochondrial locus supported the demographic expansion of the Crozet king penguin population. Sequences of 354 bp fragments of the mitochondrial DNA (mtDNA) CR were produced in 140 samples (number of haplotypes = 112; haplotypes diversity = 0.997; nucleotide diversity = 0.025) and all new haplotypes were uploaded to GenBank (accession no. KF530582 – KF530720). Demographic statistics (Tajima's D = 21.75; Ramos-Onsins & Rozas (R2) = 0.039*; Fu Fs = 2168.4*; *p , 0.05), unimodal mismatch distribution of pairwise differences (not shown), and the Bayesian Skyride analysis (supplementary material, Fig. 50 p. 346), all strongly support the hypothesis of a population expansion, thus providing an independent support to the results obtained from random sets of RAD nuclear loci. The 0.55 substitutions.site^{-1}.Myr^{-1} substitution rate (considering its upper and lower 95% CR boundaries, Millar *et al.* 2008) was then used to scale the Bayesian Skyride plot to an absolute timescale (supplementary material, Fig. 50 p. 346).

Our EBSP reconstruction based on a random set of 50 RAD loci and one mitochondrial fragment indicated that the king penguin population of 'La Baie du Marin' had a Ne of ca 2,000 individuals during the LGM, and it steeply increased at the onset of the Holocene, around 15,000 years ago. This demographic growth closely matched the trend of temperature anomalies recorded in the Epica Dome C ice core (Jouzel *et al.* 2007), which shows a rapid increase between 18,000 and 10,000 years ago (Fig. 48 p. 339). Then, the colony reached an estimated present population size of ca 170,000 individuals. Using the published mtDNA rate as a reference, the average substitution rate of loci in our dataset was estimated at 2.2.10^{-8} substitutions.site^{-1}.Myr^{-1} (2.6.10^{-7} substitutions.site^{-1}.Myr^{-1}). To obtain this estimate, we used the substitution rates estimated in BEAST for loci with different numbers of SNPs (mean values of posterior probabilities in substitutions.site^{-1}.Myr^{-1}: 0 SNP = 0.007; 1 SNP = 0.028; 2 SNPs = 0.050; 3 SNPs = 0.071; 4 SNPs = 0.092; 5 SNPs = 0.114; 6 SNPs = 0.135). Note that the number of SNPs at each locus is, in the first place, a result of the stochasticity of the mutational and coalescent process. Hence,

mutation rates estimated in BEAST for each SNP class should not be regarded as estimates of the actual substitution rates across different genomic fragments, but rather as posterior probabilities conditional to the number of SNPs at each locus. We then estimated the average substitution rate for our RAD dataset as a weighted average accounting for the frequency of each SNP class across the 66,172 loci.

Discussion

§-177 Using restriction site-associated DNA sequencing data in a coalescent-based framework. Our analyses empirically supported that RAD sequencing data can be effectively used for inferring past demography in a coalescent-based framework and that a small subset of these data (i.e. 50 loci only) is sufficient to describe the post-glacial history of the king penguin colony breeding on Crozet. This result is particularly important because, though thousands of markers can now be easily and cost-effectively sequenced in any biological system (Davey *et al.* 2011), many existing analytical tools for demographic inference are not yet optimized for genome-level data. Recently published methods, like the pairwise sequentially Markovian coalescence (Li & Durbin 2011) or DiCal (Sheehan *et al.* 2013) require phased diploid genomic data over a long fragment of the chromosome that are not readily available for most non-model species. The development of new algorithms to exploit SNP data in coalescent-based frameworks (i.e. 'SNPs and amplified fragment length polymorphisms phylogenies', see Bryant *et al.* 2012) are paving the way for a full use of genome-scan data in phylogeography and population genetics, although linkage needs to be taken into account for extensive SNP datasets.

We found that EBSP analysis is not really optimized for handling high numbers of loci (very high parametrization) and this may result in slow convergence and poor mixing of the MCMC chains. We estimated that 3–5 billion iterations would be needed to get effective sample size above 200 for all model parameters when analysing our dataset of 50 loci and eight individuals. Neverthe-

less, our EBSP demographic reconstructions were highly consistent with each other, with those produced by the diffusion approximation of the AFS (Fig. 46 p. 334) and with standard single-locus mtDNA analyses (supplementary material, Fig. 50 p. 346). The AFS analysis, based on approximation to the neutral Wright–Fisher diffusion of an allele (Gutenkunst *et al.* 2009), has been strongly criticized as theoretically unfit to distinguish between competing population histories even if strongly simplified assumptions (panmixia, infinite site mutation model and neutrality) are met in the studied system (Myers *et al.* 2008). In particular, it seems that compensating events in population dynamics are impossible to detect, thus making the analysis of complex histories unreliable. In our test case, the different analytical approaches converged on a quite simple history of sudden population growth making it a likely suitable case for AFS analysis. Both EBSP and AFS analyses, based on independent datasets (1-SNP class versus 4- to 6-SNP classes loci), produced largely similar inferences of the time and trend of the past demography of our king penguin colony. A major difference between results from the two methods was in the estimate of the current effective population size (Ne = 7,000 from AFS analysis versus Ne = 170,000 from EBSP). Both estimates are inconsistent with the direct count of breeding birds on 'La Baie du Marin' colony, Possession Island (*i.e.* 32,000 breeding birds, see Delord *et al.* 2004). However, it is likely that a certain degree of gene flow exists within the Possession Island, and that 'La Baie du Marin' colony is part of a metapopulation at the island level. According to the most recent estimate by direct count, the breeding population of Possession Island is ca 150,000 individuals (Delord *et al.* 2004). Therefore, the population size we estimated from genomic data may reflect this larger meta-population, rather than the single colony. A study investigating the level of connectivity and gene flow among the colonies of Possession Island is currently ongoing.
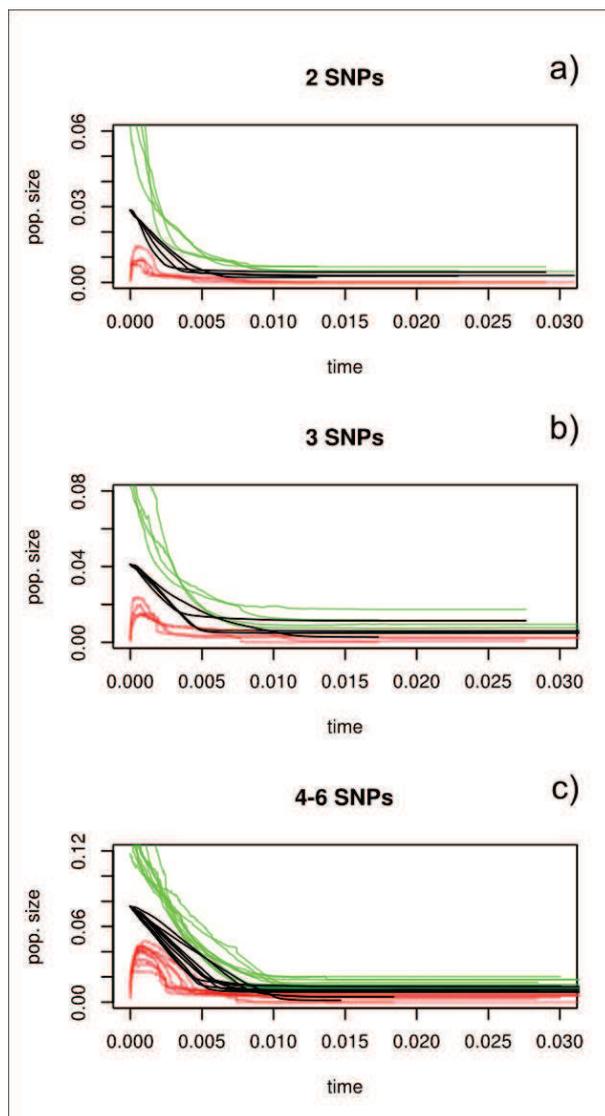
Figure 48 | Past demographic trend of the king penguin colony of 'La Baie du Marin' on Possession Island, Crozet archipelago: median value (*red*) and 95% confidence interval (*pale red*). Trend of temperature anomalies recorded in the EPICA Dome C ice core (*black* Jouzel *et al.* 2007). The LGM period is given in green.

In our test case, the demographic trend inferred from a single mitochondrial locus was consistent with a similar analysis carried out on 50 nuclear loci (Fig. 48 p. 339 and supplementary material, Fig. 50 p. 346). Nevertheless, analysing a fairly large number of (presumably) unlinked loci should be considered as best practice as it allows to us average the stochasticity of mutation and drift over many independent genealogies, thus avoiding the risk of a biased demographic inference owing to the idiosyncratic history of a single marker. In addition, when a large number of loci are genotyped, many fewer samples are needed to estimate population-level statistics and obtain demographic inferences (Felsenstein 2006; Willing *et al.* 2012).

Thanks to the inclusion of the mitochondrial marker in our genomic analyses, we were also able to propose an average substitution rate for the loci included in our RAD dataset. Our estimated rate is about one order of magnitude faster than previously reckoned in other bird species (Ellegren 2013). However, recent evidence showed that genomic substitution rates can be faster than formerly estimated from pedigree studies (O'Roak *et al.* 2012; Gibb & Hills 2013). Moreover, the RAD sequencing protocol may introduce biases in the genome representation: when using a

digestion enzyme like SbfI, whose restriction site is rich in GC, a selection for GC-rich regions occurs. Indeed, the GC content in our dataset was 50.45% that corresponds to the highest estimates for chicken microchromosomes (Hillier *et al.* 2004). Hence, our dataset is probably centred on GC-rich regions (e.g. microchromosomes), which are characterized by increased levels of gene density, recombination rate, number of CpG sites, methylation and mutation rate (Axelsson *et al.* 2005). Excess of hypermutable CpG nucleotides in GC-rich sequences has been identified as one possible explanation of increased mutation rates (Zhao & Boerwinkle 2002) so that GC-rich microchromosomes can show a 1.2–1.3 faster substitution rate than the average of the genome (Webster *et al.* 2006). This effect probably contributes, at least in part, at explaining the high mutation rate estimated for our dataset. Even if further investigation is clearly necessary, our interpretation sounds like a cautionary tale about the bias in the selection of genomic regions when using sequence-based restriction enzymes.

§-178 King penguin population history during the Last Glacial Maximum. Our genomic data from the Crozet king penguin colony contain a consistent signal of demographic expansion at all levels of variability, with very few outliers in the mismatch analysis. Our demographic reconstruction strongly supports a sudden population expansion following the LGM and starting ca 15,000 years ago. Therefore, our results show that even a cold-adapted species, such as the king penguin, was limited by colder glacial conditions, and benefited from post-glacial warming, which offered suitable breeding sites and foraging conditions in the Crozet region.

Like several other top-level predators in the Antarctic and Sub-Antarctic, king penguins depend on marine ecosystems for food and on terrestrial habitats for reproduction. This species needs a combination of two ecological factors that are both influenced by temperature: *(i)* year-round ice-free breeding grounds, and *(ii)* access to major feeding grounds (*e.g.* the Antarctic Polar Front) within swimming distance and compatible with birds' breeding duties (exchanging the egg with their fasting partner, feeding their chick). The king penguin has the longest breeding cycle

of all penguin species, spanning 14 – 16 months (Barrat 1976). This implies that the reproductive success depends on both summer and winter conditions. Yet, LGM climate strongly influenced both marine productivity and the availability of suitable breeding grounds from which feeding areas could be exploited. Lower global temperature favoured a northward expansion of both winter and summer sea ice (Gersonde *et al.* 2005; Fraser *et al.* 2009; Fraser *et al.* 2012). In turn, ice-sheet and sea ice extensions profoundly affected the location (shifted northward) and strength of oceanic fronts and circumpolar currents encircling Antarctica (Charles *et al.* 1991; Gersonde *et al.* 2005; Fraser *et al.* 2009), which determine primary productivity in the Southern Ocean (Thatje *et al.* 2008). Some polar species tracked favourable ecological niches northwards (Burckle 1984; Janko *et al.* 2007; Fraser *et al.* 2012), and suitable refugia for land-breeding species have been proposed on the Falklands, Gough Island and Southern New Zealand. Genetic evidence showed recent (re)colonizations of the sub-Antarctic islands by several taxa that drifted with the strong eastward flow of the Antarctic Circumpolar Current (Waters 2008; Fraser *et al.* 2009). However, current reconstructions of LGM conditions lack the spatial resolution to unequivocally detect the number and geographical distribution of all glacial refugia (Convey *et al.* 2009). In particular, it is not clear whether ice-free patches existed in the Crozet archipelago during the LGM (Hunt 1991).

EPICA Dome C ice core (Jouzel *et al.* 2007) data show an increase of ca 9°C between 18,000 and 10,000 years ago. In our demographic reconstruction, this interval coincides with a sustained phase of growth for the Crozet king penguin population (Fig. 48 p. 339). This growth trajectory is consistent with a threshold model, where a new colony is established as soon as all of the critical ecological requirements are met. We propose that the availability of breeding grounds within feeding-trip distance from foraging areas played the most critical role in the population expansion of Crozet king penguins after the LGM. Even if a major food resource (linked to the presence of the AFP) may have already been available within a king penguin home-range distance from the Crozet islands during the LGM, winter sea ice and possibly land glaciers, did not allow

the settlement of a viable king penguin population on the archipelago before the post-LGM warming. As soon as breeding grounds became available, the king penguin could extensively settle on Crozet and exploit the food resource. However, with growing SST temperature owing to the global warming, the AFP can soon be too far from Crozet, thus making the area unsuitable again. Extinction, beginning locally and potentially mitigated by migration events (depending on their ability to follow spatial and temporal changes in food/breeding resource availability, as seen in the Gentoo penguin *Pygoscelis papua*, see Ducklow *et al.* 2007), is a probable outcome of the ongoing climate warming.

Material and methods

§-179 Sampling, DNA extraction and quality assessment. Sampling was conducted during the 2010 breeding season in the king penguin colony of 'La Baie du Marin' on Possession Island (46°250 S, 51°8450 E), Crozet Archipelago. Blood (approx. 100 ml) was collected from the brachial vein of chicks hatched in the long-term monitored area 'ANTAVIA', transferred to a filter paper (Whatman 113), dried and later frozen at -20°C. Individuals were randomly selected along a 120 m axis at the periphery of the colony, in order to maximize separation distance. A total of 140 individuals were chosen for mtDNA CR analysis, and eight of these were randomly selected for RAD sequencing analysis. Total DNA was extracted from the filter papers using standard methods and controlled for quantity and quality.

§-180 Restriction site-associated DNA sequencing. Genomic DNA from eight king penguins was individually barcoded, pooled and genotyped by RAD sequencing (Baird *et al.* 2008) in one library sequenced on an ILLUMINA HiSeq2000 at the Norwegian Sequencing Centre, University of Oslo. Raw reads were trimmed, demultiplexed and aligned in an unreferenced catalogue using the STACKS software pipeline (Catchen *et al.* 2011) running on the server facility on the ABEL cluster, University of Oslo. Further quality filtering using custom bash and python scripts was ap-

plied to produce the final dataset used in downstream statistical analyses (detailed protocol in the supplementary material).

§-181 Genome-wide demographic analysis and calibration. Genomic RAD fragments (95 bp) were sorted into six different classes according to the number of SNPs observed (from 1 to 6 SNPs) and separate analyses were performed for each category. Minor allele frequency spectra were calculated by functions available in the R package 'adegenet' (Jombart 2008) using loci included in the 1-SNP class. The signature of the past demography in this class of polymorphism was investigated using the AFS analysis in δaδi (Gutenkunst *et al.* 2009). Using a diffusion approximation of the AFS, this analysis allows demographic inferences to be made from genetic data for testing alternative demographic scenarios in a maximum-likelihood framework. A sudden growth in population size was tested against the null hypothesis of constant population size using the '2-epoch' and the 'snc' functions, respectively. The mismatch distribution density (average mismatch distribution of pairwise differences) was then analysed to check for the same demographic pattern in the 2- to 6-SNP classes. Functions included in the R package 'ape' (Paradis *et al.* 2004) and the R standard boxplot function were used to estimate and plot the mismatch distribution density in each SNP class. Random selections of 50–100 loci in the 2- to 6-SNP classes were used to infer the past demography of the king penguin population using the coalescent-based multi-locus analysis implemented in BEAST v. 1.7.4 (Drummond & Rambaut 2007), setting the EBSP (Heled & Drummond 2008) as the tree prior model (see the supplementary material for details). The robustness of the approach was tested with respect to: *(i)* the number of SNPs per locus, *(ii)* the different random selection of loci, and *(iii)* the number of loci included in the random selection. All analyses were run on the Bioportal facility (now LifePortal) of the ABEL cluster, University of Oslo. An estimate proposed for the substitution rate of the mitochondrial CR in the Ade´lie penguins (0.55 substitutions.site^{-1}.Myr^{-1}, see Millar *et al.* 2008) was used to calibrate our demographic reconstruction. We then plotted the population trend of the last 35,000 years together with the trend of temperature anomalies (in D°C) as inferred by the analysis of the EPICA

Dome C ice core (Jouzel *et al.* 2007). Concerning the calibration of the mean genome-wide substitution rate: first, the mean of the MCMC posterior median values for each SNP class included in the selected EBSP analysis (4- to 6-SNP classes) was calculated; then, a linear regression was used to infer the substitution rate of those SNP classes excluded from the final EBSP analysis (0- to 3-SNP classes); finally, we calculated the mean genomic substitution rate weighting each SNP class according to the frequency (number of loci) of each class.

§-182 Mitochondrial DNA control region analysis. Partial sequences of the CR (354bp) were amplified a nd s equenced i n 1 40 s amples a ccording t o t he p rotocol p ublished i n H eupink *e t al.* 2012. Summary molecular statistics (Haplotype diversity: Hd; nucleotide diversity: pi), demographic parameters as Tajima's D and Fu's Fs, and the mismatch distribution of pairwise differences were calculated. This dataset was used to infer the king penguin past demography employing the Bayesian Skyride plot (Minin *et al.* 2008) reconstruction, which produces estimates of population size through time and its associated credibility intervals, combining both phylogenetic and coalescent uncertainties, as implemented in BEAST v. 1.7.4. The estimate of the CR substitution rate proposed for Adélie penguins (0.55 substitutions.site^{-1}.Myr^{-1}, see Millar *et al.* 2008) was used to calibrate our analyses.

All animals in this study were handled only once in order to mark them with a plastic tag (Floytagw), to blood-sample them, and to conduct morphological measurements. All procedures employed during this fieldwork were approved by the Ethical Committee of the French Polar Institute (Institut Paul Emile Victor 2 IPEV) and conducted in accordance with its guidelines, also complying with French laws including those relating to conservation and welfare. Authorisations to enter the breeding site (permits n82009-57 issued on the 26th of August 2009) and handle birds (permits n82009-59 issued on the 29th of August 2009) were delivered first by the French "Ministe`re de l'Amé nagement du Territoire et de l'Environnement" and then by the Terres Australes et Antarctiques Franç aises (TAAF).

1 Handled animals were removed from the colony in order to minimise the disturbance to neigh-

2 bouring birds and taken to a few meters away for manipulation. They were hooded to reduce

3 their stress and manipulations lasted between 5 and 10 minutes. All blood-sampling (quantities

4 adjusted according to the age of the chick) and tagging material was sterilized (either sealed, or

5 through chemical sterilisation). Moreover, Vétédine soap and alcoholic antiseptic solutions were

6 used to disinfect the skin before bleeding and tagging. Flesh wounds did not seem infected there-

7 after (personal observations on a subset of recaptured birds).
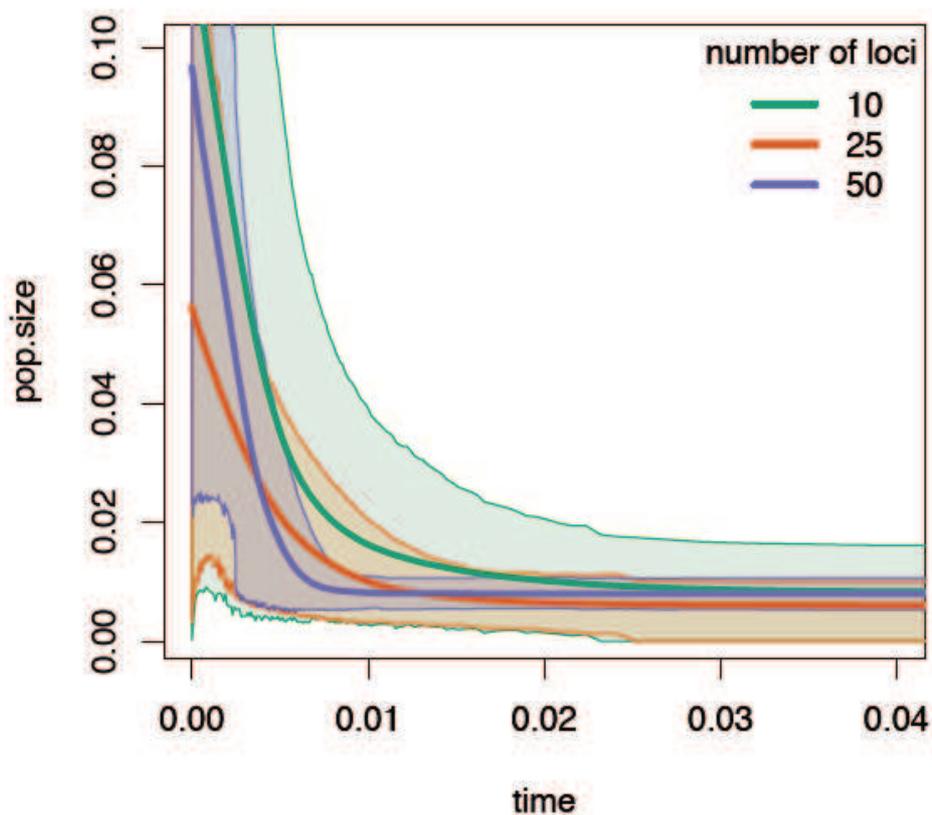
8 **Figure 49 | Demographic reconstructions of the Crozet king penguin colony** employing the Ex-
9 tended Bayesian Skyline Plot analysis. Consistency of the inference is compared across three nested datasets (10, 25
10 and 50 loci) randomly selected from the 4-6-SNP class. Population size and time are unscaled. Median (solid line)
11 and 95% upper and lower (filled areas) values are reported.

Supporting information

§-184 Sampling, DNA extraction, quality assessment. Sampling was conducted during the 2010/2011 summer season in the king penguin colony of 'La Baie du Marin' on Possession Island (46°25'S, 51°45'E) in the Crozet Archipelago. Blood (~100 µL) was collected from the brachial vein of chicks hatched in the long-term monitored area 'ANTAVIA', transferred to a filter paper (Whatman 113 ®), dried, and later frozen at -20°C. Individuals were randomly selected along a 120m-axis at the periphery of the colony,in order to maximise distance separation. A total of 140 individuals were chosen for mitochondrial DNA Control Region analysis, and 8 of these were randomly selected for restriction site-associated DNA (RAD) sequencing analysis. Total DNA were extracted from the filter papers using a Phenol-Chloroform protocol or the Qiagen DNAase blood & tissue kit according to manufacturer's instructions. After extraction, DNA quantity and quality were tested in each sample by fluorimetric-based measurement (Qubit, Invitrogen) and gel electrophoresis.

§-185 MtDNA marker analysis. Partial sequences of the Control Region (354 bp) were amplified and sequenced in 140samples according to the protocol published in Heupink *et al.* 2012. PCR products were Sanger-sequenced in the ABI-LAB at the University of Oslo. Sequences were then manually edited and aligned in Bioedit (Hall 1999). All new haplotype sequences have been uploaded to GenBank (Accession number: KF530582-KF530720). Summary molecular statistics, demographic parameters and the mismatch distribution of pairwise differences were calculated in DNAsp v5 (Rozas & Rozas 1999). This dataset was used to infer the king penguin past demogra-

phy employing the Bayesian Skyride plot (Minin *et al.* 2008), where inferred population history

is bounded by credibility intervals that combine phylogenetic and coalescent uncertainties, as im-

plemented in the BEAST 1.7.4 package (Drummond & Rambaut 2007). Analyses were per-

formed on the Bioportal facility (now LifePortal)running on the ABEL cluster, University of

Oslo. A GTR+G+I substitution model was set for the mitochondrial sequence. A relaxed uncor-

related log-normal clock prior was set for the substitution rate to take into account fluctuations

of the molecular clock along different branches of the phylogeny; a log-normal priors with mean

in the real space of 0.55substitution/site/Myr respectively were set (Millar *et al.* 2008). The

Bayesian Skyline plot was set as coalescent tree prior model. Convergence among three runs, with

a MCMC length of 30 million generations for each parameter setting was checked. Effective

sample size was checked in Tracer 1.5 (Rambaut & Drummond 2005) and plots of population

size change through time were drawn.

§-186 RAD sequencing and genome-wide demographic inference. Eight king penguin individuals

were pooled and genotyped by RAD sequencing [8] in one library sequenced on an ILLUMINA

HiSeq2000, yielding ca. 65 million 100-bp reads. All raw sequence reads are available on Gen-

Bank at the Sequence Read Archive (Run Num.:SRR942341).

After quality assessment, samples showing high molecular weight and highly concentrated DNA

were employed in next-generation sequencing (NGS) of RADtags (Baird *et al.* 2008). The follow-

ing RADseq protocol was adopted: (i) approximately 100ng of genomic DNA pers ample were

digested with the restriction enzyme SbfI (NEB); (ii) each sample was then ligated to a unique

barcoded P1 adapter prior to pooling in a single library. The library was then sheared by sonica-

tion, and gel electrophoresis of small library aliquots were run after the first 5 cycles (30'' ON –

30'' OFF) and then every 2-3 cycles of sonication; (iii) the target size range fraction (300-500

bp) was achieved after 8 cycles of sonication and was then selected by gel electrophoresis and

manual excision; (iv) before size selection on the gel,sonicated libraries were concentrated to 25

µl by DNA capture on magnetic beads (beads solution:DNA = 0.8:1), thus further reducing the carry-over of non-ligated P1 adapters; (v)capture on magnetic beads using the same beads:DNA ratio (0.8:1) was then employed in all following purification steps (after blunt-end repairing, poly-A tailing, P2 adapter ligation and library enrichment by PCR); (vi) PCR amplification was performed in 8 x 12.5 µl aliquots pooled after the amplification in order to reduce amplification bias on few loci due to random drift; (vii) the library was then quantified by a fluorimetric-based method (Qubit, Invitrogen) and molarity was checked on an Agilent Bioanalyzer chip (Invitrogen). A final volume of 20 µl with a DNA concentration of 45 ng/µl was submitted for sequencing on anILLUMINA HiSeq2000 sequencer at the Norwegian Sequencing Centre, University of Oslo.

Raw reads were then processed using the scripts included in the Stacks package (Catchen *et al.* 2013) running on our server facility on the ABEL cluster, University of Oslo. Raw reads were quality filtered and grouped according to individual barcodes. Then individual loci were retrieved and SNPs were called by a maximum-likelihood function that excluded likely sequencing errors. Several runs with different settings of read trimming parameter, quality thresholds,mismatches allowed when building the individual and the population catalogs, were performed to check for consistency of the results. The parameters setting used to build the final catalog included: -t 95 and the default values for the quality checking when using"process_radtags.pl"; -m 10, -n 7, -M 3 when running "denovo_map.pl". 101,115 loci with50X average coverage were aligned in an unreferenced catalog. A table including all loci matching the eight sequenced individuals was built using "export_sql.pl" Stacks script. This table was further filtered by python scripts (available upon request) excluding loci with missing data, with more than 2 alleles per individual, and deleveraged by Stacks algorithm.

Loci were then grouped according to the number of SNPs allowing from 0 to a maximum of 6 substitutions per locus (0 to 6-SNP classes). Loci with 4-6 SNPs were then directly checked

through the catalog web-based interface provided by Stacks. Loci with more than 2 SNPs in the last 5 base pairs or with observed heterozygosity higher than 0.6 were blacklisted and removed from the table as likely sequencing errors or paralogous loci. Only those loci hosting 1 single bi-allelic SNP were employed in AFS analysis in order to minimise linkage among the data. Not having a reference genome, we could not exclude loci produced by adjacent genomic regions or by the two sides of each restriction site. Custom python scripts (available upon request) were employed to edit this 1-SNP dataset as a suitable input file for downstream statistical analysis encoding SNPs as 0-2 when homozygote for the two alleles respectively or 1 when heterozygote. On the other hand, loci in 2 to 6-SNP classes were treated as short sequences and locus-by-locus edited using python script as NEXUS format files each containing 16 sequences 95 bp long (two sequences per individual).

Minor allele frequency spectrum was calculated by functions available in the R package "ade-genet" (Jombart 2008) using loci included in the 1-SNP class. This information was then passed to the python-based software ∂a∂i (Gutenkunst *et al.* 2009) that, using a diffusion approximation to the allele frequency spectrum, allows demographic inference from genetic data testing alternative demographic scenarios in a maximum-likelihood framework. A sudden growth in

population size was tested against the null hypothesis of constant population size using the "two_epoch" and the "snc" functions, respectively. Several runs of likelihood optimisation were performed changing the extent of the search by the "fold" parameter in the "dadi.Misc.perturb_params" function. Optimised log-likelihood and Theta values were recorded. In order to calculate effective population size from Theta values produced by ∂a∂I, a total sequence length of 1,943,510 bp (95 bp X 20,458 loci used in this analysis) was used.

Functions included in the R package "ape" (Paradis *et al.* 2004) and the R standard boxplot function[13] were used to calculate the joint mismatch distribution in the pairwise differences (from

here onwards referred to as mismatch distribution density). Calculations were performed and plotted in each 2 to 6-SNP classes separately.

Different random combinations of 50-100 loci in 2 to 6-SNP classes were compared when inferring the past demography of the king penguin population using the coalescent-theory based multi-locus analysis implemented in BEAST 1.7.4. Linkage disequilibrium was tested in all subsets using Genepop (Raymond & Rousset 1995) with the default setting in the web tool and the Bonferroni correction for multiple tests. The robustness of the approach was tested with respect to i) the number of SNPs per locus, ii) the different random selection of loci and iii)the number of loci included in the random selection: 50 loci in 2-SNP class (5 runs), 50 loci in3-SNP class (5 runs), 50 loci in 4-6-SNP class (10 runs), 10 loci in 4-6-SNP class (1 run), 25 loci in 4-6-SNP class (1 run) and 100 loci in 4-6-SNP class (1 run). Three runs showing hints of multiple optima for the demographic function were discarded. Different settings of the parameters and priors have been explored in preliminary analyses, but the following was the definitive setting: (i) markers were unlinked concerning site substitution model, clock model and tree prior model; (ii) site substitution model was set as a HKY with empirical base frequency; (iii) a strict molecular clock was estimated for each marker with a uniform prior distribution bounded within 0.5 and 0.005 sub/s/Myr; (iv) the Extended Bayesian Skyline Plot (EBSP; Heled & Drummond 2008) was selected as tree prior model and ploidy of the markers was set accordingly. Fine tuning of operators did not improve our results as running the analyses with longerMCMC simulations; 200 million iterations were set as run length.

Mitochondrial Control Region data were included in the analysis in order to test the consistency of the information provided by the two genetic dataset (genomic and mitochondrial) and to calibrate the genomic substitution rate using the mtDNA ControlRegion substitution rate as estimated in the Adélie penguin. Site substitution and clock models were set as in the analyses of the mitochondrial marker alone (see below). All analyses were run on the Bioportal facility (now

LifePortal) of the Abel cluster, University ofOslo. Results were checked on Tracer 1.5 and plot of

the EBSP data were drawn in R. An extensive study on Adélie penguin ancient DNA suggested a

fast estimate (0.88 sub/s/Myr; Lambert *et al.* 2002) for the substitution rate of the mitochondrial

Control Region. Further analyses confirmed this high figure but it was downscaled to 0.55 sub/s/

Myr (Millar *et al.* 2008). We used the more conservative 0.55 sub/s/Myr for our calibrated de-

mography. A generation time of 11.49 years (Le Bohec *in prep*) was used to convert the popula-

tion size estimates on the EBSP(given by default in effective population size * generation time).

We then plotted the population trend for the last 35,000 years together with the trend of temper-

ature anomalies as inferred by the analysis of the EPICA Dome C ice core (Jouzel *et al.* 2007).

Concerning the calibration of the mean genome-wide substitution rate: first, the mean of the me-

dian values in each SNP-ratio class included in the EBSP analysis was calculated (4 to 6-SNP

classes); then, a linear regression was used to infer the substitution rate of those SNP classes ex-

cluded from theEBSP analysis (0 to 3-SNP classes); finally, we calculated the mean genomic sub-

stitution rate weighting each SNP class accordingly with the frequency (number of loci) of each

class.

RAD-seq bench protocol optimisation.

In order to maximise sequencing yield and efficiency, we conducted thorough protocol optimisation. We used Lambda phage DNA as a control (50,000 genomic DNA, NEB): Lambda phage has 5 known restriction sizes for Sbf-I, and known restriction fragment lengths, which makes it possible to assess preparation efficiency. In order to assess potential inhibitor effects, all tests were repeated with a) lambda DNA alone, b) lambda DNA + penguin DNA at equal concentrations, c) penguin DNA alone.

(i) Digestion was tested both with the recommended NEB protocol, and with Baird *et al.* (Baird *et al.* 2008) modified protocol (reduced enzyme molarity). No difference could be found, and high-molecular-weight lambda-phage had disappeared totally in both cases. Increasing digestion time from 45min to overnight did not increase efficiency.

(ii) P1 ligation. We tested four different conditions, removing in each test condition one of the three components: (a) λ + P1 + T4, (b) λ + P1 + $\varnothing$, (c) λ + $\varnothing$ + T4, (d) a) $\varnothing$ + P1 + T4.

- Overall efficiency: ligation was first performed under recommended conditions (NEB concentrations, temperatures and times). Re-ligation of digested DNA (condition (c)) appeared sub-optimal, as only a fraction of high-molecular-weight DNA was re-formed.

- Time and temperature: tests were then repeated with three different conditions: (a) 25°C for 45 min (recommended), (b) at 16°C for 16 h (NEB test conditions) and (c) cycling between 10°C and 30°C (2°C increments every 30'') for 16 h (Lund *et al.* 1996). Under all test mixes, ligation

1 efficiency clearly increased from time conditions (a) to (c). We retained conditions (c) as optimal

2 for our updated protocol.

3 - P1 adapters dimers: in order to test the efficiency of P1 adapter ligation, we did a series of dilu-

4 tions (1:1, 1:10, 1:100) on all ligation conditions containing P1 adapters ((a) λ + P1 + T4, (b) λ

5 + P1 + Ø, and (d) a) Ø + P1 + T4). We performed 25 short cycles (25") of amplification using

6 only forward Solexa primers, that reverse-complement a section of P1 sequence. We thus expect

7 all P1-containing DNA fragments to be linearly amplified; and the band strength on a 1.5%

8 agarose gel should be proportional to initial concentration. Concentration of P1 dimers reflects

9 the efficiency of the ligation reaction. As expected, P1 dimer concentration increased from 25°C

10 incubation, to 16h cycle conditions.

11 - P1 adapter molarity: in order to test if current P1 molarity is simply limiting the reaction, we

12 performed ligation under «ideal» (cycled) conditions, with 0.1 pmol, 0.5 pmol (Baird *et al.*

13 2008), 1.0 pmol, 5 pmol, 10.0 pmol, 20 pmol, 50 pmol, and 100 pmol of P1 adapters per reac-

14 tion. In order to assess the efficiency of the P1 ligation process, we measured the molarity of

15 high-molecular-weight chimeric lambda phage re-constructs. Indeed, we consider the reaction

16 efficient when all available genomic DNA sticky-ends are ligated to a P1 adapter, which requires

17 these to be in large excess: under those conditions, genomic DNA religation should be minimal.

18 Fragment length and molarity were assessed on a TapeStation (Agilent (c)) genomic DNA chip.

19 With 0.1 pmol P1, chimeric religation is very important, but seems to decrease with increasing

20 P1 molarity. Saturation is reached at 5 pmol: chimeric DNA has disappeared, and P1 adapter

21 dimer molarity starts to increase. This new molarity is 10 times higher than recommended by

22 (Baird *et al.* 2008), and leads to enhanced library efficiency. However, when testing our stock P1

23 adapters on a BioAnalyzer DNA chip (Agilent (c)), it was found to be 10 times less concentrated

24 than expected from the manufacturer's specifications. Moreover, when using a fresh stock of

25 adapters, 0.5 pmol proved sufficient to obtain the same result. The most likely hypothesis here is

thus a manufacturer's failure - a possibility that we had not taken into account at first, but which may be worth testing on all new adapter stocks.

(iii) P2 ligation. The same set of conditions tested for P1 ligation was assessed for P2 ligation, but with no noticeable effect on library efficiency. P2 ligation was therefore considered already optimal.

(iv) Purification steps. The original protocol includes a series of purification steps, realised with a spin-column kit (Qiagen Minelute (c)). These cause massive DNA loss along the preparation. We tested an alternative protocol, in which magnetic beads (Agencourt AMPure XP (c)) are added to the library after size selection, and kept together with the library until the final purification step. Solid-state reversible immobilisation (SPRI) beads are inert, paramagnetic carboxyl-coated particles. Reversible precipitation of DNA on the beads happens under high-salt, low-DNA-solubility conditions, which are created by adding a high-salt polyethylene-glycol (PEG-8000) solution to the library. Under low-tonicity conditions, DNA is dissolved in the surrounding buffer, and beads do not interfere with enzymatic reactions. In order to implement this, we prepared a binding solution with 10 g PEG-8000, 7.3 g NaCl, and 50 mL H_2O. We calibrated its DNA precipitation efficiency by purifying 50bp DNA ladder with a gradient of binding solution to ladder ratio ranging from 0.3X to 1.4X. Purified product was assessed on a BioAnalyzer DNA 1000 chip (Agilent (c)). For our solution, a ratio of 1 (equal volumes of binding solution and target DNA solution) was found to provide the appropriate size selection for RADseqapplications, by binding all DNA fragments longer than ~200bp.

Using this updated purification method, DNA was re-immobilised on the magnetic beads 3 times (after end repair, A-tailing, and P2-ligation), and beads are removed at the final step. DNA loss was found to be greatly reduced, and library preparation efficiency (i.e. molarity of properly prepared fragments compared to initial DNA input) was approximately doubled. An additional benefit is the reduction in handling time, and in costs, given the high price of SPRI beads.

(v) Size selection. The original protocol (Baird *et al.* 2008) included a manual DNA excision from an agarose gel. This method was found to lack precision and repeatability, especially due to the inaccurate migration of several DNA ladders. It was replaced by an automated size selection system (BluePippin (c)), with higher DNA recovery and more precise size range as a result.

(vi) New protocol. All these optimisations have been gathered in a revised bench protocol *Updated RAD-sequencing protocol*, p. 357.

Updated RAD-sequencing protocol

This is a modified bench version of the original protocol by Paul D. Etter Baird *et al.* 2008. We found it to improve the overall yield and efficiency of the process, as well as speeding it up. As it is, the library preparation proper can be performed in two (long) days, not including library validation. A typical workflow would be (1) DNA extraction optimization – that may take a while. (2) On the first run, some steps need parameter optimization. This may take some time too. (3) Sample selection, library planning, DNA quantification – one day. (4) Library preparation Stage 1 – one day. (5) Library preparation Stages 2 and 3 may be combined in one day. The only limit to this is that the whole beads-in Stage 3 should not be stopped overnight, but rather performed in one stretch.

Required reagents and stock solutions

Adapter alignment buffer: Prepare a 10X stock that will be kept at +4°C.

- 500 mM NaCl

- 100 mM Tris-Cl

- adjust pH to 7.5-8.0 with H2SO4 (or NaOH).

Binding solution: Prepare a 1X stock that will be kept at +4°C. An aliquot will be brought to room temperature for library preparation. Polyethylene-glycol with high NaCl allows the re-precipitation of DNA on magnetic beads. The final concentration of NaCl determines the lower selected DNA size clip-off. Is it critical to calibrate each batch of this solution so that only DNA

fragments smaller than 200bp are left out. The ratio between the (theoretically salt-free) DNA solution and the binding solution that allows for proper size selection varies from batch to batch, we call it *k* along the protocol. *k* should be anywhere between 0.8 and 1.2.

- 10g polyethylene-glycol (PEG-8000)

- 7.3g NaCl

- 50mL H2O

- mix until the solution is totally clear.

How to calibrate that : Dilute 50bp DNA ladder to 0.5X in EB buffer, make 12*50µL aliquots. Add 75 µL AmpureXP beads to each, mix for 10min. Rinse twice in fresh 80% EtOH according to the standard protocol. Dry to near-cracking point. Resuspend each bead pellet in 50 µL EB buffer. Add binding solution in increasing volume, from 15 µL (0.3X) to 70 µL (1.4X). Mix for 10min. Repeat the rinsing and drying steps. Elute in 50 µL EB buffer. Run on a BioAnalyser DNA1000 chip. Appropriate ratio should cut the ladder around 200bp without affecting the molarity of the 250bp peak.

DNA extraction and purification: W e will n eed h igh-quality, p ure g enomic D NA - Qiagen DNeasy do fine f or a nimal b lood o r t issue s amples, b ut o ther m ethods p erform j ust a s well. Check size range on a 1% agarose gel: there should be a clear, concentrated band above 10 kb. If in doubt, perform additional bead cleaning with stringent size selection to gkeep only high molecular weight DNA.

Setting up the library: Starting setup : small pools seem better for diversity. Say 12 Gb genome per pool (*e.g.* 8 penguins of 16 tuna fishes). Take e nough for 2 s onication r uns i f p ossible, i.e. each pool should sum up to 6 µg DNA (8 samples with 750 ng each for ex).

STAGE 1 : Barcoding steps

Dilution: Prepare dilutions in PCR strips. For each sample, dilute the chosen amount of DNA up to 40 µL. If DNA concentrations range widely (more than a 1:3 ratio between the extremes), it is safer to do a pre-dilution of the more concentrated samples in EB buffer, in order to keep the Tris concentration roughly equal in all samples.

Restriction: Performed in a total volume of 50 µL with 1X NEB Cutsmart buffer. Conditions may need to be adjusted for different restriction enzymes. If the enzyme can't be heat-inactivated, it is not necessary to purify it, but one should be careful to choose P1 adapters that will not recreate the cutsite, in case there would be residual restriction activity at the lower ligation temperature. I.e. if using PstI-HF (cutting on GTGCA|C), one should avoid P1 adapters whose barcodes end with a C base, as these will reconstruct the cutsite, and P1 adapter may be re-cut as soon as ligated int he next step.

        - 5 µL 10X Cutsmart buffer

        - 4.5 µL H20 (or qsp 10 µL)

        - 0.5 µL SbfI-HF

        - 37°C for 90min (restriction)

        - 80°C for 20min (inactivation)

        - cooldown at -1°C per minute to 8°C (re-hybridization).

Ligation: Determine appropriate amount of P1 adapters. This depends on the number of cutsites and the amount of DNA. For SbfI on the penguin genome : 5 µL at 2 µM for 1 µg DNA.

How to calibrate that : in the initial setup, pick a representative sample with enough excess DNA. Prepare 8 digestions, ideally with the planned final amount of DNA (eg 750 ng). After digestion, pool them, mix, and re-aliquot into 8x50 µL reactions. Keep a sample as a digestion control. Add a gradient of P1 concentrations, starting at 0. Perform ligation on all except the digest control. Run the product on a TapeStation gDNA chip. Concentration is good when no higher-molecular-weight (religated) DNA is observed. Highest possible molecular weight should be visi-

ble in the ligation with no P1. Pay attention to the apparition of P1 dimers around 130bp : when

they start increasing noticeably, P1 has reached saturation. Just-saturated P1 is fine.

NOTE: with the Vienna adapters, use 5µL of 0.1µM adapters per sample.

Into each digested product, add the barcoded P1 adapter (it helps to prepare the P1 dilutions in

PCR strips and use a multichannel pipette to add them to the reactions).

- n µL P1.

- mix thoroughly.

Adapters must be added before the ligation premix, in order to avoid gDNA religation.

- 1 µL NEB Cutsmart buffer

- 0.6 µL rATP (100 nM)

- 0.5 µL T4 ligase (2,000,000 U/mL)

- H20 qsp (7.9-n) µL

Add (10-n) µL of this mix to each reaction. Mix throroughly by pipetting (no vortexing). Liga-

tion is done overnight with a cycle protocol :

- [10°C +2°C/30" until 30°C, then -2°C/30" until 22°C]

(96 cycles of 10min, 16h total)

- 65°C for 20'

- -1°C per minute down to 8°C.

This takes about 17 hours to run and should be performed overnight. The increase in efficiency

compared to room temperature ligation is worth it.

STAGE 2 : Shearing and selection

Pooling: At this stage, every sample is hopefully uniquely barcoded. Aliquots from each sample can be combined in a single tube, for a total of 3 µg DNA per pool. Volume will vary depending on initial DNA concentration. The rest of the samples is better not pooled in case barcoding needs to be re-done, and can be frozen until then.

Sonication: Performed on the Bioruptor at 2°C, high power. Conditions need to be calibrated for each type of organism and gDNA quality. For penguins, 7 cycles of 30"ON/30"OFF gives optimal results. Each TPX tube can sonicate a maximum of 300 µL : if the pool is larger than this, split it across several tubes.

How to calibrate that : pick a representative sample with excess DNA, take a series of 1.5 µg DNA aliquots in a volume of 200 µL, and try a range of cycle numbers (6-9-12-15 on the first try). Purify the product into 30 µL EB buffer and run on a 2% agarose gel. The best range should put the bulk of the DNA between 300 and 600bp. When the range is determined, repeat with finer steps, purify and run on a BioAnalyzer DNA chip. Optimal conditions give the highest molarity (not concentration !) between 300 and 600bp. Use the manual integration tool to obtain the molarity in the 300-600bp range and in the 600-900bp range. Calculate the M600-900/M300-600 ratio. The lowest value gives the best condition possible, as it indicates the conditions that allow most fragments to be recovered in a 300-600bp gel cut. Purify and concentrate the product in a QiaQuick column. Elute in 32 µL EB buffer.

Size selection: Prepare a BluePippin 2% DF gel cassette according to instructions. Set the machine on V1 (internal) marker, with a size selection in the 300bp to 650bp range.

- Add 10 µL Blue Pippin V1 marker solution to each sample (total 40 µL).

- Run the gel (about 90 minutes).

- Run the BluePippin according to instruction sheet.

- Take out the ~40 µL eluate into a LoBind tube.

- Replace by 40 µL EB buffer. Let stand for 5 min.

- Add these 40 µL to the eluate.

- Add EB buffer qsp. 100 µL.

STAGE 3 : Fragment preparation

Initial bead purification: The beads we add at this stage will remain in the reaction tube until the end of the library preparation. Make sure they are at room temperature and perfectly homogeneous.

- Add 80 µL AmpureXP beads.

- Mix for 10 min on a vortex or thermomixer at maximum speed.

- Place on the magnetic rack. Let stand for 5 min.

- Remove the 180 µL supernatant and discard it.

- Add 500 µL of fresh 80% ethanol and leave for 2 min.

- Remove and replace by another 500 µL 80% ethanol, leave for 2 min.

- Remove ca. 470 µL (leave a small volume at the bottom of the tube).

- Spin the beads down. Replace on the magnet.

- Remove the remaining ethanol, dry open until bead cracking point.

- Resuspend the beads in 20 µL EB buffer.

End repair: This step converts the overhangs created by sonication into phosphorylated blunt ends. We follow exactly the NEB blunting kit protocol. The reaction is performed directly in the previous tube, with the beads in, but off the magnet. To each library, add :

- 2.5 µL 10X NEB blunting buffer

- 2.5 µL dNTP mix (1 mM)

- 1 µL Blunt enzyme mix.

- Incubate at room temperature for 30min.

- Add k*26 μL binding solution.

- Mix for 10 min.

- Clean (see above) and re-suspend in 43 μL EB buffer.

A-tailing: This step adds a single 3' A-overhang on virtually every blunt end. This makes them compatible with the T-overhang on the P2 adapter. The reaction is performed directly in the previous tube, with the beads in, but off the magnet. To each library, add :

- 5 μL 10X NEB2 buffer

- 1 μL dATP (10 mM)

- 3 μL Klenow exo-

- 37°C for 30min with light mixing (300rpm)

- Cool down to RT.

- Add k*52 μL binding solution.

- Mix for 10 min.

- Clean (see above) and re-suspend in 45 μL EB buffer.

P2 ligation: This step adds the second adapter to every single A-tailed fragment available. For low plexity runs, non-barcoded adapters (P2-Ø) are fine. For higher plexities with combinatorial barcoding, use different P2 adapters (one per library pool). The reaction is performed directly in the previous tube, with the beads in, but off the magnet. To each library :

- 5.2 μL 10X NEB T4 ligase buffer

- 1 μL P2 adapters (10 μM), mix thoroughly

- 0.5 μL T4 ligase (2,000,000 U/mL)

- Incubate 45min at room temperature.

- Add k*52 μL binding solution.

- Mix for 10 min.

- Clean (see above)and elute in 52 μL EB buffer.

- Transfer to a new LoBind tube.

Mark this tube as « Template ». This is the raw library, it will need double-strand adapter conversion and enrichment before sending out for sequencing.

Library validation

Amplification test: A first non-quantitative PCR is done in order to check for correct library preparation. A successful library should amplify without problem (although the strength will vary from one library to another). For each library pool, prepare a reaction with :

- 12.5 μL NEB Phusion polymerase premix

- 7.5 μL H_20

- 1 μL Solexa primer mix (10 μM)

- 4 μL library template.

- Solexa PCR conditions : 98°C 30" ; [98°C 10" | 65°C 30" | 72°C 30"]X18 ; 72°C 5'

- Add 5 μL 6X orange loading dye,

- Load the whole product on a gel with Low Range DNA ladder.

A successful library should yield a bright, well-defined band in the 400-700bp range. If amplification is poor or absent, something probably went wrong during the prep. Good luck with that. If amplification is really good, you may want to test fewer cycles in order to reduce duplication biases to a minimum.

Qubit test: Use 2 μL of each library to measure accurately the dsDNA concentration on the Qubit. A good library with standard DNA loss should be anywhere between 6 and 10 ng.μL^{-1}. A lower concentration may indicate either a sub-optimal sonication (hence excessive DNA loss during size selection) or a generally inefficient purification steps.

Library enrichment: If everything looks good, perform a large-volume PCR with :

1   - 62.5 μL NEB Phusion polymerase premix

2   - 37.5 μL H$_2$0

3   - 5 μL Solexa primer mix (10 μM)

4   - 20 μL library template

5   - Aliquot into 5*25 μL reactions

6   - Amplify

7   - Pool together the aliquots and purify into a final 30 μL EB buffer.

8   Now, the library should consist mostly double-stranded, properly ligated fragments ready for se-

9   quencing. Though this must be checked.

10   **BioAnalyzer check:** The final library should be run together with its template on a BioAnalyzer

11   DNA chip. In order to be in roughly comparable conditions, 2 μL of template should be diluted

12   in 11.5 μL EB buffer (as this is the dilution state in the PCR reaction prior to amplification). On

13   the BioAnalyzer, the library should be at roughly twice as concentrated as the template, and

14   exhibit a clean distribution with no obvious spikes along the amplified section. Spikes indicate

15   clonal populations of highly duplicated fragements. One should also check there is no adapter

16   carryover, especially P1 dimers (which should have all been left out since size selection).

17   **qPCR check:** qPCR assay (Kappa dedicated SybrGreen Illumina kit) allows for the most exact

18   measurement of ligated fragment molarity. This is the final check before loading on the cBot.

References

A

1. Abbott CL, Double MC, Trueman JWH, Robinson A, Cockburn A (2005) An unusual source of apparent mitochondrial heteroplasmy: duplicate mitochondrial control regions in Thalassarche albatrosses. *Molecular ecology*, 14, 3605–3613.

2. Abram NJ, Gagan MK, Cole JE, Hantoro WS, Mudelsee M (2008) Recent intensification of tropical climate variability in the Indian Ocean. *Nature Geoscience*, 1, 849–853.

3. Abram NJ, Mulvaney R, Vimeux F, Phipps SJ, Turner J, England MH (2014) Evolution of the Southern Annular Mode during the past millennium. *Nature Climate Change*, 4, 564–569.

4. Ackerley D, Highwood EJ, Frame DJ (2009) Quantifying the effects of perturbing the physics of an interactive sulfur scheme using an ensemble of GCMs on the climateprediction.net platform. *J. Geophys. Res.*, 114,

5. Acosta CA (1999) Benthic dispersal of Caribbean spiny lobsters among insular habitats: implications for the conservation of exploited marine species. *Conservation Biology*, 13, 603–612.

6. Adams NJ, Klages NT (1987) Seasonal variation in the diet of the king penguin (Aptenodytes patagonicus) at sub Antarctic Marion Island. *Journal of Zoology*, 212, 303–324.

7. Aguiar D, Istrail S (2012) HapCompass: a fast cycle basis algorithm for accurate haplotype assembly of sequence data. *Journal of Computational Biology*, 19, 577–590.

8. Ahmed S, Hart T, Dawson DA, Horsburgh GJ, Trathan PN, Rogers AD (2009) Isolation and characterization of macaroni penguin (Eudyptes chrysolophus) microsatellite loci and their utility in other penguin species (Spheniscidae, AVES). *Mol Ecol Resour*, 9, 1530–1535.

9. Ainley D, Russell J, Jenouvrier S et al. (2010a) Antarctic penguin response to habitat change as Earth's troposphere reaches 2° C above preindustrial levels. *Ecological Monographs*, 80, 49–66.

10. Ainley D, Ballard G, Ackley S et al. (2007) Paradigm lost, or is top-down forcing no longer significant in the Antarctic marine ecosystem. *Antarctic Science*, 19, 283.

11. Ainley D, Ballard G, Blight LK et al. (2010b) Impacts of cetaceans on the structure of Southern Ocean food webs. *Marine Mammal Science*, 26, 482–498.

12. Ainley DG, Blight LK (2009) Ecological repercussions of historical fish extraction from the Southern Ocean. *Fish and Fisheries*,

13. Akst EP, Boersma PD, Fleischer RC (2002) A comparison of genetic diversity between the Galápagos penguin and the Magellanic penguin. *Conservation Genetics*, 3, 375–383.

14. Allendorf FW, Hohenlohe PA, Luikart G (2010) Genomics and the future of conservation genetics. *Nature Reviews Genetics*, 11, 697–709.

15. Amores A, Catchen J, Nanda I et al. (2014) A RAD-tag genetic map for the platyfish (Xiphophorus maculatus) reveals mechanisms of karyotype evolution among teleost fish. *Genetics*, 197, 625–641.

16. Amores A, Catchen J, Ferrara A, Fontenot Q, Postlethwait JH (2011) Genome evolution and meiotic maps by massively parallel DNA sequencing: spotted gar, an

outgroup for the teleost genome duplication. *Genetics*, 188, 799–808.

17.   Amos W, Harwood J (1998) Factors affecting levels of genetic diversity in natural populations. *Philos Trans R Soc Lond B Biol Sci*, 353, 177–186.

18.   Ancel A, Beaulieu M, Gilbert C (2013) The different breeding strategies of penguins: a review. *Comptes rendus biologies*, 336, 1–12.

19.   Ancel A, Beaulieu M, Le Maho Y, Gilbert C (2009) Emperor penguin mates: keeping together in the crowd. *Proc Biol Sci*, 276, 2163–2169.

20.   Ancel A, Cristofari R, Fretwell PT et al. (2014) Emperors in hiding: when icebreakers and satellites complement each other in Antarctic exploration. *PLoS One*, 9, e100404.

21.   Ancel A, Rodary D, Wienecke B, Le Maho Y, Gilbert C (1999) Exploration biologique de la polynie de Mertz. *Rapport d'Activité de l'IFRTP*, 40–44.

22.   Ancel A, Kooyman GL, Ponganis PJ et al. (1992) Foraging behaviour of emperor penguins as a resource detector in winter and summer. *Nature*, 360, 336–339.

23.   Anderson JB, Shipp SS, Lowe AL, Wellner JS, Mosola AB (2002) The Antarctic Ice Sheet during the Last Glacial Maximum and its subsequent retreat history: a review. *Quaternary Science Reviews*, 21, 49–70.

24.   Anderson MG, Rhymer JM, Rohwer FC (1992) Philopatry, dispersal, and the genetic structure of waterfowl populations. *Ecology and management of breeding waterfowl. University of Minnesota Press, Minneapolis, MN*, 365–395.

25.   Anderson RF, Ali S, Bradtmiller LI et al. (2009) Wind-driven upwelling in the Southern Ocean and the deglacial rise in atmospheric CO2. *science*, 323, 1443–1448.

26.   Arango CP, Soler-Membrives A, Miller KJ (2011) Genetic differentiation in the circum-Antarctic sea spider Nymphon australe. *Deep Sea Research Part II: Topical Studies in Oceanography*, 58, 212–219.

27.   Araya Modinger B, Duffy DC (1987) Animal introduction to Isla Chanaral, Chile; their history and effect on seabirds. *Cormorant*, 15, 3–6.

28.   Arenas M (2013) The importance and application of the ancestral recombination graph. *Front Genet*, 4, 206.

29.   Arenas M, Ray N, Currat M, Excoffier L (2012) Consequences of range contractions and range shifts on molecular diversity. *Molecular Biology and Evolution*, 29, 207–218.

30.   Armand LK, Leventer A (2010) Palaeo sea ice distribution and reconstruction derived from the geological records. In: *Sea ice*, pp. 469–530.

31.   Armitage KB (1981) Sociality as a life-history tactic of ground squirrels. *Oecologia*, 48, 36–49.

32.   Arnaud CM, Dobson FS, Murie JO (2012) Philopatry and within-colony movements in Columbian ground squirrels. *Molecular Ecology*, 21, 493–504.

33.   Arrigo K, Worthen DL, Dixon PL, Lizotte MP (1998) Primary productivity of near surface communities within Antarctic pack ice. *Antarctic Sea Ice: Biological Processes, Interactions and Variability*, 23–43.

34.   Arrigo KR, Worthen DL, Lizotte MP, Dixon P, Dieckmann G (1997) Primary production in Antarctic sea ice. *Science*, 276, 394–397.

35.   Ashok K, Guan Z, Saji NH, Yamagata T (2004) Individual and combined influences of ENSO and the Indian Ocean dipole on the Indian summer monsoon. *Journal of Climate*, 17, 3141–3155.

36. Augustin L, Barbante C, Barnes PR et al. (2004) Eight glacial cycles from an Antarctic ice core. *Nature*, 429, 623–628.

37. Auld JR, Agrawal AA, Relyea RA (2009) Re-evaluating the costs and limits of adaptive phenotypic plasticity. *Proceedings of the Royal Society of London B: Biological Sciences*, rspb20091355.

38. Avise JC, Nelson WS, Bowen BW, Walker D (2000) Phylogeography of colonially nesting seabirds, with special reference to global matrilineal patterns in the sooty tern (Sterna fuscata). *Molecular Ecology*, 9, 1783–1792.

39. Axelsson E, Webster MT, Smith NGC, Burt DW, Ellegren H (2005) Comparison of the chicken and turkey genomes reveals a higher rate of nucleotide divergence on microchromosomes than macrochromosomes. *Genome Research*, 15, 120–125.

B

40. Baird NA, Etter PD, Atwood TS et al. (2008) Rapid SNP discovery and genetic mapping using sequenced RAD markers. *PloS one*, 3, e3376.

41. Baker AJ, Tavares ES, Elbourne RF (2009) Countering criticisms of single mitochondrial DNA gene barcoding in birds. *Molecular Ecology Resources*, 9, 257–268.

42. Baker AJ, Pereira SL, Haddrath OP, Edge K-A (2006) Multiple gene evidence for expansion of extant penguins out of Antarctica due to global cooling. *Proceedings of the Royal Society B: Biological Sciences*, 273, 11–17.

43. Baker CS, Slade RW, Bannister JL et al. (2008) Hierarchical structure of mitochondrial DNA gene flow among humpback whales Megaptera novaeangliae, world-wide. *Molecular Ecology*, 3, 313–327.

44. Bakun A (2006) Wasp-waist populations and marine ecosystem dynamics: navigating the predator pit topographies. *Progress in Oceanography*, 68, 271–288.

45. Ballard G, Toniolo V, Ainley DG, Parkinson CL, Arrigo KR, Trathan PN (2010) Responding to climate change: Adélie penguins confront astronomical and ocean boundaries. *Ecology*, 91, 2056–2069.

46. Ballou JD (1997) Ancestral inbreeding only minimally affects inbreeding depression in mammalian populations. *Journal of Heredity*, 88, 169–178.

47. Balloux F, Amos W, Coulson T (2004) Does heterozygosity estimate inbreeding in real populations? *Mol Ecol*, 13, 3021–3031.

48. Balloux F, Lugon-Moulin N (2002) The estimation of population differentiation with microsatellite markers. *Molecular ecology*, 11, 155–165.

49. Banks J, Van Buren A, Cherel Y, Whitfield JB (2006) Genetic evidence for three species of rockhopper penguins, Eudyptes chrysocome. *Polar Biology*, 30, 61–67.

50. Banks SC, Peakall ROD (2012) Genetic spatial autocorrelation can readily detect sex-biased dispersal. *Molecular ecology*, 21, 2092–2105.

51. Barbante C, Barnola J-M, Becagli S et al. (2006) One-to-one coupling of glacial climate variability in Greenland and Antarctica. *Nature*, 444, 195–198.

52. Barber-Meyer SM, Kooyman GL, Ponganis PJ (2007) Estimating the relative abundance of emperor penguins at inaccessible colonies using satellite imagery. *Polar Biology*, 30, 1565–1570.

53. Barbosa A, Palacios MJ (2009) Health of Antarctic birds: a review of their parasites, pathogens and diseases. *Polar Biology*, 32, 1095–1115.

54.   Barbraud C, Gavrilo M, Mizin Y, Weimerskirch H (2011) Comparison of emperor penguin declines between Pointe Géologie and Haswell Island over the past 50 years. *Ant Sci*, 23, 461–468.

55.   Barbraud C, Jouventin P (1998) What causes body size variation in the Snow Petrel Pagodroma nivea. *Journal of Avian Biology*, 29, 161–171.

56.   Barbraud C, Weimerskirch H (2001a) Emperor penguins and climate change. *Nature*, 411, 183–186.

57.   Barbraud C, Weimerskirch H (2001b) Contrasting effects of the extent of sea ice on the breeding performance of an Antarctic top predator, the Snow Petrel Pagodroma nivea. *Journal of Avian Biology*, 32, 297–302.

58.   Barker JSFS (2008) Adaptation and Fitness in Animal Populations: Evolutionary and Breeding Perspectives on Genetic Resource Management. Adaptation and Fitness in Animal Populations, 3–14.

59.   Barlow EJ, Daunt F, Wanless S, Reid JM (2013) Estimating dispersal distributions at multiple scales: within-colony and among-colony dispersal rates, distances and directions in European Shags. *Ibis*, 155, 762–778.

60.   Barnosky AD, Hadly EA, Bascompte J et al. (2012) Approaching a state shift in Earth's biosphere. *Nature*, 486, 52–58.

61.   Baroni C, Orombelli G (1994) Abandoned penguin rookeries as Holocene paleoclimatic indicators in Antarctica. *Geology*, 22, 23–26.

62.   Barrat A (1976) Quelques aspects de la biologie et de l'écologie du manchot royal Aptenodytes patagonicus des îles Crozet. *Com. Nat. Fr. Rech. Ant*, 40, 9–51.

63.   Barron JA (1996) Diatom constraints on the position of the Antarctic Polar Front in the middle part of the Pliocene. *Marine micropaleontology*, 27, 195–213.

64.   Bathmann UV, Scharek R, Klaas C, Dubischar CD, Smetacek V (1997) Spring development of phytoplankton biomass and composition in major water masses of the Atlantic sector of the Southern Ocean. *Deep Sea Research Part II: Topical Studies in Oceanography*, 44, 51–67.

65.   Bauer S, Gienapp P, Madsen J (2008) The relevance of environmental conditions for departure decision changes en route in migrating geese. *Ecology*, 89, 1953–1960.

66.   Beaufort L, de Garidel-Thoron T, Mix AC, Pisias NG (2001) ENSO-like forcing on oceanic primary production during the late Pleistocene. *Science*, 293, 2440–2444.

67.   Beaugrand G, Edwards M, Raybaud V, Goberville E, Kirby RR (2015) Future vulnerability of marine biodiversity compared with contemporary and past changes. *Nature Clim. Change*, 5, 695–701.

68.   Beaugrand G, Reid PC, Ibanez F, Lindley JA, Edwards M (2002) Reorganization of North Atlantic marine copepod biodiversity and climate. *Science*, 296, 1692–1694.

69.   Becker BH, Beissinger SR (2006) Centennial decline in the trophic level of an endangered seabird after fisheries decline. *Conservation Biology*, 20, 470–479.

70.   Beerli P, Palczewski M (2010) Unified framework to evaluate panmixia and migration direction among multiple sampling locations. *Genetics*, 185, 313–326.

71.   Beerli P (2004) Effect of unsampled populations on the estimation of population sizes and migration rates between sampled populations. *Molecular Ecology*, 13, 827–836.

72.   Beerli P (2006) Comparison of Bayesian and maximum-likelihood infer-

ence of population genetic parameters. *Bioinformatics*, 22, 341–345.

73. Behrenfeld MJ, O Malley RT, Siegel DA et al. (2006) Climate-driven trends in contemporary ocean productivity. *Nature*, 444, 752–755.

74. Behrenfeld MJ, Randerson JT, Mc-Clain CR et al. (2001) Biospheric primary production during an ENSO transition. *Science*, 291, 2594–2597.

75. Bellard C, Bertelsmeier C, Leadley P, Thuiller… W (2012) Impacts of climate change on the future of biodiversity. *Ecology …*,

76. Berger A (2013) Milankovitch and climate: understanding the response to astronomical forcing. *Nato ASI Series*, 126,

77. Bergson H (1911) Life and consciousness.

78. Berry PM, Dawson TP, Harrison PA, Pearson RG (2002) Modelling potential impacts of climate change on the bioclimatic envelope of species in Britain and Ireland. *Global ecology and biogeography*, 11, 453–462.

79. Berthold P (1991) Genetic control of migratory behaviour in birds. *Trends in Ecology & Evolution*, 6, 254–257.

80. Bertrand R, Lenoir J, Piedallu C et al. (2011) Changes in plant community composition lag behind climate warming in lowland forests. *Nature*, 479, 517–520.

81. Bhatia G, Patterson N, Sankararaman S, Price AL (2013) Estimating and interpreting FST: the impact of rare variants. *Genome Res*, 23, 1514–1521.

82. Bicknell AWJ, Knight ME, Bilton D, Reid JB, Burke T, Votier SC (2012) Population genetic structure and long-distance dispersal among seabird populations: Implications for colony persistence. *Molecular Ecology*, 21, 2863–2876.

83. Billiard S, Lenormand T (2005) Evolution of migration under kin selection and local adaptation. *Evolution*, 59, 13–23.

84. Billing TM, Guay PJ, Peucker AJ, Mulder RA (2007) Isolation and characterization of polymorphic microsatellite loci for the study of paternity and population structure in the little penguin Eudyptula minor. *Molecular Ecology Notes*, 7, 425–427.

85. Bintanja R, van Oldenborgh GJ, Katsman CA (2015) The effect of increased fresh water from Antarctic ice shelves on future trends in Antarctic sea ice. *Annals of Glaciology*, 56, 69.

86. Bivand RS, Hauke, J., and Kossowski, T. (2013) Computing the Jacobian in Gaussian spatial autoregressive models: An illustrated comparison of available methods. *Geographical Analysis*, 45, 150–179.

87. Blais JM, Kimpe LE, McMahon D et al. (2005) Arctic seabirds transport marine-derived contaminants. *Science*, 309, 445–445.

88. Blois JL, Zarnetske PL, Fitzpatrick MC, Finnegan S (2013) Climate change and the past, present, and future of biotic interactions. *Science*, 341, 499–504.

89. Boessenkool S, Austin JJ, Worthy TH et al. (2009a) Relict or colonizer? Extinction and range expansion of penguins in southern New Zealand. *Proceedings of the Royal Society B: Biological Sciences*, 276, 815–821.

90. Boessenkool S, Star B, Waters JM, Seddon PJ (2009b) Multilocus assignment analyses reveal multiple units and rare migration events in the recently expanded yellow-eyed penguin (Megadyptes antipodes). *Molecular ecology*, 18, 2390–2400.

91. Bolnick DI, Amarasekare P, Araújo MS et al. (2011) Why intraspecific trait variation matters in community ecology. *Trends in ecology & evolution*, 26, 183–192.

92. Bonin CA, Goebel ME, Forcada J, Burton RS, Hoffman JI (2013) Unexpected genetic differentiation between recently recolonized populations of a long-lived and highly vagile marine mammal. *Ecol Evol*, 3, 3701–3712.

93. Borboroglu PG, Boersma PD (2013) Penguins: natural history and conservation.

94. Bost C-A, Delord K, Barbraud C et al. (2013) King Penguin. In: *Penguins, Natural history and conservation*, (eds Borboroglu PG, Boersma D), pp. 7–21. University of Washington Press, Seattle & London.

95. Bost CA, Cotté C, Terray P et al. (2015) Large-scale climatic anomalies affect marine predator foraging behaviour and demography. *Nat Commun*, 6, 8220.

96. Bost C-A, Cotté C, Bailleul F et al. (2009) The importance of oceanographic fronts to marine birds and mammals of the southern oceans. *Journal of Marine Systems*, 78, 363–376.

97. Both C, Bouwhuis S, Lessells CM, Visser ME (2006) Climate change and population declines in a long-distance migratory bird. *Nature*, 441, 81–83.

98. Bouckaert R, Heled J, Kuhnert D et al. (2014) BEAST 2: a software platform for Bayesian evolutionary analysis. *PLoS Comput Biol*, 10, e1003537.

99. Bouzat JL, Walker BG, Boersma PD (2009) Regional genetic structure in the Magellanic Penguin (Spheniscus magellanicus) suggests metapopulation dynamics. *The Auk*, 126, 326–334.

100. Bowen WD, Siniff DB (1999) Distribution, population biology, and feeding ecology of marine mammals. *Biology of marine mammals*, 423–484.

101. Bowler DE, Benton TG (2005) Causes and consequences of animal dispersal strategies: relating individual behaviour to spatial dynamics. *Biological Reviews*, 80, 205–225.

102. Box EEO (1981) Macroclimate and plant forms: an introduction to predictive modeling in phytogeography.

103. Boyd IL, Arnbom T (1991) Diving behaviour in relation to water temperature in the southern elephant seal: foraging implications. *Polar Biology*, 11, 259–266.

104. Braconnot P, Harrison SP, Kageyama M et al. (2012) Evaluation of climate models using palaeoclimatic data. *Nature Climate Change*, 2, 417–424.

105. Braconnot P, Harrison SP, Otto-Bliesner B, Abe-Ouchi A, Jungclaus J, Peterschmitt J-Y (2011) The paleoclimate modeling intercomparison project contribution to CMIP5. *CliVAR Exchanges*, 56, 2.

106. Bradshaw WE, Holzapfel CM (2006) Evolutionary response to rapid climate change. *Science(Washington)*, 312, 1477–1478.

107. Braudel F (1949) La Méditerranée et le monde méditerranéen à l'époque de Philippe II.

108. Braudel F (1958) La Longue durée. *Histoire et Sciences Sociales*, 13, 725–753.

109. Braudel F (1969) Ecrits sur l'histoire.

110. Bried J, Jiguet F, Jouventin P (1999) Why do Aptenodytes penguins have high divorce rates? *The Auk*, 504–512.

111. Bried J, Jouventin P (2001) The King Penguin Aptenodytes patagonicus, a non-nesting bird which selects its breeding habitat. *Ibis*, 143, 670–673.

112. Bried J, Nicolaus M, Jarne P, Dubois MP, Jouventin P (2007) Population biology of the wandering albatross (Diomedea exulans) in the Crozet and Kerguelen archipelagos, southern Indian Ocean, approached

through genetic and demographic methods. *Journal of Zoology*, 272, 20–29.

113.   Brierley AS, Fernandes PG, Brandon MA et al. (2002) Antarctic krill under sea ice: elevated abundance in a narrow band just south of ice edge. *Science*, 295, 1890–1892.

114.   Brodin A, Olsson O, Clark CW (1998) Modeling the breeding cycle of long-lived birds: Why do king penguins try to breed late? *The Auk*, 115, 767–771.

115.   Bromwich DH, Nicolas JP, Monaghan AJ et al. (2013) Central West Antarctica among the most rapidly warming regions on Earth. *Nature Geoscience*, 6, 139–145.

116.   Browning SR, Browning BL (2011) Haplotype phasing: existing methods and new developments. *Nature Reviews Genetics*, 12, 703–714.

117.   Bryant D, Bouckaert R, Felsenstein… J (2012) Inferring species trees directly from biallelic genetic markers: bypassing gene trees in a full coalescent analysis. *Molecular biology and …*,

118.   Budd GM (1961) The biotopes of emperor penguin rookeries. *Emu*, 61, 171–189.

119.   Budd GM (1962) Population studies in rookeries of the Emperor Penguin Aptenodytes forsteri. Proceedings of the Zoological Society of London 139, 365–388.

120.   Budd GM (2000) Changes in Heard Island glaciers, king penguins and fur seals since 1947. Papers and Proceedings of the Royal Society of Tasmania 133, 47–60.

121.   Burckle LH (1984) Diatom distribution and paleoceanographic reconstruction in the Southern Ocean Present and Last Glacial Maximum. *Marine Micropaleontology*, 9, 241–261.

122.   Burg TM, Croxall JP (2004) Global population structure and taxonomy of the wandering albatross species complex. *Molecular Ecology*, 13, 2345–2355.

123.   Burridge CP, Peucker AJ, Valautham SK, Styan CA, Dann P (2015) Nonequilibrium Conditions Explain Spatial Variability in Genetic Structuring of Little Penguin (Eudyptula minor). *Journal of Heredity*, 106, 228–237.

124.   Burrows MT, Schoeman DS, Buckley LB et al. (2011) The pace of shifting climate in marine and terrestrial ecosystems. *Science*, 334, 652–655.

125.   Burrows MT, Schoeman DS, Richardson AJ et al. (2014) Geographical limits to species-range shifts are suggested by climate velocity. *Nature*, 507, 492–495.

C

126.   Cabré A, Marinov I, Bernardello R, Bianchi D (2015) Oxygen minimum zones in the tropical Pacific across CMIP5 models: mean state differences and climate change trends. *Biogeosciences Discussions*, 12,

127.   Cain ML, Milligan BG, Strand AE (2000) Long-distance seed dispersal in plant populations. *American Journal of Botany*, 87, 1217–1227.

128.   Cairns DK (1988) Seabirds as indicators of marine food supplies. *Biological Oceanography*,

129.   Calvo E, Pelejero C, De Deckker P, Logan GA (2007) Antarctic deglacial pattern in a 30 kyr record of sea surface temperature offshore South Australia. *Geophysical Research Letters*, 34,

130.   Cariou M, Duret L, Charlat S (2013) Is RAD-seq suitable for phylogenetic inference? An in silico assessment and optimization. *Ecol Evol*, 3, 846–852.

131.   Carr MH, Neigel JE, Estes JA, Andelman S, Warner RR, Largier JL (2003) Comparing marine and terrestrial ecosys-

tems: implications for the design of coastal marine reserves. *Ecological Applications*, 13, 90–107.

132. Carr M-E, Friedrichs MAM, Schmeltz M et al. (2006) A comparison of global estimates of marine primary production from ocean color. *Deep Sea Research Part II: Topical Studies in Oceanography*, 53, 741–770.

133. Catchen JM, Amores A, Hohenlohe P, Cresko W, Postlethwait JH (2011) Stacks: building and genotyping loci de novo from short-read sequences. *G3: Genes, Genomes, Genetics*, 1, 171–182.

134. Catchen JM, Hohenlohe PA, Bassham S, Amores A, Cresko WA (2013) Stacks: an analysis tool set for population genomics. *Molecular ecology*, 22, 3124–3140.

135. Celia B, Claire S, Viblanc Vincent A, Helene G-N, Magali B, Le Maho Yvon LBC (2014) Inter-Annual Variability of Fledgling Sex Ratio in King Penguins. *Plos One*, 9, 1–17.

136. Chapman EW, Hofmann EE, Patterson DL, Fraser WR (2010) The effects of variability in Antarctic krill (Euphausia superba) spawning behavior and sex/maturity stage distribution on Adélie penguin (Pygoscelis adeliae) chick growth: a modeling study. *Deep Sea Research Part II: Topical Studies in Oceanography*, 57, 543–558.

137. Charles CD, Froelich PN, Zibello MA, Mortlock RA, Morley JJ (1991) Biogenic opal in Southern Ocean sediments over the last 450,000 years: Implications for surface water chemistry and circulation. *Paleoceanography*, 6, 697–728.

138. Charmantier A, McCleery RH, Cole LR, Perrins C, Kruuk LE, Sheldon BC (2008) Adaptive phenotypic plasticity in response to climate change in a wild bird population. *Science*, 320, 800–803.

139. Charrassin J-B, Bost C-A (2001) Utilisation of the oceanic habitat by king penguins over the annual cycle. *Marine Ecology Progress Series*, 221, 285–298.

140. Chen I-C, Hill JK, Ohlemüller R, Roy DB, Thomas CD (2011) Rapid range shifts of species associated with high levels of climate warming. *Science*, 333, 1024–1026.

141. Cherel Y, Pütz K, Hobson KA (2002) Summer diet of king penguins (Aptenodytes patagonicus) at the Falkland Islands, southern Atlantic Ocean. *Polar Biology*, 25, 898–906.

142. Chereskin TK, Donohue KA, Watts DR, Tracey KL, Firing YL, Cutting AL (2012) cDrake: Dynamics and transport of the Antarctic Circumpolar Current in Drake Passage. *Oceanography*, 25, 134–135.

143. Cherry-Garrard A (1922) The worst journey in the world.

144. Chevin LM, Decorzent G, Lenormand T (2014) Niche dimensionality and the genetics of ecological speciation. *Evolution*, 68, 1244–1256.

145. Chikhi L, Sousa VC, Luisi P, Goossens B, Beaumont MA (2010) The confounding effects of population structure, genetic diversity and the sampling scheme on the detection and quantification of population size changes. *Genetics*, 186, 983–995.

146. Chown SL, Clarke A, Fraser CI, Cary SC, Moon KL, McGeoch MA (2015) The changing form of Antarctic biodiversity. *Nature*, 522, 431–438.

147. Ciasto LM, Thompson DWJ (2008) Observations of large-scale ocean-atmosphere interaction in the Southern Hemisphere. *Journal of Climate*, 21, 1244–1259.

148. Clarke AL, Sæther BE, Røskaft E (1997) Sex biases in avian dispersal: a reappraisal. *Oikos*, 429–438.

149. Clarke JA, Ksepka DT, Stucchi M et al. (2007) Paleogene equatorial penguins challenge the proposed relationship between biogeography, diversity, and Cenozoic climate change. *Proceedings of the National Academy of Sciences*, 104, 11545–11550.

150. CLIMAP (1981) Seasonal Reconstructions of the Earth's surface at the Last Glacial Maximum.

151. Collins MA, Xavier JC, Johnston NM et al. (2008) Patterns in the distribution of myctophid fish in the northern Scotia Sea ecosystem. *Polar Biology*, 31, 837–851.

152. Collins M, An S-I, Cai W et al. (2010) The impact of global warming on the tropical Pacific Ocean and El Niño. *Nature Geoscience*, 3, 391–397.

153. Comte L, Murienne J, Grenouillet G (2014) Species traits and phylogenetic conservatism of climate-induced range shifts in stream fishes. *Nat Commun*, 5, 5023.

154. Convey P, Barnes DKA, Griffiths HJ, Grant SM, Linse K, Thomas DN (2012) Biogeography and regional classifications of Antarctica. *Antarctic Ecosystems: An extreme environment in a changing world*, 469–491.

155. Convey P, Morton A, Poncet J (1999) Survey of marine birds and mammals of the South Sandwich Islands. *Polar Record*, 35, 107–124.

156. Convey P, Stevens MI, Hodgson DA et al. (2009) Exploring biological constraints on the glacial history of Antarctica. *Quaternary Science Reviews*, 28, 3035–3048.

157. Cooper CB, Daniels SJ, Walters JR (2008) Can we improve estimates of juvenile dispersal distance and survival. *Ecology*, 89, 3349–3361.

158. Coria NR, Montalti D (2000) A newly discovered breeding colony of emperor penguins Aptenodytes forsteri. *Marine Ornithology*, 28, 119–120.

159. Cornet C (2014) The adaptive capacities of seabirds to face environmental variability: the role of heterogeneity within populations. PhD.

160. Cortés Labra M (2007) Ajustes fisiologicos para la nidificacion en cuevas: el caso de Pelecanoides garnotii, un enfoque evolutivo. Magister.

161. Coté SD (2000) Aggressiveness in king penguins in relation to reproductive status and territory location. *Anim Behav*, 59, 813–821.

162. Coulson JC (2002) Colonial breeding in seabirds. In 'Biology of Marine Birds.(Eds EA Schreiber and J. Burger.) pp. 87-113.

163. Cowie RH, Holland BS (2006) Dispersal is fundamental to biogeography and the evolution of biodiversity on oceanic islands. *Journal of Biogeography*, 33, 193–198.

164. Crawford TJ (1984) The estimation on neighbourhood parameters for plant populations. *Heredity*, 52, 273–283.

165. Cressey D (2015) World's whaling slaughter tallied. *Nature*, 519, 140–141.

166. Croxall JP, Butchart SHM, Lascelles B et al. (2012) Seabird conservation status, threats and priority actions: a global assessment. *Bird Conservation International*, 22, 1–34.

167. Croxall JP, Silk JRD, Phillips RA, Afanasyev V, Briggs DR (2005) Global circumnavigations: tracking year-round ranges of nonbreeding albatrosses. *Science*, 307, 249–250.

168. Croxall JP, Trathan PN, Murphy EJ (2002) Environmental change and Antarctic seabird populations. *Science*, 297, 1510.

169. Cruaud A, Gautier M, Galan M et al. (2014) Empirical assessment of RAD sequencing for interspecific phylogeny. *Mol Biol Evol*, 31, 1272–1274.

170.   Cury PM, Boyd IL, Bonhommeau S et al. (2011) Global seabird response to forage fish depletion—one-third for the birds. *Science*, 334, 1703–1706.

D

171.   Damerau M, Matschiner M, Salzburger W, Hanel R (2012) Comparative population genetics of seven notothenioid fish species reveals high levels of gene flow along ocean currents in the southern Scotia Arc, Antarctica. *Polar biology*, 35, 1073–1086.

172.   Danchin E, Wagner RH (1997) The evolution of coloniality: the emergence of new perspectives. *Trends in Ecology & Evolution*, 12, 342–347.

173.   Danecek P, Auton A, Abecasis G et al. (2011) The variant call format and VCFtools. *Bioinformatics*, 27, 2156–2158.

174.   Darwin C (1859) On the origin of species.

175.   Davey JW, Blaxter ML (2010) RAD-Seq: next-generation population genetics. *Briefings in Functional Genomics*, 9, 416.

176.   Davey JW, Hohenlohe PA, Etter PD, Boone JQ, Catchen JM, Blaxter ML (2011) Genome-wide genetic marker discovery and genotyping using next-generation sequencing. *Nature Reviews Genetics*, 12, 499–510.

177.   Davis AJ, Jenkinson LS, Lawton JH, Shorrocks B, Wood S (1998) Making mistakes when predicting shifts in species range in response to global warming. *Nature*, 391, 783–786.

178.   Davis MB, Shaw RG (2001) Range shifts and adaptive responses to Quaternary climate change. *Science*, 292, 673–679.

179.   De Boer AM, Toggweiler JR, Sigman DM (2008) Atlantic dominance of the meridional overturning circulation. *Journal of Physical Oceanography*, 38, 435–450.

180.   de Bruyn M, Hall BL, Chauke LF, Baroni C, Koch PL, Hoelzel AR (2009) Rapid response of a marine mammal species to holocene climate and habitat change. *PLoS Genet*, 5, e1000554.

181.   De Dinechin M, Dobson S, Zehtindjiev P et al. (2012) The biogeography of Gentoo Penguins. *Can. J. Zool*, 90, 353–361.

182.   De Dinechin M, Ottvall R, Quillfeldt P, Jouventin P (2008) Speciation chronology of rockhopper penguins inferred from molecular, geological and palaeoceanographic data. *Journal of Biogeography*, 36, 693–702.

183.   de Lavergne C, Palter JB, Galbraith ED, Bernardello R, Marinov I (2014) Cessation of deep convection in the open Southern Ocean under anthropogenic climate change. *Nature Climate Change*, 4, 278–282.

184.   Dearborn DC, Anders AD, Schreiber EA, Adams RMM, Mueller UG (2003) Inter-island movements and population differentiation in a pelagic seabird. *Molecular Ecology*, 12, 2835–2843.

185.   Delord K, Barbraud C, Weimerskirch H (2004) Long-term trends in the population size of king penguins at Crozet archipelago: environmental variability and density dependence? *Polar Biology*, 27, 793–800.

186.   Delord K, Roudaut G, Guinet C, Barbraud C, Bertrand S, Weimerskirch H (2015) Kite aerial photography: a low cost method for monitoring seabird colonies. *Journal of Field Ornithology*, 86, 173–179.

187.   Deng J, Shoemaker R, Xie B et al. (2009) Targeted bisulfite sequencing reveals changes in DNA methylation associated with nuclear reprogramming. *Nature biotechnology*, 27, 353–360.

188.   Denton GH, Hughes TJ (2002) Reconstructing the Antarctic ice sheet at the Last Glacial Maximum. *Quaternary Science Reviews*, 21, 193–202.

189. DePristo MA, Banks E, Poplin R et al. (2011) A framework for variation discovery and genotyping using next-generation DNA sequencing data. *Nature genetics*, 43, 491–498.

190. Descamps S, Gauthier-Clerc M, Gendner JP, Le Maho Y (2002) The annual breeding cycle of unbanded king penguins Aptenodytes patagonicus on Possession Island (Crozet). *Avian Science*, 2, 87–98.

191. Descamps S, Le Bohec C, Le Maho Y, Gendner JP, Gauthier-Clerc M (2009) Relating demographic performance to breeding-site location in the King Penguin. *The Condor*, 111, 81–87.

192. Díaz S, Fargione J, Chapin FS, Tilman D (2006) Biodiversity loss threatens human well-being. *PLoS biology*, 4, 1300–1305.

193. Dickinson MG, Orme CD, Suttle KB, Mace GM (2014) Separating sensitivity from exposure in assessing extinction risk from climate change. *Sci Rep*, 4, 6898.

194. Diffenbaugh NS, Field CB (2013) Changes in ecologically critical terrestrial climate conditions. *Science*, 341, 486–492.

195. Dingle H, Drake VA (2007) What is migration. *Bioscience*, 57, 113–121.

196. Doak DF, Morris WF (2010) Demographic compensation and tipping points in climate-induced range shifts. *Nature*, 467, 959–962.

197. Dong S, Sprintall J, Gille ST (2006) Location of the Antarctic polar front from AMSR-E satellite sea surface temperature measurements. *Journal of Physical Oceanography*, 36, 2075–2089.

198. Double MC, Peakall R, Beck NR, Cockburn A (2005) Dispersal, philopatry, and infidelity: dissecting local genetic structure in superb fairy-wrens (Malurus cyaneus). *Evolution*, 59, 625–635.

199. Drummond AJ, Rambaut A, Shapiro B, Pybus OG (2005) Bayesian coalescent inference of past population dynamics from molecular sequences. *Molecular Biology and Evolution*, 22, 1185.

200. Drummond AJ, Rambaut A (2007) BEAST: Bayesian evolutionary analysis by sampling trees. *BMC evolutionary biology*, 7, 214.

201. Du Plessis CJ, Van Heezik YM, Seddon PJ (1994) Timing of king penguin breeding at Marion Island. *Emu*, 94, 216–219.

202. Ducklow HW, Baker K, Martinson DG et al. (2007) Marine pelagic ecosystems: the west Antarctic Peninsula. *Philosophical Transactions of the Royal Society B: Biological Sciences*, 362, 67–94.

203. Duffy DC, Siegfried WR (1987) Historical variations in food consumption by breeding seabirds of the Humboldt and Benguela upwelling regions. *Seabirds: feeding ecology and role in marine ecosystems*, 327–346.

204. Dugger KM, Ainley DG, Lyver POB, Barton K, Ballard G (2010) Survival differences and the effect of environmental instability on breeding dispersal in an Adélie penguin meta-population. *Proceedings of the National Academy of Sciences*, 107, 12375–12380.

205. Dugger KM, Ballard G, Ainley DG, Barton KJ (2006) Effects of flipper bands on foraging behavior and survival of adélie penguins (Pygoscelis adeliae). *The Auk*, 123, 858–869.

206. Dunford C (1977) Kin selection for ground squirrel alarm calls. *The American Naturalist*, 111, 782–785.

207. Dunn CW (2005) Complex colony level organization of the deep sea siphonophore Bargmannia elongata (Cnidaria, Hydrozoa) is directionally asymmetric and arises by the subdivision of pro

buds. *Developmental dynamics*, 234, 835–845.

208.   Dunn PO, Winkler DW, Møller AP, Fiedler W, Berthold P (2010) Effects of climate change on timing of breeding and reproductive success in birds. *Effects of climate change on birds*, 113–128.

209.   Dunn PO, Winkler DW, Whittingham LA, Hannon SJ, Robertson RJ (2011) A test of the mismatch hypothesis: How is timing of reproduction related to food abundance in an aerial insectivore. *Ecology*, 92, 450–461.

210.   Durner GM, Douglas DC, Nielson RM et al. (2009) Predicting 21st-century polar bear habitat distribution from global climate models. *Ecological Monographs*, 79, 25–58.

E

211.   Earl DA (2012) Structure Harvester: a website and program for visualizing Structure output and implementing the Evanno method. *Conservation genetics resources*, 4, 359–361.

212.   Edwards AWF (2008) GH Hardy (1908) and Hardy Weinberg Equilibrium. *Genetics*, 179, 1143–1150.

213.   Ehrlén J, Morris WF (2015) Predicting changes in the distribution and abundance of species under environmental change. *Ecol Lett*, 18, 303–314.

214.   Eichhorn G, Drent RH, Stahl J, Leito A, Alerstam T (2009) Skipping the Baltic: the emergence of a dichotomy of alternative spring migration strategies in Russian barnacle geese. *Journal of Animal Ecology*, 78, 63–72.

215.   Ellegren H (2013) The evolutionary genomics of birds. *Annual Review of Ecology, Evolution, and Systematics*, 44, 239–259.

216.   Ellis JC (2005) Marine birds on land: a review of plant biomass, species richness, and community composition in seabird colonies. *Plant Ecology*, 181, 227–241.

217.   Emerson KJ, Merz CR, Catchen JM et al. (2010) Resolving postglacial phylogeography using high-throughput sequencing. *Proceedings of the National Academy of Sciences*, 107, 16196–16200.

218.   Emslie SD, Coats L, Licht K (2007) A 45,000 yr record of Adélie penguins and climate change in the Ross Sea, Antarctica. *Geol*, 35, 61.

219.   Epperson BK (2005) Estimating dispersal from short distance spatial autocorrelation. *Heredity*, 95, 7–15.

220.   Esler D, Iverson SA, Rizzolo DJ (2006) Genetic and demographic criteria for defining population units for conservation: the value of clear messages. *The Condor*, 108, 480–483.

221.   Evanno G, Regnaut S, Goudet J (2005) Detecting the number of clusters of individuals using the software Structure: a simulation study. *Mol Ecol*, 14, 2611–2620.

222.   Ewens WJ (1979) Mathematical Population Genetics.

223.   Ewins PJ (1986) The ecology of black guillemots (Cepphus grylle) in Shetland.

224.   Excoffier L, Dupanloup I, Huerta-Sanchez E, Sousa VC, Foll M (2013) Robust demographic inference from genomic and SNP data. *PLoS Genet*, 9, e1003905.

225.   Excoffier L, Laval G, Schneider S (2005) Arlequin (version 3.0): an integrated software package for population genetics data analysis. *Evol Bioinform Online*, 1, 47–50.

226.   Excoffier L, Smouse PE, Quattro JM (1992a) Analysis of molecular variance inferred from metric distances among DNA haplotypes: application to human mitochon-

drial DNA restriction data. *Genetics*, 131, 479–491.

227.   Excoffier L, Foll M (2011) Fastsimcoal: a continuous-time coalescent simulator of genomic diversity under arbitrarily complex evolutionary scenarios. *Bioinformatics*, 27, 1332–1334.

228.   Excoffier L, Smouse PE, Quattro JM (1992b) Analysis of molecular variance inferred from metric distances among DNA haplotypes: application to human mitochondrial DNA restriction data. *Genetics*, 131, 479–491.

F

229.   Fahrbach E, Rohardt G, Schröder M, Strass V (1994) Transport and structure of the Weddell Gyre. Annales Geophysicae 12, 840–855.

230.   Falla RA (1937) Birds of the British, Australian, and New Zealand Antarctic Research Expedition (1929-1931) and of the Australasian Antarctic Expedition (1911-1914).

231.   Falush D, Stephens M, Pritchard JK (2003) Inference of population structure using multilocus genotype data: linked loci and correlated allele frequencies. *Genetics*, 164, 1567–1587.

232.   Felsenstein J (2006) Accuracy of coalescent likelihood estimates: do we need more sites, more sequences, or more loci. *Molecular biology and evolution*, 23, 691–700.

233.   Fernández Zamora C (2011) Midiendo la densidad reproductiva del petrel buceador (Pelecanoides garnotii) antes de la erradicación de conejos europeos sobre las islas de Coquimbo, Chile. Postgrado.

234.   Fernández-Chacón A, Genovart M, Pradel R et al. (2013) When to stay, when to disperse and where to go: survival and dispersal patterns in a spatially structured seabird population. *Ecography*, 26, 1–10.

235.   Fernandez C, Miranda Urbina D, Portflitt Toro M, Luna Jorquera G (2014) Estimación de la densidad reproductiva del yunco Pelecanoides garnotii en Isla Choro. *XI Congreso Chileno de Ornitologia*, 24.

236.   Figueroa J, Stucchi M (2008) Peruvian diving petrels Pelecanoides garnotii on Lobos de afuera islands, Peru. *Marine Ornithology*, 36, 189–190.

237.   Figueroa J, Suazo E, Santillan L (2011) Registros actuales e históricos del Potoyunco peruano *Pelecanoides Garnotii* en el Perú. *The Biologist*,

238.   Fischer H, Wahlen M, Smith J, Mastroianni D, Deck B (1999) Ice core records of atmospheric CO2 around the last three glacial terminations. *Science*, 283, 1712–1714.

239.   Fogt RL, Bromwich DH (2006) Decadal variability of the ENSO teleconnection to the high-latitude South Pacific governed by coupling with the Southern Annular Mode. *Journal of Climate*, 19, 979–997.

240.   Fogt RL, Bromwich DH, Hines KM (2011) Understanding the SAM influence on the South Pacific ENSO teleconnection. *Climate dynamics*, 36, 1555–1576.

241.   Forcada J, Trathan PN (2009) Penguin responses to climate change in the Southern Ocean. *Global Change Biology*, 15, 1618–1630.

242.   Fordyce RE, Jones CM, Davis LS, Darby JT (1990) Penguin history and new fossil material from New Zealand. *Penguin biology*, 419, 446.

243.   Frankham R (1995) Inbreeding and extinction: a threshold effect. *Conservation Biology*, 9, 792–799.

244.   Frankham R (2005) Stress and adaptation in conservation genetics. *Journal of Evolutionary Biology*, 18, 750–755.

245. Fraser CI, Nikula R, Ruzzante DE, Waters JM (2012) Poleward bound: biological impacts of Southern Hemisphere glaciation. *Trends in ecology & evolution*, 27, 462–471.

246. Fraser CI, Nikula R, Spencer HG, Waters JM (2009) Kelp genes reveal effects of subantarctic sea ice during the Last Glacial Maximum. *Proceedings of the National Academy of Sciences*, 106, 3249–3253.

247. Fraser CI, Nikula R, Waters JM (2011) Oceanic rafting by a coastal community. *Proceedings of the Royal Society B: Biological Sciences*, 278, 649–655.

248. Frederiksen M, Petersen A (1999) Philopatry and dispersal within a Black guillemot colony. *Waterbirds*, 22, 274–281.

249. Frederiksen M, Edwards M, Richardson AJ, Halliday NC, Wanless S (2006) From plankton to top predators: bottom up control of a marine food web across four trophic levels. *Journal of Animal Ecology*, 75, 1259–1268.

250. Frederiksen M, Harris MP, Daunt F, Rothery P, Wanless S (2004) Scale dependent climate signals drive breeding phenology of three seabird species. *Global Change Biology*, 10, 1214–1221.

251. Freer JJ, Mable BK, Clucas G et al. (2015) Limited genetic differentiation among chinstrap penguin (*Pygoscelis antarctica*) colonies in the Scotia Arc and Western Antarctic Peninsula. *Polar Biology*, 1–10.

252. Fretwell PT, Trathan PN, Wienecke B, Kooyman GL (2014) Emperor penguins breeding on iceshelves. *PloS one*, 9, e85285.

253. Fretwell PT, Larue MA, Morin P et al. (2012) An emperor penguin population estimate: the first global, synoptic survey of a species from space. *PLoS One*, 7, e33751.

254. Fretwell PT, Trathan PN (2009) Penguins from space: faecal stains reveal the lo-cation of emperor penguin colonies. *Global Ecology and Biogeography*, 18, 543–552.

255. Friesen VL (2015) Speciation in seabirds: why are there so many species and why aren t there more. *Journal of Ornithology*, 1–13.

256. Friesen VL, Burg TM, McCoy KD (2007) Mechanisms of population differentiation in seabirds. *Molecular Ecology*, 16, 1765–1785.

257. Froget G, Gautier-Clerc M, Le Maho Y, Handrich Y (1998) Is penguin banding harmless? *Polar Biology*, 20, 409–413.

258. Frolking S, Roulet NT (2007) Holocene radiative forcing impact of northern peatland carbon accumulation and methane emissions. *Global Change Biology*, 13, 1079–1088.

259. Fumagalli M, Vieira FG, Korneliussen TS et al. (2013) Quantifying population genetic differentiation from next-generation sequencing data. *Genetics*, 195, 979–992.

260. Fumagalli M, Vieira FG, Linderoth T, Nielsen R (2014) ngsTools: methods for population genetics analyses from Next-Generation Sequencing data. *Bioinformatics*, 1–2.

261. Furness RW (1978) Energy requirements of seabird communities: a bioenergetics model. *The Journal of Animal Ecology*, 39–53.

G

262. Gagnaire PA, Normandeau E, Pavey SA, Bernatchez L (2013a) Mapping phenotypic, expression and transmission ratio distortion QTL using RAD markers in the Lake Whitefish (Coregonus clupeaformis). *Molecular Ecology*, 22, 3036–3048.

263. Gagnaire P, Pavey SA, Normandeau E, Bernatchez L (2013b) The genetic archi-

tecture of reproductive isolation during speciation-with-gene-flow in lake whitefish species pairs assessed by rad sequencing. *Evolution*, 67, 2483–2497.

264. Gales R, Pemberton D (1988) Recovery of the king penguin, Aptenodytes-patagonicus, population on Heard Island. *Wildlife Research*, 15, 579–585.

265. García-Godos I, Goya E (2006) Diet of the Peruvian diving petrel Pelecanoides garnotii at La Vieja island, Peru, 1997-2000: potential fishery interactions and conservation implications. *Marine Ornithology*, 34, 33–41.

266. Gaspar P, Benson SR, Dutton PH et al. (2012) Oceanic dispersal of juvenile leatherback turtles: going beyond passive drift modeling. *Marine Ecology Progress Series*, 457, 265.

267. Gauthier-Clerc M, Mangin S, Le Bohec C, Gendner JP, Le Maho Y (2003) Comparison of behaviour, body mass, haematocrit level, site fidelity and survival between infested and non-infested king penguin Aptenodytes patagonicus by ticks Ixodes uriae. *Polar Biology*, 26, 379–382.

268. Gauthier–Clerc M, Gendner JP, Ribic CA et al. (2004) Long–term effects of flipper bands on penguins. *Proceedings of the Royal Society of London. Series B: Biological Sciences*, 271, S423.

269. Gavryushkina A, Heath TA, Ksepka DT, Stadler T, Welch D, Drummond AJ (2015) Bayesian total evidence dating reveals the recent crown radiation of penguins. *preprint (arXiv)*, 1506.04797.

270. Gendner JP, Gauthier-Clerc M, Le Bohec C, Descamps S, Le Maho Y (2005) A new application for transponders in studying penguins. *Journal of Field Ornithology*, 76, 138–142.

271. Gent PR, Danabasoglu G, Donner LJ et al. (2011) The community climate system model version 4. *Journal of Climate*, 24, 4973–4991.

272. Gersonde R, Crosta X, Abelmann A, Armand L (2005) Sea-surface temperature and sea ice distribution of the Southern Ocean at the EPILOG Last Glacial Maximum a circum-Antarctic view based on siliceous microfossil records. *Quaternary Science Reviews*, 24, 869–896.

273. Gibb GC, Hills SFK (2013) Intergenerational mutation rate does not equal long-term evolutionary substitution rate. *Proceedings of the National Academy of Sciences*, 110, E611–E611.

274. Gienapp P, Teplitsky C, Alho JS, Mills JA, Merilä J (2008) Climate change and evolution: disentangling environmental and genetic responses. *Molecular ecology*, 17, 167–178.

275. Gilbert C, Robertson G, Le Maho Y, Ancel A (2008) How do weather conditions affect the huddling behaviour of emperor penguins. *Polar Biology*, 31, 163–169.

276. Giraud T, Pedersen JS, Keller L (2002) Evolution of supercolonies: the Argentine ants of southern Europe. *Proceedings of the National Academy of Sciences*, 99, 6075–6079.

277. Goberville E, Beaugrand G, Hautekèete NC, Piquot Y, Luczak C (2015) Uncertainties in the projection of species distributions related to general circulation models. *Ecology and evolution*, 5, 1100–1116.

278. Gómez-Díaz E, González-Solís J, Peinado MA (2009) Population structure in a highly pelagic seabird, the Cory's shearwater Calonectris diomedea: an examination of genetics, morphology and ecology. *Marine Ecology Progress Series*, 382, 197–209.

279. González-Wevar CA, Nakano T, Cañete JI, Poulin E (2010) Molecular phylogeny and historical biogeography of *Na-*

cella in the Southern Ocean. *Molecular Phylogenetics and Evolution*, 56, 115–124.

280.   Gorospe KD, Karl SA (2013) Genetic relatedness does not retain spatial pattern across multiple spatial scales: dispersal and colonization in the coral, Pocillopora damicornis. *Molecular Ecology*, 22, 3721–3736.

281.   Goudet J (1995) Fstat: a computer program to calculate F-Statistics. *The Journal of Heredity*, 86, 485–486.

282.   Gould SJ, Eldredge N (1972) Punctuated equilibria: an alternative to phyletic gradualism.

283.   Gouretski V (1999) The large-scale thermohaline structure of the Ross Gyre. In: *Oceanography of the Ross Sea Antarctica*, pp. 77–100. Springer,

284.   Grassé PP (1950) Traité de Zoologie. Oiseaux.

285.   Gray GR (1844) Aptenodytes. *The Annals and Magazine of Natural History*, 13, 315.

286.   Gregg WW, Conkright ME, Ginoux P, O'Reilly JE, Casey NW (2003) Ocean primary production and climate: Global decadal changes. *Geophys. Res. Lett.*, 30, 1–4.

287.   Grémillet D, Charmantier A (2010) Shifts in phenotypic plasticity constrain the value of seabirds as ecological indicators of marine ecosystems. *Ecological Applications*, 20, 1498–1503.

288.   Greminger MP, Stölting KN, Nater A et al. (2014) Generation of SNP datasets for orangutan population genomics using improved reduced-representation sequencing and direct comparisons of SNP calling algorithms. *BMC Genomics*, 15, 16.

289.   Groenen MAM, Archibald AL, Uenishi H et al. (2012) Analyses of pig genomes provide insight into porcine demography and evolution. *Nature*, 491, 393–398.

290.   Guindon S, Dufayard J-F, Lefort V, Anisimova M, Hordijk W, Gascuel O (2010) New algorithms and methods to estimate maximum-likelihood phylogenies: assessing the performance of PhyML 3.0. *Systematic biology*, 59, 307–321.

291.   Gutenkunst RN, Hernandez RD, Williamson SH, Bustamante CD (2009) Inferring the joint demographic history of multiple populations from multidimensional SNP frequency data. *PLoS Genet*, 5, e1000695.

H

292.   Hackett SJ, Kimball RT, Reddy S et al. (2008) A phylogenomic study of birds reveals their evolutionary history. *Science*, 320, 1763–1768.

293.   Haddad NM, Brudvig LA, Clobert J et al. (2015) Habitat fragmentation and its lasting impact on Earth   's ecosystems. *Science Advances*, 1, e1500052.

294.   Hall TA (1999) BioEdit: a user-friendly biological sequence alignment editor and analysis program for Windows 95/98/NT. Nucleic acids symposium series 41, 95–98.

295.   Halpern BS, Walbridge S, Selkoe KA et al. (2008) A global map of human impact on marine ecosystems. *Science*, 319, 948–952.

296.   Hamilton M (2011) Population genetics.

297.   Handrich Y, Bevan RM, Charrassin J-B et al. (1997) Hypothermia in foraging king penguins. *Nature*, 388, 64–67.

298.   Hanna E, Navarro FJ, Pattyn F et al. (2013) Ice-sheet mass balance and climate change. *Nature*, 498, 51–59.

299.   Hanski I (1998) Metapopulation dynamics. *Nature*, 396, 41–49.

300.   Hanski I, Ovaskainen O (2000) The metapopulation capacity of a fragmented landscape. *Nature*, 404, 755–758.

301.   Harrison SP, Bartlein PJ, Izumi K et al. (2015) Evaluation of CMIP5 palaeo-simulations to improve climate projections. *Nature Clim. Change*, 5, 735–743.

302.   Hart T, Clucas G, Levy H et al. (2011) Characterization of microsatellite loci for utility in a range of penguin species (*unpublished*).

303.   Hartl DL, Clark AG, Clark AG (1988) Principles of population genetics.

304.   Harvey BP, Gwynn Jones D, Moore PJ (2013) Meta analysis reveals complex marine biological responses to the interactive effects of ocean acidification and warming. *Ecology and Evolution*, 3, 1016–1030.

305.   Hawkins BA, Diniz Filho JAF, Jaramillo CA, Soeller SA (2006) Post Eocene climate change, niche conservatism, and the latitudinal diversity gradient of New World birds. *Journal of Biogeography*, 33, 770–780.

306.   Hays C (1989) The Peruvian diving petrel in Peru. *Oryx*, 23, 102–105.

307.   Hayward BW, Scott GH, Crundwell MP et al. (2008) The effect of submerged plateaux on Pleistocene gyral circulation and sea-surface temperatures in the Southwest Pacific. *Global and Planetary Change*, 63, 309–316.

308.   Haywood AM, Smellie JL, Ashworth AC et al. (2008) Middle Miocene to Pliocene history of Antarctica and the Southern Ocean. *Developments in Earth and Environmental Sciences*, 8, 401–463.

309.   He F, Hubbell SP (2011) Species-area relationships always overestimate extinction rates from habitat loss. *Nature*, 473, 368–371.

310.   Heg D, Rothenberger S, Schürch R (2011) Habitat saturation, benefits of philopatry, relatedness, and the extent of cooperative breeding in a cichlid. *Behavioral Ecology*, 22, 82–92.

311.   Heithaus MR, Frid A, Wirsing AJ, Worm B (2008) Predicting ecological consequences of marine top predator declines. *Trends in Ecology & Evolution*, 23, 202–210.

312.   Heled J, Drummond A (2008) Bayesian inference of population size history from multiple loci. *BMC Evolutionary Biology*, 8, 289.

313.   Hellenthal G, Stephens M (2007) msHOT: modifying Hudson's ms simulator to incorporate crossover and gene conversion hotspots. *Bioinformatics*, 23, 520–521.

314.   Heupink TH, van den Hoff J, Lambert DM (2012) King penguin population on Macquarie Island recovers ancient DNA diversity after heavy exploitation in historic times. *Biol Lett*, 8, 586–589.

315.   Hewitt G (2000) The genetic legacy of the Quaternary ice ages. *Nature*, 405, 907–913.

316.   Hillier LW, Miller W, Birney E et al. (2004) Sequence and comparative analysis of the chicken genome provide unique perspectives on vertebrate evolution. *Nature*, 432, 695–716.

317.   Ho SY, Shapiro B (2011) Skyline-plot methods for estimating demographic history from nucleotide sequences. *Mol Ecol Resour*, 11, 423–434.

318.   Hoban S, Gaggiotti O, Bertorelle G (2013a) Sample Planning Optimization Tool for conservation and population Genetics (SPOTG): a software for choosing the appropriate number of markers and samples. *Methods in Ecology and Evolution*, 4, 299–303.

319.   Hoban SM, Gaggiotti OE, Bertorelle G (2013b) The number of markers and sam-

ples needed for detecting bottlenecks under realistic scenarios, with and without recovery: a simulation based study. *Molecular ecology*, 22, 3444–3450.

320. Hodell DA, Kanfoush SL, Shemesh A, Crosta X, Charles CD, Guilderson TP (2001) Abrupt cooling of Antarctic surface waters and sea ice expansion in the South Atlantic sector of the Southern Ocean at 5000 cal yr BP. *Quaternary Research*, 56, 191–198.

321. Hodgson DA, Graham AGC, Roberts SJ et al. (2014) Terrestrial and submarine evidence for the extent and timing of the Last Glacial Maximum and the onset of deglaciation on the maritime-Antarctic and sub-Antarctic islands. *Quaternary Science Reviews*, 100, 137–158.

322. Hoegh-Guldberg O, Bruno JF (2010) The impact of climate change on the world s marine ecosystems. *Science*, 328, 1523–1528.

323. Hoelzel AR (1998) Genetic structure of cetacean populations in sympatry, parapatry, and mixed assemblages: implications for conservation policy. *Journal of Heredity*, 89, 451–458.

324. Hoffman JI, Simpson F, David P et al. (2014) High-throughput sequencing reveals inbreeding depression in a natural population. *Proc Natl Acad Sci U S A*, 111, 3775–3780.

325. Hoffmann AA, Sgrò CM (2011) Climate change and evolutionary adaptation. *Nature*, 470, 479–485.

326. Hoffmann AA, Willi Y (2008) Detecting genetic responses to environmental change. *Nature Reviews Genetics*, 9, 421–432.

327. Hofmann M, Maqueda M (2011) The response of Southern Ocean eddies to increased midlatitude westerlies: A non eddy resolving model study. *Geophysical Research Letters*, 38,

328. Hohenlohe PA, Bassham S, Etter PD, Stiffler N, Johnson EA, Cresko WA (2010) Population genomics of parallel adaptation in threespine stickleback using sequenced RAD tags. *PLoS Genetics*, 6, e1000862.

329. Holsinger KE, Weir BS (2009) Genetics in geographically structured populations: defining, estimating and interpreting FST. *Nature Reviews Genetics*, 10, 639–650.

330. Hope AG, Waltari E, Payer DC, Cook JA, Talbot SL (2013) Future distribution of tundra refugia in northern Alaska. *Nature Clim. Change*, 3, 931–938.

331. Howard WE (1960) Innate and environmental dispersal of individual vertebrates. *American Midland Naturalist*, 152–161.

332. Huffaker C, Gutierrez AP (1984) Ecological entomology.

333. Hunt GL (1991) Occurrence of polar seabirds at sea in relation to prey concentrations and oceanographic factors. *Polar Research*, 10, 553–560.

334. Hunt GL, McKinnell S (2006) Interplay between top-down, bottom-up, and wasp-waist control in marine ecosystems. *Progress in Oceanography*, 68, 115–124.

335. Hunter CM, Caswell H, Runge MC, Regehr EV, Amstrup SC, Stirling I (2010) Climate change threatens polar bear populations: a stochastic demographic analysis. *Ecology*, 91, 2883–2897.

336. Hunter S (1991) The impact of avian predator-scavengers on King Penguin Aptenodytes patagonicus chicks at Marion Island. *Ibis*, 133, 343–350.

337. Huntington CE (1951) *Ortstreue* and Subspecies Formation in the Pied Flycatcher.

338. Husby A, Nussey DH, Visser ME, Wilson AJ, Sheldon BC, Kruuk LEB (2010) Contrasting patterns of phenotypic plasticity in reproductive traits in two great tit (Parus

major) populations. *Evolution*, 64, 2221–2237.

339. Huson DH, Bryant D (2006) Application of phylogenetic networks in evolutionary studies. *Molecular biology and evolution*, 23, 254–267.

340. Hutchinson GE (1957) Cold spring harbor symposium on quantitative biology. *Concluding remarks*, 22, 415–427.

341. Hyde WT, Crowley TJ, Baum SK, Peltier WR (2000) Neoproterozoic snowball Earth simulations with a coupled climate/ice-sheet model. *Nature*, 405, 425–429.

I

342. Isenmann P (1971) Contribution à l'éthologie et à l'écologie du manchot empereur (Aptenodytes forsteri Gray) à la colonie de Pointe Géologie (Terre Adélie). PhD.

343. Isenmann P, Jouventin EP (1970) Ecoéthologie du Manchot empereur (Aptenodytes forsteri) et comparaison avec le Manchot Adélie (Pygoscelis adeliae) et le Manchot royal (Aptenodytes paragonica). *Expéditions Polaires Françaises*, 322, 136–159.

J

344. Jackson JBC (2008) Ecological extinction and evolution in the brave new ocean. *Proceedings of the National Academy of Sciences*, 105, 11458–11465.

345. Jahncke J, Goya E (1998) The status of the Peruvian diving-petrel population at its main breeding areas along the coast of Peru. *Colonial Waterbirds*, 94–97.

346. Jahncke J, García-Godos A, Goya E (1999) The Diet of the Peruvian Diving-Petrel at la Vieja and San Gallan, Perú (La Dieta de Pelecanoides garnotii a la Vieja y San Gallan, Perú). *Journal of Field Ornithology*, 71–79.

347. Janko K, Lecointre G, DeVries A, Couloux A, Cruaud C, Marshall C (2007) Did glacial advances during the Pleistocene influence differently the demographic histories of benthic and pelagic Antarctic shelf fishes? Inferences from intraspecific mitochondrial and nuclear DNA sequence diversity. *BMC Evolutionary Biology*, 7, 220.

348. Jarvis ED, Mirarab S, Aberer AJ et al. (2014) Whole-genome analyses resolve early branches in the tree of life of modern birds. *Science*, 346, 1320–1331.

349. Jenouvrier S (2004) Influence de la variabilité environnementale sur les stratégies démographiques des populations de prédateurs supérieurs : La communauté d'oiseaux marins en Antarctique. PhD.

350. Jenouvrier S, Caswell H, Barbraud C, Holland M, Stroeve J, Weimerskirch H (2009) Demographic models and IPCC climate projections predict the decline of an emperor penguin population. *Proc Natl Acad Sci U S A*, 106, 1844–1847.

351. Jenouvrier S, Weimerskirch H, Barbraud C, Park YH, Cazelles B (2005) Evidence of a shift in the cyclicity of Antarctic seabird dynamics linked to climate. *Proceedings of the Royal Society B: Biological Sciences*, 272, 887.

352. Jenouvrier S, Barbraud C, Weimerskirch H (2006) Sea ice affects the population dynamics of Adélie penguins in Terre Adélie. *Polar Biol*, 29, 413–423.

353. Jenouvrier S, Holland M, Stroeve J et al. (2012) Effects of climate change on an emperor penguin population: analysis of coupled demographic and climate models. *Global Change Biology*, 18, 2756–2770.

354. Jenouvrier S, Holland M, Stroeve J et al. (2014) Projected continent-wide declines of the emperor penguin under climate change. *Nature Climate change*, 4, 715–718.

355. Jeyasingham WS, Taylor SA, Zavalaga CB, Simeone A, Friesen VL (2013) Specialization to cold water upwellings may facilitate gene flow in seabirds: new evidence from the Peruvian pelican Pelecanus thagus (Pelecaniformes: Pelecanidae). *Journal of avian biology*, 44, 297–304.

356. Johnson K (1981) Social organization in a colony of rock squirrels (*Spermophilus variegatus*). *The Southwestern Naturalist*, 237–242.

357. Jombart T (2008) adegenet: a R package for the multivariate analysis of genetic markers. *Bioinformatics*, 24, 1403–1405.

358. Jombart T, Devillard S, Balloux F (2010) Discriminant analysis of principal components: a new method for the analysis of genetically structured populations. *BMC genetics*, 11, 94.

359. Jones OR, Wang J (2012) A comparison of four methods for detecting weak genetic structure from marker data. *Ecology and Evolution*, 2, 1048–1055.

360. Jouventin P (1971a) Comportement et structure sociale chez le manchot empereur.

361. Jouventin P (1971b) Incubation et élevage itinérants chez les manchots empereurs de Pointe Géologie (Terre Adélie).

362. Jouventin P (1972a) Note sur l'existence et la signification d'une rythmicité des parades mutuelles.

363. Jouventin P (1972b) Un nouveau système de reconnaissance acoustique chez les oiseaux. *Behaviour*, 43, 176–185.

364. Jouventin P (1975) Mortality parameters in emperor penguins Aptenodytes forsteri. *The biology of penguins. London: Macmillan*, 435–446.

365. Jouventin P, Cuthbert RJ, Ottvall R (2006) Genetic isolation and divergence in sexual traits: evidence for the northern rockhopper penguin Eudyptes moseleyi being a sibling species. *Molecular Ecology*, 15, 3413–3423.

366. Jouzel J, Masson-Delmotte V, Cattani O et al. (2007) Orbital and millennial Antarctic climate variability over the past 800,000 years. *science*, 317, 793–796.

367. Jump AS, Mátyás C, Peñuelas J (2009) The altitude-for-latitude disparity in the range retractions of woody species. *Trends in ecology & evolution*, 24, 694–701.

K

368. Kanno Y, Vokoun JC, Letcher BH (2011) Fine-scale population structure and riverscape genetics of brook trout (Salvelinus fontinalis) distributed continuously along headwater channel networks. *Molecular Ecology*, 20, 3711–3729.

369. Kaplan MR, Schaefer JM, Denton GH et al. (2010) Glacier retreat in New Zealand during the Younger Dryas stadial. *Nature*, 467, 194–197.

370. Karpouzi VS, Watson R, Pauly D (2007) Modelling and mapping resource overlap between seabirds and fisheries on a global scale: a preliminary assessment. *Marine Ecology Progress Series*, 343, 87–99.

371. Kass RE, Raftery AE (1995) Bayes factors. *Journal of the American statistical association*, 90, 773–795.

372. Kauffman MJ, Frick WF, Linthicum J (2003) Estimation of habitat-specific demography and population growth for peregrine falcons in California. *Ecological Applications*, 13, 1802–1816.

373. Keller I, Largiader CR (2003) Recent habitat fragmentation caused by major roads leads to reduction of gene flow and loss of genetic variability in ground beetles. *Pro-*

ceedings of the Royal Society of London B: Biological Sciences, 270, 417–423.

374.   Keller LF, Waller DM (2002) Inbreeding effects in wild populations. *Trends in Ecology & Evolution*, 17, 230–241.

375.   Kemp AES, Grigorov I, Pearce RB, Garabato ACN (2010) Migration of the Antarctic Polar Front through the mid-Pleistocene transition: evidence and climatic implications. *Quaternary Science Reviews*, 29, 1993–2009.

376.   Kendall WL, Nichols JD (2004) On the estimation of dispersal and movement of birds. *The Condor*, 106, 720–731.

377.   Keppel G, Van Niel KP, Wardell Johnson GW et al. (2012) Refugia: identifying and understanding safe havens for biodiversity under climate change. *Global Ecology and Biogeography*, 21, 393–404.

378.   Kierkegaard S (1843) *Gjentagelsen*. Et Forsøg i den experimenterende Psychologi af Constantin Constantius.

379.   Kim SY, Lohmueller KE, Albrechtsen A et al. (2011) Estimation of allele frequency and association mapping using next-generation sequencing data. *BMC bioinformatics*, 12, 231.

380.   Kimura M (1955) Solution of a process of random genetic drift with a continuous model. *Proc Natl Acad Sci*, 41, 144.

381.   Kimura M (1983) The neutral theory of molecular evolution.

382.   Kimura M, Crow JF (1964) The number of alleles that can be maintained in a finite population. *Genetics*, 49, 725.

383.   Kingman JFC (1982) On the genealogy of large populations. *Journal of Applied Probability*, 27–43.

384.   Kingman JFC (2000) Origins of the coalescent: 1974-1982. *Genetics*, 156, 1461–1463.

385.   Kinsky FC, Falla RA (1976) A sub-specific revision of the Australasian blue penguin (Eudyptula minor) in the New Zealand area.

386.   Kirin M, McQuillan R, Franklin CS, Campbell H, McKeigue PM, Wilson JF (2010) Genomic runs of homozygosity record population history and consanguinity. *PloS one*, 5, e13996.

387.   Knorr G, Lohmann G (2014) Climate warming during Antarctic ice sheet expansion at the Middle Miocene transition. *Nature Geoscience*, 7, 376–381.

388.   Kohfeld KE, Graham RM, de Boer AM et al. (2013) Southern Hemisphere westerly wind changes during the Last Glacial Maximum: paleo-data synthesis. *Quaternary Science Reviews*, 68, 76–95.

389.   Kooyman GL (1993) Breeding habitats of emperor penguins in the western Ross Sea. *Antarctic Science*, 5, 143–148.

390.   Kooyman GL, Ponganis PJ (1998) The physiological basis of diving to depth: birds and mammals. *Annual Review of Physiology*, 60, 19–32.

391.   Kooyman GL, Ponganis PJ (2014) Chick production at the largest emperor penguin colony decreases by 50% from 2008–10. *Antarctic Science*, 26, 33–37.

392.   Korneliussen TS, Albrechtsen A, Nielsen R (2014) ANGSD: Analysis of Next Generation Sequencing Data. *BMC Bioinformatics*, 15, 356.

393.   Koudil M, Charrassin J-B, Le Maho Y, Bost C-A (2000) Seabirds as monitors of upper-ocean thermal structure. King penguins at the Antarctic polar front, east of Kerguelen sector. *Comptes Rendus de l'Académie des Sciences-Series III-Sciences de la Vie*, 323, 377–384.

394.   Krebs CJ (2013) Ecology: The Experimental Analysis of Distribution and Abundance.

395.   Krehenwinkel H, Rödder D, Tautz D (2015) Eco-genomic analysis of the poleward range expansion of the wasp spider Argiope bruennichi shows rapid adaptation and genomic admixture. *Glob Chang Biol*, 21, 4320–4332.

396.   Kucera M, Rosell-Melé A, Schneider R, Waelbroeck C, Weinelt M (2005) Multiproxy approach for the reconstruction of the glacial ocean surface (MARGO). *Quaternary Science Reviews*, 24, 813–819.

397.   Kuhlbrodt T, Rahmstorf S, Zickfeld K et al. (2009) An integrated assessment of changes in the thermohaline circulation. *Climatic Change*, 96, 489–537.

398.   Kusahara K, Sato T, Oka A et al. (2015) Modelling the Antarctic marine cryosphere at the Last Glacial Maximum. *Annals of Glaciology*, 56, 425.

399.   Kusch A, Marín M (2012) Sobre la distribución del Pingüino Rey Aptenodytes Patagonicus (Aves: Spheniscidae) en Chile. Anales del Instituto de la Patagonia 40, 157–163.

L

400.   Lack DL (1968) Ecological adaptations for breeding in birds.

401.   Lam F, Tarpine R, Istrail S (2010) The imperfect ancestral recombination graph reconstruction problem: upper bounds for recombination and homoplasy. *Journal of Computational Biology*, 17, 767–781.

402.   Lambert DM, Ritchie PA, Millar CD, Holland B, Drummond AJ, Baroni C (2002) Rates of evolution in ancient DNA from Adélie penguins. *Science*, 295, 2270.

403.   Langham GM, Schuetz JG, Distler T, Soykan CU, Wilsey C (2015) Conservation Status of North American Birds in the Face of Future Climate Change. *PLoS One*, 10, e0135350.

404.   Langmead B, Salzberg SL (2012) Fast gapped-read alignment with Bowtie 2. *Nature methods*, 9, 357–359.

405.   LaRue MA, Kooyman G, Lynch HJ, Fretwell P (2015) Emigration in emperor penguins: implications for interpretation of long-term studies. *Ecography*, 38, 114–120.

406.   Laubscher RK, Perissinotto R, McQuaid CD (1993) Phytoplankton production and biomass at frontal zones in the Atlantic sector of the Southern Ocean. *Polar biology*, 13, 471–481.

407.   Le Boeuf BJ, Crocker DE, Costa DP, Blackwell SB, Webb PM, Houser DS (2000) Foraging ecology of northern elephant seals. *Ecological monographs*, 70, 353–382.

408.   Le Bohec C (2008) Stratégies d'histoire de vie d'un oiseau longévif: le manchot royal (Aptenodytes patagonicus). PhD.

409.   Le Bohec C, Durant JM, Gauthier-Clerc M et al. (2008) King penguin population threatened by Southern Ocean warming. *Proc Natl Acad Sci U S A*, 105, 2493–2497.

410.   Le Bohec C, Gauthier-Clerc M, Grémillet D et al. (2007) Population dynamics in a long-lived seabird: I. Impact of breeding activity on survival and breeding probability in unbanded king penguins. *Journal of Animal Ecology*, 76, 1149–1160.

411.   Le Maho Y (1977) The Emperor Penguin: A Strategy to Live and Breed in the Cold: Morphology, physiology, ecology, and behavior distinguish the polar emperor penguin from other penguin species, particularly from its close relative, the king penguin. *American Scientist*, 680–693.

412.   Le Maho Y, Saraux C, Durant JM et al. (2011) An ethical issue in biodiversity science: The monitoring of penguins with flipper bands. *C R Biol*, 334, 378–384.

413.   Le Vaillant M, Ropert-Coudert Y, Le Maho Y, Le Bohec C (2015) Individual parameters shape foraging activity in breeding

king penguins. *Behavioral Ecology*, 00, 1–11.

414.   Lê S, Josse J, Husson F (2008) FactoMineR: an R package for multivariate analysis. *Journal of statistical software*, 25, 1–18.

415.   Lea M, Soper T (2005) Discovery of the first Emperor penguin *Aptenodytes forsteri* colony in Marie Byrd Land, Antarctica. *Marine Ornithology*, 33, 59–60.

416.   Leaper R, Cooke J, Trathan P, Reid K, Rowntree V, Payne R (2006) Global climate drives southern right whale (Eubalaena australis) population dynamics. *Biology Letters*, 2, 289–292.

417.   Lecomte N, Kuntz G, Lambert N et al. (2006) Alloparental feeding in the king penguin. *Animal behaviour*, 71, 457–462.

418.   Lecomte N, Gauthier G, GIROUX JEAN, Milot E, Bernatchez L (2009) Tug of war between continental gene flow and rearing site philopatry in a migratory bird: the sex-biased dispersal paradigm reconsidered. *Molecular Ecology*, 18, 593–602.

419.   Lefebvre W (2004) Influence of the Southern Annular Mode on the sea ice-ocean system. *J. Geophys. Res.*, 109, 1–12.

420.   Legrand M, Feniet-Saigne C, Sattzman ES, Germain C, Barkov NI, Petrov VN (1991) Ice-core record of oceanic emissions of dimethylsulphide during the last climate cycle.

421.   Lenormand T (2002) Gene flow and the limits to natural selection. *Trends in Ecology & Evolution*, 17, 183–189.

422.   Lewis Smith RI, Tallowin JRB (1979) The distribution and size of king penguin rookeries on South Georgia. *Br Antarct Surv Bull*, 49, 259–276.

423.   Lewison RL, Crowder LB, Read AJ, Freeman SA (2004) Understanding impacts of fisheries bycatch on marine megafauna. *Trends in Ecology & Evolution*, 19, 598–604.

424.   Li C, Zhang Y, Li J et al. (2014) Two Antarctic penguin genomes reveal insights into their evolutionary history and molecular changes related to the Antarctic environment. *Gigascience*, 3, 27.

425.   Li H, Durbin R (2009) Fast and accurate short read alignment with Burrows–Wheeler transform. *Bioinformatics*, 25, 1754–1760.

426.   Li H, Durbin R (2011) Inference of human population history from individual whole-genome sequences. *Nature*, 475, 493–496.

427.   Li H, Handsaker B, Wysoker A et al. (2009) The sequence alignment/map format and SAMtools. *Bioinformatics*, 25, 2078–2079.

428.   Lindsay BG (1988) Composite likelihood methods. *Contemporary mathematics*, 80, 221–239.

429.   Lisiecki LE, Raymo ME (2005) A Pliocene Pleistocene stack of 57 globally distributed benthic 18O records. *Paleoceanography*, 20,

430.   Liu J, Curry JA (2010) Accelerated warming of the Southern Ocean and its impacts on the hydrological cycle and sea ice. *Proceedings of the National Academy of Sciences*, 107, 14987–14992.

431.   Liu N, Chen L, Wang S, Oh C, Zhao H (2005) Comparison of single-nucleotide polymorphisms and microsatellites in inference of population structure. *Bmc Genetics*, 6, S26.

432.   Liu N, Zhao H (2006) A non-parametric approach to population structure inference using multilocus genotypes. *Hum Genomics*, 2, 353.

433.   Liu X, Fu Y-X (2015) Exploring population size changes using SNP frequency spectra. *Nature genetics*, 47, 555–559.

434. Livermore R, Eagles G, Morris P, Maldonado A (2004) Shackleton Fracture Zone: no barrier to early circumpolar ocean circulation. *Geology*, 32, 797–800.

435. Livermore R, Nankivell A, Eagles G, Morris P (2005) Paleogene opening of Drake passage. *Earth and Planetary Science Letters*, 236, 459–470.

436. Livezey BC, Zusi RL (2007) Higher-order phylogeny of modern birds (Theropoda, Aves: Neornithes) based on comparative anatomy. II. Analysis and discussion. *Zool J Linn Soc*, 149, 1–95.

437. Lovenduski NS, Gruber N (2005) Impact of the Southern Annular Mode on Southern Ocean circulation and biology. *Geophysical Research Letters*,

438. Lucas I, Palakodeti A, Jiang Y et al. (2007) High throughput mapping of origins of replication in human cells. *EMBO reports*, 8, 770–777.

439. Luna-Jorquera G, Fernández CE, Rivadeneira MM (2012) Determinants of the diversity of plants, birds and mammals of coastal islands of the Humboldt current systems: implications for conservation. *Biodiversity and Conservation*, 1–20.

440. Luna-Jorquera G, Simeone A, Aguilar R (2003) Ecofisiología de animales endotermos en un desierto cálido y un mar frío: el caso de las aves marinas de la corriente de Humboldt. *Fisiología ecológica y evolutiva. Teoría y casos de estudios en animales*, 297–316.

441. Lund AH, Duch M, Pedersen FS (1996) Increased cloning efficiency by temperature-cycle ligation. *Nucleic acids research*, 24, 800–801.

442. Lynch HJ, Naveen R, Trathan PN, Fagan WF (2012) Spatially integrated assessment reveals widespread changes in penguin populations on the Antarctic Peninsula. *Ecology*, 93, 1367–1377.

443. Lynch M, Conery JS (2003) The origins of genome complexity. *science*, 302, 1401–1404.

M

444. Mackintosh NA (1946) The Antarctic Convergence and the distribution of surface temperatures in Antarctic waters.

445. Mahlstein I, Daniel JS, Solomon S (2013) Pace of shifts in climate regions increases with global temperature. *Nature Clim. Change*, 3, 739–743.

446. Majumdar A, Gries C, Walker J (2011) A non-stationary spatial generalized linear mixed model approach for studying plant diversity. *Journal of Applied Statistics*, 38, 1935–1950.

447. Mallory ML, Robinson SA, Hebert CE, Forbes MR (2010) Seabirds as indicators of aquatic ecosystem conditions: A case for gathering multiple proxies of seabird health. *Marine Pollution Bulletin*, 60, 7–12.

448. Mangin S, Gauthier-Clerc M, Frenot Y, Gendner J-P, Le Maho Y (2003) Ticks Ixodes uriae and the breeding performance of a colonial seabird, king penguin Aptenodytes patagonicus. *J Avian Biol*, 34, 30–34.

449. MARGO (2009) Constraints on the magnitude and patterns of ocean cooling at the Last Glacial Maximum. *Nature Geoscience*, 2, 127–132.

450. Marshall GJ (2003) Trends in the Southern Annular Mode from observations and reanalyses. *Journal of Climate*, 16, 4134–4143.

451. Marshall J, Speer K (2012) Closure of the meridional overturning circulation through Southern Ocean upwelling. *Nature Geoscience*, 5, 171–180.

452. Martínez Garcia A, Rosell Melé A, Geibert W et al. (2009) Links between iron supply, marine productivity, sea surface tem-

perature, and CO2 over the last 1.1 Ma. *Paleoceanography*, 24,

453. Martínez Meyer E, Townsend Peterson A, Hargrove WW (2004) Ecological niches as stable distributional constraints on mammal species, with implications for Pleistocene extinctions and climate change projections for biodiversity. *Global Ecology and Biogeography*, 13, 305–314.

454. Martinez Palma P (2014) Reporte Anual Regional del cumplimiento de las actividades del Plan de Conservacion de la especie Pelecanoides garnotii (Yunco). *Departamento de Areas Silvestres Protegidas, region Coquimbo*.

455. Massom RA, Hill K, Barbraud C et al. (2009) Fast ice distribution in Adélie Land, East Antarctica: interannual variability and implications for emperor penguins Aptenodytes forsteri. *Marine Ecology Progress Series*, 374, 243–257.

456. Mathews G (1911) The Birds of Australia.

457. Matschiner M (2015) Fitchi: Haplotype genealogies based on Fitch distances.

458. Matschiner M, Hanel R, Salzburger W (2009) Gene flow by larval dispersal in the Antarctic notothenioid fish Gobionotothen gibberifrons. *Molecular Ecology*, 18, 2574–2587.

459. Mattern T, Ellenberg U, Luna-Jorquera G (2002) A South American marine otter Lontra felina preys upon chicks of the Peruvian diving petrel Pelecanoides garnotii. *Marine Ornithology*, 30, 95–96.

460. Matthiopoulos J, Harwood J, Thomas L (2005) Metapopulation consequences of site fidelity for colonially breeding mammals and birds. *Journal of Animal Ecology*, 74, 716–727.

461. Mayr E (1963) Animal species and evolution.

462. Mayr E (1970) Populations, species, and evolution: an abridgment of animal species and evolution.

463. Mayr E (1982) The growth of biological thought: diversity, evolution, and inheritance.

464. Mayr E, Provine WB (1998) The evolutionary synthesis: perspectives on the unification of biology.

465. McCauley DJ, DeSalles PA, Young HS et al. (2012) From wing to wing: the persistence of long ecological interaction chains in less-disturbed ecosystems. *Scientific Reports*, 2,

466. McCauley DJ, Pinsky ML, Palumbi SR, Estes JA, Joyce FH, Warner RR (2015) Marine defaunation: Animal loss in the global ocean. *Science*, 347, 1255641.

467. McElhany P, Ruckelshaus MH, Ford MJ, Wainwright TC, Bjorkstedt EP (2000) Viable salmonid populations and the recovery of evolutionarily significant units. US Dept. Commer. *NOAA Tech. Memo. NMFS-NWFSC*, 42, 156.

468. McGlone MS, Turney CSM, Wilmshurst JM, Renwick J, Pahnke K (2010) Divergent trends in land and ocean temperature in the Southern Ocean over the past 18,000 years. *Nature Geoscience*, 3, 622–626.

469. McGuigan K, Nishimura N, Currey M, Hurwit D, Cresko WA (2010) Quantitative genetic variation in static allometry in the threespine stickleback. *Integrative and comparative biology*, 50, 1067–1080.

470. McKay R, Naish T, Carter L et al. (2012) Antarctic and Southern Ocean influences on Late Pliocene global cooling. *Proceedings of the National Academy of Sciences*, 109, 6423–6428.

471. McKechnie AE, Freckleton RP, Jetz W (2006) Phenotypic plasticity in the scaling of avian basal metabolic rate. *Proceed-*

ings of the Royal Society of London B: Biological Sciences, 273, 931–937.

472. McMahon CR, Burton HR (2005) Climate change and seal survival: evidence for environmentally mediated changes in elephant seal, Mirounga leonina, pup survival. Proceedings of the Royal Society of London B: Biological Sciences, 272, 923–928.

473. McVean GAT, Cardin NJ (2005) Approximating the coalescent with recombination. Philosophical Transactions of the Royal Society B: Biological Sciences, 360, 1387–1393.

474. Meijers AJS (2014) The Southern Ocean in the Coupled Model Intercomparison Project phase 5. Philosophical Transactions of the Royal Society of London A: Mathematical, Physical and Engineering Sciences, 372, 20130296.

475. Meinshausen M, Smith SJ, Calvin K et al. (2011) The RCP greenhouse gas concentrations and their extensions from 1765 to 2300. Climatic change, 109, 213–241.

476. Melick D, Bremmers W (1995) A recently discovered breeding colony of emperor penguins (Aptenodytes forsteri) on the Budd Coast, Wilkes Land, East Antarctica. Polar Record, 31, 426–427.

477. Meredith MP, Locarnini RA, Van Scoy KA, Watson AJ, Heywood KJ, King BA (2000) On the sources of Weddell Gyre Antarctic bottom water. Journal of Geophysical Research: Oceans (1978 2012), 105, 1093–1104.

478. Mesak F, Tatarenkov A, Earley RL, Avise JC (2014) Hundreds of SNPs vs. dozens of SSRs: which dataset better characterizes natural clonal lineages in a self-fertilizing fish. Frontiers in Ecology and Evolution, 2, 74.

479. Midgley GF, Bond WJ (2015) Future of African terrestrial biodiversity and ecosystems under anthropogenic climate change. Nature Clim. Change, 5, 823–829.

480. Millar CD, Dodd A, Anderson J et al. (2008) Mutation and evolutionary rates in Adélie penguins from the Antarctic. PLoS Genetics, 4, e1000209.

481. Miller JA (2012) Species distribution models: Spatial autocorrelation and non-stationarity. Progress in Physical Geography, 37, 161–177.

482. Miller MR, Dunham JP, Amores A, Cresko WA, Johnson EA (2007) Rapid and cost-effective polymorphism identification and genotyping using restriction site associated DNA (RAD) markers. Genome research, 17, 240–248.

483. Miller W, Schuster SC, Welch AJ et al. (2012) Polar and brown bear genomes reveal ancient admixture and demographic footprints of past climate change. Proceedings of the National Academy of Sciences, 109, E2382–E2390.

484. Mills LS, Allendorf FW (1996) The one-migrant-per-generation rule in conservation and management. Conservation Biology, 1509–1518.

485. Milot E, Weimerskirch H, Bernatchez L (2008) The seabird paradox: dispersal, genetic structure and population dynamics in a highly mobile, but philopatric albatross species. Molecular ecology, 17, 1658–1673.

486. Minin VN, Bloomquist EW, Suchard MA (2008) Smooth skyride through a rough skyline: Bayesian coalescent-based inference of population dynamics. Mol Biol Evol, 25, 1459–1471.

487. Möbius KA (1877) Die Auster und die Austernwirthschaft.

488. Moe B, Stempniewicz L, Jakubas D et al. (2009) Climate change and phenological responses of two seabird species breed-

ing in the high-Arctic. *Mar Ecol Prog Ser*, 393, 235–246.

489.   Molfetti E, Vilaca ST, Georges JY et al. (2013) Recent demographic history and present fine-scale structure in the Northwest Atlantic leatherback (Dermochelys coriacea) turtle population. *PLoS One*, 8, e58061.

490.   Møller AP, Fiedler W, Berthold P (2010) Effects of climate change on birds.

491.   Møller AP, Rubolini D, Lehikoinen E (2008) Populations of migratory bird species that did not show a phenological response to climate change are declining. *Proceedings of the National Academy of Sciences*, 105, 16195–16200.

492.   Montecino V, Strub PT, Chavez F, Thomas A, Tarazona J, Baumgartner T (2006) Bio-physical interactions off western South-America. *The sea*, 14, 329–390.

493.   Moore GJ, Robertson G, Wienecke B (1998) Food requirements of breeding king penguins at Heard Island and potential overlap with commercial fisheries. *Polar Biology*, 20, 293–302.

494.   Moore JK, Abbott MR, Richman JG (1999) Location and dynamics of the Antarctic Polar Front from satellite sea surface temperature data. *Journal of Geophysical Research*, 104,

495.   Morin PA, Parsons KM, Archer FI et al. (2015) Geographic and temporal dynamics of a global radiation and diversification in the killer whale. *Mol Ecol*, 24, 3964–3979.

496.   Moritz C, Agudo R (2013) The future of species under climate change: resilience or decline. *Science*, 341, 504–508.

497.   Mortazavi A, Williams BA, McCue K, Schaeffer L, Wold B (2008) Mapping and quantifying mammalian transcriptomes by RNA-Seq. *Nature methods*, 5, 621–628.

498.   Moss RH, Edmonds JA, Hibbard KA et al. (2010) The next generation of scenar-ios for climate change research and assessment. *Nature*, 463, 747–756.

499.   Mougin J-L, Van Beveren M (1979) Structure et dynamique de la population de Manchots empereurs Aptenodytes forsteri de la colonie de l'archipel de Pointe Géologie, Terre Adélie.

500.   Moy CM, Seltzer GO, Rodbell DT, Anderson DM (2002) Variability of El Niño/ Southern Oscillation activity at millennial timescales during the Holocene epoch. *Nature*, 420, 162–165.

501.   Mulvaney R, Abram NJ, Hindmarsh RCA et al. (2012) Recent Antarctic Peninsula warming relative to Holocene climate and ice-shelf history. *Nature*, 489, 141–144.

502.   Munafò MR, Clark TG, Flint J (2004) Assessing publication bias in genetic association studies: evidence from a recent meta-analysis. *Psychiatry research*, 129, 39–44.

503.   Murphy EJ, Watkins JL, Trathan PN et al. (2007a) Spatial and temporal operation of the Scotia Sea ecosystem: a review of large-scale links in a krill centred food web. *Philosophical Transactions of the Royal Society B: Biological Sciences*, 362, 113–148.

504.   Murphy EJ, Trathan PN, Watkins JL et al. (2007b) Climatically driven fluctuations in Southern Ocean ecosystems. *Proceedings of the Royal Society of London B: Biological Sciences*, 274, 3057–3067.

505.   Murphy RC (1915) The penguins of SOuth Goergia. *Brooklyn museum bulletin*, 5, 103–133.

506.   Murphy RC (1936) Oceanic birds of South America: a study of species of the related coasts and seas, including the American quadrant of Antarctica, based upon the Brewster-Sanford collection in the American Museum of Natural History.

507.   Murrell DJ, Travis JMJ, Dytham C (2002) The evolution of dispersal distance in

spatially-structured populations. *Oikos*, 97, 229–236.

508. Myers RA, Worm B (2003) Rapid worldwide depletion of predatory fish communities. *Nature*,

509. Myers S, Fefferman C, Patterson N (2008) Can one learn history from the allelic spectrum? *Theoretical population biology*,

510. Myrcha A (2006) Eocene penguins of Seymour Island, Antarctica: Taxonomy. *Pol. Polar Res*, 27, 3–62.

N

511. Nash SB (2011) Persistent organic pollutants in Antarctica: current and future research priorities. *Journal of Environmental Monitoring*, 13, 497–504.

512. Nathan R (2006) Long-distance dispersal of plants. *Science*, 313, 786–788.

513. Nathan R, Muller-Landau HC (2000) Spatial patterns of seed dispersal, their determinants and consequences for recruitment. *Trends in ecology & evolution*, 15, 278–285.

514. Nathan R, Schurr FM, Spiegel O, Steinitz O, Trakhtenbrot A, Tsoar A (2008) Mechanisms of long-distance seed dispersal. *Trends in Ecology & Evolution*, 23, 638–647.

515. Navarro J, Cardador L, Brown R, Phillips RA (2015) Spatial distribution and ecological niches of non-breeding planktivorous petrels. *Sci Rep*, 5, 12164.

516. Navarro J, Votier SC, Aguzzi J, Chiesa JJ, Forero MG, Phillips RA (2013) Ecological segregation in space, time and trophic niche of sympatric planktivorous petrels. *PLoS One*, 8, e62897.

517. Nei M, Li W-H (1979) Mathematical model for studying genetic variation in terms of restriction endonucleases. *Proceedings of the National Academy of Sciences*, 76, 5269–5273.

518. Neil HL, Carter L, Morris MY (2004) Thermal isolation of Campbell Plateau, New Zealand, by the Antarctic Circumpolar Current over the past 130 kyr. *Paleoceanography*, 19,

519. Nesterova AP, Le Bohec C, Beaune D, Pettex E, Le Maho Y, Bonadonna F (2010) Do penguins dare to walk at night? Visual cues influence king penguin colony arrivals and departures. *Behavioral Ecology and Sociobiology*, 64, 1145–1156.

520. Nicol S, Clarke J, Romaine SJ, Kawaguchi S, Williams G, Hosie GW (2008) Krill (Euphausia superba) abundance and Adélie penguin (Pygoscelis adeliae) breeding performance in the waters off the Béchervaise Island colony, East Antarctica in 2 years with contrasting ecological conditions. *Deep Sea Research Part II: Topical Studies in Oceanography*, 55, 540–557.

521. Nicol S, Pauly T, Bindoff NL et al. (2000) Ocean circulation off east Antarctica affects ecosystem structure and sea-ice extent. *Nature*, 406, 504–507.

522. Nicotra AB, Atkin OK, Bonser SP et al. (2010) Plant phenotypic plasticity in a changing climate. *Trends in plant science*, 15, 684–692.

523. Nielsen R, Korneliussen T, Albrechtsen A, Li Y, Wang J (2012) SNP calling, genotype calling, and sample allele frequency estimation from new-generation sequencing data. *PloS one*, 7, e37558.

524. Nielsen R, Paul JS, Albrechtsen A, Song YS (2011) Genotype and SNP calling from next-generation sequencing data. *Nat Rev Genet*, 12, 443–451.

525. Nielsen R, Williamson S, Kim Y, Hubisz MJ, Clark AG, Bustamante C (2005) Genomic scans for selective sweeps using SNP data. *Genome research*, 15, 1566–1575.

526. Nielsen SHH, Koç N, Crosta X (2004) Holocene climate in the Atlantic sector of the Southern Ocean: Controlled by insolation or oceanic circulation. *Geology*, 32, 317–320.

527. Nikula R, Fraser CI, Spencer HG, Waters JM (2010) Circumpolar dispersal by rafting in two subantarctic kelp-dwelling crustaceans. *Mar Ecol Prog Ser*, 405, 221–230.

528. Nikula R, Spencer HG, Waters JM (2013) Passive rafting is a powerful driver of transoceanic gene flow. *Biology letters*, 9, 20120821.

529. Nong GT, Najjar RG, Seidov D, Peterson WH (2000) Simulation of ocean temperature change due to the opening of Drake Passage. *Geophysical Research Letters*, 27, 2689–2692.

530. Norberg J, Urban MC, Vellend M, Klausmeier CA, Loeuille N (2012) Eco-evolutionary responses of biodiversity to climate change. *Nature Clim. Change*, 2, 747–751.

531. Nunn GB, Stanley SE (1998) Body size effects and rates of cytochrome b evolution in tube-nosed seabirds. *Molecular Biology and Evolution*, 15, 1360–1371.

532. Nussey DH, Postma E, Gienapp P, Visser ME (2005) Selection on heritable phenotypic plasticity in a wild bird population. *Science*, 310, 304–306.

O

533. O'Connell J, Gurdasani D, Delaneau O et al. (2014) A general approach for haplotype phasing across the full spectrum of relatedness. *PLoS Genet*, 10, e1004234.

534. O'Roak BJ, Vives L, Girirajan S et al. (2012) Sporadic autism exomes reveal a highly interconnected protein network of de novo mutations. *Nature*, 485, 246–250.

535. Olsson O (1998) Divorce in king penguins: asynchrony, expensive fat storing and ideal free mate choice. *Oikos*, 574–581.

536. Olsson O, Bonnedahl J, Anker-Nilssen P (2001) Mate switching and copulation behaviour in king penguins. *Journal of avian biology*, 32, 139–145.

537. Olsson O, Brodin A (1997) Changes in King Penguin breeding cycle in response to food availability. *Condor*, 994–997.

538. Olsson O, van der Jeugd HP (2002) Survival in king penguins Aptenodytes patagonicus: temporal and sex-specific effects of environmental variability. *Oecologia*, 132, 509–516.

539. Onley D, Scofield P (2013) Albatrosses, petrels and shearwaters of the world.

540. Orsi AH, Whitworth T, Nowlin WD (1995) On the meridional extent and fronts of the Antarctic Circumpolar Current. *Deep Sea Research Part I: Oceanographic Research Papers*, 42, 641–673.

541. Osborne PE, Foody GM, Suárez-Seoane S (2007) Non-stationarity and local approaches to modelling the distributions of wildlife. *Diversity and Distributions*, 13, 313–323.

542. Overeem RL, Peucker AJ, Austin CM, Dann P, Burridge CP (2008) Contrasting genetic structuring between colonies of the World's smallest penguin, Eudyptula minor (Aves: Spheniscidae). *Conservation genetics*, 9, 893–905.

P

543. Pachauri RK, Allen MR, Barros VR et al. (2014) Climate Change 2014: Synthesis Report. Contribution of Working Groups I, II and III to the Fifth Assessment Report of the Intergovernmental Panel on Climate Change.

544.   Pacifici M, Foden WB, Visconti P et al. (2015) Assessing species vulnerability to climate change. *Nature Climate change*, 5, 215–224.

545.   Paetkau D, Slade R, Burden M, Estoup A (2003) Genetic assignment methods for the direct, real-time estimation of migration rate: a simulation-based exploration of accuracy and power. *Molecular Ecology*, 13, 55–65.

546.   Pakhomov EA, Perissinotto R, McQuaid CD (1996) Prey composition and daily rations of myctophid fishes in the Southern Ocean. *Marine ecology progress series. Oldendorf*, 134, 1–14.

547.   Pan Z, Trikalinos TA, Kavvoura FK, Lau J, Ioannidis JPA (2005) Local literature bias in genetic epidemiology: an empirical evaluation of the Chinese literature. *PLoS Medicine*, 2, 1309.

548.   Paradis E, Claude J, Strimmer K (2004) APE: analyses of phylogenetics and evolution in R language. *Bioinformatics*, 20, 289–290.

549.   Park YH, Durand I, Kestenare E et al. (2014) Polar Front around the Kerguelen Islands: An up to date determination and associated circulation of surface/subsurface waters. *Journal of Geophysical Research: Oceans*, 119, 6575–6592.

550.   Parmesan C, Yohe G (2003) A globally coherent fingerprint of climate change impacts across natural systems. *Nature*, 421, 37–42.

551.   Parsons M, Mitchell I, Butler A et al. (2008) Seabirds as indicators of the marine environment. *ICES Journal of Marine Science*, 65, 1520–1526.

552.   Peakall R, Smouse PE (2006) GENALEX 6: genetic analysis in Excel. Population genetic software for teaching and research. *Molecular Ecology Notes*, 6, 288–295.

553.   Pearce JM, Blums P, Lindberg MS (2008) Site fidelity is an inconsistent determinant of population structure in the hooded merganser (Lophodytes cucullatus): evidence from genetic, mark-recapture, and comparative data. *The Auk*, 125, 711–722.

554.   Pearce JM (2007) Philopatry: A return to origins. *The Auk*, 124, 1085–1087.

555.   Pearce JM, Talbot SL, Petersen MR, Rearick JR (2005) Limited genetic differentiation among breeding, molting, and wintering groups of the threatened Steller's eider: the role of historic and contemporary factors. *Conservation Genetics*, 6, 743–757.

556.   Pearson RG, Dawson TP (2003) Predicting the impacts of climate change on the distribution of species: are bioclimate envelope models useful. *Global ecology and biogeography*, 12, 361–371.

557.   Pelletier F, Reale D, Garant D, Coltman DW, Festa-Bianchet M (2007) Selection on heritable seasonal phenotypic plasticity of body mass. *Evolution*, 1969–1979.

558.   Pereira HM, Leadley PW, Proença V et al. (2010) Scenarios for global biodiversity in the 21st century. *Science*, 330, 1496–1501.

559.   Péron C, Weimerskirch H, Bost C-A (2012) Projected poleward shift of king penguins'(Aptenodytes patagonicus) foraging range at the Crozet Islands, southern Indian Ocean. *Proceedings of the Royal Society of London B: Biological Sciences*, 279, 2515–2523.

560.   Peter HU, Buesser C, Mustafa O, Pfeiffer S (2008) Risk assessment for the Fildes Peninsula and Ardley Island and the development of management plans for designation as Antarctic Specially Protected or Managed Areas. *Federal Envirnonmental Agency, Texte*, 20, 508.

561.   Peterson RG, Whitworth T (1989) The Subantarctic and Polar Fronts in relation to deep water masses through the southwest-

ern Atlantic. *Journal of Geophysical Research: Oceans (1978 2012)*, 94, 10817–10838.

562. Petit J-R, Jouzel J, Raynaud D et al. (1999) Climate and atmospheric history of the past 420,000 years from the Vostok ice core, Antarctica. *Nature*, 399, 429–436.

563. Petit RJ, Hu FS, Dick CW (2008) Forests of the past: a window to future changes. *science*, 320, 1450–1452.

564. Peucker AJ, Dann P, Burridge CP (2009) Range-wide phylogeography of the little penguin (Eudyptula minor): evidence of long-distance dispersal. *The Auk*, 126, 397–408.

565. Pfuhl HA, McCave IN (2005) Evidence for late Oligocene establishment of the Antarctic Circumpolar Current. *Earth and Planetary Science Letters*, 235, 715–728.

566. Piatt JF, Nettleship DN (1985) Diving depths of four alcids. *The Auk*, 293–297.

567. Pickrell JK, Pritchard JK (2012) Inference of population splits and mixtures from genome-wide allele frequency data. *PLoS Genet*, 8, e1002967.

568. Pistorius PA, Baylis A, Crofts S, Pütz K (2012) Population development and historical occurrence of king penguins at the Falkland Islands. *Antarctic Science*, 24, 435–440.

569. Pithan F, Mauritsen T (2014) Arctic amplification dominated by temperature feedbacks in contemporary climate models. *Nature Geoscience*, 7, 181–184.

570. Poloczanska ES, Brown CJ, Sydeman WJ et al. (2013) Global imprint of climate change on marine life. *Nature Clim. Change*, 3, 919–925.

571. Ponchon A, Garnier R, Grémillet D, Boulinier T (2015) Predicting population responses to environmental change: the impor-tance of considering informed dispersal strategies in spatially structured population models. *Diversity and Distributions*, 21, 88–100.

572. Poulin E, González-Wevar C, Díaz A, Gérard K, Hüne M (2014) Divergence between Antarctic and South American marine invertebrates: What molecular biology tells us about Scotia Arc geodynamics and the intensification of the Antarctic Circumpolar Current. *Global and Planetary Change*, 123, 392–399.

573. Prévost J (1961) L'Ecologie du manchot empereur.

574. Price AL, Patterson NJ, Plenge RM, Weinblatt ME, Shadick NA, Reich D (2006) Principal components analysis corrects for stratification in genome-wide association studies. *Nature genetics*, 38, 904–909.

575. Primeau F (2005) Characterizing transport between the surface mixed layer and the ocean interior with a forward and adjoint global ocean transport model. *Journal of Physical Oceanography*, 35, 545–564.

576. Pritchard JK, Stephens M, Donnelly P (2000) Inference of population structure using multilocus genotype data. *Genetics*, 155, 945–959.

577. Prugnolle F, De Meeûs T (2002) Inferring sex-biased dispersal from population genetic tools: a review. *Heredity*, 88, 161–165.

578. Przybylo R, Sheldon BC, Merilä J (2000) Climatic effects on breeding and morphology: evidence for phenotypic plasticity. *Journal of animal ecology*, 69, 395–403.

579. Purcell S, Neale B, Todd-Brown K et al. (2007) PLINK: a tool set for whole-genome association and population-based linkage analyses. *Am J Hum Genet*, 81, 559–575.

580. Purkey SG, Johnson GC (2010) Warming of global abyssal and deep South-

ern Ocean waters between the 1990s and 2000s: contributions to global heat and sea level rise budgets. *Journal of Climate*, 23, 6336–6351.

581. Pütz K, Cherel Y (2005) The diving behaviour of brooding king penguins (Aptenodytes patagonicus) from the Falkland Islands: variation in dive profiles and synchronous underwater swimming provide new insights into their foraging strategies. *Marine Biology*, 147, 281–290.

582. Pütz K (2002) Spatial and temporal variability in the foraging areas of breeding king penguins. *The Condor*, 104, 528–538.

583. Pybus OG, Rambaut A, Harvey PH (2000) An integrated framework for the inference of viral population history from reconstructed genealogies. *Genetics*, 155, 1429–1437.

Q

584. Queiroz AD (2005) The resurrection of oceanic dispersal in historical biogeography. *Trends in ecology & evolution*, 20, 68–73.

585. Quilty PG (2007) Origin and evolution of the sub-Antarctic islands: the foundation. *Papers and Proceedings of the Royal Society of Tasmania*, 141, 35–58.

586. Quinlan AR, Hall IM (2010) BEDTools: a flexible suite of utilities for comparing genomic features. *Bioinformatics*, 26, 841–842.

R

587. Rahmstorf S (2007) A semi-empirical approach to projecting future sea-level rise. *Science*, 315, 368–370.

588. Raine JI, Askin RA (2001) Terrestrial palynology of Cape Roberts Project Drillhole CRP-3, Victoria Land Basin, Antarctica. *Terra Antartica*, 8, 389–400.

589. Raj A, Stephens M, Pritchard JK (2014) fastSTRUCTURE: Variational Inference of Population Structure in Large SNP Data Sets. *Genetics*, 197, 573–589.

590. Rambaut A, Drummond A (2005) Tracer version 1.3: a program for analyzing results from Bayesian MCMC programs such as BEAST and MrBayes. *Distributed by the authors at: http://evolove. zoo. ox. ac. uk/software. html*.

591. Rambaut A, Grass NC (1997) Seq-Gen: an application for the Monte Carlo simulation of DNA sequence evolution along phylogenetic trees. *Computer applications in the biosciences*, 13, 235–238.

592. Rasmussen MD, Hubisz MJ, Gronau I, Siepel A (2014) Genome-wide inference of ancestral recombination graphs.

593. Raybaud V, Beaugrand G, Dewarumez J-M, Luczak C (2015) Climate-induced range shifts of the American jackknife clam Ensis directus in Europe. *Biological Invasions*, 17, 725–741.

594. Raybaud V, Beaugrand G, Goberville E et al. (2013) Decline in kelp in west Europe and climate. *PloS one*, 8, e66044.

595. Raymond M, Rousset F (1995) GENEPOP (version 1.2): population genetics software for exact tests and ecumenicism. *Journal of heredity*, 86, 248–249.

596. Réale D, McAdam AG, Boutin S, Berteaux D (2003) Genetic and plastic responses of a northern mammal to climate change. *Proceedings of the Royal Society of London B: Biological Sciences*, 270, 591–596.

597. Reich D, Thangaraj K, Patterson N, Price AL, Singh L (2009) Reconstructing Indian population history. *Nature*, 461, 489–494.

598. Reich DE, Cargill M, Bolk S et al. (2001) Linkage disequilibrium in the human genome. *Nature*, 411, 199–204.

599. Rex MA, Stuart CT, Hessler RR, Allen JA, Sanders HL, Wilson GDF (1993) Global-scale latitudinal patterns of species diversity in the deep-sea benthos. *Nature*, 365, 636–639.

600. Reynolds J, Weir B, Cockerham CC (1983) Estimation of the coancestry coefficient: basis for a short-term genetic distance. *Genetics*, 105, 767–779.

601. Reynolds RW, Rayner NA, Smith TM, Stokes DC, Wang W (2002) An improved in situ and satellite SST analysis for climate. *Journal of climate*, 15, 1609–1625.

602. Richardson JL, Urban MC, Bolnick DI, Skelly DK (2014) Microgeographic adaptation and the spatial scale of evolution. *Trends in ecology & evolution*, 29, 165–176.

603. Riesch R, Barrett-Lennard LG, Ellis GM, Ford JKB, Deecke VB (2012) Cultural traditions and the evolution of reproductive isolation: ecological speciation in killer whales. *Biological Journal of the Linnean Society*, 106, 1–17.

604. Rintoul S, Hughes C, Olbers D (2001) The Antarctic circumpolar current system. In: *Ocean Circulation and Climate*, (eds Siedler G, Church J, Gould J), pp. 271–302.

605. Ritland K (1996) Estimators for pairwise relatedness and individual inbreeding coefficients. *Genetical Research*, 67, 175–186.

606. Ritz MS, Millar C, Miller GD et al. (2008) Phylogeography of the southern skua complex-rapid colonization of the southern hemisphere during a glacial period and reticulate evolution. *Mol Phylogenet Evol*, 49, 292–303.

607. Rivers NM, Butlin RK, Altringham JD (2005) Genetic population structure of Natterer's bats explained by mating at swarming sites and philopatry. *Molecular Ecology*, 14, 4299–4312.

608. Roeder AD, Marshall RK, Mitchelson AJ et al. (2001) Gene flow on the ice: genetic differentiation among Adélie penguin colonies around Antarctica. *Molecular Ecology*, 10, 1645–1656.

609. Rogers AD (2007) Evolution and biodiversity of Antarctic organisms: a molecular perspective. *Philosophical Transactions of the Royal Society B: Biological Sciences*, 362, 2191–2214.

610. Rolland C, Danchin E, Fraipont MD (1998) The evolution of coloniality in birds in relation to food, habitat, predation, and life-history traits: a comparative analysis. *The American Naturalist*, 151, 514–529.

611. Roman J, Palumbi SR (2003) Whales before whaling in the North Atlantic. *Science*, 301, 508–510.

612. Romiguier J, Gayral P, Ballenghien M et al. (2014) Comparative population genomics in animals uncovers the determinants of genetic diversity. *Nature*, 515, 261–263.

613. Rosenthal Y, Boyle EA, Labeyrie L (1997) Last glacial maximum paleochemistry and deepwater circulation in the Southern Ocean: Evidence from foraminiferal cadmium. *Paleoceanography*, 12, 787–796.

614. Rounsevell DE, Copson GR (1982) Growth rate and recovery of a king penguin, Aptenodytes patagonicus, population after exploitation. *Wildlife Research*, 9, 519–525.

615. Rozas J, Rozas R (1999) DnaSP version 3: an integrated program for molecular population genetics and molecular evolution analysis. *Bioinformatics*, 15, 174–175.

616. Ruzzante DE, Hansen MM, Meldrup D (2002) Distribution of individual inbreeding coefficients, relatedness and influence of stocking on native anadromous brown trout

(Salmo trutta) population structure. *Molecular Ecology*, 10, 2107–2128.

617. Ryman N, Palm S, André C et al. (2006) Power for detecting genetic divergence: differences between statistical methods and marker loci. *Molecular Ecology*, 15, 2031–2045.

S

618. Saether BE, Lande R, Engen S et al. (2005) Generation time and temporal scaling of bird population dynamics. *Nature*, 436, 99–102.

619. Sæther B-E, Engen S, Lande R (1999) Finite metapopulation models with density dependent migration and stochastic local dynamics. *Proceedings of the Royal Society of London B: Biological Sciences*, 266, 113–118.

620. Saji NH, Goswami BN, Vinayachandran PN, Yamagata T (1999) A dipole mode in the tropical Indian Ocean. *Nature*, 401, 360–363.

621. Saji NH, Yamagata T (2003) Possible impacts of Indian Ocean dipole mode events on global climate. *Climate Research*, 25, 151–169.

622. Saraux C, Le Bohec C, Durant JM et al. (2011a) Reliability of flipper-banded penguins as indicators of climate change. *Nature*, 469, 203–206.

623. Saraux C, Viblanc VA, Hanuise N, Le Maho Y, Le Bohec C (2011b) Effects of Individual Pre-Fledging Traits and Environmental Conditions on Return Patterns in Juvenile King Penguins. *PloS one*, 6, e20407.

624. Saraux C, Friess B, Le Maho Y, Le Bohec C (2012) Chick-provisioning strategies used by king penguins to adapt to a multiseasonal breeding cycle. *Animal Behaviour*, 84, 675–683.

625. Sarmiento JL, Gruber N, Brzezinski MA, Dunne JP (2004) High-latitude controls of thermocline nutrients and low latitude biological productivity. *Nature*, 427, 56–60.

626. Scheffer M, Carpenter S, Foley JA, Folke C, Walker B (2001) Catastrophic shifts in ecosystems. *Nature*, 413, 591–596.

627. Schiffels S, Durbin R (2014) Inferring human population size and separation history from multiple genome sequences. *Nature genetics*, 46, 919–927.

628. Schloss CA, Nuñez TA, Lawler JJ (2012) Dispersal will limit ability of mammals to track climate change in the Western Hemisphere. *Proceedings of the National Academy of Sciences*, 109, 8606–8611.

629. Schlosser JA, Dubach JM, Garner TWJ et al. (2009) Evidence for gene flow differs from observed dispersal patterns in the Humboldt penguin, Spheniscus humboldti. *Conservation Genetics*, 10, 839–849.

630. Schmitt T (2007) Molecular biogeography of Europe: Pleistocene cycles and postglacial trends. *Frontiers in zoology*, 4, 1–13.

631. Seehausen O, Butlin RK, Keller I et al. (2014) Genomics and the origin of species. *Nature Reviews Genetics*, 15, 176–192.

632. Serrano D, Forero MG, Donázar JA, Tella JL (2004) Dispersal and social attraction affect colony selection and dynamics of lesser kestrels. *Ecology*, 85, 3438–3447.

633. Serreze MC, Francis JA (2006) The Arctic amplification debate. *Climatic Change*, 76, 241–264.

634. Shackleton EH (1919) South: The Endurance Expedition.

635. Sheehan S, Harris K, Song YS (2013) Estimating variable effective population sizes from multiple genomes: a sequentially Markov conditional sampling distribution approach. *Genetics*, 194, 647–662.

636. Shendure J, Ji H (2008) Next-generation DNA sequencing. *Nature biotechnology*, 26, 1135–1145.

637. Shepherd LD, Lambert DM (2005) Mutational bias in penguin microsatellite DNA. *J Hered*, 96, 566–571.

638. Shirihai H, Kirwan GM (2008) Complete guide to Antarctic wildlife. *agris.fao.org*,

639. Shu Q, Song Z, Qiao F (2015) Assessment of sea ice simulations in the CMIP5 models. *The Cryosphere*, 9, 399–409.

640. Simeone A, Hiriart-Bertrand L, Reyes-Arriagada R et al. (2009) Heterospecific Pairing and Hybridization between Wild Humboldt and Magellanic Penguins in Southern Chile. *The Condor*, 111, 544–550.

641. Simeone A, Luna-Jorquera G, Bernal M et al. (2003) Breeding distribution and abundance of seabirds on islands off north-central Chile. *Revista Chilena de Historia Natural*, 76, 323–333.

642. Simmonds I, Jacka TH (1995) Relationships between the interannual variability of Antarctic sea ice and the Southern Oscillation. *Journal of Climate*, 8, 637–647.

643. Simpson GG (1975) Fossil penguins.

644. Skotte L, Korneliussen TS, Albrechtsen A (2013) Estimating individual admixture proportions from next generation sequencing data. *Genetics*, 195, 693–702.

645. Slack KE, Jones CM, Ando T et al. (2006) Early penguin fossils, plus mitochondrial genomes, calibrate avian evolution. *Molecular Biology and Evolution*, 23, 1144–1155.

646. Smagulova F, Gregoretti IV, Brick K, Khil P, Camerini-Otero RD, Petukhova GV (2011) Genome-wide analysis reveals novel molecular features of mouse recombination hotspots. *Nature*, 472, 375–378.

647. Smetacek V, Nicol S (2005) Polar ocean ecosystems in a changing world. *Nature*, 437, 362–368.

648. Smith AL, Monteiro L, Hasegawa O, Friesen VL (2007) Global phylogeography of the band-rumped storm-petrel (Oceanodroma castro; Procellariiformes: Hydrobatidae). *Molecular phylogenetics and evolution*, 43, 755–773.

649. (2007) The Physical Science Basis, Contribution of Working Group I to the Fourth Assessment Report of the Intergovernmental Panel on Climate Change.

650. Song YS, Hein J (2005) Constructing minimal ancestral recombination graphs. *Journal of Computational Biology*, 12, 147–169.

651. Soong K, Lang JC (1992) Reproductive integration in reef corals. *The Biological Bulletin*, 183, 418–431.

652. Soulé ME, Estes JA, Berger J, Del Rio CM (2003) Ecological effectiveness: conservation goals for interactive species. *Conservation Biology*, 17, 1238–1250.

653. Staab PR, Zhu S, Metzler D, Lunter G (2015) scrm: efficiently simulating long sequences using the approximated coalescent with recombination. *Bioinformatics*, 31, 1680–1682.

654. Stamatakis A (2014) RAxML version 8: a tool for phylogenetic analysis and post-analysis of large phylogenies. *Bioinformatics*, 30, 1312–1313.

655. Stammerjohn SE, Martinson DG, Smith RC, Yuan X, Rind D (2008) Trends in Antarctic annual sea ice retreat and advance and their relation to El Niño–Southern Oscillation and Southern Annular Mode variability. *J. Geophys. Res.*, 113, 1–20.

656. Stearns SC (1992) The evolution of life histories.

657.   Steele JH (1985) A comparison of terrestrial and marine ecological systems. *Nature*, 313, 355–358.

658.   Steiner UK (2005) Reproductive consequences of natal dispersal in a highly philopatric seabird. *Behavioral Ecology*, 16, 634–639.

659.   Stenseth NC, Durant JM, Fowler MS et al. (2015) Testing for effects of climate change on competitive relationships and co-existence between two bird species. *Proceedings of the Royal Society of London B: Biological Sciences*, 282, 20141958.

660.   Stevens EL, Heckenberg G, Roberson ED, Baugher JD, Downey TJ, Pevsner J (2011) Inference of relationships in population data using identity-by-descent and identity-by-state. *PLoS Genet*, 7, e1002287.

661.   Stocker T, Qin D, Plattner GK, Tignor M, Allen SK (2014) Climate change 2013: The physical science basis.

662.   Stonehouse B (1960) The King penguin: Aptenodytes patagonica, of South Georgia.

663.   Stonehouse B, Glenister TW (1953) The Emperor Penguin, *Aptenodytes Forsteri*.

664.   Stuecker MF, Timmermann A, Jin F-F, McGregor S, Ren H-L (2013) A combination mode of the annual cycle and the El Niño/Southern Oscillation. *Nature Geoscience*, 6, 540–544.

665.   Subramanian S, Lingala SG, Swaminathan S, Huynen L, Lambert D (2014) Second generation DNA sequencing of the mitogenome of the Chinstrap penguin and comparative genomics of Antarctic penguins. *Mitochondrial DNA*, 25, 271–272.

666.   Subramanian S, Beans-Picón G, Swaminathan SK, Millar CD, Lambert DM (2013) Evidence for a recent origin of penguins. *Biology letters*, 9, 20130748.

667.   Sydeman WJ, Thompson SA, Kitaysky A (2012) Seabirds and climate change: roadmap for the future. *Marine Ecology Progress Series*, 454, 107–117.

T

668.   Tajima F (1989) Statistical method for testing the neutral mutation hypothesis by DNA polymorphism. *Genetics*, 123, 585–595.

669.   Taschetto AS, Wainer I (2008) The impact of the subtropical South Atlantic SST on South American precipitation. Annales geophysicae: atmospheres, hydrospheres and space sciences 26, 3457.

670.   Tasker ML, Camphuysen CJ, Cooper J, Garthe S, Montevecchi WA, Blaber SJM (2000) The impacts of fishing on marine birds. *ICES Journal of Marine Science: Journal du Conseil*, 57, 531–547.

671.   Taylor CM, Norris DR (2007) Predicting conditions for migration: effects of density dependence and habitat quality. *Biology Letters*, 3, 280–284.

672.   Taylor KE, Stouffer RJ, Meehl GA (2012) An overview of CMIP5 and the experiment design. *Bulletin of the American Meteorological Society*, 93, 485–498.

673.   Taylor SA, Zavalaga CB, Luna-Jorquera G, Simeone A, Anderson DJ, Friesen VL (2010) Panmixia and high genetic diversity in a Humboldt Current endemic, the Peruvian Booby (Sula variegata). *Journal of Ornithology*, 1–8.

674.   Tchernia P, Jeannin PF (1980) Observations on the Antarctic East Wind Drift using tabular icebergs tracked by satellite Nimbus F (1975 1977). *Deep Sea Research Part A. Oceanographic Research Papers*, 27, 467–474.

675.   Techow NMSM, O'Ryan C, Phillips RA et al. (2010) Speciation and phylogeography of giant petrels Macronectes. *Molecu-*

lar phylogenetics and evolution, 54, 472–487.

676. Terauds A, Chown SL, Morgan F et al. (2012) Conservation biogeography of the Antarctic. *Diversity and Distributions*, 18, 726–741.

677. Thatje S, Hillenbrand C-D, Mackensen A, Larter R (2008) Life hung by a thread: endurance of Antarctic fauna in glacial periods. *Ecology*, 89, 682–692.

678. Thiebot J-B, Lescroël A, Barbraud C, Bost C-A (2013) Three-dimensional use of marine habitats by juvenile emperor penguins Aptenodytes forsteri during post-natal dispersal. *Antarctic Science*, 25, 536–544.

679. Thiel M, Macaya EC, Acuna E et al. (2007) The Humboldt Current System of northern and central Chile: oceanographic processes, ecological interactions and socioeconomic feedback. *Oceanography and Marine Biology*, 45, 195–344.

680. Thomas CD, Cameron A, Green RE et al. (2004) Extinction risk from climate change. *Nature*, 427, 145–148.

681. Thomas DN, Dieckmann GS (2008) Sea ice: an introduction to its physics, chemistry, biology and geology.

682. Thomas DB, Ksepka DT, Fordyce RE (2011) Penguin heat-retention structures evolved in a greenhouse Earth. *Biology Letters*, 7, 461–464.

683. Thouzeau C, Le Maho Y, Froget G et al. (2003) Spheniscins, avian β-defensins in preserved stomach contents of the king penguin, Aptenodytes patagonicus. *Journal of Biological Chemistry*, 278, 51053.

684. Thuiller W, Richardson DM, PY EK PETR, Midgley GF, Hughes GO, Rouget M (2005) Niche based modelling as a tool for predicting the risk of alien plant invasions at a global scale. *Global Change Biology*, 11, 2234–2250.

685. Todd FS, Adie S, Splettstoesser JF (2004) First ground visit to the emperor penguin Aptenodytes forsteri colony at Snow Hill Island, Weddell Sea, Antarctica. *Marine Ornithology*, 32,

686. Toggweiler JR, Samuels B (1998) On the ocean's large-scale circulation near the limit of no vertical mixing. *Journal of Physical Oceanography*, 28, 1832–1852.

687. Tolstoy L (1869) War and Peace.

688. Tomczak M, Godfrey JS (2003) Regional oceanography: an introduction.

689. Trathan PN, Fretwell PT, Stonehouse B (2011) First recorded loss of an emperor penguin colony in the recent period of Antarctic regional warming: implications for other colonies. *PloS one*, 6, e14738.

690. Travis JMJ, Dytham C (1999) Habitat persistence, habitat availability and the evolution of dispersal. *Proceedings of the Royal Society of London. Series B: Biological Sciences*, 266, 723–728.

691. Trivelpiece WZ, Hinke JT, Miller AK, Reiss CS, Trivelpiece SG, Watters GM (2011) Variability in krill biomass links harvesting and climate warming to penguin population changes in Antarctica. *Proceedings of the National Academy of Sciences*, 108, 7625.

692. Trucchi E, Facon B, Gratton P et al. (2015) Long live the alien: studying the fate of the genomic diversity along the long-term dynamics of an extremely successful invader, the crested porcupine. *bioRxiv*, 016493.

693. Trucchi E, Gratton P, Whittington JD et al. (2014) King penguin demography since the last glaciation inferred from genome-wide data. *Proceedings of the Royal Society B: Biological Sciences*, 281, 20140528.

694. Turchin P (1998) Quantitative analysis of movement: measuring and modeling

population redistribution in animals and plants.

695. Turner J, Barrand NE, Bracegirdle TJ et al. (2014) Antarctic climate change and the environment: an update. *Polar Record*, 50, 237–259.

696. Turner J, Bracegirdle TJ, Phillips T, Marshall GJ, Hosking JS (2013) An initial assessment of Antarctic sea ice extent in the CMIP5 models. *Journal of Climate*, 26, 1473–1484.

697. Tynan CT (1998) Ecological importance of the southern boundary of the Antarctic Circumpolar Current. *Nature*, 392, 708–710.

V

698. Valverde Romero MB (2006) First record of the endangered Peruvian diving-petrel Pelecanoides garnotii breeding on Corcovado island, Peru. *Marine Ornithology*, 34, 75–76.

699. Van Buskirk J, Steiner UK (2009) The fitness costs of developmental canalization and plasticity. *Journal of evolutionary biology*, 22, 852–860.

700. Van der Putten N, Verbruggen C, Ochyra R, Verleyen E, Frenot Y (2010) Sub-antarctic flowering plants: pre glacial survivors or post glacial immigrants. *Journal of biogeography*, 37, 582–592.

701. Van Heerwaarden B, Hoffmann AA (2007) Global warming: fly populations are responding rapidly to climate change. *Current Biology*, 17, R16–R18.

702. VanDerWal J, Murphy HT, Kutt AS et al. (2013) Focus on poleward shifts in species' distribution underestimates the fingerprint of climate change. *Nature Clim. Change*, 3, 239–243.

703. Viblanc VA, Gineste B, Stier A, Robin J-P, Groscolas R (2014) Stress hormones in relation to breeding status and territory location in colonial king penguin: a role for social density? *Oecologia*, 1–10.

704. Vilina YA (1992) Status of the peruvian diving petrel, Pelecanoides garnotii, on Chañaral Island, Chile. *Colonial Waterbirds*, 137–139.

705. Viot CR, Jouventin P, Bried J (1993) Population genetics of southern seabirds. *Marine Ornithology*, 21, 1–25.

706. Virkkala R, Heikkinen RK, Leikola N, Luoto M (2008) Projected large-scale range reductions of northern-boreal land bird species due to climate change. *Biological Conservation*, 141, 1343–1353.

707. Visser ME, Both C (2005) Shifts in phenology due to global climate change: the need for a yardstick. *Proceedings of the Royal Society of London B: Biological Sciences*, 272, 2561–2569.

708. Visser ME, Van Noordwijk AJ, Tinbergen JM, Lessells CM (1998) Warmer springs lead to mistimed reproduction in great tits (Parus major). *Proceedings of the Royal Society of London B: Biological Sciences*, 265, 1867–1870.

709. Vogl C, Karhu A, Moran G, Savolainen O (2002) High resolution analysis of mating systems: inbreeding in natural populations of Pinus radiata. *Journal of Evolutionary Biology*, 15, 433–439.

710. Von Haartman L (1949) Der Trauerfliegenschnäpper. *Acta Zoologica Fennica*, 56, 104.

711. Vucetich JA, Waite TA (2000) Is one migrant per generation sufficient for the genetic management of fluctuating populations. *Animal Conservation*, 3, 261–266.

W

712.   Wagner A (2008) Neutralism and selectionism: a network-based reconciliation. *Nature Reviews Genetics*, 9, 965–974.

713.   Wagner EL, Boersma PD (2011) Effects of fisheries on seabird community ecology. *Reviews in Fisheries Science*, 19, 157–167.

714.   Wahlund S (1928) Zusammensetzung von Populationen und Korrelationserscheinungen vom Standpunkt der Vererbungslehre aus betrachtet. *Hereditas*, 11, 65–106.

715.   Wainer I, Prado LF, Khodri M, Otto-Bliesner B (2014) Reconstruction of the South Atlantic Subtropical Dipole index for the past 12,000 years from surface temperature proxy. *Sci Rep*, 4, 5291.

716.   Wall JD, Tang LF, Zerbe B et al. (2014) Estimating genotype error rates from high-coverage next-generation sequence data. *Genome research*, 24, 1734–1739.

717.   Wallberg A, Han F, Wellhagen G et al. (2014) A worldwide survey of genome sequence variation provides insight into the evolutionary history of the honeybee Apis mellifera. *Nat Genet*, 46, 1081–1088.

718.   Walther G-R, Post E, Convey P et al. (2002) Ecological responses to recent climate change. *Nature*, 416, 389–395.

719.   Wang C, Zhang L, Lee S-K, Wu L, Mechoso CR (2014) A global perspective on CMIP5 climate model biases. *Nature Climate Change*, 4, 201–205.

720.   Wang J (2011) COANCESTRY: a program for simulating, estimating and analysing relatedness and inbreeding coefficients. *Mol Ecol Resour*, 11, 141–145.

721.   Wang J (2004) Application of the one migrant per generation rule to conservation and management. *Conservation Biology*, 18, 332–343.

722.   Waples RS (1998) Separating the wheat from the chaff: patterns of genetic differentiation in high gene flow species. *Journal of Heredity*, 89, 438–450.

723.   Waples RS, Gaggiotti O (2006) What is a population? An empirical evaluation of some genetic methods for identifying the number of gene pools and their degree of connectivity. *Molecular ecology*, 15, 1419–1439.

724.   Warnock RCM, Parham JF, Joyce WG, Lyson TR, Donoghue PCJ (2015) Calibration uncertainty in molecular dating analyses: there is no substitute for the prior evaluation of time priors. *Proceedings of the Royal Society of London B: Biological Sciences*, 282, 20141013.

725.   Warnock RCM, Yang Z, Donoghue PCJ (2012) Exploring uncertainty in the calibration of the molecular clock. *Biology letters*, 8, 156–159.

726.   Warren R, VanDerWal J, Price J et al. (2013) Quantifying the benefit of early climate change mitigation in avoiding biodiversity loss. *Nature Clim. Change*, 3, 678–682.

727.   Waser PM, Jones WT (1983) Natal philopatry among solitary mammals. *Quarterly review of biology*, 58, 355.

728.   Waters JM (2008) Driven by the West Wind Drift? A synthesis of southern temperate marine biogeography, with new directions for dispersalism. *Journal of Biogeography*, 35, 417–427.

729.   Watson JEM, Iwamura T, Butt N (2013) Mapping vulnerability and conservation adaptation strategies under climate change. *Nature Climate change*, 3, 989–994.

730.   Watterson GA (1975) On the number of segregating sites in genetical models without recombination. *Theoretical population biology*, 7, 256–276.

731.   Weber ME, Clark PU, Kuhn G et al. (2014)   Millennial-scale   variability   in

Antarctic ice-sheet discharge during the last deglaciation. *Nature*, 510, 134–138.

732. Webster MT, Axelsson E, Ellegren H (2006) Strong regional biases in nucleotide substitution in the chicken genome. *Molecular biology and evolution*, 23, 1203–1216.

733. Weimerskirch H, Stahl JC, Jouventin P (1992) The breeding biology and population dynamics of king penguins Aptenodytes patagonica on the Crozet Islands. *Ibis*, 134, 107–117.

734. Weimerskirch H, Tarroux A, Chastel O, Delord K, Cherel Y, Descamps S (2015) Population-specific wintering distribution of adult south polar skua over three oceans. *Marine Ecology Progress series*, 538, 229–237.

735. Weimerskirch H (2013) Seabirds-individuals in colonies. *Science*, 341, 35–36.

736. Weimerskirch H, Catard A, Prince PA, Cherel Y, Croxall JP (1999) Foraging white-chinned petrels (Procellaria aequinoctialis) at risk: from the tropics to Antarctica. *Biological Conservation*, 87, 273–275.

737. Weimerskirch H, Louzao M, De Grissac S, Delord K (2012) Changes in wind pattern alter albatross distribution and life-history traits. *Science*, 335, 211–214.

738. Weir BS, Cockerham CC (1984) Estimating F-statistics for the analysis of population structure. *evolution*, 1358–1370.

739. Weir BS (1990) Genetic data analysis. Methods for discrete population genetic data.

740. Welch AJ, Yoshida AA, Fleischer RC (2011) Mitochondrial and nuclear DNA sequences reveal recent divergence in morphologically indistinguishable petrels. *Molecular Ecology*, 20, 1364–1377.

741. Westerhold T, Bickert T, Röhl U (2005) Middle to late Miocene oxygen isotope stratigraphy of ODP site 1085 (SE Atlantic): new constrains on Miocene climate variability and sea-level fluctuations. *Palaeogeography, Palaeoclimatology, Palaeoecology*, 217, 205–222.

742. Wheelwright NT, Mauck RA (1998) Philopatry, natal dispersal, and inbreeding avoidance in an island population of Savannah Sparrows. *Ecology*, 79, 755–767.

743. White WB, Peterson RG (1996) An Antarctic circumpolar wave in surface pressure, wind, temperature and sea-ice extent. *Nature*, 380, 699–702.

744. Whitehead H, Rendell L (2014) The cultural lives of whales and dolphins.

745. Whitehead JM (2003) Pliocene summer sea surface temperature reconstruction using silicoflagellates from Southern Ocean ODP Site 1165. *Paleoceanography*, 18, 1–11.

746. Whitlatch RB, Lohrer AM, Thrush SF et al. (1998) Scale-dependent benthic recolonization dynamics: life stage-based dispersal and demographic consequences. In: *Recruitment, Colonization and Physical-Chemical Forcing in Marine Biological Systems*, pp. 217–226. Springer,

747. Whitlock MC, McCauley DE (1999) Indirect measures of gene flow and migration: FST≠ 1/(4Nm+1). *Heredity*, 82, 117–125.

748. Wienecke B (2009a) Emperor penguin colonies in the Australian Antarctic Territory: how many are there. *Polar Record*, 45, 304–312.

749. Wienecke B (2009b) The history of the discovery of emperor penguin colonies. *Polar Record*, 46, 271–276.

750. Wienecke B (2010) The history of the discovery of emperor penguin colonies. *Polar Record*,

751. Wienecke B (2012) Emperor penguins at the West Ice Shelf. *Polar biology*, 35, 1289–1296.

752. Wienecke B, Robertson G (2002) Foraging areas of king penguins from Macquarie Island in relation to a marine protected area. *Environmental management*, 29, 662–672.

753. Wienecke BC, Lawless R, Rodary D et al. (2000) Adélie penguin foraging behaviour and krill abundance along the Wilkes and Adélie land coasts, Antarctica. *Deep Sea Research Part II: Topical Studies in Oceanography*, 47, 2573–2587.

754. Wiens JA, Stralberg D, Jongsomjit D, Howell CA, Snyder MA (2009) Niches, models, and climate change: assessing the assumptions and uncertainties. *Proceedings of the National Academy of Sciences*, 106, 19729–19736.

755. Wiens JJ, Ackerly DD, Allen AP et al. (2010) Niche conservatism as an emerging principle in ecology and conservation biology. *Ecology letters*, 13, 1310–1324.

756. Williams JW, Jackson ST, Kutzbach JE (2007) Projected distributions of novel and disappearing climates by 2100 AD. *Proceedings of the National Academy of Sciences*, 104, 5738–5742.

757. Williams TD (1995) The penguins.

758. Willing EM, Dreyer C, van Oosterhout C (2012) Estimates of genetic differentiation measured by F(ST) do not necessarily require large sample sizes when using many SNP markers. *PLoS One*, 7, e42649.

759. Wilson GJ (1983) Distribution and abundance of Antarctic and sub-Antarctic penguins: a synthesis of current knowledge.

760. Wilson PR, Ainley DG, Nur N et al. (2001) Adélie penguin population change in the pacific sector of Antarctica: relation to sea-ice extent and the Antarctic Circumpolar Current. *Marine ecology progress series*, 213, 301–309.

761. Winters JB, Waser PM (2003) Gene dispersal and outbreeding in a philopatric mammal. *Molecular Ecology*, 12, 2251–2259.

762. Wiuf C, Hein J (1999) Recombination as a point process along sequences. *Theoretical population biology*, 55, 248–259.

763. Woehler EJ (2001) A statistical assessment of the status and trends of Antarctic and Subantarctic seabirds.

764. Woehler EJ, Croxall JP (1997) The status and trends of Antarctic and sub-Antarctic seabirds. *Marine Ornithology*, 25, 43–66.

765. Wolff EW, Rankin AM, Röthlisberger R (2003) An ice core indicator of Antarctic sea ice production. *Geophysical Research Letters*, 30,

766. Wolff EW, Fischer H, Fundel F et al. (2006) Southern Ocean sea-ice extent, productivity and iron flux over the past eight glacial cycles. *Nature*, 440, 491–496.

767. Wright S (1931) Evolution in Mendelian populations. *Genetics*, 16, 97–159.

768. Wright S (1943) Isolation by distance. *Genetics*, 28, 114.

769. Wright S (1946) Isolation by distance under diverse systems of mating. *Genetics*, 31, 39.

770. Wright S (1950) Genetical structure of populations. *Nature*, 166, 247–249.

771. Wright S (1965) The interpretation of population structure by F-statistics with special regard to systems of mating. *Evolution*, 19, 395–420.

772. Wright S (1978) Evolution and the Genetics of Populations: A Treatise in Four Volumes.

X

773. Xu S, Song M, Liu J et al. (2013) Simulation of sea ice in FGOALS-g2: Climatology and late 20th century changes. *Advances in Atmospheric Sciences*, 30, 658–673.

Y

774. Yang Z (2007) PAML 4: phylogenetic analysis by maximum likelihood. *Molecular biology and evolution*, 24, 1586–1591.

775. Yeakel JD, Guimarães PR, Bocherens H, Koch PL (2013) The impact of climate change on the structure of Pleistocene food webs across the mammoth steppe. *Proceedings of the Royal Society of London B: Biological Sciences*, 280, 20130239.

776. Younger JL, Clucas GV, Kooyman G et al. (2015) Too much of a good thing: sea ice extent may have forced emperor penguins into refugia during the last glacial maximum. *Glob Chang Biol*, 21, 2215–2226.

Z

777. Zarnetske PL, Skelly DK, Urban MC (2012) Biotic multipliers of climate change. *Science*, 336, 1516–1518.

778. Zavalaga CB, Alfaro-Shigueto J, Dell Omo G (2010) First GPS-track of Peruvian diving-petrels and inca terns in Southern Peru.

779. Zavalaga CB, Jahncke J (1997) Maximum dive depths of the Peruvian diving-petrel. *Condor*, 1002–1004.

780. Zerbino DR, Birney E (2008) Velvet: algorithms for de novo short read assembly using de Bruijn graphs. *Genome research*, 18, 821–829.

781. Zhang G, Lambert D, Wang J, (2011a) Genomic data from the Adélie penguin (Pygoscelis adeliae). *10K Genome Project.*

782. Zhang G, Lambert D, Wang J, (2011b) Genomic data from the Emperor penguin (Aptenodytes forsteri). *10K Genome Project.*

783. Zhang G, Li C, Li Q et al. (2014) Comparative genomics reveals insights into avian genome evolution and adaptation. *Science*, 346, 1311–1320.

784. Zhang J (2007) Increasing Antarctic Sea Ice under Warming Atmospheric and Oceanic Conditions. *J. Climate*, 20, 2515–2529.

785. Zhang Y-X, Perry K, Vinci VA, Powell K, Stemmer WPC, del Cardayré SB (2002) Genome shuffling leads to rapid phenotypic improvement in bacteria. *Nature*, 415, 644–646.

786. Zhao Z, Boerwinkle E (2002) Neighboring-nucleotide effects on single nucleotide polymorphisms: a study of 2.6 million polymorphisms across the human genome. *Genome research*, 12, 1679–1686.

787. Zhou Q, Zhang J, Bachtrog D et al. (2014) Complex evolutionary trajectories of sex chromosomes across bird taxa. *Science*, 346, 1246338.

788. Zink RM, Barrowclough GF (2008) Mitochondrial DNA under siege in avian phylogeography. *Molecular Ecology*, 17, 2107–2121.

Annexe 5 : Introduction (traduction française)

Populations, philpatrie et dispersion.

§-1 Les espèces: type et répétition. La description systématique des espèces peut être conçue comme un cas extrême de médiation de l'*individual* et du *collectif*. Un échantillon singulier, l'*holotype*, est d'ordinaire choisi pour référence, et légitime seul l'attribution du nom de l'espèce à chaque autre specimen - au delà de cet holotype, le reste n'est que *répétition*, dans le temps et dans l'espace. Mais aucune répétition n'est parfaite (Kierkegaard 1843) : la variation, ou *diversité*, joue un rôle essentiel tant dans le temps que dans l'espace (Mayr 1982). La variabilité phénotypique intraspé-cifique entre dans le champs de la biologie sous le nom de «*différences individuelles*» dans l'œuvre de Darwin, célèbre pour y avoir trouvé «*le matériau sur lequel la sélection naturelle agit et s'accu-mule*» (Darwin 1859): les fondements génétiques de cette diversité sont désormais au centre de la *théorie synthétique de l'évolution* (Mayr & Provine 1998; Seehausen *et al.* 2014). Cette variation ne sert aucun but prédéfini : elle peut pourtant être *a posteriori* organisée le long d'un spectre, qui s'étend de la diversité *adaptative* à la diversité *neutre* (Kimura 1983; Wagner 2008). A l'échelle moléculaire, la variation adaptative se définit comme l'apparition de mutations aux effets phéno-typiques avantageux, qui sont positivement sélectionnés dans la population (Mayr 1963), tandis que la variation neutre est faite de mutations ne semblant offir aucune prise à la sélection na-turelle (Kimura 1983). Nous ne prendrons pas position quant à l'importance relative de la varia-tion neutre et adaptative dans l'évolution moléculaire (un sujet au cœur de continuels débats,

1   voir par ex. Wagner 2008) : mais c'est essentiellement sur la variation neutre que s'appuiera notre

2   travail, car elle offre une perspective inégalée sur les processus écologiques non-moléculaires.

3   L'organisation de la variation moléculaire dans l'espace et le temps est au coeur de la génétique

4   des populations (Wright 1978; Kingman 2000) - une discipline que l'on pourrait définir comme

5   l'étude de la diversité génétique à l'intérieur des limites spatio-temporelles conventionnelles de

6   l'espèce - cette « *combinaison tout artificielle, faite par commodité* » (Darwin 1859). L'ampleur et

7   l'organisation de cette diversité reflètent certains caractères essentiels de l'espèce : la diversité

8   génétique elle-même a été expliquée par plusieurs paramètres, tels que la complexité de l'organ-

9   isme (Lynch & Conery 2003), la taille et l'histoire de ses populations (Amos & Harwood 1998),

10   ou sa biodémographie (Romiguier *et al.* 2014) - quant à son organisation dans le temps et l'es-

11   pace, elle est avant tout le fruit de l'histoire démographique et migratoire de l'espèce (un point

12   abordé en détail au §41). Ainsi l'étude des espèces en tant que système de populations nous

13   pertmet-elle de saisir non seulement leur inhérente diversité taxonomique, mais aussi la variété de

14   leurs dynamiques écologiques et évolutives.

15   Un aspect remarquable (et lourd de conséquences méthodologiques) de la façon dont la géné-

16   tique des populations aborde la diversité intraspécifique est - pour ce qui est du moins des méta-

17   zoaires - la place nécessairement ambivalente qu'y occupe l'*individu*. La génétique des popula-

18   tions reste prétrie de l'idée d'une irréductible singularité : comme l'écrit Ernst Mayr, « *où que nous*

19   *regardions, nous trouvons l'unique, et l'unique est diversité* » (Mayr 1982). L'individu, en tant qu'il

20   est combinaison singulière (et vraisemblablement unique) d'allèles, est la seule forme sur laquelle

21   peut s'opérer l'évaluation des *valeurs sélectives*[1], et, de ce fait, la seule forme *efficace* de la diversité

22   génétique. En ce sens, une population, ou *ressource génétique*[2], n'est rien d'autre que la représenta-

23   tion abstraite de ce qui n'est, en réalité, qu'un assemblage d'individus singuliers. Et bien que les

24   concepts d'espèce et de population (voir §2) soient des outils essentiels à la compréhension des

25   processus comportementaux, démographiques ou évolutifs, la seule unité *atomique* observable et

---

1.   Nous traduosons aisni d'anglais *fitness*.

2.   Selon la traduction de l'anglais *gene pool* par la Convention sur la Diversité Biologique.

1 non-interprétée de la vie des animaux demeure l'individu. Dès lors, l'on comprend que toute

2 étude empirique qui d'appuie sur l'échantillonnage de groupes ou de populations ne fait, en réal-

3 ité, qu'assembler une théorie d'individus uniques : leur attribution à tel ou tel groupe n'est qu'une

4 décision postérieure de l'observateur (ce qui pose entre autres de réellees questions pour la con-

5 ception d'expériences - voir entre autres *Fine scale structure*, p.135).

6 Et pourtant, l'*individu* se dissout soit *verticalement*, soit *transversalement*, dans toute la théorie de

7 la génétique des populations. La notion essentielle de *fréquence allélique* (voir §45), par exemple,

8 n'existe que par l'analyse transversale (c'est à dire, à un point donné du temps) d'un grand nom-

9 bre de chromosomes, à une position génomique donnée, sans plus retenir aucune information

10 quant aux associations particulières des allèles au sein des individus : ont peut ainsi la concevoir

11 comme l'abolition des frontières *synchroniques* entre individus - une idée qui trouve d'ailleurs sa

12 consécration mathématique dans l'approximation de la dérive génétique par les équations de

13 diffusion (voir §39). La théorie du *coalescent* (voir §40), quant à elle, se fonde sur l'analyse verti-

14 cale (c'est à dire transgénérationnelle) des séquences : dès lors, l'avènement et la disparition de

15 l'individu (ou la *génération*) devient un accident, et une simple mesure du temps. Ainsi la notion

16 même de coalescence réclame l'abolition des frontières *diachroniques* entre individus : un concept

17 que formalise la représentation en temps continu du coalescent, qui écarte totalement les notions

18 d'individu ou de génération (voir §45).

19 Cette représentation paradoxale du singulier dans le cadre de la génétique des populations forme

20 un contraste frappant avec la forme que prend d'ordinaire l'individu tant dans le cadre de la sys-

21 tématique (où la singularité est réduite à la dispersion autour de l'holotype dans l'espace

22 morphologique), que dans celui de l'écologie (où la diversité est soit remplacée par des paramètres

23 démographiques homogènes tels que la densité - voir Bolnick *et al.* 2011 - ou au contraire de-

24 vient le point focal de l'étude des choix d'histoire de vie - voir Le Bohec 2008; Weimerskirch

25 2013). L'un des défis de la théorie synthétique de l'évolution reste donc la réconciliation de ces

26 différents paradigmes, en dépit de la divergence de leurs fondations. En particulier, la différence

27 entre les concepts de *taille de population* ou *taux de migration* dans le paradigme écologique et

1   celui de la génétique des populations (voir §41 et Fig. 1) rend ardue l'intégration de sources in-

2   terdisciplinaire (voir *The Emperor s ynnome* p. 2 11). N on m oins a rdue e st l a r éconciliation des

3   différentes é chelles d e t emps d ans l esquelles c es p aradigmes s'inscrivent: p ar b ien d es aspects,

4   lagénétique des populations occupe une position intermédiaire entre la systématique (qui opère à

5   l'échelle « géologique » des spéciations) et l'écologie (qui s'occupe de la vie discrète des individus).

6   Si la synthèse de ces différents modes dépasse le cadre de ce travail, les questions qui nous occu-

7   pent ici, parce qu'elles sont au croisement de l'écologie et de la génétique des populations, pren-

8   nent tout leur sens à travers cette inévitable ambivalence.

9   *§-2 Population, dème, colonie.* Tout comme la distribution des positions individuelles dans les es-

10   paces morphologiques, comportementaux ou génétiques définit la forme de la diversité spatiale et

11   temporelle d'une espèce, l'étendue du recouvrement entre la zone de mouvement d'un individu,

12   et la répartition totale de l'espèce définit un spectre de structures spatiales allant de formes ho-

13   mogènes et *panmictiques* à des ensembles hétérogènes et fragmentés. L'architecture particulière

14   d'une espèce intègre des processus qui se déploient à des échelles très diverses : et sa description

15   change selon le cadre théorique dans lequel l'observateur se place (Esler *et al.* 2006). La définition

16   d'une *population* - un concept pourtant central en génétique des populations - change radicale-

17   ment selon qu'on se positionne dans le paradigme écologique ou génétique (Waples & Gaggiotti

18   2006). Dans le paradigme écologique, les critères retenus sont d'ordinaire la géographie (par ex-

19   emple la co-occurrence d'individus *au même endroit*, voir Krebs 2013), les interactions entre indi-

20   vidus (comme le partage de ressources en nourriture, voir Huffaker & G utierrez 1 984), o u, de

21   façon plus importante, l'indépendance démographique des groupes étudiés (c'est à dire, si la mi-

22   gration entre ces groupes suffit à les ramener à une unique trajectoire démographique commune,

23   ou à influencer le risque d'extinction d'un de ces groupes - voir McElhany *et al.* 2000). Wapples

24   and Gaggiotti (2006) résument de la façon suivante la définition écologique : « *un groupe d'indi-*

25   *vidus de la même espèce qui se trouvent au même point de l'espace et du temps, et ont l'occasion d'in-*

26   *teragir les uns avec les autres* » - une définition qui se base sur l'étude de la distribution, la démo-

graphie, et le comportement d'une espèce à une échelle de temps observable - c'est à dire du même ordre de grandeur que la vie de l'observateur.

Dans le paradigme génétique (ou « évolutionniste » - voir Waples & Gaggiotti 2006), une population est définie comme une communauté reproductrice, c'est à dire comme un groupe d'individus qui ont une plus grande probabilité de se reproduire entre eux, plutôt qu'avec un individu d'un autre groupe (Hartl *et al.* 1988), soit, par conséquent, un groupe d'individus dont les génotypes sont corrélés. L'aspect quantitatif de la corrélation minimale nécessaire pour obtenir le statut de « population » est quant à lui matière à débat : mais la plupart des indicateurs retenus se fondent sur la comparaison des influences relatives de la migration et de la dérive dans l'évolution de la diversité génétique d'un groupe (voir §39 et §41). Par exemple, un seuil d'un *migrant efficace* par génération a été proposé dans plusieurs études empiriques (voir Mills & Allendorf 1996; Vucetich & Waite 2000; Wang 2004) : si deux groupes échangent plus d'un migrant efficace par génération, ils ne peuvent être considérés séparés. Des seuils moins restrictifs ont été proposés - par exemple un maximum de 5 ou de 25 mingrants efficaces (Waples & Gaggiotti 2006 en donnent un résumé). Puisque ces critères se concentrent sur des paramètres évalués par générations, ils s'appliquent uniquement en moyenne, sur une fenêtre de plusieurs générations - c'est à dire, à une échelle bien plus longue que la définition écologique.

La relation entre les concepts de population dans le paradigme écologique et évolutionniste n'est pas simple. Quoiqu'il puisse sembler que l'isolation comportementale et géographique d'un groupe d'individus doive naturellement mener à une réduction du flux génique et à l'isolation génétique, le passage d'échelles de temps courtes à des échelles plus longues n'est pas nécessairement direct : la cohérence des groupes peut être hétérogène dans le temps, et donner lieu à l'apparente contradiction de groupes très structurés d'un point de vue comportemental, mais parfaitement mélangés d'un point de vue génétique (c'est par exemple le cas de l'Arlequin plongeur *Histrionicus histrionicus*, voir Esler *et al.* 2006, ou de l'Albatros hurleur *Diomedea exulans*, voir Milot *et al.* 2008). Pour distinguer clairement ces différents paradigmes, dans cette étude, nous

aurons recours à trois termes apparentés, mais non équivalents : le *dème*, la *population*, et la *colonie*.

Un *dème* répond à la définition génétique d'un groupe d'individus. On pourrait le décrire comme « *le plus grand espace, ou le plus grand ensemble d'individus, à l'intérieur duquel la reproduction est, en moyenne, aléatoire* » (Hamilton 2011). Cette définition n'inclut pas nécessairement de composante spatiale, puisque plusieurs groupes d'individus se reproduisant de façon homogène peuvent co-exister en sympatrie (par exemple les orques *Orcinus orca*, voie Riesch *et al.* 2012). Par ailleurs, un dème n'a pas nécessairement de frontières (spatiales ou comportementales), et peut être défini comme une « fenêtre coulissante », comme c'est typiquement le cas des systèmes d'« isolation par la distance », où chaque individu est le centre d'un groupe ou « voisinage génétique » (Crawford 1984), à l'intérieur duquel les fréquences alléliques sont fortement corrélées, et qui se dégrade progressivement avec la distance. Dans ce cas, le dème est l'approximation spatiale d'un plus vaste système d'autocorrélation (Double *et al.* 2005; Epperson 2005). Un seuil de 5% sur la probailité de se reproduire a été proposé pour fixer les limites d'un dème (Hamilton 2011) - mais ici encore, ce seuil est arbitraire, et le concept fait surtout sens pour des espèces à distribution discrète, avec de fortes discontinuités dans leur distribution de probabilité de reproduction. Ainsi, lorsque l'on définit un dème, considère-t'on *a priori* que dans l'ensemble en considération, la mutation et la dérive, et non la migration, sont les principaux garants de la diversité génétique.

Une *colonie* - et tout particulièrement pour les oiseaux de mer, voir §18 - est le pendant conceptuel du dème : il s'agit en effet d'un concept purement géographique et comportemental, qui décrit l'aggrégation d'individus reproducteurs pendant une période de temps donnée, et ne pose aucune hypothèse quant aux structures génétiques ou processus évolutifs sous-jacents. Le terme est couramment utilisé pour de nombreux organismes, allant du polype (par exemple les coraux ou les siphonophores) aux insectes (comme les fourmis, voir Giraud *et al.* 2002) - avec, à chaque fois, des caractéristiques différentes (en particulier en ce qui concerne l'intégration fonctionnelle, qui est extrême chez les siphonophores - voir Dunn 2005, mais minime chez les coraux - voir Soong & Lang 1992). La colonialité est aussi très répandue chez les vertébrés terrestres, qu'il

s'agisse des mammifères (comme le spermophile, voir Armitage 1981; Johnson 1981), ou des

oiseaux (voir Rolland *et al.* 1998). La colonialité de certians oiseaux s'étend à tous les aspects de

leur vie (comme c'est le cas de l'étourneau *Sturnus vulgaris*), mais dans la plupart des cas, elle se

limite à la période reproductrice (Lack 1968). C'est en particulier le cas des oiseaux de mer (voir

§18) qui passent le plus clair de leur temps à s'alimenter au large, en petits groupes, mais se

rassemblent en grandes colonies sur la terre ferme au début de la saison de reproduction. Para-

doxalement, la plupart des oiseaux de mer a une forte tendance à la philopatrie (§5) : bien que

chaque oiseau vagabonde au large durant ses voyages d'alimentation, et ne revient, de fait, jamais

à la côte, tous gardent un lien intérieur avec une parcelle de terre bien particulière, et y revien-

nent régulièrement pour s'y reproduire. Pour certaines espèces dont l'espace d'alimentation est

limité, cette a-parcelle est souvent la seule terre disponible (c'est par exemple souvent le cas du

Guillemot à Miroir *Cepphus grylle*, Ewins 1986). Mais pour les espèces qui voyagent loin au large,

comme les grands Albatros (*Diomedea sp.*) ou les grands Manchots (*Aptenodytes sp.*), la colonialité

devient une idée tout abstraite : la zone d'alimentation entre saisons de reproduction recouvre

largement celle d'autres colonies (et peut d'ailleurs, dans certains cas, s'étendre tout autour du

monde - voir Croxall *et al.* 2005), et pourtant chaque oiseau revient avec une étonnante régular-

ité à son lieu de naissance. L'apprentissage individuel, et le transfer horizontal, ou *culturel* (*sensu*

Whitehead & Rendell 2014) d'information entre oiseaux qui se reproduisent au même endroit

peut même donner naissance à des idiosyncrasies locales - par exemple différentes zones d'alimen-

tation pour des colonies pourtant proches (Weimerskirch 2013). Ainsi la colonie peut-elle être

conçue comme la représentation la plus extrême du concept de population dans le paradigme

écologique : c'est une aggrégation d'individus, stable dans le temps comme dans l'espace, que l'on

peut aisément observer, définir et délimiter (quoique non sans une série de parti-pris conceptuels,

voir §41) - mais sans caractéristiques génétiques particulières.

Notre emploi du mot *population*, dans se travail, se trouve à l'intersection du *dème* et de la

colonie. Une population y sera définie comme un ensemble délimité à la fois dans les espaces géo-

graphiques, démographiques, et génétiques - en d'autres termes une colonie, ou un groupe de

1 colonies, constituant un dème. Il y a là plus en effet qu'une coïncidence anecdotique : parler de

2 *population* implique que les processus observés à l'échelle écologique (par exemple le regroupe-

3 ment spatial d'individus, l'utilisation de ressources communes, ou la philopatrie) sont assez puis-

4 sants et assez stables dans le temps pour influencer les mécanismes évolutifs - de sorte que les par-

5 adigmes évolutifs et génétiques en viennent à se recouper. Ainsi, à l'opposé d'un dème, notre

6 définition d'une population a une composante spatiale : et contrairement à la colonie, elle de-

7 mande aussi une composante génétique.

8 Ainsi deux forces antagonistes interagissent-elles dans la définition de la diversité des architectures

9 possibles des espèces : la *dispersion* (ou capacité active ou passive qu'ont les individus à se déplacer

10 à travers leur habitat), et la *philopatrie*, ou tendance qu'a un individu à demeurer ou revenir là où

11 il est né (lorsqu'elle est absolument passive, cette tendance s'appelle *inertie*). Ensemble, ces deux

12 forces déterminent la *fluidité* et la *viscosité* d'une espèce.

13 *§-3 Qu'est-ce qu'un Synnome ?* L'architecture particulière que nous retrouvons chez les deux es-

14 pèces du genre *Aptenodytes* échappent à tout concept déjà défini. Comme nous le présenterons

15 par la suite en détails (voir en particulier *The King synnome*, et *The Emperor synnome*), les deux

16 grands manchots nous forcent à opérer une médiation difficile entre la définition de population

17 dans les paradigmes ecologiques et génétiques. La structure coloniale est poussée à l'extrême, faite

18 de concentrations locales extreêment discontinues, et qui semblent stables à travers le temps - du

19 moins à l'échelle des siècles. La philopatrie est forte (§19) et l'on considère souvent qu'elle ne se

20 limite pas à la colonie, mais jusqu'au lieu de naissance précis à l'intérieur de la colonie (voir *Fine*

21 *scale structure*). Les colonies font montre en apparence d'un fort degré d'indépendance démo-

22 graphique - comme semblent l'indiquer les trajectoires divergentes des différentes colonies de l'île

23 de la Possession, dans l'Archipel des Crozets (voir Delord *et al.* 2004). Cependant, aucun des

24 critères génétiques n'est satisfait : la fluidité de l'espèce, sur le long terme, semble contrecarrer

25 toute trace de structure génétique, et la migration apparaît comme une force majeure dans l'évo-

26 lution de l'espèce. Une telle structure se distingue d'un système de métapopulations (Hanski

27 1998), dans lequel les populations sont, dans une certaine mesure, séparées génétiquement - mais

1   il se distingue aussi d'un système panmictique, car l'extrême discontinuité dans la distribution des

2   individus et leur forte philpatrie contredisent l'hypothèse de la reproduction aléatoire à l'échelle

3   d'une génération. Quoique de nombreuses recherches soient encore nécessaires afin d'en com-

4   prendre els mécanismes sous-jacents, il est possible que des processus démographiques

5   hétérogènes soient impliqués : par exemple, une dispersion pulsatile, qui impliquerait des événe-

6   ments d'exode local catastrophiques durant certaines générations, équilibrés par des générations

7   où la philopatrie totale serait de règle (voir *Empirical evidence of heterogeneous dispersal* pour un

8   possible exemple de ce phénomène). Afin de décrire cette structure paradoxale, dans cette étude,

9   nous proposons le terme *synnome*, que nous dérivons du grec σύννομος, une «*pâture commune*» -

10 qui a en particulier été utilisé pour décrire les vols d'oiseaux[1], et de façon plus géénérale pour

11 désiger les *réunions*, les *rassemblements*, et même la *parentèle* (vois §123). Le concept central de *pâ-

12 *ture commune* rend compte avec précision de l'importance de la prospection alimentaire cen-

13 tripète[2] dans la structure coloniale de l'espèce, tout en la distinguant d'un système de métapopu-

14 lations fragmentées. Ces différentes significations, prises ensemble, capturent la particularité du

15 système pbservé chez les grands manchots, que nous définirons ici comme «*un ensemble d'indi-*

16 *vidus unique et homogène, distribué de façon extrêment hérétogène et discontinue dans son aire de ré-*

17 *partition. Les concentrations locales, ou colonies, sont très cohérentes à l'échelle de quelques générations,*

18 *et à cette échelle la philopatrie est la norme. Pourtant, la migration entre ces zones est assez forte pour*

19 *maintenir un parfaite homogénéité dans les ressources génétiques de l'espèce, de sorte qu'à une échelle*

20 *micro-évolutive, la seule unité pertinente est l'espèce entière*».

21 *§-4 Dispersion et migration.* Comme nous l'avons mentionné plus haut, une population peut être

22 définie dans deux paradigmes divergents - l'un écologique, l'autre génétique (voir §2). Dans ces

23 deux paradigmes, une population est un ensemble *délimité* - géographiquement ou génétique-

24 ment, elle est définie par son aspect autarcique. Toute forme de mouvement entre groupes œuvre

25 à l'encontre de cette autarcie. Démographiquement, le mouvement couple les trajectoires des

---

1.   Voir en particulier *Les Oiseaux* d'Aristophane, v. 1755 sqq.

2.   A défaut d'une meilleure traduction pour l'expression *central place foraging*.

populations, et contrecarre l'évolution de l'indépendance démographique. Génétiquement, le mouvement cause le transfer d'allèles entre dèmes, et travaille à homogénéiser la variation génétique et les fréquences alléliques. Cependant, la distinction entre les paradigmes écologiques et génétiques s'appplique aussi aux mouvements entre groupes - là encore, cette distinction a motivé le choix de termes différents. Une difficulté particulière, et qu'il s'agit de clarifier d'emblée, est le choix convergent du mot « migration » pour désigner deux phénomènes très différents.

Le sens le plus courant du mot « migration », et ce tout particulièrement dans le contexte de la biologie des oiseaux, est le mouvement pendulaire saisonnier, souvent de colonies entières, entre des terrains d'hiver et des terrains de reproduction estivale. Les espèces migratrices, en ce sens, ont dévelopé des adaptations particulières (voir par ex. Berthold 1991) qui leur permettent de synchroniser leurs trajets, afin de suivre tout au long de l'année les environnements les plus favorables. Il est à noter que le comportement de migration pose un défi pour la définition des populations selon le paradigme écologique, puisque chaque groupe peut changer ses frontières démographiques et géographiques entre ses aires d'hiver et d'été. Cependant, la migration entendue en ce sens ne sera pas examinée dans notre étude, tout simplement parce qu'elle n'est pas observable de façon classique dans notre système (quoique les voyages de prospection ailmentaires des manchots, entre leurs périodes de reproduction, puisse être comparés à des migrations).

Un mouvement plus simple, et unidirectionnel, est la *dispersion* des individus qui quittent leur groupe d'origine. La dispersion fut originellement décrite par Howard (1960) comme « *le mouvement que fait un animal de son point de naissance au point où il se reproduit* ». Du point de vue de chaque individu, c'est donc « *la distance maximale à laquelle il transmet ses caractéristiques génétiques, plutôt que la distance maximale qu'il lui arrivera de parcourir au cours de sa vie depuis son lieu de naissance* ». La dispersion peut être définie tant dans le paradigme écologique que dans le paradigme génétique. Ecologiquement, la dispersion est la force qui pousse au couplage démographique des populations - un excès de juvéniles à un endroit peut par exemple compenser un

faible recrutement ailleurs. Génétiquement, un événement de dispersion est «l'unité» du flux

génique - chaque individu dispersant apporte ses allèles d'un lieu à un autre.

Le second sens de *migration*, que nous utiliserons dans ce travail, a été défini par Dingle & Drake

(2007) dans un contexte biogéographique comme «*l'expansion de la distribution des faunes et des*

espèces», comme «*l'extension vers le Nord des aires de répartition après la retraite des glaciers à la fin*

des périodes glaciaires». Plus spécifiquement, dans le contexte de la génétique des populations, le

paramètre migratoire M est défini par les mêmes auteurs comme «*l'échange de gènes entre popula-*

tions par n'importe quel moyen, incluant, mais de façon non exclusive, la migration au sens où nous

l'entendons ici». C'est en ce sens que le terme est utilisé dans le cadre de al théorie du coalescent

par Beerli et al. (Beerli 2004; Beerli & Palczewski 2010, voir aussi §41). En ce sens, la migration

est la moyenne, sur le long terme, de la fréquence des événements de dispersion. Et tandis que la

dispersion et un phénomène à l'échelle de l'individu et de la génération, qui peut être directe-

ment observé, la migration est une moyenne dans le temps, à l'échelle des populations, et unique-

ment observable par des méthodes indirectes, comme par exemple la reconstruction du flux

génique. Ainsi, tandis que la dispersion appartient à la théorie des traits d'histoire de vie, et est

variable selon les caractéristiques de l'individu et du moment, la migration est une caractéristique

structurelle du système étudié, et devrait varier lentement avec les changements do'rganisation de

l'espèce.

§-5 Philopatrie et fidélité au site. La philopatrie est définie pour la première fois sous le nom

d'*Ortstreue* (ou «fidélité au lieu») par von Haartman (1949), comme la tendance qu'à le Gobe-

mouche à collier *Ficedula hypoleuca* à se reproduire près de son lieu de naissance. Le concept est

généralisé comme *philopatrie* par Huntington (1951) comme «*la tendance qu'a un animal à*

revenir à son lieu de naissance ou de reproduction». Ainsi, quoique le terme est été occasionnelle-

ment employé pour décrire la pure fidélité au lieu de nidification (Andersion *et al.* 1992), il décrit

au sens strict la fidélité des adultes à leur propre lieu de naissance, ou «philoaptrie natale» - et

c'est ce sens premier que nous emploierons ici (Pearce 2007). La philopatrie *stricto sensu* a des

conséquences importantes sur les processus génétiques qui informent l'architecture des espèces.

1 La tendance à se reproduire près de son lieu de naissance contredit l'idée de panmixie, puisque la

2 probabilité de se reproduire, pour deux individus choisis au hasard, devient inversement propor-

3 tionnelle à leur distance à la naissance. A un faible degré, ceci est à l'origine d'isolation par la dis-

4 tance : la parenté entre deux individus est fonction de leur distance géographique (Wright 1943;

5 Wright 1946). A plus forte indensité, la philopatrie peut mener à la consanguinité et à la frag-

6 mentation des populations (Mayr 1963; Avise *et al.* 2000). Les bénéfices de la philopatrie sont

7 pour autant considérables. Ces bénéfices sont comportementaux - comme une meilleure connais-

8 sance des sites et partenaires de meilleure qualité (Wheelwright & Mauck 1998; Heg *et al.* 2011;

9 Arnaud *et al.* 2012), une meilleure valeur sélective d'un comprtement défensif de proximité

10 (Dunford 1977) ou de l'alloparentalité (Lecomte *et al.* 2006) par sélection de parentèle. Mais ils

11 sont aussi génétiques : par exemple, la promotion de la microadaptation locale (Richardson *et al.*

12 2014). Un comportement philopatrique est à la base de la colonialité (Bowler & Benton 2005).

13 Cependant, là encore, les échelles de temps génétiques et écologiques divergent. A une échelle

14 écologique, le taux de retour moyen des juvéniles à leur colonie natale est do'rdinaire considéré

15 comme un estimateur de la philopatrie. Chez plusieurs espèces, en particulier d'oiseaux de mer,

16 les très forts taux de retour que l'on observe semblent incohérents avec le manque de structure

17 génétique entre colonies - le soi-disant *paradoxe des oiseaux marins* de Milot *et al.* (2008). Cepen-

18 dant, des études *in silico* ont montré que de faibles taux de migration (de 5 à 10%) suffisaient à

19 contrecarrer entièrement les effets de la dérive génétique locale à de plus longues échelles de

20 temps (Waples & Gaggiotti 2006). De plus, la notion que la philopatrie est un processus station-

21 naire chez les espèces coloniales, et que le taux de retour moyen doit, à long term, converger vers

22 la philopatrie générale de l'espèce ne prend pas en compte la possibilité d'événements de disper-

23 sion pulsatile, susceptibles de redistribuer entièrement les ressources génétiques de l'espèce. La

24 philopatrie, par opposition à la probabilité instantanée de fidélité au site (F) ou de dispersion (1-

25 F), n'est donc pas un paramètre directement estimable (Kendall & Nichols 2004; Pearce 2007),

26 mais plutôt un trait comportemental de long terme de l'espèce, qui peut, ou pas, amener l'indi-

27 vidu à un choix de fidélité au site, en fonction des conditions environnementales prévalentes.

1 *§-6 Philopatrie et dispersion dans les systèmes océaniques.* En ce qui concerne la disersion, la dy-

2 namique des structures océaniques diffère radicalement des structures terrestres (Steele 1985).

3 Bien qu'aux plus bas niveaux du système trophique, la dispersion passive sur de longues distances

4 soit également prévalente dans les écosystèmes marins et terrestres (les courants atmosphériques y

5 jouent en effet le même rôle que les courants marins pour la dispersion des graines et propagules -

6 voir Cain *et al.* 2000; Nathan & Muller-Landau 2000; Cowie & Holland 2006; Nathan 2006;

7 Nathan *et al.* 2008; Nikula *et al.* 2013), les différences d'organisation spatiale deviennent évi-

8 dentes pour les organismes de plus grande taille, en particulier les vertébrés (Carr *et al.* 2003). Les

9 écosystèmes terrestres montrent de façon typique un plus fort degré de fragmentation, mois de

10 dispersion et de flux génique, et des systèmes globalement plus fermés (Waser & Jones 1983;

11 Turchin 1998; Carr *et al.* 2003) : l'interaction entre les gradients latitudinaux et altitudinaux a

12 pour résultat une distribution complexe des habitats, en contraste avec les habitats pélagiques

13 volontiers zonaux (Burrows *et al.* 2014). Par ailleurs, les océans peuvent être considérés comme

14 un *paysage fluide* dans lequel la dispersion (active ou passive) prend place à grande échelle

15 (Queiroz 2005; Cowie & Holland 2006; Nikula *et al.* 2013). La fragmentation des habitats,

16 quoique documentée (Acosta 1999; González-Wevar *et al.* 2010) s'y restreint d'ordinaire aux

17 zones côtières ou aux espèces benthiques aux niches très spécialisées (Rex *et al.* 1993; Whitlatch *et*

18 *al.* 1998; Poulin *et al.* 2014). La dispersion passive de longue distance (mue par le courant) a été

19 observée chez des organismes allant du plancton (par exemple les stades vagiles des laminaires,

20 voir Fraser *et al.* 2009; Nikula *et al.* 2010) aux vertébrés supérieurs, en particulier dans leurs pre-

21 miers stades de développement (comme c'est le cas chez les tortues marines, Gaspar *et al.* 2012).

22 La dispersion active des vertébrés est courante à des échelles transocéaniques (Bowen & Siniff

23 1999; Le Boeuf *et al.* 2000).

24 Dans les systèmes océaniques caractérisés par de forts courants (comme le Courant Circumpo-

25 laire Antarctique ou ACC, voir §7 - ou le courant de Humboldt, voir §147), la dispersion active

26 comme passive sont des caractères généraux des écosystèmes. Dans l'ACC, une forte dispersion a

27 été mise en évidence pour des espèces allant des algues et petits invertébrés (Nikula *et al.* 2010)

aux invertébrés benthiques (Arango *et al.* 2011) et aux poissons (Matschiner *et al.* 2009; Damerau *et al.* 2012). Cependant, la diversité génétique le long des distributions circumpolaires demeure variable entre taxons, et semble dépendre largement du potentiel de dispersion et des traits d'histoire de vie (Rogers 2007). Dans de nombreux cas, des discontinuités telles que la Péninsule Antarctique (qui s'étend au Nord jusqu'à presque 62°S) rompt ces systèmes de dispersion homogène, et apparaît comme une province biogéographique distincte, en terme de climat (Mulvaney *et al.* 2012) comme de biogéographie (Terauds *et al.* 2012).

La pouvoir de dispersion active qu'ont les vertébrés a néanmoins une conséquence paradoxale : leur plus grande capacité de mouvement leur permet de *ne pas* disperser avec le courant. Tandis que les espèce sessiles résistent à la dispersion par la pure force de leur inertie, les nageurs actifs et les oiseaux font preuve de philopatrie (§5 - voir aussi Frederiksen & Petersen 1999; Steiner 2005; Bicknell *et al.* 2012; Fernández-Chacón *et al.* 2013), qui s'oppose à la grande fluidité des environnements océaniques par un mouvement actif. La philopatrie permet donc la perpétuation de dèmes relativement stables (par exemple chez l'otarie, Bonin *et al.* 2013), de groupes faliliaux (comme chez l'orque, Hoelzel 1998), ou de colonies (comme chez la plupart des oiseaux marins, Friesen *et al.* 2007). De fait, dans la plupart des cas, le comportement philopatrique est assez fort pour mener à la différentiation génétique entre des population qui se recouvrent pourtant largement dans leurs aires d'alimentation (Dearborn *et al.* 2003; Friesen *et al.* 2007; Smith *et al.* 2007). De telles structures ont été observées chez les mammifères marins (cétacés ou pinnipèdes, voir Hoelzel 1998; Baker *et al.* 2008; Bonin *et al.* 2013), chez les tortues marines (par ex. Molfetti *et al.* 2013), et chez la plupart des oiseaux de mer (Friesen *et al.* 2007; Bicknell *et al.* 2012). Les déplacements libres et rapides permis par les systèmes océaniques ont donc la conséquence inattendue de permettre de forts taux de retour au lieux de naissance pour la plupart des vertébrés, plutôt que de favoriser le brassage génétique.

L'Antarctique et l'Océan Austral

§-7 Océanographie et géographie. On nomme Océan Austral la vaste masse d'eau qui entoure le continent Antarctique, et qui constitue l'un des points d'échange thermique majeurs entre l'océan, l'atmosphère et la cryosphère (Hofmann & Maqueda 2011; Meijers 2014). Bien que sa définition officielle fixe sa limite septentrionale à 60°S (International Hydrographic Organization 2000), sa définition fonctionnelle s'étend d'habitude au moins jusqu'au Front Polaire Antarctique (APF), aux alentours de 55°S (Moore *et al.* 1999; Gersonde *et al.* 2005), latitude à laquelle il se fond dans les Océans Atlantique Sud, Indien, et Pacifique Sud (voir Fig. 6).

L'océanographie de l'Océan Austral est dominée par l'influence des vents planétaires de la cellule de Ferrell australe (De Boer *et al.* 2008; Kohfeld *et al.* 2013) qui soufflent continuellement aux latitudes intermédiaires, sans être interrompus par aucune terre dans l'hémisphère Sud, et qui mettent en mouvement les eaux de surface. Le Courant d'Ouest (*West Wind Drift* ou Courant Circumpolaire Antarctique, ACC) qui en résulte est l'un des courants les plus puissants sur terre, avec un transport moyen de 105 à 140 Svedrups - et c'est le seul qui connecte directement les trois bassins océaniques majeurs (Rintoul *et al.* 2001). Le principal effet des vents d'Ouest est de causer la dérive vers l'Est des eaux de surface dans l'ACC : mais ils sont aussi responsables du transport d'Ekman (dans l'hémisphère Sud, une déviation antihoraire allant jusqu'à 90° du courant de surface par rapport à la direction du vent, voir Toggweiler & Samuels 1998), qui pousse les eaux de surface vers l'Equateur. Dans la région antarctique, le refroidissement dû au vent et à l'évaporation, causés par les vents katabatiques, et la surconcentration de sel dûe au rejet de la saumure durant la congélation de la surface autour des polynyes (voir Thomas & Dieckmann 2008 et §18) rendent les eaux de surface particulièrement froides et salées - et par conséquent denses. Durant leur transport vers le Nord, ces masses d'eaux rencontrent des eaux plus chaudes et moins denses : les isopycnaux[1] se redressent, et les eaux de surface antarctiques coulent vers le fond, sur la zone de convergence de l'APF, pour former les Eaux Profondes Antarctiques (AABW, voir Rintoul *et al.* 2001). Au sud de l'APF, par conséquent, le transport d'Ekman est divergent : il provoque la résurgence des eaux profondes plus chaudes (*Warm Deep Water*, WDW, et

---

1.   Isolignes de densité constante

1   *Circumpolar Dee Water*, CDW - voir Sarmiento *et al.* 2004; Anderson *et al.* 2009 pour plus de

2   détails) au sud de l'APF.

3   Au Nord de l'APF s'étend la zone subantarctique, limitée au Nord par la convergence subtropi-

4   cale (STC) où les eaux subantarctiques et subtropicales se stratifient sous les eaux tropicales de

5   surface, aux alentours de 40°S. Quoiqu'elle soit loin d'être aussi nette que l'APF, la STC peut être

6   définie par la disparition du thermocline[1] permanent (Tomczak & Godfrey 2003) : au Nord de la

7   STC, la température chute rapidement de la surface vers le fond, jusqu'à environs 1000 m. Au

8   Sud de la STC, par contre, e gradient de température entre la surface et le fond s'estompe, avec

9   parfois moins d'1°C de différence dans toute la colonne d'eau en Antarctique. L'APF, cependant,

10 conserve un thermocline saisonnier à la limite inférieure de la couche mixte (le SMC, voir Char-

11 rassin & Bost 2001). Au Sud de l'ACC, plus près du continent Antarctique, le Courant Côtier

12 Antarctique, ou dérive d'Est, forme un contrecourant sur l'étroi plateau continental (Tchernia &

13 Jeannin 1980; Fahrbach *et al.* 1994). Ces deux courants se combinent dans les grandes gyres de

14 l'Océan Austral, dans les mers de Ross et de Weddell (Gouretski 1999; Meredith *et al.* 2000), qui

15 ont des caractéristiques océanographiques particulières - par exemple la résurgence d'eaux

16 chaudes profondes en mer de Weddell, qui y entretient une polynye à chaleur sensible (c'est à

17 dire une polynye causée par la température de l'eau, et non par le stress éolien - voir Thomas &

18 Dieckmann 2008).

19 L'importance de l'Océan Austral et de l'ACC dépasse largement leurs effets régionaux. Avec le

20 Pacifique Nord, l'ACC est la plus grande zone de résurgence d'eaux profondes anciennes

21 (Primeau 2005; Marshall & Speer 2012), et de ce fait un moteur majeur de la circulation ther-

22 mohaline mondiale (ou MOC, de l'anglais *Meridional Overturning Circulation* - voir Marshall &

23 Speer 2012), ce qui lui donne un rôle central dans les échanges thermiques globaux. Dans la

24 mesure où c'est l'une des rares zones où les eau profondes affleurent directement à la surface,

---

1.   Le *thermocline* est la zone de transition entre la couche mixte de surface, où les radiations solaires et le mixage dû au vent et à la marée résultent en des températures relativement homogènes et chaudes, et les eaux profondes plus froides. Le thermocline est caractérisé par un gradient serré de température dans la colonne d'eau.

1 l'ACC joue aussi un rôle essentiel dans les échanges gazeux entre l'océan profond et l'atmosphère

2 : une augmentation de l'activité de résurgence a en effet été reliée à une augmentation de CO_2 at-

3 mosphérique dans l'Océan Austral (Anderson *et al.* 2009). La résurgence de l'Océan Austral a

4 aussi été identifiée comme l'une des voies majeures de retour à la surface des nutriments après

5 leur plongée aux basses latitudes - ce qui en fait une pièce essentielle de la pompe biologique, et

6 rend compte de près des trois quarts de la productivité au nord de 30°S (Sarmiento *et al.* 2004).

7 Enfin, puisque c'est la seule masse d'eau zonalement illimitée sur terre, et qu'il se mêle aux trois

8 grands bassins océaniques, l'Océan Austral joue le rôle de mécanisme de couplage central entre

9 des masses d'eau autrement presque indépendantes, et permet la téléconnexion entre les différents

10 bassins (White & Peterson 1996; Rintoul *et al.* 2001). L'Océan Austral se prolonge aussi au Nord

11 dans les courants de limite Est de l'hémisphère Sud (le courant de Humboldt dans le Pacifique -

12 voir §160, le courant de Benguela en Altantique, et le plus marginal courant d'Australie

13 occidentale).

14 L'influence locale de l'ACC et de l'APF sur les processus biologiques est conséquente. La résur-

15 gence d'eau profondes chargées de nutriments, qui s'oxygènent dans la couche mixte, est à l'orig-

16 ine d'une productivité primaire massive dans la zone de l'APF (jusqu'à 20% de la productivité

17 primaire marine mondiale, voir Laubscher *et al.* 1993; Bathmann *et al.* 1997; Carr *et al.* 2006).

18 Cette productivité nourrit de vastes populations de krill (*Euphausia sp.*, voir Murphy *et al.* 2007a)

19 et de poisson (Pakhomov *et al.* 1996) - ceux-cis dominés par les myctophidés (en particulier *Elec-*

20 *trona sp.*, *Protomyctophum sp.*, *Gymnoscopelus sp.* and *Krefftichthys sp.*, voir Collins *et al.* 2008).

21 Plusieurs prédateurs supérieurs tirent avantage de cette concentration de proies sur l'APF - par ex-

22 emple l'Elephant de mer *Mirounga leonina* (Boyd & Arnbom 1991), ou le Manchot royal (Char-

23 rassin & Bost 2001). A la limite sud de l'ACC, la couverture de glace hivernale assure des flo-

24 raisons de productivité saisonnière : les années de grande glace ont les plus fortes biomasses de

25 krill (Nicol *et al.* 2008), avec des conséquences directs sur les populations de prédateurs

26 supérieurs (comme le Manchot Adélie *Pygoscelis adeliæ*, Nicol *et al.* 2008), ce qui fait de la zone

27 des glaces flottantes un aire de grande productivité (Tynan 1998).

1 *§-8 Variabilité climatique de l'Océan Austral.* La structure complexe et les connexions planétaires

2 de l'Océan Austral font qu'il répond fortement auxprincipaux modes de variabilité dans l'hémis-

3 phère austral : le Mode Annulaire Austral (SAM), et les dipoles subtropicaux - dont le plus im-

4 portant est l'ENSO (*El Niño Southern Oscillation*), mais qui incluent aussi le dipole Indien

5 (SIOD, *Southern Indian Ocean Dipole*) et le SASD (*South Atlantic Subtropical Dipole*).

6 Le SAM est la différence moyenne de pression entre les latitudes moyennes et le centre de

7 l'Antarctique. La circulation atmosphérique qui en résulte est la cause principale de variabilité cli-

8 matique dans l'Océan Austral (Marshall 2003; Abram *et al.* 2014), avec une forte cyclicité décen-

9 nale, et de plus lentes oscillations séculaires (Abram *et al.* 2014). Le SAM a des effets inversés

10 dans les zones polaires et subtropicales. Durant les phases positives du SAM, le déplacement vers

11 le pôle des vents d'Ouest renforce le transport d'Ekman dans l'ACC, et a pour résultat un dé-

12 placement vers le Nord de l'APF, une activité de résurgence renforcée au sud de l'APF, et une aug-

13 mentation de la productivité dans la zone frontale (Lovenduski & Gruber 2005) - tandis que

14 dans la zone subtropicale, les anomalies positives de température de surface ont pour résultat une

15 diminution de la productivité marine. En revanche, durant les phases négatives (c'est à dire

16 lorsque les vents d'Ouest se déplacent vers le Nord), la productivité de l'Océan Austral décroit,

17 avec des effets importants sur les prédateurs supérieurs (Forcada & Trathan 2009; Bost *et al.*

18 2015).

19 Tandis que l'impact du SAM se fait principalment sentir dans l'Océan Austral, chaque bassin

20 océanique est aussi sujet aux effect splus locaux - quoique téléconnectés - des dipoles subtropi-

21 caux. Bien que l'ENSO diffère significativement du SIOD et du SASD, en particulier par son

22 ampleur, la structure générale de ces trois systèmes est l'oscillation de température entre l'Est et

23 l'Ouest de la zone subtropicale de chaque bassin. Un gradient important de température garantit

24 de forts alizés et une importante circulation de Walker[1]. Dans le cas de l'ENSO, la diminution

25 périodique de la circulation atmosphérique le long de la côte Ouest d'Amérique du Sud diminue

---

1. C'est à dire, une circulation zonale des masses d'air sous les tropiques, mue principalement par des différences est-ouest de température et de pression.

1   la résurgence d'eaux froides profondes, et par conséquent la différence de température entre l'Est

2   et l'Ouest du Pacifique Sud : la circulation de Walker s'en trouve réduite, ce qui ramène les pré-

3   cipitations vers l'Amérique du Sud, et élève la température de surface dans tout le Pacifique Sud

4   (Tomczak & Godfrey 2003; Stuecker *et al.* 2013). Récemment, des phénomènes similaires ont

5   été mis en évidence dans l'Océan Indien, avec le SIOD (Saji *et al.* 1999) et l'Atlantique Sud avec

6   le SASD (Taschetto & Wainer 2008; Wainer *et al.* 2014). Leur lien avec l'ENSO et leur télé-

7   connexions globales sont cependant encore mal compris (Saji & Yamagata 2003; Ashok *et al.*

8   2004; Abram *et al.* 2008). Ensemble, le SAM, l'ENSO, le SIOD et le SASD contribuent à la

9   variabilité de la glace de mer autour d'Antarctique (Simmonds & Jacka 1995; Lefebvre 2004;

10   Stammerjohn *et al.* 2008).

11   Les effets combinés du SAM, de l'ENSO et des dipoles ont pour résultat des modes de variabilité

12   complexes dans l'Océan Austral (Fogt & Bromwich 2006; Ciasto & Thompson 2008; Fogt *et al.*

13   2011), qui influencent profondément les communautés biologiques. La productivité primaire de

14   l'Océan Austral réagit aussi bien au SAM (Lovenduski & Gruber 2005) qu'à l'ENSO (Beaufort *et*

15   *al.* 2001; Behrenfeld *et al.* 2001), la plupart du temps à travers les changements de température

16   de surface, de glace de mer, et de disponibilité des nutriments. Les changements dans les pro-

17   priétés physiques des eaux de surface, et dans les interactions trophiques, se répercutent à tous les

18   niveaux trophiques au dessus du phytoplancton - par exemple sur le krill (Murphy *et al.* 2007b) :

19   à leur tour, ces effets se transfèrent aux niveaux plus élevés, par exemple au baleines mysticètes

20   (Leaper *et al.* 2006), aux éléphants de mer (McMahon & Burton 2005) ou aux manchots (Bost *et*

21   *al.* 2015). Quoique la variabilité climatique soit un phénomène tout à fait naturel, et ne doive pas

22   menacer la résilience des espèces, la grande intégration des mécanismes climatiques de l'Océan

23   Austral le rendent susceptible de rétroactions importantes, et y amplifie les effets du changement

24   climatique (voir §12). Il est donc de toute première importance de comprendre ces processus

25   eux-mêmes, ainsi que leurs effets sur les communautés biologiques.

26   *§-9 Histoire climatique de l'Océan Austral.* L'Océan Austral est supposé avec pris son aspect actuel

27   au début du Pliocène (il y a ~5.2 Ma). La séparation physique entre l'Antarctique et l'Amérique

du Sud se produit entre l'Eocène moyen (~41 Ma, Livermore *et al.* 2005) et la transition

Oligocène-Miocène (~23 Ma, Pfuhl & McCave 2005), avec le début des conditions glaciales

(dont l'ouverture du passage de Drake a peut être été l'une des causes - Nong *et al.* 2000; Liver-

more *et al.* 2004). L'ACC (voir §7) se met en place au Miocène supérieur (Pfuhl & McCave

2005), mais les frontières actuelles des masses d'eau semblent s'être établies plus tard, peut-être

aux alentours de la Transition climatique du Miocène moyen (MMCT, ~16-11.5 Ma, voir Hay-

wood *et al.* 2008; Knorr & Lohmann 2014). Cette idée semble confirmée par la date de radiation

évolutive de plusieurs taxa, inférée génétiquement, et dont les clades Antarctiques et Subantarc-

tiques semblent avoir été isolés depuis la MMCT (Poulin *et al.* 2014) - ce qui coincide aussi avec

la radiation évolutive des manchots modernes (voir §21).

Le Miocène marque la transition entre les conditions de serre, et les conditions glaciales actuelles.

La calotte glacière antarctique replace la toundra jusque là dominante au début du Miocène

(Raine & Askin 2001), et se développe jusqu'à atteindre ses dimensions actuelles à la fin de la

période (Westerhold *et al.* 2005). Malgré un forte variabilité (encore mal comprise), les condi-

tions en mer sont globalement plus chaudes au Pliocène qu'à présent (Haywood *et al.* 2008) -

mais avec néanmoins une forte productivité. La température de surface est environs 5°C

supérieures aux moyennes actuelles dans l'Océan Austral (Whitehead 2003) et l'APF se situe 6°

au Sud de sa position présente au milieu deu Pliocène (Barron 1996). La circulation thermoha-

line semble pourtant avoir été plus forte qu'à présent (Haywood *et al.* 2008). A la fin du Pliocène

(~2.5 Ma), cependant, le refroidissement s'accentue en Antarctique, et les vents d'Ouest accrus

accompagnent une migration septentrionale de l'APF, accompagnée d'une possible réduction de

la criculation thermohaline (McKay *et al.* 2012).

La plupart des îles subantarctiques se forment durant cette période. Mis à part les archipels conti-

nentaux de Géorgie du Sud et des Malouines (qui sont des reliques du Gondwana, tout comme

l'Amérique du Sud voisine), et du plateau subcontinental des Kerguelen (formé durant

l'Oligocène), les îles subantarctiques sont principalement de jeunes formations volcaniques, qui

s'élèvent directement au-dessus de la plaine abyssale. Crozet, Heard et Macquarie apparaissent en-

1 tre le Pliocène et le Pléistocène (voir un exposé complet dans Quilty 2007). Ainsi, que ce soit en

2 termes d'océanographie ou de géographie, il semble que l'Océan Austral n'ait pris sa forme

3 actuelle qu'au début du Pleistocène.

4 Quoique mieux connue, l'histoire de l'Océan Austral au Pléistocène (~2.6 Ma - 11.7 Ka) et à

5 l'Holocène (~11.7 Ka - présent) est toujours incertaine. Généralement, la reconstruction des

6 processus atmosphériques et océanographiques à ces périodes relativement récentes repose sur

7 deux approches différentes. D'abord, des indices directs ou indirects peuvent être obtenus par le

8 biais de carottes, soit dans le sédiment marin, soit dans la calotte glaciaire, soit dans la tourbe des

9 îles subantarctiques. Par ailleurs, les modèles de circulation générale (GCM) développés pour la

10 période historique peuvent donner de bons résultats pour le passé récent, puisque les caractéris-

11 tiques les plus importantes de la circulation océan-atmosphère peuvent être considérées stables

12 durant cette période : ainsi le Coupled Model Intercomparison Project phase 5 (CMIP5, voir

13 §50) inclut-il des expériences dédiées au Pléistocène et à l'Holocène moyen (voir §50 pour le dé-

14 tail de ces expériences). Les indices sédimentologiques nous fournissent des marqueurs chim-

15 iques, physiques et biostratigraphiques qui servent de révélateurs pour un certain nombre de vari-

16 ables (Gersonde *et al.* 2005; Armand & Leventer 2010; Hodgson *et al.* 2014), soit directement

17 au site de la carotte (comme c'est le cas pour les carottes de sédiment terrestre ou marin - voir

18 Gersonde *et al.* 2005; Martínez Garcia *et al.* 2009; Armand & Leventer 2010), ou pour une com-

19 binaison de sources locales et distantes (Wolff *et al.* 2003; Wolff *et al.* 2006). Les assemblages de

20 diatomées et de foraminifères dans le sédiment marin offrent un indice précis de l'état des masses

21 d'eau de surface, et peuvent être utilisés pour identifier la position de l'APF (comme cela a été fait

22 sur le Plateau de Campbell, voir Neil *et al.* 2004, ou dans l'Océan Indien et l'Atlantique, voir

23 Kemp *et al.* 2010), ou l'étendue de la glace de mer (Hodell *et al.* 2001; Gersonde *et al.* 2005). Les

24 pollens fossiles dans le sédiment marin et terrestre sont aussi de bons révélateurs des conditions

25 climatiques locales (McGlone *et al.* 2010). Des indicateurs chimiques peuvent être extraits de

26 carottes de glace comme de sédiment. Ces différents moyens sont utilisés soit directement, soit

27 comme conditions initiales pour un modèle numérique de climat, pour reconstituer les condi-

tions globales. Cependant, la réconciliation des différentes sources disponibles demeure problématique, tant les signaux peuvent être confondus entre les environnements glaciaires, marins et terrestres (voir Armand & Leventer 2010; McGlone *et al.* 2010).

Malgré des variations locales et des conditions divergentes dans les différents bassins océaniques, il est possible d'identifier quatre périodes majeures dans l'histoire récente de l'Océan Austral - périodes qui semblent cohérentes à l'échelle globale. (i) les conditions du Quaternaire (du Pléistocène moyen à 22 Ka), (ii) le Dernier Maximum Glaciaire (LGM - 21-18 Ka), (iii) la déglaciation de la fin du Pléistocène et l'Optimum Climatique de l'Holocène (17-9 Ka), et (iv) les conditions hypsithermales et néoglaciales de la fin de l'Holocène (8-0 Ka) - voir §101 pour plus de détails sur ces périodes.

§-10 Biogéographie de l'Océan Austral. L'Océan Austral actuel a une biogéographie relativement simple, faite de systèmes généralement zonaux, mais qui abritent pourtant une biodiversité étonnante (Smetacek & Nicol 2005; Chown *et al.* 2015). Quatre régions distinctes se distinguent : (i) la zone *subantarctique*, qui dépasse l'Océan Austral au sens strict, mais lui appartient d'un point de vue biogéographique, et est limitée au sud par l'APF, et au nord par la STC, (ii) la zone de l'*océan antarctique*, au sud de la zone subantarctique, et limitée au sud par la limite sud de l'ACC, (iii) la zone *côtière antarctique* qui inclut le contrecourant antarctique et le plateau continental, aisni que la zone des glaces côtières, et (iv) la *péninsule antarctique* (Convey *et al.* 2012; Terauds *et al.* 2012). Dans cette étude, nous nous concentrerons surtout sur les trois premières zones concentriques. La région Subantarctique se caractérise par des températures plus modérées, d'importantes précipitations, aucune glace de mer, et de forts vents d'Ouest. Les îles sont couvertes de tourbières et de végétation rase, ou un habitat périglaciaire. Les îles subantarctiques sont rares et espacées (du Pacifique vers l'Atlantique : Macquarie, Heard-et-McDonald, Kerguelen, Crozet, Marion-et-Prince-Edward, Bouvet, Sandwichs du Sud, Géorgie du Sud, Terre de Feu et Malouines), et concentrent oiseaux et pinnipèdes. L'Océan antarctique, au sud de l'APF, se caractérise par des eaux de surface beaucoup plus froides, et une importante couverture de glace hivernale - les îles y sont rares et couvertes de glace (Peter I, Scott, Balleny et les Orcades du Sud). La

végétation est rase et limitée aux lichens, hépatiques et mousses (Convey *et al.* 2012). La zone antarctique côtière (Tynan 1998) est quant à elle un environnement de plateau continental, car-actérisé par une couverture de glace quasi-permanente, et une forte influence de la calotte glaciaire antarctique. La végétation y est presque absente, et y fait preuve d'adaptation extrêmes, et la faune vertébrée se limite à un epoignée d'espèces : les manchots Empereur et Adélie, le pétrel des neiges, le pétrel géant, le pétrel antarctique, le fulmar antarctique, le damier du cap, l'océanite de Wilson, le labbe antarctique, et quelques espèces de pinnipèdes. De toutes ces espèces, seul le Manchot Empereur se reproduit l'hiver austral.

Les ressources alimentaires proviennent principalement de deux sources. Comme mentionné plus haut (§7), les vastes zones de résurgence assocées à l'APF sont d'importants contributeurs à la productivité marine globale (Laubscher *et al.* 1993; Bathmann *et al.* 1997; Carr *et al.* 2006), et attirent de nombreuses espèces comme le Manchot royal (Péron *et al.* 2012). La zone de glaces flottantes concentre aussi une vaste productivité primaire (Arrigo *et al.* 1997; Arrigo *et al.* 1998), et constituent une ressource alimentaire importante pour les espèces côtières antarctiques comme le Pétrel des neiges (Barbraud & Weimerskirch 2001) ou le Manchot Adélie (Wienecke *et al.* 2000). Les zones de résurgence côtière d'eau libre dans les polynyes qui bordent la côte (voir §18) sont particulièrement propices à la productivité de plancton, et constituent des zones d'alimenta-tion privilégiées pour plusieurs espèces (Ancel *et al.* 1992; Ancel *et al.* 1999). Ainsi l'une des car-actéristiques les plus remarquables de la biogéographie de l'Océan Austral est-elle son lien presque immédiat avec les caractéristiques climatiques générales. Contrairement aux environnements terrestres, où les complexes interactions de la latitude et de l'altitude ont pour résultat des motifs très hétérogènes (Burrows *et al.* 2011), la structure zonale de l'Océan Austral en accord avec ses grandes structures de circulation annulaires et circumpolaires. La conséquence en est que la distri-bution de ces zones est en lien direct avec les modes de circulation généraux (voir §18).

Réponse des espèces aux changements climatiques

§-11 Le Climat change. Les reconstitutions paléoclimatiques nous apprennent que le changement climatique est, en lui-même, un phénomène naturel et inévitable à l'échelle millénaire (voir §9), et est partiellement lié à des forçages extérieurs (comme les changements dans l'activité solaire, les cycles orbitaux dits de Milankovitch - et leurs rétroactions positives, comme la boucle de la « terre boule de neige », voir Hyde *et al.* 2000; Berger 2013), ou à des modifications biogéniques internes dans la composition de l'atmosphères (voir Frolking & Roulet 2007). Cependant, ces changements se font lentement. Même le dernier maximum glaciaire l'a pas change significativement la structure ou la composition des communautés en Europe (voir Yeakel *et al.* 2013). Les changements climatiques actuels, par contre, se caractérisent par des changements du même ordre que la transition Pléistocène-Holocène, mais sur des intervalles de temps de l'ordre de la décennie, et non du millénaire. Le changement climatique a donc été défini de façon non ambiguë par l'Intergovernmental Panel on Climate Change (IPCC) comme « *un changement dans l'état du climat qui peut être identifié (par exemple par des tests statistiques) par des changements dans l'état moyen et/ou la variance de ses propriétés, et qui persiste pour une longue période de temps, typiquement des décennies ou plus. Le changement climatique peut être dû à des processus naturels internes, ou des forçages externes comme des modulations des cycles solaires, des éruptions volcaniques, ou des changements anthropogéniques persistants dans la composition de l'atmosphère et l'utilisation du territoire* » (Solomon *et al.* 2007). Durant les dernières décennies du XXème siècle, les preuves accumulées montrent clairement l'aspect unique des rapides changements dont nous sommes actuellement témoins, et qui commencent peu de temps après la Révolution industrielle du XIXème siècle. La combinaison de déforestation et d'utilisation à grande échelle de combustibles fossiles a mené l'augmentation de la production, et à la diminution de la fixation, des gaz à effet de serre (GHG), en particulier du dioxyde de carbone et du méthane, au point que « *les concentrations atmosphériques de dioxyde de carbone, et méthane et de protoxyde d'azote sont sans précédent depuis au moins 800,000 ands* » (Pachauri *et al.* 2014). Une concentration accrue de GHG a pour résultat une augmentation de l'effet de serre, c'est à dire du forçage radiatif efficace sur le climat global. De sorte que tous les indices actuels montrent qu'il est « *extrêmement probable que l'influence hu-*

1 *maine a été la cause déterminante du réchauffement observé depuis le milieu du XXème siècle»* (Stock-

2 er *et al.* 2014).

3 Des efforts intenses et coordonnés sont en œuvre à présent pour comprendre les mécanismes

4 sous-jacents, et les issues possibles des changemens actuels (voir §50 pour une présentation des

5 efforts de l'IPCC) - malheureusement, il n'en va pas de même des efforts politiques. Le résultat de

6 cet effort scientifique est une connaissance croissante de l'articulation entre trois différents do-

7 maines : le changement climatique, le changement environnemental, et la météorologie. Quoique

8 profondément connectés, ces trois paradigmes ne devraient pas être confondus. Le Changement

9 climatique est seul l'objet de la définition de l'IPCC, et se limite aux effets visibles dans la circula-

10 tion océan-atmosphère - c'est à dire aux changements de long terme de la température, des pré-

11 cipitations, du régime des vents, etc. Ces phénomènes peuvent être précisément décrits et saisis

12 avec les méthodes de la physiques, comme les modèles de circulation générale océan-atmosphère

13 (AO-GCM, voir §50), dont les limites résident surtout dans notre compréhension de la nature

14 des processus physiques à l'œuvre, ainsi que dans les hypothèses socio-économiques qui gouver-

15 nent nos projections des futures concentrations de GHG. Quoique les AO-GCMs soient de plus

16 en plus efficaces pour prédire l'environnement physique de la Terre au XXIème siècle, la réponse

17 des communautés biologiques, ou «changement environnemental», est un sujet plus complexe

18 (voir §13 sqq. pour un aperçu de ces difficultés), à la fois par manque d'un exemple passé

19 (quoique le réchauffement de l'Holocène soit souvent utilisé comme exemple, son rythme est en

20 effet beaucoup plus lent - voir Petit *et al.* 2008; Blois *et al.* 2013; Moritz & Agudo 2013). Les

21 divers mécanismes par lesquels ces changements affectent les écosystèmes les rendent particulière-

22 ment difficiles à prévoir. Ces effets vont du dérèglement des processus dévelopementaux des

23 organismes de bas niveau trophique par le rachauffement de l'eau (Gregg *et al.* 2003; Behrenfeld

24 *et al.* 2006) ou son acidification (Harvey *et al.* 2013), qui se répercutent aux niveaux trophiques

25 supérieurs (McMahon & Burton 2005), jusqu'au changement des aires de distributions et des

26 réductions de biodiversité qui en résultent (par exemple chez les copépodes arctiques, voir

27 Beaugrand *et al.* 2002). Les écosystèmes marins, tout comme les écosystèmes terrestres, sont déjà

sévèrement affectés apr l'exploitation humaine, qui diminue leur résilience aux changements climatiques (Halpern *et al.* 2008; Watson *et al.* 2013; McCauley *et al.* 2015). L'effondrement de la biodiversité prédit par les scénarios les plus sombres (voir §50) pourrait ainsi toucher de 50 à 70% des océans plus fortement que tous les changements qui ont eu lieu depuis le Pléistocène (Beaugrand *et al.* 2015).

Par ailleurs, de nombreuses études ont étudié les effets du changement climatique en prenant pour modèle la variabilité cyclique du climat, qui est particulièrement prévalente dans les systèmes océaniques (voir §8). Ces études ont souvent exploité le for contraste entre les phases positives et négatives de l'ENSO (par exemple, Le Bohec *et al.* 2008), du SAM (Weimerskirch *et al.* 2012) ou de l'Oscillation d'Atlantique Nord (NAO, Frederiksen *et al.* 2004). C'est souvent une approximation raisonnable, et, de façon importante, souvent la seule possible - cependant, ces oscillations météorologiques ne devraient pas être complètement assimilées au changement climatique. La météorologie, qui est surtout en jeu dans ce cas, est seulement l'interface entre le changement climatique et les espèces. Les phases chaues de l'ENSO reproduisent peut-être précisément les conditions d'une planète réchauffée dans l'Océan Austral, mais pas les mécanismes de téléconnexion plus vastes, par exemple avec l'hémisphère Nord : et ce malgré le fait que le couplage Arctique-Antarctique soit sans conteste un aspect central du changement climatique au sens strict (Barbante *et al.* 2006). Si l'approximation météorologique est souvent une nécessité méthodologique, il convient de garder à l'esprit la différence essentielle entre changement météorologique et changement climatique.

§-12 Particularités du changement climatique dans les régions polaires. Les effets du changement climatique sont particulièrement visibles dans les régions polaires, un fait dû à leurs caractéristiques climatologiques, mais aussi à la structure de leurs communautés biologiques. D'un point de vue purement climatologique (ou «abiotique», voir §49), les régions polaires apparaissent différentes du reste de la planète. Les singularités de la circulation Océan-Atmosphère dans l'Arctique - et tout particulièrement l'abrupt changement d'albedo selon l'étendue de la glace - donne lieu à un phénomène d'*amplification arctique* (Serreze & Francis 2006; Pithan & Mauritsen 2014).

1 L'Antarctique, d'un autre côté, semble plus ambigüe : tandis que la partie orientale paraît « résis-

2 ter » au changement (potentiellement grâce à l'effet tampon de l'Océan Austral, voir Mulvaney *et*

3 *al.* 2012 - quoique les incertitudes liées aux méthodes d'observation puissent masquer la tendance

4 réelle, voir Hanna *et al.* 2013), la partie occidentale et la Péninsule sont au nombre des régions

5 connaissant le réchauffement le plus rapide sur Terre (Mulvaney *et al.* 2012; Bromwich *et al.*

6 2013). Dans l'Océan Austral, le réchauffement accéléré des eaux de surface (Liu & Curry 2010)

7 comme des eaux profondes (Purkey & Johnson 2010) a été directement observé, et es effets de

8 l'influx d'eau douce en provenance de la calotte antarctique sur l'activité de résurgence a de même

9 déjà été documentée (de Lavergne *et al.* 2014). Les connexions globales fondamentales de

10 l'Océan Austral le rendent aussi particulièrement sensible aux changements dans la circulation

11 tropicale, comme l'ENSO (voir §8 et Collins *et al.* 2010). De sorte qu'un effet globalement accru

12 du changement climatique est à craindre.

13 Outre ses caractéristiques physiques, la biogéographie de l'Océan Austral le rend aussi partic-

14 ulièrement sensible aux changements climatiques. Tandis que les habitats devraient généralement

15 se déplacer vers les pôles en réponse au réchauffement (Williams *et al.* 2007; Fraser *et al.* 2012 et

16 §15), les écosystèmes polaires ont relativement peu de marge pour se déplacer, et les hautes lati-

17 tudes devraient devenir des zones de « subduction cilmatique » (Burrows *et al.* 2014), où les habi-

18 tats se contractent et finissent par disparaître, plutôt que de se déplacer plus avant (§15). Ce

19 phénomène est encore compliqué par le fait que l'activité humaine a fortement influencé l'Océan

20 Austral depuis le bas de la chaine trophique (c'est à dire *via* le changement climatique anthro-

21 pogène et la réduction de productivité primaire associée), comme depuis le haut (par le massacre

22 des prédateurs supérieurs - baleines, phoques ou manchots - voir Ainley *et al.* 2007), ce qui

23 donne lieu à des effets combinés et complexes (Smetacek & Nicol 2005 - voir aussi l'exemple

24 concret et spectaculaire donné par Trivelpiece *et al.* 2011).

25 Par conséquent, les régions polaires, en apparence intactes, concentrent désormais en réalité les

26 effets du changement climatique. De nombreuses années durant, l'opinion générale fut que les

27 écosystèmes polaires étaient plus simples, et basés sur des chaines trophiques plus courtes, que les

1 écosystèmes des basses latitudes - menant aisni à des bouleversements plus facilement intelligi-

2 bles. Cependant, il est à présent admis que la diversité taxonomique et la complexité du réseau

3 trophique sont aussi élevés que dans les régions tempérées (Smetacek & Nicol 2005; Chown *et al.*

4 2015 et Fig. 6), et il est probable que la particularité apparente des régions polaires ne soit dûe à

5 rien d'autre qu'à leur destruction plus tardive, garantie par leur inaccessiblité - et non à quelque

6 caractéristique particulière qui y favoriserait la mégafaune, par exemple. Smetacek & Nicol 2005

7 ont ainsi proposé que ces régions soient considérées comme un vestige des écosystèmes marins

8 préhistoriques - un «*Serengetis des mers*». De sorte que les processus que nous voyons à l'œuvre

9 dans les régions polaires ont déjà eu lieu depuis longtemps sous les tropiques, et sont les mêmes

10 qui sont à l'œuvre en Afrique continentale, avec le déclin de la macrofaune mammifère et son

11 remplacement par l'exploitation humaine omniprésente.Une question cependant reste en suspens

12 - le changement climatique est-il spécial en lui même dans les régions polaires, au delà de son ry-

13 thme accéléré ; ou ses effets sur les communautés biologiques sont-ils surtout le résultat de la rela-

14 tive intégrité de ces communautés encore peu anthropisées ?

15 *§-13 Réponse des espèces au changement climatique.* L'importance des changements globaux actuels

16 sur les communautés biologiques est reconnu par l'ensemble de la communauté scientifique (voir

17 §11 et Thomas *et al.* 2004; Warren *et al.* 2013; Pacifici *et al.* 2015), mais le détail de leurs im-

18 pacts est encore matière à débat (Pereira *et al.* 2010; He & Hubbell 2011; Pacifici *et al.* 2015).

19 Les différents niveaux auxquels les impacts se produisent (qui vont de la physiologie à l'organisa-

20 tion des communautés, voir §11), la complexité des interactions biotiques (Davis *et al.* 1998;

21 Norberg *et al.* 2012; Midgley & Bond 2015), et le caractère idiosyncratique de la sensibilité et de

22 l'exposition de chaque espèce (Moritz & Agudo 2013; Comte *et al.* 2014; Dickinson *et al.* 2014)

23 contribuent à l'apparente hétérogénéité des réponses au niveau des écosystèmes (Parmesan &

24 Yohe 2003). La plupart des études, cependant, s'accordent sur l'idée que trois mécanismes fonda-

25 mentaux interagissent dans la détermination de la réponse d'une espèce au changement : (i) la

26 microévolution adaptative par sélection naturelle (Bradshaw & Holzapfel 2006; Hoffmann &

27 Sgrò 2011), (ii) la plasticité phénotypique et en particulier les changements de phénologie (Char-

mantier *et al.* 2008; Hoffmann & Sgrò 2011) et (iii) les changements de distribution pour suivre les isohabitats (Walther *et al.* 2002; Chen *et al.* 2011; VanDerWal *et al.* 2013).

§-14 Micro-évolution et plasticité phénotypique. La micro-évolution et la plasticité phénotypique partagent une structure commune : afin de s'adapter à son environnement local, une espèce change ses caractéristiques physiologiques, phénologies, ou généralement comportementales (Hoffmann & Sgrò 2011). Les mécanismes impliqués, par contre, sont très différents. Une réponse micro-évolutive nécessite un certain nombre de générations, par sélection des traits héritables conférant un meilleur avantage (et déterminés soit génétiquement, soit épigénétiquement) : c'est donc un processus de population. La plasticité phénotypique, par contre, est un phénomène individuel. Soit par des modifications développementales, soit par des processus purement comportementaux, chaque individu optimise sa valeur sélective dans les conditions présentes - mais son nouvel état n'est pas héritable, si nous laissons de côté la relativement marginale (dans l'état actuel des connaissances) transmission culturelle des comportements (Whitehead & Rendell 2014).

Des réponses évolutives au changement lcimatique anthropogénique ont déjà été mises en évidence chez plusieurs espèces à temps de génération court, comme les moustiques (Gienapp *et al.* 2008; Hoffmann & Sgrò 2011). Cependant, aucune étude conduite sur des vertébrés n'a encore pu mettre au jour de processus évolutif clair (soir Møller *et al.* 2010 pour un exposé complet chez les oiseaux). Le décalage entre le rythme rapide du changement, les temps de génération plus longs des vertébrés, et leurs stratégies reproductices généralement de type K, rend la tâche ardue pour la sélection naturelle.

La plasticité, d'un autre côté, joue un rôle important dans la réponse de court terme de nombreuses espèces (Charmantier *et al.* 2008; Hoffmann & Sgrò 2011). Elle affecte en priorité la phénologie, afin de conserver une synchronisation avec les conditions météorologiques, et en particulier le pic de nutriments, comme cela a été démontré chez la mésange charbonnière *Parus major* (Charmantier *et al.* 2008; Husby *et al.* 2010) ou le Gobemouche à collier (*Ficedula hypoleuca*,

Dunn *et al.* 2010), mais aussi chez certaines plantes (Anderson *et al.* 2012). Mais elle affecte aussi les traits métaboliques (McKechnie *et al.* 2006; Nicotra *et al.* 2010) ou la morphologie (Przybylo *et al.* 2000). La structure hautement dynamique de l'Océan Austral fait de la phénologie un mécanisme central pour al survie de la plupart des espèces. Les variations saisonnières de la température causent un déplacement cyclique de l'APF (voir §7), et changent ainsi la distance entre les terrains d'alimentation et les aires de reproduction pour de nombreuses espèces (Massom *et al.* 2009; Bost *et al.* 2015). Elles déterminent la force des résurgences et par conséquent la productivité marine, jusque dans le courant de Humboldt (Thiel *et al.* 2007). Ainsi, tout comme la synchronisation avec le pic d'abondance des insectes est un facteur de succès reproducteur crucial pour de nombreux oiseaux terrestres (Dunn *et al.* 2010), les variations saisonnières des aires d'alimentation dans les systèmes océaniques sont probablement une contrainte majeure pour leur phénologie, et son évolution devrait amener un changement dans la phénologie de plusieurs espèces. De tels changements, cependant, ont un coût (Van Buskirk & Steiner 2009), et augmentent la probabilité d'une désynchronisation entre différentes contraines écologiques (Both *et al.* 2006) - la plasticité a donc ses limites (Visser & Both 2005; Both *et al.* 2006; Møller *et al.* 2008).

En résumé, les réponses micro-évolutives, qui nécessitent une sélection, à une échelle multigénérationnelle, de variantes génétiques pré-existantes, sont un processus de temps long. Elles ont été mises en évidence chez plusieurs espèces à courte durée de vie (Van Heerwaarden & Hoffmann 2007; Hoffmann & Willi 2008; Hoffmann & Sgrò 2011; Krehenwinkel *et al.* 2015), mais l'extrême vélocité des changements actuels (Mahlstein *et al.* 2013; Poloczanska *et al.* 2013; Burrows *et al.* 2014) est und éfi majeur pour les espèces à longues générations (Hoffmann & Sgrò 2011) et faible diversité génétique (Norberg *et al.* 2012), et ce d'autant plus que ces deux caractères sont souvent corrélés (Romiguier *et al.* 2014). La mmicro-évolution et la plasticité sont, de plus, interconnectés : et seule l'ampleur de l'héritabilité permet actuellement de les distinguer (Réale *et al.* 2003), d'autant plus que la plasticité elle-même est un trait héritable (Nussey *et al.* 2005; Pelletier *et al.* 2007).

1 Dans cette étude, cependant, le rythme des changements et les traits d'histoire de vie des oiseaux

2 de mer excluent, a priori, toute réponse évolutive forte. Une réponse plastique est possible, et

3 même souhaitable. Mais son étude dépasse le cadre de ce travail, puisqu'elle décessite des données

4 transgénérationnelles actuellement indisponibles. Jusqu'à présent, des indices convaiquants ont

5 été trouvés chez des espèces à courtes génératiosn (Charmantier *et al.* 2008) - mais des décennies

6 d'observation phénologiques et comportementales seront nécessaires pour construire une image

7 claire chez les oiseaux marins.

8 *§-15 Déplacement d'habitat et de distributions.* Les déplacements de distributions semblent de plus

9 en plus centraux dans les réponses de court terme au changement climatique (Davis & Shaw

10 2001; Chen *et al.* 2011; Burrows *et al.* 2014). Quoique l'expression principale de la réponse plas-

11 tique se concentre sur la phénologie (§14), c'est à dire sur le cadre *temporel* du cycle reproducteur

12 des espèces ou des populations, les déplacements de distributions représentent un changement de

13 son cadre *spatial*. Par opposition à la micro-évolution et à la plasticité, ce déplacemnt implique

14 uniquement un changement géographique, a priori sans contraintes physiologiques ou autres -

15 cependant, les cas de déplacements «pur», non associés à des changements de phénologie, sont

16 rares (Møller *et al.* 2010). Les déplacements de distributions sont l'expression de facteurs allant

17 de l'échelle de l'individu à celle de l'espèce. A un niveau fonctionnel, le *conservatisme de niche*

18 peut être défini comme la tendance, pour un individu, à demeurer à l'intérieur de sa zone de con-

19 fort physiologique et écologique (Wiens *et al.* 2010). Selon la largeur de cette niche, et le po-

20 tentiel d'évolution de l'espèce, le conservatisme de niche peut se vérifier pendant de très longues

21 périodes. Par exemple, les oiseaux du Nouveau Monde sont un exemple frappant de conser-

22 vatisme de niche à l'échelle géologique, dans la mesure où les taxa les plus apomorphiques occu-

23 pent les niches les plus spécialisées (Hawkins *et al.* 2006), tandis que des structures similaires

24 s'observent aussi chez les poissons d'eau douce (Comte *et al.* 2014) ou les mammifères terrestres

25 (Martínez Meyer *et al.* 2004). Ce conservatisme de niche dans le temps long signifie que les

26 préférences d'habitat ne évoluent lentement, et peuvent être héritées phylogénétiquement dans

27 un taxon, ralentissant la colonisation de nouveaux habitats.

A des échelles de temps plus courtes, au contraire, le conservatisme de niche est la force principale qui pousse les individus à suivre leur habitat plutôt qu'à s'adapter à de nouvelles conditions. En ce sens, les espèces *suivent leur habitat* - un mouvement par lequel une population entière se déplace avec ses conditions environnementales. Le suivi d'habitat, observé depuis une perspective humaine, résulte dans le *déplacement des distributions*, une modification globale de la distribution géographique de l'espèce en réponse aux tendances de son habitat. Le réchauffement climatique, par exemple, a pour résultat typique (quoique schématique) un déplacement des habitats et des espèces vers les pôles, ou les sommets (Jump *et al.* 2009; Fraser *et al.* 2012).

Dans un système idéal, on peut s'attendre à ce que les espèces suivent leur habitat de façon linéaire (Scheffer *et al.* 2001). Cependant, le caractère anisotropique des biozones implique que les habitats ne se transforment pas de façon homogène (Diffenbaugh & Field 2013), et que les changements sont vraisemblablement doubelemtn hétérogènes - entre écosystèmes, et entre espèces à l'intérieur des écosystèmes. Une étude récente sur les oiseaux australiens (VanDerWal *et al.* 2013), par exemple, a montré que durant les 60 dernières années, les déplacements de distributions ont suivi des trajectoires majoritairement idiosyncratiques à l'échelle du continent, et qui ne reflètent que partiellement les déplacements d'habitats. Un tel exemple montre l'importance des interactions biotiques dans la détermination de la distribution des espèces : plusieurs relations interspécifiques peuvent être affectées simultanément par le changement climatique (par exemple le comportement alimentaire - voir Charmantier *et al.* 2008, ou la compétition - voir Stenseth *et al.* 2015), avec pour résultat des réponses non linéaires et parfois paradoxales (comme c'est le cas pour la Bernache nonnette *Branta leucopsis*, voir Bauer *et al.* 2008; Eichhorn *et al.* 2009). Ainsi, la compréhension des distributions présentes et futures est presque impossible si l'on se limite à l'étude d'une seule espèce (par exemple dans une approche de type «envelope climatique», voir Pearson & Dawson 2003), et doit au contraire être étendue pour intégrer les interactions biotiques les plus importantes (un point développé au §49).

L'hétérogénéité et l'idiosyncrasie des déplacements de distributions est exacerbé à chaque fois que les discontinuités de l'environnement provoquent des *convergences d'habitat* (Burrows *et al.* 2014)

ou «subductions», par exemple lorsque des corridors climatiques où les déplacements d'habitats pourraient, en théorie, se faire de façon linéaire, sont interrompus par des barrières osit naturelles, soit anthropogéniques. La fragmentation des habitats, qui est souvent le résultat des influences humaines (mais qui peut être naturelle, voir par ex *The King synnome*) interagit donc avec le changement climatique pour donner lieu à des conséquences souvent imprévisibles. Ceci est particulièrement vrai autour des «gouffres climatiques» où les condition slocales disparaissent tout de bon (Burrows *et al.* 2014). De plus, les espèces elles-mêmes ne répondent aps nécessairement de façon linéaire aux déplacements d'habitats : des capacités de dispersion insuffisantes, par exemple, peuvent conduire à des déplacements décalés (Bertrand *et al.* 2011; Schloss *et al.* 2012), une compétition accrue autour des zones de gouffre peut empêcher l'expansion de la distribution de certaines espèces (Norberg *et al.* 2012), et des mécanismes compensatoires peuvent masquer pour un temps les effets du changement jusqu'à atteindre un point de bascule (Doak & Morris 2010). Ces effets retardés peuvent nous pousser à sous-estimer l'importance des changements à l'œuvre, et placer les espèces en situation de dette climatique, laissant finalement place à des effondrements d'écosystèmes (Scheffer *et al.* 2001; Hoegh-Guldberg & Bruno 2010; Barnosky *et al.* 2012).

Ainsi, les régions polaires, qui traversent une période de changements accélérés (Serreze & Francis 2006; Turner *et al.* 2014; Chown *et al.* 2015) et ont une marge de manœuvre très limitée pour les déplacements d'habitats sont un exemple emblématique de ces problèmes (Williams *et al.* 2007). Détecter les réponses délayées avant d'atteindre leur point de bascule est une priorité si nous voulons développer des stratégies de mitigation appropriées, et prédire avec précision les distributions d'espèces futures pour y préparer des réserves environnementales (Keppel *et al.* 2012; Hope *et al.* 2013; Watson *et al.* 2013), en particulier pour les prédateurs supérieurs, qui déterminent dans une large mesure les propriétés de résilience des écosystèmes (Soulé *et al.* 2003; Heithaus *et al.* 2008) afin de développer des stratégies de conservation et de gestion efficaces. Ainsi, la prédiction des changements de distribution apparaitêlle encore comme un défi majeur dans le domaine de la modélisation biologique.

Objectifs de cette étude

§-16 Les Echelles du changement. L'un des aspects les plus déroutants de la biologie du changement climatique est le labyrinthe d'échelles dans lesquelles il se déploie. Les études actuelles oscillent souvent entre deux extrêmes : une approche de « temps long », dans lequel les changements climatiques « géologiques » (tels que la transition Pléistocène-Holocène) sont prises pour exemple des changements anthropogéniques actuels, et une de « temps court », dans lequel la stochasticité météorologique comme ses phénomènes cycliques (par exempl l'Oscillation d'Atlantique Nord, ou NAO) sont utilisés à la même fin. Dans ce contexte, ce qui rend particulièrement difficile la compréhension des changements climatiques actuels est qu'ils se déroulent à une échelle pour laquelle nous n'avons que peu de concepts, parce qu'ils n'ont pas de précédent dans l'histoire de la Terre : ils nous forcent à trouver un intermédiaire entre le temps écologique et le temps évolutionniste. Une question centrale est donc de savoir si les observations que nous pouvons obtenir sur le temps long (par exemple en paléodémographie) sont de même nature que celles que nous obtenons sur le temps court (par exemple du suivi de terrain) - et si l'une ou l'autre de ces observations peut expliquer et prédire les événements résultat des changements climatiques anthropogéniques. Par bien des aspects, il semble que les observations quasi-instantanées que nous pouvons faire sur des populations d'étude, et qui s'étendent, au mieux, sur quelques générations, sont dominées par plusieurs niveaux de stochasticité et de forçages mixtes - la stochasticité et les cycles de la météorologie autour des grandes tendances du climat, la stochasticité de la démographie autour des trajectoires générales des populations et des espèces, la restructuration lente mais chaotique des écosystèmes alors que leurs éléments évoluent dans des directions différentes - tous ces signaux contradictoires peuvent masquer pour quelques temps la tendance inévitablement directionnelle du changement climatique. De l'autre côté de ce spectre, pourtant, la paléodémographie, qui lisse tous ces événements stochastiques, et ces cycles de hautes fréquences, n'en conserve que les motifs les plus lents, comme la lente pulsation des glaciations du Pléistocène, qui laissent

1 à l'évolution le temps de se réaliser. Mais elle pourrait, de ce fait, être totalement impuissante à

2 saisir le mouvement relativement rapide des changements actuels.

3 Pour ces raisons, ce qui se passe réellement dans une situation telle que les changements clima-

4 tiques anthropogéniques actuels peut être conçu comme une disruption du rythme et de la

5 manière selon laquelle ces différentes échelles sont articulées, et une probabilité croissante de dé-

6 calage entre les différents niveaux de variation spatiale et temporelle. La durée d'une génération,

7 par exemple, peut de façon simpliste être considérée comme le laps de temps durant lequel les

8 conditions environnementales sont intégrées par un individu qui est soumis à la sélection na-

9 turelle : cette durée est suffisante pour faire la moyenne des saisons, voire des modes climatiques -

10 mais assez courte pour qu'un grand nombre de générations s'écoulent afin de laisser place à l'évo-

11 lution au long des changements géologiques. Un changement au rythme plus serré a de fortes

12 chances de mettre à mal cette synchronisation. De même, l'organisation dans l'espace des indi-

13 vidus et des espèces reflète l'étendue au sein de laquelle les conditions les rendent les mieux adap-

14 tés (voir §49), et la taille et la mobilité des individus est adaptée à cet espace : là encore, la con-

15 vergence ou la divergence des habitats brise cet équilibre. Ainsi, par bien des aspects, il semble

16 que la clef de la compréhension des changements climatiques contemporains soit la façon dont

17 les différents paradigmes chronologiques et spatiaux s'articulent pour les écosystèmes, les espèces

18 et les individus.

19 *§-17 Comprendre les échelles do'rganisation des oiseaux de mer.* Le but principal de notre travail sera

20 de comprendre l'organisation des différentes échelles spatiales et temporelles dans la démographie

21 et la dynamique des espèces d'oiseaux de mer - un groupe aux premières lignes du changement

22 climatique (voir §18) - en se basant sur le contraste de trois espèces : le manchot Royal (*Apten-*

23 *odytes patagonicus*), le manchot Empereur (*Aptenodytes forsteri*) et la puffinure de Garnot (*Pele-*

24 *canoides garnotii*). Si notre étude se place principalement dans une perspective évolutioniste, en

25 s'appuyant sur les outils de la génétique des populations, nous explorerons aussi une large gamme

26 d'approches complémentaires - comme le suivi par marquage individuel, ou la modélisation

27 d'habitats. Pour chacune des deux espèces du genre *Aptenodytes*, nous présentons deux études

complémentaires - l'une centrée sur des processus globaux, et ancrée dans les données de la génomique (voir *The King Synnome* et *The Emperor Synnome*), et l'une centrée sur les phénomènes de corut terme, à l'échelle de la génération (voir *Fine-scale structure* et *Empirical evidence for heterogeneous dispersal*). Ces deux approches sont combinées dans l'étude plus exploratoire de la Puffinure de Garnot (*Unexpected philopatry*).

(i) La biogéographie comparée de ces trois espèces sert de base à l'étude. Une première tâche sera donc de comprendre comment la distribution de chaque espèce s'organise, à des échelles allant de la diversité intra-coloniale, à l'île, à la distribution complète - et d'établir ce qui semble être l'unité d'étude démographique la plus pertinente pour l'étude des changements passés, présents et futurs. Cette première direction impliquera aussi une révision des estimations de taille de population, de structure, et, dans le cas du manchot Royal, de la diversité taxonomique.

(ii) Des prédictions plutôt sombres ont été formulées pour ces trois espèces, face au changement environnemental. Le manchot Empereur a récemment été déclaré condamné dans toutes son aire de distribution (Jenouvrier *et al.* 2014), la colonie principale, et la mieux étudiée, du manchot Royal semble montrer des perspective pessimistes (Le Bohec *et al.* 2008; Péron *et al.* 2012), et la Puffinure de Garnot a été classée *Menacée* en 1994 sur la liste rouge de l'IUCN. Cependant, afin d'obtenir une meilleure compréhension de la dynamique des populations d'oiseaux de mer, nous devrons procéder à une ré-évaluation critique de ces prédicitons, et à une intégration des différentes méthodes qui y ont conduit. Dans ce but, nous utilisons toute l'information disponible sur la mieux connue de ces trois espèces, le manchot Royal, et proposons une interprétation alternative de la réponse du manchot Empereur aux changements de l'Océan Austral. Dans ces deux cas, nous tenterons de proposer une projection consensuelle, basée à la fois sur des observations de long terme et de court terme, comme une tentative de solution au délicat problème de l'intégration des données écologiques et évolutives dans le contexte du changement climatique.

Robin CRISTOFARI

Structure and dynamics of the penguin synnomes

Résumé

L'Océan austral est l'un des pivot des écosystèmes et du climat de notre planète, qui concentre plus de 20% de la productivité primaire marine mondiale. La complexité de ses réseaux trophiques et son inacessibilité rendent plus encore qu'ailleurs nécessaire l'utilisation d'espèces bio-indicatrices. Plusieurs espèces de manchots (comme le Manchot Royal et le Manchot Empereur) sont ainsi l'objet de programmes de suivi à long terme.

Dans cette étude, nous utilisons les données offertes par la génomique des populations (« RAD-sequencing » couvrant le génome de centaines d'individus issus couvrant la distribution de ces deux espèces) et les représentations numériques du climat de l'IPCC-CMIP5 pour calibrer dans le temps long les analyses démographique plus précises réalisées à l'échelle de quelques générations dans le cadre de suivis démographiques, et mieux comprendre la réponse des manchots au changement climatique.

Au-delà de ses conséquences immédiates pour l'étude des Manchots en tant que sentinelles de l'Océan Austral, cette étude montre l'intérêt d'une plus forte intégration de la génomique des populations dans les études démographiques et comportementales.

Mots-clefs : *génétique des populations, RAD-sequencing, océan austral, sphéniscidés, changement climatique.*

Résumé en anglais

The Southern Ocean plays a central role in the regulation of the Earth's climate and ecosystems, and accounts for more than 20% of the world's marine productivity. The complexity of its trohpic networks and its sheer inaccessibility make the use of bioindicator species more necessary there than anywhere else. Several penguin species (such as the King and the Emperor penguin) are therefore the focus of long-term monitoring programs.

In this study, we use the information from population genomics (« RAD-sequencing » data covering the genome of hundreds of individuals from the two species' full distribution) and from IPCC-CMIP5 numerical climate models to calibrate in the long time the more precise demographic analyses realised in the framework of field surveys, and understand penguin responses to cliamte change.

Beyond its implications for the study of penguins as sentinels of the Southern Ocean, our work demonstrates the interest of a stronger integration of population genomics in demographic and behavioural investigation.

Keywords: *population genetics, RAD-sequencing, Southern Ocean, spheniscids, climate change.*